Dynamical Congestion Control Strategies for a Network of Multi-Agent Systems Subject to Differentiated Services Traffic

Ruiru Chen

A Thesis

in

The Department

of

Electrical and Computer Engineering

Presented in Partial Fulfillment of the Requirements

for the Degree of Doctor of Philosophy at

Concordia University

Montréal, Québec, Canada

February 2011

CONCORDIA UNIVERSITY
SCHOOL OF GRADUATE STUDIES

This is to certify that the thesis prepared

By: **Ruiru Chen**

Entitled: **Dynamical Congestion Control Strategies for a Network of Multi-Agent Systems Subject to Differentiated Services Traffic**

and submitted in partial fulfillment of the requirements for the degree of

Doctor of Philosophy

complies with the regulations of the University and meets the accepted standards with respect to originality and quality.

Signed by the final examining committee:

Dr. T. Fevens	Chair
Dr. S. M. Djouadi	External Examiner
Dr. W. F. Xie	External to Program
Dr. S. Hashtrudi Zad	Examiner
Dr. M. K. Mehmet Ali	Examiner
Dr. L. Rodrigues	Examiner
Dr. K. Khorasani	Thesis Supervisor

Approved by

Dr. M. Kahrizi
Chair of Department or Graduate Program Director

Dr. R. Drew
Dean of Faculty

ABSTRACT

Dynamical Congestion Control Strategies for a Network of Multi-Agent Systems
Subject to Differentiated Services Traffic

Ruiru Chen, Ph. D.

Concordia Unviersity, 2011

This research focuses on the congestion control problem for a network of multi-agent
systems (NMAS) having differentiated services (Diff-Serv) traffic. Our goal is to present
a formal framework for design of a control theoretic and rigorous solution to this problem
by taking advantage of recent advances in multi-agent systems. The congestion control
problem is defined as the one dealing with fair, effective and dynamic regulation of the
network resources for avoiding the loss of Quality of Service (QoS) requirement. The
dynamic approaches presented in this work utilize concepts and scheme from nonlinear
control theory, robust adaptive estimation techniques, switching control techniques, and
quadratic regulation methodologies. The traffic transmission, propagation, processing,
and queuing latencies of the network are incorporated and manifested as unknown and
time-varying delay variables in the dynamic models of the NMAS. The limitations on
the physical resources of the communication network such as the buffer size, bandwidth,
and link capacity are all taken into account and incorporated as constraints on inputs and
network states. Consequently, the congestion control problem of each traffic type (namely,
the Premium services and the Ordinary services) in the Diff-Serv NMAS is casted as the
control of a nonlinear constrained system with multiple and unknown time-varying delays.
Two different strategies, namely the *switching congestion control* (SCC) approach and
the *guaranteed cost congestion control* (GCC) approach are proposed, developed, and
compared in this thesis.

In the *switching congestion control* (SCC) approach, the physical constraints of the
network are considered *before* the controller design. A set of fixed structured controllers

are designed that are switched according to the overall system operating conditions. The closed-loop system is shown to experience multiple modes. The stability and performance requirements of the closed-loop switched system are then guaranteed by satisfying a corresponding set of Linear Matrix Inequality (LMI) conditions. On the other hand, in the *guaranteed cost congestion control* (GCC) approach, the physical constraints are considered *after* the controller design, as a group of complementary stability and stabilization conditions. A quadratic cost function containing measures of both the queuing errors and the control effort is introduced for each traffic class (namely, the Premium traffic and the Ordinary traffic). Lyapunov theory is used to ensure that an upper bound of the corresponding cost function is obtained. This will guarantee that a specified QoS is achieved with a bounded cost. The resulting congestion control synthesis method is known as the *guaranteed cost control*. Corresponding to the SCC and GCC approaches, three different control schemes namely, (a) centralized, (b) decentralized, and (c) distributed control are developed, respectively. The overall organization of the thesis is as follows.

First, centralized and decentralized switching congestion control (SCC) strategies are proposed for a Diff-Serv network subject to resource constraints and unknown multiple and time-varying delays having a fixed network topology. The proposed congestion control strategies are then generalized to the mobile network application. The changes of the network topology are modeled stochastically by a Markovian jump process. Subsequently, a mode-dependent congestion control strategy is proposed and developed for each traffic class.

Second, centralized and decentralized guaranteed cost congestion control (GCC) schemes are developed for a Diff-Serv network subject to resource constraints that can ensure a robust performance in presence of unknown multiple and time-varying delays for fixed network as well as mobile network topologies.

Third, by incorporating the scenario where the controllers are communicating among them, a *distributed* congestion control scheme is proposed and developed for mobile networks with Diff-Serv traffic. The proposed distributed congestion controller is shown to be equivalent to a local state-feedback law that is augmented with a nearest neighboring

controller having a proportional adjustable gains. The proposed distributed congestion control strategy is then evaluated and compared with the centralized and decentralized control approaches as far as the QoS performance and control efforts metrics are concerned.

Finally, the robustness of the proposed SCC and GCC strategies for both fixed and mobile networks are evaluated with respect to uncertainties in the system parameters and unmodeled dynamics in the queuing models. The robustness performance properties of the centralized, the decentralized, and the distributed schemes for both the fixed and the mobile networks, as well as for the premium and the ordinary traffics are investigated and evaluated extensively through simulation studies.

Dedicated to

My parents, Shangheng Chen and Airong Chen

My husband, Qingyuan Li

with love and gratitude.

ACKNOWLEDGEMENTS

TABLE OF CONTENTS

List of Figures

xvi

List of Tables

List of Symbols and Abbreviations

NMAS	Network of Multi-Agent System
DiffServ	Differentiated Services
IETF	Internet Engineering Task Force
LMI	Linear Matrix Inequality
SN	Sensor Network
SAN	Sensor Actuator Network
S-DM-A	Sensor, Decision Maker, Actuator Netowrk
MAHN	mobile Ad Hoc Network
UAV	Unmanned Aerial Vehicles
UGV	Unmanned Ground Vehicles
UUV	Unmanned Underwater Vehicles
NASA	National Aeronautics and Space Administration
QoS	Quality of Serive
QoP	Quality of Performance
AQM	Active Queue Management
VBR	Variable Bit Rate Traffic
CBR	Constant Bit Rate Traffic
IDCC	Integrated Dynamic Congestion Controller
SCC	Switching Congestion Control
GCCC	Guaranteed Cost Congestion Control

Chapter 1

Introduction

Efficient and reliable information communication has become an important consideration in both military and commercial applications, as more and more coordinations and exchanges are required to realize and accomplish tasks over a large area with a number of geometrically distributed devices. The technological advances in embedded systems and communication networks have given birth to devices with sensing, processing, actuating, and communicating capabilities. These kind of devices are usually refereed to as "intelligent agents". An intelligent agent is defined as an autonomous entity which observes and acts upon an environment and directs its activity towards achieving goals. The important characteristics of an intelligent agent are [4], [5], [6]:

1. Intelligence. Intelligent agents have a certain degree of specific domain knowledge with which they are capable of reasoning and learning. This capability requires the agent to have access to a knowledge base, as well as an inference engine for reasoning. The capability of learning determines the adaptive behavior of an agent in the sense that it can effectively handle new situations or contexts.

2. Autonomy. Intelligent agent act autonomously without the involvement of human. Autonomous behavior means that agents are not only passively driven by external events from the environment, but also be able to perform a serials of actions that is in line with the objectives it is supposed to pursue.

3. Mobility. Since the agents are not restricted and have to move to the destination place where they are supposed to carry out tasks, the intelligent agents may have a certain degree of mobility. In the context of distributed processing and load balancing, mobility is an attractive capability. Another advantage of mobility is that the possibility of having agents keeping functional after the location it originated from has gone off-line.

4. Communicative or social behavior. Intelligent agents are able to interact with other agents. Social ability connotes more than the simple passing of data between different software and hardware entities. It connotes the ability to negotiate and interact in a cooperative manner. The communications among intelligent agents is normally created by an agent communication language (ACL) [7], which allows agents to converse rather than simply pass data.

When the intelligent agents exist in a distributed fashion and communicate over networks, they can be used to monitor and control a remote physical environment without an extensive involvement of humans. This kind of system is referred to by the term **Network of Multi-Agent Systems (NMAS)**. Over the past few years, NMAS has become a crucial technology for effectively exploiting the increasing availability of diverse, heterogeneous and distributed information sources. The main challenge in NMAS is that the agents in the network must be able to perceiving, reasoning, learning, evolving, interacting and cooperating with their environment and with other nodes in order to achieve system wide goals. These challenges have been in the heart of NMAS research from its inception.

The NMAS are able to solve the problems which are difficult or impossible for individual agent to solve. During the past few years, considerable efforts and investments have been made to provide suitable and satisfactory solutions to the technological problems associated with the networks of multi-agent systems in fields of industrial automation, process control and networked unmanned vehicles. To study communication over NMAS, each agent is regarded as a single node. Each node which may consist of several

2
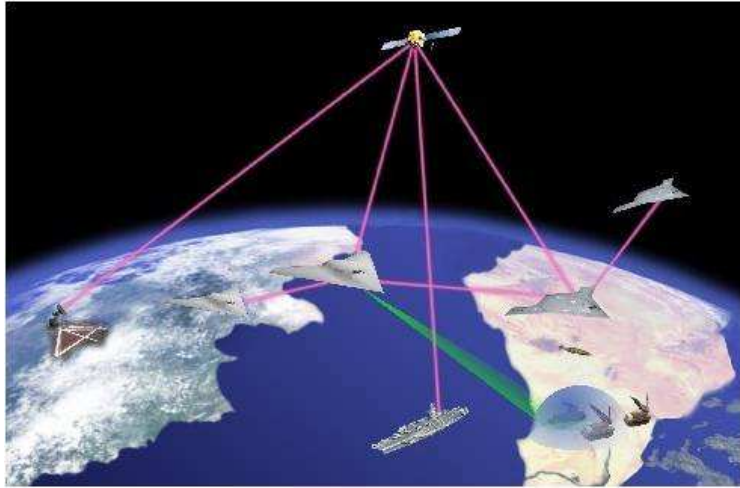
Figure 1.1: A network of unmanned vehicles [1]

sensors, actuators and decision makers, should communicate and exchange information, process the received information and make a decision autonomously while collaborating with other nodes to accomplish a mission. In this sense, the NMAS can be reviewed as a sensor/decision maker/actuator network, where sensors collect data from environment and actuators process the data and perform actions. Usually the sensors and actuators are highly mobile and have powerful energy resources, processor and memory to perform both decision making and actuation.

1.1 Motivation and Applications

Among the large number of applications for NMAS, networked unmanned vehicles, such as unmanned aerial vehicles (UAV), unmanned ground vehicles (UGV), and unmanned underwater vehicles (UUV), is one of the most complicated domains and of significant interest by governmental agencies and military services in the world. Figures 1.1 and 1.2 show a simulated framework for a NMAS that is composed of UAVs, UUVs and UGVs, where the autonomous systems from space, air, ocean and land cooperate with one other. In this system, the unmanned vehicles expand tactical missions such as search and rescue, surveillance, localization and tracking. The group of UAVs can carry payloads to
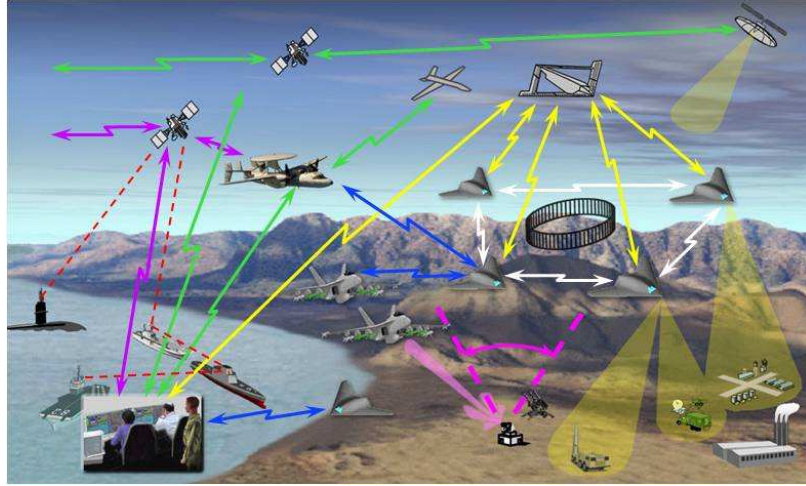
Figure 1.2: A network of unmanned vehicles [2]

areas where it might be dangerous for a human to go, and they can transit between operating stations at high speeds, allowing for quick response to changing situations. The space-to-ground collaborations among the vehicles create a robotic mission system to perform complex tasks over large unknown areas. In such an arrangement, effectiveness is increased by utilizing the benefits of UAVs and UGVs or UUVs. Therefore, major challenges are present for communication and control among multiple networks with different network sizes and transmission speeds. As the number of vehicles increase in the system to cover a larger interested area and to accomplish more sophisticated tasks, the information exchanges among vehicles become more complicated and challenging. Actually, each unmanned vehicle is responsible for multiple operations of sensing, processing and actuating. Therefore, how to guarantee the efficient and reliable communication among the vehicles is a necessary and a critical objective for the NMAS to guarantee flexible operations and successful mission accomplishments.

1.2 Research Challenges

The applications of NMAS have raised serval research problems in various domains. Among them are the following main challenges:

1. **Platforms**. NMAS consists of intelligent agents which may include groups of sensors, decision makers and actuators. The necessity to develop these devices that can interact with each other is fundamental to the development of flexible, extensible and open architectures. For this reason, platform choice is extremely important for NMAS. Many research groups in both academia and industry have devoted to the development of such platform. Such as the TinyOS for sensor networks which is developed by the Berkeley motes [8]; the NesC [9] which is a C language extension of TinyOS; and the Java Agent Development Framework (JADE) developed by the authors in [10], [11] .

2. **Localization**. When data is obtained from a certain node in the NMAS, its physical position is associated with where the data is obtained. Therefore, the position of the node is essential for analyzing and controlling of the system. The location information is essential in various problems of NMAS such as location based routing [12], vision-based formation control [13] and pursuit-evasion games (PEG) [14].

3. **Security**. Due to the peer-to-peer communication among agents, security is another important aspect of design for the NMAS, since it may operate in a hostile environment. There must be measures to determine the level of trust among agents and the security of messaging [15]. Communication between two agents is open to attacks such as sender spoofing (the message claims to be from a more trusted agent) and message modification (a message is changed while traveling between agents, particularly in negotiation situations).

4. **Power consumption**. Power consumption is a central design consideration for autonomous systems whether they are powered using batteries or energy harvesters, since the power consumption strategy affects the overall system life-cycle, mission management, design, dimensioning and requirement tradeoff. Additionally, the power capacity of each node influences the communication capability of the network, and consequently the network performance. Though technologies in micro electronics enable the design of cheap, small, highly reconfigurable devices which

consume less energy. However, communications among nodes strongly dominate the power consumption besides the other node functionalities such as sensing and processing. Specially, when a transmitted packet is corrupted it has to be discarded, and the follow-on retransmissions increase the possibility of congestion and consequently energy consumption. Therefore, developing new concepts for reducing power requirements, regulating energy consumption in NMAS is needed.

5. **Communication**. Guaranteeing reliable communication is one of the most important and key problems of communication networks. This is due to the fact that efficient and safe information exchange are essential not only for the task accomplishment but also for the network lifetime and security. Each node in a NMAS has to share its information and cooperate with others to achieve the mission objectives while maintaining the minimum resources consumption. Since the NMAS is usually applied to highly comprehensive tasks through cooperation of numerous agents in a large scala area, the communication is much more complicated and challenging due to the large amount of complex data information and the continuous changes in the network topology. As the number of nodes and complexity of the traffic in the network increase, more reliable and efficient communication solutions is required. The main issues in the communication problems in NMAS can be listed as follows:

   (a) ***Traffic Compression***. NMAS applications require sending of large amounts of relevant data from one point of the network to another. This necessitates a fast and robust traffic processing protocol which performs data compression without substantial loss in accuracy, addresses considerations of storage and facilitates quick retrieval of attributes. An excessive number of agent nodes can easily congest the network, flooding it with information. The prevailing solution to this problem is to process the traffic flow and then transmit compressed data to the next node. Different traffic compression approaches influence when and how much of the data in the network should be compressed.

   (b) ***Routing***. Routing problem can be defined as that of determining a route for

6

packets from a given source to a destination through other nodes. During the past decades, large amount of routing protocols have been proposed [16], [17], [18], [19], where the network topology changes frequently because of the node failures and communication conditions. The authors in [17] propose an architecture that is geared towards one shot frequent queries in sensor networks. Their approach aims at reducing the total energy cost of query resolution as opposed to searching for high quality routes. In [19], the authors classify a selection of algorithms proposed for ad hoc networks according to their relevance and efficiency. A spatial position node from GPS or other coordination mechanisms can be used for geographic routing and there have been many proposals using this methodology, such as those in [20], [21], [22]. Survey papers [19], [6] contain useful details on routing protocols in wireless sensor networks (WSNs).

(c) *Congestion Control*. Congestion control concerns controlling of traffic entry into a network (such as telecommunications network, urban and air traffic network [5], and all networks that consist of links and switches, and the controls that govern their operation and that allow for data transfer among links). Due to the limited communication resources, such as buffer size and link capacity, the QoS of network will degrade when the saturation of resources occurs. To avoid congestive problems, the network needs to take a set of actions to minimize the intensity, spread and duration of data collisions. In this case, the routing paths are fixed and predefined, and congestion is avoided by allocating the network resources and adjusting the traffic flow. In the following subsection, several issues concerning the congestion control of NMAS are introduced in more detail.

1.2.1   Congestion Control Problem in Multi-Agent Systems

Congestion control is designed to support Quality of Service (QoS) in a network [3], [23], [24]. For the traditional TCP/IP network, a large number of congestion control schemes have been designed [25], [26], [27] which have shown excellent performance and have been

7

demonstrated to be robust in a variety of scenarios. However, when they are applied to wireless environment and mobile ad hoc networks, it has been shown that by simply relying on the TCP congestion control algorithms and scaling up with ad hoc techniques, the QoS requirements that are expected by the NMAS cannot be fully realized [27]. This problem is more challenging in the networks consisting of nodes with stringent constraints such as sensors, decision makers, and actuators. The major features of NMAS that challenge the QoS provisions are listed as follows.

1. **Resource Constraints**. [28] As in a network of multi-agent systems, each agent may consists of sensors, decision makers and actuators. The physical resources such as buffer size and link capacity of each node are limited. Specially, the sensor nodes are usually low-cost, low-power, small devices that are equipped with only limited data processing capability, transmission rate, battery energy, and memory. For example, the MICAz mote from Crossbow based on a 8-bit micro controller can provide only up to 8MHz clock frequency, 128kb flash program memory and 4kb EPROM, and the transmit data rate is limited to 250kbps [14]. Moreover, due to the limitation on the transmission power, the available bandwidth and the radio range of the wireless channel are often limited. Although the actuator nodes may have stronger computation and communication capabilities and more energy budget relative to the sensors, however the actuators are usually responsible for task execution and need to move longer distances than the sensor nodes. Therefore, resource constraints apply to both sensors and actuators. In the presence of resource constraints, the network QoS may suffer from the unavailability of computing and/or communication resources. For instance, a number of nodes that want to transmit messages over the same network have to compete for the limited bandwidth that the network is able to provide. As a consequence, some data transmissions will possibly experience large delays, resulting in low level of QoS. Due to the limited memory size, data packets may be dropped before the nodes successfully send them to the destination. Therefore, it is of critical importance to use the available resources in the network in a very efficient way.

2. **Platform Heterogeneity**. As mentioned above, sensors and actuators do not share the same level of resource constraints. Possibly designed using different technologies and with different goals, they are different from each other in many aspects such as computing and communication capabilities, functionality, and number. In a large-scale NMAS, the hardware and networking technologies used in the network may differ from one subsystem to another. This is true because of the lack of relevant standards dedicated to the wireless sensor networks, and hence commercially available products often have disparate features. This platform heterogeneity makes it very difficult to make full use of the resources available in the integrated system. Consequently, resource efficiency cannot be maximized in many situations. In addition, the platform heterogeneity also makes it challenging to achieve real-time and reliable communication among different nodes.

3. **Dynamic Network Topology**. The nodes in a NMAS is usually mobile, therefore the node's neighboring sets are time-varying. In fact, node mobility is an intrinsic nature in many applications of NMAS such as, autonomous unmanned vehicles and networked robot systems. During runtime, new sensors or actuators may be added; the state of a node is possibly changed to or from sleeping mode by the employed power management mechanism; some nodes may even die due to exhausted battery energy. All of these factors may potentially cause the network topologies of NMAS change dynamically. Dealing with the inherent dynamics of NMAS, the network control mechanism (such as routing and congestion control) needs to work in dynamic and even unpredictable environments. In this context, QoS adaptation becomes necessary, that is, the congestion control scheme of NMAS must be adaptive and flexible at runtime with respect to changes in network topology and available resources.

4. **Mixed Traffic**. NMAS may need to deal with diverse applications, inducing both periodic and aperiodic data. This feature will become increasingly evident as the scale of network grows. Some sensors may be used to create the measurements

of certain physical variables in a periodic manner for the purpose of monitoring and/or control. Meanwhile, some others may be deployed to detect critical events. For instance, in a smart home, some sensors are used to sense the temperature and lighting, while some others are responsible for reporting events like the entering or leaving of a person. Furthermore, different kinds of traffic have different level of requirements in QoS. For example, a security surveillance signal (such as a video camera) has more stringent requirements in delay and packet lost rate than the daily recording data (such as temperature). Along with the development of more intelligent agents and more applications of NMAS in various domains, the complexity of mixed traffic will increase. Hence, a congestion control algorithm for the NMAS needs to support the characteristics of data traffic.

5. **Data Processing**. Information processing is another essential and critical aspect that is related to the network congestion. The nodes in a NMAS collaborate with each other to collect and process data for generating useful information. The degree of information sharing between nodes and how nodes fuse the information from other nodes will affect the bandwidth required for transmission. Processing data from more sensors generally result in better performance but require more communication resources and energy. Therefore, one needs to consider the tradeoffs between performance and robustness. Simple fusion rules are robust but suboptimal while more sophisticated and higher performance fusion rules may be sensitive to the underlying models.

1.3 Literature Review

In a network with shared resources, where multiple senders compete for link bandwidth, it is necessary to adjust the capacity allocated to and the data rate used by each sender in order not to overload the network. If no appropriate control is activated and performed this can lead to a congestion collapse of the network, where almost no data is successfully delivered. In this section, an overview of the congestion control problem and approaches

in the literature for the traditional TCP/IP network and the sensor/actuator network are given. The main contributions and proposed approaches from the control prospective and control community for the congestion control problem are also presented.

1.3.1   Congestion Control of TCP/IP Networks

Congestion control problem was first introduced for the TCP/IP network in 1980's [29]. Packets that arrive at a router and cannot be forwarded are dropped, consequently an excessive amount of packets arriving at a network bottleneck leads to many packet drop outs. These dropped packets might already have traveled a long distance in the network and thus consumed significant resources. Additionally, the lost packets often trigger retransmissions, which implies that even more packets are sent into the network. Thus network congestion can severely deteriorate the network throughput. Such situations have occurred in the early Internet, leading to the development of the TCP congestion control mechanism [30], [31], [32]. During the 1980's TCP/IP links on the Internet became increasingly congested and a new concept of "conservation of packets" was presented in [33], where when "conservation of packets" is observed then TCP flows are generally stable. This "conservation of packets" was implemented by a congestion window where further packets would not be sent once the congestion window was full until another packet was removed. This congestion window could be dynamically realized as the connection was established and as conditions change. These changes are widely credited with preventing ongoing TCP collapse. Over the past few years, large amount of research have been conducted for developing a combination of end-to-end rate (window) adaptation and network-layer dropping or signaling techniques for the TCP/IP and ATM networks to ensure that the network can operate without collapsing due to congestion. However, it has become clear that existing TCP congestion avoidance mechanisms, while necessary and powerful, are not sufficient to provide good service in all circumstances. Most of the current congestion control methods are based on intuition and ad hoc control techniques together with extensive simulations to demonstrate their performance. The problem with these approaches is that very little is known about why these methods work and very little explanation can

11

be given about when they fail due to the ad hoc nature of many of these schemes.

In the existing TCP/IP networks, the most studied and used mechanisms to address the congestion problem are the Active Queue Management (AQM) algorithms. These techniques attempt to prevent congestion and regulate the queue length by sending congestion signals (i.e., dropping packets) in a proactive manner. The AQM algorithms are based on a first in first out (FIFO) queue system, and the basic idea is to calculate and update the packet drop probability. Therefore, the incoming packets to a queue can be dropped before the buffer overflows. The work in [34] present an AQM algorithm for routers and an explicit congestion notification (ECN) control for the IP. The authors in [35] takes it a step further for the internet and propose backward ECN (BECN) and multi-level ECN (MECN), in which feedback signals can include information on severity of the congestion. The similarity in concept with explicit rate (ER) based schemes advocated by the ATM forum traffic management specification for managing available bit rate (ABR) traffic should be noted. ATM switches can calculate the maximum ER that they can accept over the next control interval, so that the ABR traffic into the network can be regulated, for effective use of the available resources.

Among the numerous proposals on AQM the random early detection (RED) algorithm is probably the most widely studied and applied one [25]. The basic idea of RED is to use the average queue length to calculate the packet drop probability and to regulate the queue length accordingly. An exponentially weighted average of the queue length is used to calculate the dropping probability. Specifically, when the average queue length is less than a minimum threshold value no packets are dropped and when this average exceeds a maximum threshold value all incoming packets are dropped. When the average queue length is between these thresholds, packets are then dropped with a probability that is a function of the average queue length.

Despite the simplicity of RED, the optimal configuration for the weighting parameter remains a daunting task. Hence, a large number of work has been published during the past decades to enhance its performance. The self configuring RED (SRED) [36] and adaptive RED (ARED) [37] have been introduced to adaptively configure the parameters. The

12

BLUE [38], calculates the packet drop probability based on only two events, namely, buffer overflow and buffer emptiness, and whereas adaptive settings in such a complex system are still difficult. Recently, a loss ratio-based RED (LRED) algorithm was presented in [39], which employs the packet loss ratio as a complement to the queue length for the AQM. The use of packet loss ratio enables LRED to cope with network dynamics in time, thus achieving fast control response and better performance in terms of good-put, average queue length, and packet loss ratio. Another approach, namely adaptive virtual queue (AVQ) algorithm, presented in [30], uses the input traffic rate to control packet drop and to achieve an expected link utility. Through maintaining a virtual queue, AVQ deterministically drops packets upon each new packet arrival, realizing the same effect of probabilistic packet drop. AVQ achieves lower average queue length and higher link utility than the RED and its variants.

During the past few years, other advanced algorithms have been studied by using the queue length and input rate jointly to achieve better performance. One example is the proportional-integral (PI) controller [31], which regulates the queue length to an expected reference value according to the queue mismatch and its integral. The latter is closely related to the input rate mismatch. If the network states are known *a priori*, optimal parameters of the PI can be determined through a control theoretic model. However, in dynamic networks, PI controllers may have to use a conservative setting to ensure stability, yielding large response times. Another derivation of the AQM algorithm is the REM [32], which uses a linear combination of the queue mismatch and input rate mismatch to calculate the drop probability, and the input rate mismatch is equivalently simplified to the queue variance between two adjacent queue length samples.

1.3.2 Congestion Control of Sensor-Actuator Networks

During the past few years, sensor networks have received extensive attention in research and applications due to their capability of self organization and distributed computing. However, sensors are passive devices that can only collect data from the environment without interaction. Therefore, actuators are introduced to make decisions and perform

13

appropriate actions according to the sensor measurements, which leads to the notion of sensor-actuator networks (SAN). The actuators are usually highly mobile and need to carry out execution activities. Hence, it is required that the actuators have powerful battery, processor and memory to perform both decision making and actuation. As mentioned earlier, a network of multi-agent systems (NMAS) is composed of a number of distributed intelligent agents. Each agent may consist of a group of sensors, decision makers and actuators. The exchange of information and process of decision making are made autonomously. In this sense, the NMAS can be viewed as a wireless sensor-actuator network (SAN)

Among the many research issues in sensor-actuator networks, congestion control is one of the most predicament problems that needs to be solved. Although, the existing TCP/IP congestion control algorithms perform quite well on the Internet, the unique properties of the sensor-actuator networks requires the design of appropriate protocols and protocol stacks in general, and of a congestion control mechanism in particular. The congestion control algorithms for SAN need to be highly energy-efficient, to prolong system lifetime, improve fairness, and improve QoS in terms of throughput (or link utilization) and packet loss ratio along with the packet delay. A SAN consists of one or more sinks and perhaps tens or thousands of sensor nodes scattered in a large area of interest. Congestion restraint generally follows two steps: congestion detection and congestion control.

1. **Congestion Detection**. Accurate and efficient congestion detection plays a vital role in congestion control in sensor networks. There are various detection techniques that have low cost in terms of energy and computation complexity. An energy efficient congestion detection method known as CODA discussed in [40] deals with various degrees of congestion depending on the sensing application. In a hop-by-hop back-pressure congestion detection [41], if the sink is congested, back-pressure spatially spreads the congestion and helps alleviate congestion quickly. In addition, hop-by- bop control supports in-network data processing. Once congestion is detected, the receiver will broadcast a suppression message to its neighbors. The hop-by-hop back-pressure can immediately response to the congestion at the intermediate node

14

without incurring the round trip delay that reduces feedback effectiveness.

Queue occupancy [42] is another simple way to detect congestion that relies on monitoring a node's buffer queue length. In the implementations of [42], if the fraction of space available in the output queue falls below a threshold (20-25% of the output queue size), the congestion bit of routed packets is set until the available queue size goes up. In this thesis, the threshold is selected as 10% of the output queue size based on the experimental simulation results that reported subsequently. In the event to sink reliable transport [43], a sensor sets a congestion notification bit in the packet header if its buffer is full. The sink periodically computes a new reporting rate based on the reliability measurement, that is the received congestion notification bits and the previous reporting rate. An intelligent congestion detection method proposed in [44] measures the local congestion level at each intermediate node, the packet inter-arrival time and the packet service time at the MAC layer.

2. **Congestion Control**. Once the congestion at a node is detected, the node informs its source nodes of the congestion and a series of actions are performed at the node side or at the sink side to remedy the congestions. A proportional access method presented in [45] gives more access to a node carrying a higher amount of traffic. Therefore, downstream nodes obtain higher access to the medium than the upstream nodes. In this method one avoids the packet drop due to congestion by not allowing upstream nodes to transmit, if there is no available buffer. In [46], a priority based rate adjustment (PRA) technique is presented. A node priority index is introduced to reflect the importance of each node. The authors in [42] present two congestion control approaches. The first one is a short term control method in which when node experiences congestion, its immediate downstream node split the real-time traffic on to its alternate upstream node in proportion to their weight factor. This approach will eventually carry the newly created real-time data flows at a slower rate along the primary route, allowing the congested node to be relieved and thus alleviate the congestion. The second method in [42] is the so-called long-term congestion control

in that the source node will dynamically adjust to the changing conditions and select the best upstream node as its primary route to send further packets. Consequently, both the real-time and non-real-time data flows will follow the changed or updated primary route. The pump slowly fetch quickly (PSFQ) method is another method worth mentioning that is developed for the sensor networks [47]. It requires the source node to pace data at a relatively slow speed ("pump slowly"), but allows nodes that experience data losses to fetch (i.e., recover) any missing segments from immediate neighbors very aggressively (local recovery, "fetch quickly"). In [48], the authors proposed a light weight buffer management mechanism which is an effective approach that prevents data packets from overflowing the buffer space of the intermediate sensors. This approach automatically adapts the sensors' forwarding rates to nearly optimal values without causing congestion.

1.3.3 Congestion Control Schemes in the Control Community

The control systems community has shown a growing interest in and has made important contributions by addressing the challenges in the congestion control area. Since the early congestion control concept was introduced in [33], several attempts at control theoretic-based schemes have been made in the literature by using approaches such as optimal control [49]; linear control [50]; fuzzy and neural control [51], [52]; predictive adaptive control [53]; and nonlinear control techniques [54], [55].

Several new congestion control schemes for Diff-Serv networks [56] (briefly introduced in the next Chapter) whose performance can be analytically established have been presented in the literature by using sliding mode control [57], [58] and robust adaptive control [3] techniques. The results developed in these works are interesting. However, the above solutions have serious drawbacks. First, the nature of discontinuities of the sliding mode controller may result and introduce unavoidable and undesirable oscillations in the closed-loop system [59], and therefore reduce the effectiveness of the developed congestion

16

control solution. On the other hand, the adaptive congestion control scheme in [3] is designed for a *cascade network* of switches and considered the bottleneck switch as a single node. Consequently, the presence of unknown and time-varying delays and latencies are not considered in the design of the congestion controller. The lack of explicit consideration of the delays will yield a critical challenge and even an instability when the approach is applied to a large scale network consisting of many nodes [60] structured in *arbitrary configurations*. In [3], [61], [62], a Integrated Dynamic Congestion Control (IDCC) strategy was proposed by utilizing the nonlinear control theory and the robust adaptive control techniques. The IDCC approach is developed based on analytical network models and has been shown great performance when applied to ATM networks. In this thesis, the IDCC approach is used as a benchmark strategy for comparative studies. The details of the IDCC approach can be found in Appendix A.

Extensive studies on congestion control have been conducted and a large body of results are available in the literature [37], [38], [3], [44], [45], [39], [56], [58] . To model and analyze the performance of a network, such as throughput, queuing delay, and packet loss rate in a formal, quantitative, and analytical manner are not easy tasks, since their effects on the congestion are significantly nonlinear. The congestion control problem may become unmanageable unless analytical, effective and robust methods are developed. Moreover, when the number of nodes in the NMAS increases and the nodes become mobile, and in addition the differentiated services traffic and unknown time-varying delays are considered, the complexity of the congestion control problem become even more challenging. Therefore, systematical modeling, synthesis, and analysis considerations are mandatary for the design of congestion control strategies for the NMAS. The development of such effective congestion control protocols will require integration of advanced networking and control techniques.

1.4 Proposed Research

This thesis aims to develop a dynamic congestion control strategy for a network of multi-agent systems (NMAS) by taking advantages of control theory machinery. The proposed framework is based on an analytical queuing model of the traffic network which is derived based on the fluid flow theory. The traffic flow in the network is classified into different classes according to the differentiated services architecture [56], namely the premium service, the ordinary service, and the best-effort service. The control objectives of each traffic class is defined based on their corresponding quality of service (QoS) specifications. The propagating, transmitting and processing delays are considered as inherent characteristics in the queuing models. Therefore, from a control aspect, the congestion control problem is defined as designing a stabilizing controller for a dynamical system with unknown multiple and time-varying delays.

It has been widely known that time-delays in a system is one of the leading sources of instability. Complications arise in practical cases where there is limited *a priori* knowledge about transmitting, propagating, and processing delays and the fact that they vary according to the traffic flow and other disturbances in the network. Random changes in the network topology makes the system dynamics time-varying and more challenging to describe. In addition to the uncertain delays, the physical constraints of the communication network such as limited link capacity and limited buffer size makes the congestion control problem of NMAS more complicated to investigate.

The proposed research in this thesis considers the congestion control problem of the NMAS corresponding to two methodologies and approaches, namely:

- *Switching congestion control (SCC) approach, and*

- *Guaranteed cost congestion control (GCC) approach.*

In the *switching congestion control (SCC) approach*, the physical constraints of the network are transformed into the constraints of the inputs and states of the queuing models. A group of fixed structured controllers are then defined according to the maximum and the minimum bounds of the input signals. In our proposed *switching congestion*

control approach, we name the maximum and the minimum values of the inputs as the *edge controllers* and the medium values of the input within the safe operation range as the *normal controller*. For each traffic class, a supervisor mechanism is applied to generate switching signals based on the system state. The closed-loop system will experience multiple modes with respect to the different choices of the control input. The strategy under the *edge modes* is to regulate the system parameters so to force the system states to change, towards the safe operation mode. Once the system enters the safe operation mode the normal controller will be selected, where the stability of the closed-loop system will be guaranteed by satisfying a set of linear matrix inequality (LMI) conditions.

On the other hand, in the *guaranteed cost congestion control (GCC) approach*, the controller is first designed without the consideration of the physical constraints. A linear quadratic cost function is proposed with the measures of the queuing error and input. Our proposed guaranteed cost congestion controller will then guarantee the stability of the system and an upper bound on the cost in the presence of unknown multiple and time-varying delays is obtained. Indeed, the LMI specification which can deal with convex and quasi-convex optimization problems with a variety of design specifications and constraints has been the main motivation for developing this method in solving the congestion control problem. The physical constraints of the network are considered as the complementary stability conditions which are then represented by a group of additional LMIs. By applying the guaranteed cost congestion control approach, the QoS specifications, such as the packet loss rate, and the efficiency and the cost of control effort are guaranteed simultaneously.

Towards this end, this research has been conducted in four parts. In Part I, a dynamic switching congestion control (SCC) strategy is proposed for multi-agent network systems with differentiated services traffic. A centralized control scheme is proposed for networks with fixed topology in the presence of multiple unknown, time-varying delays and network physical constraints. Our proposed centralized control scheme is then modified to a decentralized strategy. Unlike most of the existing work in the literature, delay functions are considered to be unknown *a priori*. Therefore, our proposed decentralized congestion control strategy not only guarantees the congestion avoidance for a single node

in the presence of the unknown time-varying delays, but also is scalable to potentially large scale networks. In both the above two approaches, the congestion control problem of the differentiated services are formulated as a multi-level switching control problem of time-delay systems. A state feedback controller with proportional plus integral action embedded with an adaptation law is then presented for the premium and the ordinary traffic, respectively. We next consider the mobile networks and the proposed switching congestion controllers (SCC) are extended such that they can also incorporate the changes in the network topology. To deal with changing network topology, we model the changes of the topology as a memoryless stochastic process, which can be described by a Markov chain. Consequently, the congestion control problem of a mobile network can be formulated as a hybrid switching control of a Markovian jump system with time-delays.

In Part II, the dynamic queuing models of the fixed and mobile networks are considered again. A guaranteed cost congestion control (GCC) strategy is proposed for both centralized and decentralized frameworks. By utilizing a quadratic cost function, the congestion control problem of the NMAS is recast as a robust control of a nonlinear system with uncertain time-delays. By solving the corresponding LMI conditions, the stability of the system is ensured and the upper bound of the cost function is guaranteed with all admissible time-delays.

In Part III, a different control scheme, namely a *distributed control scheme*, is considered for the congestion control problem. Since the nodes in a NMAS are usually distributed geographically, the congestion control efficiency of each node is affected by the queuing state and the traffic rate of its neighboring nodes. Actually, due to the inter cluster traffic, the queuing model of a single node in NMAS is highly coupled in the presence of unknown time-varying delays. Therefore, a purely decentralized congestion control algorithm is difficult to cope with the unknown states of its neighboring nodes with delays. To tackle this problem, by incorporating the possibility of the communication among the controllers a *distributed* congestion control scheme is proposed for the fixed as well as the mobile network problems. The proposed congestion control strategy is shown to be in fact equivalent to a local state feedback control plus a nearest neighboring controller that are adjusted

with proportional gains. The resulting optimal congestion control problem is then cast as a quadratic regulation problem of a time-delay system with free parameters (gains) that need to be selected. Both centralized and decentralized weight selection approaches are considered such that certain cost function is minimized. By including the nearest neighboring controllers' adjustment mechanism, the distributed control approach yields an algorithm that significantly enhances the scalability of the centralized algorithm and improves the performance of the decentralized approach to a large scale traffic network. By proper selection of the distributed gains, other external effects from the nearest neighboring nodes, such as the queuing lengths and external traffic flows, can be considered and managed separately. In the distributed control framework, the cooperation among the nodes (agents) can be considered in the sense of "cooperation for resolution" and can also permit the agents to mutually increase their knowledge by exchanging information periodically about their states. Moreover, the nodes can take local decisions immediately when they have no access to other nodes. When the network is not heavily loaded, it is possible to exchange information on the life of the network to update and improve the node's performance. This implies that the nodes are able to cooperate and make better decisions as compared to the decentralized control approach.

Finally in Part IV, the robustness of all the proposed methods are investigated and evaluated through a comprehensive set of simulations. The performance of the switching congestion control (SCC) and the guaranteed cost congestion control (GCC) are compared for both fixed and mobile networks.

Investigation and derivations of the work in each of the above parts are given in the subsequent chapters of this thesis.

1.4.1 Performance Metrics

The congestion control problem is usually considered as an optimal problem in utilizing the network resources while maintaining reasonable fairness among network users with acceptable QoS. Serval control objectives have been identified in the congestion control problems. Typical performance metrics include the throughput, delay, response time,

fairness etc. It is worth noting that the congestion control problem is indeed defined as finding a trade-off among the various competing goals. All the existing algorithms that reviewed earlier support at least one of the following goals in evaluating the congestion control protocols.

1. **Queuing Delay.** Whenever the networks are free of congestion, the transmission capability of the network is greater than the amount of the traffic flow in the channel. In such cases, the queuing delay is very low. Once congestion starts to build up in the channel, the packets are forced to wait and queues are created waiting to be serviced. In these cases, queuing delay can be very high and pose a major problem to the dynamics of the channel. Since the network operation is fast, queuing delays are usually measured in milliseconds (ms). Congested channels have numerous packets waiting to be transmitted and this in turn reduces the transmission capacity of the channel which leads to higher queuing delay and even worse situation of congestions.

2. **Packet Loss Rate.** Losses occur when there is congestion in the transmission channel and these channels are forced to drop the packets since it is almost impossible to transfer them forward to their destination nodes. Packet loss rates can be measured as network-based or as flow-based metric. When evaluating the effects of the packet losses on the performance of a congestion control mechanism for an individual flow researchers often use both the packet loss/mark rate for that connection and the congestion event rate (also called the loss event rate), where a congestion event or loss event consists of one or more lost or marked packets in one round-trip time [63]. Other users may be concerned with the packet loss rate only in so far as it affects per-connection transfer times, while other users may be concerned with the packet loss rates directly. In some cases, it is useful to distinguish between packets dropped at nodes due to buffer overflow and packets lost in the network due to traffic flow regulation. One network-related reason for avoiding high steady-state packet loss rates is to avoid congestion collapse in environments containing paths with multiple

22

congested links. In such environments, high packet loss rates could result in congested links wasting scarce bandwidth by carrying packets that will only be dropped downstream before being delivered to the receiver [64].

3. **Energy.** [28] Energy is an issue in every engineering design. In congestion control problem, limited energy supply is an important factor. This is especially crucial for wireless sensor networks where the battery life in each node is very limited. An efficient congestion control algorithm should consume minimum energy and keep the nodes alive as long as possible. Indeed, most of the energy consumption of a node is due to communication which is the total energy consumed for sensing, transmitting and receiving. The total energy should not exceed the available energy for each sensor node [65], [66].

1.5 Thesis Contributions

The research conducted in this thesis attempts to investigate the following issues. The main contributions of the thesis are also stated below.

- **Communication Models of NMAS Subject to Diff-Serv Traffic**

  To successfully realize missions and tasks, the communication among the network of multi-agent systems need to be conducted efficiently. The specific characteristics and the unique research challenges in the network of multi-agent systems may render the communication problems more complex. Furthermore, dealing with differentiated services traffic flow in the network is expected to be very complex and nonstationary in nature. Therefore, an analytical and quantitative model with a more detailed and accurate description of the NMAS characteristics are needed for the development of congestion control strategies. In contrast with the dynamic models that are used in conventional congestion control approaches, the main contributions of the presented dynamic model are stated as follows:

  1. We extended the model of a single node system to a model of large scale

networks where the inter-node traffic is considered explicitly with unknown and time-varying delays.

2. The dynamic models are developed in two different frameworks, namely the centralized and decentralized formulations. In the centralized model, the entire network is considered as one for each traffic class. The unknown and time-varying delays are considered as inherent characteristics in the model. In the decentralized model, the dynamics of each node is modeled as a coupled system with unknown an time-varying delays in the coupling states and inputs from the neighboring nodes.

3. Unlike other work in the literature, we allow and consider traffic data compressions during the design of the congestion control system. The compression gains are incorporated at the output port of each node as a free parameter that needs to be selected through analysis and stability considerations.

4. The centralized and decentralized models are extended to a mobile network environment by modeling the changes of network topologies stochastically.

- **Congestion Control of Large Scale Diff-Serv Networks with Multiple Time-Varying Delays**

Our research work have led to several congestion control frameworks and strategies. In these strategies, the queue length is used as a feedback information to control the network performance for congestion avoidance. The control objective for each traffic class is presented based on the QoS specifications and represented as quadratic cost functions. The transmission, propagation, processing, and queuing delays are considered in the dynamic queuing models as unknown multiple and time-varying parameters. The physical constraints of the communication network, such as the buffer size and the link capacity are considered as the constraints of inputs and states. The congestion control problem of Diff-Serv networks with multiple time-varying delays and physical constraints is considered and the following two congestion control approaches are proposed in this thesis, namely:

1. **Switching Congestion Control (SCC) of Diff-Serv Networks**

   The first congestion control approach proposed in this thesis is the switching congestion control (SCC) strategy. The physical constraints of the inputs are considered for the controller design. The congestion control problem of each traffic class is then recast as a switching controller based on the system operation condition. For the switching congestion control strategy, multiple controllers are designed in advance, and are then switched by a supervisor according to the system state so that the closed-loop system experiences multiple modes. The stability of the system is guaranteed by satisfying a group of Linear Matrix Inequality (LMI) conditions. For each traffic class, centralized and decentralized switching congestion control strategies are developed. Furthermore, the proposed SCC approach is extended to mobile Diff-Serv networks. The changes of the network topology due to nodes mobility, addition of new nodes, or deletion of nodes due to their low energy or faults/failures is modeled stochastically by a Markovian jump process. A Markovian jump switching congestion controller (MJ-SCC) is then proposed for each traffic class based on the switching control strategies for the first time in the literature.

2. **Guaranteed Cost Congestion Control (GCC) of Diff-Serv Traffic**

   The second congestion control approach proposed in this thesis is the guaranteed cost congestion control (GCC) strategy. The congestion control problem is recast as a guaranteed cost control problem of a nonlinear system with unknown time-varying delays, subject to constrained inputs and states. By applying the GCC approach, the congestion controller can first be developed without considering the physical constraints. The robust stability of the closed-loop system is guaranteed by satisfying an associated set of linear matrix inequality (LMI) conditions. The physical constraints of the system are then considered by including a set of complementary LMIs. The proposed guaranteed cost congestion controller is also extended to the mobile networks. The resulting guaranteed cost control problem for each traffic class is considered as a jump

linear quadratic regulation (JLQR) problem and a Markovian jump guaranteed cost congestion control (MJ-GCC) strategy is proposed for the fist time in the literature.

- **Combined Bandwidth Allocation and Flow Rate Regulation for Fully Connected Networks with Diff-Serv Traffic**

In this thesis, three different congestion control architectures are presented, namely decentralized, centralized, and distributed. Each of the proposed congestion controllers maintain the average queuing length of a buffer in the network by dynamically allocating the bandwidth and regulating the flow rate. In additions to the contributions on the centralized and distributed congestion controllers, the decentralized switching congestion control strategy (SCC) developed in this work is an improved version of the strategy that is proposed in [3], having the following main features and novelties:

1. The approach in [3] is designed for a *cascade network* of switches and consider the bottleneck switch as a single node. Consequently, the presence of unknown and time-varying delays are *not* considered in the design of the congestion controller. The lack of explicit consideration of the delays yields a critical challenge and even an instability when the approach is applied to a large scale network, such as the NMAS. To the contrary, our proposed decentralized congestion controller is developed for either a fully or nearly-fully connected network topology. The coupling effects from the neighboring nodes are included in the dynamic model of each node with explicit consideration of the delays. Hence, the resulting congestion controller shows a significant improvement in robustness to the unknown and time-varying delays.

2. The approach in [3] only controls the flow rate of the ordinary traffic (the second class of the traffic that is defined in this thesis and will be described in Chapter 2), by allocating the full leftover server capacity from the premium traffic (the first traffic class). Unlike the approach in [3], we have applied a

combined bandwidth allocation and flow rate regulation to the ordinary traffic in our proposed congestion control strategy. Consequently, the performance of the ordinary traffic congestion control is shown to be significantly improved.

- **Distributed Guaranteed Cost Congestion Control (DGCC) of Large Scale Mobile Diff-Serv Networks**

  The proposed centralized and decentralized approaches are evaluated and compared on a given performance index in terms of both the QoS and the control criteria, for the fixed and the mobile networks. The distinct advantages of each approach have revealed that an alternative mixed control scheme can benefit from these control approaches. Consequently, a distributed congestion control strategy is developed, by incorporating the possibility of communication among only the controllers. The distributed congestion control strategy is in fact equivalent to a local state feedback control plus a nearest neighboring controller that are adjusted with proportional gains. The resulting congestion control problem is then cast as a quadratic regulation problem of a Markovian jump time-delay system subject to constrained inputs and states. By considering the nearest neighboring controllers' adjustment mechanism, the distributed control approach yields an algorithm that significantly enhances the scalability of the centralized algorithm and improves the performance of the decentralized approach to a large scale traffic network. The proposed novel distributed guaranteed cost congestion control (DGCC) approach is then evaluated and compared with the centralized and decentralized congestion control approaches in terms of the QoS performance of and control criteria.

1.6   Thesis Organization

The remainder of this thesis is organized as follows: In Chapter 2, the basic definitions and concepts on the switching control and guaranteed cost control as well as the LMI techniques are briefly reviewed. A description of the differentiated services architecture is also presented. The centralized and decentralized dynamic models for the differentiated

services traffic are derived for both the fixed and mobile network of multi-agent systems (NMAS). The rest of this thesis is divided into four parts.

Part I, consisting of Chapter 3 and Chapter 4, deals with the switching congestion control approach. Chapter 3 provides centralized as well as decentralized switching congestion control strategies for the NMAS with fixed network topology. The simulation results obtained for our introduced congestion control algorithm for fixed NMAS is then compared with the benchmark congestion control algorithm in the literature known as the integrated dynamic congestion controller (IDCC) [3]. In Chapter 4, the dynamics of mobile NMAS are modeled by a Markovian jump switching system. The decentralized and centralized switching congestion control strategies in Chapter 3 are then extended to the mobile NMAS for each traffic class. Extensive comparisons of the centralized and the decentralized approaches are conducted in both Chapters 3 and 4, for the fixed and mobile networks, respectively.

Part II, consisting of Chapter 5 and Chapter 6, treats the guaranteed cost congestion control approach of the NMAS with fixed network topology. In Chapter 5, centralized and decentralized guaranteed cost congestion control strategies are proposed. In Chapter 6, the mobile NMAS is considered, and the GCC strategies in Chapter 5 are generalized to these networks.

Part III, consisting of Chapter 7, handles the distributed congestion control scheme for the mobile NMAS subject to differentiated services traffic, by applying the guaranteed cost control approach. The performance of the proposed distributed guaranteed cost congestion controller (DGCC) is evaluated and compared with the decentralized and the centralized congestion control schemes, which are presented in the previous chapters.

Part IV, consisting of Chapter 8 and Chapter 9, deals with the robustness evaluations of all the previously proposed congestion control strategies and proposes some future direction of research, respectively. In Chapter 8, the robustness of our proposed congestion control algorithms with respect to a) uncertainties in the network traffic model, and b) unmodeled dynamics in the queuing models, are studied through extensive simulation

scenarios. The robustness performance of the centralized, the decentralized, and the distributed approaches for both fixed and mobile networks, as well as for the premium and the ordinary traffics are investigated and evaluated. Finally, in Chapter 9, conclusions and future direction of research are presented.

Chapter 2

Problem Formulation

In this chapter, the analytical representation of the network of multi-agent systems (NMAS) is expressed according to a fluid flow model for both the fixed and mobile networks. These dynamics are formulated into a nonlinear state space representation with time-varying delays. For the purpose of differentiated services (Diff-Serv) traffic control, the dynamical model for each traffic class is obtained separately.

This chapter is organized as follows. In Section 2.1, a brief introduction to the Diff-Serv traffic, queuing theory, data aggregation, stability of time-delay systems, feedback linearization technique, guaranteed cost control theory, and the linear matrix inequality (LMI) are provided. The dynamical models of the NMAS are given subsequently in Section 2.2.

2.1 Basic Definitions and Concepts

2.1.1 Differentiated Services (Diff-Serv) Traffic

With the increasing demand of multimedia applications, differentiated services have been considered in many applications of communication networks. Internet Engineering Task Force (IETF) proposed the differentiated services (Diff-Serv) architecture [56] to deliver aggregated quality of service (QoS) in IP networks. The main idea is to assign different

priorities to different kinds of services (video/audio, control command etc.). The traffic is forwarded by using one of the three IETF defined per-hop behavior (PHB) mechanisms. This approach allows traffic with similar service characteristics to be passed with similar traffic guarantees across multiple networks, even if multiple networks do not provide the same service in the same way. This is an important feature because the Internet is really a network of multiple service providers.

According to the definitions by IETF, Diff-Serv is a protocol for specifying and controlling network traffic by class so that certain types of traffic can get precedence, for example the voice traffic which requires a relatively uninterrupted flow of data over other kinds of traffic.

Prior to the use of Diff-Serv, Tail-Drop [67] was the standard behavior of router queues on the Internet. Tail-drop works by queuing up packets to a limit, then dropping all the traffic that exceeds that limit. This is not a good practice as it leads to retransmit synchronization. When retransmit synchronization occurs, the sudden burst of drops from a router that has reached its maximum limit will cause a delayed burst of retransmits, which will over fill the congested router again. In order to adjust with the transient congestion on links, backbone routers will often use large queues. Unfortunately, while these queues are good for throughput, they can substantially increase latency and cause TCP connections to behave very "burstily" during congestion. On the other hand, traditional IP networks offer users best-effort service. In this kind of service, all packets compete equally for network resources. However, this best-effort service cannot provide any predictability and reliability in packet delivery, making it unsuitable for real-time applications.

The Diff-Serv architecture has become the preferred method to address QoS issues in IP networks. This packet-marking based approach to IP QoS is attractive due to its simplicity and ability to scale [68], [69]. An end-to-end differentiated service is obtained by concatenation of per-domain services and Service Level Agreements (SLAs) between adjoining domains along the path that the traffic crosses in passing from the source to the destination [55], [70]. Per domain services are realized by traffic conditioning at the edge

and simple differentiated forwarding mechanisms at the core of the network.

Two broad aggregate behavior groups of forwarding mechanisms are adopted by the IETF, these are the Expedited Forwarding (EF) [71] and the Assured Forwarding (AF) Per Hop Behaviors (PHB) [72]. Traffic conditioning includes classification, metering, policing and shaping. The EF-PHB can be used to build a low loss, low latency, low jitter, and assured bandwidth service, hence it can indirectly guarantee the QoS. On the other hand, the AF-PHB is appealing, as it proposes simple mark and drop mechanisms to realize IP QoS. The AF approach provides better QoS than the best-effort service by controlling the drop preference of packets at the time of congestion. The AF-PHB draft proposes four classes and three drop preferences per class, hence each class can provide different levels of bandwidth and buffer guarantees.

In this thesis, we follow the same spirit of Diff-Serv and divide the traffic into three groups, namely the premium service, the ordinary service and the best effort service [3]. The premium traffic belongs to the first class of EF-PHB, whereas the ordinary traffic belongs to the first class of the AF-PHB, and the best-effort traffic belongs to the last class of EF-PHB. The QoS of these three traffics are listed below.

- Premium Service. The premium service is chosen for applications with stringent delay and loss requirements that can specify upper bounds on their traffic needs and required quality of service. It is envisaged that the user may contract with the network. The only commitment required by the user is to not exceed the peak rate. The network contract then guarantees that the contracted bandwidth will be available when the traffic is sent. Typical applications of the premium traffic services include control command, audio and video conferencing, etc.

- Ordinary Service. The ordinary service is intended for applications that have relaxed delay requirements and allow their rate into the network to be controlled. This kind of traffic use any left over capacity from the premium traffic. It should be noted that to ensure there is bandwidth leftover from the premium traffic service, a minimum bandwidth might be assigned for the ordinary traffic, e.g., by using bandwidth

allocation between services or connection admission. Typical applications of this kind of service include image retrieval, event based applications, etc.

- Best effort service. Finally, the best effort traffic has no delay or loss expectations. It opportunistically uses any instantaneous leftover capacity from both premium and ordinary traffic services.

2.1.2 Queuing Theory

We have seen that as a network gets congested, the queuing delay in the system increases. A good understanding of the relationship between congestion and delay is essential for designing effective congestion control algorithms. Queuing theory provides all the tools that are needed for this analysis. According to the Little's theorem [73], the average number of customers N can be determined by $N = \lambda * T$, where λ is the average arrival rate and T is the average service time for a packet. With Little's theorem, the basic understanding of a queuing system can be illustrated by three essential characteristics of a queue, namely the arrival process, the service process, and the number of servers. The arrival process defines the probability density distribution that the packets arrive to the node, and the service process indicates the probability density function of the service time in the node. Finally the number of servers indicates how many available servers are connected to the output port of a node. Therefore, a queuing system can be represented by the following convention: $A/S/n$, where A denotes the arrival process, S denotes the service process and n denotes the number of servers. A and S can be any of the following [74]

- M (Markov): exponential probability density;

- D (Deterministic): all customers have the same value;

- G (General): any arbitrary probability distribution.

A typical example of queuing system is the M/M/1 queue, where the arrival and service times are negative exponentially distributed (Poisson process). The system consists of only one server. This queuing system can be applied to a wide variety of problems as

any system with a very large number of independent customers can be approximated by a Poisson process. The distribution of the Poisson process can be described by the following distribution function:

$$f(x|\lambda) = \frac{\lambda^x e^{-\lambda}}{x!} \tag{2.1}$$

where λ is the expected number of "events" or "arrivals" that occur per unit time and x is the number of occurrences of an event. In this thesis, we also assume that the packets arrive to the network according to a Poisson process, and consequently an M/M/1 queue is considered for the following research.

2.1.3 Traffic Flow Compression and Processing

Each agent in a network of multi-agent systems may consist of several sensors, actuators and decision makers. These devices are resource constrained in terms of power supply, communication bandwidth, processing speed, and memory. One possible approach to achieve the maximum utilization of these resources is to apply traffic compression on data. Usually, processing data consumes much less power than transmitting data in communication medium [75], so it is effective to apply compression before transmitting data for reducing the total power consumption. By doing so, the life time of the network is extended [76]. By reducing the data size less bandwidth will be required for sending and receiving data, and hence the risk of congestion is decreased. Traffic compression and processing have shown significant improvements for network performance in the literature, especially for the traffic containing video and graphics [77]. However, applying data compression will require more processing power. Determination of an optimal or minimum feasible traffic compression rates is critical for the purpose of overall network control.

In this thesis, we assign a traffic flow compression mechanism at the output port of each node, represented by a time-varying design parameter to be selected. Each node can process and compress the traffic before sending it to the next node. This parameter indicates the level of the data compression rate and can vary from 0 to 1. By incorporating our proposed traffic flow compression one can simultaneously ensure (a) reduction of the queued and transmitted traffic, and (b) avoidance of the overall network congestion.

Introducing the traffic compression mechanism represents an important novel aspect of our proposed congestion control design.

2.1.4 Feedback Linearization Technique

The mathematical modeling of most physical systems yields a nonlinear system representation. The synthesis and control of nonlinear systems are important research topics in both academic and industrial domains. Among all the critical problems of nonlinear control systems, the stabilization problem is among the most important ones. In the stabilization problem, a controller is to be designed so that the closed-loop system achieves certain specified objectives. Various formal tools have been developed for nonlinear system stabilization in the literature, which can be broadly divided into two categories, namely a) linear and b) nonlinear feedback control. The former one is based on an approximate linearized model of a nonlinear system about an operating on equilibrium point, while the later one is based on the actual nonlinear system directly. Among the various types of direct nonlinear control techniques, *feedback linearization* [78] is an approach which has attracted a great deal of research interest. The central idea of the approach is to transform the nonlinear system dynamics into (fully or partly) linear one, so that linear control techniques can then be applied [78]. This approach differs from conventional Taylor's series linearization in that feedback linearization is achieved by exact state space coordinate transformation and feedback, hence the transformed exact linear system is *equivalent* to the original nonlinear system.

Input-State Linearization

Consider the problem of designing the control input u for the nonlinear system of the form:

$$\dot{x}(t) = f(x, u, t) \tag{2.2}$$

The input-state linearzation technique solves the problem in two steps. First, one need to find a state space coordinate transformation and a diffeomorphism $z(t) = \phi(x, t)$ and

an input transformation $u = \psi(x, \bar{u}, t)$ such that the nonlinear system dynamics is transformed into a equivalent *linear system*, in the standard form of $\dot{z} = Az + B\bar{u}$. Second, conventional linear control techniques can then be applied to design the new controller $\bar{u}$.

2.1.5 Stability of Time-delay Systems

The growing interest in improving performances and quality of service of communication networks is at the origin of the development of various control algorithms that use deterministic or stochastic, continuous or discrete-time model representations of the network. Independent of the representation, these models should take into consideration a number of resources of delays, including the propagation, the transmission, and the processing delays. These network induced delays can be a cause of instability and performance degradation. Among the research topics of time-delay systems, stabilization is one of the most crucial problems. During the few decades, a number of publications have appeared in the literature, among which two main approaches are considered. The first is the frequency domain approach [79], [80] and the second is the time domain approach [81], [82]. The frequency analysis method utilizes analytical tools to find roots of the characteristic equation for the system where stability of the system can be analyzed according to standard control theories. In addition, standard graphical methods such as root locus, Bode plot, and Nyquist diagram can also be modified and applied to analyze delayed polynomials and transform functions. However, in contrast to conventional control systems, delays in the characteristic equation of time-delay systems appear as exponential functions. Therefore, Taylor and Pade approximations have to be used in developing analytical techniques to obtain solutions. These approximations may yield conservative results and sometimes lead to difficulties in ensuring acceptable stability conditions.

On the other hand, time domain approaches have advantages in dealing with nonlinearity and time-varying uncertainties. Depending on how one considers delay as a parameter, stability criteria may be divided into two types, namely *delay-independent* [83], [84] and *delay-dependent* [81], [85] stability conditions. In the delay-independent approach, no

a priori knowledge about the delay is required but the results tend to generally be conservative. In the delay-dependent approach, the stability conditions guarantee stability for all delays satisfying $0 < \tau < h$, where h is an upper bound on the delay. Hence, to design a delay-dependent controller, the upper bound of the delay should be known. The basic idea behind delay-dependent stability criteria is to transform the original system with discrete delays into a system with distributed delays where a Lyapunov-Krasovskii functional can be applied to derive the stability conditions. In most practical cases, the delays are not only unknown, but also time-varying. Treating time-varying delays requires a more involved and deeper analysis since their presence may induce further complex behaviors.

Linear Matrix Inequality

The LMI methodology for solving convex and quasi-convex optimization problems in the presence of design constraints has attracted a great deal of interest in the past decade. LMI techniques have emerged as powerful design tools in control engineering. The applications range from control engineering such as multi-model/multi objective state feedback design, robust pole placement, control of stochastic systems, multi-criterion LQG/LQR, optimal control, system identification and structural design [86]. The main factors that make LMI techniques appealing can be stated as follows [87]:

- A variety of design specifications and constraints can be expressed in terms of LMI feasibility conditions which make it suitable for multi-objective optimization problems.

- LMI algorithms formulate the problem in terms of a convex optimization problem. Hence, usually exact solutions can be found [87].

- While most of the problems with multiple constraints or objectives lack analytical solutions in terms of matrix equations, they often remain tractable in the LMI framework. This makes LMI-based design a valuable alternative to classical analytical methods.

2.1.6 Centralized, Decentralized and Distributed Control Schemes

Different definitions are available given for centralized and decentralized controllers in the literature [88], [89], [90]. To avoid ambiguity, the following definitions are adopted for these concepts in this thesis.

Definition 2.1. *A controller is classified as centralized if a central (global) controller is responsible for making decisions for the entire system. The controller needs to have access to the information on the entire system.*

Definition 2.2. *A controller is classified as decentralized if the controller for each subsystem (through the partitioning of the overall system into reduced order subsystems) is capable of making decisions using only local information.*

Definition 2.3. *A controller is classified as distributed if the controller for each subsystem is capable of communicating with the controllers of the other subsystems and the decisions of each controller can use both the local information (as in the decentralized controller) and its nearest neighboring controllers.*

2.2 Dynamic Communication Network Model

The "fluid flow" conservation principle [74], [91], [92] states that the rate of change of information queued in the buffer is equal to the difference between the arriving input and the outgoing output information rates. This is the basis of a static model of the traffic network that is used for developing some early congestion control algorithms. However, in communication networks, the customer arrival process is non-stationary with the arrival process parameters depending on the time [93]. Communication networks in particular are subject to a variety of phenomena that give rise to transient/non-stationary conditions such as load sharing, changes in the routing and flow control parameters, failure of links, nodes or other network resources and most commonly, non-stationary input loads. There is an empirical evidence that the user demand for communication is non-stationary in

many networks, varying with time [94]. Furthermore, as communication networks evolve to encompass differentiated services (Diff-Serv) which are utilized to transport complex traffic types with various quality of service (QoS) requirements, the traffic in the network is expected to be very bursty and non-stationary in nature. Therefore, using a dynamical model can provide a more precise description of the network operations and gives us an opportunity to develop control techniques whose properties can be studied analytically.

As discussed in Chapter 1, the main QoS specifications and performance metrics of a congestion control mechanism include both the node throughput as well as the delay and packet loss rates [95], [96]. Due to the trade-offs among these performance metrics it is important to consider them all together. Since the trade-offs are most clearly expressed and represented in terms of the queue management mechanism [95], an analytical and a quantitative model which has the queuing length as a state and network resources, such as the bandwidth, as control inputs would be the most appropriate model for our desired congestion control design.

In [97], the authors have proposed an approximation model of non-stationary queues based on the conservation laws of traffic flow and developed a fluid flow model to describe the dynamical queuing behaviors. In [62], the concept of guaranteed traffic and available bit rate (ABR) traffic are introduced to describe the *external* and *internal* traffic flows in a network, and based on the fluid flow model developed in [62], the authors developed an integrated connection admission control (CAC), flow rate, and bandwidth control for the ATM network. In [3], a Diff-Serv network is considered and a decentralized congestion controller is proposed to guarantee the queuing length and delays for an ATM network. In [98], a stochastic version of the fluid flow model presented in [62] is developed as the network model and a Lyapunov control theory was employed to solve the dynamic "cell" level bandwidth allocation problem. In [57], [58], a sliding mode-based congestion controller is developed by using the fluid flow model of a single node. In [99], a fluid flow control scheme for a large scale network is proposed based on the model presented in [62] where it is assumed that all the delays satisfy a saturation based Lipschitz-like condition.

However, none of the transmission, propagation, processing, and queuing delays were

considered in the above approaches and the congestion control schemes proposed therein are for fixed networks. Since the sending rate and scheduling is determined online, the network delay is not negligible and which will deteriorate the performance of the system in practice, and may even lead to instability. Moreover, the mobility of the network nodes can result in a time-varying topology, which requires new comprehensive models for effective congestion control design.

In this thesis, motivated from the existing works we extend the dynamical model that is presented in [62] to the NMAS. In the model considered here the delays are unknown and time-varying which makes it more realistic for real-world traffic network applications. The network induced delays could vary significantly due to unpredictable circumstances such as unpredicted traffic flows and congestion. In this thesis, the following types of delays are considered in the dynamic model of the networks:

- Transmitting delay: The time between starting and ending the transmission of a message. It depends on the length of the message.

- Propagating delay: The time for propagating a message on each link.

- Processing delay: The time that each message from upstream nodes or outside of the network should spend at each node to be received, identified by its destination, inserted to the appropriate queue, and performed the routing calculations (in dynamic routing).

The remainder of this section is focused on the selection and development of the dynamic models of NMAS with Diff-Serv traffic. We first give the fluid flow model of a single node, then describe the dynamical model for centralized, decentralized and mobile traffic networks that are considered in this thesis.

2.2.1 Fluid Flow Model

Consider a single node queue with non-stationary arrival process. Let us define $x(t)$ as the queuing state representing the ensemble average number in the node at time t. From

the fluid flow conservation principle, the rate of change of the queuing length is given as follows:

$$\dot{x}(t) = -f_{out}(t) + f_{in}(t) \tag{2.3}$$

The above type of equation can be used to model a wide range of queuing and contention systems [74], [91] and is often called a *fluid flow model*.

Assuming that the queue storage capacity is unlimited and the traffic arrives at the queue with the rate of $\lambda(t)$, then $f_{in}(t)$ is simply the offered load rate $\lambda(t)$. The flow out of the node, $f_{out}(t)$, can be related to the ensemble average utilization of the link by $f_{out}(t) = C(t)\rho(t)$, where $C(t)$ is the link capacity. Note that $\rho(t)$ is the probability that the number of packets in the queue is not zero (i.e. $\rho(t) = P(N(t)) > 0$, where $N(t)$ is the number of packets in the queue). Therefore, equation (2.3) becomes:

$$\dot{x}(t) = -C(t)\rho(t) + \lambda(t) \tag{2.4}$$

In general, determining an exact expression for $\rho(t)$ is quite difficult even for the simplest queues [100]. Hence, an approximate method is generally applied. We assume that $\rho(t)$ can be approximated by a function of the state $G(x(t))$. Thus, the dynamics of the queue can be represented by the following nonlinear differential equation

$$\dot{x}(t) = -C(t)G(x(t)) + \lambda(t) \tag{2.5}$$

with the initial condition $x(0) = x_0$. The expression for $G(x(t))$ which will accurately model the system is dependent on the type of the queue that one chooses for study.

Different approaches can be used for determining $G(x(t))$. If experimental data from an existing system can be obtained, then $G(x(t))$ can be determined based on the data statistics. However, such data are normally unavailable and one must determine $G(x(t))$ through other means, such as an approximation procedure. The simplest and the most commonly used approach for determining $G(x(t))$ is to match the steady-state equilibrium point of (2.5) with that of an equivalent queuing theory model, where the meaning of the term "equivalent" depends on the queuing discipline assumed.

This method has been validated through simulations for a number of network systems and for different queuing models in [74], [101]. In addition, the explicit relationship

41

between the queuing state $x(t)$ and the network resource (i.e., the link capacity $C(t)$ and the flow rate $\lambda(t)$) in (2.5) makes it to be the most appropriate model for our control design and analysis. Therefore, in this thesis, we adopt the *fluid flow model* as the basis for development of our congestion control design.

As stated earlier, the characteristics of $G(x(t)$ is dependent on the queuing system that is under study. Serval different analytical queuing models have been derived according to the approximation method that is described above and can be found in the literature [100], such as M/M/1, M/D/1, and D/M/1 queues. Each of these dynamical queuing models is developed based on the particular assumptions of the queuing discipline. It is worth noting that although the G/G/n queue is the most general queuing system, where the arrival and service time processes are both arbitrary, there is no known explicit analytical solution for this queuing system in the literature.

In this thesis, we represent the dynamics of a queue as an M/M/1 since the resulting queuing system can be applied to describe a wide variety of queuing models as found in systems with a very large number of independent customers/nodes that can be approximated as a Poisson process. In the following sections, the studied congestion control strategies will be based on the M/M/1 model. For an M/M/1 queue by matching the steady state of the queuing length $x(t) = \lambda/(\mu C - \lambda)$ to the steady state of the fluid flow model (2.5), the dynamics of a single node can consequently be expressed as

$$\dot{x}(t) = -\mu \frac{x(t)}{1 + x(t)} C(t) + \lambda(t) \tag{2.6}$$

where $x(t)$ is the queuing length; $C(t)$ is the output link capacity; $\lambda(t)$ is the average rate of incoming traffic; and μ is the average queue service rate. Based on the above fluid flow conservation principle and the M/M/1 queuing systems, a decentralized dynamic model for the Diff-Serv network is first developed and then extended to a centralized model in the following section.
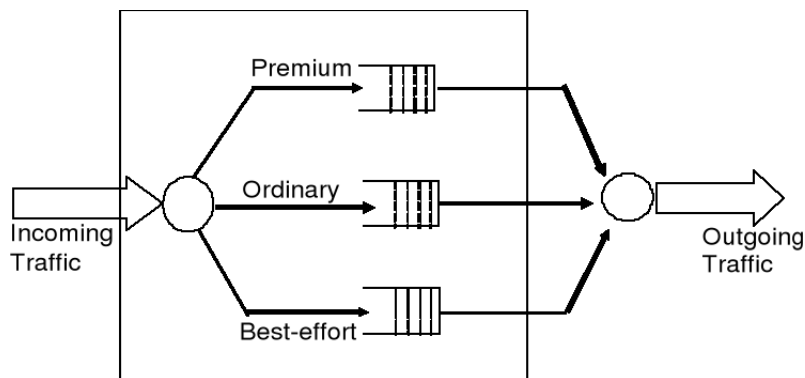
Figure 2.1: A DiffServ node with the premium, the ordinary, and the best-effort traffic.

2.2.2 Decentralized Model of Diff-Serv Network

In this section, the dynamic model of differentiated services (Diff-Serv) network is derived and the congestion control problem is formulated in a decentralized control framework. Generally speaking, the congestion control problem is in fact concerned with allocating the output bandwidth and regulating the flow rate of each queue. However, for the differentiated services (Diff-Serv) network, as presented in Section 2.1, the premium traffic requires no loss, no latency, no jitter, assured bandwidth service for all the incoming packets. That is, the incoming flow rate of the premium traffic is unnegotiable in the congestion control level. On the other hand, the ordinary traffic has relaxed delay requirements and allow their rate into the network to be regulated, which implies that the bandwidth and the incoming traffic rate of the ordinary traffic flow are both accessible for control. Finally, in the best-effort traffic there is no control activities but one opportunistically uses any instantaneous leftover resources. Therefore, the state space representations of the Diff-Serv traffic must be formulated in different ways according to the different control frameworks for the congestion control problem. The decentralized model of the premium and the ordinary traffic are now presented as follows.

Consider a Diff-Serv network consisting of n nodes. Each node has three separate buffers associated with the premium, the ordinary, and the best-effort traffic classes as shown in Fig. 2.1. Each node receives messages from both the neighboring nodes within the

network and from outside the network. It is assumed that the network is *fully connected*, that is each node of the network has a direct link with other nodes. Based on the flow conservation principle (2.3), the queuing state of each node can be expressed as follows

$$\dot{x}_i(t) \quad = \quad -f_i^{out}(t) + f_i^{in}(t) \qquad i = 1, ..., n \tag{2.7}$$

where x_i is the queuing length, $f_i^{in}(t)$ and f_i^{out} are the incoming and the outgoing traffic of node i, respectively. Unlike the single node, the incoming traffic $f_i^{in}(t)$ of the node in a networked system includes two parts, namely the traffic flow from i) external to the network, and ii) the neighboring nodes to node i within the network, that is

$$f_i^{in}(t) \quad = \quad f_i^{external}(t) + f_i^{internal}(t) \tag{2.8}$$

$$f_i^{external}(t) \quad = \quad \lambda_i(t)$$

$$f_i^{internal}(t) \quad = \quad \sum_{\substack{j=1 \\ j \neq i}}^{n} f_j^{out}(t - \tau_{ji}(t))g_{ji}(t)$$

where

$\lambda_i(t)$: external traffic rate entering node i,

$\tau_{ji}(t)$: total unknown time-varying and bounded delay in transmitting, propagating, and processing of messages from node j to node i,

$g_{ji}(t)$: time varying gains indicating the data compression rate between the nodes j and i, and

n: number of the nodes in the network.

According to the dynamics of M/M/1 queue (2.6), we have that

$$f_i^{out}(t) \quad = \quad \mu \frac{x_i(t)}{1 + x_i(t)} C_i(t) \tag{2.9}$$

$$f_j^{out}(t - \tau_{ji}(t)) \quad = \quad \mu \frac{x_j(t - \tau_{ji}(t))}{1 + x_j(t - \tau_{ji}(t))} C_j(t - \tau_{ji}(t)) \tag{2.10}$$

where $C_i(t)$ is the link capacity of node i. Therefore, the dynamic fluid flow model corresponding to each node in the network is governed by

$$\dot{x}_i(t) = -\mu \frac{x_i(t)}{1 + x_i(t)} C_i(t) + \lambda_i(t) + \sum_{\substack{j=1 \\ j \neq i}}^{n} \mu \frac{x_j(t - \tau_{ji}(t))}{1 + x_j(t - \tau_{ji}(t))} C_j(t - \tau_{ji}(t))g_{ji}(t) \tag{2.11}$$

It is worth noting that the model (2.11) is an extension of the M/M/1 queuing model (2.6) with explicit expression of the internal traffic flow $f_i^{internal}(t)$. The above model (2.11) can be used to represent all possible internal traffic paths for any origin destination pair. It has been shown to be reasonably accurate in comparison to discrete event simulations with a variety of scenarios [97], [62], [100], [61], [102].

Assumptions on The Delay

The delay $\tau_{ji}(t)$ in equation (2.11) is modeled as a *time-varying and unknown* signal which satisfies the following assumptions:

- Heterogeneous. The delays are heterogeneous where the delays between any node i and node j can have *different* values,

- Bounded. The delays are assumed to be lower and upper bounded with heterogeneous bounds as follows:

$$\tau_{ij}^{min} \leq \tau_{ij}(t) \leq \tau_{ij}^{max} \qquad i,j = 1,...,n \qquad (2.12)$$

  and the minimum lower bound and the maximum upper bound in the overall network are given by the following constant values:

$$0 = min\{\tau_{ij}^{min}\}$$

$$h = max\{\tau_{ij}^{max}\} \qquad i,j = 1,...,n \qquad (2.13)$$

  where 0 is the minimum value of the lower bound of the delay and h is a known constant indicating the maximum value of the upper bound of the delays, and

- Equivalent. Without loss of generality and for simplicity the bidirectional delays between any two pair of nodes are assumed to be equal, that is

$$\tau_{ij}(t) = \tau_{ji}(t) \qquad i,j = 1,...,n \qquad (2.14)$$

Physical Constraints

Certain *physical constraints* such as buffer size, link capacity and maximum supported transmission rate have to be considered. A NMAS may consist of a number of sensors,

decision makers, and actuators. Usually, sensors have the least communication recourses such as bandwidth capacity and buffer size. This is due to the fact that sensors are usually small devices with limited power supply and physical components which are not replaceable. Compared with sensors, decision makers are more powerful and need larger buffer and capacity to deal with comprehensive analysis and decision making. Finally, actuators are the nodes with execution functionalities and equipments. They are highly mobile and need to keep communication with both sensors and decision makers at most of the times. Therefore, each node in the NMAS may have very different levels of resources and, consequently have different values of physical constraints.

Let us define $C_{server,i}$ as the link capacity and $x_{buffer,i}$ as the buffer size of each node. The following constraints are therefore required to be satisfied:

- **Bandwidth constraints:** The bandwidth that is utilized in the output link of each node cannot exceed the capacity of that link capacity, that is

$$0 \leq C_i(t) \leq C_{server,i} \qquad i = 1, ..., n \qquad (2.15)$$

- **Buffer size constraints:** To avoid packet loss, the queuing length at any time must not exceed the maximum buffer size specified for the node, that is

$$0 \leq x_i(t) \leq x_{buffer,i} \qquad i = 1, ..., n \qquad (2.16)$$

- **Transmitter constraints:** Each node has a transmitter which can support a maximum transmission rate of λ_i^{max}. Therefore, the instantaneous traffic transmission rate at each node should satisfy

$$\lambda_i(t) \leq \lambda_i^{max} \leq C_{server,i} \qquad i = 1, ..., n \qquad (2.17)$$

Each node in the NMAS has three separate buffers for the premium, the ordinary, and the best-effort traffic class, respectively. Hence, the decentralized queuing model (2.11) is applicable for each of these three traffic classes. However, as stated in Section 2.1.1, each traffic class in the Diff-Serv network has different levels of QoS specifications, and consequently has different control variables. Specifically, the premium service is designed

for applications with the highest QoS requirements among the three classes. The incoming traffic rate of the premium traffic is unknown and not negotiable, the only network contract for the premium traffic is that the bandwidth will be available when the traffic is sent. Therefore, form the queuing model (2.11), the only available control variable for the premium traffic is the bandwidth capacity $C_i(t)$. On the other hand, the ordinary service is designed for applications with relaxed delay requirements that allow their traffic rate to be regulated. That is, both the bandwidth capacity $C_i(t)$ and the incoming traffic rate $\lambda_i(t)$ with respect to the ordinary traffic are available for control. Finally, since there is no specific QoS for the best-effort traffic, there is no control issue for this class. It opportunistically uses any leftover capacities from the premium and the ordinary traffic classes.

To design a congestion control strategy for the Diff-Serv traffic, one needs to consider the dynamic model of each traffic class and clarify the control objectives separately. In the rest of this section, we reformulate the decentralized queuing model (2.11) for the premium and the ordinary traffic classes, with their corresponding physical constraints, respectively.

1. Premium Traffic Model

The decentralized queuing model (2.11) with respect to the premium traffic is rewritten here again

$$\dot{x}_{pi}(t) = -\mu \frac{x_{pi}(t)}{1 + x_{pi}(t)} C_{pi}(t) + \lambda_{pi}(t) + \sum_{\substack{j=1 \\ j \neq i}}^{n} \mu \frac{x_{pj}(t - \tau_{ji}(t))}{1 + x_{pj}(t - \tau_{ji}(t))} C_{pj}(t - \tau_{ji}(t)) g_{ji}^{p}(t) \quad (2.18)$$

where "p" denotes the premium traffic. The congestion control problem of the *premium traffic* is actually concerned with allocating the bandwidth $C_{pi}(t)$, according to the network information, such that certain QoS objectives are satisfied.

Let us define

$$f(x_{pi}(t)) = \mu \frac{x_{pi}(t)}{1 + x_{pi}(t)} \quad (2.19)$$

$$u_{pi}(t) = C_{pi}(t), \qquad i = 1, ... n \quad (2.20)$$

47

In view of the above notations, equation (2.18) can be rewritten in the following state space representation

$$\dot{x}_{pi}(t) = -f(x_{pi}(t))u_{pi}(t) + \sum_{\substack{j=1 \\ j \neq i}}^{n} f(x_{pj}(t - \tau_{ji}(t)))u_{pj}(t - \tau_{ji})g_p^{ji}(t) + \lambda_{pi}(t) \qquad (2.21)$$

The above dynamic model is a nonlinear system with unknown external signal and time-varying delays in the coupled states. Based on this model, the decentralized control objective for the premium traffic is now to select the controller $u_{pi}(t)$ so that the system (2.21) is ultimately bounded and the closed-loop performance cost is guaranteed subject to all the admissible delays. Details of the congestion control development will be presented in Chapter 3.

- **Physical constraints of The Premium Traffic**

  The constraints (2.15)-(2.17) are now reformulated for the premium traffic model (2.21) as follows:

  $$0 \leq x_{pi}(t) \leq x_{pi}^{buffer} \qquad (2.22)$$

  $$0 \leq u_{pi}(t) \leq C_{server,i}, \qquad i = 1, ...n \qquad (2.23)$$

  where x_{pi}^{buffer} is the premium buffer size of node i.

2. Ordinary Traffic Model

The decentralized queuing model (2.11) with respect to the ordinary traffic is rewritten as follows

$$\dot{x}_{ri}(t) = -\mu\frac{x_{ri}(t)}{1 + x_{ri}(t)}C_{ri}(t) + \lambda_{ri}(t) + \sum_{\substack{j=1 \\ j \neq i}}^{n} \mu\frac{x_{rj}(t - \tau_{ji}(t))}{1 + x_{rj}(t - \tau_{ji}(t))}C_{rj}(t - \tau_{ji}(t))g_{ji}^{r}(t) \ (2.24)$$

where "r" represents the ordinary traffic. Since the ordinary traffic allows their incoming traffic rate to be regulated, hence the control strategies for this class are to regulate the incoming traffic $\lambda_{ri}(t)$ and the link capacity $C_{ri}(t)$ so that the queuing length $x_{ri}(t)$ behaves as desired. Therefore, for the ordinary queue of each node, there are two available control inputs. Similar to the premium traffic, let us we define

$$f(x_{ri}(t)) \quad = \quad \mu \frac{x_{ri}(t)}{1 + x_{ri}(t)}$$

$$u_{ri}^1(t) \quad = \quad C_{ri}(t) \tag{2.25}$$

$$u_{ri}^2(t) \quad = \quad \lambda_{ri}(t) \tag{2.26}$$

Therefore, the queuing model (2.24) for the ordinary traffic can be reformulated as follows

$$\dot{x}_{ri}(t) = -f(x_{ri}(t))u_{ri}^1(t) + u_{ri}^2(t) + \sum_{\substack{j=1 \\ j \neq i}}^{n} f(x_{rj}(t - \tau_{ji}(t)))u_{rj}^1(t - \tau_{ji})g_r^{ji}(t) \tag{2.27}$$

Equation (2.27) indicates that the dynamic model of the ordinary traffic is a non-linear system with multiple inputs and time-varying delays with the coupled states. The congestion control problem for the ordinary traffic is now to select the controllers $u_{ri}^1(t)$ and $u_{ri}^2(t)$ so that the system (2.27) is asymptotically stable and the closed-loop system performance is guaranteed subject to any admissible delays.

- **Physical Constraints of The Ordinary Traffic**

  The ordinary traffic can only utilize the leftover capacity from the premium traffic. That is, the maximum allowable bandwidth for the ordinary traffic is a time-varying variable depending on the value of $C_{server,i} - u_{pi}(t)$. Therefore, the physical constraints (2.15)-(2.17) for the ordinary traffic of each node can be described accordingly

$$0 \leq x_{ri}(t) \leq x_{ri}^{buffer} \tag{2.28}$$

$$0 \leq u_{ri}(t) \leq c_{ri}(t) \qquad i = 1, ..., n \tag{2.29}$$

  where x_{ri}^{buffer} is the buffer size for the ordinary traffic at node i, and $c_{ri}(t) = C_{server,i} - u_{pi}(t)$ is the instantaneous leftover capacity of node i from the premium traffic.

2.2.3 Centralized Model of Diff-Serv Network

According to the definitions given in Section 2.1.7, the centralized controller needs to know the information of the entire system. For the congestion control problem, the information

of the system are the queuing lengthes of each node. In this section, we consider all the nodes of the network together, so that the queuing dynamics of the entire network is formulated and the control objectives of each traffic class are described in a centralized framework.

Consider a Diff-Serv network with n nodes which is *fully connected*. Based on the decentralized queuing model of each node (2.11), let us define

$$x(t) \quad = \quad vec\{x_i(t)\} \tag{2.30}$$

$$C(t) \quad = \quad vec\{C_i(t)\} \tag{2.31}$$

$$\lambda(t) \quad = \quad vec\{\lambda_i(t)\} \tag{2.32}$$

$$f(x_i(t)) \quad = \quad \mu \frac{x_i(t)}{1 + x_i(t)} \tag{2.33}$$

$$F(x(t)) \quad = \quad \begin{bmatrix} f(x_1(t)) & 0 & 0 \\ 0 & \ddots & 0 \\ 0 & 0 & f(x_n(t)) \end{bmatrix} \quad i = 1, ..., n \tag{2.34}$$

where the operation *vec* stands for a vector. Consequently, the fluid flow model of the entire network can be give as follows

$$\dot{x}(t) = -F(x(t))C(t) + \lambda(t) + \sum_{l=1}^{m} G_l F(x(t - \tau_l(t)))C(t - \tau_l) \tag{2.35}$$

where m denotes the number of possible delays in the network, and $G_l \in R^{n \times n}$ is the matrix indicating data compression gains among the nodes in the network. In fact

$$\sum_{l=1}^{m} G_l = \begin{bmatrix} 0 & g_{21} & \cdots & g_{n1} \\ g_{12} & 0 & \cdots & g_{n2} \\ \vdots & \vdots & \ddots & \vdots \\ g_{1n} & \cdots & \cdots & 0 \end{bmatrix} \tag{2.36}$$

The following example is provided to clarify the definitions of m and G_l.

Example 2.1. *Consider the network given in Fig. 2.2. The network has 3 nodes and is fully connected. According to the equivalent assumption of delays (2.14), the time-varying delays in the network has 3 different values, that is $m = 3$. Let us define*

50
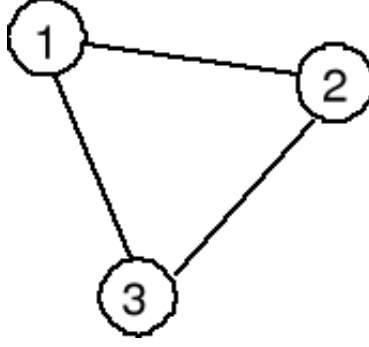
Figure 2.2: A network with three nodes.

$$
\begin{aligned}
\tau_1(t) &= \tau_{12}(t) = \tau_{21}(t) \\
\tau_2(t) &= \tau_{23}(t) = \tau_{32}(t) \\
\tau_3(t) &= \tau_{13}(t) = \tau_{31}(t)
\end{aligned}
$$

Corresponding to the above definition, G_l, $l = 1, .., 3$ are given by

$$
G_1 = \begin{bmatrix} 0 & g_{21} & 0 \\ g_{12} & 0 & 0 \\ 0 & 0 & 0 \end{bmatrix}, G_2 = \begin{bmatrix} 0 & 0 & g_{31} \\ 0 & 0 & 0 \\ g_{13} & 0 & 0 \end{bmatrix}, G_3 = \begin{bmatrix} 0 & 0 & 0 \\ 0 & 0 & g_{32} \\ 0 & g_{23} & 0 \end{bmatrix}
$$

∎

Based on the centralized model (2.35) and the QoS specifications of each traffic class, the centralized queuing model for the premium and the ordinary traffic are described in the remainder of this section. The physical constraints are reformulated for each traffic class in a centralized framework also.

1. Premium Traffic Model

In the centralized model (2.35), define $u_p(t) = C_p(t)$. Then the centralized model of the premium traffic can be written as

$$
\dot{x}_p(t) = -F(x_p(t))u_p(t) + \lambda_p(t) + \sum_{l=1}^{m} G_l F(x_p(t - \tau_l(t)))u_p(t - \tau_l) \tag{2.37}
$$

where p stands for the premium. The control objective of the premium traffic is to design the centralized controller $u_p(t)$ so that the system (2.37) is ultimately bounded and certain adequate performance level is guaranteed with respect to all the admissible delays.

- *Physical Constraints of The Premium Traffic*

In a centralized control, all the nodes in the network need to satisfy the physical constraints (2.15)-(2.17), simultaneously. Hence, the following definition of a vector inequality is needed.

Definition 2.4. *[103]* Consider two vectors $a = (a_1, ..., a_n)$ and $b = (b_1, ..., b_n)$, where a_i and b_i are real numbers for $i = 1, ..., n$. Then,

$$a < b \iff a_i < b_i, \qquad i = 1, ..., n \qquad (2.38)$$

By using the above definition, the constraints (2.15)-(2.17) for the centralized model of the premium traffic can be expressed as:

$$0 \le x_p(t) \le x_p^{buffer} \qquad (2.39)$$

$$0 \le u_p(t) \le C_{server} \qquad (2.40)$$

where $x_p^{buffer} = vec\{x_{pi}^{buffer}\}$ and $C_{server} = vec\{C_{server,i}\}$.

2. Ordinary Traffic Model

In the centralized model (2.35), let us define

$$u_{r1}(t) = C_r(t) \qquad (2.41)$$

$$u_{r2}(t) = \lambda_r(t) \qquad (2.42)$$

$$C_r(t) = vec\{C_{ri}(t)\} \qquad (2.43)$$

$$\lambda_r(t) = vec\{\lambda_{ri}(t)\} \qquad (2.44)$$

where r refers to the ordinary traffic. Consequently, the centralized model of the ordinary traffic with inputs can be written as follows

$$\dot{x}_r(t) = -F(x_r(t))u_{r1}(t) + u_{r2}(t) + \sum_{l=1}^{m} G_l F(x_r(t - \tau_l(t)))u_{r1}(t - \tau_l) \qquad (2.45)$$

For the above nonlinear system, the control objective is now to select the centralized controller $u_r(t) = vec\{u_{ri}(t) \ u_{r2}(t)\}$ so that the system (2.45) is asymptotically stable and certain adequate performance level of corresponding closed-loop system is guaranteed subject to all the admissible delays.

- *Physical Constraints of The Ordinary Traffic*

  The physical constraints (2.15)-(2.17) for the ordinary traffic of the entire network can be described accordingly

  $$0 \leq x_r(t) \leq x_r^{max} \qquad (2.46)$$

  $$0 \leq u_r(t) \leq c_r(t) \qquad (2.47)$$

  where $x_r^{max} = vec\{x_{ri}^{buffer}\}$ denotes the buffer size constraints of the network, and $c_r(t)$ is the vector of instantaneous leftover capacities of all the nodes from the premium traffic. In fact, $c_r(t)$ equals to $C_{server} - u_p(t)$ and is a time-varying bound.

It worth noting that the constraints of the centralized model, for the premium traffic (2.37) and the ordinary traffic (2.45), respectively, are more conservative then those in the decentralized models (2.21) and (2.27). The reason for this is that in a centralized control, the dynamics of all the nodes in the network are considered simultaneously. Since the centralized controller needs all the system information. Violating the physical constraints of a single node may substantially lead to instability of the entire network. Therefore, the physical constraints of all the nodes have to be guaranteed at all the times.

2.2.4 Dynamical Model of Mobile Diff-Serv Network

Recently, wireless communication technologies have stimulated a large body of research activity on self-organizing networks such as mobile ad-hoc networks. In mobile ad hoc network, there is no stationary infrastructure for the network. The nodes in a mobile network can move arbitrarily, thus the topology of the network is expected to change often and unpredictably. In addition to mobility, loss of node power, or addition of new nodes will also lead to changing network topology. Consequently, the neighboring sets of each node is also changing. To achieve an efficient congestion control strategy certain physical parameters such as the distance between the nodes or maximizing the nodes lifetime, and fading nodes should be considered in defining the neighborhood sets. In [100], the impact of mobility and the resulting link failures and additions are represented by an adjacency variable, which is set to be either 1 or 0, depending on the distance between

53

every two nodes. If the distance is less than or equal to their radio range, R, then the nodes are connected and the adjacency variable is set to 1. Otherwise, the adjacency variable is set to 0. In [104], the definition of the adjacency variable in [100] is extended by defining a threshold on the distance between two nodes, which is a function of the maximum output power of the transmitter antenna.

In view of the above, the congestion control problem is more challenging for mobile ad hoc networks that are subject to fast and unpredictable network topology changes. Therefore, highly adaptive congestion control algorithms are required. In this thesis, the congestion control problem for mobile Diff-Serv networks is considered according to two approaches based on the available network information and the communication capability of the controllers. These are (a) the centralized and the decentralized, and (b) the distributed control strategies. Towards this end, the dynamic model of the mobile ad hoc network is formulated in 1) decentralized, and 2) centralized for the premium and the ordinary traffic, in the following two sections, respectively. These models are subsequently used to design the corresponding centralized, decentralized and distributed control strategies in the following chapters.

Decentralized Model of The Mobile Network

Consider a mobile Diff-Serv network with n nodes. Due to the mobility, the dynamics of the queuing system (2.11) is now modified to the following representation for mobile networks

$$\dot{x}_i(t) = -\mu \frac{x_i(t)}{1 + x_i(t)} C_i(t) + \lambda_i(t) + \sum_{j \in \wp_i(\alpha(t))} \mu \frac{x_j(t - \tau_{ji}(t))}{1 + x_j(t - \tau_{ji}(t))} C_j(t - \tau_{ji}(t)) g_{ji}(t) \quad (2.48)$$

where $\wp_i$ denotes the neighboring set of node i and $\alpha(t)$ denotes a function representing the rule for changing the neighboring sets.

The time-varying function $\alpha(t)$ is also referred to as a *mode* of the network with the corresponding topology at instant t. It is known that the link connectivity between two nodes at time $t + \Delta t$ is only dependent on the nodes' position, velocity and the direction of movement at time t. Therefore, the future connection of two nodes is independent of

54

its history, but dependent only on the current state of the connectivity. Therefore, the changes of the network topology is a memoryless stochastic process which can be described by a stochastic process, namely the Markov chain. In this thesis, the rule for changing network topology $\alpha(t)$ (sometimes denoted as α_t) is defined according to the Markov chain as below.

Given a complete probability space $\{\Omega, \mathcal{F}, P\}$, where Ω is the sample space, $\mathcal{F}$ is the σ-algebra of subsets of the sample space, and P is the probability measure on $\mathcal{F}$, the stochastic process $\alpha(t)$ can be defined as a continuous-time Markov process. The variable $\alpha(t)$ takes values in a finite set $\mathcal{S} = \{1, ..., M\}$ with the transition probability matrix $\Pi = \{\pi_{kl}\}$ given as follows:

$$P[\alpha_{t+\Delta} = k \mid \alpha_t = l] = \begin{cases} \pi_{kl}\Delta + o(\Delta), & k \neq l; \\ 1 + \pi_{kk}\Delta + o(\Delta), & k = l. \end{cases} \tag{2.49}$$

where $\pi_{kl} \geq 0$ is the transition rate from mode k to mode l, $\pi_{kk} = -\sum_{l=1, l \neq k}^{M} \pi_{kl}$, and $o(\Delta)$ is a function satisfying $\lim_{\Delta \to 0} \frac{o(\Delta)}{\Delta} = 0$.

In the stochastic system (2.48), the same assumptions regarding the multiple and time-varying delays (2.12)-(2.14) and the physical constraints as defined in equations (2.15)-(2.17) are applicable to mobile networks also. The decentralized model for the premium and the ordinary traffic in the mobile networks are described as follows.

- **Premium Traffic Model**

  Following the same definition of input $u_{pi}(t) = C_{pi}(t)$, let us define $f(x_{pi}(t)) = \mu \frac{x_{pi}(t)}{1+x_{pi}(t)}$ as in the fixed network. Therefore, the decentralized queuing dynamics of the mobile network (2.48) with respect to the premium traffic can be written as follows

  $$\dot{x}_{pi}(t) = -f(x_{pi}(t))u_{pi}(t) + \sum_{j \in \wp_i(\alpha(t))} f(x_{pj}(t - \tau_{ji}(t)))u_{pj}(t - \tau_{ji})g_p^{ji}(t) + \lambda_{pi}(t) \tag{2.50}$$

  where

  p: denotes the premium traffic,

  $x_{pi}(t)$: is the queuing length of node i,

$u_{pi}(t)$: is the bandwidth allocated to the premium traffic in node i,

$\lambda_{pi}(t)$: is the traffic flow external to the network, and

$g_p^{ji}(t)$: is the data compression rate of the premium traffic between nodes j and i.

The control objective now is to design the mode dependent controller $u_{pi}(\alpha(t))$ associate with each mode $\alpha(t)$ so that the stochastic system (2.50) is ultimately bounded and the closed-loop system performance is guaranteed with respect to any admissible delays.

  – **Physical Constraints of The Premium Traffic**

   In a mobile network, the link capacity of each node is changing due to the nodes mobility. Therefore, the capacity constraint of each node is dependent on the *mode* $\alpha(t)$ of mobile networks, and the premium traffic model (2.50) needs to satisfy the following physical constraints

$$0 \le x_{pi}(t) \le x_{pi}^{buffer} \tag{2.51}$$

$$0 \le u_{pi}(t) \le C_{server,i}(\alpha(t)), \qquad i = 1, ...n \tag{2.52}$$

   where $C_{server,i}(\alpha(t))$ denotes the time-varying link capacity that is dependent on the network topology and the instantaneous neighboring set.

- **Ordinary Traffic Model**

  Let us define $u_{ri}^1 = C_{ri}(t)$, $u_{ri}^2(t) = \lambda_{ri}(t)$ and $f(x_{ri}(t)) = \mu \frac{x_{ri}(t)}{1+x_{ri}(t)}$, so that the decentralized queuing model (2.48) for the ordinary traffic is modified as follows

$$\dot{x}_{ri}(t) = -f(x_{ri}(t))u_{ri}^1(t) + u_{ri}^2(t) + \sum_{j \in \wp_i(\alpha(t))} f(x_{rj}(t - \tau_{ji}(t)))u_{rj}^1(t - \tau_{ji})g_r^{ji}(t) \tag{2.53}$$

  where r represents the ordinary traffic, $x_{ri}(t)$ is the ordinary queuing length, $u_{ri}^1(t)$ denotes the allocated bandwidth and $u_{ri}^2(t)$ is the regulated traffic rate of the ordinary traffic into node i. The above model represents a nonlinear system with time-varying delays, where the control objective is to select a controller $u_{ri}(t) = vec\{u_{ri}^1 \ u_{ri}^2\}$ associated with each different mode $\alpha(t)$ so that the closed-loop system

of (2.53) is asymptotically stable with a guaranteed performance cost corresponding to all admissible delays.

- – *Physical Constraints of The Ordinary Traffic*

  The bandwidth constraint and the buffer size constraint of the ordinary traffic are now modified as follows

$$0 \leq x_{ri}(t) \leq x_{ri}^{buffer} \tag{2.54}$$

$$0 \leq u_{ri}(t) \leq c_{ri}(\alpha(t)), \qquad i = 1, ...n \tag{2.55}$$

  where $c_{ri}(\alpha(t))$ denotes the instantaneous leftover capacity of the node i from the premium traffic which is actually equals to $C_{server,i}(\alpha(t)) - u_{pi}(\alpha(t))$.

Centralized Model of The Mobile Network

Consider the queuing dynamics (2.48) of all the nodes in the same neighboring set simultaneously. Based on the definition of the neighboring set $\wp_i$ and the changing rule $\alpha(t)$ of the network topology, the centralized model for both the premium traffic and the ordinary traffic are now modified for the mobile networks as follows:

- **Premium Traffic Model**

  The queuing dynamics of the premium traffic for a mobile ad hoc network can be written as follows

$$\dot{x}_p(t) = -F(x_p(t))u_p(t) + \lambda_p(t) + \sum_{l=1}^{m(\alpha(t))} G_l F(x_p(t - \tau_l(t)))u_p(t - \tau_l) \tag{2.56}$$

  where $x_p(t)$ is the premium queuing length of the nodes in the network, $u_p(t)$ is the input vector of the allocated bandwidth of all the nodes in the network, $m(\alpha(t))$ is the number of possible delays in the network, depending on the network topology at time t, and which in turn is a function of the changing rule $\alpha(t)$. The following example is presented to illustrate the definition of $m(\alpha(t))$.

  Example 2.2. *Consider the same network as in Example 2.1, except that all the nodes are mobile now. As shown in Figure 2.3, the three nodes are expected to*
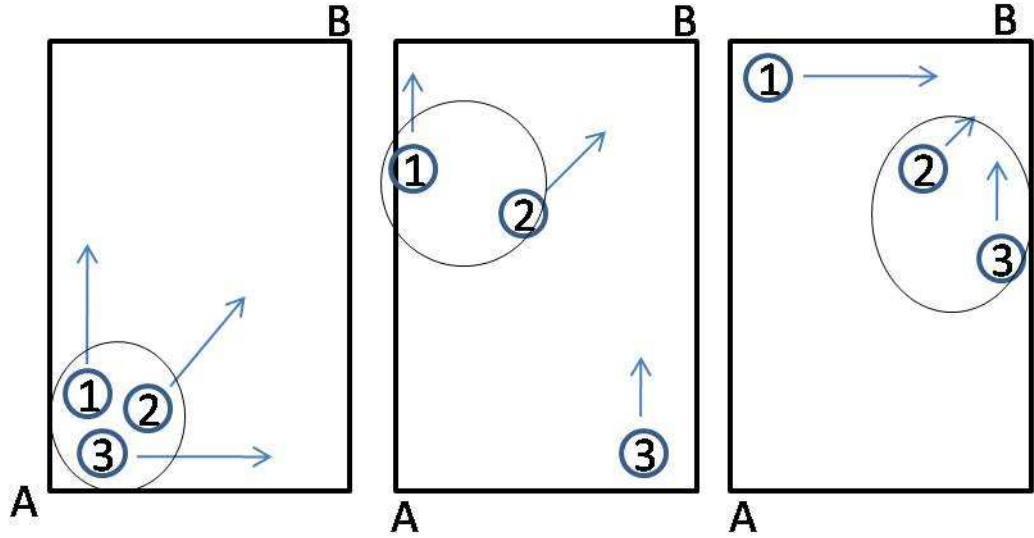
Figure 2.3: The schematic of the network configuration for three "typical" modes of a three node network.

explore a rectangular area of interest by moving from position A to position B. Node 1 moves towards north first and then towards east; node 2 moves towards northeast directly; and node 3 moves towards east and then towards north. Figure 2.3 depicts the configuration of the network at three distinct modes during the exploration.

Therefore, in mode 1, the time-varying delays in the network have 3 different values, that is $m = 3$, where we may define

$$
\begin{aligned}
\tau_1(t) &= \tau_{12}(t) = \tau_{21}(t) \\
\tau_2(t) &= \tau_{23}(t) = \tau_{32}(t) \\
\tau_3(t) &= \tau_{13}(t) = \tau_{31}(t)
\end{aligned}
$$

However, in mode 2, node 3 is outside of the neighboring set of nodes 1 and 2, and hence is not communicating with any of these two nodes. There is only one type of delay in the network here, that is $m = 1$, where we can define

$$
\tau_1(t) = \tau_{12}(t) = \tau_{21}(t)
$$

Finally in mode 3, the neighboring set is reformulated between nodes 2 and 3 and node 1 is now isolated. Therefore, $m = 1$ and the delay in the network can be defined

as

$$\tau_1(t) \quad = \quad \tau_{23}(t) = \tau_{32}(t)$$

- **Ordinary Traffic Model**

  The dynamics of the ordinary traffic in a mobile ad hoc network can be given as follows

  $$\dot{x}_r(t) = -F(x_r(t))u_{r1}(t) + u_{r2}(t) + \sum_{l=1}^{m(\alpha(t))} G_l F(x_r(t - \tau_l(t)))u_{r1}(t - \tau_l) \quad (2.57)$$

  where $u_{r1}(t)$ is the vector of bandwidth allocated to the ordinary traffic in the network, and $u_{r2}(t)$ is the vector of the regulated ordinary traffic flow rate for the nodes.

It should be noted that the change of the neighboring set will not only change the number of delays in the network, but also change the number of connections of each node. Consequently, the internal traffic flow in the same neighboring set will become time-varying and mode-dependent. The queuing models of the mobile networks do now represent as switching systems due to the changes in the mode function $\alpha(t)$. Therefore, to cope with the changing network topologies, the associated congestion control strategies must be made and designed to be mode-dependent also.

2.3 Main Methodologies

As presented earlier, the dynamical models of the NMAS are highly nonlinear systems having unknown multiple and time-varying delays, and are subject to a group of input and state constraints. During the past decades, the control of constrained systems have received great attention and a large number of work has been published in the literature. In this thesis, we mainly consider the following two methodologies:

- *Switching control approach.* In this method, the system constraints are adjoined to the controller design process. The control strategy is derived incorporating the conditions of constrained inputs or states. The control input switches among a set

of controllers that are designed according to the system constraints. The stability of closed-loop system with respect to each controller is then analyzed and derived.

- *Guaranteed cost control approach.* In this method, the controller is first synthesis without consideration of the system constraints. The control input is designed according to the guaranteed cost control technique. The stability of closed-loop system is derived as a LMI conditions. The physical constraints of the network are then expressed as a set of complementary LMIs also.

Details of these two methodologies are presented as follows.

2.3.1 Switching Control Approach

As presented earlier, the dynamical model of each traffic class in a Diff-Serv network is described by a nonlinear time-varying delay system that is subject to a group of physical constraints. These physical constraints are manifested in the system model as inputs and states constraints that may lead to performance deterioration and even instability. It is well-known that violations of such constraints drastically degrade the system performances and even lead to instability if not properly accounted for in the design procedure [105]. During the past decade, switching control related approaches for constrained systems have been developed [106], [107], [108], [109], [110], [111]. Specially, control laws that utilize switching of fixed-structure controllers, although are relatively simple, can actually achieve significant performance enhancements [105], [108], [112], [113], [114].

In [111], a switching control law for constrained systems is proposed where a supervisor selects the highest performance controller that is "safe" for the current state of the plant. However, the supervisory logic in [111] is conservative from the safety point of view. The switching controllers conservativeness is reduced by employing the strategy that is based on the maximal constrained positively invariant (CPI) set property as proposed in [108], and which is utilized in the analysis of constrained systems [106], [107], [109]. It has been shown that by employing the switching control approach the constraints of the system can be properly accounted for in the design procedure, and hence the risk of
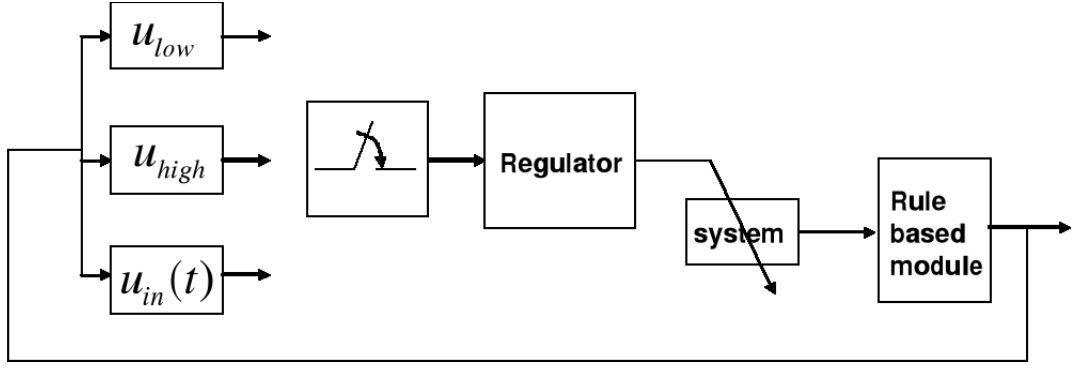
Figure 2.4: Schematic of the switching control scheme of a constrained system.

instability due to the control boundary can be avoided. The switching control law of a constrained system can be described as follows [115].

Consider a system having the control signal $u(t)$ that is lower and upper bounded by physical constraints to u_{low} and u_{high}, respectively. The switching control law can then be defined as:

$$
u(t) = \begin{cases} u_{low}, & \text{if } u_{in}(t) < u_{low}; \\ u_{in}(t), & \text{if } u_{low} \leq u_{in}(t) \leq u_{high}; \\ u_{high}, & \text{if } u_{in}(t) > u_{high}. \end{cases}
\tag{2.58}
$$

The above switching law indicates that when the value of the input signal $u_{in}(t)$ exceeds the physical constraints, the controller switches to the boundary value which are usually constant. On the other hand, when the input signal satisfies the constraints, it remains the same as the designed control input. For a constrained system, the safe operating range is when the input signal satisfies $u_{low} < u(t) < u_{high}$. In synthesizing a switching control strategy, it is important to ensure that the system remains in the safe operating mode for the given set of constraints.

Fig. 2.4 shows a block diagram of a switching control scheme for a constrained system. By utilizing this switching scheme the closed-loop system will experience multiple modes with respect to the controller and the stability under each mode must then be guaranteed so that the entire system is ensured to be stable. In this thesis, the first and the last modes in equation (2.58) are designated as *edge modes* and the second mode in

61

equation (2.58) is designated as *normal control mode.* The control input switches among the three controllers which are selected automatically by the *rule based module.* We expect that the system remains in the normal control mode (safe operation) as long as possible so that the desired control input $u(t)$ can take on its most effect. As shown in Fig. 2.4, when the control input reaches its boundaries an additional regulator is employed to adjust the system parameters. Hence, the system state is forced to change towards the direction of safe operating range. Therefore, after a finite time the desired controller $u(t)$ will be selected.

On the other hand, the control objective of the normal control mode is to select the control input $u(t)$, based on the nonlinear dynamical queuing models presented in Section 2.2, so that the closed-loop system is stable. The details of the proposed switching congestion control (SCC) strategies are presented in Chapter 3.

2.3.2   Guaranteed Cost Control Approach

The problem of designing a robust controller for a system with uncertainties has drawn considerable attention in the control systems literature. Much effort has been directed towards finding a controller that guarantees robust stability. However, when controlling a real plant it is also desirable to design a system that is not only stable but also guarantees an adequate level of performance. One approach to this problem is the *guaranteed cost control* (GCC) which was first introduced in [116]. The GCC approach is proposed as an extension to the classical LQR regulation problem for linear systems with parametric uncertainties, subject to the following quadratic cost function

$$J = \int_0^\infty (x^T(t)Qx(t) + u^T(t)Ru(t))dt \tag{2.59}$$

where x is the state of the system, u is the control input, and Q and R are given positive definite matrices. The conceptual objective of the GCC is to design a feedback controller such that for all admissible uncertainties the closed-loop system is asymptotically stable and an upper bound on the quadratic cost function (2.59) is guaranteed [117], [118], [119].

Based on this idea, a number of significant results have been proposed in the literature. In particular, the authors in [117] have presented a Riccati equation approach for designing a quadratic guaranteed cost controller. In [120], a linear matrix inequality (LMI) approach for the design of guaranteed cost controller is presented. The main idea is to obtain a controller through the solution of an LMI optimization problem [119], [121]. This allows a computationally efficient and practical solution to the GCC problems.

The GCC approach has recently been extended to time-delay systems. In [122], [120], delay-independent design methods are applied to derive the guaranteed costs, and in [123], [124], delay-dependent design methods for guaranteed cost control via state feedback are presented for uncertain continuous-time systems. According to the above references, the definition of a *guaranteed cost control* of a *time-delay system* can be described as follows.

Consider the following linear time-delay system:

$$\dot{x}(t) = A_0 x(t) + A_1 x(t - \tau(t)) + Bu(t) \tag{2.60}$$

where x is the state vector, u is the control input vector, $\tau(t)$ is the unknown time-varying delay, and A_0, A_1 and B_0 are the system matrices. Associated with the cost function (2.59), the following definition is now given.

Definition 2.5. *[125] For the system (2.60) and the performance cost function (2.59), if there exist a control law $u^*(t)$ and a positive scalar J^* such that the closed-loop system is asymptotically stable and the closed-loop performance cost J satisfies*

$$J \leq J^* \tag{2.61}$$

then J^* is the guaranteed cost *and $u^*(t)$ is the* guaranteed cost control *law for the system (2.60).*

In this thesis, the transmission, the processing, and the propagation delays in the NMAS are considered as unknown and time-varying delays in the dynamical system model. The guaranteed cost control approach is then applied for the synthesis and development of the congestion control strategies. The details of the proposed guaranteed cost congestion control (GCC) strategies are provided in Chapter 5 and 6. Moreover, in this thesis the

guaranteed cost controller is obtained to guarantee asymptomatic stability or ultimate boundedness of the closed-loop system. The notation of an ultimate boundedness is defined as follows:

Ultimate Boundedness

Consider the following system

$$\dot{x}(t) = f(x, t) \tag{2.62}$$

where $f : [0, \infty) \times D \rightarrow R^n$ is piecewise continuous in t and locally Lipschitz in x on $[0, \infty) \times D$ and $D \subset R^n$ is a domain that contains the origin.

Definition 2.6. *[78] The solutions of (2.62) are said to be uniformly ultimately bounded with an ultimate bound b if there exist positive constants b and c, independent of $t_0 \geq 0$, and for every $a \in (0, c)$, there is $T = T(a, b) \geq 0$, independent of t_0, such that*

$$\|x(t_0)\| \leq a \Rightarrow \|x(t)\| \leq b, \quad \forall t \geq t_0 + T \tag{2.63}$$

2.4 Conclusions

In this chapter, after revisiting some basic definitions and concepts, the dynamic model of the Diff-Serv traffic is presented based on the fluid flow model for both the fixed and mobile network of multi-agent systems and according to both decentralized and centralized frameworks. The network traffic dynamics are presented as a standard nonlinear state space representations where the transiting, the propagating and the processing delays are considered as unknown time varyings delays present in the system.

Based on the dynamical models, two main approaches are introduced in this thesis for the congestion control problem of NMAS. The first approach utilizes switching of fixed-structure controllers that are derived by satisfying the system physical constraints. The congestion control problem of each traffic class is then recast as a switching control problem of a constrained system. In the second approach, a guaranteed cost control technique is applied to deal with the uncertainties in network delays. By considering a quadratic cost

function having the measures of state and input, the congestion control problem is to select a state feedback controller such that the closed-loop system is stable and a certain performance level is guaranteed subject to all the admissible time delays .

Part I

Switching Congestion Control Approach

Chapter 3

Switching Congestion Control of DiffServ Networks with Fixed Topology

The aim of this chapter is to develop a congestion control strategy for a network of multi-agent systems (NMAS) with a fixed topology, by utilizing the switching control approach. In the Diff-Serv architecture the traffic is aggregated into different classes of flows and the congestion control strategies are to be applied to the traffic classes according to their QoS requirements and specifications. As presented in Chapter 2, the queuing dynamics of each traffic class is modeled as a nonlinear dynamical system subject to physical constraints and unknown time-varying delays. It is well-known that the constrained systems are difficult to stabilize by smooth (continuous) feedback control since the control laws have to switch between boundary points of the admissible control set [126]. Any violation of the constraints may degrade the system performance and in the worst case scenario, the system could become unstable. Furthermore, maintaining stability of time-delayed feedback systems in general is not a trivial problem owing to the infinite dimensional nature of time-delay systems. On the other hand, the nonlinearities of the system make the synthesis and design more difficult. To tackle this problem, one of the promising

approaches would be to switch the controller based on the system operating range [115]. In this *switching control* system, multiple controllers are designed in advance, the control input switches among these fixed structured controllers according to the state of the system in order to not violate the constraints.

As presented in Section 2.3, the switching control scheme for constrained systems can be expressed by equation (2.58). The control input switches among three controllers, namely, 1) the maximum boundary u_{high}; 2) the minimum boundary u_{low}, (u_{high} and u_{low} are usually constant values determined by the physical constraints), and 3) the normal control input $u(t)$, that is designed based on the system state. The schematic of the switching control scheme is shown in Fig. 2.4, the control input switches among three controllers according to the system constraints. The congestion control problem for each traffic class can then be recast as a switching control problem of a nonlinear system with multiple and time-varying delays. The controller switches among the above three choices based on the physical constraints of the system. However, we expect that the normal controller $u(t)$ to take effect for as long time as possible. The reason is that by staying too long in the edge situations (u_{high} and u_{low}) may result in low efficiency and utilization of the control authority.

Therefore, in this thesis we add an extra regulation mechanism to adjust the system under the edge situations. Fig. 2.4 shows the idea of this regulation. When the controller switches to its boundaries (u_{low} or u_{high}), it enters the corresponding designated *edge modes*. In this case, the regulation mechanism adjusts the system parameters so that its state trajectory is forced to move towards the *safe operating range*. When the state enters the safe operating range, the normal controller $u(t)$ will then be selected and the system enters the so-called *normal control mode*. Therefore, the control objective under the edge modes is to design the regulation strategies. Specifically, in our congestion control problem, the traffic compression gains among the nodes are the system parameter that can be regulated under the edge modes. A nonlinear feedback controller based on the feedback linearization technique and robust adaptive control theory is designated for the normal controller under the normal control mode, for both the premium and the ordinary

68

traffic.

The remainder of this chapter is structured as follows. In Section 3.1, a centralized switching congestion control (SCC) strategy is presented for each traffic class based on the dynamical queuing models that are given in Chapter 2. The proposed congestion control algorithms guarantee the stability of the closed-loop system and maintain the safe operation of the system subject to the given physical constraints. In Section 3.2, the centralized SCC approach is extended to the decentralized switching congestion control strategy in order to enhance the scalability of our proposed solutions. Simulation results and performance comparisons are given in Section 3.3. Finally, the conclusions are provided in Section 3.3.

3.1   Centralized Congestion Control Scheme

A centralized control strategy is attractive due to its high accuracy and reliability, economic installation features and overall better performance. Fig. 3.1 shows a centralized control framework of a networked multi-agent system (NMAS) with three nodes. In the centralized control scheme, there is only one commander and control center. The control command is localized in one place and the action of each node depends on the information that is provided to the central command and control to all other nodes in the team. Since the centralized control requires exchange of large amount of information over communication channels particularly when the number of nodes in the network is large, it is often used in small-scale system. A distinguished benefit of the centralized control in a small-scale network is that it can effectively employ the entire network information. In this section, we first consider the congestion control problem of a small-scale Diff-Serv network in a centralized control framework. The centralized queuing models given in Chapter 2 are considered and a centralized switching control strategy based on the physical constraints of the system is developed for the premium and the ordinary traffic.

Recall the centralized dynamical model of the traffic network that is presented in Chapter 2. By considering the fluid flow conservation law, the network traffic dynamics
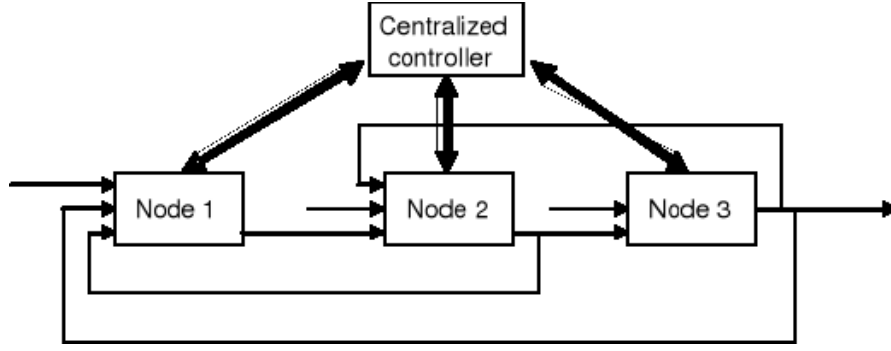
Figure 3.1: The centralized control framework for a NMAS with three nodes.

is expressed in the following standard state space representation for the premium traffic (2.37) and the ordinary traffic (2.45):

$$\dot{x}_p(t) = -F(x_p(t))u_p(t) + \lambda_p(t) + \sum_{l=1}^{m} G_l F(x_p(t - \tau_l(t)))u_p(t - \tau_l) \quad (3.1)$$

$$\dot{x}_r(t) = -F(x_r(t))u_{r1}(t) + u_{r2}(t) + \sum_{l=1}^{m} G_l F(x_r(t - \tau_l(t)))u_{r1}(t - \tau_l) \quad (3.2)$$

where "p" stands for the premium traffic and "r" represents the ordinary traffic, x_p and x_r are the queuing length of the premium and the ordinary traffic in the nodes, $u_p(t)$ and $u_r(t)$ are the input signals, $\lambda_p(t)$ is the unknown but bounded external incoming premium traffic, $\tau_l(t)$ is the unknown time-varying delays, for $l = 1, ..., m$, m is the number of delays in the network, and $F(x_p(t))$, $F(x_r(t))$ and G_l are the system matrices as defined in equations (2.30) and (2.36).

It should be noted that the centralized congestion control algorithm is practically applicable only to small-scale networks. Also, it is assumed that the multiple delays in the network satisfy the *bounded* and the *heterogeneous* assumptions that are given by equations (2.12)-(2.14) in Chapter 2 and are reproduced in detail as follows.

Assumption 3.1. *The unknown multiple and time-varying delays $\tau_l(t)$ are upper bounded where the maximum upper bound h is known. Namely, h is the maximum allowable delay in the network, that is*

$$0 \leq \tau_l(t) \leq h_l \quad (3.3)$$

$$h = max\{h_l\} \qquad l = 1, ..., m$$

70

3.1.1 Premium Traffic Control Strategy

The physical constraints for the premium traffic class are listed below:

$$0 \leq x_p(t) \leq x_p^{buffer} \tag{3.4}$$

$$0 \leq u_p(t) \leq C_{server} \tag{3.5}$$

$$0 \leq \lambda_p(t) \leq \lambda_p^{max} \tag{3.6}$$

where x_p^{buffer} is the buffer size, C_{server} is the link capacity, and λ_p^{max} is the maximum allowable traffic rate induced by the transmitter constraint (3.6).

Considering the premium traffic model (3.1), the switching control problem for the premium traffic becomes a nonlinear feedback controller that stabilizes the system (3.1) and will not exceed the above physical constraints. Towards this end, the switching congestion control strategy for the premium traffic is selected as follows:

$$u_p(t) \quad = \quad \begin{cases} 0, & \text{if } \bar{u}_p(t) < 0; \\ \bar{u}_p(t), & \text{if } 0 \leq \bar{u}_p(t) \leq C_{server}; \\ C_{server}, & \text{if } \bar{u}_p(t) > C_{server}. \end{cases} \tag{3.7}$$

where the first and the third cases in the above switching controller are refereed to as the *edge modes* and the second case with the to be designed controller $\bar{u}_p(t)$ is designated as *normal control mode*.

Since the queuing dynamics of the premium traffic model (3.1) is nonlinear with respect to the queuing state, the following nonlinear feedback controller based on the input-state linearization technique is considered:

$$\bar{u}_p(t) = F^{-1}(x_p, t)K_p\bar{x}_p(t) \tag{3.8}$$

where $\bar{x}_p(t) = x_p(t) - x_p^{ref}$, x_p^{ref} is the reference queuing length of the premium traffic in the nodes selected by the network operator, and K_p is the state feedback control gain.

However, due to the unknown nature of the external incoming traffic $\lambda_p(t)$, a pure state feedback controller may require a high gain controller which is clearly undesirable in the presence of high-frequency unmodeled dynamics and noise [127]. In principle, the system may become unstable for any finite control gain in presence of nonzero external

signals. In this case, an adaptive estimator $\hat{\lambda}_p(t)$ is applied to estimate the unknown external incoming traffic $\lambda_p(t)$ and compensate its effect via feedback. Thus, the nonlinear feedback controller (3.8) for the premium traffic is modified to the following

$$\bar{u}_p(t) = F^{-1}(x_p, t)[K_p \bar{x}_p(t) + \hat{\lambda}_p(t)] \tag{3.9}$$

where $\hat{\lambda}_p(t)$ is a online estimate of the external incoming traffic $\lambda_p(t)$. Motivated from the robust adaptive control theory [128], the updating rule of $\hat{\lambda}_p(t)$ is selected as follows:

$$\dot{\hat{\lambda}}_p(t) = \begin{cases} \Delta_p \bar{x}_p(t) - \Pi_p \hat{\lambda}_p(t), & \text{if } 0 \leq \hat{\lambda}_p(t) \leq \lambda_p^{max} \text{ or} \\ & \qquad \hat{\lambda}_p(t) = 0, \ \bar{x}_p(t) \geq 0 \text{ or} \\ & \qquad \hat{\lambda}_p(t) = \lambda_p^{max}, \ \bar{x}_p(t) \leq 0 \\ -\Pi_p \hat{\lambda}_p(t), & \text{otherwise} \end{cases} \tag{3.10}$$

where Δ_p and Π_p are the adaptive control gains that are positive definite matrices.

It should be noted that the centralized switching congestion control strategy (3.7)-(3.10) has two levels of switchings. The first switching is induced by the physical constraint of the input in (3.7). The control input $u_p(t)$ switches among three values, namely $u_{low} = 0$, $u_{high} = C_{server}$, and $u_{in}(t) = \bar{u}_p(t)$. According to the switching control scheme shown in Fig. 2.4, when the edge controllers u_{low} or u_{high} is selected, the regulation mechanism will adjust the system parameters to force the system state trajectory to move towards the safe operating range, and after some finite time the system state changes and the normal controller $u_{in}(t)$ is selected. Next, the system switches to the second level which is induced by the updating laws of the adaptive estimator (3.10).

Therefore, after applying the switching congestion controller (3.7), the dynamics of the premium traffic (3.1) will experience multiple modes depending on the different choices of the controllers in (3.7). Specifically, we have that

1. When $x_p(t)$ is sufficiently large, then $\bar{u}_p(t) \geq C_{server}$, which leads to $u_p(t) = C_{server}$,

2. When $x_p(t)$ is sufficiently small, then $\bar{u}_p(t) \leq 0$, which leads to $u_p(t) = 0$, or

3. When $0 < \bar{u}_p(t) < C_{server}$, then we have $u_p(t) = \bar{u}_p(t)$.

Cases (1) and (2) are referred to as the *edge modes* and case (3) is denoted as the *normal control mode*. Therefore, we now need to select the regulation rule under the edge modes so that the system will move towards the normal control mode. The detailed analysis of the multiple modes is presented below.

- **Edge Mode (i):** If $u_p(t) = 0$ at some time $t = t_1$, it follows that the queuing length of the nodes are sufficiently small at this time. In this case, the closed-loop system of (3.1) is governed by

$$\dot{x}_p(t) \quad = \quad \lambda_p(t) + \sum_{l=1}^{m} G_l F(x_p(t - \tau_l(t))) u_p(t - \tau_l) \tag{3.11}$$

  According to the buffer constraint of the queue (3.4) and given that the delayed input $u_p(t - \tau_l(t))$ also satisfies the switching law (3.7), one can conclude that the derivative of the queue $\dot{x}_p(t)$ in the above equation is positive. That is, the queuing state $x_p(t)$ will increase with time. Until some time $t_2 > t_1$ when the queuing length is sufficiently large and the normal control input satisfies $\bar{u}_p(t) > 0$, the controller $\bar{u}_p(t)$ that is defined in (3.9) will then take effect.

- **Edge Mode (ii):** If the controller $u_p(t) = C_{server}$ at some time $t = t_3$, then according to equation (3.9) it implies that the queuing length $x_p(t)$ of all the nodes in the network are sufficiently large. It follows that:

$$\dot{x}_p(t) \quad = \quad -F(x_p(t)) C_{server} + \lambda_p(t) + \sum_{l=1}^{m} G_l F(x_p(t - \tau_l(t))) u_p(t - \tau_l)$$

$$\approx \quad -C_{server} + \lambda_p(t) + \sum_{l=1}^{m} G_l F(x_p(t - \tau_l(t))) u_p(t - \tau_l) \tag{3.12}$$

  Note that $F(x_p(t - \tau_l(t))) u_p(t - \tau_l)$ is nothing but the incoming traffic from the neighboring nodes with time delay. Therefore, according to the transmitter constraint of the premium traffic (3.6), we have that

$$\dot{x}_p(t) \quad \leq \quad -C_{server} + \lambda_p^{max} + \sum_{l=1}^{m} G_l \lambda_p^{max}$$

  Therefore, the regulation strategy in this mode is to regulate the system parameter, that is the traffic compression gain G_l, so that the derivative of the queuing

73

state $x_p(t)$ is negative. Therefore, the regulation strategy for the premium traffic compression gain is selected as follows:

$$0 \le \sum_{l=1}^{m} G_l < (C_{server} - \lambda_p^{max})(\lambda_p^{max})^{+} \tag{3.13}$$

where $+$ denotes the Moor-Penrose inverse [103] of a non-square matrix. Consequently, the queuing length $x_p(t)$ will decrease with time and after some time $t_4 > t_3$ the normal controller $\bar{u}_p(t)$ will then take effect.

- **Normal Control Mode (iii):** If the normal controller $u_p(t) = \bar{u}_p(t)$ takes effect at some time $t = t_5$, the closed-loop system of (3.1) will become

$$\dot{x}_p(t) = -K_p \bar{x}_p(t) - \hat{\lambda}_p(t) + \lambda_p(t) + \sum_{l=1}^{m} G_l F(x_p(t - \tau_l(t))) u_p(t - \tau_l(t)) \tag{3.14}$$

Now we need to analyze the incoming traffic $u_p(t - \tau_l(t))$ from the neighboring nodes with delay, which is also governed by the switching control law (3.7) depending on the value of the delayed queuing state $x_p(t - \tau_l(t))$. Therefore, the equation (3.14) can be written as

$$\begin{aligned} \dot{x}_p(t) &= -K_p \bar{x}_p(t) - \hat{\lambda}_p(t) + \lambda_p(t) + \sum_{l=1}^{m_1} G_l C_{server} \\ &\quad + \sum_{l=1}^{m_2} G_l [K_p \bar{x}_p(t - \tau_l(t)) + \hat{\lambda}_p(t - \tau_l(t))] \end{aligned} \tag{3.15}$$

where m_1 is the number of neighbor nodes which take the maximum value of the controller C_{server}, m_2 is the number of neighbor nodes which take the value of the normal controller $\bar{u}_p(t - \tau_l(t))$, and the other neighbors which take the minimum values of the controller 0 are included in equation (3.15). Therefore, the above system can be written by the following state space representation:

$$\begin{aligned} \dot{x}_p(t) &= -K_p \bar{x}_p(t) - \hat{\lambda}_p(t) + \lambda_p(t) + \sum_{l=1}^{m} G_l B_c C_{server} \\ &\quad + \sum_{l=1}^{m} G_l B_l [K_p \bar{x}_p(t - \tau_l(t)) + \hat{\lambda}_p(t - \tau_l(t))] \end{aligned} \tag{3.16}$$

where the system matrices B_c and B_l are defined as follows:

$$B_c = \begin{cases} I, & \text{if } u_p(t - \tau_l(t)) = C_{server} \\ 0, & \text{otherwise} \end{cases}$$

$$B_l = \begin{cases} I, & \text{if } u_p(t - \tau_l(t)) = \bar{u}_p(t - \tau_l(t)) \\ 0, & \text{otherwise} \end{cases}$$

Therefore, by applying the switching controller (3.8) and the selection strategy of the traffic compression gains (3.13), the dynamic queuing system of the premium traffic (3.1) will enter the *normal control mode* and can be expressed by the linear time-delay system given in (3.16). The system (3.16) with the adaptive estimator $\hat{\lambda}_p(t)$ as given in (3.11) is a linear switching time-delay system with arbitrary switchings. The stability analysis of the above closed-loop system is presented in the next section.

3.1.2 Stability Analysis of the Premium Traffic

For the purpose of stability analysis, let us review the adaptive estimator (3.10) as a new state and introduce the following coordinate system, namely

$$\bar{\lambda}_p(t) = \hat{\lambda}_p(t) - \lambda_p(t)$$
$$z_p(t) = \begin{bmatrix} \bar{x}_p^T(t) & \bar{\lambda}_p^T(t) \end{bmatrix}^T$$

Consequently, the resulting closed-loop system of (3.1) can be written as

$$\dot{z}_p(t) = D_k z_p(t) + \sum_{l=1}^{m} F_l z_p(t - \tau_l(t)) + \sum_{l=1}^{m} H_l v_l(t) \tag{3.17}$$
$$z_p(t) = \varphi(t), t \in [-h, 0]$$
$$k \in \wp, \wp = 1, 2$$

where $\varphi(t)$ is the initial condition of the delay system, $k \in \wp, \wp = 1, 2$ is the switching signal defined in the set $\wp$ with two values, $v_l(t)$ is the external signal, and D_k, F_l, H_l are

the system matrices that are defined as follows:

$$
D_1 = \begin{bmatrix} -K_p & -I \\ \Delta_p & -\Pi_p \end{bmatrix} \qquad D_2 = \begin{bmatrix} -K_p & -I \\ 0 & -\Pi_p \end{bmatrix} \qquad F_l = \begin{bmatrix} G_l B_l K_p & G_l B_l \\ 0 & 0 \end{bmatrix}
$$

$$
H_l = \begin{bmatrix} 0 & 0 & G_l B_l & G_l B_c \\ -\Pi_p & -I & 0 & 0 \end{bmatrix} \qquad v_l^T(t) = \begin{bmatrix} \lambda_p(t) & \dot{\lambda}_p(t) & \lambda_p(t - \tau_l(t)) & C_{server} \end{bmatrix}
$$

The above system is a linear switched system with multiple and time-varying delays. The switchings in the system is arbitrary. The feedback control gain K_p and the adaptive control gains Δ_p and Π_p are present in the system matrices D_k and F_l. Therefore, the objective of the congestion control problem for the premium traffic is to find the control gains that will guarantee the stability of the closed-loop system (3.17). First, the following lemma is presented to derive the stability conditions of the closed-loop system (3.17).

Lemma 3.1. *The switched time-delay system (3.17) is uniformly ultimately bounded if there exist symmetric positive definite matrices P, S_l, Q, R, and positive definite matrices M and N of appropriate dimensions, for $l = 1, ..., m$, such that the following matrix inequality conditions are satisfied:*

$$
W_k = \begin{bmatrix} 2Q^T(D_k + F_l) + M & P - Q^T + (D_k + F_l)^T R & -hQ^T F_l \\ * & -R - R^T + S_l + N & -hR^T F_l \\ * & * & -S_l \end{bmatrix} < 0 \qquad (3.18)
$$

Under these conditions, in steady state the ultimate bound of the system states has a radius of $r = max(r_1,\ r_2)$ with $r_k = \frac{\lambda_{max}(\Phi_l)}{\lambda_{min}(-W_k)} \|v_l(t)\|^2$, $k = 1, 2$, where $\lambda_{max}(.)$ and $\lambda_{min}(.)$ are the maximum and the minimum eigenvalue of the corresponding matrix, respectively and
$$
\Phi_l = H_l^T(QM^{-1}Q + RN^{-1}R^T)H_l \qquad (3.19)
$$

Proof: The switched time-delay system (3.17) can be expressed in an equivalent descriptor form [85] as follows

$$
\begin{aligned}
\dot{z}_p(t) &= y(t) \\
y(t) &= (D_k + \sum_{l=1}^{m} F_l)z_p(t) - \sum_{l=1}^{m} F_l \int_{t-\tau_l(t)}^{t} y(s)ds + \sum_{l=1}^{m} H_l v_l(t) \qquad (3.20)
\end{aligned}
$$

Consider the following Lyapunov function candidate with symmetric positive definite matrices P and S_l,

76

$$V(z_t) = z_p^T(t)Pz_p(t) + \sum_{l=1}^{m} \frac{1}{h} \int_{-h}^{0} \int_{t+\theta}^{t} y^T(s)S_l y(s)\,ds\,d\theta \qquad (3.21)$$

Noting that $0 \leq \tau_l(t) \leq h$, the time derivative of V along the trajectories of (3.17) is given by

$$
\begin{aligned}
\dot{V} &= 2z_p^T(t)Py(t) + \sum_{l=1}^{m} y^T(t)S_l y(t) - \frac{1}{h}\sum_{l=1}^{m}\int_{t-h}^{t} y^T(s)S_l y(s)\,ds \\
&= 2[z_p^T(t)\ y^T(t)]
\begin{bmatrix} P & Q^T \\ 0 & R^T \end{bmatrix}
\begin{bmatrix} y(t) \\ \dot{z}_p(t) - y(t) \end{bmatrix}
+ \sum_{l=1}^{m} y^T(t)S_l y(t) \\
&\quad - \frac{1}{h}\sum_{l=1}^{m}\int_{t-h}^{t} y^T(s)S_l y(s)\,ds \\
&= 2z_p^T(t)Py(t) + (2z_p^T(t)Q^T + 2y^T(t)R^T)(\dot{z}_p(t) - y(t)) + \sum_{l=1}^{m} y^T(t)S_l y(t) \\
&\quad - \frac{1}{h}\sum_{l=1}^{m}\int_{t-h}^{t} y^T(s)S_l y(s)\,ds \qquad (3.22)
\end{aligned}
$$

where Q and R are symmetric positive definite matrices. By introducing the positive matrices Q and R, there is no cross product of the Lyapunov matrix P and the system matrices D_k and F_l, hence it will be adapted for the controller design.

By submitting equation (3.20) into (3.22), we will have that

$$
\begin{aligned}
\dot{V} &\leq 2z_p^T(t)Py(t) + 2z_p^T(t)Q^T(D_k + \sum_{l=1}^{m} F_l)z_p(t) \\
&\quad - 2z_p^T(t)Q^T\sum_{l=1}^{m} F_l \int_{t-\tau_l(t)}^{t} y(s)\,ds + 2z_p^T(t)Q^T\sum_{l=1}^{m} H_l v_l(t) \\
&\quad + 2y^T(t)R^T(D_k + \sum_{l=1}^{m} F_l)z_p(t) - 2y^T(t)R^T\sum_{l=1}^{m} F_l \int_{t-\tau_l(t)}^{t} y(s)\,ds \\
&\quad + 2y^T(t)R^T\sum_{l=1}^{m} H_l v_l(t) \\
&\quad - 2z_p^T(t)Q^T y(t) - 2y^T(t)R^T y(t) \\
&\quad + \sum_{l=1}^{m} y^T(t)S_l y(t) - \frac{1}{h}\sum_{l=1}^{m}\int_{t-\tau_l(t)}^{t} y^T(s)S_l y(s)\,ds
\end{aligned}
$$

$$
= \begin{bmatrix} z_p(t) \\ y(t) \end{bmatrix}^T \begin{bmatrix} 2Q^T(D_k + \sum\limits_{l=1}^{m} F_l) & P - Q^T + (D_k + \sum\limits_{l=1}^{m} F_l)^T R \\ * & -R - R^T + \sum\limits_{l=1}^{m} S_l \end{bmatrix} \begin{bmatrix} z_p(t) \\ y(t) \end{bmatrix}
$$

$$
+ \frac{1}{h} \sum_{l=1}^{m} \int_{t-\tau_l(t)}^{t} \begin{bmatrix} z_p(t) \\ y(t) \\ y(s) \end{bmatrix}^T \begin{bmatrix} 0 & 0 & -hQ^T F_l \\ * & 0 & -hR^T F_l \\ * & * & -S_l \end{bmatrix} \begin{bmatrix} z_p(t) \\ y(t) \\ y(s) \end{bmatrix} ds
$$

$$
+ 2z_p^T(t)Q^T \sum_{l=1}^{m} H_l v_l(t) + 2y^T(t)R^T \sum_{l=1}^{m} H_l v_l(t)
$$

$$
\leq \sum_{l=1}^{m} \frac{1}{\tau_l(t)} \int_{t-\tau_l(t)}^{t} \begin{bmatrix} z_p(t) \\ y(t) \end{bmatrix}^T \begin{bmatrix} 2Q^T(D_k + F_l) & P - Q^T + (D_k + F_l)^T R \\ * & -R - R^T + S_l \end{bmatrix} \begin{bmatrix} z_p(t) \\ y(t) \end{bmatrix} ds
$$

$$
+ \sum_{l=1}^{m} \frac{1}{\tau_l(t)} \int_{t-\tau_l(t)}^{t} \begin{bmatrix} z_p(t) \\ y(t) \\ y(s) \end{bmatrix}^T \begin{bmatrix} 0 & 0 & -hQ^T F_l \\ * & 0 & -hR^T F_l \\ * & * & -S_l \end{bmatrix} \begin{bmatrix} z_p(t) \\ y(t) \\ y(s) \end{bmatrix} ds
$$

$$
+ 2z_p^T(t)Q^T \sum_{l=1}^{m} H_l v_l(t) + 2y^T(t)R^T \sum_{l=1}^{m} H_l v_l(t) \tag{3.23}
$$

For the last two terms in equation (3.23), the following inequality known as the Park's inequality is used for bounding the last two cross terms, namely given $a, b \in R^n$ and a positive definite matrix R we can always write

$$
2a^T b \leq a^T R a + b^T R^{-1} b \qquad R > 0 \tag{3.24}
$$

The above inequality was presented and shown in [129].

Therefore, by applying the Park's inequality (3.24) to the last two terms in $\dot{V}$, one can obtain:

$$
\begin{aligned}
2z_p^T(t)Q^T \sum_{l=1}^{m} H_l v_l(t) &\leq z_p^T(t)M z_p(t) + \sum_{l=1}^{m} v_l^T(t)H_l^T Q M^{-1} Q^T H_l v_l(t) \\
2y^T(t)R^T \sum_{l=1}^{m} H_l v_l(t) &\leq y^T(t)N y(t) + \sum_{l=1}^{m} v_l^T(t)H_l^T R N^{-1} R^T H_l v_l(t)
\end{aligned}
$$

where M and N are positive definite matrices. Therefore,

$$
\dot{V} \leq \sum_{l=1}^{m} \frac{1}{\tau_l(t)} \int_{t-\tau_l(t)}^{t} [\xi^T(t,s)W_k \xi(t,s) + v_l^T(t)\Phi_l v_l(t)] ds \tag{3.25}
$$

where

$$W_k = \begin{bmatrix} 2Q^T(D_k + F_l) + M & P - Q^T + (D_k + F_l)^T R & -hQ^T F_l \\ * & -R - R^T + S_l + N & -hR^T F_l \\ * & * & -S_l \end{bmatrix}$$

$$\xi^T(t,s) = [z_p^T(t) \ y^T(t) \ y^T(s)]$$

$$\Phi_l = H_l^T(QM^{-1}Q^T + RN^{-1}R^T)H_l \qquad l = 1,...,m$$

Consequently, if $W_k < 0$ and for any $\xi^T(t,s)$ that satisfies:

$$-\xi^T(t,s)W_k\xi(t,s) \geq v_l^T(t)\Phi_l v_l(t) \tag{3.26}$$

one will have

$$\dot{V} \leq 0 \tag{3.27}$$

Therefore, the system (3.17) is ultimately bounded when $W_k < 0$, and the radius of the ultimately bounded region is given by:

$$\frac{\lambda_{max}(\Phi_l)}{\lambda_{min}(-W_k)}\|v_l(t)\|^2 \tag{3.28}$$

where λ_{max} and λ_{min} denote the maximum and the minimum eigenvalue of the corresponding matrices, respectively. This completes the proof of the lemma. ∎

Lemma 3.1 shows that the nonlinear feedback controller $\bar{u}_p(t)$ is a stabilization control law of the system (3.1) under the normal control mode and provides the stability conditions for the closed-loop system (3.17). However, the matrix W_k in equation (3.26) is not linear with respect to the system matrices. To tackle this problem, we need to transform the matrix inequality W_k into an equivalent linear matrix inequality (LMI). The following lemma is now presented to in order to derive the control gains through the expressions of the system matrices by solving the transformed LMI conditions.

Lemma 3.2. *Consider the system (3.17), if there exist symmetric positive definite matrices Y_1, Y_2, Y_3, $\bar{R}$, $\bar{S}$, positive definite matrices $\bar{M}$, $\bar{N}$, and matrices U_k, $\bar{U}_k$, T_l, $\bar{T}_l$, $\bar{Q}_l$ of appropriate dimensions, $k = 1, 2$ and $l = 1, ..., n$, such that the following LMI conditions are satisfied:*

$$\Omega_k = \begin{bmatrix} 2(U_k + T_l) + \bar{M} & Y_1^T - Y_2 + \bar{U}_k & -h\bar{T}_l \\ * & -\bar{R} - \bar{R}^T + \bar{S} + \bar{N} & -h\bar{Q}_l \\ * & * & -Y_{3l} \end{bmatrix} < 0 \qquad (3.29)$$

then the matrix inequality condition (3.18) in lemma 3.1 holds and the system (3.17) is ultimately bounded. The system matrices are then given by $D_k = U_k Y_1^{-1}$ and $F_l = T_l Y_1^{-1}$.

Proof: As far as the matrix inequality condition $W_k < 0$ that is given in lemma 3.1 is concerned, let us define

$$Y_1^{-1} = Q$$

$$Y_2^{-1} = P$$

$$Y_{3l}^{-1} = S_l$$

$$\Lambda^T = diag\{Y_1^T \ Y_2^T \ Y_{3l}^T\}$$

Then, by multiplying W_k with Λ^T and Λ from the left and the right, respectively, we will have

$$\begin{aligned} \Omega_k &= \Lambda^T W_k \Lambda \\ &= \begin{bmatrix} 2(U_k + T_l) + \bar{M} & Y_1^T - Y_2 + \bar{U}_k & -h\bar{T}_l \\ * & -\bar{R} - \bar{R}^T + \bar{S} + \bar{N} & -h\bar{Q}_l \\ * & * & -Y_{3l} \end{bmatrix} \end{aligned} \qquad (3.30)$$

where

$$D_k = U_k Y_1^{-1} \qquad\qquad F_l = T_l Y_1^{-1}$$

$$\bar{M} = Y_1^T M Y_1 \qquad\qquad \bar{N} = Y_2^T N Y_2$$

$$\bar{R} = Y_2^T R Y_2 \qquad\qquad \bar{S}_l = Y_2^T S_l Y_2$$

$$\bar{T}_l = T_l Y_1^{-1} Y_{3l} \qquad\qquad \bar{Q}_l = Y_2^T R^T \bar{T}_l$$

$$\bar{U}_k = (U_k + T_l)^T R Y_2$$

Therefore, if $\Omega_k < 0$ then one will also have $W_k < 0$. Consequently, by using the LMI conditions (3.29) one can guarantee the ultimate boundedness of the switched time-delay system (3.17). This completes the proof of the lemma. ∎

Lemma 3.2 gives the expressions of the control gains that are incorporated in the system matrices D_k and F_l. It should be noted that Lemma 3.1 only gives the stability condition of the system (3.1) under the normal control mode. The stability of the system under the edge modes is guaranteed by the regulation strategy of the traffic compression gains (3.13). The following remarks are presented to clarify our proposed congestion control strategies.

Remark 3.1. *The values of the traffic compression gains are initially assigned by the network operator, however during the network operation it may be regulated to avoid congestion. Specifically when the entire link capacity C_{server} is allocated to the premium traffic, as shown in the edge mode (ii), this implies a high likelihood of congestion so that the network is required to lower its traffic load by resetting the traffic compression gains according to the regulation rule (3.13). In this case, more packets are forced to be dropped out and the throughput of the entire network will decrease.*

Remark 3.2. *As per Lemma 3.1, the ultimate boundary region of the premium traffic is a time-varying function:*

$$\|\xi(t,s)\|^2 = max\{r_1, r_2\}$$
$$r_k = \frac{\lambda_{max}(\Phi_l)}{\lambda_{min}(-W_k)}\|v_l(t)\|^2 \tag{3.31}$$

From the above equation one can note that if the external signal $v_l(t)$ decreases, the ultimate boundary of the premium traffic will also decrease. However, the external signal $v_l(t)$ is given by

$$v_l^T(t) \quad = \quad \left[\begin{array}{cccc} \lambda_p(t) & \dot{\lambda}_p(t) & \lambda_p(t - \tau_l(t)) & C_{server} \end{array} \right] \tag{3.32}$$

therefore, the minimum boundary of the premium traffic can be expressed as

$$\|\xi(t,s)\|^2_{min} = \frac{\lambda_{max}(\Phi_l)}{\lambda_{min}(-W_k)}\|C_{server}\|^2 \tag{3.33}$$

where $\|C_{server}\|^2$ is the l_2 norm of the server capacity which includes the output capacities of all the nodes in the network.

Therefore, the results above with the LMI conditions in Lemma 3.2 can be summarized by the following theorem.

Theorem 3.1. *The dynamic queuing model of the premium traffic (3.1) is ultimately bounded with the application of the switching congestion controller (3.8) and the regulation strategy of the traffic compression gain (3.13), if the LMI conditions in Lemma 3.2 are satisfied. Furthermore, the physical constraints of the premium traffic (3.4) is ensured by the switching congestion control strategy.*

Proof: The proof follows from the constructive analysis that is given in this section.

∎

3.1.3 Ordinary Traffic Control Strategy

The physical constraints (2.15)-(2.17) for the ordinary traffic of the entire network is written here again:

$$0 \le x_r(t) \le x_r^{max} \tag{3.34}$$

$$0 \le u_{r1}(t) \le c_r(t) \tag{3.35}$$

$$0 \le u_{r2}(t) \le \lambda_r^{max} < c_r(t) \tag{3.36}$$

where $x_r^{max} = vec\{x_{ri}^{buffer}\}$ denotes the buffer size constraints of the network, λ_r^{max} is the maximum allowable traffic rate of the ordinary traffic induced by the transmitter constraint, and $c_r(t)$ is the instantaneous leftover capacity from the premium traffic which equals to $C_{server} - u_p(t)$ and is a time-varying bound.

Recall that the dynamic queuing model of the ordinary traffic (3.2). Since the incoming traffic of the ordinary traffic is available for control, the congestion control problem for the ordinary traffic is to regulate the traffic rate $u_{r2}(t)$ and to allocate the bandwidth capacity $u_{r1}(t)$ of the ordinary traffic so that the system (3.2) is stable and the physical constraints (3.34)-(3.36) are guaranteed. Therefore, according to the switching control approach, the congestion control strategy of the ordinary traffic is selected as follows:

$$u_{r1}(t) = \begin{cases} 0, & \text{if } \bar{u}_{r1}(t) < 0; \\ \bar{u}_{r1}(t), & \text{if } 0 \le \bar{u}_{r1}(t) \le c_r(t); \\ c_r(t), & \text{if } \bar{u}_{r1}(t) > c_r(t). \end{cases} \tag{3.37}$$

$$u_{r2}(t) = \begin{cases} \lambda_r^{max}, & \text{if } \lambda_r(t) \geq \lambda_r^{max}; \\ \lambda_r(t), & \text{if } \lambda_r(t) < \lambda_r^{max}. \end{cases} \qquad (3.38)$$

where $c_r(t) = C_{server} - u_p(t)$ is the leftover capacity from the premium traffic.

As shown in the above switching control strategy, the regulation rule of the input $u_{r2}(t)$ is to guarantee that the incoming traffic rate of the ordinary traffic $\lambda_r(t)$ will not exceed the maximum allowable rate which is bounded by the leftover capacity from the premium traffic, that is the time-varying bound $c_r(t)$. When the incoming traffic $\lambda_r(t)$ is within the threshold, the control strategy is to allocate the bandwidth capacity $u_{r1}(t)$ of the ordinary traffic without adjusting the incoming traffic rate $\lambda_r(t)$ anymore. By doing so, the ordinary traffic will receive as large as possible traffic rate and left as much as possible bandwidth for the best-effort traffic class. In the meantime, the physical constraint of the bandwidth $u_{r1}(t)$ is also guaranteed by the switching controller (3.37).

Given the nonlinearity of the dynamic queuing model of the ordinary traffic (3.2), the nonlinear feedback controller $\bar{u}_{r1}(t)$ is selected according to the following feedback linearization rule:

$$\bar{u}_{r1}(t) = F^{-1}(x_r(t))[K_r \bar{x}_r(t) + \hat{\lambda}_r(t)] \qquad (3.39)$$

where K_r is the state feedback control gain, and $\hat{\lambda}_r(t)$ is a time-varying signal to compensate for the external signal $\lambda_r(t)$. The time-varying signal $\hat{\lambda}_r(t)$ is selected according to the *modified parameter projection method* as follows:

$$\dot{\hat{\lambda}}_r(t) = \begin{cases} \Delta_r \bar{x}_r(t) - \Pi_r \hat{\lambda}_r(t), & \text{if } 0 \leq \hat{\lambda}_r(t) \leq \lambda_r^{max} \text{ or} \\ & \qquad \hat{\lambda}_r(t) = 0, \ \bar{x}_r(t) \geq 0 \text{ or} \\ & \qquad \hat{\lambda}_r(t) = \lambda_r^{max}, \ \bar{x}_r(t) \leq 0 \\ -\Pi_r \hat{\lambda}_r(t), & \text{otherwise} \end{cases} \qquad (3.40)$$

where Δ_r and Π_r are the adaptive control gains for the ordinary traffic class.

The congestion control scheme of the ordinary traffic has three levels of switchings. The first switching level is caused by the regulation strategy of the incoming traffic (3.38). Provided that the incoming traffic rate satisfies it upper bound λ_r^{max} the bandwidth controller (3.37) is applied which induces the second switching level. The bandwidth controller

$u_{r1}(t)$ switches among three values, namely $u_{r1}^{low} = 0$, $u_{r1}^{high} = c_r(t)$, and $u_{r1}^{in}(t) = \bar{u}_{r1}(t)$. According to the switching scheme shown in Fig. 2.4, whenever the bandwidth controller $u_{r1}(t)$ switches to the boundary values, 0 or $c_r(t)$, an extra regulator is applied to adjust the system parameters so to ensure that after some finite time the normal controller $\bar{u}_{r1}(t)$ will take effect. Subsequently, the system will operate on the third switching level that is introduced by the adaptive estimator given in (3.38).

Therefore, after applying the switching congestion control strategies (3.37)-(3.38), the closed-loop system for the ordinary traffic will experience multiple modes. However, since the constraint of the ordinary traffic $c_r(t)$ is time-varying, we first need to analyze the following two cases depending on the different values of the time-varying bound $c_r(t)$, namely

- **Case (i):** If $c_r(t) = 0$ at some time $t = t_1$, that is $C_{server} - u_p(t) = 0$, implying that there is no leftover capacity from the premium traffic class, from equation (3.37) it then follows that $u_{r1}(t) = 0$ and $u_{r2}(t) = 0$.

  Therefore, the dynamical system for the ordinary traffic becomes

$$\dot{x}_r(t) = \sum_{l=1}^{m} G_l F(x_r(t - \tau_l(t))) u_{r1}(t - \tau_l(t)) \tag{3.41}$$

  Since there is no leftover capacity available for the ordinary traffic at this time, no incoming ordinary traffic is allowed and the ordinary queuing state $x_r(t)$ must remain unchanged until there is any capacity available. Therefore, the traffic compression gains G_l is set to $G_l = 0$. This implies that any incoming traffic from the neighboring nodes are forced to be dropped out until there is an available capacity.

- **Case (ii):** If $c_r(t) > 0$ at some time $t = t_2$, by applying the flow rate regulator (3.38), the ordinary incoming traffic $\lambda_r(t) = u_{r2}(t)$ is guaranteed to be bounded. That is, $0 \leq \lambda_r(t) \leq \lambda_r^{max}$. Consequently, the following three submodes depending on different choices of the bandwidth controller $u_{r1}(t)$ are need to be considered:

  - **(a) Edge Mode:** Let $u_{r1}(t) = 0$ at some time $t = t_2$, then it follows that the queuing length of the ordinary traffic in each node is sufficiently small so

that one have $\bar{u}_{r1}(t) < 0$. Therefore, the closed-loop of dynamical model (3.2) becomes:

$$\dot{x}_r(t) \quad = \quad \lambda_r(t) + \sum_{l=1}^{m} G_l F(x_r(t - \tau_l(t))) u_{r1}(t - \tau_l(t)) > 0 \qquad (3.42)$$

It now follows that the ordinary queuing state $x_r(t)$ will increase. After some finite time $t_3 > t_2$, one will have $u_{r1}(t) > 0$ and $u_{r1}(t - \tau_l(t)) > 0$, and therefore the controller $\bar{u}_{r1}(t)$ will take effect.

- **(b) Edge Mode:** If $u_{r1}(t) = c_r(t)$ at some time $t = t_4$, then it implies that the queuing length $x_r(t)$ is sufficiently large. The closed-loop system corresponding to (3.2) is now governed by

$$
\begin{aligned}
\dot{x}_r(t) \quad = \quad & -F(x_r(t))c_r(t) + u_{r2}(t) + \sum_{l=1}^{m} G_l F(x_r(t - \tau_l(t))) u_{r1}(t - \tau_l(t)) \\
\leq \quad & -F(x_r(t))c_r(t) + \lambda_r^{max} + \sum_{l=1}^{m} G_l F(x_r(t - \tau_l(t))) u_{r1}(t - \tau_l(t))
\end{aligned}
$$

Recall that $F(x_r(t - \tau_l(t))) u_{r1}(t - \tau_l(t))$ represents the internal incoming ordinary traffic among the nodes with time delays $\tau_l(t)$. Therefore, according to the transmitter constraint, we will have

$$\dot{x}_r(t) \quad \leq \quad -F(x_r(t))c_r(t) + \lambda_r^{max} + \sum_{l=1}^{m} G_l \lambda_r^{max} \qquad (3.43)$$

The objective under this case is to regulate the system design variable, that is the traffic compression gain G_l, so that the derivative of the queuing state $\dot{x}_r(t)$ is negative, and hence the queuing length $x_r(t)$ will decrease with the time. Therefore, the following conditions for the traffic compression gain matrix G_l can be obtained:

$$0 \leq \sum_{l=1}^{m} G_l \leq (F(x_r(t))c_r(t) - \lambda_r^{max})(\lambda_r^{max})^+ \qquad (3.44)$$

so that the right hand side of equation (3.43) is negative indicating that $\dot{x}_r(t) < 0$. Consequently, the ordinary queuing length $x_r(t)$ will decrease until $u_{r1}(t)$ becomes $< c_r(t)$, at some time $t_5 > t_4$, and the controller $\bar{u}_{r1}(t)$ will take effect.

– **(c) Normal Control Mode:** If $u_{r1}(t) = \bar{u}_{r1}(t)$ at some time $t = t_6$, then the closed-loop of the ordinary traffic (3.2) can be written as

$$\dot{\bar{x}}_r(t) = -K_r \bar{x}_r(t) - \hat{\lambda}_r(t) + \lambda_r(t) + \sum_{l=1}^{m} G_l F(x_r(t - \tau_l(t))) u_{r1}(t - \tau_l(t)) \quad (3.45)$$

We now need to check the value of the delayed incoming traffic $u_{r1}(t - \tau_l(t))$. Similar to the analysis in the normal control mode of the premium traffic, multiple submodes of the system (3.44) with respect to different choices of the delayed inputs $u_{r1}(t - \tau_l(t))$ need to be considered. However, the multiple submodes can be written together in one state space representation as follows:

$$\begin{aligned} \dot{\bar{x}}_r(t) &= -K_r \bar{x}_r(t) - \hat{\lambda}_r(t) + \lambda_r(t) + \sum_{l=1}^{m} G_l^r B_c^r c_r(t) \quad (3.46) \\ &+ \sum_{l=1}^{m} G_l^r B_l^r [K_r \bar{x}_r(t - \tau_l(t)) + \hat{\lambda}_r(t - \tau_l(t))] \end{aligned}$$

if we define the system matrices B_c^r and B_l^r as shown below

$$B_c^r = \begin{cases} I & \text{if } u_r(t - \tau_l(t)) = c_r(t) \\ 0 & \text{otherwise} \end{cases} \quad (3.47)$$

$$B_l^r = \begin{cases} I & \text{if } u_r(t - \tau_l(t)) = \bar{u}_r(t - \tau_l(t)) \\ 0 & \text{otherwise} \end{cases} \quad (3.48)$$

Therefore, after applying the switching congestion controller (3.37)-(3.38) and the regulation strategy of the traffic compression gains (3.44), the dynamic queuing of the ordinary traffic (3.2) will eventually reduce to the normal control mode. The closed-loop ordinary traffic system (3.46) with the adaptive estimator (3.40) is a linear arbitrary switched system with multiple and time-varying delays. The stability analysis of this system is given in the next section.

3.1.4 Stability Analysis of the Ordinary Traffic

For the stability analysis of the ordinary traffic, we consider the adaptive estimator $\hat{\lambda}_r(t)$ as a new state and define the following revised state space representation:

$$\bar{\lambda}_r(t) = \hat{\lambda}_r(t) - \lambda_r(t)$$

$$\bar{z}_r(t) = vec\{\bar{x}_r(t), \bar{\lambda}_r(t)\}$$

The closed-loop ordinary traffic system can be expressed by the following standard linear time-delay switching system:

$$\dot{z}_r(t) = D_k^r z_r(t) + \sum_{l=1}^{m} F_l^r z_r(t - \tau) + \sum_{l=1}^{m} H_l^r v_l(t) \tag{3.49}$$

$$z_r(t) = \phi(t), \phi(t) = [-h, 0]$$

$$k \in \wp, \wp = 1, 2$$

where the system matrices D_k^r, F_l^r, H_l^r are defined as follows:

$$D_1^r = \begin{bmatrix} -K_r & -I \\ \Delta_r & -\Pi_r \end{bmatrix} \qquad D_2^r = \begin{bmatrix} -K_r & -I \\ 0 & -\Pi_r \end{bmatrix} \qquad F_l^r = \begin{bmatrix} G_l^r B_l^r K_r & G_l^r B_l^r \\ 0 & 0 \end{bmatrix}$$

$$H_l^r = \begin{bmatrix} 0 & 0 & G_l^r B_l^r & G_l^r B_c^r \\ -\Pi_r & -I & 0 & 0 \end{bmatrix} \qquad v_l^r(t) = \begin{bmatrix} \lambda_r(t) & \dot{\lambda}_r(t) & \lambda_r(t - \tau_l(t)) & c_r(t) \end{bmatrix}^T$$

The control objective of the ordinary traffic is then to derive the feedback control gain K_r and the adaptive control gains Δ_r and Π_r, as incorporated in the system matrices D_k^r and F_l^r, so that closed-loop system (3.49) is stable.

When the above system is compared with the closed-loop system of the premium traffic (3.17), one can conclude that the closed-loop of the ordinary traffic system (3.49) has a similar structure to that of the premium traffic class. Therefore, similar to the Lemma 3.1, the stability conditions of the closed-loop system (3.49) are given by the following lemma.

Lemma 3.3. *The switched time-delay system (3.49) is uniformly ultimately bounded if there exist symmetric positive definite matrices P, S_l, Q, R, and positive definite matrices M and N of appropriate dimensions for $l = 1, ..., m$, such that the following matrix inequality conditions are satisfied:*

$$W_k^r = \begin{bmatrix} 2Q^T(D_k^r + F_l^r) + M & P - Q^T + (D_k^r + F_l^r)^T R & -hQ^T F_l^r \\ * & -R - R^T + S_l + N & -hR^T F_l^r \\ * & * & -S_l \end{bmatrix} < 0 \tag{3.50}$$

87

and the radius of the ultimately bounded region is given by:

$$r = max(r_1, \ r_2)$$

$$r_k = \frac{\lambda_{max}(\Phi_l^r)}{\lambda_{min}(-W_k^r)} \|v_l^r(t)\|^2$$

$$\Phi_l^r = (H_l^r)^T (QM^{-1}Q + RN^{-1}R^T) H_l^r$$

where $\lambda_{max}(.)$ and $\lambda_{min}(.)$ are the maximum and the minimum eigenvalue of the corresponding matrix, respectively.

Proof: The proof follows along the same lines as in the proof of Lemma 3.1 by considering the system matrices of the ordinary traffic. ∎

Lemma 3.3 shows that the closed-loop system (3.49) is ultimately bounded under the normal control mode. However, the matrix inequality condition (3.50) is not linear with respect to the system matrices, so that the gains of the congestion controller can not be derived directly. Therefore, the following lemma is presented to derive the expressions of the control gains through solving an equivalent LMI condition of the matrix inequality in Lemma 3.3.

Lemma 3.4. *Consider the matrix inequality condition (3.50). If there exists symmetric positive definite matrices Y_1, Y_2, Y_3, $\bar{R}$, $\bar{S}$, positive definite matrices $\bar{M}$, $\bar{N}$, and matrices U_k^r, $\bar{U}_k^r$, T_l^r, $\bar{T}_l^r$, $\bar{Q}_l^r$ of appropriate dimensions, $k = 1, 2$ and $l = 1, ..., n$, such that the following LMI conditions are satisfied:*

$$\Omega_k^r = \begin{bmatrix} 2(U_k^r + T_l^r) + \bar{M} & Y_1^T - Y_2 + \bar{U}_k^r & -h\bar{T}_l^r \\ * & -\bar{R} - \bar{R}^T + \bar{S} + \bar{N} & -h\bar{Q}_l^r \\ * & * & -Y_{3l} \end{bmatrix} < 0 \qquad (3.51)$$

then the matrix inequality condition (3.50) is valid and the system (3.49) is ultimately bounded. The system matrices of the ordinary traffic are then given by $D_k^r = U_k^r Y_1^{-1}$ and $F_l^r = T_l^r Y_1^{-1}$.

Proof: The proof follows along the same lines as that in the proof of Lemma 3.2 by considering the system matrices of the ordinary traffic. ∎

Lemma 3.4 shows that the nonlinear feedback $\bar{u}_{r1}(t)$ of the ordinary traffic is a stabilizing control law for the system (3.2) under the normal control mode. The stability

of the dynamic queuing system (3.2) under the edge modes are guaranteed by regulating the traffic compression gains according to (3.40). Similar to the analysis in the premium traffic, the following remarks are noted for the switching congestion control strategy of the ordinary traffic.

Remark 3.3. *The traffic compression gains are initially assigned by the network operator and will be set to 0 when there is no leftover capacity from the premium traffic (that is the case (i)). For the ordinary traffic, when there is no leftover capacity from the premium traffic, as described in case (i), the network is required to block all the links in the network and wait until there is an available capacity. In this case, the centralized control algorithm will be conservative since all the packets in the network are forced to be dropped out. As seen in the next section, this conservatism will be relaxed in the decentralized control algorithm.*

Remark 3.4. *When the entire leftover capacity $c_r(t) = C_{server} - u_p(t)$ is utilized, a potential congestion will occur if the queuing length keeps increasing. The proposed regulation strategy for the traffic compression gains (3.44) can guarantee that traffic load in the network is decreased so that the queuing length of the ordinary traffic will decrease. In this case, more packets are dropped out and the throughput of the entire network will also decrease.*

Remark 3.5. *As mentioned in Lemma 3.3, the radius of the ultimately bounded region for the ordinary traffic is given by a time-varying function, namely*

$$r = max\{r_1, r_2\}$$
$$r_k = \frac{\lambda_{max}(\Phi_l^r)}{\lambda_{min}(-W_k^r)}\|v_l^r(t)\|^2 \qquad (3.52)$$

As the external signal $v_r(t)$ decreases, the ultimate boundary of the system will also decrease. Specifically, when $v_r = 0$ we will have

$$r_{min} = 0 \qquad (3.53)$$

and the queuing error of the ordinary traffic will convergence to 0 as $t \to \infty$. That is, the system is asymptotically stable.
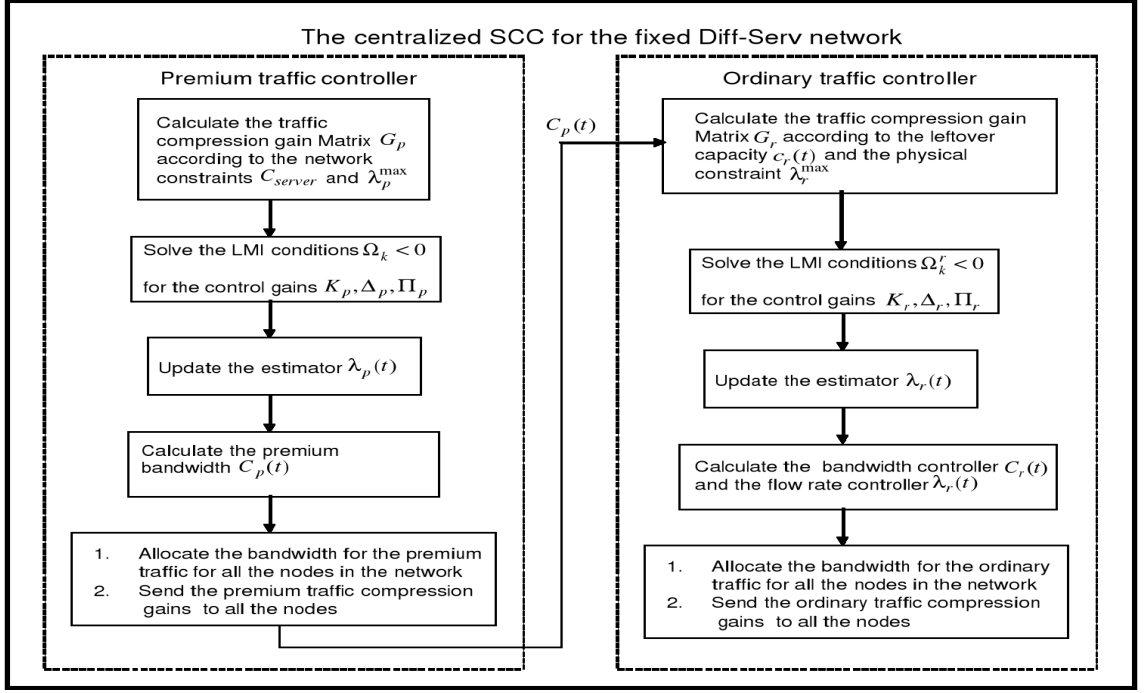
Figure 3.2: The flow chart of the centralized switching congestion control (SCC) for Diff-Serv network with a fixed topology.

The following theorem is now presented to summarize the above results as well as the stability conditions that are given in Lemma 3.4.

Theorem 3.2. *The dynamic queuing model of the ordinary traffic (3.2) is ultimately bounded when the switching congestion controller (3.37) and the regulation strategy of the traffic compression gain (3.44) are applied, and if the LMI conditions in Lemma 3.4 are satisfied. Furthermore, all the physical constraints of the ordinary traffic (3.34)-(3.36) are ensured by the switching congestion control strategy.*

Proof: The proof follows from the constructive analysis and results that are given in this subsection.   ∎

The centralized switching congestion control algorithms for the premium and the ordinary traffic classes presented in this section are summarized by the flow chart that is given in Fig. 3.2.

As shown in Fig. 3.2, given a fixed topology Diff-Serv network with n nodes, the

90

premium traffic controller first selects the traffic compression gain matrix G_p of the premium traffic based on the physical constraints of the network according to (3.13), where G_p is defined as follows

$$G_p = \sum_{l=1}^{m} G_l = \begin{bmatrix} 0 & g_{21} & \cdots & g_{n1} \\ g_{12} & 0 & \cdots & g_{n2} \\ \vdots & \vdots & \ddots & \vdots \\ g_{1n} & \cdots & \cdots & 0 \end{bmatrix} \tag{3.54}$$

Then, the premium traffic controller solves the LMI conditions Ω_k so that the state feedback control gain K_p and the adaptive control gains Δ_p and Π_p are obtained. Therefore, the adaptive estimator $\hat{\lambda}_p(t)$ can be updated based on the instant queuing state and the switching conditions in (3.10). The value of the allocated bandwidth for the premium traffic $C_p(t)$ can be calculated according to $C_p(t) = u_p(t)$. Finally, the centralized controller sends the value of the allocated bandwidth for the premium traffic flow $C_{pi}(t)$ to each node as well as the traffic compression gains g_{ji}^p. Each node in the network will adjust its allocated bandwidth and the data compression rates in the next communication cycle.

On the other hand, provided that the premium traffic bandwidth $C_p(t)$ is given, the ordinary traffic controller first calculates the leftover capacity in the network from $c_r(t) = C_{server} - C_p(t)$ and then the traffic compression gain matrix G_r for the ordinary traffic is selected according to the regulation strategy (3.44). By solving the LMI conditions Ω_k^r in Lemma 3.4, the control gains K_r, Δ_r and Π_r are now obtained. The allocated bandwidth $C_r(t)$ and the regulated flow rate $\lambda_r(t)$ for the ordinary can also be obtained.

3.2 Decentralized Congestion Control Scheme

As mentioned earlier, the centralized control approach requires exchange of large amount of information over the communication channels which may not be always feasible and reliable, and it does impose and extensive computational burden particularly when the number of nodes in the network is large. Therefore, although the centralized control solution may be economic and may achieve high performance, it is very difficult to implement it in large-scale networks. In these cases, decentralized control approach is more suitable
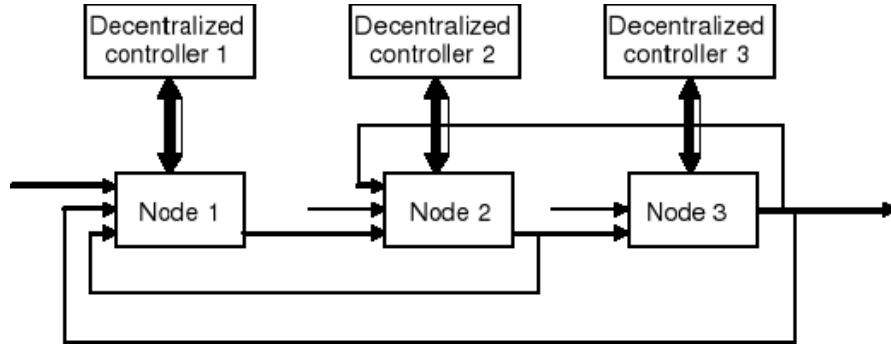
Figure 3.3: The decentralized control framework for a NMAS with three nodes.

and can reduce the complexity of the controller design. From the communication point of view, the decentralized control approach can greatly reduce the communication burden, and from the implementation point of view, decentralized controllers are easy to deploy. As shown in Fig. 3.3, in the decentralized control a local controller is attached to each node and the control action is only based on the local information.

In this section, we consider the congestion control problem of a large-scale Diff-Serv network. The centralized switching congestion control strategies that are proposed in the previous section are extended to the decentralized framework based on the decentralized dynamic queuing models that are presented in Chapter 2. The control objective for the premium traffic is to allocate the output capacity of each node $C_{pi}(t)$ by considering its physical constraints. The control objective pursued for the ordinary traffic is to simultaneously regulate the incoming flow rate of each node $\lambda_{ri}(t)$ and allocate its capacity $C_{ri}(t)$ under the constraints of the ordinary traffic. In the next two subsections, decentralized switching congestion control strategies will be developed for the premium and the ordinary traffic, respectively.

3.2.1 Premium Traffic Control Strategy

Consider a large-scale network with n nodes. Let us re-write the decentralized model of the premium traffic (2.37) for convenience as shown below

$$\dot{x}_{pi}(t) = -f(x_{pi}(t))u_{pi}(t) + \sum_{\substack{j=1 \\ j \neq i}}^{n} f(x_{pj}(t - \tau_{ji}(t)))u_{pj}(t - \tau_{ji})g_p^{ji}(t) + \lambda_{pi}(t) \qquad (3.55)$$

where $x_{pi}(t)$ is the queuing state of node i, $u_{pi}(t)$ is the control input, $g_{ji}^p(t)$ is the traffic compression gains of the premium traffic between node j and i, and $\tau_{ji}(t)$ is the time-varying delay from node j to node i which satisfy the assumption (2.12)-(2.14).

The physical constraints of the premium traffic are also given below:

$$0 \leq x_{pi}(t) \leq x_{pi}^{buffer}$$

$$0 \leq u_{pi}(t) \leq C_{server,i},$$

$$0 \leq \lambda_{pi}(t) < \lambda_{pi}^{max} \leq C_{server,i} \qquad\qquad i = 1, ...n$$

where x_{pi}^{buffer} is the premium buffer size of node i, $C_{server,i}$ is the total link capacity of node i, and λ_{pi}^{max} is the maximum allowable external incoming traffic which is introduced by the transmitter constraint of node i.

The decentralized congestion control problem for the premium traffic is to design the control input $u_{pi}(t)$ so that system (3.55) is stable and the physical constraints (3.56) are satisfied. According to the switching control approach of the constrained system, the decentralized controller for the premium traffic is select as follows:

$$u_{pi}(t) \;\; = \;\; \begin{cases} 0 & \text{if } \bar{u}_{pi}(t) < 0 \\ \bar{u}_{pi}(t) & \text{if } 0 \leq \bar{u}_{pi}(t) \leq C_{server,i} \\ C_{server,i} & \text{if } \bar{u}_{pi}(t) > C_{server,i} \end{cases} \qquad (3.56)$$

Furthermore, since system (3.55) is nonlinear with respect to the queuing state $x_{pi}(t)$, and the incoming traffic $\lambda_{pi}(t)$ is unknown. The nonlinear feedback controller $\bar{u}_{pi}(t)$ is selected according to the feedback linearization technique and robust adaptive control theory [128], namely

$$\bar{u}_{pi}(t) \;\; = \;\; f^{-1}(x_{pi}, t)[k_{pi}\bar{x}_{pi}(t) + \hat{\lambda}_{pi}(t)] \qquad (3.57)$$

where k_{pi} is the state feedback control gain that affects the convergence rate of the controller, and $\hat{\lambda}_{pi}(t)$ is the adaptive estimator that is used to estimate the incoming traffic $\lambda_{pi}(t)$ and is designed according to the *modified parameter projection method* as shown below:

$$
\dot{\hat{\lambda}}_{pi}(t) =
\begin{cases}
\delta_{pi}\bar{x}_{pi}(t) - \beta_{pi}\hat{\lambda}_{pi}(t) & \text{if } 0 \leq \hat{\lambda}_{pi}(t) \leq \lambda_{pi}^{max} \text{ or} \\
& \qquad \hat{\lambda}_{pi}(t) = 0, \ \bar{x}_{pi}(t) \geq 0 \text{ or} \\
& \qquad \hat{\lambda}_{pi}(t) = \lambda_{pi}^{max}, \ \bar{x}_{pi}(t) \leq 0 \\
-\beta_{pi}\hat{\lambda}_{pi}(t) & \text{otherwise}
\end{cases}
\tag{3.58}
$$

where δ_{pi} and β_{pi} are design parameters. Compared with the centralized estimator $\hat{\lambda}_p(t)$ in the centralized control framework of the premium traffic, the switching laws of the decentralized congestion controller (3.56) and the update rule of the adaptive estimator (3.58) are only dependent on the local information of each node. Unlike in the centralized control approach, the performance of the decentralized congestion control is evaluated at each local node. Therefore, although each node in the network will eventually become stable, but that may be achieved at different transient time rates.

It should be noted that the decentralized congestion control strategies (3.56)-(3.58) have two levels of switchings. Similar to the centralized control, the first level of switching is introduced by the physical constraints of the system. The control input switches among three values, namely $u_{pi}^{low} = 0$, $u_{pi}^{high} = C_{server,i}$, and $u_{pi}^{in}(t) = \bar{u}_{pi}(t)$. If the controller switches to its boundary values, a regulator is applied to adjust the system parameters so that the system will move towards the safe operation mode. After the normal controller $\bar{u}_{pi}(t)$ is selected, the second level of switching is activated by the adaptive estimator as defined in (3.58) and the system will operate at this level.

Therefore, according to the *switching* control law (3.56), the decentralized controller $u_{pi}(t)$ of each node has three different choices over time, that is 0, $\bar{u}_{pi}(t)$, and $C_{server,i}$ depending on the changes in $x_{pi}(t)$. The analysis corresponding to these three operational modes are described in detail below.

- **Edge State (i):** Suppose that $u_{pi}(t) = 0$ at some time $t = t_1$ which implies that $\bar{x}_{pi} < 0$, and which indicates that $x_{pi}(t_1)$ is sufficiently small. The dynamic queuing

94

system (3.55) can then be written as follows:

$$\dot{x}_{pi}(t) = \sum_{\substack{j=1 \\ j \neq i}}^{n} f(x_{pj}(t - \tau_{ji}(t)))u_{pj}(t - \tau_{ji})g_p^{ji}(t) + \lambda_{pi}(t) > 0 \qquad (3.59)$$

The state $x_{pi}(t)$ will increase until some finite time $t_2 > t_1$, when $\bar{u}_{pi}(t_2) > 0$, and the controller $u_{pi}(t) = \bar{u}_{pi}(t)$ will then take effect afterwards.

- **Edge State (ii):** If $u_{pi}(t) = C_{server,i}$ at some time $t = t_3$, this indicates that $x_{pi}(t_1)$ is sufficiently large. Therefore, $f(x_{pi}(t))C_{server,i} \approx C_{server,i}$, and the premium queuing state is now governed by

$$
\begin{aligned}
\dot{x}_{pi}(t) &\approx -C_{server,i} + \lambda_{pi}(t) + \sum_{\substack{j=1 \\ j \neq i}}^{n} \lambda_{pj}(t - \tau_{ji}(t))g_{ji}(t) \\
&\leq -C_{server,i} + \sum_{\substack{j=1 \\ j \neq i}}^{n} \lambda_{pj}^{max} g_{ji}(t) + \lambda_{pi}^{max}
\end{aligned}
\qquad (3.60)
$$

The regulation strategy in this case is to reset the traffic compression gains $g_{ji}^p(t)$ so that the derivative of the local queuing state $x_{pi}(t)$ will be negative. Hence, the queuing length will decrease with the time and after some finite time $t_4 > t_3$, the normal controller $\bar{u}_{pi}(t)$ will take effect. Therefore, according to the state equation (3.60), the regulation strategy for the traffic compression gains are selected as

$$0 \leq g_{ji}^p(t) < \frac{C_{server,i} - \lambda_{pi}^{max}}{\sum_{j \in \wp_i} \lambda_{pj}^{max}} \qquad (3.61)$$

- **Normal Control State (iii):** At some time $t = t_5$, the premium controller $\bar{u}_{pi}(t)$ as defined in (3.80) will take effect. The governing premium queuing equation (3.55) is now given by

$$\dot{x}_{pi}(t) = -k_{pi}\bar{x}_{pi}(t) - \hat{\lambda}_{pi}(t) + \lambda_{pi}(t) + \sum_{\substack{j=1 \\ j \neq i}}^{n} f(x_{pj}(t - \tau_{ji}(t)))u_{pj}(t - \tau_{ji}(t))g_{ji}(t)$$

One now needs to check the incoming traffic from each neighboring node j. Certain node controllers may be given by $u_{pj}(t - \tau_{ji}(t)) = C_{server,j}$ for $j = 1, ..., n_1$, and others may be given by $u_{pk}(t - \tau_{ki}(t)) = \bar{u}_{pk}(t - \tau_{ki}(t))$ for $k = 1, ..., n_2$, and yet

95

others may be given by $u_{pl}(t - \tau_{li}(t)) = 0$ for $l = 1, ..., n_3$, where $n = n_1 + n_2 + n_3$.

Therefore, the state equation (3.55) may be approximated as follows:

$$
\begin{aligned}
\dot{x}_{pi}(t) &= -[k_{pi}\bar{x}_{pi}(t) + \hat{\lambda}_{pi}(t)] + \lambda_{pi}(t) + \sum_{j=1}^{n_2} C_{server,j} g_{ji}^p(t) \\
&+ \sum_{j=1}^{n_1} [k_{pj}\bar{x}_{pj}(t - \tau_{ji}(t)) + \hat{\lambda}_{pj}(t - \tau_{ji}(t))] g_{ji}^p(t)
\end{aligned}
\tag{3.62}
$$

In contrast to the closed-loop system in the centralized control, the above system is a linear switching system with multiple time-varying delays with coupled states from the neighboring nodes. The decentralized control objective of the premium traffic can be recast as that of selecting the state feedback control gains k_{pi} and the adaptive control gain δ_{pi} and β_{pi} such that the above system is stable. The stability conditions of such a system is presented in the next subsection.

3.2.2 Stability Analysis of the Premium Traffic

To derive the stability conditions of the system (3.62) and select the control gains of the premium traffic, let us re-write the adaptive estimator as a new state and define the new state space as follows:

$$
\begin{aligned}
\bar{\lambda}_{pi}(t) &= \hat{\lambda}_{pi}(t) - \lambda_{pi}(t) \\
z_{pi}(t) &= \begin{bmatrix} \bar{x}_{pi}(t) & \bar{\lambda}_{pi}(t) \end{bmatrix}^T
\end{aligned}
\tag{3.63}
$$

The closed-loop system of each node can be re-written in the following standard linear switching form with time-varying delays, namely

$$
\dot{z}_{pi}(t) = D_i^k z_{pi}(t) + \sum_{\substack{j=1 \\ j \neq i}}^{n} F_j z_{pj}(t - \tau_{ji}(t)) + H_i v_{pi}(t) \quad i = 1, ..., n
\tag{3.64}
$$

$$
z_{pi}(t) = \varphi_i(t) \quad \varphi_i(t) \in [-h, 0]
$$

$$
k \in \wp, \quad \wp = 1, 2
$$

where $\varphi_i(t)$ defines the initial condition of the system, $\wp$ is the switching signal that is introduced by the adaptive estimator, $v_{pi}(t)$ is the external signal to the system, and D_i^k,

F_j, H_i, for $i, j = 1, ..., n$, are the system matrices that are defined as follows:

$$D_i^1 = \begin{bmatrix} -k_{pi} & -1 \\ \delta_{pi} & -\beta_{pi} \end{bmatrix} \qquad D_i^2 = \begin{bmatrix} -k_{pi} & -1 \\ 0 & -\beta_{pi} \end{bmatrix}$$

$$F_j = \begin{bmatrix} k_{pj}g_{ji}^p & g_{ji}^p \\ 0 & 0 \end{bmatrix} \qquad H_i = \begin{bmatrix} 0 & 0 & G_{ji} \\ -\beta_{pi} & -1 & 0 \end{bmatrix}$$

$$v_{pi}(t) = \begin{bmatrix} \lambda_{pi}(t) & \dot{\lambda}_{pi}(t) & \Lambda_{pj}(t - \tau_{ji}(t)) \end{bmatrix}^T$$

$$\Lambda_{pj}(t - \tau_{ji}(t)) = [vec\{\lambda_{pj}(t - \tau_{ji}(t))\}, vec\{C_{server,j}\}]$$

$$G_{ji} = vec\{g_{ji}^p(t)\}$$

The system (3.64) is a switching system with coupled states and time-varying delays. The control objective is to determine the control gains k_{pi}, β_{pi}, and δ_{pi} as presented in the system matrix D_i^k, in order to guarantee the stability of the closed-loop system (3.64). The following lemma is now presented to derive the stability conditions of the closed-loop system (3.64).

Lemma 3.5. *The system (3.64) is ultimately bounded if there exist symmetric positive definite matrices P_i, S_i, $i = 1, ..., n$, and positive definite matrices M_i, N_i, Q_i, R_i, such that the following matrix inequality condition is satisfied:*

$$W_{ik} = \begin{bmatrix} 2M_i^T D_i^k + Q_i & P_i - M_i^T + (D_i^k)^T N_i^T & -M_i^T F_{ji} & 0 \\ * & -N_i^T - N_i + R_i + S_i & -N_i^T F_{ji} & 0 \\ * & * & 0 & 0 \\ * & * & * & -S_i \end{bmatrix} < 0 \qquad (3.65)$$

where $F_{ji} = vec\{F_j\}$, and the radius of the ultimately bounded region is given by:

$$r = max\{r_1, \ r_2\}$$

$$r_k = \frac{\lambda_{max}(\Phi_i)}{\lambda_{min}(-W_{ik})}\|v_{pi}(t)\|^2 \qquad (3.66)$$

where $\Phi_i = H_i^T(M_iQ_i^{-1}M_i^{-1} + N_iR_i^{-1}N_i^{-1})H_i$, and λ_{min} and λ_{max} denotes the maximum and minimum eigenvalue of the corresponding matrix.

Proof: The switching system (3.64) can be re-written into the following descriptor system [81]:

$$\dot{z}_{pi}(t) = y_i(t)$$

$$y_i(t) = D_i^k z_{pi}(t) + \sum_{\substack{j=1 \\ j \neq i}}^{n} F_j z_{pj}(t) - \sum_{\substack{j=1 \\ j \neq i}}^{n} F_j \int_{t-\tau_{ji}(t)}^{t} y_j(s)ds + H_i v_{pi}(t)$$

The following Lyapunov-Krasovskii functional candidate is now considered:

$$V_i = V_{i1} + V_{i2}$$

$$V_{i1} = z_{pi}^T(t) P_i z_{pi}(t) \tag{3.67}$$

$$V_{i2} = \frac{1}{h} \int_{-h}^{0} \int_{t+\theta}^{t} y_i^T(s) S_i y_i(s) ds d\theta \tag{3.68}$$

where P_i and S_i are sympatric positive definite matrices. Therefore, the time derivative of V_i along the trajectories of the system (3.64) can be obtained as:

$$
\begin{aligned}
\dot{V}_{i1} &= 2 z_{pi}^T(t) P_i y_i(t) \\
&= 2[z_{pi}^T(t)\ y_i^T(t)] \begin{bmatrix} P_i & M_i^T \\ 0 & N_i^T \end{bmatrix} \begin{bmatrix} y_i(t) \\ \dot{z}_{pi}(t) - y_i(t) \end{bmatrix} \\
&= 2 z_{pi}^T(t)(P_i - M_i^T)y_i(t) - 2 y_i^T N_i^T y_i(t) \\
&\quad + 2 z_{pi}^T M_i^T D_i^k z_{pi} + 2 z_{pi}^T M_i^T \sum_{\substack{j=1 \\ j \neq i}}^{n} F_j z_{pj}(t - \tau_{ji}(t)) + 2 z_{pi}^T M_i^T H_i v_{pi}(t) \\
&\quad + 2 y_i^T N_i^T D_i^k z_{pi} + 2 y_i^T N_i^T \sum_{\substack{j=1 \\ j \neq i}}^{n} F_j z_j(t - \tau_{ji}(t)) + 2 y_i^T N_i^T H_i v_{pi}(t) \\
&= \begin{bmatrix} z_{pi}^T(t) \\ y_i^T(t) \\ Z_j^T(t - \tau_{ji}(t)) \end{bmatrix}^T \begin{bmatrix} 2M_i^T D_i^k & P_i - M_i^T + (D_i^k)^T N_i^T & M_i^T F_{ji} \\ * & -2N_i^T & N_i^T F_{ji} \\ * & * & 0 \end{bmatrix} \begin{bmatrix} z_{pi}(t) \\ y_i(t) \\ Z_j(t - \tau_{ji}(t)) \end{bmatrix} \\
&\quad + 2 z_{pi}^T(t) M_i^T H_i v_{pi}(t) + 2 y_i^T N_i^T H_i v_{pi}(t) \\
\dot{V}_{i2} &= y_i^T(t) S_i y_i(t) - \frac{1}{h} \int_{t-h}^{t} y_i^T(s) S_i y_i(s) ds
\end{aligned}
$$

where M_i and N_i are symmetric positive definite matrices, and $Z_j(t - \tau_{ji}(t))$ and F_{ji} are defined as follows:

$$Z_j(t - \tau_{ji}(t)) = vec\{z_j(t - \tau_{ji}(t))\} \tag{3.69}$$

$$F_{ji} = vec\{F_j\} \tag{3.70}$$

Now, by applying the Park's inequality (3.24) [129] to the last two terms of $\dot{V}_{i1}$, the

following inequalities hold for any positive definite matrices R_i and Q_i:

$$2z_{pi}^T(t)M_i^T H_{ji} v_{pi}(t) \leq z_{pi}^T(t)Q_i z_{pi}(t) + v_{pi}^T H_i^T M_i Q_i^{-1} M_i^T H_i v_{pi}$$

$$2y_i^T(t)N_i^T H_{ji} v_{pi}(t) \leq y_i^T(t)R_i y_i(t) + v_{pi}^T H_i^T N_i R_i^{-1} N_i^T H_i v_{pi}$$

Therefore, the time derivative of V_{i1} becomes

$$\dot{V}_{i1} \leq \begin{bmatrix} z_{pi}^T(t) \\ y_i^T(t) \\ Z_j^T(t - \tau_{ji}(t)) \end{bmatrix}^T \begin{bmatrix} 2M_i^T D_i^k + Q_i & P_i - M_i^T + (D_i^k)^T N_i^T & M_i^T F_{ji} \\ * & -2N_i^T + R_i & N_i^T F_{ji} \\ * & * & 0 \end{bmatrix} \begin{bmatrix} z_{pi}(t) \\ y_i(t) \\ Z_j(t - \tau_{ji}(t)) \end{bmatrix}$$
$$+ v_{pi}^T H_i^T (M_i Q_i^{-1} M_i^T + N_i R_i^{-1} N_i^T) H_i v_{pi}$$

and $\dot{V}_i$ can be written as

$$\dot{V}_i \leq \frac{1}{h} \int_{t-h}^{t} (\xi_i^T(t,s) W_{ik} \xi_i(t,s) + v_{pi}^T \Phi_i v_{pi}) ds \tag{3.71}$$

where $\xi_i^T(t,s) = [z_{pi}^T(t) \ y_i^T(t) \ Z_j^T(t - \tau_{ji}(t)) \ y_i^T(s)]^T$, $\Phi_i = H_i^T(Q_i^{-1} + R_i^{-1})H_i$, and

$$W_{ik} = \begin{bmatrix} 2M_i^T D_i^k + Q_i & P_i - M_i^T + (D_i^k)^T N_i^T & -M_i^T F_{ji} & 0 \\ * & -2N_i^T + R_i + S_i & -N_i^T F_{ji} & 0 \\ * & * & 0 & 0 \\ * & * & * & -S_i \end{bmatrix} \tag{3.72}$$

Therefore, according to the definition of the ultimate boundedness stability, the system (3.64) is ultimately bounded if $W_{ik} < 0$ and the radius of the ultimately bounded region is given by:

$$r = max\{r_1, \ r_2\}$$
$$r_k = \frac{\lambda_{max}(\Phi_i)}{\lambda_{min}(-W_{ik})} \|v_{pi}(t)\|^2 \tag{3.73}$$

where λ_{min} and λ_{max} indicate the maximum and minimum eigenvalue of the corresponding matrix, respectively. This completes the proof of Lemma. ∎

Lemma 3.5 gives the stability conditions of the system (3.64). However, the matrix inequality condition in Lemma 3.5 is not linear with respect to the system matrix, and hence can not yield the control gains directly. Similar as before, we need to transform the matrix inequality condition $W_{ik} < 0$ into an equivalent linear matrix inequality (LMI)

99

condition through fundamental matrix operations. The following lemma is now presented to solve this problem and provide the expression of the system matrix D_i^k which contains the control gains k_{pi}, δ_{pi}, and β_{pi}.

Lemma 3.6. *Consider the matrix inequality condition (3.65) in Lemma 3.5. If there exists symmetric positive definite matrices Y_{1i}, Y_{2i}, Y_{3i}, $\bar{Q}_i$, $\bar{N}_i$, $\bar{R}_i$, $\bar{S}_i$, and matrices U_{ik}, L_{ik}, V_i, T_i of appropriate dimensions, for $k = 1, 2$ and $i = 1, ..., n$, such that the following LMI conditions are satisfied:*

$$
\Omega_{ik} = \begin{bmatrix} 2U_{ik} + \bar{Q}_i & Y_{1i} - Y_{2i} + L_{ik} & -V_i & 0 \\ * & -2\bar{N}_i + \bar{R}_i + \bar{S}_i & -T_i & 0 \\ * & * & 0 & 0 \\ * & * & * & -Y_{3i} \end{bmatrix} < 0 \tag{3.74}
$$

then the matrix inequality condition (3.65) holds and the system (3.64) is ultimately bounded. The system matrix of the premium traffic is now given by $D_i^k = U_{ik} Y_{1i}^{-1}$.

Proof: Consider the matrix W_{ik} in Lemma 3.5, and let us define

$$
Y_{1i} = M_i^{-1} \qquad\qquad Y_{2i} = P_i^{-1}
$$
$$
Y_{3i} = Y_{4i} = S_i^{-1} \qquad\qquad \Lambda_i = diag\{Y_{1i}\ Y_{2i}\ I\ Y_{3i}\}
$$

By pre and post multiplying the matrix W_{ik} with Λ_i^T and Λ_i, respectively, we obtain

$$
\begin{aligned}
\Omega_{ik} &= \Lambda_i^T W_{ik} \Lambda_i \\
&= \begin{bmatrix} 2U_{ik} + \bar{Q}_i & Y_{1i} - Y_{2i} + L_{ik} & -V_i & 0 \\ * & -2\bar{N}_i + \bar{R}_i + \bar{S}_i & -T_i & 0 \\ * & * & 0 & 0 \\ * & * & * & -Y_{3i} \end{bmatrix}
\end{aligned}
$$

where:

$$
\begin{aligned}
\bar{Q}_i &= Y_{1i}^T Q_i Y_{1i} & \bar{N}_i &= Y_{2i}^T N_i Y_{2i} \\
\bar{R}_i &= Y_{2i}^T R_i Y_{2i} & \bar{S}_i &= Y_{2i}^T S_i Y_{2i} \\
V_i &= F_{ji} & T_i &= Y_{2i}^T N_i^T F_{ji} \\
U_{ik} &= D_i^k Y_{1i} & L_{ik} &= U_{ik}^T N_i^T Y_{2i}
\end{aligned}
$$

Therefore, if $\Omega_{ik} < 0$ we will obtain $W_{ik} < 0$ and the system (3.64) is ultimately bounded. This completes the proof of Lemma. ■

3.2.3 Ordinary Traffic Control Strategy

Recall that the decentralized dynamic queuing model of the ordinary traffic (2.27) is given by:

$$\dot{x}_{ri}(t) = -f(x_{ri}(t))u_{ri}^1(t) + u_{ri}^2(t) + \sum_{\substack{j=1 \\ j \neq i}}^{n} f(x_{rj}(t - \tau_{ji}(t)))u_{rj}^1(t - \tau_{ji})g_r^{ji}(t) \qquad (3.75)$$

Since the ordinary traffic has a less restrictive QoS requirements and lower priority than the premium traffic, the control specifications and objectives of the ordinary traffic are different from those of the premium traffic and are now defined in terms of regulating the incoming traffic rate while monitoring the link capacity that is leftover after its utilization by the premium traffic.

A typical set of the physical constraints of the ordinary traffic are listed as follows:

$$0 \leq x_{ri}(t) \leq x_{ri}^{buffer} \qquad (3.76)$$

$$0 \leq u_{ri}^1(t) \leq c_{ri}(t) \qquad (3.77)$$

$$0 \leq u_{ri}^2 \leq \lambda_{ri}^{max} < c_{ri}(t) \qquad (3.78)$$

where $c_{ri}(t)$ denotes the instantaneous leftover capacity of node i from the premium traffic which is actually equal to $C_{server,i} - u_{pi}(t)$.

The congestion control procedure for the ordinary traffic is divided into two steps, namely 1) *flow rate regulation*, and 2) *bandwidth allocation*. In the next two subsections, we will address the *flow rate control* and the *bandwidth allocation control* problems for the ordinary traffic as governed by the dynamic queuing model (3.75) subject to the constraints (3.76)-(3.78).

1. *Flow Rate Regulation*: At the start of each measurement cycle, we calculate the maximum allowable capacity $c_{ri}(t)$ from equation (3.76) and compare it with the ordinary incoming traffic $\lambda_{ri}(t)$. If the incoming traffic $\lambda_{ri}(t)$ is greater than the

available capacity, that is $\lambda_{ri}(t) > c_{ri}(t)$, then the traffic needs to be regulated first and the *flow rate control* is adopted as follows

$$u_{ri}^2(t) = \begin{cases} \lambda_{ri}^{max} & \text{if } u_{ri}^2(t) \geq \lambda_{ri}^{max} \\ \lambda_{ri}(t) & \text{if } u_{ri}^2(t) < \lambda_{ri}^{max} \end{cases} \tag{3.79}$$

Once the above regulator is invoked, the ordinary incoming traffic $\lambda_{ri}(t)$ is guaranteed to be bounded by $0 \leq \lambda_{ri}(t) \leq c_{ri}(t)$.

2. *Bandwidth Allocation*: Provided that $0 \leq \lambda_{ri}(t) \leq c_{ri}(t)$, the ordinary traffic capacity controller $u_{ri}^1(t)$ is selected as

$$u_{ri}^1(t) = \begin{cases} 0 & \text{if } \bar{u}_{ri}^1(t) < 0 \\ \bar{u}_{ri}^1(t) & \text{if } 0 \leq \bar{u}_{ri}^1(t) \leq c_{ri}(t) \\ c_{ri}(t) & \text{if } \bar{u}_{ri}^1(t) > c_{ri}(t) \end{cases} \tag{3.80}$$
$$\bar{u}_{ri}^1(t) = f^{-1}(x_{ri}, t)[k_{ri}\bar{x}_{ri}(t) + \hat{\lambda}_{ri}(t)]$$

where $\bar{x}_{ri}(t) = x_{ri}(t) - x_{ri}^{ref}$, x_{ri}^{ref} denotes the desired reference ordinary queuing length that is specified by the network manager, k_{ri} is the state feedback control gain, $\hat{\lambda}_{ri}(t)$ is a time-varying signal used to estimate the incoming traffic $\lambda_{ri}(t)$ to compensate for its effects via feedback. The time-varying signal $\hat{\lambda}_{ri}(t)$ is selected according to the robust adaptive control theory [128] as follows:

$$\dot{\hat{\lambda}}_{ri}(t) = \begin{cases} \delta_{ri}\bar{x}_{ri}(t) - \beta_{ri}\hat{\lambda}_{ri}(t), & \text{if } 0 \leq \hat{\lambda}_{ri}(t) \leq \lambda_{ri}^{max} \text{ or} \\ & \qquad \hat{\lambda}_{ri}(t) = 0, \ \bar{x}_{ri}(t) \geq 0 \text{ or} \\ & \qquad \hat{\lambda}_{ri}(t) = \lambda_{ri}^{max}, \ \bar{x}_{ri}(t) \leq 0 \\ -\beta_{ri}\hat{\lambda}_{ri}(t), & \text{otherwise} \end{cases} \tag{3.81}$$

where δ_{ri} and β_{ri} are the adaptive control gains.

It should be noted that the switching congestion controller for the ordinary traffic has three levels of switchings. The first level of switching is incurred by the flow rate controller (3.79) and the second level of switching is induced by the bandwidth controller (3.80). The bandwidth controller switches among three values, namely $u_{ri}^{1,low} = 0$, $u_{ri}^{1,high} = c_{ri}(t)$, and $u_{ri}^{1,in}(t) = \bar{u}_{ri}^1(t)$. When the controller switches to its boundary values, that is 0 and

102

$c_{ri}(t)$, an extra regulator is applied to adjust the system parameters so that the system trajectory will move towards the safe operating mode so that the normal controller $\bar{u}_{ri}^1(t)$ will take effect. According to the switching control strategies above, the system (3.75) will experience the following possible operational modes as described next.

- **Case (i):** If $c_{ri}(t) = 0$ at some time $t = t_1$, implying that there is no leftover capacity for the ordinary traffic, then from equation (3.80) it follows that $u_{ri}^1(t) = 0$ and $u_{ri}^2(t) = 0$. The closed-loop system dynamics (3.75) reduces to

$$\dot{x}_{ri}(t) = \sum_{\substack{j=1 \\ j \neq i}}^{n} f(x_{rj}(t - \tau_{ji}(t))) u_{rj}^1(t - \tau_{ji}(t)) g_r^{ji}(t) \tag{3.82}$$

  since there is no incoming traffic allowed, the ordinary queuing state $x_{ri}(t)$ should remain constant until there is an available capacity. Therefore, the regulation strategy for the transmission gains $g_{ji}^r(t)$ in this case is selected as $g_{ji}^r = 0$. This implies that the neighboring nodes are *forced to* drop all their outgoing traffic packets. At a subsequent time $t_2 > t_1$, when $c_{ri}(t) > 0$ the following cases should be considered.

- **Case (ii):** If $0 < c_{ri}(t) \leq C_{server,i}$ at some time $t = t_3$, then the switching controller $u_{ri}^1(t)$ will be able to take effect. Provided that $\lambda_{ri}(t) < c_{ri}(t)$, the closed-loop system of the ordinary traffic will experience the following multiple modes:

  - **Edge Mode (i):** If $u_{ri}^1(t) = 0$ at some time $t = t_3$, this implies that the instantaneous queuing length $x_{ri}(t)$ is sufficiently small so that $\bar{u}_{ri}^1(t) < 0$. The dynamical system (3.75) then becomes

$$\dot{x}_{ri}(t) = \lambda_{ri}(t) + \sum_{\substack{j=1 \\ j \neq i}}^{n} f(x_{rj}(t - \tau_{ji}(t))) u_{rj}^1(t - \tau_{ji}(t)) g_r^{ji}(t) > 0 \tag{3.83}$$

    Therefore, the ordinary queuing length $x_{ri}(t)$ will increase with the time, and after some finite time $t_4 > t_3$ one will get $\bar{u}_{ri}^1(t) > 0$ and the controller $\bar{u}_{ri}^1(t)$ will then take effect.

  - **Edge Mode (ii):** If $u_{ri}^1(t) = c_{ri}(t)$ at some time $t = t_5$, this implies that the normal controller $\bar{u}_{ri}^1(t) > c_{ri}(t)$. The closed-loop system of (3.75) can be

103

expressed as follows:

$$
\begin{aligned}
\dot{x}_{ri}(t) &= -f(x_{ri}(t))c_{ri}(t) + \lambda_{ri}(t) + \sum_{\substack{j=1 \\ j \neq i}}^{n} f(x_{rj}(t - \tau_{ji}(t)))u_{rj}^{1}(t - \tau_{ji}(t))g_r^{ji}(t) \\
&= -f(x_{ri}(t))c_{ri}(t) + \lambda_{ri}(t) + \sum_{\substack{j=1 \\ j \neq i}}^{n} \lambda_{rj}(t - \tau_{ji}(t))g_r^{ji}(t) \\
&\leq -f(x_{ri}(t))c_{ri}(t) + \lambda_{ri}^{max}(t) + \sum_{\substack{j=1 \\ j \neq i}}^{n} \lambda_{rj}^{max} g_{ji}^{r}(t) \quad (3.84)
\end{aligned}
$$

The regulation strategy in this case is to select the traffic compression gains $g_{ji}^{r}(t)$ so that the queuing length $x_{ri}(t)$ will decrease, and hence after some finite time one will get $\bar{u}_{ri}^{1}(t) < c_{ri}(t)$. Therefore, the traffic compression gains are selected as follows:

$$
0 \leq g_{ji}^{r}(t) < \frac{f(x_{ri}(t))c_{ri}(t) - \lambda_{ri}^{max}}{\sum\limits_{j \in \wp_i} \lambda_{j}^{max}} \quad (3.85)
$$

Consequently, the derivative of the queuing state $x_{ri}(t)$ in (3.84) will be negative, and the queuing length $x_{ri}(t)$ will decrease. After some finite time $t_6 > t_5$ the normal controller $\bar{u}_{ri}^{1}(t)$ will then take effect.

– **Normal Control Mode (iii):** If $u_{ri}^{1}(t) = \bar{u}_{ri}^{1}(t)$ at some time $t = t_7$, then the dynamical system (3.49) becomes

$$
\begin{aligned}
\dot{x}_{ri}(t) &= -k_{ri}\bar{x}_{ri}(t) - \hat{\lambda}_{ri}(t) + \lambda_{ri}(t) \\
&\quad + \sum_{\substack{j=1 \\ j \neq i}}^{n} f(x_{rj}(t - \tau_{ji}(t)))u_{rj}^{1}(t - \tau_{ji}(t))g_r^{ji}(t) \quad (3.86)
\end{aligned}
$$

Now we need to analyze the value of the neighboring controllers $\bar{u}_{pj}^{1}(t - \tau_{ji}(t))$. Similar to the analysis in mode (iii) of the premium traffic control, after applying the switching congestion controller (3.80) to the neighboring controllers and selecting the traffic compression gains according to (3.85), the normal controllers of the neighboring nodes $\bar{u}_{pj}^{1}(t - \tau_{ji}(t))$ will take effect after some finite time $t_8 > t_7$. As a sequence, the closed-loop system (3.75) can be written as

$$
\begin{aligned}
\dot{x}_{ri}(t) &= -k_{ri}\bar{x}_{ri}(t) - \hat{\lambda}_{ri}(t) + \lambda_{ri}(t) \\
&\quad + \sum_{\substack{j=1 \\ j \neq i}}^{n} (k_j \bar{x}_{rj}(t - \tau_{ji}(t)) + \hat{\lambda}_{rj}(t - \tau_{ji}(t)))g_r^{ji}(t) \quad (3.87)
\end{aligned}
$$

The above system is a linear switching system with coupled states and time-varying delays. The control objective of the ordinary traffic is then to select the state feedback control gain k_{ri} and the adaptive control gains δ_{ri} and β_{ri} so that the system (3.87) is stable.

In the following subsection, the stability conditions of the system (3.87) as well as the expressions of the control gains are presented .

3.2.4 Stability Analysis of the Ordinary Traffic

For the purpose of stability analysis, the closed-loop system (3.87) and the adaptive estimator (3.81) are considered together and the following new state space is defined:

$$
\begin{aligned}
\bar{\lambda}_{ri}(t) &= \hat{\lambda}_{ri}(t) - \lambda_{ri}(t) \\
z_{ri}(t) &= \left[\begin{array}{cc} \bar{x}_{ri}(t) & \bar{\lambda}_{ri}(t) \end{array} \right]^T
\end{aligned}
$$

Therefore, the closed-loop system of the ordinary traffic (3.87) with the adaptive estimator (3.81) can be re-written as follows:

$$
\dot{z}_{ri}(t) = D_{ir}^k z_{ri}(t) + \sum_{\substack{j=1 \\ j \neq i}}^{n} F_j^r z_{rj}(t - \tau_{ji}(t)) + H_i^r v_{ri}(t) \quad i = 1, ..., n \quad (3.88)
$$

$$
z_{ri}(t) = \phi_i(t) \quad \phi_i(t) \in [-h, 0]
$$

$$
k \in \wp, \qquad \wp = 1, 2
$$

where $v_{ri}(t)$ is the external signal to the system, and D_{ri}^k, F_j^r, H_i^r are the system matrices that are defined as follows:

$$
D_{ri}^1 = \left[\begin{array}{cc} -k_{ri} & -1 \\ \delta_{ri} & -\beta_{ri} \end{array} \right] \qquad D_{ri}^2 = \left[\begin{array}{cc} -k_{ri} & -1 \\ 0 & -\beta_{ri} \end{array} \right]
$$

$$
F_j^r = \left[\begin{array}{cc} k_{rj} g_{ji}^r & g_{ji}^r \\ 0 & 0 \end{array} \right] \qquad H_i^r = \left[\begin{array}{ccc} 0 & 0 & G_{ji} \\ -\beta_{ri} & -1 & 0 \end{array} \right]
$$

$$
v_{ri}(t) = \left[\begin{array}{ccc} \lambda_{ri}(t) & \dot{\lambda}_{ri}(t) & \Lambda_{rj}(t - \tau_{ji}(t)) \end{array} \right]^T
$$

$$
\Lambda_{rj}(t - \tau_{ji}(t)) = vec\{\lambda_{rj}(t - \tau_{ji}(t))\}
$$

$$
G_{ji} = vec\{g_{ji}^r(t)\}
$$

105

The state feedback control gain k_{ri} and the adaptive control gains δ_{ri} and β_{ri} are incorporated in the system matrix D_{ir}^k. The control objective is now to select the matrix D_{ri}^k for each node so that system (3.88) is stable. If we compare the system (3.88) with the closed-loop system of the premium traffic (3.64), one can see that the structure of the two systems are the same, expect for the different values of the control gains. Therefore, Lemmas 3.5 and 3.6 for the premium traffic can be modified for the ordinary traffic as shown next.

Lemma 3.7. *The system (3.88) is ultimately bounded if there exist symmetric positive definite matrices P_i, S_i, $i = 1, ..., n$, and positive definite matrices M_i, N_i, Q_i, R_i, such that the following matrix inequality condition is satisfied:*

$$
W_{ik}^r = \begin{bmatrix}
2M_i^T D_{ri}^k + Q_i & P_i - M_i^T + (D_{ri}^k)^T N_i^T & -M_i^T F_{ji}^r & 0 \\
* & -N_i^T - N_i + R_i + S_i & -N_i^T F_{ji}^r & 0 \\
* & * & 0 & 0 \\
* & * & * & -S_i
\end{bmatrix} < 0 \quad (3.89)
$$

where $F_{ji}^r = vec\{F_j^r\}$, and the radius of the ultimately bounded region is given by:

$$
r_r = max\{r_{r1}, r_{r2}\}
$$

$$
r_{rk} = \frac{\lambda_{max}(\Phi_i^r)}{\lambda_{min}(-W_{ik}^r)} \|v_{ri}(t)\|^2 \quad (3.90)
$$

where $\Phi_i^r = (H_i^r)^T (Q_i^{-1} + R_i^{-1}) H_i^r$, and λ_{min} and λ_{max} denote the maximum and minimum eigenvalue of the corresponding matrix.

    Proof: The proof follows along the same lines as that in the proof of Lemma 3.5 by substituting the system matrices of the ordinary traffic. ∎

    Lemma 3.7 shows that the normal controller $\bar{u}_{ri}^1(t)$ as defined in (3.80) is a stabilizing control law for the system (3.75). The following lemma is presented to transform the matrix inequality in Lemma 3.7 into an equivalent LMI condition and gives the expressions for the control gains of the ordinary traffic.

Lemma 3.8. *Consider the matrix inequality condition (3.89) in Lemma 3.7. If there exists symmetric positive definite matrices Y_{1i}, Y_{2i}, Y_{3i}, $\bar{Q}_i$, $\bar{N}_i$, $\bar{R}_i$, $\bar{S}_i$; and matrices U_{ik}^r,*
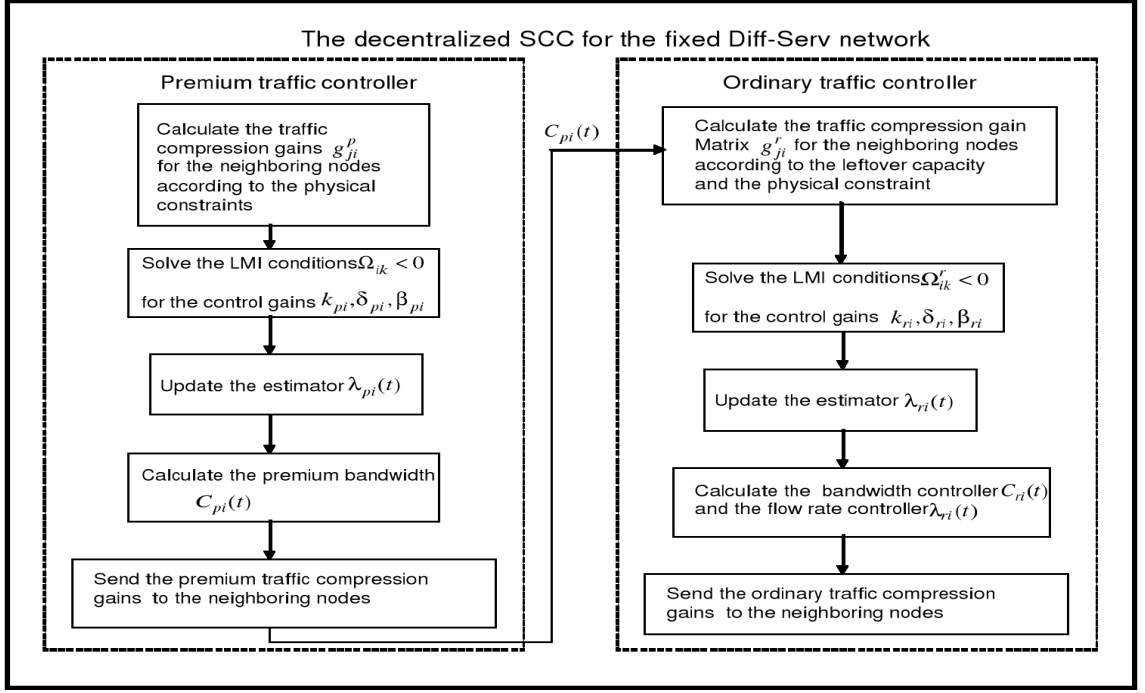
Figure 3.4: The flow chart of the decentralized switching congestion controller (SCC) for the Diff-Serv network with a fixed topology.

L_{ik}^r, V_i^r, T_i^r of appropriate dimensions, for $k = 1, 2$ and $i = 1, ..., n$, such that the following LMI conditions are satisfied:

$$
\Omega_{ik}^r = \begin{bmatrix} 2U_{ik} + \bar{Q}_i & Y_{1i} - Y_{2i} + L_{ik} & -V_i & 0 \\ * & -2\bar{N}_i + \bar{R}_i + \bar{S}_i & -T_i & 0 \\ * & * & 0 & 0 \\ * & * & * & -Y_{3i} \end{bmatrix} < 0 \tag{3.91}
$$

then the matrix inequality condition (3.65) holds and the system (3.64) is ultimately bounded. The system matrix of the premium traffic is given by $D_{ri}^k = U_{ik}^r Y_{1i}^{-1}$.

Proof: The proof follows closely along the lines that are presented in the proof of Lemma 3.6 by substituting the system matrices of the ordinary traffic. ∎

The decentralized switching congestion control (SCC) strategy for the premium and the ordinary traffic derived in this section can be illustrated with the flow chart of Fig. 3.4.

As shown in Fig. 3.4, the premium traffic controller of each node selects the traffic compression gains for its neighboring nodes g_{ji}^p according to the physical constraints and solves the LMI conditions Ω_{ik} for the local control gains k_{pi}, δ_{pi} and β_{pi}. The adaptive estimator $\hat{\lambda}_{pi}(t)$ is then updated according to equation (3.58). Consequently, the bandwidth allocated for the premium traffic at each node $C_{pi}(t)$ can be obtained. On the other hand, given the premium traffic bandwidth $C_{pi}(t)$, the ordinary traffic controller of each node calculates the leftover capacity $c_{ri}(t) = C_{server,i} - C_{pi}(t)$ and selects the traffic compression gains for the ordinary traffic g_{ji}^r according to the regulation strategy (3.85). By solving the LMI conditions Ω_{ik}^r for each node, the ordinary traffic control gains k_{ri}, δ_{ri} and β_{ri} can then be obtained. Finally, the bandwidth controller $C_{ri}(t)$ and the flow rate controller $\lambda_{ri}(t)$ are calculated at each node i.

3.3 Simulation Results and Comparisons

In this section, the results obtained by applying our proposed centralized switching congestion control strategy is compared with those of the decentralized schemes as well as another state-of-the-art model based congestion control scheme in the control community, known as the Integrated Dynamic Congestion Control (IDCC) method. The IDCC approach is derived based on the dynamic fluid flow model and was developed in a decentralized framework. The IDCC approach has shown good performance when applied to single node or cascade networks [61], [62], [53], [3]. Therefore, it is selected as a benchmark congestion control algorithm in this thesis for comparison and evaluation purposes. The detailed description of the IDCC algorithm can be found in Appendix A. The following section introduces the performance metrics that are utilized in this thesis.

3.3.1 Performance Metrics

According to the specifications of the congestion control algorithms presented in Chapter 1, the following two metrics are presented to evaluate and measure the performance of the proposed congestion control strategies, namely, the packet loss rate (PLR) and the

average queuing delay. These are defined formally next.

- *Packet Loss Rate (PLR):*

  In this thesis one assume that in a fixed network no packet will be lost during the transmission process. The packet loss occurs for the premium traffic only due to the node's buffer overflow. For the ordinary traffic, packet loss is caused by both the buffer overflow and an inadequate flow rate regulation. Therefore, the packet loss rate (PLR) for the premium traffic in this thesis is defined as

  $$PLR_{pi}(t) = \frac{max\{0, \lambda_{pi}(t) + \sum\limits_{j \in \wp_i} \lambda_{ji}(t)g_{ji}(t) - (x_{buffer,i} - x_{pi}(t))\}}{\lambda_{pi}(t) + \sum\limits_{j \in \wp_i} \lambda_{ji}(t)g_{ji}(t)} \quad (3.92)$$

  and the PLR for the ordinary traffic is defined according to

  $$PLR_{ri}(t) = \frac{P_b(t) + P_f(t)}{\lambda_{ri}(t) + \sum\limits_{j \in \wp_i} \lambda_{ji}^r(t)g_{ji}^r(t)} \quad (3.93)$$

  with $P_b(t) = max\{0, \lambda_{ri}(t) + \sum\limits_{j \in \wp_i} \lambda_{ji}^r(t)g_{ji}^r(t) - (x_{buffer,i} - x_{ri}(t))\}$, $P_f(t) = \lambda_{ri}^a(t) - \lambda_{ri}(t)$, and where P_b is the packet loss due to the buffer overflow, P_f is the packet loss due to the inadequate flow rate regulation, λ_{ri}^a is the actual incoming traffic of node i before regulation, and λ_{ri} is the desired regulated flow rate of the incoming traffic that can be obtained from equation (3.75).

- *Average Queuing Delay:*

  The queuing delay is the time a packet waits in a queue until it can be executed. During network congestion the queuing delay is considered infinite. In this section, the objective of our proposed congestion control is to regulate the node's buffer size as close as possible to a reference set point value so that a bound on the queuing delay in the network can be ensured indirectly. Therefore, the average queuing delay, as denoted by T_q, is considered as our second metric for performance evaluation purposes.

  According to the Little's theorem [73], the average number of customers (N) in a queue can be determined from the following equation

  $$E\{T\} = \frac{E\{N\}}{\lambda} \quad (3.94)$$

109

In the above expression, λ is the average customer arrival rate and $E\{T\}$ is the average time spent by a customer in a queuing system (waiting and being served). By applying the Little's formula (3.94) to our system, the average queuing delay T_q can be formally defined as follows

$$E\{T_q^i\} = \frac{E\{x_i(t)\}}{E\{\lambda_i(t)\} + \sum_{j \in \wp_i} E\{\lambda_{ji}(t)g_{ji}(t)\}} \tag{3.95}$$

where $E\{T_q^i\}$ is the average queuing delay and $x_i(t)$ is the present queuing state for node i.

Based on the above performance metrics definitions, we formally present the simulation results and comparisons of our proposed switching congestion control strategies and the IDCC approach in the following three subsections.

3.3.2 Decentralized SCC vs the Decentralized IDCC

Consider the network shown in Fig. 3.5. There are three clusters and each cluster has five nodes. In each cluster, one of the five nodes act as the decision maker and the other four nodes act as sensors. Only the decision makers can communicate with each other to share the information among the three clusters. This network configuration is quite general and can be found in many applications such as sensor/actuator networks, cooperative team of unmanned vehicles [60], [130], [131], [132], and high speed Ethernet networks. The link capacities of the three decision makers are set to $C_{server,1} = 20$ Mb, $C_{server,2} = 10$ Mb, and $C_{server,3} = 5$ Mb, while the capacities of the other sensor nodes are set to $C_{server} = 100$ Mb. Using the above specifications, we assume that each node has three separate logical buffers that are collecting the premium, ordinary and the best-effort traffic. The buffer size for each traffic is set to 5 Mb.

For our simulation studies we implement the network behavior by an event-based simulator tool known as QualNet [133] software environment. In this event-based framework the system entity is the *node-queue*, the system events are *packets-arrival* and *packets-departure*, and the system state which is changed according to and by these events is the *number-of-packets-in-the-queue*. This is represented as a discrete-event system with
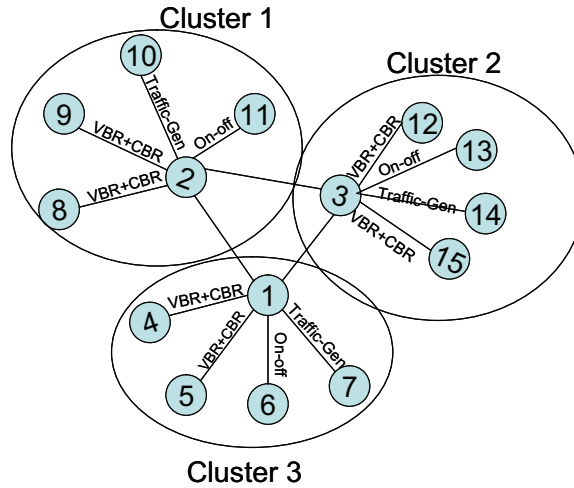
Figure 3.5: The schematic of a traffic network consisting of three clusters and 15 nodes that is used in simulation studies.

continuous-time state space representation. The random variables that need to be specified to model this system stochastically are *packet-size* and *packet-inter-arrival-time*, which are the characteristics of the incoming traffic. Since we do not consider the node mobility and the MAC control issues in this chapter, the only entities that will change the events (*packets-arrival* and *packets-departure*) are the *traffic generator* that are invoked in the application layer of the QualNet software. Once the variables are set, such as the *packet-size* and *average-inter-arrival-time*, the packets characteristics are subsequently determined. In other words, the chronological sequence of events are determined.

Therefore, our approach to this problem is to first construct a simulation scenario and generate the traffic by using the QualNet software environment, and then convert the packet characteristics, as determined by the entities set in the QualNet, into data flows with the form that is required by the fluid flow model. The fluid flow analytical model will make use of these data flows and other parameters to obtain network statistics by solving the corresponding differential equations. In particular, the queue lengths of the nodes are obtained. The fluid flow model is the part that is implemented in Matlab. Therefore, we can state that the discrete behavior of the packets as generated by the QualNet software environment is integrated with the fluid flow model that is implemented by the Matlab
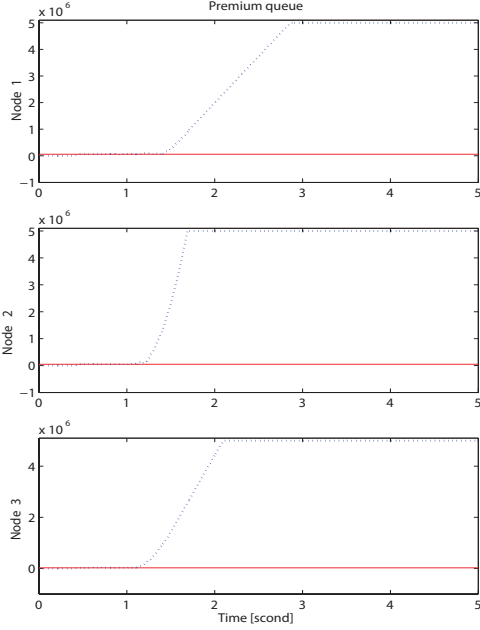
Figure 3.6: Premium queuing lengths (bits) by utilizing the decentralized IDCC method [3] corresponding to Case 1. The solid lines denote the set point references and the dashed lines denote the actual queuing lengths.
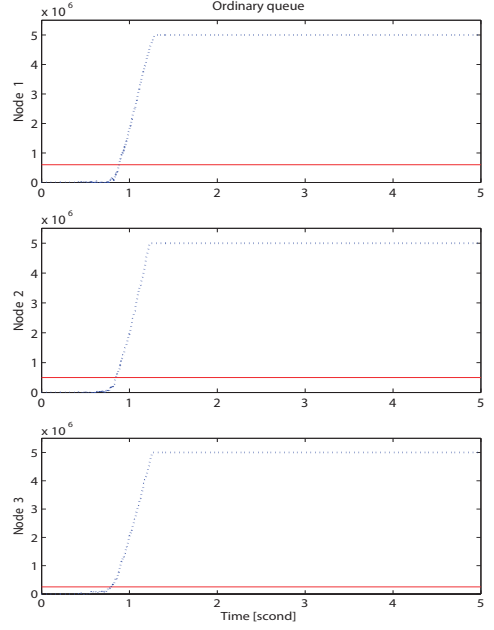
Figure 3.7: Ordinary queuing lengths (bits) by utilizing the decentralized IDCC method [3] corresponding to Case 1. The solid lines denote the set point references and the dashed lines denote the actual queuing lengths.

software environment.

As shown in Fig. 3.5, the premium and the ordinary traffic in each cluster are generated by the source nodes dynamically. In the simulation results presented below all the source traffic are simulated by the applications that are defined in QualNet. In each cluster, there are two premium traffic source nodes that simultaneously generate a variable bit rate traffic (VBR) and a constant bit rate traffic (CBR) (i.e. VBR+CBR). As defined according to the IETF Diff-Serv architecture [56], the premium traffic is used mainly for voice, video and other real-time constrained services that need to be strictly controlled. For example, in cluster 1, nodes 4 and 5 are the premium traffic sources, where both nodes generate VBR and CBR traffic to node 1. Typical networks will limit the premium traffic to no more than 30% of the total link capacity, and often indeed to much lower levels. Therefore, the VBR source is simulated by generating packets with an average size of 512 bytes and pace the packets into the network every 4 *ms*. The average rate of the VBR traffic is 1 Mbps. The CBR source generates 0.5 Mbps and paces the packets into the
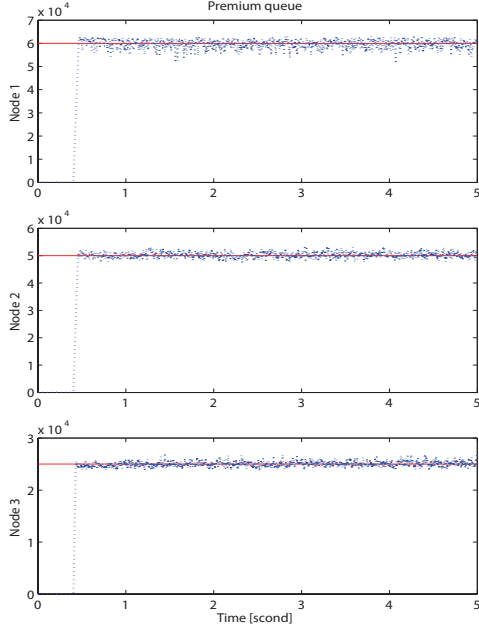
Figure 3.8: Premium queuing lengths (bits) by utilizing the proposed decentralized SCC corresponding to Case 1. The solid lines denote the set point references and the dashed lines denote the actual queuing lengths.
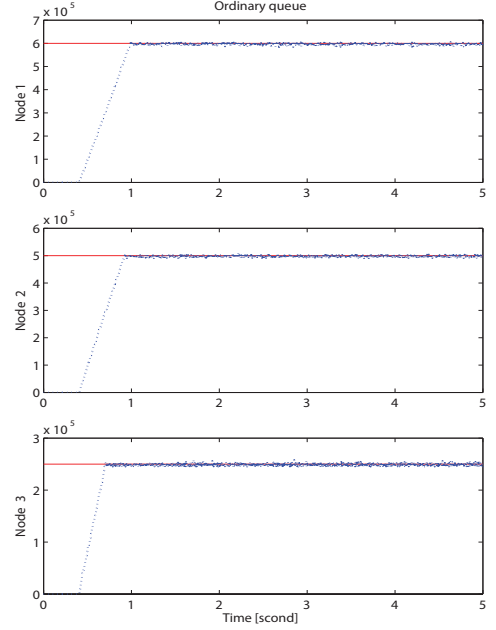
Figure 3.9: Ordinary queuing lengths (bits) by utilizing the proposed decentralized SCC corresponding to Case 1. The solid lines denote the set point references and the dashed lines denote the actual queuing lengths.

network constantly.

In each cluster, there is also one ordinary traffic source. For example, in cluster 3 node 13 is the ordinary traffic source. The ordinary traffic source is implemented by an on-off traffic. The on-off traffic is typically represented in networks for periodic surveillance or monitoring messages over an area of interest or in networks with measurement messages from a sensor. In our simulations, the on-off traffic is implemented by invoking the Supper application module in the QualNet software [133]. During the off-time period no packets are generated. The off-time period is generated from an exponential distribution with a mean period of 2 ms. During the on-time period each ordinary source generates a series of packets with the size of 512 bytes. The number of packets generated in each on-time period is determined by an exponential distribution with the mean value of 20 packets.

Finally there is also one best-effort traffic source in each cluster, for example, in cluster 1 node 7 is the best-effort traffic source node. The best-effort source generates a random traffic that is implemented by invoking the Traffic-Gen application module in the
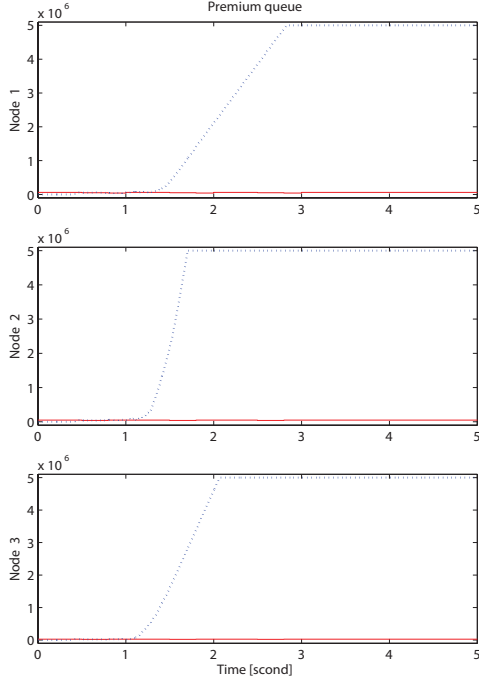
Figure 3.10: Premium queuing lengths (bits) by utilizing the decentralized IDCC method [3] corresponding to Case 2. The solid lines denote the set point references and the dashed lines denote the actual queuing lengths.
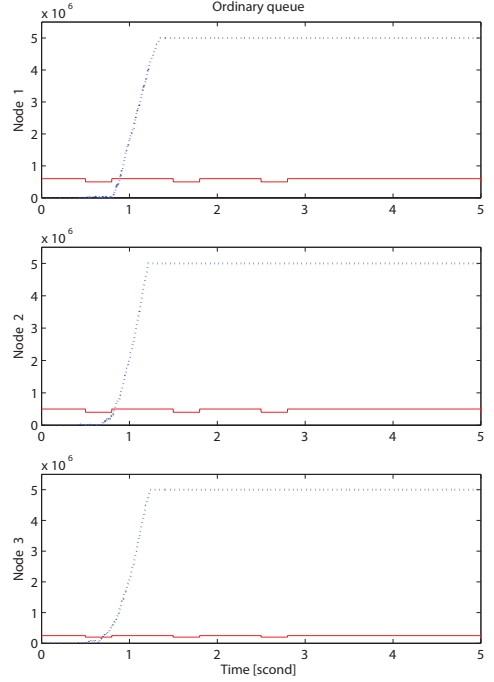
Figure 3.11: Ordinary queuing lengths (bits) by utilizing the decentralized IDCC method [3] corresponding to Case 2. The solid lines denote the set point references and the dashed lines denote the actual queuing lengths.

QualNet software. Each best-effort source generates packets whose length is exponentially distributed with an average of 512 bytes, and the inter-arrival time is also exponentially distributed with an average period of 4 ms.

The heterogeneous delays corresponding to any link connecting a node i to node j are considered as *randomly generated* signals (using a Gaussian distribution) that are lower and upper bounded by 0 s and 40 ms corresponding to all the traffic. The expression of this random signal is given as below

$$h \sim N(\mu, \sigma^2) \tag{3.96}$$

$$\tau = min\{0, max\{h_{max}, h\}\} \tag{3.97}$$

where $\mu = 20$ ms is the mean value of delay, $\sigma^2 = 10$ ms is the standard deviation, and $h_{max} = 40$ ms is the maximum value of delay.

The average value of the traffic compression gains during the network operation are

114

given as follows:

$$
\bar{G}_p = \begin{bmatrix} 0 & \bar{g}_{21}^p & \bar{g}_{31}^p \\ \bar{g}_{12}^p & 0 & \bar{g}_{32}^p \\ \bar{g}_{13}^p & \bar{g}_{23}^p & 0 \end{bmatrix} = \begin{bmatrix} 0 & 0.48 & 0.50 \\ 0.70 & 0 & 0.50 \\ 0 & 0.50 & 0 \end{bmatrix}
$$

$$
\bar{G}_r = \begin{bmatrix} 0 & \bar{g}_{21}^r & \bar{g}_{31}^r \\ \bar{g}_{12}^r & 0 & \bar{g}_{32}^r \\ \bar{g}_{13}^r & \bar{g}_{23}^r & 0 \end{bmatrix} = \begin{bmatrix} 0 & 0.50 & 0.50 \\ 0.50 & 0 & 0.50 \\ 0 & 0.30 & 0 \end{bmatrix}
$$

Control Parameters

According to the specifications of the network model given above, the maximum upper bounds for the adaptive controllers of the three bottleneck nodes 1, 2, 3 are set to $\lambda_1^{max} = 15$ Mb, $\lambda_2^{max} = 8$ Mb, and $\lambda_3^{max} = 4$ Mb, for the premium and the ordinary traffic classes. The state feedback control gains and the adaptive control gains that are derived according to Theorem 3.1 and Theorem 3.2 are given as follows:

$$
\begin{array}{lll}
k_{p1} = 5276 & k_{p2} = 7100 & k_{p3} = 2.63 * 10^4 \\
\delta_{p1} = 1.43 & \delta_{p2} = 0.834 & \delta_{p3} = 1.2 * 10^{-4} \\
\beta_{p1} = 0.505 & \beta_{p2} = 0.643 & \beta_{p3} = 1.532 \\
k_{r1} = 2054 & k_{r2} = 5165 & k_{r3} = 6732 \\
\delta_{r1} = 1.43 & \delta_{r2} = 1.50 & \delta_{r3} = 1.12 \\
\beta_{r1} = 1.506 & \beta_{r2} = 0.437 & \beta_{r3} = 1.320
\end{array}
$$

Based on the network model and the congestion control parameters obtained above, we first implement the integrated dynamic congestion controller (IDCC) scheme [3] and use the results obtained as a benchmark for comparative analysis with our proposed control strategies. For the sake of making an unbiased and fair evaluation and comparison, we actually do apply the same setting for the parameters as well as the same maximum delays in the IDCC algorithm as those that are selected for our proposed scheme as presented in the subsection of *Control Parameters*. In order to evaluate the performance of our proposed controllers under both stationary and dynamic conditions, we compare the performance
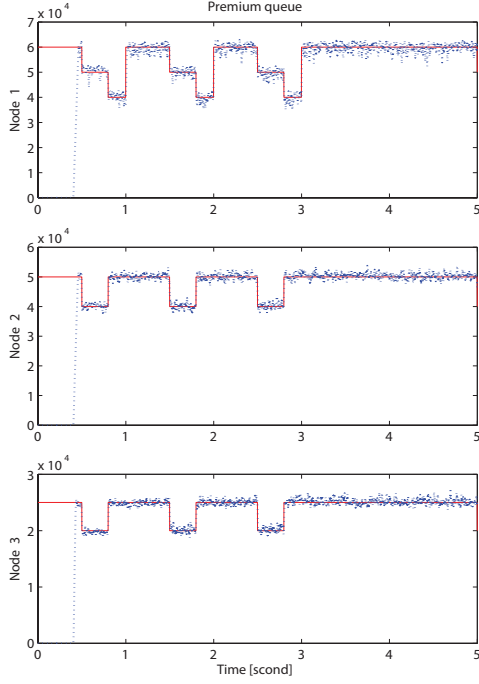
Figure 3.12: Premium queuing lengths (bits) by utilizing the proposed decentralized SCC corresponding to Case 2. The solid lines denote the set point references and the dashed lines denote the actual queuing lengths.
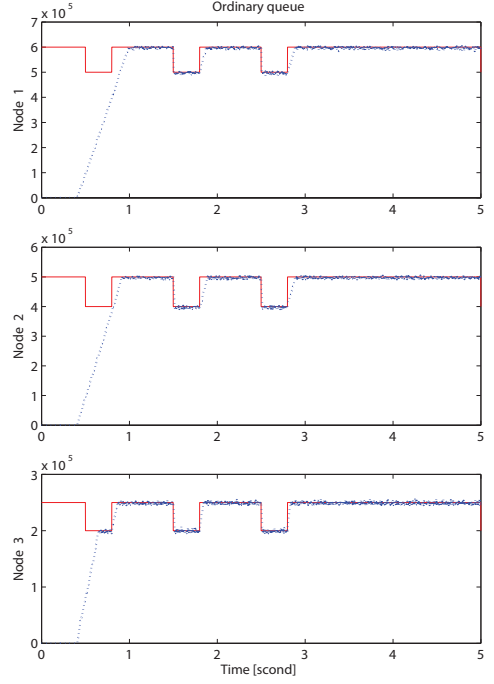
Figure 3.13: Ordinary queuing lengths (bits) by utilizing the proposed decentralized SCC corresponding to Case 2. The solid lines denote the set point references and the dashed lines denote the actual queuing lengths.

of the three bottleneck links and nodes under the following two cases:

- *Case 1: Fixed reference set point*. The reference set points for the queuing lengths are considered to be constant during the simulation period, that is

$$x_{p,1}^{ref} = 60 \; Kbits, \quad x_{p,2}^{ref} = 50 \; Kbits, \quad x_{p,3}^{ref} = 25 \; Kbits$$

$$x_{r,1}^{ref} = 600 \; Kbits, \quad x_{r,2}^{ref} = 500 \; Kbits, \quad x_{r,3}^{ref} = 250 \; Kbits$$

- *Case 2: Variable reference set point*. The reference set points for the queuing length are considered to be time-varying. During the time interval $0 \leq t < 0.5s$, the reference set points are assigned to

$$x_{p,1}^{ref} = 60 \; Kbits, \quad x_{p,2}^{ref} = 50 \; Kbits, \quad x_{p,3}^{ref} = 25 \; Kbits$$

$$x_{r,1}^{ref} = 600 \; Kbits, \quad x_{r,2}^{ref} = 500 \; Kbits, \quad x_{r,3}^{ref} = 250 \; Kbits$$

and during the time interval $0.5s \leq t < 0.8s$, the reference set points are assigned to

116

Table 3.1: Packet loss rate by utilizing the decentralized IDCC and the SCC approaches with $h_{max} = 40$ ms.

Premium	IDCC [3]	SCC
Node 1	92.96%	0
Node 2	93.86%	0
Node 3	93.27%	0
Ordinary	IDCC [3]	SCC
Node1	87.93%	5.66%
Node 2	96.08%	4.65%
Node 3	96.13%	2.34%

Table 3.2: Average queuing delay by utilizing the decentralized IDCC and the SCC approaches with $h_{max} = 40$ ms.

Premium	IDCC [3]	SCC
Node 1	∞	48.8 ms
Node 2	∞	44.9 ms
Node 3	∞	22.5 ms
Ordinary	IDCC [3]	SCC
Node 1	∞	67.8 ms
Node 2	∞	138.1 ms
Node 3	∞	178.5 ms

$$x_{p,1}^{ref} = 50 \ Kbits, \quad x_{p,2}^{ref} = 40 \ Kbits, \quad x_{p,3}^{ref} = 20 \ Kbits$$

$$x_{r,1}^{ref} = 500 \ Kbits, \quad x_{r,2}^{ref} = 400 \ Kbits, \quad x_{r,3}^{ref} = 200 \ Kbits$$

and finally during the time interval $0.8s \leq t < 1s$, the reference set points are assigned to

$$x_{p,1}^{ref} = 40 \ Kbits, \quad x_{p,2}^{ref} = 50 \ Kbits, \quad x_{p,3}^{ref} = 25 \ Kbits$$

$$x_{r,1}^{ref} = 600 \ Kbits, \quad x_{r,2}^{ref} = 500 \ Kbits, \quad x_{r,3}^{ref} = 250 \ Kbits$$

The simulations are conducted and validated for the duration of 5 seconds by repeating the above reference set points during the time intervals $[0s, 1s]$, $[1s, 2s]$, and $[2s, 5s]$, respectively. Figures 3.6 and 3.7 illustrate the resulting queuing lengths (bits) by utilizing the IDCC method [3] corresponding to Case 1. As can be seen from these figures, the queuing states of all the nodes are *unstable*, that is the buffers for both the premium and the ordinary traffics *do not* converge to their desired set point values but instead have overflown and reached their upper bound buffer sizes. One explanation for this undesired behavior is due to the presence of the time-varying *heterogeneous* delays that are not explicitly taken into account by the IDCC controller. On the other hand, as shown in Figures 3.8 and 3.9, by applying our proposed congestion controllers with the parameters that are derived from the LMI conditions discussed earlier and quantified in the *Control Parameters* subsection above, the queuing lengths do indeed converge to their desired set points and the overall performance of the network is greatly improved as compared to that of the IDCC method.
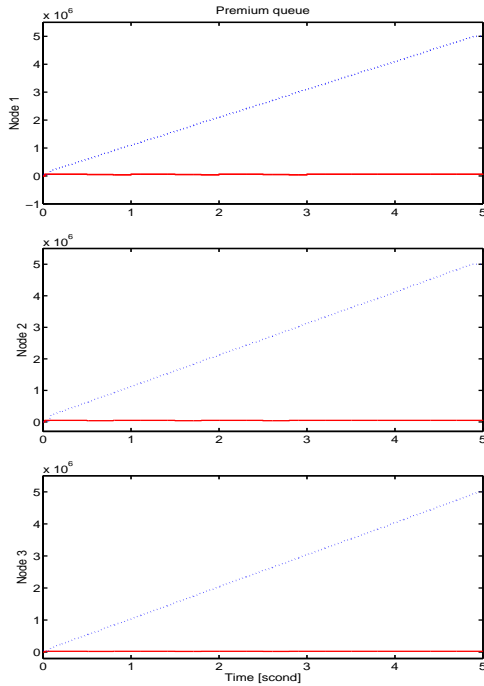
Figure 3.14: Premuim queuing lengths (bits) by utilizing the centralized IDCC. The solid lines denote the set point references and the dashed lines denote the actual queuing lengths.
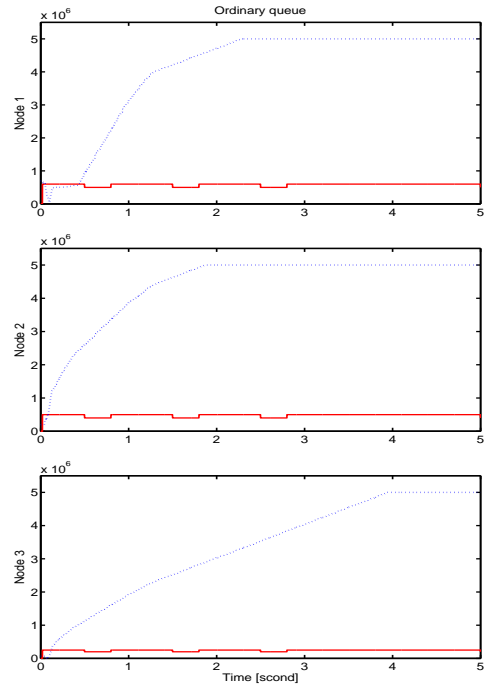
Figure 3.15: Ordinary queuing lengths (bits) by utilizing the centralized IDCC. The solid lines denote the set point references and the dashed lines denote the actual queuing lengths.

Figures 3.10-3.11 depict the simulation results by applying the IDCC approach to the network corresponding to the Case 2. As one can see from the queuing behavior of the three edges nodes, the performance of the IDCC method is similar to those in the Case 1. The buffers for both the premium and the ordinary traffics are again overflown and the queuing lengths become *unstable*. On the contrary, by utilizing our proposed method, as shown in Figures 3.12 and 3.13, the overall performance of the network is greatly improved and the queuing lengths converge to their desirable variable set points.

A quantitative comparison related to the packet loss rate (PLR) metric for the Case 2 is now provided and summarized in Table 3.1. As can be seen from Table 3.1, by utilizing the IDCC method a large number of the premium and the ordinary packets to the three nodes are lost. This is due to the fact that the buffer size of the nodes are overflown and all the incoming packets have to be discarded. However, by utilizing our proposed congestion control approach the performance of the average packet loss rate is significantly improved when compared to that of the IDCC approach. By utilizing our proposed method the
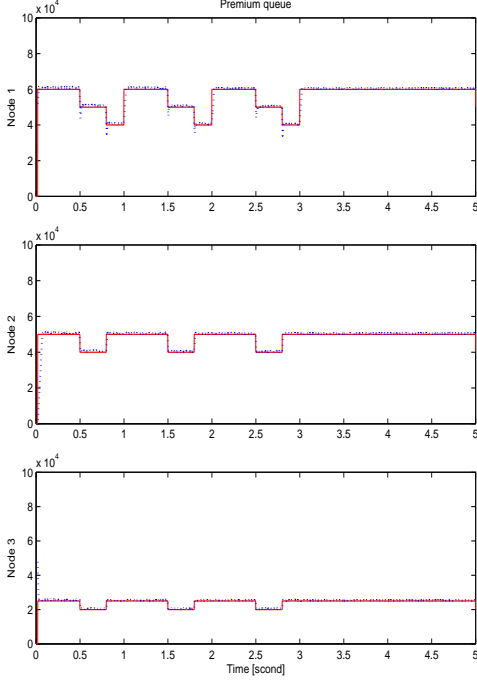
Figure 3.16: Premium queuing lengths (bits) by utilizing the proposed centralized SCC. The solid lines denote the set point references and the dashed lines denote the actual queuing lengths.
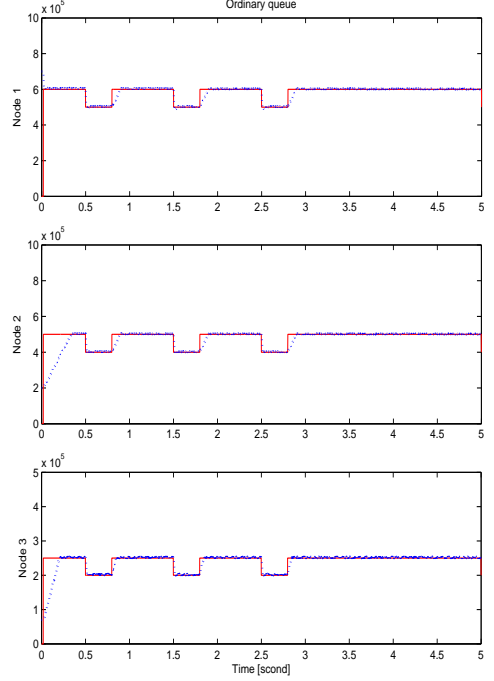
Figure 3.17: Ordinary queuing lengths (bits) by utilizing the proposed centralized SCC. The solid lines denote the set point references and the dashed lines denote the actual queuing lengths.

premium traffic has <u>no</u> packet losses and the ordinary traffic's loss rate is *less than* 6%. Table 3.2 provides the comparative results corresponding to the average queuing delays. As can be seen from Table 3.2 by utilizing the IDCC method the queuing delays are *infinite* due to the buffer overflow and packet losses. However, by utilizing our proposed congestion control method the performance of the network is significantly improved. The queuing delays remain bounded to less than 50 *ms* for the premium and 200 *ms* for the ordinary traffic.

3.3.3 Centralized SCC vs the Centralized IDCC Approaches

In order to evaluate the performance more fairly, in this section we generalized the IDCC algorithm to a centralized framework, with exactly the same control strategies as presented in [61]. The detailed derivation of the centralized IDCC algorithm can be found in Appendix B. We compare now the performance of our proposed SCC algorithm with the centralized IDCC as follows.

119

Table 3.3: Packet loss rate by utilizing the centralized IDCC and the SCC approaches with $h_{max} = 40$ ms.

Premium	IDCC [3]	SCC
Node 1	84.63%	0
Node 2	83.23%	0
Node 3	88.70%	0
Ordinary	IDCC [3]	SCC
Node 1	38.34%	1.61%
Node 2	62.95%	0.94%
Node 3	73.68%	1.43%

Table 3.4: Average queuing delay by utilizing the centralized IDCC and the SCC approaches with $h_{max} = 40$ ms.

Premium	IDCC [3]	SCC
Node 1	∞	45.3 ms
Node 2	∞	43.7 ms
Node 3	∞	21.4 ms
Ordinary	IDCC [3]	SCC
Node 1	∞	57.1 ms
Node 2	∞	116.6 ms
Node 3	∞	132.8 ms

Consider the same network model that is shown in the Fig. 3.5 and the same configuration of the incoming traffic and delays as defined in Section 3.3.2. The state feedback control gains that are and the adaptive control gains derived from Theorem 3.2 are given as $K_p = diag\{3680\ 4210\ 1780\}$, $K_r = diag\{574\ 3211\ 1994\}$, $\Delta_p = diag\{5.2 \times 10^{-3}\ 3.2 \times 10^{-3}\ 1.6 \times 10^{-3}\}$, $\Delta_r = diag\{1.7 \times 10^{-3}\ 1.2 \times 10^{-3}\ 1.3 \times 10^{-3}\}$, $\Pi_p = diag\{0.87\ 1.24\ 3.59\}$, and $\Pi_r = diag\{0.5\ 0.2\ 0.9\}$. The average traffic compression gain matrices G during the network operation are given as

$$\bar{G}_p = \begin{bmatrix} 0 & 0.23 & 0.31 \\ 0.42 & 0 & 0.21 \\ 0 & 0.30 & 0 \end{bmatrix} \qquad \bar{G}_r = \begin{bmatrix} 0 & 0.41 & 0.25 \\ 0.52 & 0 & 0.12 \\ 0 & 0.28 & 0 \end{bmatrix}$$

The performance of our proposed centralized SCC and the centralized IDCC approaches are shown in Figures 3.14-3.17. As we can see from Fig. 3.14 and Fig. 3.15, the premium and the ordinary queuing lengthes are unstable by utilizing the centralized IDCC approach. On the contrary, by utilizing our proposed centralized SCC algorithm, both the premium and the ordinary queues in each node do converge to their reference values. The numerical comparisons of the packet loss rate and the average queuing delays over the simulation time of 30 seconds are given in Tables 3.3 and 3.4.

According to the simulation results and the comparisons presented in Sections 3.3.1 and 3.3.2, one can see that by utilizing our proposed switching congestion control strategies the performance of the congestion control problem of the differentiated services are greatly improved when compared with the IDCC approach, in both the decentralized and

120

centralized frameworks. Therefore, we can conclude that for a Diff-Serv network with fixed topology, subject to multiple time-varying delays and physical constraints, the switching congestion control strategy yields a more desirable solution than the IDCC approah.

3.3.4 Centralized SCC vs the Decentralized SCC Approaches

As presented above for the congestion control problem of Diff-Serv networks with multiple time-varying delays and constraints, the performance of our proposed switching congestion control (SCC) approach has obvious strengthes, advantages, and better performance than the IDCC approach. In this section, we will evaluate and compare the performance of the centralized SCC and the decentralized SCC according to the performance metrics of PLR and the queuing delay.

Consider the network configuration that is shown in Fig. 3.18, where the communication channels among the nodes can be classified into two groups based on their different functionalities, namely:

- Forward channel. This is the channel from the sensor to the actuator which is responsible for sending the collected data and execution commands.

- Feedback channel. This is the channel from the actuator to the sensor which is responsible for sending feedback regulation and adjustments.

Therefore, the simulations are conducted in two cases, namely 1) the forward channel dominate and 2) the feedback channel dominate. In the first case, the traffic compression gains in the forward channel are set to be higher than that in the feedback channels; while in the second case it is vise versa. We consider the network model as shown in Fig. 3.18. There are three nodes in the network, each node has three different kinds of sources, namely the premium traffic, the ordinary traffic, and the best effort traffic. Each node has three buffers for the three kinds of traffic, respectively, and buffer size is set to be 10 Mb. The link capacity of each node is set to $C_{server,i} = 20$ Mbps and the transmitter constraint of each node is selected as $\lambda_i^{max} = 15$ Mbps.
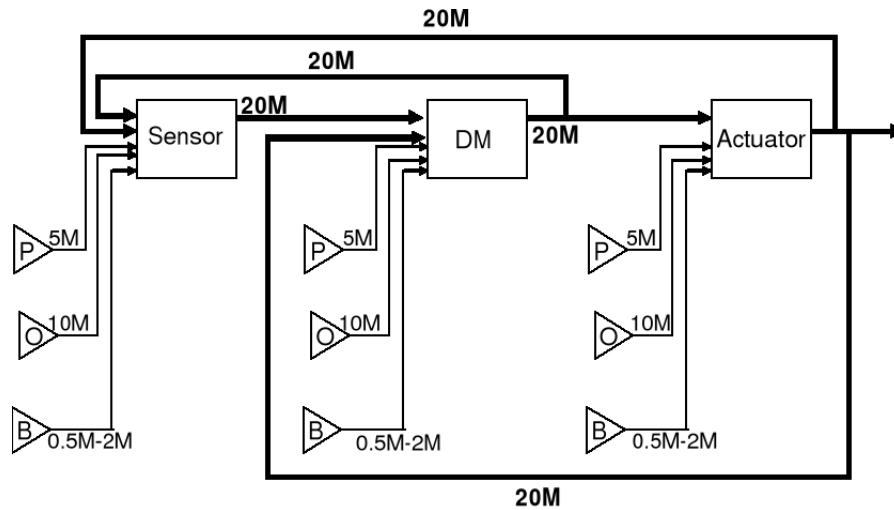
Figure 3.18: The simulation framework

The time evolutions of the three incoming traffic are shown in Fig. 3.19. The premium traffic is modeled as a sum of one variable bit rate traffic (VBR) and one constant bit rate traffic (CBR). As defined by the IETF Diff-Serv architecture [56], the premium traffic is used for voice, video and other real time services, which need to be strictly controlled. Typical networks will limit premium traffic to no more than 30%, and often much less, of the capacity of a link. Therefore, we select the premium traffic with an average bit rate of 1 Mbps and peak bit rate of 1.5 Mpbs. The ordinary traffic, which is modeled as an on-off source, is a typical kind of traffic in the network of multi-agent systems (NMAS) such as periodic surveillance over an area and measurement of a sensor node. The bit rate of the ordinary traffic is measurable and can be regulated by the controller. In our case the peak bit rate of the ordinary traffic is selected to be 10 Mbps. Finally, the best effort traffic does not have any QoS guarantee. It utilizes any instantaneous left over capacity from the premium and the ordinary traffic for transmission. Any traffic that does not meet the requirements of other possible defined classes of traffic is placed in this group. In our case, the bit rate of the best effort traffic is varying from 0.5 Mbps to 2 Mbps.

Since the premium traffic has stringent maximum delay bound and loss requirements,
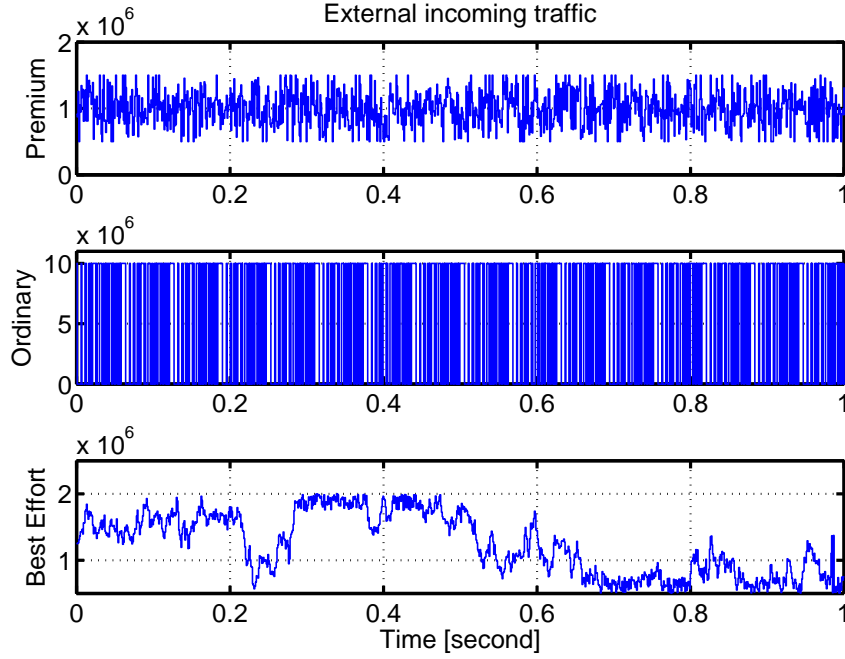
Figure 3.19: The three classes of incoming traffic.

the reference point of the queue length is set to be less than 10% of its buffer size (10 Mbits). For the ordinary traffic, since it can accept larger delays than the premium traffic, we set the reference value of the queue length as 10 times of the premium traffic, and within 60% of the buffer size (10 Mbits). Therefore, the reference values of these two kinds of traffic for each node are given as follows:

During the interval $0 \leq t < 0.5s$, we set the reference points as follows

$$x_{p,1}^{ref} = 60 \ Kbits, \quad x_{p,2}^{ref} = 50 \ Kbits, \quad x_{p,3}^{ref} = 25 \ Kbits$$

$$x_{r,1}^{ref} = 600 \ Kbits, \quad x_{r,2}^{ref} = 500 \ Kbits, \quad x_{r,3}^{ref} = 250 \ Kbits$$

After $t = 0.5s$, the reference set points are set as

$$x_{p,1}^{ref} = 50 \ Kbits, \quad x_{p,2}^{ref} = 40 \ Kbits, \quad x_{p,3}^{ref} = 20 \ Kbits$$

$$x_{r,1}^{ref} = 500 \ Kbits, \quad x_{r,2}^{ref} = 400 \ Kbits, \quad x_{r,3}^{ref} = 200 \ Kbits$$
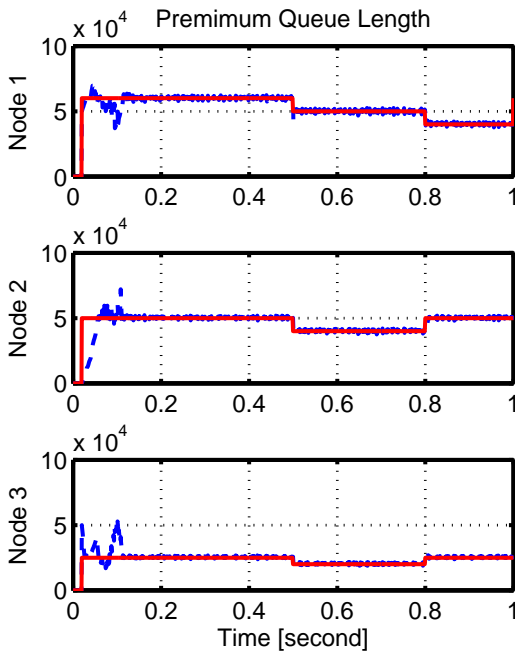
Figure 3.20: Case 1: Premium queuing length by utilizing the centralized SCC.
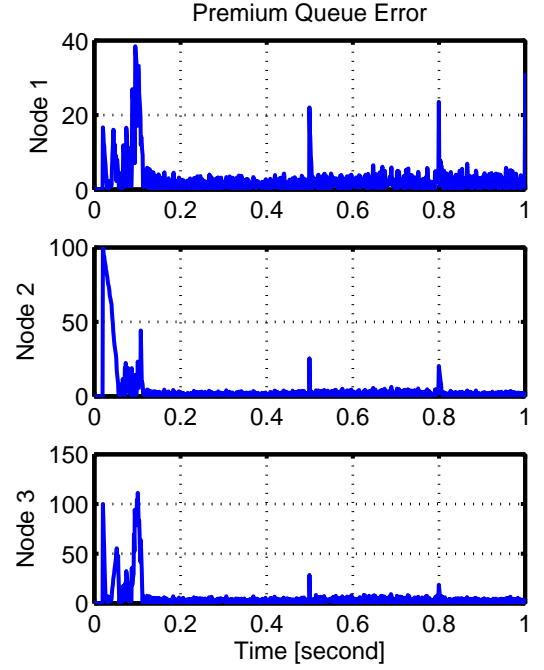
Figure 3.21: Case 1: Premium queuing error by utilizing the centralized SCC.

Finally, after $t = 0.8s$, the reference set points are assigned to be

$$x_{p,1}^{ref} = 60 \ Kbits, \quad x_{p,2}^{ref} = 50 \ Kbits, \quad x_{p,3}^{ref} = 25 \ Kbits$$

$$x_{r,1}^{ref} = 600 \ Kbits, \quad x_{r,2}^{ref} = 500 \ Kbits, \quad x_{r,3}^{ref} = 250 \ Kbits$$

Based on the definitions of the feedback channel and the feed forward channel, the following two scenarios are selected for simulations, namely the *forward channel dominate scenario* and the *feedback channel dominate scenario*. In the forward channel dominate scenario, we assume that the information in the forward channel is more important than that in the feedback channels. Hence, the traffic compression gains in the forward channel are selected to be relatively large. On the other hand, this is vice versa in the feedback channel dominate scenario.

- *Case 1: Forward Channel Dominate*. In this case, the traffic compression gains are initially set to be $g_{ij} = 0.9$ in the forward channel, and $g_{ij} = 0.2$ in the feedback channel. The majority of the incoming traffic to each node is assumed to contain valuable information such as images, videos, and etc. So that the traffic compression

124
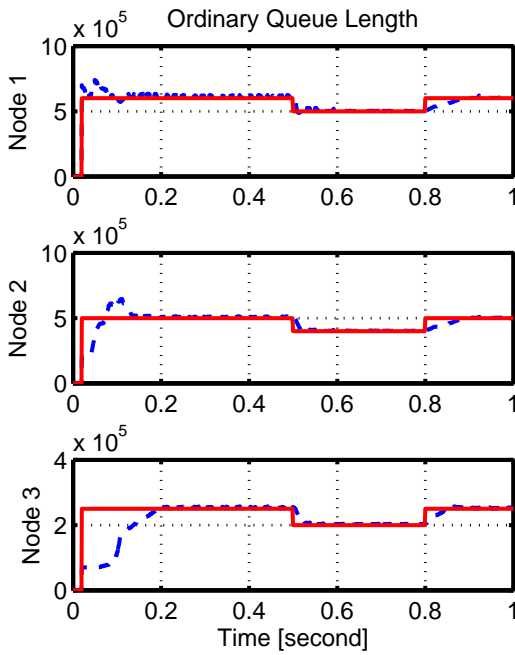
Figure 3.22: Case 1: Ordinary queuing length by utilizing the centralized SCC.
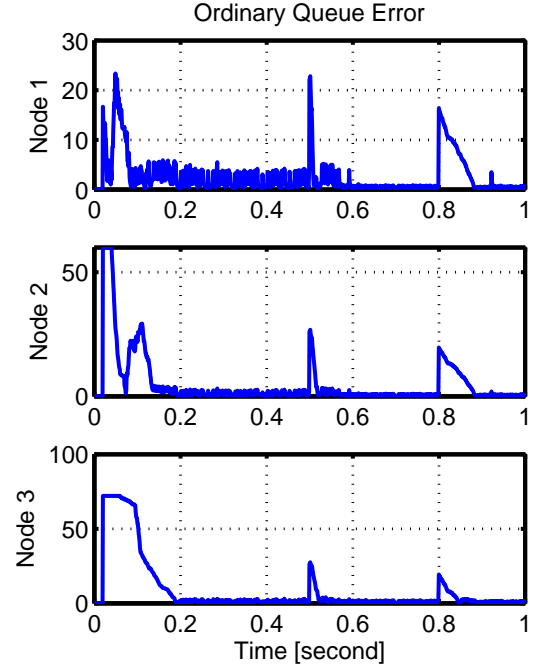
Figure 3.23: Case 1: Ordinary queuing error by utilizing the centralized SCC.

gains in the forward channel are selected to be relatively larger then that in the feedback channel. For each input flow, the delay is taken as a random signal with a normal distribution function of $\tau = min\{0, max\{h_{max}, h\}\}$, where $h_{max} = 20$ ms is the maximum value of delay, $h \sim N(\mu, \sigma^2)$ is a normal distributed random signal with the mean value of $\mu = 10$ ms and the standard derivation of $\sigma^2 = 5$ ms.

The queuing length and the queuing errors of the premium and the ordinary traffic in the nodes are shown in the Fig. 3.20 to Fig. 3.27, by utilizing the centralized and the decentralized switching congestion controller (SCC) algorithms, respectively. From the performances that are illustrated in the figures, one can see that the premium and the ordinary queuing length of all the nodes do converge to their corresponding reference values. One compare the settling time and the mean percentage error of the two algorithms as given in Table. 3.5. The settling time of each node by using the centralized control approach is larger than that by using the decentralized algorithm, especially for the ordinary traffic. The main reason of this behavior may due to the coupling effects of the centralized controller where the command to each
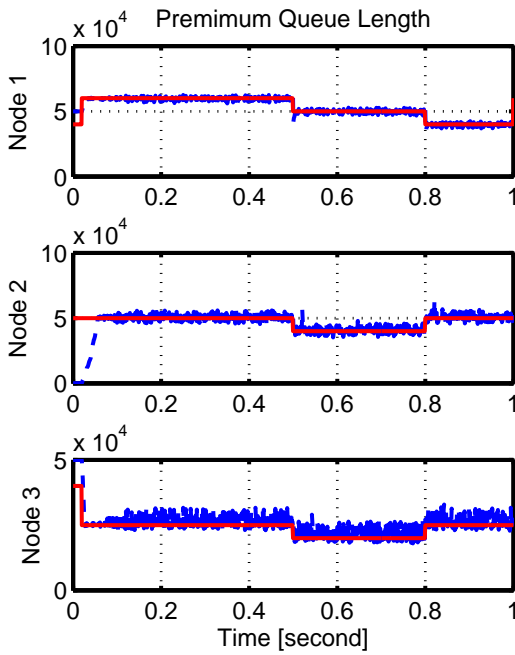
Figure 3.24: Case 1: Premium queuing length by utilizing the decentralized SCC.
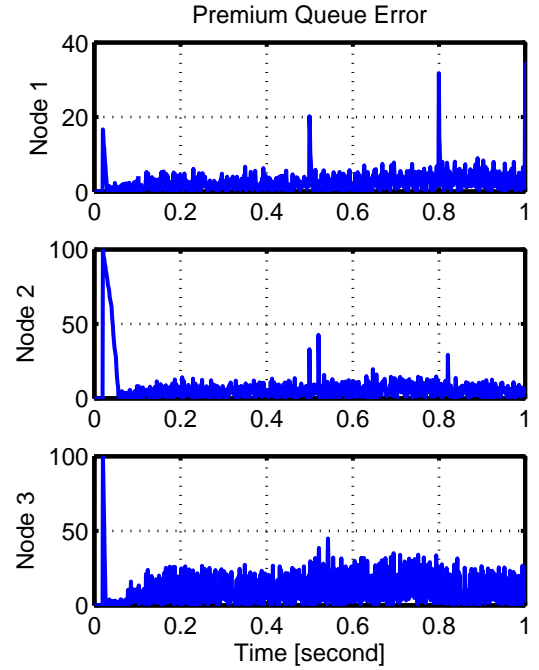
Figure 3.25: Case 1: Premium queuing error by utilizing the decentralized SCC.

node is affected by states of the other nodes in the network, and hence the queue response is slower than the decentralized one.

Note that one can observe that after the convergence, the average percentage error of the queuing length at each node by utilizing the centralized SCC algorithm is much smaller than the queuing errors by utilizing the decentralized SCC. This result is reasonable because in the decentralized control algorithm, each controller only has access to the local information. Moreover, the queuing state of each node is highly coupled with the states of its neighboring nodes. On the contrary, in the centralized SCC algorithm, the controller is based on the queuing state of all the nodes in the network. Therefore, it can achieve more accurate control than the decentralized SCC algorithm after the convergence.

- *Case 2: Feedback Channel Dominate*. In this case, we assume that the incoming traffic to the sensor contains more noise as the sensor is operating in a noisy environment, and hence it needs to filter and compress the raw data before sending the
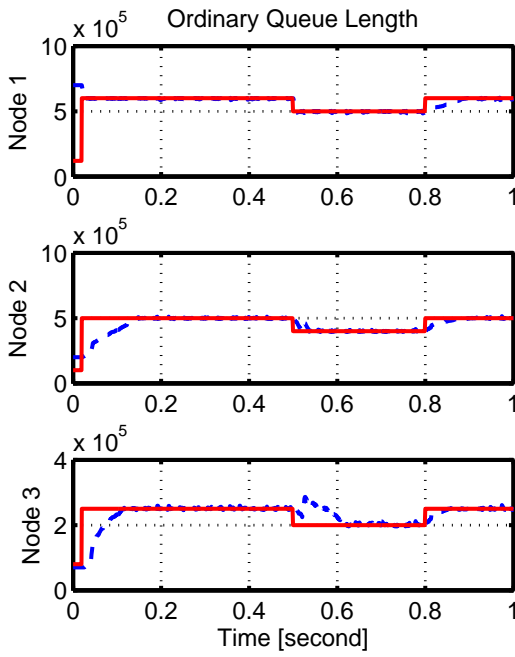
Figure 3.26: Case 1: Ordinary queuing length by utilizing the decentralized SCC.
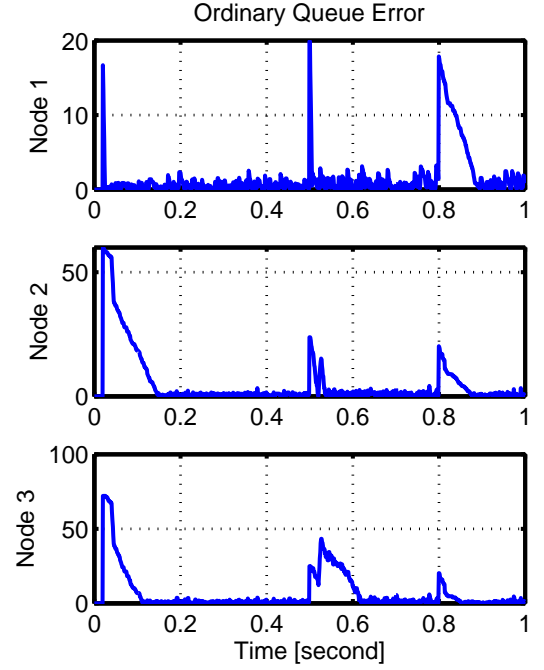
Figure 3.27: Case 1: Ordinary queuing length by utilizing the decentralized SCC.

valuable information to the decision maker and actuator. Therefore, the traffic compression gains are initially set to be $g_{ij} = 0.2$ in the forward channel and $g_{ij} = 0.9$ in the feedback channel, respectively. The time delay among the nodes is taken as the normal distributed function $\tau = min\{0, max\{h_{max}, h\}\}$ and $h \sim N(5ms, 1ms)$, where $h_{max} = 10$ ms is the maximum bound of the delays in the network. The performance of the queuing length in all the nodes by utilizing the proposed switching congestion control strategies are illustrated in Fig. 3.28-Fig. 3.31 and Fig. 3.32-Fig. 3.35, for the centralized and the decentralized SCC algorithms, respectively.

As can be seen from these figures the queuing length of the premium and the ordinary traffic do convergence to their reference values under both approaches. The average percentage error and the settling time of each node, with respect to the premium and ordinary traffic are summarized in the Table. 3.6. As can be seen from the comparative results in Table. 3.6 the centralized SCC algorithm can achieve higher accuracy in the steady state with respect to the decentralized SCC approach. However, the queuing state of each node by utilizing the decentralized SCC algorithm

Table 3.5: The comparisons between the centralized and the decentralized SCC approaches corresponding to Case 1.

$h_{max} = 20$ ms	Centralized SCC				Decentralized SCC			
	Mean Error		Settling Time		Mean Error		Settling Time	
	P	O	P	O	P	O	P	O
Node 1	1.83%	0.94%	$0.06s$	$0.28s$	2.50%	1.54%	$0.02s$	$0.03s$
Node 2	2.31%	2.99%	$0.08s$	$0.31s$	7.09%	5.04%	$0.05s$	$0.15s$
Node 3	2.45%	2.20%	$0.09s$	$0.35s$	9.57%	6.86%	$0.04s$	$0.12s$

Table 3.6: The comparison between the centralized and the decentralized SCC approaches corresponding to Case 2.

$h_{max} = 10ms$	Centralized SCC				Decentralized SCC			
	Mean Error		Settling Time		Mean Error		Settling Time	
	P	O	P	O	P	O	P	O
Node 1	1.76%	0.93%	$0.07s$	$0.30s$	8.58%	1.69%	$0.02s$	$0.02s$
Node 2	2.30%	3.04%	$0.06s$	$0.32s$	7.34%	8.27%	$0.02s$	$0.25s$
Node 3	2.45%	2.18%	$0.08s$	$0.35s$	5.36%	6.25%	$0.03s$	$0.18s$

have relatively faster convergence speed.

From the simulation results and the comparisons of the performance of the proposed centralized and the decentralized SCC algorithms, it follows that both of two approaches are effective congestion control algorithms for the Diff-Serv networks with fixed topology. Each congestion control approach has distinct advantages and disadvantages. When the scale of the network is small, such as a small team of UAVs, the centralized SCC algorithm is more suitable due to the resulting high accuracy performance. However, if the number of nodes in the network is large, such as sensor-actuator networks, a centralized controller may not be feasibly implementable and the decentralized SCC algorithm should be selected.
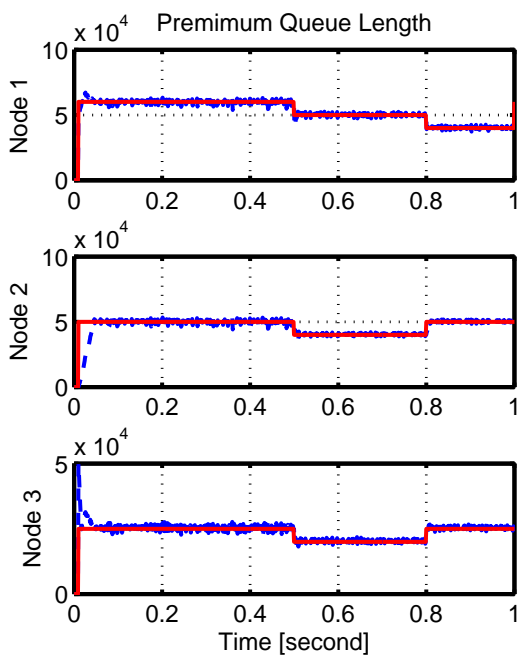
Figure 3.28: Case 2: Premium queuing length by utilizing the centralized SCC.
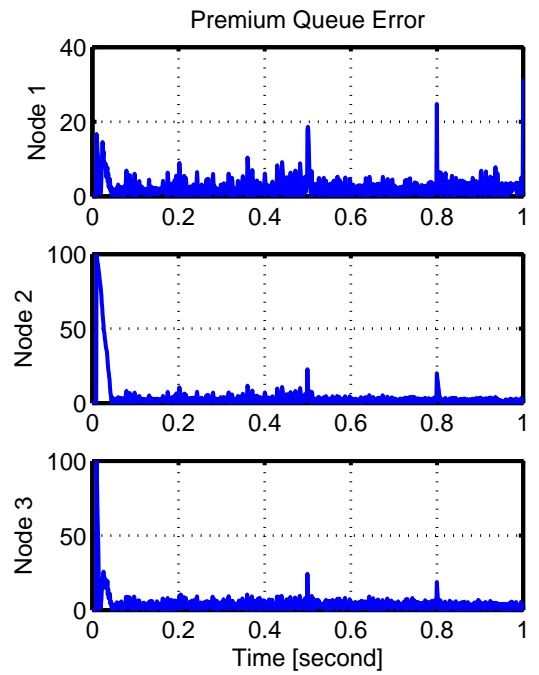
Figure 3.29: Case 2: Premium queuing error by utilizing the centralized SCC.
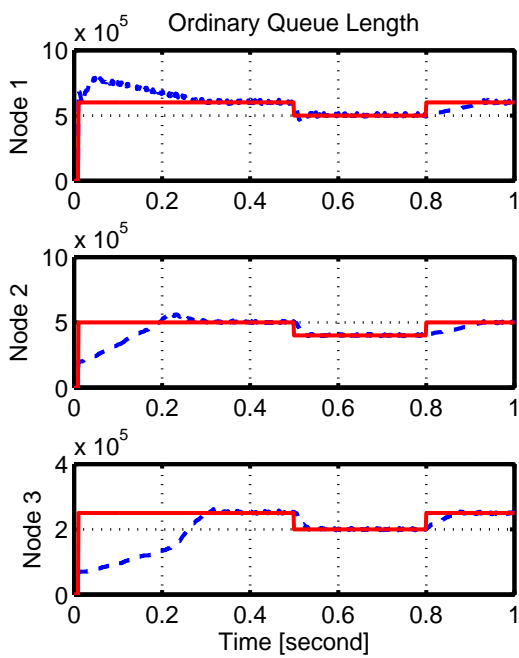
Figure 3.30: Case 2: Ordinary queuing length by utilizing the centralized SCC.
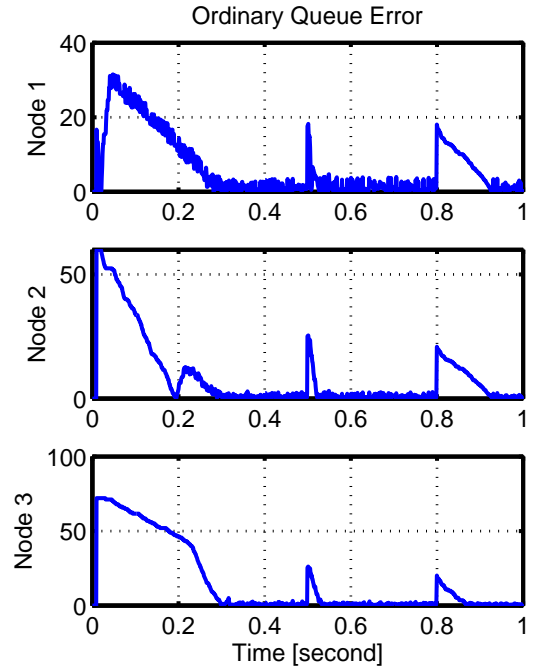
Figure 3.31: Case 2: Ordinary queuing length by utilizing the centralized SCC.

129

3.4   Conclusions

In this chapter a new methodology for analytical solutions to centralized and decentralized congestion control problems of Diff-Serv networks with fixed topology was proposed. The method incorporates queuing dynamics and physical constraints that exist in the traffic network. The transmitting, propagating, and processing delays considered in the dynamics of the network are assumed to be unknown and time-varying. By employing switching control strategy, the proposed congestion control schemes resolve the conflict in the design of congestion controllers, that is by meeting performance requirements such as fast response and satisfactory disturbance rejection while simultaneously avoiding violations of the specified constraints. The switching congestion control (SCC) problem is formulated as a multi-mode regulation framework corresponding to the *edge modes* and the *normal control mode.* By regulating the system parameters, the edge mode states are forced to behave similar to the normal control mode state where the system states are forced to change toward the safe operating range (normal control mode). It is shown that the system experiences multiple modes and the stability conditions of the closed-loop system are formulated in the LMI framework. Simulation results presented do indeed confirm and demonstrate the effectiveness of the proposed switching congestion control strategies. Numerical results demonstrate that the network packet loss rates and its corresponding stability conditions are significantly improved by utilizing our proposed control strategies when compared to the other available method (that is the IDCC) in the literature.
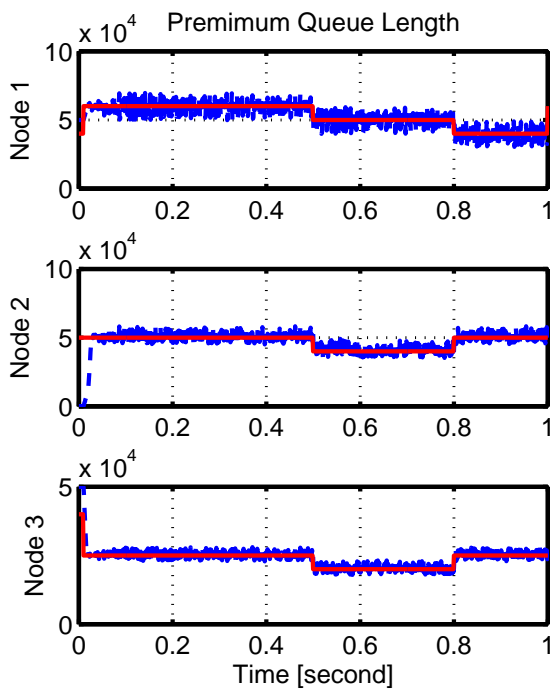
Figure 3.32: Case 2: Premium queuing length by utilizing the decentralized SCC.
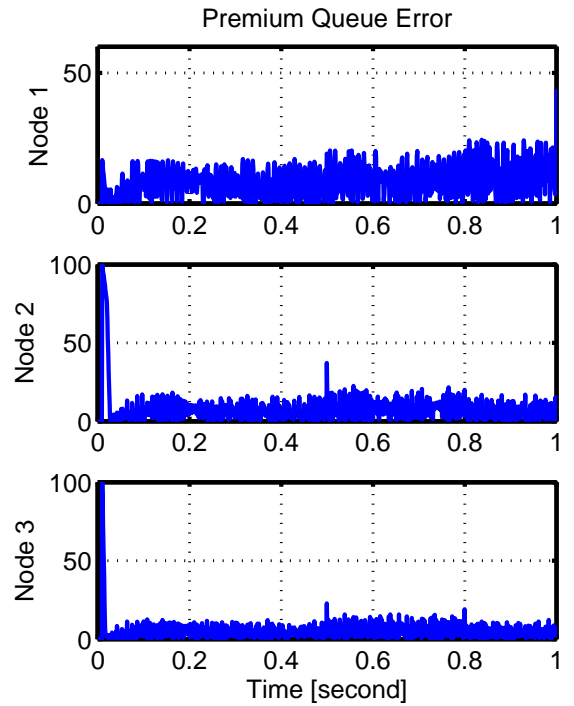
Figure 3.33: Case 2: Premium queuing error by utilizing the decentralized SCC.
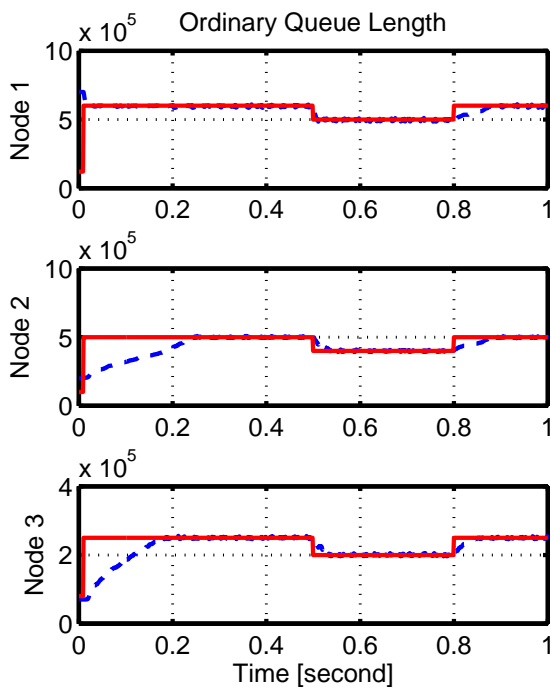
Figure 3.34: Case 2: Ordinary queuing length by utilizing the decentralized SCC.
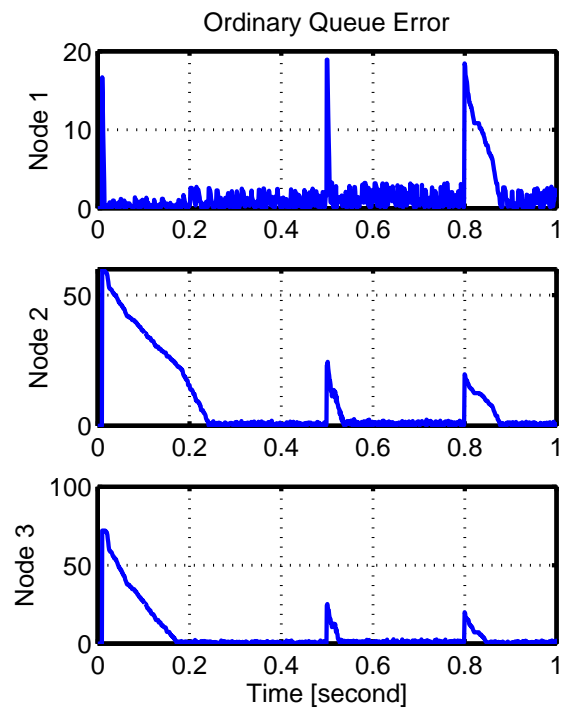
Figure 3.35: Case 2: Ordinary queuing length by utilizing the decentralized SCC.

131

Chapter 4

Switching Congestion Control of Mobile DiffServ Networks

In Chapter 3, the switching congestion control strategies for the Diff-Serv networks with fixed topology are developed. However, in most applications of the network of multi-agent systems (NMAS), such as space missions, pursuit and rescue missions, and networked robots, the nodes in the network are usually highly mobile and the network topology will in turn become time-varying. The movement of nodes will produce random sequence of on-off link changes, and the associated network topology will change unpredictably. Thus, there is no stationary infrastructure in the mobile ad hoc networks. It should be pointed out that in addition to the mobility, loss of node power, deleting or addition of new nodes will also lead to changes in the network topology.

Unlike the cellular networks, both ends (transmitter and receiver) in a mobile ad hoc network are free to move. The connectivity between two nodes is determined by the radio range of both ends which is a function of the antenna pattern, the power level, and the geographic terrain of each node. Therefore, in mobile networks, each node can only effectively communicate with certain nearest nodes, typically those that lie in its vicinity or in its so-called neighboring set. The changing of the network topology will result in the changing of the neighboring set of each node. Therefore, the queuing dynamics of each

node in the mobile network will also be affected by the changing neighboring set.

Furthermore, due to the restrictive physical constraints of the communication network, such as the link capacity and the buffer size constraints, performing congestion control in mobile ad hoc networks is not a trivial problem. Moreover, the changing of the neighboring set will change the number of links at the output of each node, hence the link capacity of the node becomes time-varying. Therefore, the physical constraints of the mobile network is also time-varying and the congestion control problem is more challenging now.

The objective of this chapter is to develop efficient congestion control algorithms for mobile Diff-Serv networks, subject to the multiple time-varying delays and time-varying physical constraints. To achieve this goal, the changing of the neighborhood sets must be defined. As mentioned in Chapter 2, the connection between the nodes is dependent on certain physical parameters such as the distance between the nodes and the maximum of the nodes life-time. Since the link connectivity between two nodes at time $t + \Delta t$ is only dependent on the nodes' position, velocity and the direction of movement at time t, hence the future connection of two nodes is independent of its history, but dependent only on the current state of the connectivity. Therefore, the changes of the network topology is a memoryless stochastic process which can be described by a Markov chain.

During the past two decades, the Markov chains have been considered in modeling the abrupt variations of systems and have been widely applied in many applications [134], [135], [136], [137], [138]. In this chapter, we adopt the concept of the Markov chain and model the changes of the neighboring set stochastically as a Markovian process. The switching congestion control algorithms proposed in Chapter 3 are now generalized for the congestion control problem of mobile Diff-Serv networks. Both a centralized and a decentralized control scheme are considered for the premium and the ordinary traffic, respectively.

The remainder of this chapter is organized as follows. In Section 4.1, a brief introduction of the Markovian jump linear system (MJLS) with time-delay is presented. The definitions of stochastic stability and the stochastic stabilization are given. In Section

133

4.2, the switching control approach for MJLS with constraints is described. In Section 4.3, a novel centralized Markovian Jump Switching Congestion Controller (MJ-SCC) for the premium and the ordinary traffic flows are proposed. In Section 4.4, the centralized MJ-SCC algorithm is then extended to a decentralized framework. In Section 4.5, the performance of the proposed MJ-SCC is evaluated through comprehensive simulations. Finally, conclusions are stated in Section 4.6.

4.1 Markovian Jump Linear Systems with Time-Delay

Markovian jump linear systems (MJLSs) are a special class of hybrid systems with two components in their vector states, namely $x(t)$ and α_t. The first is referred to as the state and the second is refereed to as the mode. The MJLS jumps abruptly from on mode to another in a random manner that makes it a stochastic system. The switchings between the modes is governed by a continuous/discrete Markov time process with definite state space. On the other hand, the state in each mode is represented by a system of differential/difference equations. Therefore, when the system mode is fixed, the system evolves like a deterministic linear system.

The MJLS has the advantage more accurately representing physical systems with abrupt variations, such as manufacturing systems, power systems, communication networks, economic systems, etc. During the past two decades, the MJLS has attracted large attention with an increasing interest in both theoretical and application domains [134], [137], [135], [138], [136]. In [139], [140], [141], [142], [143], [57], [144], [145], the authors extensively investigated problems such as stability, stabilizability, H_∞ control, and their robustness. In [146], the authors presented a state estimation algorithm for the Markovian jump singular systems. In [147], a decentralized stabilization approach for an uncertain Markovian large scale system was developed. More recently, the MJLS with time-delays has attracted attention in control community. Researchers in [148], [149], [150] have made contributions on the control problem of MJLS with time-delays. The methods used were

mostly based on Lyapunov-Krasovskii functions, which are quite general and lead to a linear matrix inequality (LMI) conditions.

In this chapter, a novel congestion control strategy based on the switching control approach is developed for the Markovian jump systems. By solving certain linear matrix inequalities (LMIs), sufficient conditions for stochastic stabilization are derived for the resulting closed-loop systems with Markovian jumping parameters. Below we fist give the definitions of the stochastic stability.

A mathematical representation of a MJLS with multiple and time-varying delays can be given by the following dynamics:

$$
\begin{aligned}
\dot{x}(t) &= A(\alpha_t)x(t) + \sum_{j=1}^{n} A_d(\alpha_t)x(t - \tau_j(t)) \\
&\quad + B(\alpha_t)u(t) + \sum_{j=1}^{n} B_d(\alpha_t)u(t - \tau_j(t)) + B_w(\alpha_t)w(t) \qquad (4.1) \\
x(t) &= \phi(t), t \in [-h, 0]
\end{aligned}
$$

where $x(t)$ and $u(t)$ are the state and the control input of the system, respectively; $A(\alpha_t)$, $A_d(\alpha_t)$, $B(\alpha_t)$, $B_d(\alpha_t)$ and $B_w(\alpha_t)$ are the system matrices with appropriate dimensions which are dependent on the Markov process α_t, and $\phi(t)$ is a continuously differentiable function that represents the initial condition of the time-delay system. The multiple and time-varying delay $\tau_j(t)$ satisfy the following assumption:

$$
0 \le \tau_j(t) \le h_j \qquad (4.2)
$$

$$
h = max\{h_j\} \qquad j = 1, ..., n \qquad (4.3)
$$

where h is the maximum bound of the delays in the network, and n is the number of delays in the network. Therefore, given a complete probability space $\{\Omega, \mathcal{F}, P\}$, where Ω is the sample space, $\mathcal{F}$ is the σ-algebra of subsets of the sample space, and P is the probability measure on $\mathcal{F}$, the stochastic process α_t can be defined as a continuous-time Markov process. The variable α_t takes values in a finite set $\mathcal{S} = \{1, ..., M\}$ with the transition probability matrix $\Pi = \{\pi_{kl}\}$ given as follows:

$$
P[\alpha_{t+\delta} = k \mid \alpha_t = l] = \begin{cases} \pi_{kl}\Delta + o(\Delta), & k \ne l; \\ 1 + \pi_{kk}\Delta + o(\Delta), & k = l. \end{cases} \qquad (4.4)
$$

where $\pi_{kl} \geq 0$ is the transition rate from mode k to mode l, $\pi_{kk} = -\sum_{l=1,l\neq k}^{M} \pi_{kl}$, and $o(\Delta)$ is a function satisfying $\lim_{\Delta \to 0} \frac{o(\Delta)}{\Delta} = 0$. The following definitions of stochastic stability, stochastic stabilizability can now be stated for the MJLS (4.1) [135].

Definition 4.1. *[135]: System (4.1) with $u(t) \equiv 0$ and $w(t) \equiv 0$ is said to be stochastically stable (SS) if there exists a constant $T(\phi(.), r_0)$ such that the following holds for any initial condition $(\phi(.), r_0)$:*

$$E[\int_0^\infty \|x(t)\|^2 dt \mid \phi(.), r_0] \leq T(\phi(.), r_0) \tag{4.5}$$

where ϕ is the initial condition function.

Definition 4.2. *[135]: System (4.1) is said to be stochastically stabilizable if there exist a state feedback controller $u(t) = K(\alpha_t)x(t)$ such that the closed-loop system is stochastically stable (SS), where $K(\alpha_t)$ is constant gain matrix for any given $\alpha_t \in \mathcal{S}$.*

The following lemma will be applied in the subsequent stability analysis of the congestion control algorithms and is presented next. The proof of the lemma can be found in [151].

Lemma 4.1. *[151]: For any symmetric positive definite matrix $W > 0$, scalar $a > 0$ and vector function: $x : [0; a] \to R^n$ such that the integrations concerned are well-defined, the following inequality holds:*

$$(\int_0^a x(s)ds)^T W (\int_0^a x(s)ds) \leq a \int_0^a x^T(s)Wx(s)ds \tag{4.6}$$

4.2 Switching Control of MJLS with Constraints

As presented above, the Markovian jump linear system (MJSL) (4.1) has a group of modes $\alpha_t \in \mathcal{S}$, and jumps among the modes that take place stochastically according to the switching rule (4.4). At each instant time, only one mode is operated. In this section, we consider the switching control problem of MJLS (4.1) with constraints. That is, for each mode α_t, the MJLS has the following physical constraint:
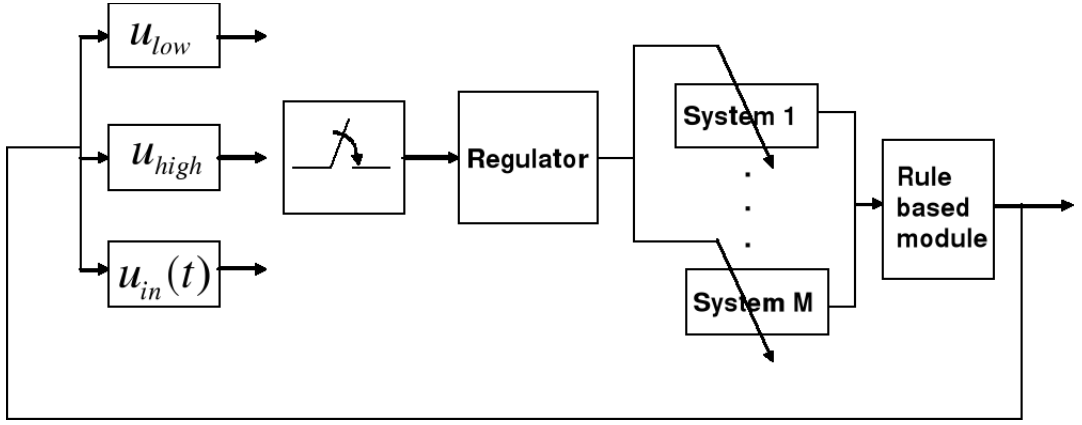
Figure 4.1: The framework of the switching control of MJLS with constrained input.

$$u_{low} \leq u(t) \leq u_{high} \qquad (4.7)$$

where u_{low} and u_{high} are the minimum and maximum bound of the input signal. According to the switching control, as presented in Chapter 2, the switching controller for the MJLS system (4.1) with the constraint (4.7) is selected as

$$u(t) \quad = \quad \begin{cases} u_{low} & \text{if } u_{in}(t) < u_{low}; \\ u_{in}(t) & \text{if } u_{low} \leq u_{in}(t) \leq u_{high}; \\ u_{high} & \text{if } u_{in}(t) > u_{high}. \end{cases} \qquad (4.8)$$

Therefore, the control input of the system (4.1) will switch among three different values. The closed-loop of the MJLS (4.1) will then have two levels of switchings, one stochastic switching as defined in (4.4) and one deterministic switching as defined in (4.8). The switching control framework of the MJLS is shown in the Fig. 4.1. As shown in Fig. 4.1, the first level of switching is caused by the Markovian chain $\alpha_t \in \mathcal{S}$. The probability of switching among the different modes α_t is determined by the probability distribution function (4.4). Each mode α_t is corresponded to a specific topology of the mobile network. Therefore, the total number of possible network topologies is M. The second level of switching is induced by the switching controller $u(t)$. That is, for each network topology $\alpha_t \in \mathcal{S} = \{1, ..., M\}$ the control input $u(t)$ switches among the three values, namely u_{low}, u_{high}, and $u_{in}(t)$.

137

We define the closed-loop system with the control signal u_{low} or u_{high} as the *edge modes* and the closed-loop system with the input $u(t)$ as the *normal control mode*. Obviously, for each subsystem $\alpha_t \in \mathcal{S}$, one expects that the system will remain in the normal control mode as long as possible. Therefore, similar as before, an extra regulator is added to adjust the system parameters to force it to move towards the safe operating range. The regulation strategy is also dependent on the Markovian chain α_t.

In the remaining of this chapter, the above switching control approach is applied to the congestion control problem of mobile Diff-Serv networks with physical constraints. For each traffic class, the switching congestion controller (SCC) is developed based on its corresponding physical constraints. The multiple modes of the closed-loop system need to be then analyzed for deriving the regulation strategies of the traffic compression gains. The detailed synthesis and analysis of the centralized and the decentralized SCC are presented in the following two sections.

4.3 Centralized Markovian Jump Switching Congestion Control (MJ-SCC) Scheme

The centralized dynamic model of the mobile ad hoc networks as given in Chapter 2 are re-written here again:

$$\dot{x}_p(t) = -F(x_p(t))u_p(t) + \lambda_p(t) + \sum_{l=1}^{m(\alpha_t)} G_l F(x_p(t - \tau_l(t)))u_p(t - \tau_l(t)) \qquad (4.9)$$

$$\dot{x}_r(t) = -F(x_r(t))u_{r1}(t) + u_{r2}(t) + \sum_{l=1}^{m(\alpha_t)} G_l F(x_r(t - \tau_l(t)))u_{r1}(t - \tau_l(t)) \quad (4.10)$$

where $m(\alpha_t)$ is the number of possible delays in the network, depending on the network topology at time t, $x_p(t)$ and $x_r(t)$ denote the queuing states of the premium and the ordinary traffic, respectively, $u_p(t)$ and $u_r(t)$ denotes the input signals for the premium and the ordinary traffic, respectively, $\lambda_p(t)$ is the unknown but bounded external incoming premium traffic, and $\tau_l(t)$ are the unknown multiple and time-varying delays.

The physical constraints of the premium and the ordinary traffic in the mobile

network are listed as

$$0 \leq x_p(t) \leq x_p^{max} \tag{4.11}$$

$$0 \leq u_p(t) \leq C_{server}(\alpha_t) \tag{4.12}$$

$$0 \leq \lambda_p(t) \leq \lambda_p^{max} < C_{server}(\alpha_t) \tag{4.13}$$

$$0 \leq x_r(t) \leq x_r^{max} \tag{4.14}$$

$$0 \leq u_{r1}(t) \leq c_r(\alpha_t) \tag{4.15}$$

$$0 \leq u_{r2}(t) \leq \lambda_r^{max} < c_r(\alpha_t) \tag{4.16}$$

$$c_r(\alpha_t) = C_{server}(\alpha_t) - u_p(t) \tag{4.17}$$

where x_p^{max} and x_r^{max} denote the buffer size of the premium and the ordinary traffic, respectively, $C_{server}(\alpha_t)$ is the mode-dependent link capacity, λ_p^{max} and λ_r^{max} denote the maximum allowable traffic rate of the premium and the ordinary traffic, respectively, and $c_r(\alpha_t)$ is the leftover capacity from the premium traffic which is also dependent on the mode α_t.

The congestion control problem of mobile Diff-Serv networks is then to select the controllers $u_p(t)$ and $u_r(t)$, which have considered the physical constraints (4.11), so that the queuing length of the premium and the ordinary traffic will convergence to their corresponding reference values. It should be noted that since the physical constraints of the mobile network $C_{server}(\alpha_t)$ and $c_r(\alpha_t)$ are mode-dependent, the switching congestion controller and the regulation strategy of the system under the edge modes are indeed mode-dependent which is clearly more complicated than the control of fixed Diff-Serv networks. In the following subsections, the centralized switching congestion control strategy for the premium and the ordinary traffic will be presented based on the dynamic queuing models of mobile networks.

4.3.1 Centralized MJ-SCC of Premium Traffic in Mobile Networks

According to the switching control approach, the congestion control strategy for the premium traffic is selected as

$$
u_p(t) = \begin{cases} 0 & \text{if } \bar{u}_p(t) < 0 \\ \bar{u}_p(t) & \text{if } 0 \leq \bar{u}_p(t) \leq C_{server}(\alpha_t) \\ C_{server}(\alpha_t) & \text{if } \bar{u}_p(t) > C_{server}(\alpha_t) \end{cases} \tag{4.18}
$$

where the first and the third controllers are refereed to as the *edge modes*, and the second controller is refereed to as the *normal control mode*. Due to the nonlinearity of the system and the unknown input traffic $\lambda_p(t)$, the normal controller $\bar{u}_p(t)$ is designed according to the feedback linearization technique [78] and the robust adaptive control theory [128] and is selected as

$$
\bar{u}_p(t) = F^{-1}(x_p, t)[K_p(\alpha_t)\bar{x}_p(t) + \hat{\lambda}_p(t)] \tag{4.19}
$$

where $\bar{x}_p(t) = x_p(t) - x_p^{ref}$, x_p^{ref} is the reference queuing lengthes of the premium traffic in the nodes selected by the network operator, $K_p(\alpha_t)$ is the mode dependent control gain, and $\hat{\lambda}_p(t)$ is the adaptive estimator used to estimate the unknown external incoming traffic $\lambda_p(t)$ to compensate for its effect via feedback. The updating rule of $\hat{\lambda}_p(t)$ is defined as follows:

$$
\dot{\hat{\lambda}}_p(t) = \begin{cases} \Delta_p(\alpha_t)\bar{x}_p(t) - \Pi_p(\alpha_t)\hat{\lambda}_p(t) & \text{if } 0 \leq \hat{\lambda}_p(t) \leq \lambda_p^{max} \text{ or} \\ & \quad \hat{\lambda}_p(t) = 0, \ \bar{x}_p(t) \geq 0 \text{ or} \\ & \quad \hat{\lambda}_p(t) = \lambda_p^{max}, \ \bar{x}_p(t) \leq 0 \\ -\Pi_p(\alpha_t)\hat{\lambda}_p(t) & \text{otherwise} \end{cases} \tag{4.20}
$$

where $\Delta_p(\alpha_t)$ and $\Pi_p(\alpha_t)$ are the mode dependent adaptive control gains which need to be selected.

It should be noted that the dynamic queuing system (4.9) and the physical constraints (4.11) of the mobile network are mode dependent. The above congestion controller (4.18) and the adaptive estimator (4.20) need to be updated at each time when the

network topology is changed. That is, the control gains $K_p(\alpha_t)$, $\Delta_p(r_r)$, and $\Pi_p(\alpha_t)$ are also dependent on the Markovian chain α_t.

Moreover, after applying the switching congestion control strategy (4.18), the dynamics of the mobile network (4.9) will experience multiple modes depending on the different choices of the controller in (4.18). The detailed analysis of each mode is given below.

- **Edge Mode (i):** If $u_p(t) = 0$ at some time $t = t_1$ for the mode $\alpha_t = k$, $k \in \mathcal{S}$, this implies that the queuing state $x_p(t)$ of the mode k is sufficiently small. The closed-loop system of the premium traffic (4.9) will become

$$\dot{x}_p(t) \;=\; \lambda_p(t) + \sum_{l=1}^{m(k)} G_l F(x_p(t - \tau_l(t))) u_p(t - \tau_l) > 0 \tag{4.21}$$

Since $\dot{x}_p(t) > 0$, the queuing length will increase with the time. Therefore, after some finite time $t_2 > t_1$, one will have $\bar{u}_p(t) > 0$ and the normal controller $\bar{u}_p(t)$ will be chosen and take effect. The traffic compression gains G_l need not be regulated under this mode. The above analysis holds for any mode $\alpha_t \in \mathcal{S}$.

- **Edge Mode (ii):** If $u_p(t) = C_{server}(\alpha_t)$ for the mode $\alpha_t = k$, $k \in \mathcal{S}$, at some time $t = t_3$, this implies that the queuing state $x_p(t)$ of the mode k is sufficiently large. The closed-loop system of (4.9) will now be governed by:

$$
\begin{aligned}
\dot{x}_p(t) \;&=\; -F(x_p(t)) C_{server}(k) + \lambda_p(t) + \sum_{l=1}^{m(k)} G_l F(x_p(t - \tau_l(t))) u_p(t - \tau_l) \\
&\approx\; -C_{server}(k) + \lambda_p(t) + \sum_{l=1}^{m(k)} G_l F(x_p(t - \tau_l(t))) u_p(t - \tau_l) \\
&\leq\; -C_{server}(k) + \lambda_p^{max} + \sum_{l=1}^{m(k)} G_l \lambda_p^{max}
\end{aligned}
\tag{4.22}
$$

where λ_p^{max} is the maximum allowable traffic rate induced by the transmitter constraint (2.17) of the nodes.

The control strategy in this mode is to regulate the traffic compression gains G_l, so that the queuing state $x_p(t)$ will decrease. According to the dynamic equation

141

(4.22), the traffic compression gains for the mode α_t are selected as

$$0 \leq \sum_{l=1}^{m(k)} G_l < (C_{server}(k) - \lambda_p^{max})(\lambda_p^{max})^+ \tag{4.23}$$

where $+$ denotes the Moor-Penrose inverse [103] of the vector λ_p^{max}. The queuing length $x_p(t)$ of the mode α_t will decrease, and after some time $t_4 > t_3$ the normal controller $\bar{u}_p(t)$ will take effect.

It should be noted that the regulation strategy (4.23) is derived based on the mode k. Suppose that the network has switched from mode k to another mode $\alpha_t = j$, $j \in \mathcal{S}$, at some time $t = t_5$, before the normal controller $\bar{u}_p(t)$ takes effect. Then it implies that:

$$\bar{u}_p(t_5) > C_{server}(k) \tag{4.24}$$

Since the network topology has changed, the switching controller (4.18) will be recalculated with respect to the mode j and the following two cases may be considered:

- If $C_{server}(j) < C_{server}(k)$, this implies that certain nodes move away from the network and the number of links in the network decreases. We will now have

$$\bar{u}_p(t_5) > C_{server}(j) \tag{4.25}$$

  According to (4.23), the traffic compression gains will be recalculated as

$$0 \leq \sum_{l=1}^{m(j)} G_l < (C_{server}(j) - \lambda_p^{max})(\lambda_p^{max})^+ \tag{4.26}$$

  It turns out in this case since the link capacity of the nodes decreases, the traffic compression gains are required to decrease too. Hence, the traffic load in the network will reduce and the threat of congestion will be alleviated.

- If $C_{server}(j) > C_{server}(k)$, this implies that extra nodes move into the network and the link capacity of the nodes increases. Therefore, we will have

$$u_p(t) = \begin{cases} \bar{u}_p(t) & \text{if } \bar{u}_p(t) < C_{server}(j) \\ C_{server}(j) & \text{otherwise} \end{cases} \tag{4.27}$$

  Therefore, the normal controller $\bar{u}_p(t)$ will take effect in case there is enough capacity. On the other hand, if there is still not enough capacity, the regulation strategy (4.26) will than be applied.

Therefore, after some finite time, the normal controller $\bar{u}_p(t)$ will take effect for the modes $\alpha_t \in \mathcal{S}$.

- **Normal Control Mode (iii):** If $u_p(t) = \bar{u}_p(t)$ at some time $t = t_5$ for the mode $\alpha_t = k$, $k \in \mathcal{S}$, the closed-loop system of (4.9) will become

$$\dot{x}_p(t) = -K_p(k)\bar{x}_p(t) - \hat{\lambda}_p(t) + \lambda_p(t) + \sum_{l=1}^{m(k)} G_l F(x_p(t - \tau_l(t)))u_p(t - \tau_l(t)) \quad (4.28)$$

Now we need to analyze the incoming traffic from the neighboring nodes. The equation (4.24) can be written as

$$\begin{aligned}
\dot{x}_p(t) &= -K_p(k)\bar{x}_p(t) - \hat{\lambda}_p(t) + \lambda_p(t) \quad &(4.29) \\
&\quad + \sum_{l=1}^{m_1(k)} G_l C_{server} + \sum_{l=1}^{m_2(k)} G_l[K_p(k)\bar{x}_p(t - \tau_l(t)) + \hat{\lambda}_p(t - \tau_l(t))]
\end{aligned}$$

where $m_1(k)$ is the number of neighbor nodes which take the maximum value of the controller $C_{server}(k)$, $m_2(k)$ is the number of neighbor nodes which take the value of the normal controller $\bar{u}_p(t - \tau_l(t))$, and the other neighbors which take the minimum value of the controller 0 are included in the equation (4.25). The above system can be written in the following state space representation

$$\begin{aligned}
\dot{x}_p(t) &= -K_p(k)\bar{x}_p(t) - \hat{\lambda}_p(t) + \lambda_p(t) \quad &(4.30) \\
&\quad + \sum_{l=1}^{m(k)} G_l B_c C_{server} + \sum_{l=1}^{m(k)} G_l B_l[K_p(k)\bar{x}_p(t - \tau_l(t)) + \hat{\lambda}_p(t - \tau_l(t))]
\end{aligned}$$

where the system matrices B_c and B_l are defined as

$$B_c = \begin{cases} I & \text{if } u_p(t - \tau_l(t)) = C_{server}(k) \\ 0 & \text{otherwise} \end{cases}$$

$$B_l = \begin{cases} I & \text{if } u_p(t - \tau_l(t)) = \bar{u}_p(t - \tau_l(t)) \\ 0 & \text{otherwise} \end{cases}$$

Now all the operational modes of the system (4.9) is completed after applying the switching controller (4.18). By selecting the traffic compression gains according to (4.23), the dynamic model of the premium traffic for the mobile network (4.9) will operate under the *normal control mode* and can be expressed as the Markovian jump linear system with multiple and time-varying delays (4.30).

Let us compare the above regulation strategies of the traffic compression gains with that of the fixed network, as presented in the Section 3.1.1. One can note that for the fixed network we only need to calculate the traffic compression gain matrix G_l once, according to (3.13). On the contrary, for the mobile network, since the network topology is dependent on the Markov chain α_t, one needs to check the link capacity whenever the network topology is changed. The traffic compression gains G_l have to be then re-calculated again so to guarantee that the system (4.9) with respect to each mode α_t will operate in the safe range (normal control mode).

The centralized switching congestion control strategy for the premium traffic in mobile networks has two levels of switchings. As shown in Fig. 4.1, the first level switching induced by the change of network topology is represented by the Markov chain $\alpha_t \in \mathcal{S}$, $\mathcal{S} = \{1, ..., M\}$. The switchings among different modes α_t are governed by the probability function (4.4). For each mode α_t, the control input switches among three values according to the network constraints. When the control input switches to the edge mode, 0 or $C_{server}(\alpha_t)$, the regulation mechanism will adjust the traffic compression gains within the network to force the queuing states change toward the normal control mode. After some finite time, the normal controller $\bar{u}_p(\alpha_t)$ will then be selected.

Now, let us we define the estimation error of the unknown external incoming traffic $\bar{\lambda}_p(t) = \hat{\lambda}_p(t) - \lambda_p(t)$ as a new state and define the a new state space as $z_p(t) = \begin{bmatrix} \bar{x}_p^T(t) & \bar{\lambda}_p^T(t) \end{bmatrix}^T$. The closed-loop system (4.30) together with the adaptive estimator (4.20) can be expressed as

$$\dot{z}_p(t) = D_k(\alpha_t)z_p(t) + \sum_{l=1}^{m(\alpha_t)} F_l(\alpha_t)z_p(t - \tau_l(t)) + \sum_{l=1}^{m(\alpha_t)} H_l(\alpha_t)v_l(\alpha_t) \quad (4.31)$$

$$z_p(t) = \varphi(t), t \in [-h, 0]$$

$$k \in \wp, \wp = 1, 2$$

$$\alpha_t \in \mathcal{S}, \mathcal{S} = 1, ..., M$$

where $\varphi(t)$ is a continuous function representing the initial condition of the delay system, $k \in \wp, \wp = 1, 2$ is the deterministic switching introduced from the adaptive estimator $\hat{\lambda}_p(t)$, and is defined in the set $\wp$ with two values, α_t is the stochastic switching that is

induced by the changes of the neighboring set, $v_l(t)$ is the external signal, and $D_k(\alpha_t)$, $F_l(\alpha_t)$, $H_l(\alpha_t)$ are the system matrices that are defined as follows:

$$D_1(\alpha_t) = \begin{bmatrix} -K_p(\alpha_t) & -I \\ \Delta_p(\alpha_t) & -\Pi_p(\alpha_t) \end{bmatrix} \qquad D_2(\alpha_t) = \begin{bmatrix} -K_p(\alpha_t) & -I \\ 0 & -\Pi_p(\alpha_t) \end{bmatrix}$$

$$F_l = \begin{bmatrix} G_l B_l K_p(\alpha_t) & G_l B_l \\ 0 & 0 \end{bmatrix} \qquad H_l(\alpha_t) = \begin{bmatrix} 0 & 0 & G_l B_l & G_l B_c \\ -\Pi_p(\alpha_t) & -I & 0 & 0 \end{bmatrix}$$

$$v_l^T(\alpha_t) = \begin{bmatrix} \lambda_p(t) & \dot{\lambda}_p(t) & \lambda_p(t - \tau_l(t)) & C_{server}(\alpha_t) \end{bmatrix}$$

The above system is a hybrid system with multiple and time-varying delays. There are two levels of switchings in the system (4.31). The first switching level is represented by the Markov chain α_t, and the second switching level is given by the arbitrary switching parameter k. Therefore, the congestion control problem for the premium traffic of mobile networks is to select the control gains $K_p(\alpha_t)$, $\Delta_p(\alpha_t)$, and $\Pi_p(\alpha_t)$ so that the closed-loop system (4.31) is stable.

The control objective for the premium traffic is now to select the mode-dependent control gain $K_p(\alpha_t)$ and the adaptive control gains $\Delta_p(\alpha_t)$ and $\Pi_p(\alpha_t)$, as presented in the system matrices $D_k(\alpha_t)$ and $F_l(\alpha_t)$, so that the closed-loop system (4.31) is stable. The following lemma provides the stability conditions of the system (4.31).

Lemma 4.2. *Consider the system (4.31). If there exist symmetric positive definite matrices $P(\alpha_t)$, $Q(\alpha_t)$, R, and positive definite matrices $M(\alpha_t)$ and $N(\alpha_t)$ such that the following matrix inequality condition is satisfied for all the modes $\alpha_t \in \mathcal{S}$, $\mathcal{S} = \{1, ..., M\}$:*

$$W_k(\alpha_t) = \begin{bmatrix} w_{k1}(\alpha_t) & w_{k2}(\alpha_t) & R \\ * & w_3(\alpha_t) & 0 \\ * & * & -R - (1-h)Q_{\alpha_t} \end{bmatrix} < 0 \quad k = 1, 2 \quad (4.32)$$

where

$$w_{k1}(\alpha_t) = (2P(\alpha_t) + h^2 D_k^T(\alpha_t)R)D_k(\alpha_t) + \sum_{l=1}^{M} \pi_{\alpha_t l} P(l) + (1+h)Q(\alpha_t) - R + M(\alpha_t)$$

$$w_{k2}(\alpha_t) = (h^2 D_k^T(\alpha_t)R + P(\alpha_t))F(\alpha_t)$$

$$w_3(\alpha_t) = h^2 F^T(\alpha_t)(R + N(\alpha_t))F(\alpha_t)$$

145

then the system (4.31) is stochastically ultimately bounded. The radius of the stochastic bounded region is $max\{\rho_k(\alpha_t)\}|_k = \frac{\lambda_{min}(\Psi(\alpha_t))}{\lambda_{max}(-W_k(\alpha_t))}\|v(\alpha_t)\|^2$, $k = 1, 2$, where λ_{max} and λ_{min} indicate the maximum and the minimum eigenvalues of the corresponding matrices, respectively.

Proof: Consider the following stochastic Lyapunov-Krasovskii functional:

$$V(z_p(t), \alpha_t) = V_1 + V_2 + V_3 + V_4 \tag{4.33}$$

$$V_1 = z_p(t)^T P(\alpha_t) z_p(t) \tag{4.34}$$

$$V_2 = \int_{t-h}^t z_p^T(s) Q(\alpha_t) z_p(s) ds \tag{4.35}$$

$$V_3 = h \int_{-h}^0 \int_{t+\theta}^t \dot{z}_p^T(s) R \dot{z}_p(s) ds d\theta \tag{4.36}$$

$$V_4 = \int_{-h}^0 \int_{t+\theta}^t z_p^T(s) Q(\alpha_t) z_p(s) ds d\theta \tag{4.37}$$

where $P(\alpha_t)$, $Q(\alpha_t)$, R are positive definite matrices with appropriate dimensions. Let $\mathcal{L}$ denote the infinitesimal generator of $z_t, \alpha_t, t \geq 0$. Then, for each $\alpha_t = k \in \mathcal{S}$ we have

$$
\begin{aligned}
\mathcal{L}V_1 &= \lim_{\Delta \to 0^+} \frac{1}{\Delta} \{E[V_1(z_p(t+\Delta), \alpha_{t+\delta}, t+\Delta)|z_p(t), \alpha_t = k] - V_1(z_p(t), k, t)\} \\
&= \lim_{\Delta \to 0^+} \frac{1}{\Delta} \{\sum_{l \neq k} (\pi_{lk}\Delta + o(\Delta) z_p^T(t+\Delta) P(\alpha_{t+\delta}) z_p(t+\Delta) \\
&\quad + (1 + \pi_{kk}\Delta + o(\Delta)) z_p^T(t+\Delta) P(\alpha_{t+\delta}) z_p(t+\Delta)) - z_p^T(t) P(\alpha_t) z_p(t)\} \\
&= 2z_p^T(t) P(\alpha_t) \dot{z}_p(t) + \sum_{k=1}^M \pi_{\alpha_t k} z_p^T(t) P(k) z_p(t) \\
&= 2z_p^T(t) P(\alpha_t) [D_k(\alpha_t) z_p(t) + \sum_{l=1}^{m(\alpha_t)} F_l(\alpha_t) z_p(t - \tau_l(t))] \\
&\quad + z_p^T(t) \sum_{k=1}^M \pi_{\alpha_t k} P(k) z_p(t) + 2z_p^T(t) P(\alpha_t) \sum_{l=1}^{m(\alpha_t)} H(\alpha_t) v_l(\alpha_t) \\
\mathcal{L}V_2 &= \int_{t-h}^t 2z_p^T(s) Q(\alpha_t) \dot{z}_p(s) ds + \int_{t-h}^t z_p^T(s) \sum_{k=1}^M \pi_{\alpha_t k} Q(k) z_p(s) ds \\
&= z_p^T(t) Q(\alpha_t) z_p(t) - (1 - h) z_p^T(t - h) Q(\alpha_t) z_p(t - h) \\
&\quad + \int_{t-h}^t z_p^T(s) \sum_{k=1}^M \pi_{\alpha_t k} Q(k) z_p(s) ds
\end{aligned}
$$

146

$$\mathcal{L}V_3 = h^2 \dot{z}_p^T(t)R\dot{z}_p(t) - h\int_{t-h}^{t} \dot{z}_p^T(s)R\dot{z}_p(s)ds$$

$$= h^2[D_k(\alpha_t)z_p(t) + \sum_{l=1}^{m(\alpha_t)} F_l(\alpha_t)z_p(t-\tau_l(t)) + \sum_{l=1}^{m(\alpha_t)} H_l(\alpha_t)v_l(\alpha_t)]^T R$$

$$[D_k(\alpha_t)z_p(t) + \sum_{l=1}^{m(\alpha_t)} F_l(\alpha_t)z_p(t-\tau_l(t)) + \sum_{l=1}^{m(\alpha_t)} H_l(\alpha_t)v_l(\alpha_t)]$$

$$-h\int_{t-h}^{t} \dot{z}_p^T(s)R\dot{z}_p(t)ds$$

$$\mathcal{L}V_4 = hz_p^T(t)Q(\alpha_t)z_p(t) - \int_{t-h}^{t} z_p^T(s)\sum_{k=1}^{M} \pi_{\alpha_t k}Q(k)z_p(s)ds$$

Now, by applying Lemma 4.1 to $\mathcal{L}V_3$ one obtains

$$h\int_{t-h}^{t} \dot{z}_p^T(s)R\dot{z}_p(s)s \geq (z_p(t) - z_p(t-h))^T R(z_p(t) - z_p(t-h)) \qquad (4.38)$$

Combining the above, we get

$$\mathcal{L}V \leq z_p^T(t)(2P(\alpha_t)D_k(\alpha_t) + \sum_{k=1}^{M} \pi_{\alpha_t k}P(k) + (1+h)Q(\alpha_t))z_p(t)$$

$$+h^2 z_p^T(t)(D_k^T(\alpha_t)RD_k(\alpha_t) - R)z_p(t)$$

$$+2z_p^T(t)(h^2 D_k^T(\alpha_t)R + P(\alpha_t))\sum_{l=1}^{m(\alpha_t)} F_l(\alpha_t)z_p(t-\tau_l(t))$$

$$+h^2(\sum_{l=1}^{m(\alpha_t)} F_l(\alpha_t)z_p(t-\tau_l(t)))^T R(\sum_{l=1}^{m(\alpha_t} F_l(\alpha_t)z_p(t-\tau_l(t)))$$

$$+2z_p^T(t)Rz_p(t-h) - z_p^T(t-h)(R + (1-h)Q(\alpha_t))z_p(t-h)$$

$$+h^2(\sum_{l=1}^{m(\alpha_t)} H_l(\alpha_t)v_l(\alpha_t))^T R(\sum_{l=1}^{m(\alpha_t)} H_l(\alpha_t)v_l(\alpha_t))$$

$$+2z_p^T(t)(h^2 D_k(\alpha_t)R + P(\alpha_t))\sum_{l=1}^{m(\alpha_t)} H_l(\alpha_t)v_l(\alpha_t)$$

$$+2h^2(\sum_{l=1}^{m(\alpha_t)} F_l(\alpha_t)z_p(t-\tau_l(t)))^T(\sum_{l=1}^{m(\alpha_t)} H_l(\alpha_t)v_l(\alpha_t))$$

By using the fact that

$$\sum_{l=1}^{m(\alpha_t)} F_l(\alpha_t)z_p(t-\tau_l(t)) = F(\alpha_t)z_p(t-\tau) \quad \text{and} \quad \sum_{l=1}^{m(\alpha_t)} H_l(\alpha_t)v_l(\alpha_t) = H(\alpha_t)v(\alpha_t) \;(4.39)$$

where

$$F(\alpha_t) = vec\{F_l(\alpha_t)\} \qquad v_t(\alpha_t) = vec\{v_l^T(\alpha_t)\}$$

$$H(\alpha_t) = vec\{H_1(\alpha_t)\} \qquad z_p(t-\tau) = vec\{z_p^T(t-\tau_l(t))\} \quad l = 1,...,m(\alpha_t)$$

147

and defining $Y(\alpha_t) = h^2 D_k(\alpha_t)R + P(\alpha_t)$, and applying the Park's inequality (3.24) [129] to the last two terms in $\mathcal{L}V$, one can obtain

$$2z_p^T(t)Y(\alpha_t)H(\alpha_t)v(\alpha_t) \leq z_p^T(t)M(\alpha_t)z_p(t) + (H(\alpha_t)v(\alpha_t))^T Y^T(\alpha_t)M^{-1}(\alpha_t)Y(\alpha_t)H(\alpha_t)v(\alpha_t)$$

$$2(F(\alpha_t)z_p(t-\tau))^T H(\alpha_t)v(\alpha_t) \leq (F(\alpha_t)z_p(t-\tau))^T N(\alpha_t)F(\alpha_t)z_p(t-\tau)$$

$$+(H(\alpha_t)v(\alpha_t))^T N^{-1}(\alpha_t)H(\alpha_t)v(\alpha_t)$$

where M_{rt} and $N(\alpha_t)$ are arbitrary positive definite matrices. Therefore, the infinitesimal generator of the Lyapunov function $V(z_p(t), \alpha_t)$ will become

$$
\begin{aligned}
\mathcal{L}V \leq\; & z_p^T(t)(2P(\alpha_t)D_k(\alpha_t) + \sum_{k=1}^{M}\pi_{\alpha_t l}P(k) + (1+h)Q(\alpha_t))z_p(t) \\
& +h^2 z_p^T(t)(D_k^T(\alpha_t)RD_k(\alpha_t) - R + M(\alpha_t))z_p(t) \\
& +2z_p^T(t)(h^2 D_k^T(\alpha_t)R + P(\alpha_t))F(\alpha_t)z_p(t-\tau) \\
& +h^2(F(\alpha_t)z_p(t-\tau))^T(R + N(\alpha_t))(F(\alpha_t)z_p(t-\tau)) \\
& +2z_p^T(t)Rz_p(t-h) - z_{t-h}^T(R + (1-h)Q_{rt})z_p(t-h) \\
& +h^2(H(\alpha_t)v(\alpha_t))^T RH(\alpha_t)v(\alpha_t) + (H(\alpha_t)v(\alpha_t))^T Y^T(\alpha_t)M^{-1}(\alpha_t)Y(\alpha_t)H(\alpha_t)v(\alpha_t) \\
& +h^2(H(\alpha_t)v(\alpha_t))^T N^{-1}(\alpha_t)H(\alpha_t)v(\alpha_t) \\
=\; & z_p^T(t)(2P(\alpha_t)D_k(\alpha_t) + \sum_{k=1}^{M}\pi_{\alpha_t l}P(k) + (1+h)Q(\alpha_t))z_p(t) \\
& +h^2 z_p^T(t)(D_k^T(\alpha_t)RD_k(\alpha_t) - R + M(\alpha_t))z_p(t) \\
& +2z_p^T(t)(h^2 D_k^T(\alpha_t)R + P(\alpha_t))F(\alpha_t)z_p(t-\tau) \\
& +h^2 z_{t-\tau}^T F^T(\alpha_t)(R + N(\alpha_t))F(\alpha_t)z_p(t-\tau) \\
& +2z_p^T(t)Rz_p(t-h) - z_{t-h}^T(R + (1-h)Q(\alpha_t))z_p(t-h) \\
& +v^T(\alpha_t)H^T(\alpha_t)(h^2 R + Y^T(\alpha_t)M^{-1}(\alpha_t)Y(\alpha_t) + h^2 N^{-1}(\alpha_t))H(\alpha_t)v(\alpha_t) \\
=\; & \eta^T(t,\tau,h)W_k(\alpha_t)\eta(t,\tau,h) + v^T(\alpha_t)\Psi(\alpha_t)v(\alpha_t) \qquad\qquad (4.40)
\end{aligned}
$$

where

$$
W_k(\alpha_t) = \begin{bmatrix} w_{k1}(\alpha_t) & w_{k2}(\alpha_t) & R \\ * & w_3(\alpha_t) & 0 \\ * & * & -R - (1-h)Q(\alpha_t) \end{bmatrix}
$$

148

$$w_{k1}(\alpha_t) = (2P(\alpha_t) + h^2 D_k^T(\alpha_t)R)D_k(\alpha_t) + \sum_{l=1}^{M} \pi_{\alpha_t l}P(l) + (1+h)Q(\alpha_t) - R + M(\alpha_t)$$

$$w_{k2}(\alpha_t) = (h^2 D_k^T(\alpha_t)R + P(\alpha_t))F(\alpha_t)$$

$$w_3(\alpha_t) = h^2 F^T(\alpha_t)(R + N(\alpha_t))F(\alpha_t)$$

$$\Psi(\alpha_t) = H^T(\alpha_t)(h^2 R + Y^T(\alpha_t)M^{-1}(\alpha_t)Y(\alpha_t) + h^2 N^{-1}(\alpha_t))H(\alpha_t)$$

$$\eta(t,\tau,h) = \left[\begin{array}{ccc} z_p^T(t) & z^T(t-\tau) & z^T(t-h) \end{array} \right]^T$$

Since $W_k(\alpha_t) < 0$, for any $\eta(t,\tau,h)$ that satisfies:

$$-\eta^T(t,\tau,h)W_k(\alpha_t)\eta(t,\tau,h) \geq v^T(\alpha_t)\Psi(\alpha_t)v(\alpha_t) \tag{4.41}$$

we will have

$$\mathcal{L}V \leq 0 \tag{4.42}$$

Therefore, according to the Definition.4.1, the system (4.9) is stochastically ultimately bounded. The radius of the ultimately bounded region is given by:

$$\rho_k(\alpha_t) = \frac{\lambda_{max}(\Psi(\alpha_t))}{\lambda_{min}(-W_k(\alpha_t))}\|v(\alpha_t)\|^2 \tag{4.43}$$

and this completes the proof of Lemma. ∎

Lemma 4.2 shows that the switching controller (4.18)-(4.20) together with the regulation strategy (4.23) is a stabilizing control strategy for the Markovian jump system (4.9). But the stability condition (4.32) is not linear with respect to the system matrices, which contains the control gains $K_p(\alpha_t)$, $\Delta_p(\alpha_t)$, and $\Pi_p(\alpha_t)$. Hence, it can not be solved directly. To tackle this problem, the following lemma is presented to transform the nonlinear matrix inequality $W_k(\alpha_t)$ into a standard linear matrix inequality (LMI) condition which therefore gives the expression of the controllers.

Lemma 4.3. *Consider the system (4.31). If there exist symmetric positive definite matrices $X(\alpha_t)$, $N(\alpha_t)$, $\bar{Q}(\alpha_t)$, R, Z, and matrices $U_k(\alpha_t)$, $\bar{V}_k(\alpha_t)$, $\bar{R}_k(\alpha_t)$, for $k = 1, 2$,*

$\alpha_t \in S = \{1, \ldots, M\}$ such that the following LMI conditions are satisfied:

$$\Omega_k(\alpha_t) = \begin{bmatrix} \theta_{k1}(\alpha_t) & \theta_{k2}(\alpha_t) & X^T(\alpha_t) \\ * & \theta_3(\alpha_t) & 0 \\ * & * & -Z - (1-h)\bar{Q}_{\alpha_t} \end{bmatrix} < 0 \qquad (4.44)$$

$$\theta_{k1}(\alpha_t) = U_k(\alpha_t) + U_k^T(\alpha_t) + h^2 \bar{R}_k(\alpha_t) + (1 + h + \sum_{l=1}^{M} \pi_{\alpha_t l}) X^T(\alpha_t)$$

$$\theta_{k2}(\alpha_t) = \bar{V}_k(\alpha_t) + I$$

$$\theta_3(\alpha_t) = h^2 (R + N(\alpha_t))$$

then the matrix inequality condition in Lemma 4.2 holds and the system (4.31) is ultimately bounded.

Proof: Consider the nonlinear matrix $W_k(\alpha_t)$, and let us define the following matrices:

$$X(\alpha_t) = P^{-1}(\alpha_t)$$

$$Y(\alpha_t) = F^{-1}(\alpha_t)$$

$$Z = R^{-1}$$

$$\Lambda(\alpha_t) = diag\{X(\alpha_t), Y(\alpha_t), Z\}$$

Then, by pre and post multiplying (4.32) with $\Lambda(\alpha_t)$ and $\Lambda^T(\alpha_t)$, respectively, the matrix $W_k(\alpha_t)$ becomes

$$\begin{aligned} \Omega_k(\alpha_t) &= \Lambda^T(\alpha_t) W_k(\alpha_t) \Lambda(\alpha_t) \\ &= \begin{bmatrix} \theta_{k1}(\alpha_t) & \theta_{k2}(\alpha_t) & X^T(\alpha_t) \\ * & \theta_3(\alpha_t) & 0 \\ * & * & -Z - (1-h)\bar{Q}_{\alpha_t} \end{bmatrix} \qquad (4.45) \end{aligned}$$

where

$$\theta_{k1}(\alpha_t) = U_k(\alpha_t) + U_k^T(\alpha_t) + h^2 \bar{R}_k(\alpha_t) + (1 + h + \sum_{l=1}^{M} \pi_{\alpha_t l}) X^T(\alpha_t)$$

$$\theta_{k2}(\alpha_t) = \bar{V}_k(\alpha_t) + I$$

$$\theta_3(\alpha_t) = h^2 (R + N(\alpha_t))$$

$$D_k(\alpha_t) = U_k(\alpha_t) X^{-1}(\alpha_t) \quad ; \quad \bar{R}_k(\alpha_t) = U_k(\alpha_t)^T R U_k(\alpha_t)$$

$$M(\alpha_t) = R \quad ; \quad Q(\alpha_t) = P(\alpha_t)$$

$$\bar{V}_k(\alpha_t) = U_k(\alpha_t)^T R \quad ; \quad \bar{Q}(\alpha_t) = Z^T Q(\alpha_t) Z$$

Therefore, if $\Omega_k(\alpha_t) < 0$ one will have $W_k(\alpha_t) < 0$, and hence the system (4.31) is ultimately bounded, and the system matrix $D_k(\alpha_t)$ is given by $D_k(\alpha_t) = U_k(\alpha_t)X^{-1}(\alpha_t)$. This completes the proof of Lemma 4.3. ∎

Remark 4.1. *According to Lemma 4.2 and Lemma 4.3, the stability condition (4.32) and (4.44) of the closed-loop system (4.31) is dependent on the Markov chain $\alpha_t \in \mathcal{S}$, for $\mathcal{S} = \{1, ..., M\}$. That is, at each time when the network topology is changed, one needs to re-calculate the state feedback control gain $K_p(\alpha_t)$, as well as the mode-dependent adaptive control gains $\Delta_p(\alpha_t)$ and $\Pi_p(\alpha_t)$. The congestion controller $u_p(t)$ and the adaptive estimator $\hat{\lambda}_p(t)$ are then updated with the new parameters.*

Furthermore, as pointed out earlier, when the network topology is changed, one needs to also check the new link capacities of all the nodes in the network $C_{server}(\alpha_t)$, and re-select the switching congestion controller $u_p(t)$ according to the conditions of new physical constraints.

Remark 4.2. *According to equation (4.40), the ultimately bounded region of the premium traffic in a mobile network is given by:*

$$\rho(\alpha_t) = max[\rho_k(\alpha_t)], \qquad k = 1, 2$$

$$\rho_k(\alpha_t) = \frac{\lambda_{max}(\Psi(\alpha_t))}{\lambda_{min}(-W_k(\alpha_t))}\|v(\alpha_t)\|^2 \qquad (4.46)$$

where λ_{min} and λ_{max} denote the minimum and maximum eigenvalue of a matrix, respectively. As one can see from (4.46), the system (4.31) with respect to each mode α_t may have different radius of the ultimately bounded region.

4.3.2 Centralized MJ-SCC of Ordinary Traffic in Mobile Networks

The dynamic model of the ordinary traffic in a mobile network is given by

$$\dot{x}_r(t) = -F(x_r(t))u_{r1}(t) + u_{r2}(t) + \sum_{l=1}^{m(\alpha_t)} G_l F(x_r(t - \tau_l(t)))u_{r1}(t - \tau_l) \quad (4.47)$$

where $u_{r1}(t)$ is the bandwidth controller and $u_{r2}(t)$ is the flow rate controller of the ordinary traffic.

The control objective for the ordinary traffic is to select the controllers $u_{r1}(t)$ and $u_{r2}(t)$ so that the queuing length of the ordinary traffic $x_r(t)$ in the mobile network environment will be as close as possible to its reference value x_r^{ref}. According to the physical constraints of the ordinary traffic class, as given in (4.11), the control strategy for the flow rate controller $u_{r2}(t)$ is to ensure that the ordinary incoming traffic rate $\lambda_r(t) = u_{r2}(t)$ will not exceed the maximum allowable rate $c_r(\alpha_t)$, and hence is selected as follows

$$u_{r2}(t) = \begin{cases} \lambda_r^{max} & \text{if } \lambda_r(t) \geq \lambda_r^{max}; \\ \lambda_r(t) & \text{if } \lambda_r(t) < \lambda_r^{max}. \end{cases} \tag{4.48}$$

When the incoming traffic rate $\lambda_r(t)$ is guaranteed to be within the bound, the control strategy for the bandwidth controller $u_{r1}(t)$ is designed as follows:

$$u_{r1}(t) = \begin{cases} 0 & \text{if } \bar{u}_{r1}(t) < 0 \\ \bar{u}_{r1}(t) & \text{if } 0 \leq \bar{u}_{r1}(t) \leq c_r(\alpha_t) \\ c_r(\alpha_t) & \text{if } \bar{u}_{r1}(t) > c_r(\alpha_t) \end{cases} \tag{4.49}$$

$$\bar{u}_{r1}(t) = F^{-1}(x_r, t)[K_r(\alpha_t)\bar{x}_r(t) + \hat{\lambda}_r(t)] \tag{4.50}$$

where $K_r(\alpha_t)$ is the mode-dependent feedback control gain, $\hat{\lambda}_r(t)$ is a time-varying signal used to compensate for the effects of the external signal $\lambda_r(t)$ via feedback, and is selected according to the robust adaptive control theory [128] as follows:

$$\dot{\hat{\lambda}}_r(t) = \begin{cases} \Delta_r(\alpha_t)\bar{x}_r(t) - \Pi_r(\alpha_t)\hat{\lambda}_r(t) & \text{if } 0 \leq \hat{\lambda}_r(t) \leq \lambda_r^{max} \text{ or} \\ & \qquad \hat{\lambda}_r(t) = 0, \ \bar{x}_r(t) \geq 0 \text{ or} \\ & \qquad \hat{\lambda}_r(t) = \lambda_r^{max}, \ \bar{x}_r(t) \leq 0 \\ -\Pi_r(\alpha_t)\hat{\lambda}_r(t) & \text{otherwise} \end{cases} \tag{4.51}$$

where $\Delta_r(\alpha_t)$ and $\Pi_r(\alpha_t)$ are the mode-dependent adaptive control gains which need to be designed. After applying the switching congestion controller (4.48), the closed-loop Markovian jump system (4.47) will experience multiple modes depending on the different choices of the switching controller in (4.48). Similar to the analysis in the premium traffic, the following operational modes for the ordinary traffic are considered.

- **Case (i):** If $c_r(\alpha_t) = 0$ at some time $t = t_1$, for the mode $\alpha_t = k$, $k \in \mathcal{S}$, this implies that:

152

$$C_{server}(k) - u_p(t) = 0 \qquad (4.52)$$

so that there is no leftover capacity in the network. According to the switching controller (4.48), we will have

$$u_{r1}(t) = 0, \qquad u_{r2}(t) = 0$$

Therefore, the dynamic system of the ordinary traffic (4.47) becomes:

$$\dot{x}_r(t) = \sum_{l=1}^{m(k)} G_l F(x_r(t - \tau_l(t))) u_{r1}(t - \tau_l(t)) > 0 \qquad (4.53)$$

The queuing length of the ordinary traffic will increase with the time. However, since there is no leftover capacity in the network, increasing queuing length will result in a buffer overflow and in turn cause congestion in a short time. Therefore, the only way to avoid congestion, in this case, is to reset the traffic compression gains to $G_l = 0$. Any incoming traffic from neighboring nodes are forced to be dropped out until there is an available capacity for the ordinary traffic.

- **Case (ii):** If $c_r(\alpha_t) > 0$, at some time $t = t_2$, for the mode $\alpha_t = k$, $k \in \mathcal{S}$, then the following three operational modes of the system (4.30) depend on the different choices of the bandwidth controller $u_{r1}(t)$ that are considered next.

  - **Edge Mode (i):** Suppose that $u_{r1}(t) = 0$ at some time $t = t_2$, for the mode $\alpha_t = k$, $k \in \mathcal{S}$. This implies that the ordinary queuing length of the mode k is sufficiently small and the closed-loop system of (4.30) is governed by:

  $$\dot{x}_r(t) = \lambda_r(t) + \sum_{l=1}^{m(k)} G_l F(x_r(t - \tau_l(t))) u_{r1}(t - \tau_l(t)) > 0 \qquad (4.54)$$

  Hence, the ordinary queuing length $x_r(t)$ will increase and after some finite time $t_3 > t_2$ the normal controller $\bar{u}_{r1}(t)$ will take effect for the mode k.

  - **Edge Mode (ii):** If $u_{r1}(t) = c_r(\alpha_t)$ at some time $t = t_4$, for the mode $\alpha_t = k$, $k \in \mathcal{S}$, then it follows that the ordinary queuing length $x_r(t)$ is sufficiently large and $\bar{u}_{r1}(t) > c_r(\alpha_t)$. The dynamical queuing model of the ordinary

traffic (4.30) then becomes:

$$
\begin{aligned}
\dot{x}_r(t) &= -F(x_r(t))c_r(k) + \lambda_r(t) + \sum_{l=1}^{m(k)} G_l F(x_r(t - \tau_l(t))) u_{r1}(t - \tau_l(t)) \\
&\leq -F(x_r(t))c_r(k) + \lambda_r^{max} + \sum_{l=1}^{m(k)} G_l F(x_r(t - \tau_l(t))) u_{r1}(t - \tau_l(t)) \\
&\leq -F(x_r(t))c_r(k) + \lambda_r^{max} + \sum_{l=1}^{m(k)} G_l \lambda_r^{max} \quad\quad\quad\quad (4.55)
\end{aligned}
$$

Therefore, the regulation strategy in this case is to regulate the traffic compression gain G_l so that the queuing length $x_r(t)$ of the mode k will decrease, and after some finite time the normal controller $\bar{u}_{r1}(t)$ will take effect. Hence, the following regulation rule for G_l is considered:

$$
0 \leq \sum_{l=1}^{m(k)} G_l \leq (F(x_r(t))c_r(k) - \lambda_r^{max})(\lambda_r^{max})^+ \quad\quad\quad\quad (4.56)
$$

Similar to the analysis in the premium traffic control, although the regulation rule (4.56) is derived based on the mode k, it is valid for all the modes $\alpha_t \in \mathcal{S}$. If the network has switched from mode k to another mode $\alpha_t = j$, $j \in \mathcal{S}$ before the normal controller $\bar{u}_{r1}$ takes effect, the switching controller $u_{r1}(t)$ will be re-compared with the link capacity $c_r(j)$ with respect to the mode j. The regulation strategy (4.56) will then be applied if there is still not enough capacity, but with respect to the variables $m(j)$ and $c_r(j)$. Consequently, after some finite time, the normal controller $\bar{u}_{r1}(t)$ will take effect for all the modes $\alpha_t \in \mathcal{S}$.

– **Normal Control Mode:** If $u_{r1}(t) = \bar{u}_{r1}(t)$ at some time $t = t_6$, for the mode $\alpha_t = k$, $k \in \mathcal{S}$, the dynamic system (4.30) becomes

$$
\dot{\bar{x}}_r(t) = -K_r(k)\bar{x}_r(t) - \hat{\lambda}_r(t) + \lambda_r(t) + \sum_{l=1}^{m(k)} G_l F(x_r(t - \tau_l(t))) u_{r1}(t - \tau_l(t))
$$

We now need to check the neighboring controllers $u_{r1}(t - \tau_l(t))$. Similar to the analysis in the premium traffic, certain nodes in the neighboring set may take the maximum value of the control $c_r(k)$, while others may take the minimum

value of the control 0, and yet the others may take the value of the normal control $\bar{u}_{r1}(t)$. However, the dynamic queuing system of the ordinary traffic for the entire network can be expressed in one state space representation as follows:

$$\dot{\bar{x}}_r(t) = -K_r(k)\bar{x}_r(t) - \hat{\lambda}_r(t) + \lambda_r(t) \tag{4.57}$$
$$+ \sum_{l=1}^{m(k)} G_l^r B_c^r c_r(k) + \sum_{l=1}^{m(k)} G_l^r B_l^r [K_r(k)\bar{x}_r(t - \tau_l(t)) + \hat{\lambda}_r(t - \tau_l(t))]$$

if we define the system matrices B_c^r and B_l^r as

$$B_c^r = \begin{cases} I & \text{if } u_r(t - \tau_l(t)) = c_r(t) \\ 0 & \text{otherwise} \end{cases}$$

$$B_l^r = \begin{cases} I & \text{if } u_r(t - \tau_l(t)) = \bar{u}_r(t - \tau_l(t)) \\ 0 & \text{otherwise} \end{cases} \tag{4.58}$$

Therefore, after applying the switching congestion controller (4.48)-(4.49), and selecting the traffic compression gains according to (4.56), the normal controller of the ordinary traffic $\bar{u}_{r1}(t)$ will eventually take effect for all the modes $\alpha_t \in \mathcal{S}$ and the Markovian jump system (4.30) will become the Markovian jump linear system (MJLS) with multiple and time-varying delays (4.57). The control objective for the ordinary traffic in the mobile network is to select the control gains $K_r(\alpha_t)$, $\Delta_r(\alpha_t)$, and $\Pi_r(\alpha_t)$ for each mode $\alpha_t \in \mathcal{S}$, so that the closed-loop system (4.57) is stable. Therefore, the following section will be focused on the stability analysis of the closed-loop system (4.57).

For the stability analysis of the Markovian jump linear system (4.57), let us define the new state space $\bar{z}_r(t) = vec\{\bar{x}_r(t), \bar{\lambda}_r(t)\}$, where $\bar{\lambda}_r(t) = \hat{\lambda}_r(t) - \lambda_r(t)$. The closed-loop system of the ordinary traffic (4.57) and the adaptive estimator (4.51) can then be written in the following form

$$\dot{z}_r(t) = D^r(\alpha_t)(\alpha_t)z_r(t) + \sum_{l=1}^{m(\alpha_t)} F_l^r(\alpha_t)z_r(t - \tau_l(t)) + \sum_{l=1}^{m(\alpha_t)} H_l^r(\alpha_t)v_l(\alpha_t) \tag{4.59}$$

$$z_r(t) = \phi(t), \phi(t) = [-h, 0]$$

$$k \in \wp, \wp = 1, 2$$

$$\alpha_t \in \mathcal{S}, \mathcal{S} = 1, ...M$$

155

where $\phi(t)$ is the initial condition of the time-delay system, k is the deterministic switching parameter of the system induced by the adaptive estimator (4.51), α_t is the Markov chain indicating the changes of the neighboring set, and $D^r(\alpha_t)(\alpha_t)$, $F_l^r(\alpha_t)$, $H_l^r(\alpha_t)$ are the mode-dependent system matrices that are defined as follows:

$$D_1^r(\alpha_t) = \begin{bmatrix} -K_r(\alpha_t) & -I \\ \Delta_r(\alpha_t) & -\Pi_r(\alpha_t) \end{bmatrix} \qquad D_2^r(\alpha_t) = \begin{bmatrix} -K_r(\alpha_t) & -I \\ 0 & -\Pi_r(\alpha_t) \end{bmatrix}$$

$$F_l^r(\alpha_t) = \begin{bmatrix} G_l^r B_l^r K_r(\alpha_t) & G_l^r B_l^r \\ 0 & 0 \end{bmatrix} \qquad H_l^r(\alpha_t) = \begin{bmatrix} 0 & 0 & G_l^r B_l^r & G_l^r B_c^r \\ -\Pi_r(\alpha_t) & -I & 0 & 0 \end{bmatrix}$$

$$v_l^r(t) = \begin{bmatrix} \lambda_r(t) & \dot{\lambda}_r(t) & \lambda_r(t - \tau_l(t)) & c_r(\alpha_t) \end{bmatrix}^T$$

The control objective of the ordinary traffic is then to select the mode-dependent control gains $K_r(\alpha_t)$, $\Delta_r(\alpha_t)$, $\Pi_r(\alpha_t)$, as presented in the system matrices $D^r(\alpha_t)(\alpha_t)$ and $F_l^r(\alpha_t)$, so that closed-loop system (4.59) is stable.

Comparing the closed-loop system of the ordinary traffic (4.59) with the closed-loop system of the premium traffic (4.31), one can conclude that the structure of the two dynamics are similar. Therefore, the same technique and theory which were applied in the stability analysis of the premium traffic class can be utilized for the ordinary traffic also. Therefore, the following two lemmas can be obtained.

Lemma 4.4. *Consider the closed-loop system of the ordinary traffic (4.59). If there exist symmetric positive definite matrices* $P(\alpha_t)$, $Q(\alpha_t)$, R, *and positive definite matrices* $M(\alpha_t)$ *and* $N(\alpha_t)$ *such that the following matrix inequality condition is satisfied for all the modes* $\alpha_t \in \mathcal{S}$, $\mathcal{S} = \{1, ..., M\}$:

$$W_k^r(\alpha_t) = \begin{bmatrix} w_{k1}^r(\alpha_t) & w_{k2}^r(\alpha_t) & R \\ * & w_3^r(\alpha_t) & 0 \\ * & * & -R - (1-h)Q_{\alpha_t} \end{bmatrix} < 0 \quad k = 1, 2 \quad (4.60)$$

where

$$w_{k1}^r(\alpha_t) = (2P(\alpha_t) + h^2(D_k^r(\alpha_t)^T)R)D_k^r(\alpha_t) + \sum_{l=1}^{M} \pi_{\alpha_t l} P(l) + (1+h)Q(\alpha_t) - R + M(\alpha_t)$$

$$w_{k2}^r(\alpha_t) = (h^2(D_k^r(\alpha_t))^T R + P(\alpha_t))F^r(\alpha_t)$$

$$w_3^r(\alpha_t) = h^2(F^r(\alpha_t))^T(R + N(\alpha_t))F^r(\alpha_t)$$

156

then the system (4.59) is ultimately bounded, and the radius of the ultimately bounded region is given by:

$$\rho^r(\alpha_t) = max[\rho_k^r(\alpha_t)], \qquad k = 1, 2$$

$$\rho_k^r(\alpha_t) = \frac{\lambda_{max}(\Psi^r(\alpha_t))}{\lambda_{min}(-W_k^r(\alpha_t))} \|v^r(\alpha_t)\|^2 \qquad (4.61)$$

where

$$\Psi^r(\alpha_t) = H_r^T(\alpha_t)(h^2 R + Y_r^T(\alpha_t)M^{-1}(\alpha_t)Y_r(\alpha_t) + h^2 N^{-1}(\alpha_t))H_r(\alpha_t)$$

Proof: The proof follows along the same lines as in the proof of Lemma 4.2 by substituting the appropriate system matrices of the ordinary traffic. ∎

Lemma 4.5. *Consider the system (4.59). If there exist symmetric positive definite matrices $X(\alpha_t)$, $N(\alpha_t)$, $\bar{Q}(\alpha_t)$, R, Z, and matrices $U_k^r(\alpha_t)$, $\bar{V}_k^r(\alpha_t)$, $\bar{R}_k^r(\alpha_t)$, for $k = 1, 2$, $\alpha_t \in S = \{1, \ldots, M\}$ such that the following LMI conditions are satisfied:*

$$\Omega_k^r(\alpha_t) = \begin{bmatrix} \theta_{k1}^r(\alpha_t) & \theta_{k2}^r(\alpha_t) & X^T(\alpha_t) \\ * & \theta_3^r(\alpha_t) & 0 \\ * & * & -Z - (1-h)\bar{Q}_{\alpha_t} \end{bmatrix} < 0 \qquad (4.62)$$

$$\theta_{k1}^r(\alpha_t) = U_k^r(\alpha_t) + (U_k^r(\alpha_t))^T + h^2 \bar{R}_k^r(\alpha_t) + (1 + h + \sum_{l=1}^{M} \pi_{\alpha_t l})X^T(\alpha_t)$$

$$\theta_{k2}^r(\alpha_t) = \bar{V}_k^r(\alpha_t) + I$$

$$\theta_3^r(\alpha_t) = h^2(R + N(\alpha_t))$$

then the matrix inequality condition in Lemma 4.4 holds and the system (4.59) is ultimately bounded.

Proof: The proof follows along the same lines as in the proof of Lemma 4.3 by substituting the appropriate system matrices of the ordinary traffic. ∎

The centralized switching congestion control (SCC) strategies for the mobile Diff-Serv network that are proposed in this section can be summarized in the flow chart shown in Fig. 4.2.

As shown in the Fig. 4.2, given a mobile Diff-Serv network with the changing network topology represented by the Markov chain $\alpha_t = \mathcal{S} = \{1, ..., M\}$, the premium

traffic controller first needs to determine the traffic compression gains among the nodes in the entire network, based on the network constraints under the current mode α_t. Given the traffic compression gain matrix $G_p(\alpha_t)$, the premium traffic controller will then solve the LMI conditions so that the mode-dependent control gain $K_p(\alpha_t)$ and the adaptive control gain $\Delta_p(\alpha_t)$ and $\Pi_p(\alpha_t)$ can be obtained. Adaptive estimator $\hat{\lambda}_p(t)$ is then updated based on the value of the queuing state and the switching conditions as given in (4.20). After updating the adaptive estimator, the bandwidth controller $C_p(\alpha_t)$ can be obtained as

$$C_p(\alpha_t) = max\{C_{server}(\alpha_t), min\{F^{-1}[K_p(\alpha_t)(x_p(t) - x_p^{ref}) + \hat{\lambda}_p(t)], 0\}\} \quad (4.63)$$

where $x_p(t)$ is the premium queuing length, x_p^{ref} is the reference of queuing length selected by the network operator, $F(x_p(t)) = diag\{f(x_{pi}(t))\}$ and $f(x_{pi}(t)) = \mu\frac{x_{pi}(t)}{1+x_{pi}(t)}$ can also be calculated with the queuing state. The bandwidth of the premium traffic are then allocated to all the nodes in the network. At the same time, the centralized controller sends the traffic compression gains $g_{ji}^p(t)$ to each corresponding node in the network, and each node will adjust its traffic compression rate in the next communication cycle.

On the other hand, given the premium traffic controller $C_p(t)$, the centralized ordinary traffic controller first calculates the traffic compression gains for the ordinary traffic based on the leftover capacity $c_r(\alpha_t) = C_{server}(\alpha_t) - C_p(\alpha_t)$ under the current network mode α_t. Then, by solving the centralized LMI conditions, the centralized control gain $K_r(\alpha_t)$ and the adaptive control gain $\Delta_r(\alpha_t)$ and the $\Pi_r(\alpha_t)$ will be obtained, so that the adaptive estimator can be updated. The bandwidth controller and the flow rate regulator for the ordinary traffic are then calculated as follows:

$$\lambda_r(t) = max\{c_r(\alpha_t), \lambda_r(t)\} \quad (4.64)$$

$$C_r(\alpha_t) = max\{c_r(\alpha_t), min\{F^{-1}[K_r(\alpha_t)(x_r(t) - x_r^{ref}) + \hat{\lambda}_r(t)], 0\}\} \quad (4.65)$$

It should be noted that different from the centralized switching congestion control algorithm of the fixed network, as shown in Fig. 3.2, the Markovian jump switching congestion control (MJ-SCC) algorithm need to recalculate all the mode-dependent parameters, such as the traffic compression gains, the state feedback control gains $K_p(\alpha_t)$ and $K_r(\alpha_t)$,
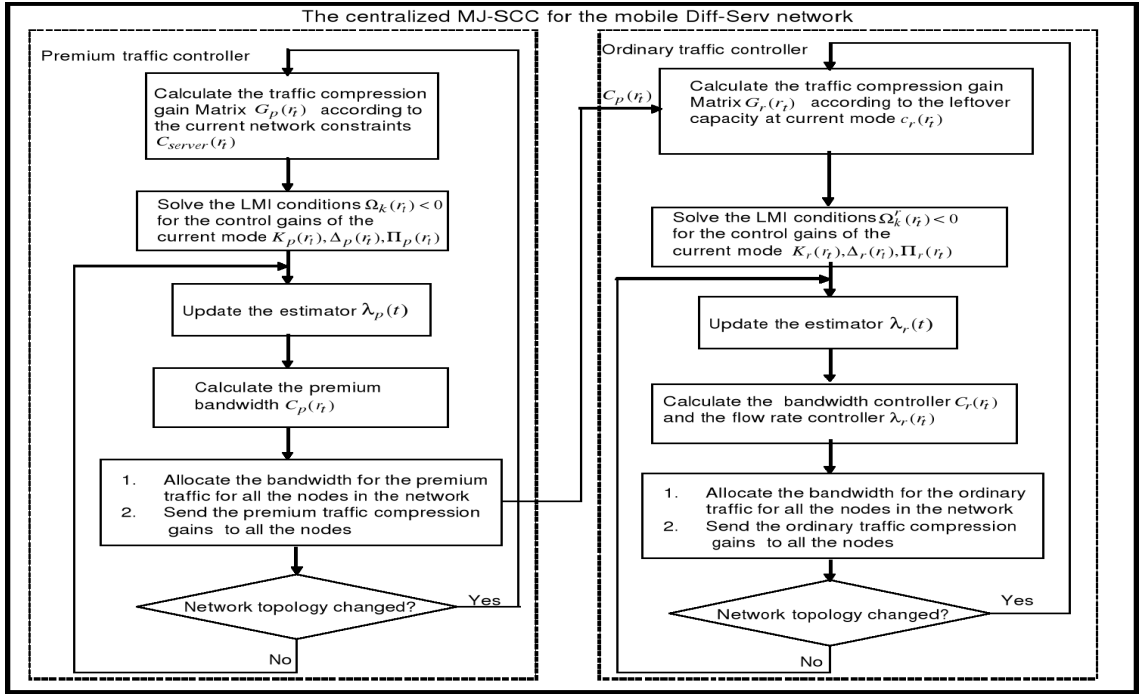
Figure 4.2: The flow chart of the centralized Markovian jump switching congestion controller (MJ-SCC) for the mobile Diff-Serv network.

at each time when the network topology is changed. The congestion controllers will then be updated based on the new control gains.

4.4 Decentralized Markovian Jump Switching Congestion Control (MJ-SCC) Scheme

When the number of nodes in the network is large, a centralized control scheme may become impractical. Especially, in mobile ad hoc networks, the connections between the centralized controller and the nodes may get disconnected during the changes of the network topology. Hence, the centralized control decision will be incorrect and this can even result in instability. Therefore, in this section we consider the decentralized control scheme for the congestion control problem in mobile Diff-Serv networks.

Recall the dynamical models of the premium and the ordinary traffic in mobile

159

networks as given by (2.57)-(2.57), that is

$$\dot{x}_{pi}(t) = -f(x_{pi}(t))u_{pi}(t) + \sum_{j \in \wp_i(\alpha_t)} f(x_{pj}(t - \tau_{ji}(t)))u_{pj}(t - \tau_{ji}(t))g_p^{ji} + \lambda_{pi}(t) \quad (4.66)$$

$$\dot{x}_{ri}(t) = -f(x_{ri}(t))u_{ri}^1(t) + u_{ri}^2(t) + \sum_{j \in \wp_i(\alpha_t)} f(x_{rj}(t - \tau_{ji}(t)))u_{rj}^1(t - \tau_{ji}(t))g_r^{ji} \quad (4.67)$$

where $\wp_i(\alpha_t)$ is the neighboring set of the node i that depends on the mode α_t, α_t is a Markov chain that represents the rule for changing the neighboring sets with the distribution function defined by (4.4), $x_{pi}(t)$ and $x_{ri}(t)$ denote the premium and the ordinary queuing state of node i, respectively, $\tau_{ji}(t)$ is the *unknown* but bounded *time-varying* delays from node j to node i, and $g_{ji}(t)$ is the traffic compression gain between the nodes i and j.

Therefore, the decentralized congestion control problem of mobile Diff-Serv networks is to select the switching congestion controllers $u_{pi}(t)$ and $u_{ri}(t)$ for the node i so that the queuing length of the premium and the ordinary traffic at the node i, respectively, will be as close as possible to their reference values. The physical constraints of each node, such as the link capacity and the buffer size need to also be considered in the controller design and have to be satisfied for each node. The detailed development of the decentralized switching congestion control strategy for the premium and the ordinary traffic are presented in the following subsections.

4.4.1 Decentralized MJ-SCC of the Premium Traffic in Mobile Networks

The typical set of physical constraints for the premium traffic in mobile networks can be given as follows:

$$0 \le x_{pi}(t) \le x_{pi}^{buffer} \quad (4.68)$$

$$0 \le u_{pi}(t) \le C_{server,i}(\alpha_t), \qquad i = 1, ...n \quad (4.69)$$

where $C_{server,i}(\alpha_t)$ denotes the time-varying link capacity that is dependent on the network topology and the instantaneous neighboring set. It should be noted that in a mobile

network, the link capacity of each node is changing due to the nodes mobility. Therefore, the capacity constraint of each node is also mode dependent.

Therefore, the control objective is to select the controller $u_{pi}(t)$ subject to each mode α_t, by considering the physical constraints (4.4). The switching congestion control strategy is now selected as follows:

$$u_{pi}(\alpha_t) = \begin{cases} 0 & \text{if } \bar{u}_{pi}(\alpha_t) < 0 \\ \bar{u}_{pi}(\alpha_t) & \text{if } 0 \leq \bar{u}_{pi}(\alpha_t) \leq C_{server,i}(\alpha_t) \\ C_{server,i}(\alpha_t) & \text{if } \bar{u}_{pi}(\alpha_t) > C_{server,i}(\alpha_t) \end{cases} \tag{4.70}$$

$$\bar{u}_{pi}(\alpha_t) = f^{-1}(x_{pi}, t)[k_{pi}(\alpha_t)\bar{x}_{pi}(t) + \hat{\lambda}_{pi}(t)] \tag{4.71}$$

where $\bar{x}_{pi}(t) = x_{pi}(t) - x_{pi}^{ref}(t)$ is the queuing error, $x_{pi}^{ref}(t)$ denotes the desired queuing length specified by the network manager, $k_{pi}(\alpha_t)$ is the state feedback control gain, and $\hat{\lambda}_{pi}(t)$ is a time-varying signal that is used to estimate the incoming traffic $\lambda_{pi}(t)$. Motivated from the robust adaptive control techniques in [128], the time-varying sginal $\hat{\lambda}_{pi}(t)$ is designed according to the *modified parameter projection method* and is applied to system (4.66) to estimate the unknown but bounded incoming traffic $\lambda_{pi}(t)$ as follows:

$$\dot{\hat{\lambda}}_{pi}(t) = \begin{cases} \delta_{pi}(\alpha_t)\bar{x}_{pi} - \beta(\alpha_t)_{pi}\hat{\lambda}_{pi}(t) & \text{if } 0 \leq \hat{\lambda}_{pi}(t) \leq \lambda_{pi}^{max} \text{ or} \\ & \qquad \hat{\lambda}_{pi}(t) = 0,\ \bar{x}_{pi} \geq 0 \text{ or} \\ & \qquad \hat{\lambda}_{pi}(t) = \lambda_{pi}^{max},\ \bar{x}_{pi} \leq 0 \\ -\beta_{pi}(\alpha_t)\hat{\lambda}_{pi}(t) & \text{otherwise} \end{cases} \tag{4.72}$$

where $\delta_{pi}(\alpha_t)$ and $\beta_{pi}(\alpha_t)$ are constant design parameters.

According to the switching laws in (4.5), the premium traffic controller $u_{pi}(\alpha_t)$ has the following three possible values over time under each mode α_t, namely

$$u_{pi}(\alpha_t) = 0, \quad \text{or} \quad u_{pi}(\alpha_t) = C_{server,i}, \quad \text{or} \quad u_{pi}(\alpha_t) = \bar{u}_{pi}(\alpha_t) \tag{4.73}$$

Therefore, the closed-loop system will experience multiple modes after applying the switching controller (4.5). Detailed analysis of each mode is given below.

- **Edge Mode i:** If $u_{pi}(\alpha_t) = 0$ at some time $t = t_1$, for $\alpha_t = k$, $k \in \mathcal{S}$, it then follows that the queuing length $x_{pi}(t_3)$ is sufficiently small. The closed-loop system (4.66)

can now be written as

$$\dot{x}_{pi}(t) \;=\; \lambda_{pi}(t) + \sum_{j \in \wp_i(k)} f(x_{pj}(t - \tau_{ji}(t)))u_{pj}(t - \tau_{ji}(t))g_p^{ji}(t) > 0 \quad (4.74)$$

Therefore, the queuing length $x_{pi}(t)$ will increase with the time. After some finite time $t_2 > t_1$, the normal controller $\bar{u}_{pi}(\alpha_t)$ will take effect.

- **Edge Mode (ii):** If $u_{pi}(\alpha_t) = C_{server,i}(\alpha_t)$ at some time $t = t_3$, for $\alpha_t = k$, $k \in \mathcal{S}$, this indicates that $x_{pi}(t_1)$ is sufficiently large so that the third condition $\bar{u}_{pi}(\alpha_t) > C_{server,i}(k)$ in (4.5) is satisfied. Consequently, the dynamical model (4.66) becomes

$$
\begin{aligned}
\dot{x}_{pi}(t) \;&\approx\; -C_{server,i}(k) + \lambda_{pi}(t) + \sum_{j \in \wp_i(k)} f(x_{pj}(t - \tau_{ji}(t)))u_{pj}(t - \tau_{ji}(t))g_p^{ji}(t) \\
&\leq\; -C_{server,i}(k) + \lambda_{pi}^{max} + \sum_{j \in \wp_i(k)} \lambda_{pj}^{max} g_p^{ji}(t) \quad (4.75)
\end{aligned}
$$

The regulation strategy under this case is to reset the traffic compression gains $g_p^{ji}(t)$ so that $\dot{x}_{pi}(t) < 0$, and hence the queuing length $x_{pi}(t)$ decreases. Therefore, the traffic compression gains are selected as

$$0 \leq g_p^{ji}(t) < \frac{C_{server,i}(\alpha_t) - \lambda_{pi}^{max}}{\displaystyle\sum_{j \in \wp_i(\alpha_t)} \lambda_{pj}^{max}}, \quad \alpha_t = k \quad (4.76)$$

Consequently, after some finite time $t_4 > t_3$ the controller $u_{pi}(\alpha_t)$ will take the value of $\bar{u}_{pi}(\alpha_t)$.

Although the regulation strategy (4.76) is derived based on the mode k, it is valid for all the other modes $\alpha_t \in \mathcal{S}$. The following analysis will clarify this claim.

Note that only one mode will operate at each time instant. If the network has switched from topology k to topology j before the normal controller $\bar{u}_{pi}(t)$ takes effect at node i, then the link capacity of node i will be re-calculated with respect to $\alpha_t = j$, and the normal controller $\bar{u}_{pi}(t)$ will be re-compared with $C_{servre,i}(j)$.

Therefore, if $\bar{u}_{pi}(t) \geq C_{servre,i}(j)$, which implies that there is still not enough capacity for node i in the new network topology, the traffic compression gains have to

be regulated again according to the strategy (4.76), but re-calculated based on the new network topology $\alpha_t = j$.

On the other hand, if $\bar{u}_{pi}(t) < C_{servre,i}(j)$, then the normal controller $\bar{u}_{pi}(t)$ will take effect immediately. Therefore, for either case, the normal controller $\bar{u}_{pi}(t)$ will eventually take effect after applying the regulation strategy (4.76).

- **Normal Control Mode (iii):** When the premium controller $u_{pi}(\alpha_t) = \bar{u}_{pi}(\alpha_t)$ takes effect, at some $t = t_5$, for $\alpha_t = k$, $k \in \mathcal{S}$, the queuing state equation (4.66) will become

$$\dot{x}_{pi} = -[k_{pi}(k)\bar{x}_{pi} + \hat{\lambda}_{pi}(t)] + \lambda_{pi}(t) + \sum_{j \in \wp_i(k)} f(x_{pj}(t - \tau_{ji}(t)))u_{pj}(t - \tau_{ji})g_p^{ji}(t)$$

Now, we need to check the delayed incoming traffic from the nodes in the neighboring set $\wp_i(k)$. The delayed input $\bar{u}_{pj}(t - \tau_{ji}(t)$ is governed by the switching control laws in (4.70). Similar to the analysis for the fixed network, let us define the neighboring sets as

$$\wp_i(k) = \wp_{i1}(k) \cup \wp_{i2}(k) \cup \wp_{i3}(k)$$

 where

$\wp_{i1}(k)$ denotes the subset of the neighboring set in which the delayed controllers of the mode k is equal to $C_{server,j}(k)$.

$\wp_{i2}(k)$ denotes the subset of the neighboring set in which the controllers are equal to $\bar{u}_{pj}(k)$.

$\wp_{i3}(k)$ denotes the subset of the neighboring set in which the controllers are equal to 0.

The dynamic queuing model (4.66) can then be re-written as follows:

$$\begin{aligned}
\dot{x}_{pi} &= -k_{pi}(k)\bar{x}_{pi} - \hat{\lambda}_{pi} + \lambda_{pi} + \sum_{j \in \wp_2(k)} C_{server,j}(k)g_{ji}^p(t) \\
&+ \sum_{j \in \wp_1(k)} [k_{pj}(k)\bar{x}_{pj}(t - \tau_{ji}(t)) + \hat{\lambda}_{pj}(t - \tau_{ji}(t))]g_{ji}^p(t) \qquad (4.77)
\end{aligned}$$

163

Therefore, after applying the switching congestion controller (4.70) and the regulation strategy of the traffic compression gains (4.76), the dynamic queuing model of the premium traffic for the mobile network (4.66) will enter the normal control mode and can be written as a Markovian jump linear system with multiple time-varying delays and coupled states, as given by (4.77).

It should be noted that at each instant when the network topology is changed, one needs to recheck the link capacity of each node i and the traffic compression gains from its neighboring nodes need to be re-calculated according to the new network topology. In the mean time, the control gains of the switching controller $k_{pi}(\alpha_t)$, $\delta_{pi}(\alpha_t)$, and $\beta_{pi}(\alpha_t)$ need to also be updated with respect to the new network topology.

It has been shown that the physical constraints of the premium traffic is guaranteed by the switching control strategy (4.70). However, the stability of the closed-loop system (4.77) is still dependent on the selections of the control gains $k_{pi}(\alpha_t)$, $\delta_{pi}(\alpha_t)$, and $\beta_{pi}(\alpha_t)$. Therefore, the control objective of the premium traffic is now to select the control gains for each node i, so that the closed-loop system (4.77) is stable. The detailed analysis is presented below.

For the purpose of stability analysis of the closed-loop system (4.77), we define $\bar{\lambda}_{pi}(t) = \hat{\lambda}_{pi}(t) - \lambda_{pi}(t)$ and the new state space $z_{pi}(t) = \begin{bmatrix} \bar{x}_{pi}(t) & \bar{\lambda}_{pi}(t) \end{bmatrix}^T$. The queuing dynamics of the premium traffic at each node (4.77) and the adaptive estimator (4.72) can be re-written together by the following standard Markovian jump linear system (MJLS):

$$\dot{z}_{pi}(t) = D_i^k(\alpha_t)z_{pi}(t) + \sum_{j \in \wp_1(\alpha_t)} F_j(\alpha_t)z_{pj}(t - \tau_{ji}(t)) + H_i(\alpha_t)v_{pi}(\alpha_t) \quad (4.78)$$

$$z_{pi}(t) = \varphi_i(t) \quad \varphi_i(t) \in [-h, 0]$$

$$k \in \wp, \qquad \wp = 1, 2 \qquad i, j = 1, ..., n$$

where $\varphi_i(t)$ is the initial condition function of the system, $v_{pi}(t)$ is the external signal to the system, and $D_i^k(\alpha_t)$, $F_j(\alpha_t)$, $H_i(\alpha_t)$, for $i, j = 1, ..., n$, are the system matrices that

164

are defined as follows:

$$D_i^1(\alpha_t) = \begin{bmatrix} -k_{pi}(\alpha_t) & -1 \\ \delta_{pi}(\alpha_t) & -\beta_{pi}(\alpha_t) \end{bmatrix} \qquad D_i^2(\alpha_t) = \begin{bmatrix} -k_{pi}(\alpha_t) & -1 \\ 0 & -\beta_{pi}(\alpha_t) \end{bmatrix}$$

$$F_j(\alpha_t) = \begin{bmatrix} k_{pj}(\alpha_t)g_{ji}^p(\alpha_t) & g_{ji}^p(\alpha_t) \\ 0 & 0 \end{bmatrix} \qquad H_i(\alpha_t) = \begin{bmatrix} 0 & 0 & G_{ji}(\alpha_t) \\ -\beta_{pi}(\alpha_t) & -1 & 0 \end{bmatrix}$$

$$v_{pi}(\alpha_t) = \begin{bmatrix} \lambda_{pi}(t) & \dot{\lambda}_{pi}(t) & \Gamma_{pj}(t - \tau_{ji}(t)) \end{bmatrix}^T$$

$$\Gamma_{pj}(t - \tau_{ji}(t)) = [vec\{\lambda_{pj}(t - \tau_{ji}(t)\}, vec\{C_{server,j}(\alpha_t)\}]$$

$$G_{ji}(\alpha_t) = vec\{g_{ji}^p(\alpha_t)\}$$

The system (4.78) above is a hybrid system with the deterministic switching that is given by the signal k and the stochastic switching that is governed by the Markov chain α_t. Furthermore, the system is subject to coupled states with multiple and time-varying delays. The congestion control problem of the ordinary traffic in the mobile network can then be recast as finding the state feedback control gain $k_{pi}(\alpha_t)$, the adaptive control gains $\beta_{pi}(\alpha_t)$ and $\delta_{pi}(\alpha_t)$ for each node i with respect to each mode α_t so that the system (4.78) is stable.

As far as the above coupled hybrid system with time-delay is concerned the following lemma is now provided for its stability conditions.

Lemma 4.6. *Consider the system (4.78). If there exist symmetric positive definite matrices $P_i(\alpha_t)$, $Q_i(\alpha_t)$, R_i, and positive definite matrices $M_i(\alpha_t)$ and $N_i(\alpha_t)$ such that the following condition is satisfied for all the modes $\alpha_t \in \mathcal{S}$, $\mathcal{S} = \{1, ..., M\}$:*

$$W_{ik}(\alpha_t) = \begin{bmatrix} w_{ik}^1(\alpha_t) & w_{ik}^2(\alpha_t) & R_i \\ * & w_i^3(\alpha_t) & 0 \\ * & * & -R_i - (1-h)Q_i(\alpha_t) \end{bmatrix} < 0 \qquad (4.79)$$

where

$$w_{ik}^1(\alpha_t) = (2P_i(\alpha_t) + h^2(D_i^k)^T(\alpha_t)R_i)D_i^k(\alpha_t) + \sum_{l=1}^{M} \pi_{\alpha_t l} P_i(l) + (1+h)Q_i(\alpha_t) - R_i + M_i(\alpha_t)$$

$$w_{ik}^2(\alpha_t) = (h^2(D_i^k)^T(\alpha_t)R_i + P_i(\alpha_t))F(\alpha_t)$$

$$w_i^3(\alpha_t) = h^2 F^T(\alpha_t)(R_i + N_i(\alpha_t))F(\alpha_t)$$

then the system (4.78) is ultimately bounded. The radius of the ultimately bounded region is given by $max\{\rho_{ik}(\alpha_t)\}|_k = \frac{\lambda_{max}\{\Psi_i(\alpha_t)\}}{\lambda_{min}(-W_{ik}(\alpha_t))}$, $k = 1, 2$, *where* λ_{min} *and* λ_{max} *represent the maximum and the minimum eigenvalues of the corresponding matrices.*

Proof: Consider the following stochastic Lyapunov-Krasovskii functional candidate:

$$V_i(z_{pi}(t), \alpha_t) = V_{i1} + V_{i2} + V_{i3} + V_{i4}$$

where

$$V_{i1} = z_{pi}(t)^T P_i(\alpha_t) z_{pi}(t) \tag{4.80}$$

$$V_{i2} = \int_{t-h}^{t} z_{pi}^T(s) Q_i(\alpha_t) z_{pi}(s) ds \tag{4.81}$$

$$V_{i3} = h \int_{-h}^{0} \int_{t+\theta}^{t} \dot{z}_p^T(s) R_i \dot{z}_p(s) ds d\theta \tag{4.82}$$

$$V_{i4} = \int_{-h}^{0} \int_{t+\theta}^{t} z_{pi}^T(s) Q_i(\alpha_t) z_{pi}(s) ds d\theta \tag{4.83}$$

and where $P_i(\alpha_t)$, $Q_i(\alpha_t)$, R_i are positive definite matrices with appropriate dimensions. Let $\mathcal{L}$ denote the infinitesimal generator of $\{z_{pi}(t), \alpha_t\}$, $t \geq 0$. Then, for each $\alpha_t = k \in \mathcal{S}$ we have

$$
\begin{aligned}
\mathcal{L}V_{i1} &= \lim_{\Delta \to 0^+} \frac{1}{\Delta} \{E[V_{i1}(z_{pi}(t+\Delta), \alpha_{t+\delta}, t+\Delta)|z_{pi}(t), \alpha_t = k] - V_{i1}(z_{pi}(t), k, t)\} \\
&= 2z_{pi}^T(t) P_i(\alpha_t) \dot{z}_{pi}(t) + \sum_{k=1}^{M} \pi_{\alpha_t k} z_{pi}^T(t) P_i(k) z_{pi}(t) \\
&= 2z_{pi}^T(t) P_i(\alpha_t)[D_i^k(\alpha_t) z_{pi}(t) + \sum_{j \in \wp_1(\alpha_t)} F_j(\alpha_t) z_{pj}(t - \tau_{ji}(t))] \\
&\quad + z_{pi}^T(t) \sum_{k=1}^{M} \pi_{\alpha_t k} P_i(k) z_{pi}(t) + 2z_{pi}^T(t) P_i(\alpha_t) H_i(\alpha_t) v_{pi}(\alpha_t) \\
\mathcal{L}V_{i2} &= \int_{t-h}^{t} 2z_{pi}^T(s) Q_i(\alpha_t) \dot{z}_{pi}(s) ds + \int_{t-h}^{t} z_{pi}^T(s) \sum_{k=1}^{M} \pi_{\alpha_t k} Q_i(k) z_{pi}(s) ds \\
&= z_{pi}^T(t) Q_i(\alpha_t) z_{pi}(t) - (1 - h) z_{pi}^T(t - h) Q_i(\alpha_t) z_{pi}(t - h) \\
&\quad + \int_{t-h}^{t} z_{pi}^T(s) \sum_{k=1}^{M} \pi_{\alpha_t k} Q_i(k) z_{pi}(s) ds
\end{aligned}
$$

166

$$
\begin{aligned}
\mathcal{L}V_{i3} &= h^2 \dot{z}_{pi}^T(t) R_i \dot{z}_{pi}(t) - h \int_{t-h}^t \dot{z}_{pi}^T(s) R_i \dot{z}_{pi}(s) ds \\
&= h^2 [D_i^k(\alpha_t) z_{pi}(t) + \sum_{j \in \wp_1(\alpha_t)} F_j(\alpha_t) z_{pj}(t - \tau_{ji}(t)) + H_i(\alpha_t) v_{pi}(\alpha_t)]^T R_i \\
&\quad [D_i^k(\alpha_t) z_{pi}(t) + \sum_{j \in \wp_1(\alpha_t)} F_j(\alpha_t) z_{pj}(t - \tau_{ji}(t)) + H_i(\alpha_t) v_{pi}(\alpha_t)] \\
&\quad - h \int_{t-h}^t \dot{z}_{pi}^T(s) R_i \dot{z}_{pi}(t) ds \\
\mathcal{L}V_{i4} &= h z_{pi}^T(t) Q_i(\alpha_t) z_{pi}(t) - \int_{t-h}^t z_{pi}^T(s) \sum_{k=1}^M \pi_{\alpha_t k} Q_i(k) z_{pi}(s) ds
\end{aligned}
$$

Adding up the above equations, we will have

$$
\begin{aligned}
\mathcal{L}V_i &\leq z_{pi}^T(t)(2P_i(\alpha_t) D_i^k(\alpha_t) + \sum_{k=1}^M \pi_{\alpha_t k} P_i(k) + (1+h) Q_i(\alpha_t)) z_{pi}(t) \\
&\quad + h^2 z_{pi}^T(t)((D_i^k)^T(\alpha_t) R_i D_i^k(\alpha_t) - R_i) z_{pi}(t) \\
&\quad + 2 z_{pi}^T(t)(h^2 (D_i^k(\alpha_t))^T R_i + P_i(\alpha_t)) \sum_{j \in \wp_1(\alpha_t)} F_j(\alpha_t) z_{pj}(t - \tau_{ji}(t)) \\
&\quad + h^2 (\sum_{j \in \wp_1(\alpha_t)} F_j(\alpha_t) z_{pj}(t - \tau_{ji}(t)))^T R_i (\sum_{j \in \wp_i(\alpha_t)} F_j(\alpha_t) z_{pj}(t - \tau_{ji}(t))) \\
&\quad + 2 z_{pi}^T(t) R_i z_{pi}(t - h) - z_{pi}^T(t - h)(R_i + (1-h) Q_i(\alpha_t)) z_{pi}(t - h) \\
&\quad + h^2 (H_i(\alpha_t) v_{pi}(\alpha_t))^T R_i (H_i(\alpha_t) v_{pi}(\alpha_t)) \\
&\quad + 2 z_{pi}^T(t)(h^2 D_i^k(\alpha_t) R_i + P_i(\alpha_t)) H_i(\alpha_t) v_{pi}(\alpha_t) \\
&\quad + 2 h^2 (\sum_{j \in \wp_1(\alpha_t)} F_j(\alpha_t) z_{pi}(t - \tau_{ji}(t)))^T (H_i(\alpha_t) v_{pi}(\alpha_t))
\end{aligned}
$$

Let us define

$$
\begin{aligned}
F(\alpha_t) &= vec\{F_j(\alpha_t)\} \\
H(\alpha_t) &= vec\{H_i(\alpha_t)\} \\
v(\alpha_t) &= vec\{v_{pi}^T(\alpha_t)\} \\
z_{pi}(t - \tau) &= vec\{z_{pi}^T(t - \tau_{ji}(t))\} \qquad i, j = 1, ..., n
\end{aligned}
$$

Then, the following two equations will hold

$$
\begin{aligned}
F(\alpha_t) z_{pj}(t - \tau) &= \sum_{j \in \wp_1(\alpha_t)} F_j(\alpha_t) z_{pj}(t - \tau_{ji}(t)) \\
H(\alpha_t) v(\alpha_t) &= H_i(\alpha_t) v_{pi}(\alpha_t)
\end{aligned}
$$

By substituting $F(\alpha_t)z_{pj}(t-\tau)$ and $H(\alpha_t)v(\alpha_t)$ into $\mathcal{L}V_i$, we will have

$$
\begin{aligned}
\mathcal{L}V_i \;\leq\; & z_{pi}^T(t)(2P_i(\alpha_t)D_i^k(\alpha_t) + \sum_{k=1}^{M}\pi_{\alpha_t l}P_i(k) + (1+h)Q_i(\alpha_t))z_{pi}(t) \\
& +h^2 z_{pi}^T(t)((D_i^k)^T(\alpha_t)R_i D_i^k(\alpha_t) - R_i + M_i(\alpha_t))z_{pi}(t) \\
& +2z_{pi}^T(t)(h^2(D_i^k)^T(\alpha_t)R_i + P_i(\alpha_t))F(\alpha_t)z_{pj}(t-\tau) \\
& +h^2(F(\alpha_t)z_{pj}(t-\tau))^T(R_i + N_i(\alpha_t))(F(\alpha_t)z_{pj}(t-\tau)) \\
& +2z_{pi}^T(t)R_i z_{pi}(t-h) - z_{pi}^T(t-h)(R_i + (1-h)Q_i(rt))z_{pi}(t-h) \\
& +h^2(H(\alpha_t)v(\alpha_t))^T R_i H(\alpha_t)v(\alpha_t) + (H(\alpha_t)v(\alpha_t))^T Y_i^T(\alpha_t)M_i^{-1}(\alpha_t)Y_i(\alpha_t)H(\alpha_t)v(\alpha_t) \\
& +h^2(H(\alpha_t)v(\alpha_t))^T N_i^{-1}(\alpha_t)H(\alpha_t)v(\alpha_t) \\
=\; & z_{pi}^T(t)(2P_i(\alpha_t)D_i^k(\alpha_t) + \sum_{k=1}^{M}\pi_{\alpha_t l}P_i(k) + (1+h)Q_i(\alpha_t))z_{pi}(t) \\
& +h^2 z_{pi}^T(t)((D_i^k)^T(\alpha_t)R_i D_i^k(\alpha_t) - R_i + M_i(\alpha_t))z_{pi}(t) \\
& +2z_{pi}^T(t)(h^2(D_i^k)^T(\alpha_t)R_i + P_i(\alpha_t))F(\alpha_t)z_{pj}(t-\tau) \\
& +h^2 z_{t-\tau}^T F^T(\alpha_t)(R_i + N_i(\alpha_t))F(\alpha_t)z_{pj}(t-\tau) \\
\\
& +2z_{pi}^T(t)R_i z_{pi}(t-h) - z_{t-h}^T(R_i + (1-h)Q_i(\alpha_t))z_{pi}(t-h) \\
& +v^T(\alpha_t)H^T(\alpha_t)(h^2 R_i + Y_i^T(\alpha_t)M_i^{-1}(\alpha_t)Y_i(\alpha_t) + h^2 N_i^{-1}(\alpha_t))H(\alpha_t)v(\alpha_t) \\
=\; & \eta_i^T(t,\tau,h)W_{ik}(\alpha_t)\eta_i(t,\tau,h) + v^T(\alpha_t)\Psi_i(\alpha_t)v(\alpha_t) \qquad\qquad (4.84)
\end{aligned}
$$

where $M_i(\alpha_t)$ and $N_i(\alpha_t)$ are positive definite matrices, $Y_i(\alpha_t) = h^2 D_i^k(\alpha_t)R_i + P_i(\alpha_t)$, and the matrix W_{ik} and Ψ_i are defined as

$$
W_{ik}(\alpha_t) = \begin{bmatrix} w_{ik}^1(\alpha_t) & w_{ik}^2(\alpha_t) & R_i \\ * & w_i^3(\alpha_t) & 0 \\ * & * & -R_i - (1-h)Q_i(\alpha_t) \end{bmatrix}
$$

$$
w_{ik}^1(\alpha_t) = (2P_i(\alpha_t) + h^2(D_i^k)^T(\alpha_t)R_i)D_i^k(\alpha_t) + \sum_{l=1}^{M}\pi_{\alpha_t l}P_i(l) + (1+h)Q_i(\alpha_t) - R_i + M_i(\alpha_t)
$$

$$
w_{ik}^2(\alpha_t) = (h^2(D_i^k)^T(\alpha_t)R_i + P_i(\alpha_t))F(\alpha_t)
$$

$$
w_i^3(\alpha_t) = h^2 F^T(\alpha_t)(R_i + N_i(\alpha_t))F(\alpha_t)
$$

$$
\Psi_i(\alpha_t) = H^T(\alpha_t)(h^2 R_i + Y_i^T(\alpha_t)M_i^{-1}(\alpha_t)Y_i(\alpha_t) + h^2 N_i^{-1}(\alpha_t))H(\alpha_t)
$$

$$
\eta_i(t,\tau,h) = \begin{bmatrix} z_{pi}^T(t) & z_{pj}^T(t-\tau) & z_{pi}^T(t-h) \end{bmatrix}^T
$$

168

Therefore, according to (4.79), we will have

$$\mathcal{L}V_i \leq 0 \qquad (4.85)$$

for any $\eta_i(t, \tau, h)$ that satisfies:

$$-\eta_i^T(t, \tau, h)W_{ik}(\alpha_t)\eta_i(t, \tau, h) \geq v_i^T(\alpha_t)\Psi_i(\alpha_t)v_i(\alpha_t) \qquad (4.86)$$

Therefore, according to the Definition 4.1, the system (4.78) is stochastically ultimately bounded and the radius of the bounded region is given by:

$$\rho_{ik}(\alpha_t) = \frac{\lambda_{max}\{\Psi_i(\alpha_t)\}}{\lambda_{min}(-W_{ik}(\alpha_t))} \qquad (4.87)$$

This completes the proof of Lemma 4.6. ∎

The following lemma is can then be obtained for the derivation of the control gains.

Lemma 4.7. *The matrix inequality condition in Lemma 4.6 hold if there exist symmetric positive definite matrices $X_i(\alpha_t)$, $N_i(\alpha_t)$, $\bar{Q}_i(\alpha_t)$, R_i, Z_i, and matrices $U_{ik}(\alpha_t)$, $\bar{V}_{ik}(\alpha_t)$, $\bar{R}_{ik}(\alpha_t)$, for $k = 1, 2$, $\alpha_t \in S = \{1, \dots, M\}$ such that the following LMI conditions are satisfied:*

$$\Omega_{ik}(\alpha_t) = \begin{bmatrix} \theta_{ik}^1(\alpha_t) & \theta_{ik}^2(\alpha_t) & X_i^T(\alpha_t) \\ * & \theta_i^3(\alpha_t) & 0 \\ * & * & -Z_i - (1-h)\bar{Q}_i(\alpha_t) \end{bmatrix} < 0 \qquad (4.88)$$

where

$$\theta_{ik}^1(\alpha_t) = U_{ik}(\alpha_t) + U_{ik}^T(\alpha_t) + h^2\bar{R}_{ik}(\alpha_t) + (1 + h + \sum_{l=1}^M \pi_{\alpha_t l})X_i^T(\alpha_t)$$

$$\theta_{ik}^2(\alpha_t) = \bar{V}_{ik}(\alpha_t) + I$$

$$\theta_i^3(\alpha_t) = h^2(R_i + N_i(\alpha_t))$$

Proof: The following matrices are defined in order to transform the nonlinear matrix $W_{ik}(\alpha_t)$ into an equivalent linear matrix:

$$X_i(\alpha_t) = P_i^{-1}(\alpha_t)$$

$$Y_i(\alpha_t) = F^{-1}(\alpha_t)$$

$$Z_i = R_i^{-1}$$

$$\Lambda_i(\alpha_t) = diag\{X_i(\alpha_t), Y_i(\alpha_t), Z_i\}$$

169

By pre and post multiplying $W_{ik}(\alpha_t)$ with the above matrices $\Lambda_i(\alpha_t)$ and $\Lambda_i^T(\alpha_t)$, respectively, we will have

$$
\begin{aligned}
\Omega_{ik}(\alpha_t) &= \Lambda_i^T(\alpha_t)W_{ik}(\alpha_t)\Lambda_i(\alpha_t) \\[2mm]
&= \begin{bmatrix} \theta_{ik}^1(\alpha_t) & \theta_{ik}^2(\alpha_t) & X_i^T(\alpha_t) \\[2mm] * & \theta_i^3(\alpha_t) & 0 \\[2mm] * & * & -Z_i - (1-h)\bar{Q}_i(\alpha_t) \end{bmatrix}
\end{aligned}
\tag{4.89}
$$

where

$$\theta_{ik}^1(\alpha_t) = U_{ik}(\alpha_t) + U_{ik}^T(\alpha_t) + h^2\bar{R}_{ik}(\alpha_t) + (1 + h + \sum_{l=1}^{M}\pi_{\alpha_t l})X_i^T(\alpha_t)$$

$$\theta_{ik}^2(\alpha_t) = \bar{V}_{ik}(\alpha_t) + I$$

$$\theta_i^3(\alpha_t) = h^2(R_i + N_i(\alpha_t))$$

$$D_i^k(\alpha_t) = U_{ik}(\alpha_t)X_i^{-1}(\alpha_t) \quad ; \quad \bar{R}_{ik}(\alpha_t) = U_{ik}(\alpha_t)^T R_i U_{ik}(\alpha_t)$$

$$Q_i(\alpha_t) = P_i(\alpha_t) \quad ; \quad \bar{V}_{ik}(\alpha_t) = U_{ik}(\alpha_t)^T R_i$$

$$M_i(\alpha_t) = R_i \quad ; \quad \bar{Q}_i(\alpha_t) = Z_i^T Q_i(\alpha_t)Z_i$$

Therefore, the following two inequality conditions are equivalent:

$$\Omega_{ik}(\alpha_t) < 0 \Longleftrightarrow W_{ik}(\alpha_t) < 0 \qquad \alpha_t \in \mathcal{S}, \mathcal{S} = \{1, ..., M\} \tag{4.90}$$

Hence, the system (4.78) is ultimately bounded. This completes the proof of Lemma 4.7.
∎

4.4.2 Decentralized MJ-SCC of the Ordinary Traffic in Mobile Networks

The dynamic queuing model of the ordinary traffic in mobile networks is re-written here again for convenience:

$$\dot{x}_{ri}(t) = -f(x_{ri}(t))u_{ri}^1(t) + u_{ri}^2(t) + \sum_{j \in \wp_i(\alpha_t)} f(x_{rj}(t - \tau_{ji}(t)))u_{rj}^1(t - \tau_{ji})g_r^{ji} \tag{4.91}$$

where $u_{ri}^1(t)$ is the bandwidth controller of node i, $u_{ri}^2(t)$ is the flow rate controller of the node i, $\wp_i(\alpha_t)$ is the neighboring set of the node i with respect to the mode $\alpha_t \in \mathcal{S}$, $S = 1, ..., M$, and α_t is the Markov chain representing the changes in the neighboring set with

the probability distribution function governed by (4.4). Recall the physical constraints of the ordinary traffic in the mobile network (2.57):

$$0 \leq x_{ri}(t) \leq x_{ri}^{buffer} \tag{4.92}$$

$$0 \leq u_{ri}(t) \leq c_{ri}(\alpha_t), \qquad i = 1, ...n \tag{4.93}$$

where $c_{ri}(\alpha_t)$ denotes the instantaneous leftover capacity of node i from the premium traffic which is actually equal to $C_{server,i}(\alpha_t) - u_{pi}(\alpha_t)$. In contrast to the fixed networks, the input constraint of the ordinary traffic in mobile networks is now mode-dependent. Therefore, the Markovian jump switching congestion control strategy for the ordinary traffic is designed as follows:

1. *Flow Rate Regulation*: At the start of each measurement cycle, we first calculate the maximum allowable capacity for the ordinary traffic as follows:

$$c_{ri}(\alpha_t) = \max[0, \ C_{server,i} - u_{pi}(\alpha_t)] \tag{4.94}$$

where the flow rate controller $u_{ri}^2(t)$ is selected according to

$$u_{ri}^2(t) = \begin{cases} c_{ri}(\alpha_t) & \text{if } u_{ri}^2(t) \geq c_{ri}(\alpha_t) \text{ under mode } \alpha_t \\ u_{ri}^2(t) & \text{otherwise} \end{cases} \tag{4.95}$$

Once the above regulation is invoked, the ordinary incoming traffic $\lambda_{ri}(t) = u_{ri}^2$ is guaranteed to be bounded by $0 \leq \lambda_{ri}(t) \leq c_{ri}(\alpha_t)$.

2. *Bandwidth Allocation* : Provided that $0 \leq \lambda_{ri}(t) \leq c_{ri}(\alpha_t)$, the ordinary traffic capacity controller $u_{ri}^1(\alpha_t)$ is selected according to the following switching law:

$$u_{ri}^1(\alpha_t) = \begin{cases} 0 & \text{if } \bar{u}_{ri}^1(\alpha_t) < 0 \\ \bar{u}_{ri}^1(\alpha_t) & \text{if } 0 \leq \bar{u}_{ri}^1(\alpha_t) \leq c_{ri}(\alpha_t) \\ c_{ri}(\alpha_t) & \text{if } c_{ri}(\alpha_t) > c_{ri}(\alpha_t) \end{cases} \tag{4.96}$$

$$\bar{u}_{ri}^1(\alpha_t) = f^{-1}(x_{ri}, t)[k_{ri}(\alpha_t)\bar{x}_{ri}(t) + \hat{\lambda}_{ri}(t)] \tag{4.97}$$

where $\bar{x}_{ri}(t) = x_{ri}(t) - x_{ri}^{ref}$ is the queuing error, $k_{ri}(\alpha_t)$ is the state feedback control gain, and $\hat{\lambda}_{ri}(t)$ denotes the adaptive estimator of the ordinary traffic which is

updated as follows:

$$
\dot{\hat{\lambda}}_{ri} = \begin{cases} \delta_{ri}(\alpha_t)\bar{x}_{ri} - \beta_{ri}(\alpha_t)\hat{\lambda}_{ri} & \text{if } 0 \leq \hat{\lambda}_{ri}(t) \leq \lambda_{ri}^{max} \text{ or} \\ & \hat{\lambda}_{ri} = 0, \ \bar{x}_{ri} \geq 0 \text{ or} \\ & \hat{\lambda}_{ri} = \lambda_{ri}^{max}, \ \bar{x}_{ri} \leq 0 \\ -\beta_{ri}(\alpha_t)\hat{\lambda}_{ri} & \text{otherwise} \end{cases} \tag{4.98}
$$

where $\delta_{ri}(\alpha_t)$ and $\beta_{ri}(\alpha_t)$ are the design parameters.

Similar to the analysis of the premium traffic, the closed-loop system of the ordinary traffic will experience the following multiple modes depending on the different choices of the controller $u_{ri}^1(t)$ as defined in (4.84):

- **Case (i):** If $c_{ri}(\alpha_t) = 0$ at some time $t = t_1$, for the mode $\alpha_t = k$, $k \in \mathcal{S}$, this implies that there is no leftover capacity for the ordinary traffic. According to (4.84), it follows that $u_{ri}^1(\alpha_t) = 0$ and $u_{ri}^2(t) = 0$. Hence the closed-loop system of the ordinary traffic model (4.80) is reduced to:

$$
\dot{x}_{ri} = \sum_{j \in \wp_i(k)} \lambda_{rj}(t - \tau_{ji}) g_{ji}^r(t) \tag{4.99}
$$

Since no incoming traffic is allowed to the buffer, the traffic compression gains $g_r^{ji}(t)$ are set to $g_{ji}^r = 0$. The incoming traffic from the neighboring nodes are *forced* to be dropped out. At a subsequent time $t_2 > t_1$, when $c_{ri}(\alpha_t) > 0$, the following case is then considered.

- **Case (ii):** If $c_{ri}(\alpha_t) > 0$ at some time $t = t_2$, for the mode $\alpha_t = k$, $k \in \mathcal{S}$, then there will be leftover capacity from the premium traffic, and the strong regulation conditions of the traffic compression gains $g_{ji}^r(t)$ in **case (i)** can be released. The bandwidth controller for the ordinary traffic $u_{ri}^1(\alpha_t)$ is considered next. According to the switching laws in (4.26), the following multiple submodes need to be considered.

  - **Edge Mode (i):** If $u_{ri}^1(\alpha_t) = 0$ at some time t_3, for the mode $\alpha_t = k$, $k \in \mathcal{S}$, it follows that $x_{ri}(t)$ is sufficiently small so that $\bar{u}_{ri}^1(k) \leq 0$. The dynamic queuing system (4.80) will then become

172

$$\dot{x}_{ri} = \lambda_{ri}(t) + \sum_{j \in \wp_i(k)} \lambda_{rj}(t - \tau_{ji}) g_{ji}^r(t) > 0 \qquad (4.100)$$

and the queuing length of the ordinary traffic $x_{ri}(t)$ will increase with time so that after some finite time $t_4 > t_3$, one will have $\bar{u}_{ri}^1(k) > 0$ and the normal controller $\bar{u}_{ri}^1(\alpha_t)$ will take effect.

– **Edge Mode (ii):** If $u_{ri}^1(\alpha_t) = c_{ri}(\alpha_t)$ at some $t = t_5$, for the mode $\alpha_t = k$, $k \in \mathcal{S}$, it follows that $\bar{u}_{ri}^1(k) > c_{ri}(k)$. In this case, the dynamic system (4.80) can be written as follows:

$$\begin{aligned} \dot{x}_{ri} &= -f(x_{ri}(t))c_{ri}(k) + \lambda_{ri}(t) + \sum_{j \in \wp_i(k)} \lambda_{rj}(t - \tau_{ji})g_{ji}^r(t) \\ &\leq -f(x_{ri}(t))c_{ri}(k) + \lambda_{ri}^{max} + \sum_{j \in \wp_i(k)} \lambda_{rj}^{max} g_{ji}^r(t) \qquad (4.101) \end{aligned}$$

Since the queuing length of node i is relatively large, the regulation strategy for the system (4.86) is to reset the traffic compression gains $g_{ji}^r(t)$ so that the queuing state $x_{ri}(t)$ will decrease with time. Therefore, the following regulation rule for the traffic compression gains $g_{ji}^r(t)$ can be obtained:

$$0 \leq g_{ji}^r(t) < \frac{f(x_{ri}(t))c_{ri}(\alpha_t)(t) - \lambda_{pi}^{max}}{\sum_{j \in \wp_i(\alpha_t)} \lambda_{pj}^{max}}, \qquad \alpha_t = k \qquad (4.102)$$

The derivative of the queuing state $\dot{x}_{ri}(t)$ in (4.86) is negative and the queuing length $x_{ri}(t)$ will then decrease. After some finite time $t_6 > t_5$, the normal controller $\bar{u}_{ri}^1(\alpha_t)$ will take effect for the mode k.

If the network topology has switched from mode k to mode j before the normal controller takes effect, then the leftover capacity of node i will be re-calculated. The bandwidth controller $\bar{u}_{ri}^1(t)$ will be re-compared with the new boundary $c_{ri}(j)$. If $\bar{u}_{ri}^1(t) > c_{ri}(j)$, this implies that there is still not enough capacity for the ordinary traffic in node i, hence the traffic compression gains has to be re-regulated according to (4.87) with respect to $\alpha_t = j$.

On the contrary, if $\bar{u}_{ri}^1(t) < c_{ri}(j)$, then the normal controller $\bar{u}_{ri}^1(t)$ will be applied. Therefore, one can conclude that by regulating the traffic compression gains as in (4.87), the normal controller of node i will eventually take effect.

– **Normal Control Mode (iii):** If the controller $u_{ri}^1(\alpha_t) = \bar{u}_{ri}^1(\alpha_t)$ at some time $t = t_7$, for the mode $\alpha_t = k$, $k \in \mathcal{S}$, then the closed-loop system of the ordinary traffic (4.80) will be governed by:

$$\dot{x}_{ri} = -k_{ri}(k)\bar{x}_{ri} - \hat{\lambda}_{ri}(t) + \lambda_{ri}(t) + \sum_{j \in \wp_i(k)} \lambda_{rj}(t - \tau_{ji})g_{ji}^r(t) \qquad (4.103)$$

We now need to check the incoming traffic from the neighboring nodes. Similar to the analysis of the premium traffic, different neighboring nodes may take different values of the switching controller based on the queuing state of node j at the time $t - \tau_{ji}(t)$. Therefore, the dynamic queuing system of the node i can be written as

$$
\begin{aligned}
\dot{x}_{ri} = {} & -k_{ri}(k)\bar{x}_{ri} - \hat{\lambda}_{ri} + \lambda_{ri} + \sum_{j \in \wp_2(k)} c_{rj}(k)g_{ji}^r(t) \\
& + \sum_{j \in \wp_1(k)} [k_{rj}(k)\bar{x}_{rj}(t - \tau_{ji}(t)) + \hat{\lambda}_{rj}(t - \tau_{ji}(t))]g_{ji}^r(t) \qquad (4.104)
\end{aligned}
$$

where $\wp_2(k)$ is the subset of the neighboring set in which the delayed controllers of the ordinary traffic are equal to $c_{rj}(k)$, and $\wp_1(k)$ is the subset of the neighboring set in which the delayed controllers of the ordinary traffic are equal to $\bar{u}_{ri}^1(t - \tau_{ji}(t))$.

Similar as before, we define the adaptive estimation error $\hat{\lambda}_{ri}(t) - \lambda_{ri}(t)$ as a new state and define the new state space as $z_{ri}(t) = \begin{bmatrix} \bar{x}_{ri}(t) & \bar{\lambda}_{ri}(t) \end{bmatrix}^T$. Consequently, the closed-loop system of the ordinary traffic in mobile networks can be written as

$$\dot{z}_{ri}(t) = D_{ik}^r(\alpha_t)z_{ri}(t) + \sum_{j \in \wp_1(\alpha_t)} F_j^r(\alpha_t)z_{rj}(t - \tau_{ji}(t)) + H_i^r(\alpha_t)v_{ri}(\alpha_t) \quad (4.105)$$

$$z_{ri}(t) = \varphi_i(t) \qquad \varphi_i(t) \in [-h, 0]$$

$$k \in \wp, \qquad \wp = 1, 2 \qquad i, j = 1, ..., n$$

where the system matrices $D_{ik}^r(\alpha_t)$, $F_j^r(\alpha_t)$, $H_i^r(\alpha_t)$, for $i, j = 1, ..., n$, are defined as

$$D_{i1}^r(\alpha_t) = \begin{bmatrix} -k_{ri}(\alpha_t) & -1 \\ \delta_{ri}(\alpha_t) & -\beta_{ri}(\alpha_t) \end{bmatrix} \qquad D_{i2}^r(\alpha_t) = \begin{bmatrix} -k_{ri}(\alpha_t) & -1 \\ 0 & -\beta_{ri}(\alpha_t) \end{bmatrix}$$

$$F_j^r(\alpha_t) = \begin{bmatrix} k_{rj}(\alpha_t)g_{ji}^r(\alpha_t) & g_{ji}^r(\alpha_t) \\ 0 & 0 \end{bmatrix} \qquad H_i^r(\alpha_t) = \begin{bmatrix} 0 & 0 & G_{ji}^r(\alpha_t) \\ -\beta_{ri}(\alpha_t) & -1 & 0 \end{bmatrix}$$

$$v_{ri}(\alpha_t) = \begin{bmatrix} \lambda_{ri}(t) & \dot{\lambda}_{ri}(t) & \Gamma_{rj}(t-\tau_{ji}(t)) \end{bmatrix}^T$$

$$\Gamma_{rj}(t-\tau_{ji}(t)) = [vec\{\lambda_{rj}(t-\tau_{ji}(t)\}, vec\{c_r(\alpha_t)\}]$$

$$G_{ji}^r(\alpha_t) = vec\{g_{ji}^r(\alpha_t)\}$$

Therefore, the control objective of the ordinary traffic in mobile networks is to select the mode-dependent control gains of each node i so that the closed-loop system (4.105) is stable for all modes $\alpha_t \in \mathcal{S}$. Comparing the dynamics of the closed-loop system (4.105) with the closed-loop system of the premium traffic (4.78), one can observe that the two systems have the same structure. Therefore, the Lemmas 4.6 and 4.7 can be applied for deriving the stability conditions and the control gains of the ordinary traffic, by replacing the corresponding system matrices in Lemmas 4.6 and 4.7 with that of the system (4.105).

The decentralized switching congestion control (SCC) strategies proposed in this section can be summarized in Fig. 4.3. As shown in Fig. 4.3, the decentralized premium traffic controller of each node first determines the traffic compression gains g_{ji}^p for its neighboring node based on the current network topology $\alpha_t \in \mathcal{S} = \{1, ..., M\}$. By solving the local LMI conditions of each node, the decentralized control gain $k_{pi}(\alpha_t)$ as well as the adaptive control gains $\delta_{pi}(\alpha_t)$ and $\beta_{pi}(\alpha_t)$ are then obtained. The bandwidth allocated for the premium traffic of each node is updated according to the following rule:

$$C_{pi}(t) = max\{C_{server,i}(\alpha_t), min\{f^{-1}(x_{pi}, t)[k_{pi}(\alpha_t)(x_{pi}(t) - x_{pi}^{ref}) + \hat{\lambda}_{pi}(t)], 0\}\} \quad (4.106)$$

Given the premium traffic controller $C_{pi}(\alpha_t)$, the ordinary traffic first calculates the leftover capacity $c_{ri}(\alpha_t) = C_{server,i}(\alpha_t) - C_{pi}(\alpha_t)$ and determines the traffic compression gains of the neighboring nodes. By solving the corresponding LMI conditions, the decentralized control gains and the adaptive control gains of the ordinary traffic are then obtained so that the adaptive estimator can be updated. The bandwidth controller and the flow rate controller of each node are calculated as follows:

$$\lambda_{ri}(t) = max\{c_{ri}(\alpha_t), \lambda_{ri}(t)\} \quad (4.107)$$

$$C_{ri}(t) = max\{c_{ri}(\alpha_t), min\{f^{-1}(x_{ri}, t)[k_{ri}(\alpha_t)(x_{ri}(t) - x_{ri}^{ref}) + \hat{\lambda}_{ri}(t)], 0\}\}(4.108)$$
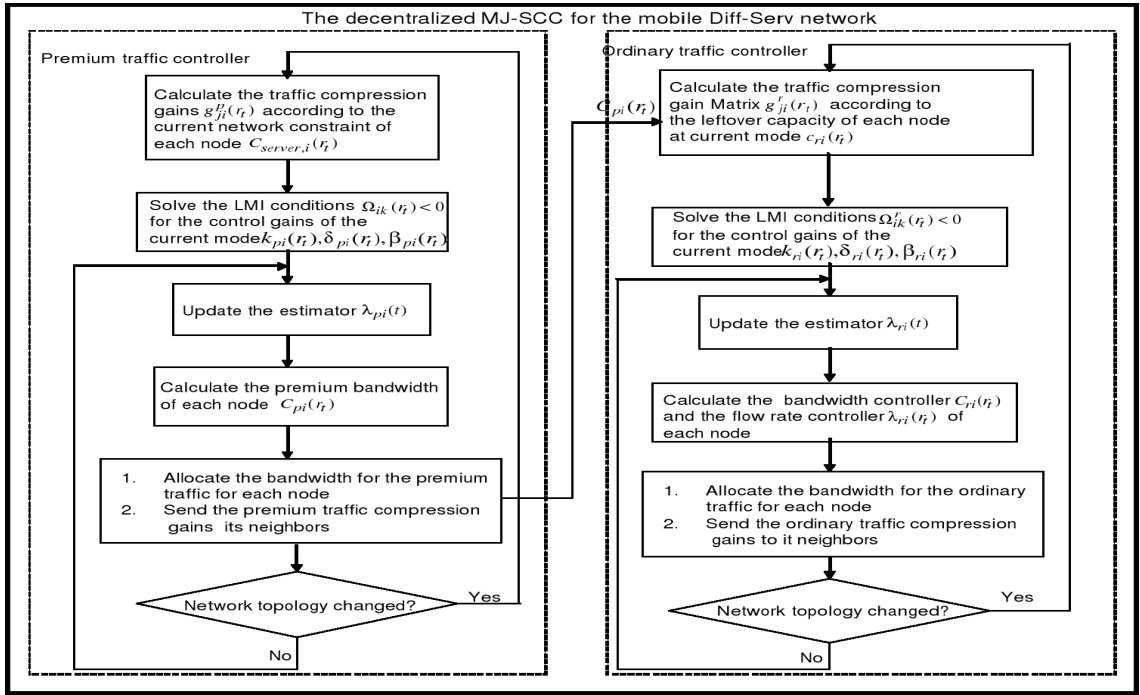
Figure 4.3: The flow chart of the decentralized Markovian jump switching congestion controller (MJ-SCC) for the mobile Diff-Serv network.

In contrast to the decentralized switching congestion control algorithm of the fixed network, as shown in Fig. 3.4, the decentralized Markovian jump switching congestion controller needs to re-calculate the mode-dependent parameters such as the traffic compression gains $g_{ji}(\alpha_t)$, the control gains $k_{pi}(\alpha_t)$ and $k_{ri}(\alpha_t)$, and the adaptive control gains $\delta_i(\alpha_t)$ and $\beta_i(\alpha_t)$, at each instant when the network topology is changed.

4.5 Simulation Results

In this section, simulation results are provided to evaluate the performance of our proposed Markovian jump switching congestion control (MJ-SCC) strategy in mobile NMAS. The results obtained by utilizing the decentralized MJ-SCC strategy are compared with those of the centralized MJ-SCC algorithm as well as the IDCC [3] approaches. In the mobile NMAS, nodes usually move in groups and exchange information among one another. Furthermore, specific nodes in one group can also communicate with the specific nodes from

176

the other groups when they move into the radio range of each other. The change of the network topology due to the nodes mobility is represented by a stochastic process which takes values from a finite set $\mathcal{S} = \{1, ..., M\}$. The probability of transition π_{ji} among different modes $\alpha_t \in \mathcal{S}$ satisfies the equation (4.4) and is assumed to be known.

4.5.1   Performance Metrics

To evaluate the performance of the Markovian jump switching congestion control (MJ-SCC) strategies proposed in this section, we adopt the same performance metrics as before, namely the packet loss rate (PLR) and the queuing delay. Besides the buffer overflow and the traffic regulation, packet loss occurs in a mobile network when the link between two nodes is disconnected. That is, the outgoing packets from node i to node k will be drop out when these two nodes are disconnected due to network topology changes.

In the simulations of this chapter, one denotes the link between nodes by a connectivity parameter $a_{ij}(\alpha_t)$ which is defined as

$$a_{ij}(\alpha_t) = \begin{cases} 1, & \text{if node } i \text{ and node } j \text{ are connected in mode } \alpha_t \\ 0, & \text{otherwise} \end{cases} \tag{4.109}$$

where α_t represents the changes of network topology with the transition probabilities as defined in equation (4.4).

Therefore, the packet loss rate (PLR) for the premium traffic in the mobile network is defined as

$$PLR_{pi}(t) = \frac{P_{bi} + P_{ci}}{\lambda_{pi}(t) + \sum\limits_{j \in \wp_i} \lambda_{ji}(t) g_{ji}(t) a_{ji}(\alpha_t)} \tag{4.110}$$

$$P_{bi}(t) = max\{0, \lambda_{pi}(t) + \sum\limits_{j \in \wp_i} \lambda_{ji}(t) g_{ji}(t) a_{ji}(\alpha_t) - (x_{buffer,i} - x_{pi}(t))\} \tag{4.111}$$

$$P_{ci}(t) = \sum\limits_{k \in \wp_i} \lambda_{ik}(t) g_{ik}(t)(1 - a_{ik}(\alpha_t)) \tag{4.112}$$

where P_{bi} is the packet loss induced by the buffer overflow and P_{ci} is the packet loss due to the network topology changes. The PLR for the ordinary traffic in the mobile network is then defined according to
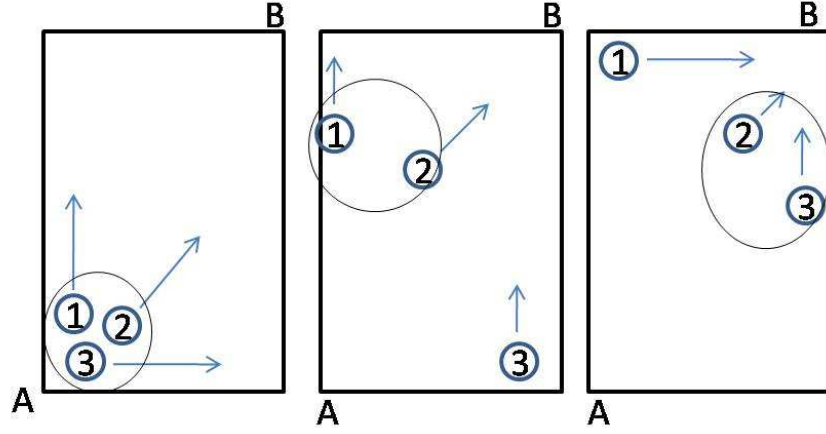
Figure 4.4: The schematic of the network configuration for three "typical" modes of a mobile network.

$$PLR_{ri}(t) = \frac{P_{bi}^r(t) + P_{fi}^r(t) + P_{ci}^r(t)}{\lambda_{ri}(t) + \sum\limits_{j \in \wp_i} \lambda_{ji}^r(t) g_{ji}^r(t) a_{ji}(\alpha_t)} \tag{4.113}$$

$$P_{bi}^r(t) = max\{0, \lambda_{ri}(t) + \sum\limits_{j \in \wp_i} \lambda_{ji}^r(t) g_{ji}^r(t) a_{ji}(\alpha_t) - (x_{buffer,i} - x_{ri}(t))\} \tag{4.114}$$

$$P_{fi}^r(t) = \lambda_{ri}^a(t) - \lambda_{ri}(t) \tag{4.115}$$

$$P_{ci}^r(t) = \sum\limits_{k \in \wp_i} \lambda_{ik}^r(t) g_{ik}^r(t)(1 - a_{ik}(\alpha_t)) \tag{4.116}$$

where P_{bi}^r is the packet loss due to the buffer overflow, P_{fi}^r is the packet loss due to the inadequate flow rate regulation, and $P_{ci}^r(t)$ is the packet loss due to disconnection.

On the other hand, the average queuing delay of the fixed network as defined in equation (3.95) can be extended to the mobile network as

$$E\{T_q^i\} = \frac{E\{x_i(t)\}}{E\{\lambda_i(t)\} + \sum\limits_{j \in \wp_i} E\{\lambda_{ji}(t) g_{ji}(t) a_{ji}(\alpha_t)\}} \tag{4.117}$$

where $E\{T_q^i\}$ is the average queuing delay and $x_i(t)$ is the present queuing state.

4.5.2 Decentralized MJ-SCC vs the Decentralized IDCC

Consider a network with three nodes as shown in Fig. 4.4. These three nodes are supposed to explore a rectangular area by moving from position A to position B. Node 1 moves towards north first and then towards east, node 2 moves towards northeast directly, and

node 3 moves towards east and then towards north. Fig. 4.4 depicts the configuration of the network at three distinct modes during the exploration. As one can see during the movement the neighboring set of each node changes depending on the distance between the nodes.

We assume that each node has three separate logical buffers that are collecting the premium, the ordinary and the best-effort traffics. The buffer size for each traffic is set to 5 Mb, the link capacity of each node is set to $C_{server} = 20$ Mb and the maximum allowable traffic rate are $\lambda^{max} = 15$ Mb. The heterogeneous time delays among the nodes are selected as a random signal with Gaussian distribution that is bounded by 0 and 20 ms. That is, $\tau = min\{0, max\{h_{max}, h\}\}$, where $h_{max} = 20$ ms is the maximum bound of delays, $h \sim N(\mu, \sigma^2)$ is a Gaussian distribution with the mean value of $\mu = 10$ ms and the standard derivation of $\sigma^2 = 5$ ms.

Based on the movement of nodes, a total of 5 switchings modes are defined based on the neighboring set as below

$$M_1 = \{1, 2, 3\}$$

$$M_2 = \{1, 2\}, \ \{3\}$$

$$M_3 = \{1\}, \ \{2, 3\}$$

$$M_4 = \{1, 3\}, \ \{2\}$$

$$M_5 = \{1\}, \{2\}, \{3\}$$

Fig. 4.4 only illustrates three *typical* modes during the movement of the network. The transition probability π_{kl} among different modes are random and is governed by the following rule

$$P[\alpha_{t+\delta} = k \mid \alpha_t = l] = \begin{cases} \pi_{kl}\Delta + o(\Delta), & k \neq l; \\ 1 + \pi_{ll}\Delta + o(\Delta), & k = l. \end{cases} \qquad (4.118)$$

where $\pi_{kl} \geq 0$ is the transition rate from mode k to mode l, $\pi_{ll} = -\sum_{k=1,k \neq l}^{M} \pi_{kl}$, and $o(\Delta)$ is a function satisfying $\lim_{\Delta \to 0} \frac{o(\Delta)}{\Delta} = 0$.

In this simulation, the transition probabilities are assumed to be

$$\Pi = \begin{bmatrix} \pi_{11} & \cdots & \pi_{15} \\ \vdots & \ddots & \vdots \\ \pi_{51} & \cdots & \pi_{55} \end{bmatrix} = \begin{bmatrix} 0.5 & 0.1 & 0.05 & 0.15 & 0.2 \\ 0.1 & 0.6 & 0.1 & 0.1 & 0.1 \\ 0.02 & 0.15 & 0.6 & 0.08 & 0.15 \\ 0.02 & 0.08 & 0.06 & 0.8 & 0.04 \\ 0.2 & 0.1 & 0.3 & 0.2 & 0.2 \end{bmatrix} \tag{4.119}$$

Remark 4.3. *The possible switching modes of a mobile network is dependent on the number of nodes in the network. The more nodes in the network, the more possible neighboring set, and hence the more possible network topologies. In the above simulation, the maximum number of possible changes of neighboring set is 5.*

Remark 4.4. *The transition probability π_{kl} indicates the probability of switching from mode l to mode k. The value of π_{kl} depends on the velocity, the communication range of nodes and the distance among them. In the above simulation, we assume different transition probabilities among the different network modes and use a Monte carlo method [152] to generate a Markov chain based on the transition matrix (4.119).*

The following two cases are considered for evaluating the performance of our proposed MJ-SCC algorithms. Using the specifications above, the traffic compression gains that are calculated from the LMI conditions have the corresponding *mean values* over the simulation time as given below

$$\bar{G}_p = \begin{bmatrix} 0 & 0.31 & 0.23 \\ 0.50 & 0 & 0.23 \\ 0 & 0.40 & 0 \end{bmatrix} \qquad \bar{G}_r = \begin{bmatrix} 0 & 0.23 & 0.23 \\ 0.50 & 0 & 0.23 \\ 0 & 0.30 & 0 \end{bmatrix}$$

A quantitative comparison between the decentralized MJ-SCC scheme and the decentralized IDCC method [3] are performed next. The performance of the premium and the ordinary queues are shown in Fig. 4.5 to Fig. 4.8. As can be seen from Fig. 4.5, the queuing states of all the nodes by utilizing the MJ-SCC strategy do converge to their desired set points with acceptable error bounds. On the contrary, the performance of the queuing length by utilizing the decentralized IDCC approach are shown in Fig. 4.9 to
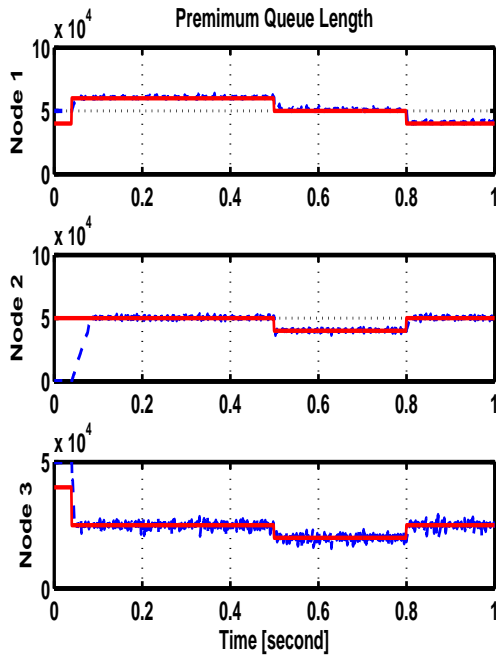
Figure 4.5: Premium queuing lengths by utilizing the proposed decentralized MJ-SCC approach.
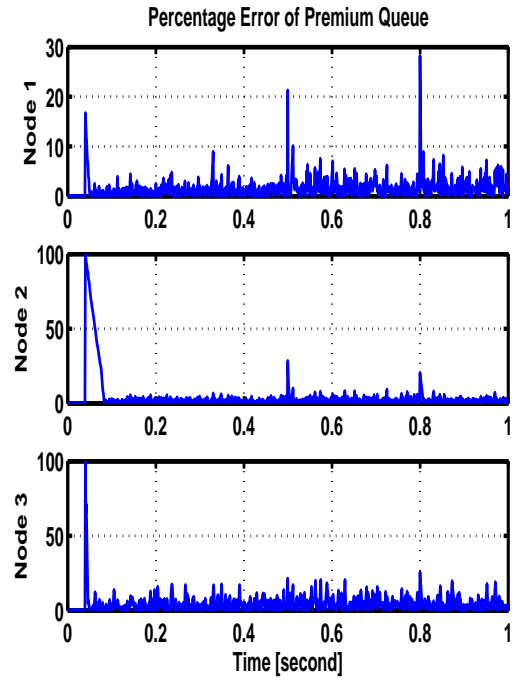
Figure 4.6: Premium queuing error by utilizing the proposed decentralized MJ-SCC approach.
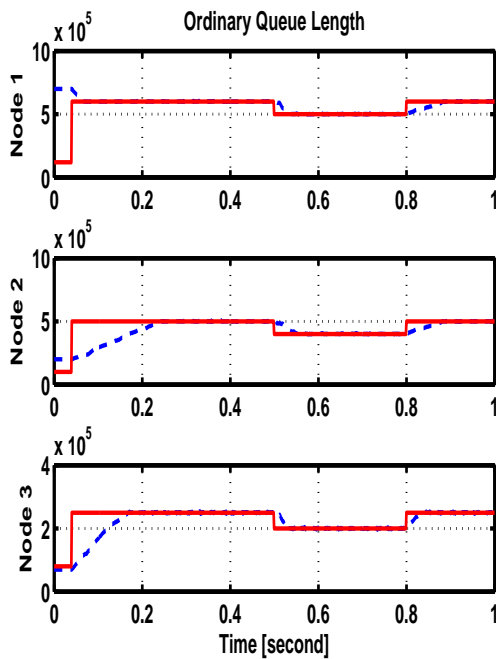
Figure 4.7: Ordinary queuing lengths by utilizing the proposed decentralized MJ-SCC approach.
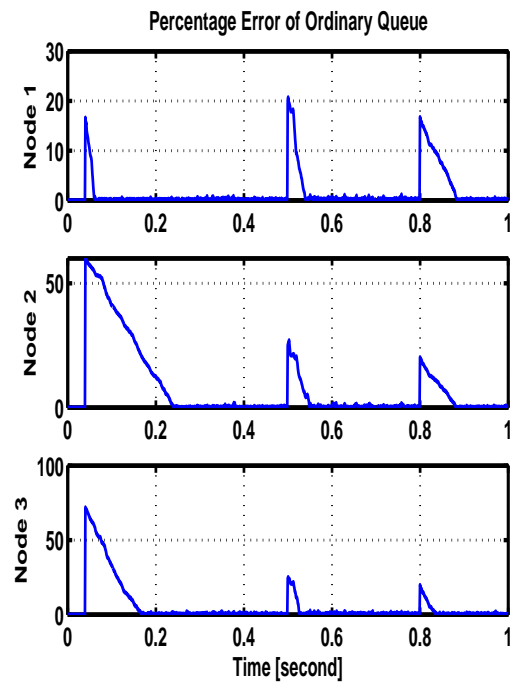
Figure 4.8: Ordinary queuing error by utilizing the proposed decentralized MJ-SCC approach.
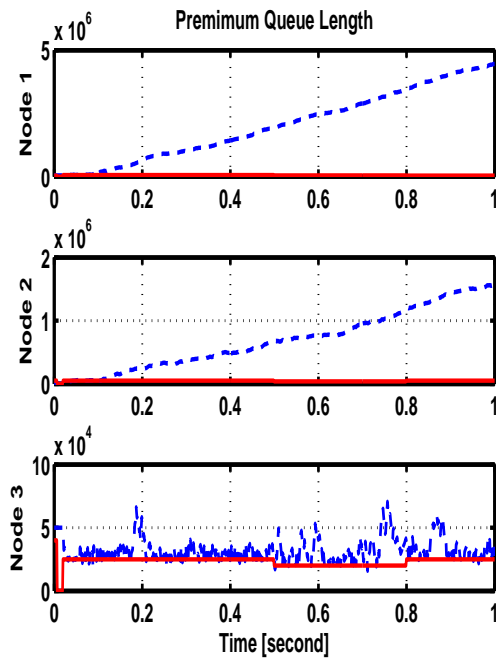
Figure 4.9: Premium queuing lengths by utilizing the decentralized IDCC [3] approach.
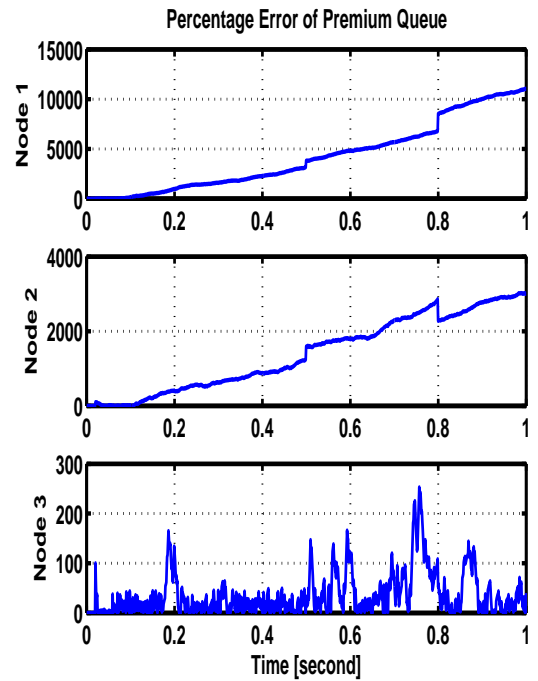
Figure 4.10: Premium queuing error by utilizing the decentralized IDCC [3] approach.
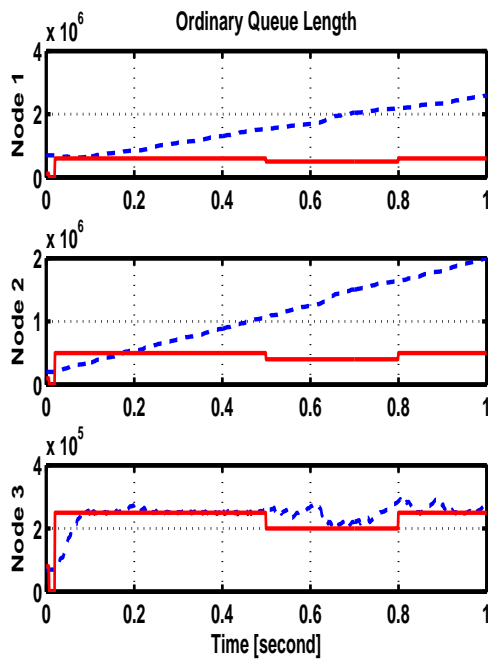
Figure 4.11: Ordinary queuing lengths (bits) by utilizing the decentralized IDCC [3] approach.
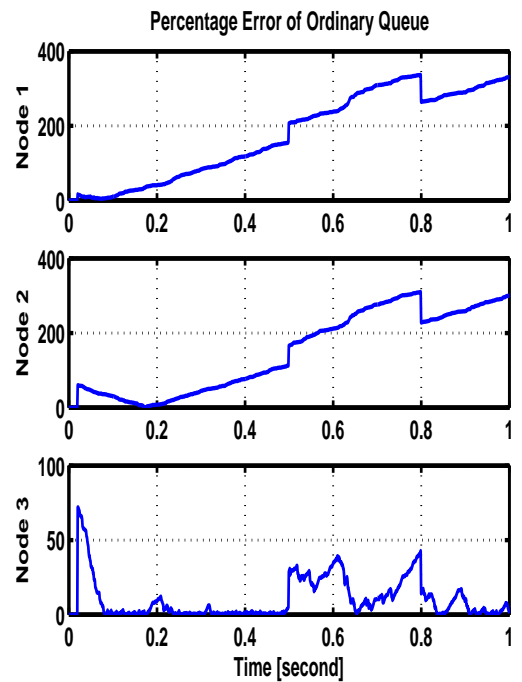
Figure 4.12: Ordinary queuing error by utilizing the decentralized IDCC [3] approach.

182

Table 4.1: Packet loss rate by utilizing the decentralized IDCC method [3] and the MJ-SCC approaches with $h_{max} = 20$ ms.

Premium	IDCC [3]	MJ-SCC
Node 1	99.33%	0.029%
Node 2	96.15%	0.034%
Node 3	93.59%	0.017%
Ordinary	IDCC [3]	MJ-SCC
Node1	89.51%	9.62%
Node 2	96.50%	9.80%
Node 3	98.85%	9.94%

Table 4.2: Average queuing delay by utilizing the decentralized IDCC method [3] and the MJ-SCC approaches with $h_{max} = 20$ ms.

Premium	IDCC [3]	MJ-SCC
Node 1	∞	52.7 ms
Node 2	∞	47.2 ms
Node 3	∞	25.6 ms
Ordinary	IDCC [3]	MJ-SCC
Node 1	∞	570.1 ms
Node 2	∞	406.3 ms
Node 3	∞	205.3 ms

Fig. 4.12. As can be seen, both the queuing sizes of the premium and the ordinary traffic become unstable and the buffer sizes are overflown.

The numerical results of the packet loss rate (PLR) and the average queuing delays are summarized in Table 4.1 and Table 4.2. As can be seen from Table 4.1, by utilizing the IDCC method a large portion of the premium and the ordinary packets to the three nodes are lost. This is due to the fact that the buffer size of the nodes are overflown and all the incoming packets have to be discarded. However, by utilizing our proposed MJ-SCC scheme the performance of the average packet loss rate is significantly improved. By utilizing the MJ-SCC scheme the packet loss of premium traffic is less than 0.05% and the ordinary traffic's loss rate is *less than* 10%. Table 4.2 provides the comparative results corresponding to the average queuing delays. As can be seen from Table 4.2 by utilizing the IDCC method the queuing delays are *infinite* due to the buffer overflow and packet losses. However, by utilizing our MJ-SCC scheme the performance of the network is significantly improved. The queuing delays remain bounded to less than 60 ms for the premium and 600 ms for the ordinary traffic.

4.5.3 Centralized MJ-SCC vs the Centralized IDCC

In this section, the performance of our proposed centralized MJ-SCC is compared with the centralized IDCC approach. Consider the same network model as in Section 4.5.1, where the changes of the network topology α_t and the transition probabilities are set to be the

Table 4.3: Packet loss rate by utilizing the centralized IDCC and the MJ-SCC approaches with $h_{max} = 20$ ms.

Premium	IDCC [3]	MJ-SCC
Node 1	91.24%	0.001%
Node 2	94.41%	0.002%
Node 3	92.13%	0.002%
Ordinary	IDCC [3]	MJ-SCC
Node1	75.25%	6.27%
Node 2	88.56%	6.40%
Node 3	89.08%	5.11%

Table 4.4: Average queuing delay by utilizing the centralized IDCC and the MJ-SCC approaches with $h_{max} = 20$ ms.

Premium	IDCC [3]	MJ-SCC
Node 1	∞	51.4 ms
Node 2	∞	44.8 ms
Node 3	∞	21.5 ms
Ordinary	IDCC [3]	MJ-SCC
Node 1	∞	240.4 ms
Node 2	∞	174.2 ms
Node 3	∞	133.4 ms

same as in equation (4.119). The time delays among nodes are generated by a random signal (using Gaussian distribution) bounded by 0 ms and 20 ms.

The simulation results corresponding to the buffer queue responses for all the nodes by utilizing the centralized IDCC are shown in Fig. 4.13 to Fig. 4.16, for the queuing length and the queuing error of the premium and the ordinary traffic services, respectively. As inspected from the results presented in these figures, one may conclude that for both services the centralized IDCC approach cannot stabilize the queues. The buffers are overflown and large amount of packets are lost.

On the other hand, the buffer queue responses of the premium and the ordinary traffic of nodes 1-3 by utilizing our proposed centralized MJ-SCC algorithm are illustrated in Fig. 4.17 to Fig. 4.20. As revealed from the simulation results, one may argue that for both services our proposed MJ-SCC strategy stabilizes the network in the presence of maximum time-delay of 40 ms and a non-stationary network topology. It can be seen that not only all the buffer queue lengths converge to their respective references, but also the transient responses are faster for the premium service than that with the IDCC approach.

Furthermore, the numerical comparisons of the packet loss rate and the average queuing delays for both traffic classes in all the nodes are given in Table 4.3 and Table 4.4, for the centralized IDCC and the centralized MJ-SCC approaches, respectively. As indicated by the comparative results, one may conclude that for both services the performance of our proposed centralized MJ-SCC strategy is better than the IDCC approach.
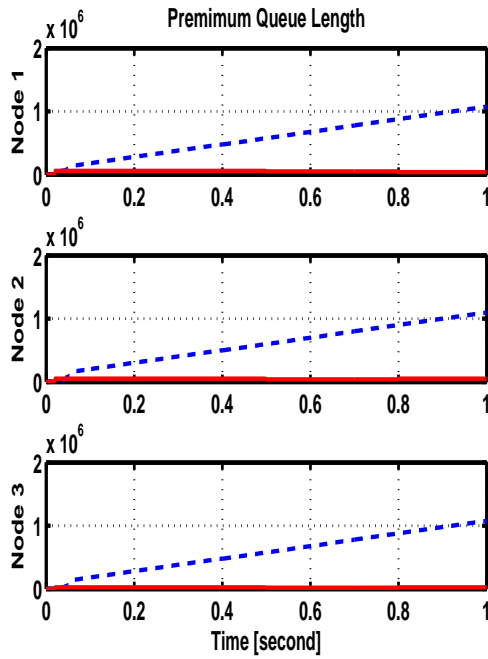
Figure 4.13: Premium queuing lengths by utilizing the centralized IDCC [3].
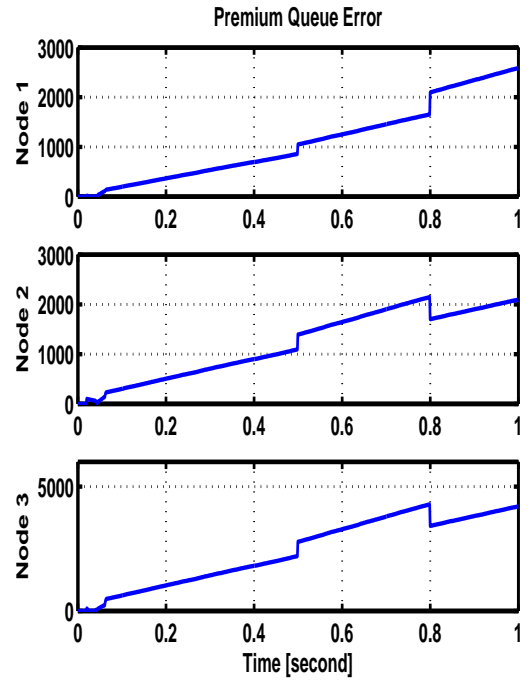
Figure 4.14: Premium queuing error by utilizing the centralized IDCC [3].
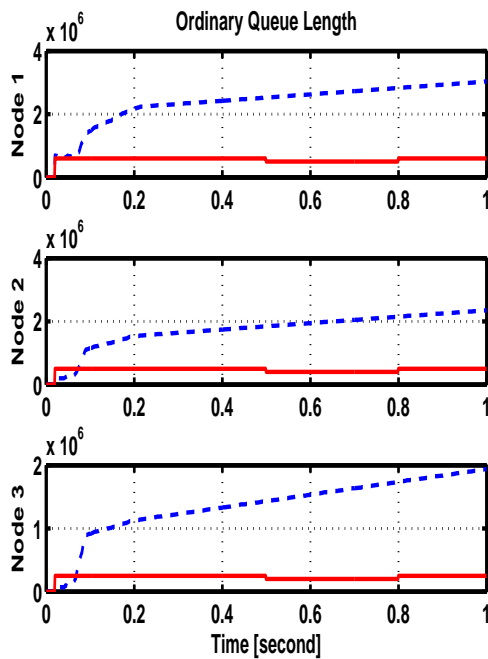
Figure 4.15: Ordinary queuing lengths by utilizing the centralized IDCC [3].
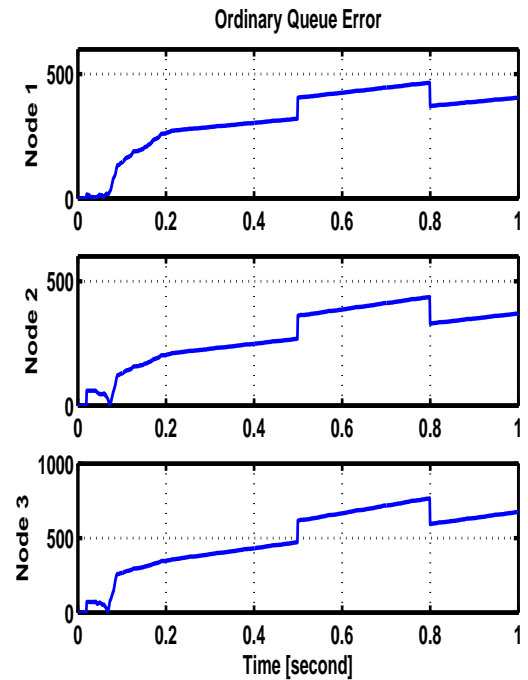
Figure 4.16: Ordinary queuing error by utilizing the centralized IDCC [3].
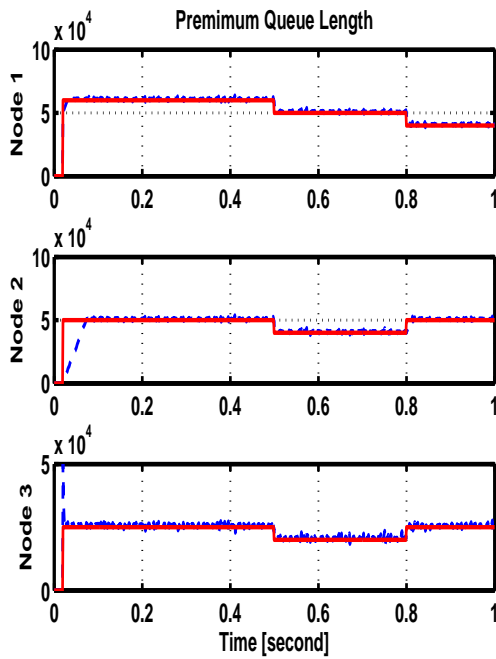
Figure 4.17: Premium queuing lengths by utilizing the proposed centralized MJ-SCC approach.
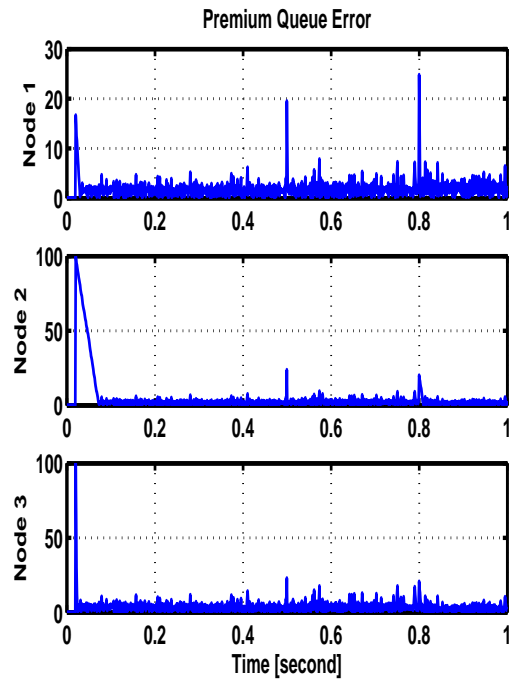
Figure 4.18: Premium queuing error by utilizing the proposed centralized MJ-SCC approach.
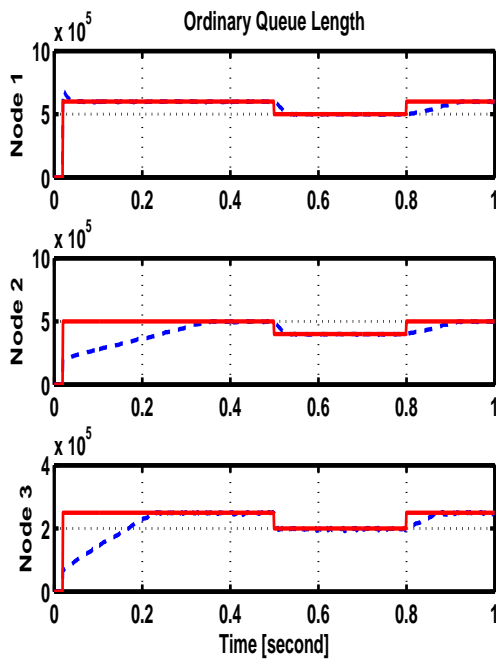
Figure 4.19: Ordinary queuing lengths by utilizing the proposed centralized MJ-SCC approach.
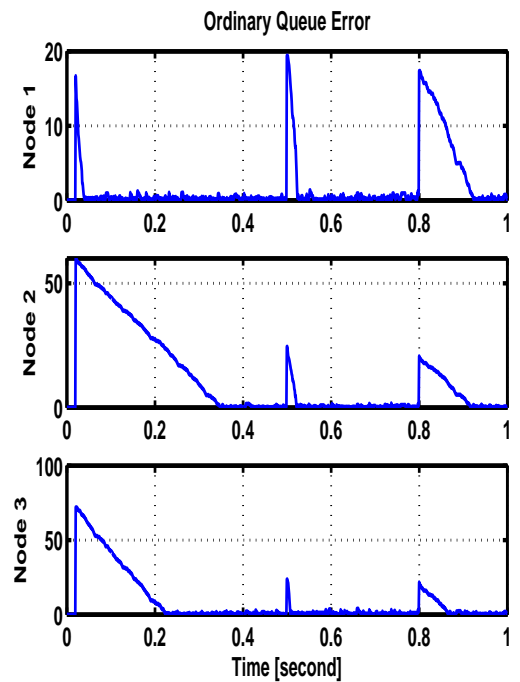
Figure 4.20: Ordinary queuing error by utilizing the proposed centralized MJ-SCC approach.

4.5.4   Centralized MJ-SCC vs the Decentralized MJ-SCC

In this section, the simulation results of the proposed centralized MJ-SCC and the decentralized MJ-SCC that are obtained in the previous two subsections are compared and analyzed. Let us compare the numerical results of the centralized MJ-SCC strategy, as given in Tables 4.3 and 4.4 with that of the decentralized approach, as given in Tables 4.1 and 4.2. One can see that the packet loss rate of the ordinary traffic and the queuing delays of both traffic classes by utilizing the centralized MJ-SCC are smaller. The reason is that in the centralized MJ-SCC approach the controls and regulations are derived based on the entire information of the network and hence is more accurate than that of the decentralized approach. However, as shown in Fig. 4.17 and Fig. 4.20, since the switching conditions of the updates and re-calculations are also based on the situations of all the nodes, the response of the centralized MJ-SCC approach is slower than that of the decentralized one.

Furthermore, in order to evaluate the performance of our proposed congestion control strategies with different level of delays. The time-varying delays are set as below

$$\tau = min\{0, max\{h_{max}, h\}\} \tag{4.120}$$

$$h \sim N(\mu, \sigma^2) \tag{4.121}$$

where h_{max} is the maximum bound of delay in the network that takes values of [20 40 80] ms and h is a random signal with Gaussian distribution of mean value $\mu = 20$ ms and standard derivation $\sigma^2 = 10$ ms.

The average percentage queuing error and the settling time for both traffic classes in node 1 corresponding to different amount of maximum delay h_{max} are given in Table 4.5 and Table 4.6. The settling time is determined as the time when the queuing error has decreased to less than 1% and remain bounded by 2% during the remaining simulation time. As can be seen from the comparison results in Table 4.5 and Table 4.6, it can be concluded that the decentralized MJ-SCC strategy could fairly compete with the performance of the centralized MJ-SCC algorithm. However, as the number of nodes increases, the dimension of the LMI conditions associated with the centralized control strategy will

Table 4.5: The comparisons between the centralized the decentralized MJ-SCC approaches with respect to the queuing error of node 1 subject to different delay levels.

	Centralized MJ-SCC		Decentralized MJ-SCC	
h_{max}	P	O	P	O
20 ms	1.19%	1.04%	1.86%	1.51%
40 ms	1.25%	1.15%	1.96%	1.54%
80 ms	1.48%	1.28%	1.98%	1.74%

Table 4.6: The comparisons between the centralized the decentralized MJ-SCC approaches with respect to the settling time of node 1 subject to different delay levels.

	Centralized MJ-SCC		Decentralized MJ-SCC	
h_{max}	P	O	P	O
20 ms	0.05 s	0.04 s	0.03 s	0.04 s
40 ms	0.06 s	0.07 s	0.06 s	0.05 s
80 ms	0.10 s	0.10 s	0.09 s	0.09 s

increase dramatically and one may not be able to easily obtain the feasible solution due to numerical ill-conditioning and/or reductions in the size of the feasibility regions. On the other hand, the decentralized strategy is scalable and would provide an acceptable performance even in networks with large amounts of delay.

4.6 Conclusions

In this chapter, a novel Markovian jump switching congestion control (MJ-SCC) algorithm for mobile Diff-Serv networks was proposed for both centralized and decentralized frameworks. The queuing dynamics of the network are modeled as a nonlinear time-delay system with Markovian jump parameters. The time-delays considered in the network include transmitting, propagating, and processing delays and are assumed to be unknown and time-varying. The changes of the network topology is viewed as a stochastic process and is modeled by a Markov chain. By taking advantage of the Markovian jump in the network dynamics, changing neighboring sets due to node mobility and changes of the

network topology can be handled.

Furthermore, by employing a switching control strategy, the mode-dependent physical constraints of the network are guaranteed to be satisfied during the congestion control process. The closed-loop system after applying the MJ-SCC algorithms becomes a hybrid system with both stochastic and deterministic switchings. A group of mode-dependent LMI conditions are developed for determining the stability conditions. The congestion control problem of mobile Diff-Serv networks is solved by guaranteeing that the LMI conditions corresponding to each mode is satisfied. The simulation results presented demonstrate that the resulting steady-state and the transient behavior of our proposed congestion control strategies are satisfactory. Numerical comparisons show that the performance of the queuing behavior by utilizing our proposed MJ-SCC algorithms are greatly improved when compared to another model-based method that is available in the literature.

Part II

Guaranteed Cost Congestion

Control Approach

Chapter 5

Guaranteed Cost Congestion Control of DiffServ Networks with Fixed Topology

In this chapter, we consider the congestion control problem of the NMAS subject to the differentiated services by using another approach, namely the *guaranteed cost control approach.* The main disadvantage of the switching congestion control approach is that one needs to regulate the traffic compression gains when the network reaches its physical constraints. However, in some cases this regulation may lead to conservative results and low quality of communication. In this chapter, we first consider the dynamic queuing models of the Diff-Serv networks without considering the physical constraints and a guaranteed cost controller is proposed based on a quadratic cost function. The physical constraints of the system will then be taken into account as extra conditions to the stability of the closed-loop system. In this chapter, the traffic compression gains among the nodes are assumed to be given and as selected by the network operator. Therefore, one does not need to regulate it anymore for stability purposes. As given in Chapter 2, the dynamic queuing models of the Diff-Serv networks are nonlinear systems with multiple and time-varying delays. It is well-known that the feedback linearization technique is a common and

widely applied methodology for nonlinear system control that can transform the original nonlinear system into an equivalent linear one. By employing the feedback linearization technique, the queuing models presented in Chapter 2 are firstly transformed into equivalent linear systems. Then, the *guaranteed cost control* (GCC) approach is applied to design state feedback controllers for each traffic class. The GCC scheme has been shown to be an efficient tool for dealing with system uncertainties and disturbances. Therefore, for the transformed linear queuing models, the congestion control problem of each traffic class is formulated as a guaranteed cost control problem of a time-delay system subject to its corresponding physical constraints.

This chapter is organized in two parts. In the first part, considering the dynamical model of the traffic network that is presented in Chapter 2, a quadratic cost function is defined for the premium and the ordinary traffic and a new centralized congestion control strategy is introduced based on the feedback linearized equivalent linear system model. The proposed congestion control algorithm guarantees the stability of the closed-loop system and can maintain a robust performance of the queuing error in presence of multiple and unknown time-varying delays. The centralized control strategy is then modified to a decentralized congestion control strategy in the second part of this chapter. Therefore, it can be implemented at the output port of each node and hence is scalable to potentially large scale traffic networks.

The remainder of this chapter is structured as follows. In Section 5.1, the traffic model introduced in Chapter 2 is briefly re-called where the input-state feedback linearization technique is applied. The centralized congestion control strategy is developed for both the premium and the ordinary traffic. The physical constraints are then formulated as LMI feasibility conditions. In Section 5.2, the decentralized queuing model is considered and the above results are subsequently extended to a decentralized congestion control strategy. By invoking the stability results derived LMI conditions are proposed that guarantee the stability as well as an optimal guaranteed cost of the traffic network. Performance evaluation and comparisons are illustrated at the end of these two sections. Finally, conclusions are presented in Section 5.3.

5.1 Centralized Guaranteed Cost Congestion Control (GCC) Scheme

In this section, we consider the congestion control problem of the entire network in a centralized control framework. A centralized cost function is considered and a guaranteed cost congestion control strategy is proposed for both the premium and the ordinary traffic.

The centralized dynamic models, as presented in Chapter 2, for the premium traffic (2.37) and the ordinary traffic (2.46) are re-written here for convenience:

$$\dot{x}_p(t) = -F(x_p(t))u_p(t) + \lambda_p(t) + \sum_{l=1}^{m} G_l F(x_p(t - \tau_l(t)))u_p(t - \tau_l) \qquad (5.1)$$

$$\dot{x}_r(t) = -F(x_r(t))u_{r1}(t) + u_{r2}(t) + \sum_{l=1}^{m} G_l F(x_r(t - \tau_l(t)))u_{r1}(t - \tau_l) \qquad (5.2)$$

where "p" denotes the premium traffic and "r" denotes the ordinary traffic, x_p and x_r are the queuing lengths of the premium and ordinary traffic in the nodes, $u_p(t)$ and $u_r(t)$ are the input vectors, $\lambda_p(t)$ is the unknown but bounded external incoming premium traffic, $\tau_l(t)$ is an unknown but bounded time-varying total delay, m is the number of delays in the network, and $F(x_p(t))$, $F(x_r(t))$ and $\sum_{l=1}^{m} G_l$ are the system matrices as defined in (2.30) and (2.36).

The multiple and time-varying delays $\tau_l(t)$ in the queuing dynamics of the premium and the ordinary traffic models (5.1)-(5.2) take into account the propagation, transmission, and processing delays in the network and are unknown. The multiple delays are assumed to be upper bounded by various upper bounds h_l where the maximum upper bound h is assumed to be known. In this chapter, the same assumptions on the time-varying delays as stated in Assumption. 3.1, are adopted in the following synthesis and analysis of the guaranteed cost congestion control algorithms.

Note that, the queuing dynamics of the premium and the ordinary traffic models (5.1)-(5.2) are nonlinear with respect to the queuing states. We observe that the nonlinear terms $F(x(t))$ is only related to the states so that the models can be transformed into equivalent linear systems through an input-state feedback linearization technique by using state and input coordinate transformations.

Feedback Linearization

According to the input-state feedback linearization procedure, the nonlinear system models (5.1)-(5.2) can be transformed into an equivalent linear system by defining the new states and inputs as follows:

$$z_p(t) = x_p(t) - x_p^{ref} \tag{5.3}$$

$$z_r(t) = x_r(t) - x_r^{ref} \tag{5.4}$$

$$u_p(t) = F^{-1}(x_p(t))\bar{u}_p(t) \tag{5.5}$$

$$u_r(t) = G^{-1}(x_r, t)\bar{u}_r(t) \tag{5.6}$$

$$u_r(t) = vec\{u_{r1}(t), u_{r2}(t)\} \tag{5.7}$$

$$\bar{u}_r(t) = vec\{\bar{u}_{r1}(t), \bar{u}_{r2}(t)\} \tag{5.8}$$

$$G(x_r, t) = \begin{bmatrix} F(x_r(t)) & 0 \\ 0 & I \end{bmatrix} \tag{5.9}$$

where x_p^{ref} and x_r^{ref} are the reference queuing length reference "trajectories" that are selected by the network operator, u_r and $\bar{u}_r$ are vectors that consist of two inputs of the ordinary traffic, and $G(x_r, t)$ is the matrix that consists of the nonlinear term of the ordinary traffic $F(x_r(t))$. By using the above transformations and definitions, the new state space representation for the premium and the ordinary traffic queuing models (5.1)-(5.2) can be re-written as follows

$$\dot{z}_p(t) = -\bar{u}_p(t) + \lambda_p(t) + \sum_{l=1}^{m} G_l \bar{u}_p(t - \tau_l(t)) \tag{5.10}$$

$$\dot{z}_r(t) = B_0 \bar{u}_r(t) + \sum_{l=1}^{m} B_l \bar{u}_r(t - \tau_l(t)) \tag{5.11}$$

where $B_0 \in R^{n \times 2n}$ and $B_l \in R^{n \times 2n}$ are the new system matrices defined as, $B_0 = vec\{-I, I\}$ and $B_l = vec\{G_l, 0\}$. The following example is presented to clarify the definitions of the matrices B_0 and B_l.

194

Example 5.1. *Consider the network that is given in Example 2.1. There are three nodes in the network. Let us define*

$$u_{r1}(t) = \begin{bmatrix} C_1(t) \\ C_2(t) \\ C_3(t) \end{bmatrix}, \qquad u_{r1}(t - \tau_l) = \begin{bmatrix} C_1(t - \tau_l) \\ C_2(t - \tau_l) \\ C_3(t - \tau_l) \end{bmatrix}$$

$$u_{r2}(t) = \begin{bmatrix} \lambda_1(t) \\ \lambda_2(t) \\ \lambda_3(t) \end{bmatrix}, \qquad u_{r2}(t - \tau_l) = \begin{bmatrix} \lambda_1(t - \tau_l) \\ \lambda_2(t - \tau_l) \\ \lambda_3(t - \tau_l) \end{bmatrix}$$

where the time-varying delays $\tau_l(t)$, $l = 1, 2, 3$ are defined as in Example 2.1. Correspondingly, the matrices B_0 and B_l are given by

$$B_0 = \begin{bmatrix} -I_{3\times3} & I_{3\times3} \end{bmatrix} \; and \qquad \sum_{l=1}^{m} B_l = \begin{bmatrix} \sum_{l=1}^{m} G_l & 0 \end{bmatrix}$$

Physical Constraints

By using the state and input transformation (5.3)-(5.9), the physical constraints for the new state dynamic models (5.10)-(5.11) are now expressed as follows:

- **Constraints for the states:** Each node has three separate buffers for the premium, the ordinary and the best-effort traffic class. The buffer size for each class is limited. Hence the queuing error has upper and lower bounds with respect to each traffic class as follows:

$$-x_p^{ref} \; \leq z_p(t) \leq \; x_p^{buffer} - x_p^{ref} \tag{5.12}$$

$$-x_r^{ref} \; \leq z_r(t) \leq \; x_r^{buffer} - x_r^{ref} \tag{5.13}$$

  where x_p^{ref} and x_r^{ref} are the reference set points of the queuing length for the premium and the ordinary traffic, respectively, and x_p^{buffer} and x_r^{buffer} are the size of the premium and ordinary buffers.

- **Constraints for the inputs:** The input signal of the premium traffic is the bandwidth capacity that is allocated to it. Since the output capacity of each node is

195

bounded, the input of the premium traffic can not exceed the maximum link capacity, that is

$$0 \quad \leq \bar{u}_p(t) \leq \quad C_{server} \tag{5.14}$$

On the other hand, the ordinary traffic model has two input signals, namely the bandwidth controller $\bar{u}_r^1(t)$ and the flow rate controller $\bar{u}_r^2(t)$. The maximum bandwidth that can be allocated to the ordinary traffic cannot exceed the maximum leftover capacity from the premium traffic class. That is, the constraint of $\bar{u}_r^1(t)$ is time-varying depending on the premium traffic controller $\bar{u}_p(t)$. Furthermore, the flow rate controller $u_r^2(t)$ has to satisfy the transmission constraint (2.17). Therefore, the constraints for the input signals of the ordinary traffic can be written together as follows:

$$0 \quad \leq \bar{u}_r^1(t) \leq \quad c_r(t)$$
$$0 \quad \leq \bar{u}_r^2(t) \leq \quad \lambda_r^{max} < c_r(t)$$
$$0 \quad \leq \bar{u}_r(t) < \quad c_r(t) \tag{5.15}$$

where $c_r(t)$ denotes the instantaneous left-over capacity from the premium traffic, which in fact is equal to $c_r(t) = C_{server} - \bar{u}_p(t)$.

- **Constraints for the external signal:** All the external incoming traffic has to satisfy the transmission constraint (2.17) due to the limitation of the nodes' communication capability, that is:

$$0 \quad \leq \lambda(t) \leq \quad \lambda^{max} \tag{5.16}$$

Based on the above new system models for the premium and the ordinary traffic (5.10)-(5.11), the congestion control problem is now to select the controller $\bar{u}_p$ and $\bar{u}_r$ so that the closed-loop systems are stable. Due to the presence of unknown multiple and time-varying delays, the performance of the closed-loop system has to be robust with respect to the uncertainties in delay, subject to the Assumption. 3.1. The guaranteed cost control approach is viable strategy and has been shown to be a powerful solution for the control design of such time-delay systems. The guaranteed cost controller can maintain

196

the stability and robustness of the closed-loop system by ensuring an upper bound of a given cost function so that the system performance degradations incurred by the delays is guaranteed to be less than this upper bound. According to the guaranteed cost control theory, as presented in Chapter 2, the performance cost function for our congestion control problem is selected as follows.

Performance Cost Function

According to the guaranteed cost control definition (2.59), our proposed congestion control scheme is now to design the controllers $\bar{u}_p(t)$ and $\bar{u}_r(t)$ that simultaneously stabilize the network and maintain a robust performance of the closed-loop system in presence of multiple and time-varying delays. As introduced in Chapter 2, the performance cost function for the premium and the ordinary traffic is selected as follows

$$J = \int_0^\infty (z^T(t)Qz(t) + \bar{u}^T(t)R\bar{u}(t))dt \tag{5.17}$$

where $z(t)$ is the state of the new space representation after applying feedback linearzation as defined in equations (5.10) and (5.11), $\bar{u}(t)$ is the input of the new space representation, and Q and R are given positive definite matrixes.

The above quadratic cost function is a real-valued, non-negative function of time histories of the states, reference trajectories and control inputs. For our congestion control problem, the time histories of the states represent the queuing errors. By properly selecting the control input $\bar{u}$, this cost function will be shown to be bounded, that is the performance degradations incurred by the unknown and time-varying delays are guaranteed to be less than this bound. Consequently, a given set of QoS performance, such as the per flow throughput, the queuing delay and the packet loss rate can be indirectly guaranteed for each traffic class. Our objective in this section is to design a centralized congestion controller for the network model (5.10)-(5.11) subject to the constraints (5.12)-(5.16), under the Assumption. 3.1, so that the closed-loop system of (5.10)-(5.11) is stable and the performance cost (5.17) is upper bounded for any admissible delay.

The control objective for the premium and the ordinary traffic is to regulate the

197

queuing lengths as close as possible to their reference set points such that the QoS performance, such as the packet loss rate, throughput, and the queuing delays can be guaranteed indirectly. However, the premium and the ordinary traffic have different levels of QoS requirements. Moreover, as shown in the system model (5.10), the premium traffic model is a linear time-delay system with unknown but bounded external signals $\lambda_p(t)$. This is due to the incoming traffic of the premium traffic that is not negotiable and thus is not trivial to regulate. The bandwidth is supposed to be allocated to the prmeium class first whenever needed, within the system physical constraints. On the other hand, the ordinary traffic model (5.11) is a linear time-delay system that takes the traffic flow rate as a control input. Therefore, different congestion control strategies have to be selected for these two traffic classes.

In order to guarantee an upper bound on the cost function (5.17), in this chapter we impose a new constraint on the external incoming traffic as given below:

Assumption 5.1. *The external incoming traffic is L_2 norm bounded, that is*

$$\int_0^\infty \|\lambda(t)\|^2 dt \leq \gamma, \qquad \gamma > 0 \tag{5.18}$$

Remark 5.1. *It should be noted that Assumption 5.1 implies that the improper integral of $\|\lambda(t)\|^2$ is convergent. Since $0 \leq \lambda(t) \leq \lambda^{max}$ and $t \in [0, \infty)$, the above condition implies that the external incoming traffic $\lambda(t)$ is asymptotically vanishing, that is*

$$\lim_{t \to \infty} \lambda(t) \to 0 \tag{5.19}$$

In the remainder of this section, we develop congestion control strategies for both the premium and the ordinary traffic.

5.1.1 Premium Traffic Control Strategy

In view of the premium traffic model (5.12), the guaranteed cost control problem for this traffic is selected as a state feedback controller of the form $\bar{u}_p(t) = Kz_p(t)$ that should stabilize the system (5.12) and guarantees the upper bound of the cost function (5.17). However, due to the unknown external incoming traffic $\lambda_p(t)$, an adaptive estimator $\hat{\lambda}_p(t)$

is applied to estimate the unknown external incoming traffic $\lambda_p(t)$ to compensate for its effect via feedback. Thus, according to the robust adaptive control theory [128], the centralized controller $\bar{u}_p(t)$ for the premium traffic is modified as follows:

$$\bar{u}_p(t) = K_1 z_p(t) + K_2 \hat{\lambda}_p(t) \tag{5.20}$$

where $\hat{\lambda}_p(t)$ is an online estimates of the unknown but bounded external traffic flow $\lambda_p(t)$. Motivated from the robust adaptive control technique [128], the time-varying signal $\hat{\lambda}_p(t)$ is now designed according to the *modified parameter projection method* which is given by

$$\dot{\hat{\lambda}}_p(t) = \begin{cases} \Delta z_p(t) - \Pi \hat{\lambda}_p(t) & \text{if } 0 < \hat{\lambda}_p(t) < \lambda_p^{max} \text{ or} \\ & \hat{\lambda}_p(t) = 0, \ z_p(t) \geq 0 \text{ or} \\ & \hat{\lambda}_p(t) = \lambda_p^{max}, \ z_p(t) \leq 0 \\ -\Pi \hat{\lambda}_p(t) & \text{otherwise} \end{cases} \tag{5.21}$$

where Δ and Π are the adaptive control gains that are positive definite matrices which need to be selected. The updating rule of the adaptive estimator $\hat{\lambda}_p(t)$ is based on a group of switching conditions. The switching laws are arbitrary and depend on the queuing states and the instantenous value of the estimates. In other words, the switching time is uncontrollable. Moreover, the switching conditions in (5.21) is centralized. Based on the definition of the inequality (2.39), the estimator will update only when all the nodes simultaneously satisfy the switching conditions.

Let us view the adaptive estimator $\hat{\lambda}_p(t)$ as an extra state so that the premium traffic model (5.10) can be modified to the following standard state space representation

$$\dot{\bar{z}}_p(t) = A_0^k \bar{z}_p(t) + B_0 \bar{u}_p(t) + \sum_{l=1}^{m} B_l \bar{u}_p(t - \tau_l(t)) + B_\lambda \lambda_p(t) \tag{5.22}$$

$$\bar{z}_p(t) = \varphi(t), \ \ t \in [-h, 0]$$

$$k \in \aleph, \aleph = 1, 2$$

where $\bar{z}_p(t) = \begin{bmatrix} z_p(t) & \hat{\lambda}_p(t) \end{bmatrix}^T$ is the new state, $\varphi(t), \ t \in [-h, 0]$ specifies the initial condition of the system, k denotes the switchings of the system which belongs to the set

$\aleph$, and A_0^k, B_0, B_l and B_λ are the system matrices that are defined as

$$A_0^1 = \begin{bmatrix} 0 & 0 \\ \Delta & -\Pi \end{bmatrix}, \quad A_0^2 = \begin{bmatrix} 0 & 0 \\ 0 & -\Pi \end{bmatrix}$$

$$B_0 = \begin{bmatrix} -I \\ 0 \end{bmatrix}, \quad \sum_{l=1}^m B_l = \begin{bmatrix} \sum\limits_{l=1}^m G_l \\ 0 \end{bmatrix}, \quad B_\lambda = \begin{bmatrix} I \\ 0 \end{bmatrix} \qquad (5.23)$$

The premium traffic model (5.30) is a linear switching time-delay system with arbitrary switchings and unknown external signals $\lambda_p(t)$. The congestion control problem for the premium traffic can be recast as a state feedback control $\bar{u}_p = K\bar{z}_p$ where $K = [K_1 \ K_2]$ so that the system (5.23) is stable and the following performance cost function is guaranteed to remain bounded

$$J_p = \int_0^\infty (\bar{z}_p^T(t)Q\bar{z}_p(t) + \bar{u}_p^T(t)R\bar{u}_p)dt \qquad (5.24)$$

The following lemma shows that indeed the state feedback controller $\bar{u}_p = K\bar{z}_p$ is a guaranteed cost controller for the system (5.23).

Lemma 5.1. *Given the system (5.23) and the cost function (5.22) and under Assumption 5.1, if there exists a matrix K, symmetric positive definite matrices P, S_l, $l = 1, ..., m$, and positive definite matrices M, N, $\bar{M}$, $\bar{N}$, such that for all the admissible time-varying delays, under the conditions of Assumption 3.1, the following matrix inequality holds:*

$$\bar{W}_k = \begin{bmatrix} Y_k & P - M^T + (A_c^k + B_c^l K)^T N & -hM^T B_c^l K \\ * & -N - N^T + S_l + \bar{N} & -hN^T B_c^l K \\ * & * & -S_l \end{bmatrix} < 0 \qquad (5.25)$$

where $A_c^k = A_0^k + B_0 K$ and $B_c^l = B_l$ are the closed-loop system matrices, and $Y_k = 2M^T(A_c^k + B_c^l K) + \bar{M} + Q + K^T RK$, then the system (5.23) is ultimately bounded with the control law $\bar{u}_p(t) = K\bar{z}_p(t)$, and the corresponding closed-loop cost function satisfies:

$$J_p < \varphi^T(0)P\varphi(0) + \sum_{l=1}^m \frac{1}{h} \int_{-h}^0 \int_\theta^0 \dot{\varphi}^T(s)S_l\dot{\varphi}(s)dsd\theta + \gamma\lambda_{max}(\Phi) = J_p^* \qquad (5.26)$$

where $\lambda_{max}(\Phi)$ is the maximum eigenvalue of the matrix Φ and $\Phi = B_\lambda^T(\bar{M}^{-1} + \bar{N}^{-1})B_\lambda$. That is, $u_p(t)$ is the guaranteed cost controller for the system (5.23).

Proof: Since the switchings in the system (5.23) is arbitrary, the following common Lyapunov-Krasovskii functional is selected for stability analysis:

$$V = V_1 + V_2$$

$$V_1 = \bar{z}_p^T(t)P\bar{z}_p(t) \tag{5.27}$$

$$V_2 = \sum_{l=1}^{m} \frac{1}{h} \int_{-h}^{0} \int_{t+\theta}^{t} y^T(s)S_l y(s)\,ds\,d\theta \tag{5.28}$$

and where P and S_l are symmetric positive definite matrices, $y(s)$ is the descriptor form of the closed-loop system which is defined by the following descriptor transformation [81]

$$\dot{\bar{z}}_p(t) = y(t)$$

$$y(t) = (A_c^k + \sum_{l=1}^{m} B_c^l K)z_p(t) - \sum_{l=1}^{m} B_c^l K \int_{t-\tau_l(t)}^{t} y(s)\,ds + B_\lambda \lambda_p(t) \tag{5.29}$$

Therefore, by considering Assumption 3.1, the time derivative of V along the trajectories of system (5.23) is given by

$$\dot{V} = \dot{V}_1 + \dot{V}_2$$

$$\dot{V}_1 = 2\bar{z}_p^T(t)Py(t)$$

$$\leq 2[\bar{z}_p^T(t)\ y^T(t)]\begin{bmatrix} P & M^T \\ 0 & N^T \end{bmatrix}\begin{bmatrix} y(t) \\ \dot{\bar{z}}_p(t) - y(t) \end{bmatrix}$$

$$\dot{V}_2 = \sum_{l=1}^{m} y^T(t)S_l y(t) - \frac{1}{h}\sum_{l=1}^{m} \int_{t-h}^{t} y^T(s)S_l y(s)\,ds$$

where M and N are positive definite matrices.

If compare the system (5.22) with the system (3.17), since the structures of the two systems are similar one can follow the similar lines as presented in Lemma 3.1. Consequently, the time derivative of the Lyapunov function becomes:

$$\dot{V} \leq \begin{bmatrix} \bar{z}_p(t) \\ y(t) \end{bmatrix}^T \begin{bmatrix} 2M^T(A_c^k + \sum_{l=1}^{m} B_c^l K) & P - M^T + (A_c^k + \sum_{l=1}^{m} B_c^l K)^T N \\ * & -N - N_k^T + \sum_{l=1}^{m} S_l \end{bmatrix} \begin{bmatrix} \bar{z}_p(t) \\ y(t) \end{bmatrix}$$

$$+ \sum_{l=1}^{m} \frac{1}{\tau_l(t)} \int_{t-\tau_l(t)}^{t} \begin{bmatrix} \bar{z}_p(t) \\ y(t) \\ y(s) \end{bmatrix}^T \begin{bmatrix} 0 & 0 & -hM^T B_c^l K \\ * & 0 & -hN^T B_c^l K \\ * & * & -S_l \end{bmatrix} \begin{bmatrix} \bar{z}_p(t) \\ y(t) \\ y(s) \end{bmatrix} ds$$

$$+ 2\bar{z}_p^T(t)M^T B_\lambda \lambda_p(t) + 2y^T(t)N^T B_\lambda \lambda_p(t)$$

201

For the last two terms in $\dot{V}$, the following Park's inequality (3.24) [129] is applied:

$$2\bar{z}_p^T(t)M^T B_\lambda \lambda_p(t) \leq \bar{z}_p^T(t)\bar{M}\bar{z}_p(t) + \lambda_p^T B_\lambda^T M\bar{M}^{-1}M^T B_\lambda \lambda_p(t) \tag{5.30}$$

$$2y^T(t)N^T B_\lambda \lambda_p(t) \leq y^T(t)\bar{N}y(t) + \lambda_p^T(t)B_\lambda^T N\bar{N}^{-1}N^T B_\lambda \lambda_p(t) \tag{5.31}$$

where $\bar{M}$ and $\bar{N}$ are positive definite matrices. Substituting (5.30) and (5.31) into $\dot{V}$, we obtain

$$\dot{V} \leq \sum_{l=1}^{m} \frac{1}{\tau_l(t)} \int_{t-\tau_l(t)}^{t} [\xi^T(t,s)W_k\xi(t,s) + \lambda_p^T(t)\Phi\lambda_p(t)]ds \tag{5.32}$$

where $\xi^T(t,s) = [\bar{z}_p^T(t) \ y^T(t) \ y^T(s)]^T$, $\Phi = B_\lambda^T(\hat{M}^{-1} + \hat{N}^{-1})B_\lambda$ $(\hat{M}^{-1} = M\bar{M}^{-1}M^T$ and $\hat{N}^{-1} = N\bar{N}^{-1}N^T)$, and

$$W_k = \begin{bmatrix} 2M^T(A_c^k + B_c^l K) + \bar{M} & P - M^T + (A_c^k + B_c^l K)^T N & -hM^T B_c^l K \\ * & -N - N^T + S_l + \bar{N} & -hN^T B_c^l K \\ * & * & -S_l \end{bmatrix}$$

Comparing the matrix W_k with $\bar{W}_k$ in (5.25), one can see that

$$W_k = \bar{W}_k - \Lambda \tag{5.33}$$

$$\Lambda = \begin{bmatrix} Q + K^T RK & 0 & 0 \\ 0 & 0 & 0 \\ 0 & 0 & 0 \end{bmatrix}$$

Hence, the following inequality of $\dot{V}$ holds

$$\dot{V} \leq \sum_{l=1}^{m} \frac{1}{\tau_l(t)} \int_{t-\tau_l(t)}^{t} [\xi^T(t,s)[\bar{W}_k - \Lambda]\xi(t,s) + \lambda_p^T(t)\Phi\lambda_p(t)]ds \tag{5.34}$$

Since $\bar{W}_k < 0$, then for all the admissible delays satisfying the Assumption 3.1, we have

$$\begin{aligned} \dot{V} &< \sum_{l=1}^{m} -\frac{1}{\tau_l(t)} \int_{t-\tau_l(t)}^{t} [\xi^T(t,s)\Lambda\xi(t,s) - \lambda_p^T(t)\Phi\lambda_p(t)]ds \\ &= -\sum_{l=1}^{m} \frac{1}{\tau_l(t)} \int_{t-\tau_l(t)}^{t} [\bar{z}_p^T(t)(Q + K^T RK)\bar{z}_p(t) - \lambda_p^T(t)\Phi\lambda_p(t)]ds \\ &= -\bar{z}_p^T(t)(Q + K^T RK)\bar{z}_p(t) + \lambda_p^T(t)\Phi\lambda_p(t) \\ &\leq -\lambda_{min}(Q + K^T RK)\|\bar{z}_p(t)\|^2 + \lambda_{max}(\Phi)\|\lambda_p(t)\|^2 \end{aligned} \tag{5.35}$$

where λ_{max} and λ_{min} denote the maximum and the minimum eigenvalue of the corresponding matrices, respectively. Therefore, for any $\bar{z}_p(t)$ that satisfies

$$\|\bar{z}_p(t)\|^2 \geq \frac{\lambda_{max}(\Phi)}{\lambda_{min}(Q + K^T RK)}\|\lambda_p(t)\|^2 \tag{5.36}$$

one will have $\dot{V} \leq 0$. Therefore, the system (5.36) is ultimately bounded. The ultimate boundary in (5.36) is time-varying and depend on the instantenous value of the external incoming premium traffic $\lambda_p(t)$. However, the external incoming traffic has to satisfy the transmission constraint (5.16) which is bounded. Consequently, the maximum value of the ultimate boundary can be written as

$$\frac{\lambda_{max}(\Phi)}{\lambda_{min}(Q + K^T R K)} \|\lambda_p^{max}\|^2 \tag{5.37}$$

Therefore, according to the ultimate boundedness Definition (2.6), the system (5.23) is ultimately bounded. Furthermore, from the inequality (5.35), we have

$$\dot{V} \quad < \quad -\bar{z}_p^T(t)(Q + K^T R K)\bar{z}_p(t) + \lambda_p^T(t)\Phi_k\lambda_p(t) \tag{5.38}$$

Integrating (5.38) on both sides from 0 to ∞, one will obtain

$$
\begin{aligned}
J_p \quad &< \quad -\int_0^\infty \dot{V}(t)dt + \int_0^\infty \lambda_p^T(t)\Phi\lambda_p(t)dt \tag{5.39}\\
&= \quad V(0) - V(\infty) + \int_0^\infty \lambda_p^T(t)\Phi\lambda_p(t)dt \\
&< \quad V(0) - V(\infty) + \int_0^\infty \lambda_{max}(\Phi)\|\lambda_p(t)\|^2 dt \\
&\leq \quad V(0) - V(\infty) + \gamma\lambda_{max}(\Phi) \\
&= \quad \varphi^T(0)P\varphi(0) + \sum_{l=1}^m \frac{1}{h}\int_{-h}^0\int_\theta^0 \dot{\varphi}^T(s)S_l\dot{\varphi}(s)dsd\theta - \bar{z}_p^T(\infty)P\bar{z}_p(\infty) + \gamma\lambda_{max}(\Phi) \\
&< \quad \varphi^T(0)P\varphi(0) + \sum_{l=1}^m \frac{1}{h}\int_{-h}^0\int_\theta^0 \dot{\varphi}^T(s)S_l\dot{\varphi}(s)dsd\theta - \lambda_{min}(P)\|\bar{z}_p(\infty)\|^2 + \gamma\lambda_{max}(\Phi)
\end{aligned}
$$

Since the system is ultimately bounded, from the ultimate bound (5.36) one can conclude that:

$$\|z_p(\infty)\|^2 = \frac{\lambda_{max}(\Phi)}{\lambda_{min}(Q + K^T R K)}\|\lambda_p(\infty)\|^2 = 0 \tag{5.40}$$

Substituting (5.40) into J_p, the upper bound of the performance cost function can be written as follows

$$J_p < \varphi^T(0)P\varphi(0) + \sum_{l=1}^m \frac{1}{h}\int_{-h}^0\int_\theta^0 \dot{\varphi}^T(s)S_l\dot{\varphi}(s)dsd\theta + \gamma\lambda_{max}(\Phi) = J_p^* \tag{5.41}$$

Therefore, the system is robust with respect to any admissible time-varying delay under the Assumption 3.1. The degradation of the closed-loop performance incurred by delay is

guaranteed to be less than the upper bound J_p^*. Consequently, the state feedback controller $\bar{u}_p = K\bar{z}_p$ is the guaranteed cost controller of the system (5.23). This completes the proof of Lemma 5.1. ∎

Lemma 5.1 shows that a memoryless state feedback control law $\bar{u}_p = K\bar{z}_p$ is a guaranteed cost controller for the system (5.23). Detailed analysis of the stability conditions and the time-varying ultimate bound will be presented in the next subsection. Here, we first derive the memoryless state feedback control gain K. The following lemma presents a procedure to select K by solving a set of corresponding LMI conditions.

Lemma 5.2. *Consider the system (5.23), Assumption 3.1, and the cost function (5.22), then the state feedback control law $\bar{u}_p = K\bar{z}_p$ is the guaranteed cost controller if there exist symmetric positive definite matrices $\tilde{P}$, $\tilde{S}_l$, positive definite matrices $\tilde{Q}$, $\tilde{R}$, $\tilde{M}$, $\tilde{N}$, $\bar{\bar{M}}$, $\bar{\bar{N}}$, $\bar{\bar{S}}_l$, $l = 1, ..., m$, and matrices X_{1k}, X_{2k}, Y_i, $i = 1, ..., 6$, such that the following LMI conditions are satisfied:*

$$\Omega_k = \begin{bmatrix} 2(X_{1k} + Y_1 + Y_2) + \bar{\bar{M}} + \tilde{Q} + \tilde{R} & \tilde{M}^T - \tilde{P} + X_{2k} + Y_3 + Y_4 & -hY_5 \\ * & -\tilde{N} - \tilde{N}^T + \tilde{S}_l + \bar{\bar{N}} & -hY_6 \\ * & * & -\bar{\bar{S}}_l \end{bmatrix} < 0 \quad (5.42)$$

Furthermore, the state feedback control gain is given by $K = Y_5^{-1} Y_2 \tilde{M}^{-1}$.

Proof: According to Lemma 5.1, the state feedback controller $\bar{u}_p(t) = K\bar{z}_p(t)$ is a guaranteed cost controller of system (5.23) if the matrix inequality (5.25) is satisfied. However, the matrix $\bar{W}_k$ in (5.25) is not linear with respect to the control gain K. To tackle this problem, we need to transform the bilinear matrix inequality (5.25) into a standard LMI condition through equivalent matrix operations. For this purpose, the following matrices are defined:

$$\tilde{M} = M^{-1} \qquad \tilde{P} = P^{-1}$$
$$\tilde{K} = K^+ \qquad \Lambda^T = diag\{\tilde{M} \ \tilde{P} \ \tilde{K}\} \qquad (5.43)$$

where the operator "+" denotes the Moore-Pentose generalized inverse [103] of the matrix K. In view of the above definitions, we pre and post multiply the matrix $\bar{W}_k$ with Λ^T and

Λ, respectively. Then, the following matrix is obtained

$$\Omega_k = \begin{bmatrix} \tilde{M}^T Y_k \tilde{M} & \tilde{M}^T - \tilde{P} + \tilde{M}^T (A_c^k + B_c^l K)^T N \tilde{P} & -h B_c^l \\ * & -\tilde{P}^T (N + N^T) \tilde{P} + \tilde{P}^T S_l \tilde{P} + \tilde{P}^T \bar{N} \tilde{P} & -h \tilde{P}^T N^T B_c^l \\ * & * & -\tilde{K}^T S_l \tilde{K} \end{bmatrix} \qquad (5.44)$$

Recall that $A_c^k = A_0^k + B_0 K$ and $B_c^l = B_l$, so that the first element in the first column of Ω_k can be written as follows

$$\begin{aligned} \tilde{M}^T Y_k \tilde{M} &= 2(A_c^k + \sum_{l=1}^m B_c^l K)\tilde{M} + \tilde{M}^T \bar{M} \tilde{M} + \tilde{M}^T Q \tilde{M} + \tilde{M}^T K^T R K \tilde{M} \\ &= 2(A_0^k + B_0 K + \sum_{l=1}^m B_l K)\tilde{M} + \tilde{M}^T \bar{M} \tilde{M} + \tilde{M}^T Q \tilde{M} + \tilde{M}^T K^T R K \tilde{M} \end{aligned}$$

Let us define

$$\begin{aligned} X_{1k} &= A_0^k \tilde{M} & \tilde{Q} &= \tilde{M}^T Q \tilde{M} \\ X_{2k} &= X_{1k}^T N \tilde{P} & \tilde{R} &= \tilde{M}^T K^T R K \tilde{M} \\ Y_1 &= B_0 K \tilde{M} & \tilde{N} &= \tilde{P}^T N \tilde{P} \\ Y_{2l} &= B_l K \tilde{M} & \tilde{S}_l &= \tilde{P}^T S_l \tilde{P} \\ Y_3 &= Y_1^T N \tilde{P} & \bar{\tilde{M}} &= \tilde{M}^T \bar{M} \tilde{M} \\ Y_4 &= Y_2^T N \tilde{P} & \bar{\tilde{N}}_k &= \tilde{P}^T \bar{N} \tilde{P} \\ Y_{5l} &= B_l & \bar{\tilde{S}}_l &= \tilde{K}^T S_l \tilde{K} \\ Y_6 &= \tilde{P}^T N^T Y_5 \end{aligned}$$

Then the matrix (5.44) becomes

$$\Omega_k = \begin{bmatrix} 2(X_{1k} + Y_1 + Y_2) + \bar{\tilde{M}} + \tilde{Q} + \tilde{R} & \tilde{M}^T - \tilde{P} + X_{2k} + Y_3 + Y_4 & -h Y_5 \\ * & -\tilde{N} - \tilde{N}^T + \tilde{S}_l + \bar{\tilde{N}} & -h Y_6 \\ * & * & -\bar{\tilde{S}}_l \end{bmatrix} \qquad (5.45)$$

By solving the LMI conditions $\Omega_k < 0$, one can obtain

$$P = \tilde{P}^{-1} \qquad (5.46)$$

$$S_l = P^T \bar{S}_l P \qquad (5.47)$$

$$A_0^k = X_{1k} \tilde{M}^{-1} \qquad (5.48)$$

$$B_l = Y_{5l} \qquad (5.49)$$

$$K = Y_5^{-1} Y_2 \tilde{M}^{-1} \qquad (5.50)$$

which completes the proof of Lemma 5.2. ∎

Stability Analysis of the Premium Traffic

Lemma 5.1 shows that the closed-loop system of the premium traffic model (5.23) with the state feedback controller $\bar{u}_p = K\bar{z}_p$ is ultimately bounded. The ultimate bound (5.37) defines a hyper surface in the state space $\bar{z}_p(t)$. When the state $\bar{z}_p(t)$ remains within the surface, we have $\dot{V} > 0$, so that the Lypapunov-Krasovskii function will increase and the system is unstable. However, whenever the state $\bar{z}_p(t)$ reaches or is beyond the hyper surface, we will have $\dot{V} \leq 0$ which implies that the states $\bar{z}_p(t)$ will converge to the boundary of this surface and will remain there.

As mentioned in the last subsection, the ultimate bound of the premium traffic is time-varying and is rewritten as follows:

$$\|\bar{z}_p(t)\|^2 \geq \frac{\lambda_{max}(\Phi)}{\lambda_{min}(Q + K^T R K)} \|\lambda_p(t)\|^2 \tag{5.51}$$

From the above equation, one can see that as the external premium traffic $\lambda_p(t)$ decreases, the ultimate bound of the system will also decrease. Specially, when $\lambda_p(t) \to 0$, the ultimate bound becomes:

$$\|\bar{z}_p(t)\|^2 \to 0 \tag{5.52}$$

which implies that:

$$\lim_{t\to\infty} \bar{z}_p(t) = 0 \tag{5.53}$$

That is, the queuing errors $\lim_{t\to\infty} \bar{z}_p(t) = 0$ and the estimates $\lim_{t\to\infty} \hat{\lambda}_p(t) = 0$. Hence, the system is asymptotically stable. Furthermore, the closed-loop cost J_p in (5.39) can actually achieve better performance when $\lambda_p(t) = 0$, that is

$$J_p|_{\lambda_p(t)=0} < \varphi^T(0)P\varphi(0) + \sum_{l=1}^{m} \frac{1}{h} \int_{-h}^{0} \int_{\theta}^{0} \dot{\varphi}^T(s) S_l \dot{\varphi}(s) ds d\theta$$

Therefore, a more accurate description of the closed-loop performance cost can be stated as follows:

$$J_p < J_p^* \tag{5.54}$$

$$J_{p,min}^* \leq J_p^* \leq J_{p,max}^*$$

$$J_{p,min}^* = \varphi^T(0)P\varphi(0) + \sum_{l=1}^{m} \frac{1}{h} \int_{-h}^{0} \int_{\theta}^{0} \dot{\varphi}^T(s)S_l\dot{\varphi}(s)dsd\theta$$

$$J_{p,max}^* = J_{p,min}^* + \gamma\lambda_{max}(\Phi)$$

In fact, for our congestion control problem, as $\lambda_p(t)$ decreases, the external incoming premium traffic decreases, which implies the network load is decreasing. Hence, a better congestion control result (queuing errors reduce) can be obtained. When $\lambda_p(t) = 0$, there is no external traffic from outside the network, so that the best congestion control result can be achieved (queuing errors = 0).

Furthermore, since the dynamic system model of the premium traffic is a switching system, the stability conditions in (5.25) contain two LMIs with respect to the two sub-systems. To ensure the stability of the entire system one needs to check the feasibility of the two LMIs at each time. However, these LMIs will only impact the control parameter embedded in matrix A_0^k. The memoryless state feedback control gain K will be the same for both LMIs.

Stability Conditions Incorporating the Physical Constraints

When looking for a feasible solution to the delay-dependent stability conditions given by the main LMI condition (5.45), the physical constraints of the system have to be considered. In this section, the physical constraints (5.12)-(5.16) are transformed into LMI conditions. These complementary LMIs, together with the stability condition (5.45) will be taken into account for determining a complete solution to the congestion control problem.

Constraints of the State

As mentioned in (5.12), the state constraints can be expressed in the terms of the transformed new state $\bar{z}_p(t)$ as follows

$$\bar{z}_p^{min} \leq \bar{z}_p(t) \leq \bar{z}_p^{max} \tag{5.55}$$

where $\bar{z}_p^{min} = vec\{-x_p^{ref} \; 0\}$ is the lower bound of the state, $\bar{z}_p^{max}$ is the upper bound of the state which is in fact a vector of the maximum queuing error $x_p^{buffer} - x_p^{ref}$ and the maximum allowable incoming traffic λ_p^{max} induced by the transmission constraint. By squaring (5.55) we get:

$$\bar{z}_p^T(t)\bar{z}_p(t) \leq \|\bar{z}_p^{max}\|^2 \tag{5.56}$$

Let us define the following ellipsoid for a selected $\epsilon_1 > 0$

$$\mathbb{F} = \{\bar{z}_p(t)|\bar{z}_p^T \tilde{P}^{-1}\bar{z}_p \leq \epsilon_1\} \tag{5.57}$$

If the stability condition (5.42) is satisfied, then it follows from the definition of V in (5.27) that,

$$\bar{z}_p^T \tilde{P}^{-1}\bar{z}_p \leq V(t) \tag{5.58}$$

since $\tilde{P}^{-1} = P$ and $P = P^T > 0$.

On the other hand, by integrating $\dot{V}$ given in (5.38), from 0 to t and considering $V(0) = 0$, one gets

$$\begin{aligned}
V(t) \quad &< \quad -\int_0^t \bar{z}_p^T(t)(Q + K^T R K)\bar{z}_p(t)dt + \int_0^t \lambda_p^T(t)\Phi\lambda_p(t)dt \\
&< \quad \int_0^t \lambda_p^T(t)\Phi\lambda_p(t)dt \\
&< \quad \int_0^\infty \lambda_p^T(t)\Phi\lambda_p(t)dt \\
&< \quad \gamma\lambda_{max}(\Phi) \tag{5.59}
\end{aligned}$$

where λ_{max} denotes the maximum eigenvalue of the matrix Φ. Therefore, $\bar{z}_p(t)$ belongs to the invariant set $\mathbb{F}$ for all $t > 0$ if:

$$\gamma\lambda_{max}(\Phi) \leq \epsilon_1 \tag{5.60}$$

Therefore, the right hand side of the constraint (5.55) will be satisfied if

$$\epsilon_1/\|\bar{z}_p^{max}\|^2 \leq \tilde{P}^{-1} \tag{5.61}$$

Applying Schur complement to (5.61), the right hand side of the state constraint (5.55) can be expressed according to the following LMI conditions

$$\Omega_{c1} \quad \triangleq \quad \gamma\lambda_{max}(\Phi) \leq \epsilon_1 \tag{5.62}$$

$$\Omega_{c2} \quad \triangleq \quad \begin{bmatrix} \tilde{P} & \tilde{P}^T \\ \tilde{P} & \|\bar{z}_p^{max}\|^2/\epsilon_1 \end{bmatrix} \geq 0 \tag{5.63}$$

On the other hand, the left hand side of the state constraint (5.55) is equal to:

$$\bar{z}_p(t) - \bar{z}_p^{min} \geq 0 \tag{5.64}$$

In order to solve the above non-negative constraint, the following definition of the non-negative system is needed:

Definition 5.1. *[153] The liner time-delay system $\dot{x} = A_0 x(t) + A_1 x(t - \tau(t))$ is said to be non-negative if and only if A_0 is essentially non-negative and A_1 is non-negative, that is, the off-diagonal entries of A_0 are non-negative and all the entries of A_1 are non-negative.*

By substituting the state feedback controller $\bar{u}_p = K\bar{z}_p$ into the premium traffic model (5.22), and noting that $\dot{\bar{z}}_p(t) - \dot{\bar{z}}_p^{min} = \dot{\bar{z}}_p(t)$, the closed-loop dynamics can be expressed as

$$\dot{\bar{z}}_p(t) - \dot{\bar{z}}_p^{min} = (A_0^k + B_0 K)\bar{z}_p(t) + \sum_{l=1}^{m} B_l K \bar{z}_p(t - \tau_l(t)) + B_\lambda \lambda_p(t) \tag{5.65}$$

Therefore, if the above system is non-negative, then the left hand side of the state constraint (5.55) is ensured. According to the Definition 5.1, we need to choose $A_0^k + B_0 K$ to be essentially non-negative and $\sum_{l=1}^{m} B_l K$ to be non-negative. By selecting the positive definite matrix $\tilde{M}$ to be a diagonal matrix and noting that $K = Y_5^{-1} Y_2 \tilde{M}^{-1}$, $A_0^k = X_{1k}$, and $\sum_{l=1}^{m} B_l = Y_5$, the non-negative conditions of the closed-loop system matrices can be expressed as follows:

$$\Omega_{c3} \triangleq (X_{1k} + B_0 Y_5^{-1} Y_2)_{ij} \geq 0, \qquad i \neq j \tag{5.66}$$

$$\Omega_{c4} \triangleq (Y_2)_{ij} \geq 0 \qquad i, j = 1, ...2n \tag{5.67}$$

Constraints of the input

The constraint of the premium traffic input due to the capacity limitation is rewritten here again:

$$0 \leq \bar{u}_p(t) \leq C_{server} \tag{5.68}$$

Using (5.53), the feedback controller $\bar{u}_p$ can be defined as follows:

$$\bar{u}_p = Y_5^{-1} Y_2 \tilde{M}^{-1} \bar{z}_p$$

209

Therefore, (5.68) can be written as below:

$$0 \leq Y_5^{-1} Y_2 \tilde{M}^{-1} \bar{z}_p \leq C_{server} \tag{5.69}$$

Adopting the similar lines that are used for the state constraint and considering the ellipsoid (5.57), the right hand side of the input constraint is satisfied if:

$$(Y_5^{-1} Y_2 \tilde{M}^{-1})^T (\epsilon_1 / \|C_{server}\|^2) Y_5^{-1} Y_2 \tilde{M}^{-1} \leq \tilde{P}^{-1} \tag{5.70}$$

which can be transformed into the following LMI condition

$$\Omega_{c5} \triangleq \begin{bmatrix} I & (Y_5^{-1} Y_2 \tilde{M}^{-1})^T \\ Y_5^{-1} Y_2 \tilde{M}^{-1} & (\|C_{server}\|^2 / \epsilon_1) \tilde{P} \end{bmatrix} \geq 0$$

$$\Leftrightarrow \begin{bmatrix} I & K^T \\ K & (\|C_{server}\|^2 / \epsilon_1) \tilde{P} \end{bmatrix} \geq 0 \tag{5.71}$$

The non-negative constraint of the input $\bar{u}_p(t) \geq 0$ can be satisfied if we specify $K_{ij} > 0$. Hence, by using $K = Y_5^{-1} Y_2 \tilde{M}^{-1}$ and noting that $\tilde{M}$ is set to be diagonal positive definite, the non-negative side of the input constraint (5.68) can now be expressed by the following LMI conditions

$$(Y_5^{-1} Y_2)_{ij} \geq 0, \qquad i, j = 1, ..., 2n \tag{5.72}$$

Noting the conditions Ω_{c4} for the non-negative constraint of the state, the above condition is equivalent to the following condition:

$$\Omega_{c6} \triangleq (Y_5^{-1})_{ij} \geq 0 \tag{5.73}$$

Remark 5.2. *The LMI condition Ω_k as given in Lemma 5.2, together with the above constraint conditions Ω_{c1} to Ω_{c6}, have the following three properties*

1. *They guarantee the ultimate boundedness of the premium traffic dynamic system (5.23).*

2. *They provide a guaranteed cost controller for the premium traffic class, that is $\bar{u}_p = K\bar{z}_p$ with the control gain $K = Y_5^{-1} Y_2 \tilde{M}^{-1}$, where the matrices Y_5, Y_2 and $\tilde{M}$ are derived based on the above conditions.*

3. *They produce the update control gains Δ_p and Π_p, as shown in the system matrix A_0^k, which is given by (5.46).*

Remark 5.3. *The condition Ω_{c3} is not linear with respect to the matrices therein, hence is difficult to be satisfied directly. In addition, noting that by satisfying Ω_{c4} and Ω_{c6} one obtains the matrices Y_5 and Y_2 with positive elements. On the other hand, since the matrix $B_0 = \begin{bmatrix} -I & 0 \end{bmatrix}^T$, then by multiplying $B_0 Y_5^{-1} Y_2$ to (5.66) lead to a square matrix with the upper half block of $-Y_5^{-1} Y_2$ and the bottom half block with zeros.*

Now, Let us first define the matrices X_{1k} and $\tilde{M}$ as the following block matrices

$$X_{1k} = \begin{bmatrix} X_{1k}^1 & X_{1k}^2 \\ X_{1k}^3 & X_{1k}^4 \end{bmatrix} \qquad \tilde{M} = \begin{bmatrix} \tilde{M}_1 & 0 \\ 0 & \tilde{M}_2 \end{bmatrix} \tag{5.74}$$

Hence, by setting the blocks $\tilde{M}_1$ and $\tilde{M}_2$ to be diagonal positive definite, $\tilde{M}$ will be diagonal definite positive too.

Therefore, recall that the control gain K is a rectangular matrix of to-be-designed parameters with the form $K = \begin{bmatrix} K_1 & K_2 \end{bmatrix}$. Since, the matrix Y_5 and Y_2 are required to be equal to:

$$Y_5 \;=\; \sum_{l=1}^{m} B_l \qquad\qquad Y_2 = \sum_{l=1}^{m} B_l K \tilde{M}$$

then, $B_0 Y_5^{-1} Y_2$ is required to be equal to:

$$B_0 Y_5^{-1} Y_2 \;=\; \begin{bmatrix} -K_1 \tilde{M}_1 & -K_2 \tilde{M}_2 \\ 0 & 0 \end{bmatrix} \tag{5.75}$$

Hence, $X_{ik} + B_0 Y_5^{-1} Y_2$ results in a square matrix which is required to be equal to

$$X_{ik} + B_0 Y_5^{-1} Y_2 = \begin{bmatrix} X_{1k}^1 - K_1 \tilde{M}_1 & X_{1k}^2 - K_2 \tilde{M}_2 \\ X_{1k}^3 & X_{1k}^4 \end{bmatrix} \tag{5.76}$$

Therefore, by selecting the positive definite matrices $\tilde{M}_1$ and $\tilde{M}_2$ to be diagonal matrices, setting $X_{1k}^1 - K_1$ and X_{1k}^4 to be essentially non-negative, and setting $X_{1k}^2 - K_2$ and X_{1k}^3 to be non-negative, the condition Ω_{c3} will be ensured indirectly.

Remark 5.4. *As stated in Remark 5.2, the LMI conditions are required to produce the update estimation gains Δ_p and Π_p through deriving the system matrices A_0^k and*

$\sum_{l=1}^{m} B_l$.Specifically, the matrix A_0^k in the premium dynamic system (5.23) is defined as follows

$$A_0^1 = \begin{bmatrix} 0 & 0 \\ -\Delta & -\Pi \end{bmatrix} \qquad A_0^2 = \begin{bmatrix} 0 & 0 \\ 0 & -\Pi \end{bmatrix} \qquad k = 1, 2$$

On the other hand, from the LMI condition in Lemma 5.2, A_0^k is required to be equal to:

$$A_0^k = X_{1k}\tilde{M}^{-1} = \begin{bmatrix} X_{1k}^1 \tilde{M}_1^{-1} & X_{1k}^2 \tilde{M}_2^{-1} \\ X_{1k}^3 \tilde{M}_1^{-1} & X_{1k}^4 \tilde{M}_2^{-1} \end{bmatrix}$$

Noting that the matrix $\tilde{M}^{-1}$ is diagonal and positive definite, the adaptive gains Δ and Π need to be positive definite, and the (essential) non-negative conditions given at the end of Remark 5.3,then it follows that the condition Ω_{c3} can be finally transformed into

$$X_{11}^1 = X_{12}^1 = 0$$

$$X_{11}^2 = X_{12}^2 = 0$$

$$X_{11}^3 > 0 \ \ and \ is \ diagonal$$

$$X_{12}^3 = 0$$

$$X_{11}^4 = X_{12}^4 < 0 \ \ and \ is \ diagonal$$

The results above together with the LMI condition Ω_k in Lemma 5.1 can be summarized by the following theorem.

Theorem 5.1. *A guaranteed cost controller K for the premium traffic class with dynamical queuing model (5.22) is obtained by solving the LMI condition Ω_k in Lemma 5.2 and the LMI conditions Ω_{c1}, Ω_{c2}, Ω_{c4}, Ω_{c5}, Ω_{c6}, subject to the following block matrices:*

$$X_{1k} = \begin{bmatrix} 0 & 0 \\ X_{1k}^3 & X_{1k}^4 \end{bmatrix} \qquad \tilde{M} = \begin{bmatrix} \tilde{M}_1 & 0 \\ 0 & \tilde{M}_2 \end{bmatrix} \tag{5.77}$$

with diagonal positive definite matrices $\tilde{M}_1$, $\tilde{M}_2$, diagonal negative definite matrices X_{1k}^4, for $k = 1, 2$, diagonal positive definite matrix X_{1k}^3 when $k = 1$, and zero matrix X_{1k}^3 when $k = 2$.

> **Proof:** The proof follows from the constructive derivations that are given above in this section. ∎

5.1.2 Ordinary Traffic Control Strategy

Let us recall the dynamic model of the ordinary traffic for convenience again

$$\dot{z}_r(t) = B_0 \bar{u}_r(t) + \sum_{l=1}^{m} B_l \bar{u}_r(t - \tau_l(t)) \tag{5.78}$$

$$z_r(t) = \phi(t), \ \ t \in [-h, 0]$$

where $u_r(t) = [u_r^1(t) \ u_r^2(t)]$ is the input signal, and $z_r(t) = \phi(t), \ \ t \in [-h, 0]$ is the initial condition of the system. Since the external incoming ordinary traffic flow $\lambda_r(t)$ represents controllable, the congestion control problem for the ordinary traffic is actually to design a state feedback controller $\bar{u}_r(t) = K z_r(t)$ so that the closed-loop system of (5.55) is asymptotically stable and the following corresponding quadratic cost function is bounded

$$J_r = \int_0^\infty (z_r^T(t) Q z_r(t) + \bar{u}_r^T(t) R \bar{u}_r(t)) dt \tag{5.79}$$

First we present a sufficient condition for the existence of a memoryless state feedback guaranteed-cost control law for the ordinary traffic model (5.55).

Lemma 5.3. *Consider the system (5.78) and the cost function (5.79) and under Assumption 5.1, the control law $u_r(t) = K z_r(t)$ is a guaranteed cost controller if there exist symmetric positive definite matrices P, S_l, $l = 1, ..., m$, and positive definite matrices M and N such that for all the admissible time-varying delays satisfying Assumption 3.1, the following matrix inequality condition holds*

$$\bar{W} = \begin{bmatrix} X & P - M^T + K^T(B_0 + B_l)^T N & -hM^T B_l K \\ * & -N - N^T + S_l & -hN^T B_l K \\ * & * & -S_l \end{bmatrix} < 0 \tag{5.80}$$

where $X = 2M^T(B_0 + B_l)K + Q + K^T R K$.

Proof: Let $u_r(t) = K z_r(t)$ be applied to (5.78), so that the resulting closed-loop system becomes

$$\dot{z}_r(t) = B_0 K z_r(t) + \sum_{l=1}^{m} B_l K z_r(t - \tau_l(t)) \tag{5.81}$$

Choose a Lyapunov-Krasovskii functional candidate for the system (5.78) as

$$V = \bar{z}_r^T(t) P \bar{z}_r(t) + \sum_{l=1}^{m} \frac{1}{h} \int_{-h}^{0} \int_{t+\theta}^{t} y^T(s) S_l y(s) ds d\theta$$

213

where P and S_l are symmetric positive definite matrices.

The above close-loop system model can be written as

$$
\begin{aligned}
\dot{z}_r(t) &= y(t) \\
y(t) &= (B_0 K + \sum_{l=1}^{m} B_l K) z_r(t) - \sum_{l=1}^{m} \int_{t-\tau_l(t)}^{t} B_l K y(s) ds
\end{aligned}
\tag{5.82}
$$

so that the time derivative of $V(t)$ along the trajectories of (5.78) becomes:

$$
\begin{aligned}
\dot{V} &= 2z_r^T(t) P y(t) + \sum_{l=1}^{m} y^T(t) S_l y(t) - \frac{1}{h} \sum_{l=1}^{m} \int_{t-h}^{t} y^T(s) S_l y(s) ds \\
&= 2[z_r^T(t)\ y^T(t)] \begin{bmatrix} P & M^T \\ 0 & N^T \end{bmatrix} \begin{bmatrix} y(t) \\ \dot{z}_r(t) - y(t) \end{bmatrix} \\
&\quad + \sum_{l=1}^{m} y^T(t) S_l y(t) - \frac{1}{h} \sum_{l=1}^{m} \int_{t-h}^{t} y^T(s) S_l y(s) ds \\
&\leq \begin{bmatrix} z_r(t) \\ y(t) \end{bmatrix}^T \begin{bmatrix} 2M^T(B_0 + \sum_{l=1}^{m} B_l)K & P - M^T + K^T(B_0 + \sum_{l=1}^{m} B_l)TN \\ * & -N_k - N^T + \sum_{l=1}^{m} S_l \end{bmatrix} \begin{bmatrix} z_r(t) \\ y(t) \end{bmatrix} \\
&\quad + \sum_{l=1}^{m} \frac{1}{\tau_l(t)} \int_{t-\tau_l(t)}^{t} \begin{bmatrix} z_r(t) \\ y(t) \\ y(s) \end{bmatrix}^T \begin{bmatrix} 0 & 0 & -hM^T B_l K \\ * & 0 & -hN^T B_l K \\ * & * & -S_l \end{bmatrix} \begin{bmatrix} z_r(t) \\ y(t) \\ y(s) \end{bmatrix} ds \\
&\leq \sum_{l=1}^{m} \frac{1}{\tau_l(t)} \int_{t-\tau_l(t)}^{t} \xi_r^T(t,s) W \xi_r(t,s) ds
\end{aligned}
\tag{5.83}
$$

where $\xi_r(t,s) = \begin{bmatrix} z_r^T(t) & y^T(t) & y^T(s) \end{bmatrix}^T$, M and N are positive definite matrices, and the matrix W is given by

$$
W = \begin{bmatrix} 2M^T(B_0 + B_l)K & P - M^T + K^T(B_0 + B_l)^T N & -hM^T B_l K \\ * & -N - N^T + S_l & -hN^T B_l K \\ * & * & -S_l \end{bmatrix}
\tag{5.84}
$$

Since $W = \bar{W} - Q - K^T R K$, the derivative of V can be re-written as follows

$$
\begin{aligned}
\dot{V} &< \sum_{l=1}^{m} \frac{1}{\tau_l(t)} \int_{t-\tau_l(t)}^{t} \xi_r^T(t,s)(\bar{W} - Q - K^T R K)\xi_r(t,s) ds \\
&< \sum_{l=1}^{m} \frac{1}{\tau_l(t)} \int_{t-\tau_l(t)}^{t} -z_r^T(t)(Q + K^T R K)z_r(t) ds \\
&= -z_r^T(t)(Q + K^T R K)z_r(t) < 0
\end{aligned}
\tag{5.85}
$$

214

Therefore, it follows that the closed-loop system (5.81) is asymptotically stable. Furthermore, by integrating both sides of the above inequality from 0 to ∞ and using the initial condition, we will have

$$
\begin{aligned}
J_r &< \int_0^\infty -\dot{V} dt \\
&= V(0) - V(\infty) \\
&= V(0) \\
&= \phi^T(0)P\phi(0) + \sum_{l=1}^m \frac{1}{h} \int_{-h}^0 \int_\theta^0 \dot{\phi}^T(s) S_l \dot{\phi}(s) ds d\theta = J_r^*
\end{aligned}
\tag{5.86}
$$

Therefore, the quadratic cost function for the ordinary traffic class (5.79) is upper bounded. The closed-loop system performance is guaranteed for any admissible unknown and time-varying delays. According to the definition of guaranteed cost control (GCC), the state feedback control law $\bar{u}_r = K z_r$ is the GCC controller of the system (5.78). This completes the proof of Lemma 5.3. ∎

In the following lemma, we show that the sufficient condition for the existence of guaranteed cost controller K is equivalent to the solvability of a system of LMIs.

Lemma 5.4. *For the system (5.78), if there exist symmetric positive definite matrices Λ_2, $\tilde{S}_l$, positive definite matrices Λ_1, $\tilde{Q}$, $\tilde{R}$, $\tilde{N}$, $\bar{\bar{S}}_l$, for $l = 1, ..., m$, and matrices θ_i, for $i = 1, ...6$, such that the following LMI condition is satisfied:*

$$
\Omega = \begin{bmatrix} 2(\theta_1 + \theta_2) + \tilde{Q} + \tilde{R} & \Lambda_1^T - \Lambda_2 + \theta_3 + \theta_4 & -h\theta_5 \\ * & -\tilde{N} - \tilde{N}^T + \tilde{S}_l & -h\theta_6 \\ * & * & -\bar{\bar{S}}_l \end{bmatrix} < 0
\tag{5.87}
$$

then the state feedback controller $\bar{u}_r = K z_r$ with the control gain $K = \theta_5^{-1} \theta_2 \Lambda_1^{-1}$ is the guaranteed cost control law of the system (5.78).

Proof: The following matrices are defined to transform the bilinear matrix $\bar{W}$ into an equivalent linear matrix Ω, namely

$$
\Lambda_1 = M^{-1} \qquad \Lambda_2 = P^{-1}
$$

$$
\Lambda_3 = K^+ \qquad \Lambda = diag\{\Lambda_1 \ \Lambda_2 \ \Lambda_3\}
$$

By pre and post multiplying the matrix $\bar{W}$ with Λ^T and Λ, respectively, one obtains

$$\Omega = \begin{bmatrix} 2(\theta_1 + \theta_2) + \tilde{Q} + \tilde{R} & \Lambda_1^T - \Lambda_2 + \theta_3 + \theta_4 & -h\theta_5 \\ * & -\tilde{N} - \tilde{N}^T + \tilde{S}_l & -h\theta_6 \\ * & * & -\bar{\bar{S}}_l \end{bmatrix} \qquad (5.88)$$

where

$$
\begin{aligned}
\theta_1 &= B_0 K \Lambda_1 & \tilde{Q} &= \Lambda_1^T Q \Lambda_1 \\
\theta_{2l} &= B_l K \Lambda_1 & \tilde{R} &= \Lambda_1^T K^T R K \Lambda_1 \\
\theta_3 &= \theta_1^T N \Lambda_2 & \tilde{N} &= \Lambda_2^T N \Lambda_2 \\
\theta_4 &= \theta_2^T N \Lambda_2 & \tilde{S}_l &= \Lambda_2^T S_l \Lambda_2 \\
\theta_{5l} &= B_l & \bar{\bar{S}} &= \Lambda_3^T S_l \Lambda_3 \\
\theta_6 &= \Lambda_2^T N^T \theta_5 &
\end{aligned}
$$

Then, by solving the LMI condition $\Omega < 0$, the state feedback control gain is obtained as

$$K = \theta_5^{-1} \theta_2 \Lambda_1^{-1}$$

$$B_l = \theta_{5l}$$

This completes the proof of Lemma 5.4. ■

Stability Analysis of the Ordinary Traffic

Let us compare the stability conditions of the ordinary traffic and the premium traffic classes, as governed by the LMIs in (5.87) and (5.42),respectively. We observe that for the ordinary traffic control, one only needs to check the feasibility of one matrix at each time. The reason is that the external incoming traffic of the ordinary traffic is known and controllable, and no estimation is need in the congestion control problem of the ordinary traffic class. Consequently, the closed-loop dynamic system does not contain any switchings. Therefore, the computational cost of the congestion controller for the ordinary traffic is lower than the premium one.

Moreover, the ordinary dynamic system can achieve asymptotic stability by using the memoryless state feedback control. However, for the premium traffic system one can only achieve this goal when there is no external incoming premium traffic flow. The

ordinary queuing error $z_r(t) = x_r(t) - x_r^{ref}$ will always converge to 0 as $t \to \infty$. The reason is that more information is available for the congestion control of ordinary traffic, so that a better stability result can be achieved.

Consequently, the upper bound of the closed-loop performance cost, as given below, is always constant which is only dependent on the system initial conditions

$$J_r^* = \phi^T(0)P\phi(0) + \sum_{l=1}^{m} \frac{1}{h} \int_{-h}^{0} \int_{\theta}^{0} \dot{\phi}^T(s)S_l\dot{\phi}(s)dsd\theta \qquad (5.89)$$

Therefore, for any unknown and time-varying delays, under Assumption 3.1, the closed-loop system is always asymptotically stable and the performance cost is guaranteed to be less than J_r^*.

Stability Conditions Incorporating the Physical Constraints

The closed-loop system of the ordinary dynamic system after applying the controller $\bar{u}_r(t) = Kz_r(t)$ can be expressed as follows

$$\dot{z}_r(t) = B_0 K z_r(t) + \sum_{l=1}^{m} B_l K z_r(t - \tau_l(t)) \qquad (5.90)$$

The physical constraints (5.12)-(5.16) for the dynamical queuing model of the ordinary traffic class is written as

$$-x_r^{ref} \quad \leq z_r(t) \quad \leq x_r^{buffer} - x_r^{ref} \qquad (5.91)$$

$$0 \quad \leq \bar{u}_r(t) \quad \leq c_r(t) \qquad (5.92)$$

where x_r^{ref} is a constant set-point indicating the reference value of the ordinary queuing length, $c_r(t)$ is the maximum allowable bandwidth for the ordinary traffic, which equals to the instantaneous leftover capacity from the premium traffic and in fact is given by $c_r(T) = C_{server} - \bar{u}_p(t)$.

Constraints of the states

For the constraints of the states (5.91), consider the following ellipsoid for a selected positive number ϵ_2

$$\mathbb{S} = \{z_r(t)|z_r^T(t)\Lambda_2^{-1}z_r(t) \leq \epsilon_2, \Lambda_2^T = \Lambda_2 > 0\}$$

From the Lyapunov-Krosovskii functional V as defined in (5.82), if the stability condition (5.87) is satisfied, then we have

$$\bar{z}_r^T(t)\Lambda_2^{-1}z_r(t) \leq V(t)$$

Noting that in (5.85), by integrating both sides of the inequality from 0 to ∞ and considering $V(0) = 0$, one can get

$$V(t) = -\int_0^t z_r^T(t)(Q + K^T R K)z_r(t)dt < 0 \tag{5.93}$$

Therefore, $z_r(t)$ belongs to the set $\mathbb{S}$ for all $t > 0$. By squaring the state constraint (5.90), we get

$$z_r^T z_r \leq \|z_r^{max}\|^2 \tag{5.94}$$

where $z_r^{max} = x_r^{buffer} - x_r^{ref}$. Therefore, the right hand side of the state constraint (5.90) will be satisfied if

$$\frac{\epsilon_2}{\|z_r^{max}\|^2} \leq \Lambda_2^{-1} \tag{5.95}$$

which can be expressed according to the following LMI condition

$$\Omega_{c1} \triangleq \begin{bmatrix} \Lambda_1 & \Lambda_1^T \\ \Lambda_1 & \|z_r^{max}\|^2/\epsilon_2 \end{bmatrix} \geq 0 \tag{5.96}$$

On the other hand, the negative side of the state constraint (5.91) can be rewritten as follows:

$$z_r(t) - z_r^{ref} \leq 0 \tag{5.97}$$

Noting that $\dot{z}_r - \dot{z}_r^{ref} = \dot{z}_r$, the non-negative condition (5.97) will be satisfied if the closed-loop system (5.90) is a non-negative system. According to the definition of non-negative system in Definition5.1, by setting $K = \theta_5^{-1}\theta_2\Lambda_1^{-1}$ and $\sum_{l=1}^m B_l = \theta_5$, with a diagonal positive definite matrix Λ_1^{-1}, the non-negative condition (5.45) will be satisfied if the following conditions hold

$$\Omega_{c2} \triangleq (B_0\theta_5^{-1}\theta_2)_{ij} \geq 0, \qquad i \neq j \tag{5.98}$$

$$\Omega_{c3} \triangleq (\theta_2)_{ij} \geq 0, \qquad i,j = 1,...2n \tag{5.99}$$

218

Constraints of the input

For the constraints of the input, by using $\bar{u}_r = Kz_r$, it can be expressed as

$$0 \le Kz_r(t) \le c_r(t) \tag{5.100}$$

Note that:

$$
\begin{aligned}
c_r(t) &= C_{server} - \bar{u}_p(t) \\
&= C_{server} - K_p \bar{z}_p(t) \tag{5.101}
\end{aligned}
$$

where K_p is the control gain of the premium traffic controller as derived in the last section. To avoid confusion, we denote K_r as the control gain for the ordinary traffic in the remainder of this section. Therefore, the input constraint (5.100) can be re-written as

$$0 \le K_r z_r(t) \le C_{server} - K_p \bar{z}_p(t) \tag{5.102}$$

From the right hand side of the above condition, we have

$$K_r z_r(t) + K_p \bar{z}_p(t) \le C_{server} \tag{5.103}$$

By squaring (5.103), we get

$$
\begin{bmatrix} z_r^T \\ \bar{z}_p^T \end{bmatrix}^T \begin{bmatrix} K_r^T \\ K_p^T \end{bmatrix} \begin{bmatrix} K_r & K_p \end{bmatrix} \begin{bmatrix} z_r \\ \bar{z}_p \end{bmatrix} \le \|C_{server}\|^2 \tag{5.104}
$$

Now, consider the ellipsoids of the premium traffic state $\mathbb{F}$ as defined in (5.57), and of the ordinary traffic state $\mathbb{S}$ as given in (5.93). Hence, the following union of the two ellipsoids can be defined

$$
\Sigma = \mathbb{F} + \mathbb{S} = \left\{ (z_r(t), \bar{z}_p(t)) \middle| \begin{bmatrix} z_r^T \\ \bar{z}_p^T \end{bmatrix}^T \begin{bmatrix} \Lambda_2^{-1} & 0 \\ 0 & \tilde{P}^{-1} \end{bmatrix} \begin{bmatrix} z_r \\ \bar{z}_p \end{bmatrix} \le \epsilon_1 + \epsilon_2 \right\} \tag{5.105}
$$

As indicated by (5.93), $z_r \in \mathbb{S}$ for all $t > 0$. Therefore, $(z_r(t), \bar{z}_p(t))$ belongs to the invariant set Σ for all $t > 0$, if the condition (5.60) is satisfied

$$\gamma \lambda_{max}(\Phi) \le \epsilon_1$$

Therefore, (5.104) will be satisfied if

$$
\begin{bmatrix} K_r^T \\ K_p^T \end{bmatrix} \frac{\epsilon_1 + \epsilon_2}{\|C_{server}\|^2} \begin{bmatrix} K_r & K_p \end{bmatrix} \le \begin{bmatrix} \Lambda_2^{-1} & 0 \\ 0 & \tilde{P}^{-1} \end{bmatrix} \tag{5.106}
$$

219

By applying the Schur complement, the upper constraint of the input due to the capacity limitation can be expressed according to the following LMI conditions

$$\Omega_{c4} \triangleq \gamma\lambda_{max}(\Phi) \leq \epsilon_1 \tag{5.107}$$

$$\Omega_{c5} \triangleq \begin{bmatrix} I & K_r & K_p \\ K_r^T & \frac{\|C_{server}\|^2}{\epsilon_1+\epsilon_2}\Lambda_2 & 0 \\ K_p^T & 0 & \frac{\|C_{server}\|^2}{\epsilon_1+\epsilon_2}\tilde{P} \end{bmatrix} \geq 0 \tag{5.108}$$

On the other hand, once the non-negative conditions Ω_{c2} and Ω_{c3} are satisfied, the system (5.90) is a non-negative system, so that $z_r(t) > 0$. Hence, the non-negative constraint of the input $\bar{u}_r(t) \geq 0$ can be satisfied if we set $(K_r)_{ij} > 0$. By setting the positive definite matrix Λ_1 to be a diagonal matrix and noting that $(\theta_2)_{ij} > 0$, as given by (5.98), the non-negative constraint of the input is satisfied if

$$\Omega_{c6} \triangleq (\theta_5^{-1})_{ij} > 0, \qquad i,j = 1,...,2n \tag{5.109}$$

Remark 5.5. *It should be noted that in order to satisfying the condition Ω_{c5}, as given in (5.107), the control gain of the premium traffic controller K_p is a known matrix by deriving the premium traffic controller first. This is also justified by the fact that the premium traffic has the highest priority and the bandwidth is allocated to it first. Moreover, the control of the premium traffic will affect the feasibility of Ω_{c5}. This is also validated by the fact that the capacity constraint of the ordinary traffic is dependent on the leftover bandwidth from the premium one. When there is no leftover capacity, we will have $\bar{u}_r(t) = 0$ which implies that no capacity is available and no incoming traffic is allowed.*

Remark 5.6. *Notice by satisfying the LMI conditions Ω_{c3} and Ω_{c6} as governed by (5.98) and (5.109), respectively, $\theta_5^{-1}\theta_2$ becomes a rectangular matrix with positive elements. On the other hand, since the elements in B_0 are -1 or 0, the condition Ω_{c2} is naturally satisfied.*

The above conditions for the centralized congestion controller of the ordinary traffic can be written in the following theorem.
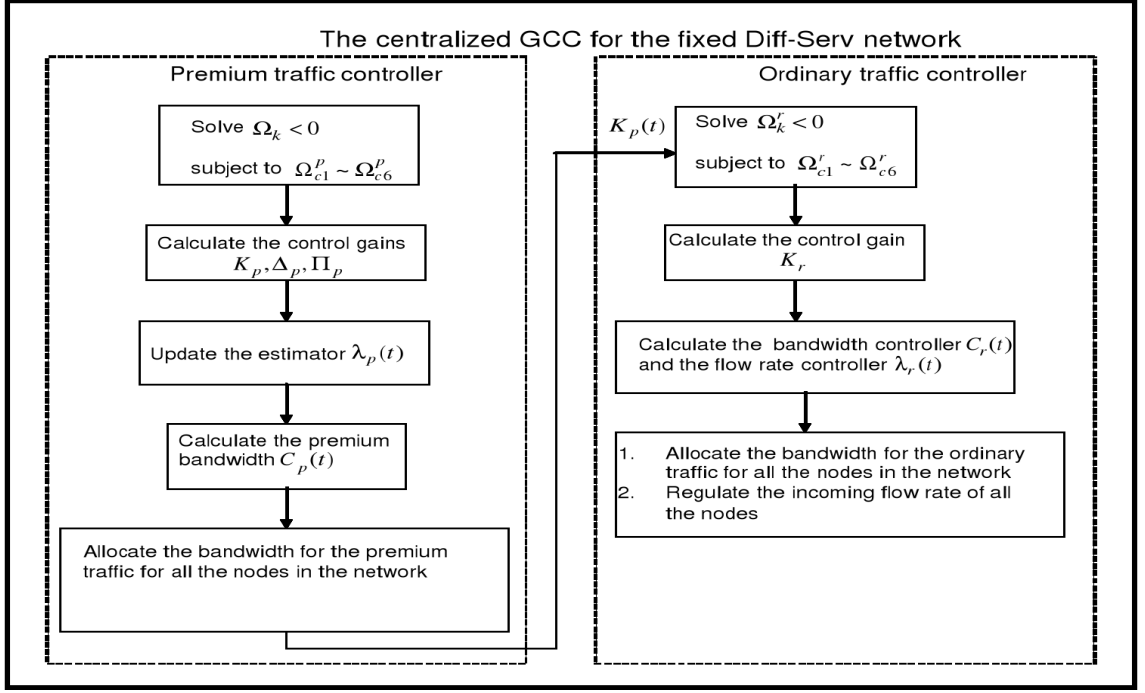
Figure 5.1: The flow chart of the centralized guaranteed cost congestion controller (GCC) for the Diff-Serv network with fixed topology.

Theorem 5.2. *A guaranteed cost congestion controller for the ordinary traffic class, as described by the dynamical queuing model (5.78), of the structure*

$$\bar{u}_r(t) = K_r z_r(t) \tag{5.110}$$

is obtained by solving the LMI condition Ω in Lemma 5.4 and the LMI conditions Ω_{c1}, Ω_{c3}, Ω_{c4}, Ω_{c5}, Ω_{c6}, as governed by equations (5.96), (5.98), (5.107), and (5.109), respectively, subject to a diagonal positive definite matrix Λ_1.

Proof: The proof follows along the same lines as those given in the above derivations. ∎

The centralized congestion control strategies of the premium and the ordinary traffic classes derived in this section are summarized in the flow chart shown in Figure 5.1. As stated in Figure 5.1, given a network of multi-agent systems (NMAS) with n nodes and a fixed network topology, the premium traffic congestion controller first solves the LMI conditions Ω_k and Ω_{c1} to Ω_{c6}, so that the memoryless state feedback control gain K,

221

and the adaptive estimation gains Δ and Π are obtained. The adaptive estimator $\hat{\lambda}_p(t)$ is updated according to the value of the queuing state and the switching conditions as given in (5.21). After obtaining the estimate of the external incoming premium traffic, the bandwidth controller $C_p(t)$ is calculated according to the following rule:

$$
\begin{aligned}
C_p(t) &= u_p(t) = F^{-1}(x_p,t)\bar{u}_p(t) \\
&= F^{-1}(x_p,t)K\bar{z}_p(t) \\
&= F^{-1}(x_p,t)K \begin{bmatrix} x_p(t) - x_p^{ref} \\ \hat{\lambda}_p(t) \end{bmatrix}
\end{aligned}
\tag{5.111}
$$

where $x_p(t)$ denotes the queuing length, x_p^{ref} denotes the reference set point of the queuing length that is selected by the network operator. Note that $F(x_p(t)) = diag\{f(x_{pi}(t))\}$ and $f(x_{pi}(t)) = \mu \frac{x_{pi}}{1+x_{pi}}$ are calculated with the given queuing states.

The bandwidth for the premium traffic flow at each node is allocated based on the values that are given by the centralized controller (5.111). On the other hand, given the premium traffic control gain K_p, the ordinary traffic congestion controller can solve the corresponding LMI conditions that are given in Lemma 5.4 and The physical constraints conditions, so that the bandwidth controller $C_r(t)$ and the flow rate regulator $\lambda_r(t)$ are calculated as follows

$$
\begin{bmatrix} C_r(t) \\ \lambda_r(t) \end{bmatrix} = F^{-1}(x_r,t)K(x_r(t) - x_r^{ref})
\tag{5.112}
$$

where $F(x_r(t)) = diag\{f(x_{ri}(t))\}$ and $F(x_r(t)) = \mu \frac{x_{ri}}{1+x_{ri}}$.

The bandwidth for the ordinary traffic is allocated at each node. The allowable incoming flow rates are sent to each node in the network so that the corresponding adjustments can be conducted during the next communication cycle.

5.2 Decentralized Guaranteed Cost Congestion Control (GCC) Scheme

The network of multi-agent systems is composed of a large number of interconnected nodes. Transmitting information among the network nodes may cause delays which adversely

affect stability and deteriorate performance of the system. Control of such large scale systems can become quite complicated owing to the high dimensionality of the system dynamics, uncertainties and time-delays. Decentralized control strategies are among the best choices for controlling such systems. In other words, each node is required to control its behavior by using its local and limited information that it receives from other nodes in the network to accomplish a global objective.

In this section, a decentralized congestion control approach is developed based on the model that is presented in Chapter 2. A guaranteed cost control method is applied to derive the congestion control strategies of each traffic class with a set of LMI constraints. Consider a NMAS with n nodes. Suppose each node has three queues corresponding to the premium, the ordinary and the best-effort traffic. The congestion controller is implemented at the output port of each node. The control objective pursued for the premium traffic is to allocate the output capacity that is denoted by $C_{pi}(t)$ by incorporating an adaptive estimator to compensate for the incoming traffic uncertainties. The ordinary traffic controller needs to simultaneously regulate the incoming flow rate that is denoted by $\lambda_{ri}(t)$ and allocate its capacity $C_{ri}(t)$. Finally, for the best-effort traffic, no explicit active control is designed since this traffic does not have any QoS requirements.

5.2.1 Premium Traffic Control Strategy

Let us recall the decentralized dynamic model of the traffic flow at each node that is given by (2.21)for covenience

$$\dot{x}_{pi}(t) = -f(x_{pi}(t))u_{pi}(t) + \sum_{\substack{j=1 \\ j \neq i}}^{n} f(x_{pj}(t - \tau_{ji}(t)))u_{pj}(t - \tau_{ji})g_p^{ji}(t) + \lambda_{pi}(t) \quad (5.113)$$

where x_{pi}, $i = 1, ..., n$ denotes the premium queuing length in node i, $u_{pi} = C_{pi}$ denotes the bandwidth capacity allocated to the premium traffic in node i, $u_{pj}(t)$ denotes the bandwidth controller of the neighboring node j, $\tau_{ji}(t)$ denotes the unknown but bounded time-varying delays in transmission, propagation, and processing, $\lambda_{pi}(t)$ denotes the external input flow for node i, and $g_p^{ji}(t)$ denotes the traffic compression gain between nodes j and i.

The set of constraints are also given by

$$0 \leq x_{pi}(t) \leq x_{pi}^{buffer}$$

$$0 \leq u_{pi}(t) \leq C_{server,i}, \qquad\qquad i = 1, ...n$$

$$0 \leq \lambda_{pi}(t) < \lambda_{pi}^{max} \leq C_{server,i} \qquad\qquad (5.114)$$

where x_{pi}^{buffer} is the premium buffer size of node i, $C_{server,i}$ is the total link capacity of node i, λ_{pi}^{max} is the maximum allowable external incoming traffic, which is introduced by the transmission constraint of node i.

Our objective is to find a stabilizing controller, u_{pi}, for each node such that the system (5.113) is stable and the closed-loop system is robust to any admissible time-varying delays satisfying assumption 3.1. Since the corresponding dynamic model is nonlinear, we first apply the feedback linearization technique to transform the original nonlinear system into an equivalent linear system and then a guaranteed cost control approach is employed to derive the state feedback control law based on the new state space representation.

Feedback linearization scheme

For the nonlinear system (5.113), the following feedback linearization scheme is proposed

$$z_{pi}(t) \;\; = \;\; x_{pi}(t) - x_{pi}^{ref} \qquad\qquad (5.115)$$

$$u_{pi} \;\; = \;\; f^{-1}(x_{pi}, t)\bar{u}_{pi} \qquad\qquad (5.116)$$

where x_{pi}^{ref} is the reference queuing length of node i. The new state equation can be described as follows

$$\dot{z}_{pi}(t) = -\bar{u}_{pi}(t) + \lambda_{pi}(t) + \sum_{\substack{j=1 \\ j \neq i}}^{n} \bar{u}_{pj}(t - \tau_{ji}(t)) g_p^{ji}(t) \qquad\qquad (5.117)$$

Due to the unknown external incoming traffic $\lambda_{pi}(t)$, an additional state $\hat{\lambda}_{pi}(t)$ is introduced to estimate $\lambda_{pi}(t)$ and to compensate for its effect through feedback. The online

updating rule of the estimation is selected based on the parameter projection method [128]

$$
\dot{\hat{\lambda}}_{pi}(t) = \begin{cases} \delta_i \bar{x}_{pi}(t) - \beta_i \hat{\lambda}_{pi}(t), & \text{if } 0 \leq \hat{\lambda}_{pi}(t) \leq \lambda_{pi}^{max} \text{ or} \\ & \hat{\lambda}_{pi}(t) = 0, \ \bar{x}_{pi}(t) \geq 0 \text{ or} \\ & \hat{\lambda}_{pi}(t) = \lambda_{pi}^{max}, \ \bar{x}_{pi}(t) \leq 0 \\ -\beta_i \hat{\lambda}_{pi}(t), & \text{otherwise} \end{cases} \tag{5.118}
$$

where $\delta_i > 0$ and $\beta_i > 0$ are constant design parameters. The open-loop system dynamics (5.109) and (5.111) can be then written as a switching system with the following two subsystems

$$
\dot{\bar{z}}_{pi}(t) = A_{i0}^k \bar{z}_{pi}(t) + B_{i0} \bar{u}_{pi}(t) + \sum_{\substack{j=1 \\ j \neq i}}^{n} B_j \bar{u}_j(t - \tau_{ji}(t)) + B_{\lambda_i} \lambda_i(t) \tag{5.119}
$$

$$
\bar{z}_{pi}(t) = \varphi_i(t) \qquad \varphi_i(t) \in [-h, 0]
$$

$$
k \in \aleph, \aleph = 1, 2
$$

where $\bar{z}_{pi}(t) = [z_{pi}(t) \ \hat{\lambda}_{pi}(t)]^T$ is the new state vector, and m_i is the number of delays in the neighboring set of node i. The new dynamic system (5.113) is a linear time-delay system with arbitrary switchings between the two subsystems that is represented by k, A_{i0}^k, B_{i0}, B_j, and B_{λ_i}, for $i, j = 1, ..., n$ are the system matrices

$$
A_{i0}^1 = \begin{bmatrix} 0 & 0 \\ \delta_i & -\beta_i \end{bmatrix} \qquad A_{i0}^2 = \begin{bmatrix} 0 & 0 \\ 0 & -\beta_i \end{bmatrix}
$$

$$
B_{i0} = \begin{bmatrix} -1 \\ 0 \end{bmatrix} \qquad B_j = \begin{bmatrix} g_{ji} \\ 0 \end{bmatrix} \qquad B_{\lambda_i} = \begin{bmatrix} 1 \\ 0 \end{bmatrix}
$$

It is worth noting that the update rule of the decentralized estimator (5.118) depends only on the local information of each node. Hence, the estimate of the external incoming traffic with respect to a single node is more efficient than that in the centralized control, since in this case one does not need to wait for the neighbors to simultaneously perform an update. This is due to the fact that in the decentralized congestion control each node is only concerned about the congestion status of itself. The congestion control decisions are made locally and the performance is also only evaluated at local nodes. Therefore,

although all the nodes in the network will become stable eventually, but this may take longer time than the centralized control. In this section, the control objective for the premium traffic is defined as that of determining a state feedback controller $\bar{u}_{pi}(t) = K_i \bar{z}_{pi}(t)$ for each node such that the system (5.113) is ultimately bounded and the following performance cost function is upper bound:

$$J_{pi} = \int_0^\infty (\bar{z}_{pi}^T(t)Q_i\bar{z}_{pi}(t) + \bar{u}_{pi}^T(t)R_i\bar{u}_{pi})dt \qquad (5.120)$$

where Q_i and R_i are given positive definite matrices. In order to guarantee an upper bound of the cost function, the following assumption of the external incoming traffic to each node is imposed in this section as presented below

Assumption 5.2. *The external incoming traffic to each node is L_2 norm bounded, that is*

$$\int_0^\infty \|\lambda_i(t)\|^2 dt \leq \gamma_i, \qquad \gamma_i > 0 \qquad (5.121)$$

Then, the following theorem is proposed to show that the memoryless state feedback control law is a guaranteed cost controller for system (5.113).

Lemma 5.5. *Given the cost function (5.120) and under the Assumption 5.2, the controller $\bar{u}_{pi}(t) = K_i\bar{z}_{pi}(t)$ is a guaranteed cost control law of system (5.113), if there exist symmetric positive definite matrices P_i, S_i, $i = 1, ..., n$, and positive definite matrices M_i, N_i, $\bar{M}_i$, $\bar{N}_i$, such that the following matrix inequality condition is satisfied*

$$\bar{W}_{ik} = \begin{bmatrix} Y_{ik} & P_i - M_i^T + (A_{ic}^k)^T N_i^T & -M_i^T B_{ji}K_{ji} & 0 \\ * & -2N_i^T + \bar{N}_i + S_i & -N_i^T B_{ji}K_{ji} & 0 \\ * & * & 0 & 0 \\ * & * & * & -S_i \end{bmatrix} < 0 \qquad (5.122)$$

where $A_{ic}^k = A_{i0}^k + B_{i0}K_i$, $Y_{ik} = 2M_i^T A_{ic}^k + \bar{M}_i + Q_i + K_i^T R_i K_i$, $B_{ji} = vec\{B_j\}$, and $K_{ji} = diag\{K_j\}$.

Proof: For the switching system (5.113), the following common Lyapunov-Krasovskii functional is selected for the stability analysis

$$V_i = V_{i1} + V_{i2} \tag{5.123}$$

$$V_{i1} = \bar{z}_{pi}^T(t)P_i\bar{z}_{pi}(t)$$

$$V_{i2} = \frac{1}{h}\int_{-h}^{0}\int_{t+\theta}^{t} y_i^T(s)S_i y_i(s)\,ds\,d\theta$$

where P_i and S_{li} are sympatric positive definite matrices, and

$$\dot{\bar{z}}_{pi}(t) = y_i(t) \tag{5.124}$$

$$y_i(t) = A_{ic}^k \bar{z}_{pi}(t) + \sum_{\substack{j=1 \\ j\neq i}}^{n} B_j K_j \bar{z}_{pj}(t) - \sum_{\substack{j=1 \\ j\neq i}}^{n} B_j K_j \int_{t-\tau_{ji}(t)}^{t} y_j(s)\,ds + B_{\lambda_i}\lambda_{pi}(t)$$

Therefore, the time derivative of V along the trajectories of system (5.113) is given by

$$\dot{V}_i = \dot{V}_{i1} + \dot{V}_{i2}$$

$$\dot{V}_{i1} = 2\bar{z}_{pi}^T(t)P_i y_i(t)$$

$$= 2[\bar{z}_{pi}^T(t)\ y_i^T(t)]\begin{bmatrix} P_i & M_i^T \\ 0 & N_i^T \end{bmatrix}\begin{bmatrix} y_i(t) \\ \dot{\bar{z}}_{pi}(t) - y_i(t) \end{bmatrix}$$

$$= \begin{bmatrix} 2\bar{z}_{pi}^T(t)P_i & 2\bar{z}_{pi}^T(t)M_i^T + 2y_i^T N_i^T \end{bmatrix}\begin{bmatrix} y_i(t) \\ -\dot{\bar{z}}_{pi}(t) + y_i(t) \end{bmatrix}$$

$$= [2\bar{z}_{pi}^T(t)P_i y_i(t) - (2\bar{z}_{pi}^T(t)M_i^T \dot{z}_i(t) + 2y_i^T N_i^T \dot{z}_i(t) - 2\bar{z}_{pi}^T(t)M_i^T y_i(t) - 2y_i^T N_i^T y_i(t)]$$

$$= [2\bar{z}_{pi}^T(t)P_i y_i(t) - 2\bar{z}_{pi}^T(t)M_i^T y_i(t) - 2y_i^T N_i^T y_i(t) + 2\bar{z}_{pi}^T(t)M_i^T(A_{ic}^k \bar{z}_{pi}(t) + \sum_{\substack{j=1 \\ j\neq i}}^{n} B_j K_j z_j(t)$$

$$- \sum_{\substack{j=1 \\ j\neq i}}^{n} B_j K_j \int_{t-\tau_{ji}(t)}^{t} y_j(s)\,ds + B_{\lambda_i}\lambda_{pi}(t))$$

$$+ 2y_i^T N_i^T(A_{ic}^k \bar{z}_{pi}(t) + \sum_{\substack{j=1 \\ j\neq i}}^{n} B_l K_j z_j(t) - \sum_{\substack{j=1 \\ j\neq i}}^{n} B_j K_j \int_{t-\tau_{ji}(t)}^{t} y_j(s)\,ds + B_{\lambda_i}\lambda_{pi}(t))]$$

$$= [2\bar{z}_{pi}^T(t)(P_i - M_i^T)y_i(t) - 2y_i^T N_i^T y_i(t)$$

$$+ 2\bar{z}_{pi}^T M_i^T A_{ic}^k \bar{z}_{pi} + 2\bar{z}_{pi}^T M_i^T \sum_{\substack{j=1 \\ j\neq i}}^{n} B_j K_j \bar{z}_j(t - \tau_{ji}(t)) + 2\bar{z}_{pi}^T M_i^T B_{\lambda_i}\lambda_{pi}(t)$$

$$+ 2y_i^T N_i^T A_{ic}^k \bar{z}_{pi} + 2y_i^T N_i^T \sum_{\substack{j=1 \\ j\neq i}}^{n} B_j K_j \bar{z}_j(t - \tau_{ji}(t)) + 2y_i^T N_i^T B_{\lambda_i}\lambda_{pi}(t)]$$

$$= \begin{bmatrix} \bar{z}_{pi}^T(t) \\ y_i^T(t) \\ \bar{Z}_j^T(t - \tau_{ji}(t)) \end{bmatrix}^T \begin{bmatrix} 2M_i^T A_{ic}^k & P_i - M_i^T + (A_{ic}^k)^T N_i^T & M_i^T B_{ji} K_{ji} \\ * & -2N_i^T & N_i^T B_{ji} K_{ji} \\ * & * & 0 \end{bmatrix} \begin{bmatrix} \bar{z}_{pi}(t) \\ y_i(t) \\ \bar{Z}_j(t - \tau_{ji}(t)) \end{bmatrix}$$
$$+ (2\bar{z}_{pi}^T(t) M_i^T B_{\lambda_i} \lambda_{pi}(t) + 2y_i^T N_i^T B_{\lambda_i} \lambda_{pi}(t))$$

where M_i and N_i are symmetric positive definite matrices, $\bar{Z}_j(t - \tau_{ji}(t))$ is a vector containing all the neighboring nodes' states with the corresponding time-varying delays, for $j = 1, ..., n$, and B_{ji} and K_{ji} are the matrices corresponding to the vector $\bar{Z}_j(t - \tau_l(t))$. In fact these three matrices are defined as follows:

$$B_{ji} = vec\{B_j\}$$

$$K_{ji} = diag\{K_j\}$$

$$\bar{Z}_j(t - \tau_{ji}(t)) = vec\{\bar{z}_j(t - \tau_{ji}(t))\}$$

The following example should clarify the definitions of these three matrices.

Example 5.2. *Suppose there are three nodes in a given network. Then for the dynamical queuing model of node 1, the neighboring nodes' states are specified as follows*

$$\bar{Z}_j(t - \tau_{ji}(t)) = [\bar{z}_2(t - \tau_{21}(t)) \ \ \bar{z}_3(t - \tau_{31}(t))]^T \quad j = 2, 3$$

The matrices B_{ji} and K_{ji} can be expressed as

$$B_{ji} = [B_2 \ B_3] = \begin{bmatrix} g_{21}^p & g_{31}^p \\ 0 & 0 \end{bmatrix} \qquad K_{ji} = \begin{bmatrix} K_2 & 0 \\ 0 & K_3 \end{bmatrix}$$

By applying the Park's inequality (3.24) [129] to the last two terms in the equation (5.125), one can obtain

$$2\bar{z}_{pi}^T(t) M_i^T B_{\lambda_i} \lambda_{pi}(t) \leq \bar{z}_{pi}^T(t) \bar{M}_i \bar{z}_{pi}(t) + \lambda_{pi}^T B_{\lambda_i}^T \bar{M}_i^{-1} B_{\lambda_i} \lambda_{pi}$$

$$2y_i^T(t) N_i^T B_{\lambda_i} \lambda_{pi}(t) \leq y_i^T(t) \bar{N}_i y_i(t) + \lambda_{pi}^T B_{\lambda_i}^T \bar{N}_i^{-1} B_{\lambda_i} \lambda_{pi}$$

where $\bar{M}_i$ and $\bar{N}_i$ are positive definite matrices. Therefore, the derivative of the Lyapunov

function V_{i1} becomes

$$
\dot{V}_{i1} \leq
\begin{bmatrix}
\bar{z}_{pi}^T(t) \\
y_i^T(t) \\
\bar{Z}_j^T(t - \tau_{ji}(t))
\end{bmatrix}^T
\begin{bmatrix}
2M_i^T A_{ic}^k + \bar{M}_i & P_i - M_i^T + (A_{ic}^k)^T N_i^T \\
* & -2N_i^T + \bar{N}_i \\
* & *
\end{bmatrix}
$$

$$
\begin{bmatrix}
M_i^T B_{ji} K_{ji} \\
N_i^T B_{ji} K_{ji} \\
0
\end{bmatrix}
\begin{bmatrix}
\bar{z}_{pi}(t) \\
y_i(t) \\
\bar{Z}_j(t - \tau_{ji}(t))
\end{bmatrix}
+ \lambda_{pi}^T B_{\lambda_i}^T (\bar{M}_i + \bar{N}_i)^{-1} B_{\lambda_i} \lambda_{pi}
$$

On the other hand, the time derivative of V_{i2} is equal to

$$
\dot{V}_{i2} \;=\; (y_i^T(t) S_i y_i(t) - \frac{1}{h}\int_{t-h}^{t} y_i^T(s) S_i y_i(s) ds)
$$

Therefore, $\dot{V}$ can be written as

$$
\dot{V}_i \;\leq\; \frac{1}{h}\int_{t-h}^{t} (\xi_i^T(t,s) W_{ik}\xi_i(t,s) + \lambda_{pi}^T \Phi_{ik}\lambda_{pi}) ds \tag{5.125}
$$

where $\xi_i(t,s) = [\bar{z}_{pi}^T(t) \; y_i^T(t) \; Z_j^T(t - \tau_{ji}(t)) \quad y_i^T(s)]^T$, $\Phi_i = B_{\lambda_i}^T(\bar{M}_i^{-1} + \bar{N}_i^{-1}) B_{\lambda_i}$, and

$$
W_{ik} =
\begin{bmatrix}
2M_i^T A_{ic}^k + \bar{M}_i & P_i - M_i^T + (A_{ic}^k)^T N_i^T & -M_i^T B_{ji} K_{ji} & 0 \\
* & -2N_{ik}^T + \bar{N}_{ik} + S_i & -N_i^T B_{ji} K_{ji} & 0 \\
* & * & 0 & 0 \\
* & * & * & -S_i
\end{bmatrix}
\tag{5.126}
$$

Since $W_{ik} = \bar{W}_{ik} - Q_i - K_i^T R_i K_i$, the following inequality holds for $\dot{V}_i$, namely

$$
\begin{aligned}
\dot{V}_i \;&\leq\; \frac{1}{h}\int_{t-h}^{t} (\xi_i^T(t,s)(\bar{W}_{ik} - Q_i - K_i^T R_i K_i)\xi_i(t,s) + \lambda_{pi}^T \Phi_i \lambda_{pi}) ds \\
&=\; -\frac{1}{h}\int_{t-h}^{t} [\bar{z}_{pi}^T(t)(Q_i + K_i^T R_i K_i)\bar{z}_{pi}(t) + \lambda_{pi}^T \Phi_i \lambda_{pi}] ds \\
&=\; -\bar{z}_{pi}^T(t)(Q_i + K_i^T R_i K_i)\bar{z}_{pi}(t) + \lambda_{pi}^T \Phi_i \lambda_{pi} \tag{5.127}
\end{aligned}
$$

Therefore, for any $\bar{z}_{pi}(t)$ that satisfies $\bar{z}_{pi}^T(t)(Q_i + K_i^T R_i K_i)\bar{z}_{pi}(t) \geq \Phi_i \lambda_{pi}^2(t)$, we have $\dot{V}_i < 0$. Therefore, according to the definition of the ultimate boundedness stability, the system (5.113) is ultimately bounded and the ultimate bound is given by

$$
\|\bar{z}_{pi}(t)\|^2 \geq \frac{\Phi_i}{\lambda_{min}(Q_i + K_i^T R_i K_i)} \lambda_{pi}^2(t) \tag{5.128}
$$

Integrating both sides of (5.125) from 0 to ∞, one obtains the upper bound of the performance cost function J as follows

$$
\begin{aligned}
J_{pi} \quad &< \quad V_i(0) - V_i(\infty) + \int_0^\infty \lambda_{pi}^T(t)\Phi_i\lambda_{pi}(t)dt \\
&< \quad V_i(0) - V_i(\infty) + \Phi_i \int_0^\infty \|\lambda_{pi}(t)\|^2 dt \\
&< \quad V_i(0) - V_i(\infty) + \gamma_i\Phi_i \\
&= \quad \varphi_i^T(0)P_i\varphi_i(0) + \frac{1}{h}\int_{-h}^0\int_\theta^0 \dot{\varphi}_i^T(s)S_i\dot{\varphi}_i(s)dsd\theta \qquad (5.129) \\
&\quad -\bar{z}_{pi}^T(\infty)P_i\bar{z}_{pi}(\infty) + \gamma_i\Phi_i
\end{aligned}
$$

Therefore, the upper bound of the cost function J_{pi} is given by (since $z_{pi}(\infty) \geq 0$)

$$
J_{pi} < \varphi_i^T(0)P_i\varphi_i(0) + \frac{1}{h}\int_{-h}^0\int_\theta^0 \dot{\varphi}_i^T(s)S_i\dot{\varphi}_i(s)dsd\theta + \gamma_i\Phi_i = J_{pi}^* \qquad (5.130)
$$

Therefore, the closed-loop system performance is guaranteed to be less than the upper bound, and the controller $\bar{u}_{pi}(t) = K_i\bar{z}_{pi}(t)$ is the guaranteed cost controller of the system (5.113). This completes the proof of Lemma 5.5. $\blacksquare$

Lemma 5.5 shows that the decentralized memoryless state feedback control law $\bar{u}_{pi} = K_i\bar{z}_{pi}$ is a guaranteed cost controller for the switching time-delay system (5.113). However, the matrix inequality (5.117) is not linear with respect to either the system matrices A_{i0}^k and B_{i0}, or the control gain K_i. Moreover, the inequality (5.117) contains the control gains of the neighboring nodes K_j which are not available to the node i in the decentralized control approach. Therefore, one needs to find a way to eliminate the neighboring nodes' parameters K_j and transform the bilinear matrix inequality into a standard LMI condition so that the control parameters and the control gains can be calculated and obtained easily.

Lemma 5.6. *Given the cost function (5.115), if there exist symmetric positive definite matrices $\tilde{P}_i$, $\tilde{S}_i$, positive matrices $\tilde{M}_i$, $\tilde{N}_i$, $\tilde{Q}_i$, $\tilde{R}_i$, $\bar{\bar{M}}_i$ $\bar{\bar{N}}_i$, and matrices X_{ik}, Y_{ik}, U_i, T_i, V_i, for $i = 1,...,n$, $k = 1,2$, such that the following LMI condition is satisfied*

$$
\bar{\Omega}_{ik} \quad = \quad
\begin{bmatrix}
2(X_{ik} + U_i) + \bar{\bar{M}}_i + \tilde{Q}_i + \tilde{R}_i & \tilde{M}_i - \tilde{P}_i + Y_{ik} & -V_i \\
* & -2\tilde{N}_i + \bar{\bar{N}}_i + \bar{S}_i & -T_i \\
* & * & 0
\end{bmatrix} < 0
$$

then $\bar{u}_{pi} = K_i \bar{z}_{pi}$ *is the guaranteed cost controller for the system (5.113) and the decentralized gain is given by* $K_i = B_{i0}^+ U_i \tilde{M}_i^{-1}$.

Proof: Based on the matrix inequality $\bar{W}_{ik} < 0$ that is given in (5.117), one needs to derive the state feedback control gain K_i, and the control parameters δ_i, β_i, and g_{ji}^p. Note that the parameters δ_i, β_i and g_{ji}^p are included in the closed-loop system matrix A_{i0}^k and B_{ji}. Therefore, the objective is to solve the matrix inequality (5.117) so that one obtains these system matrices as well as the Lyapunov function matrices P_i and S_{li}.

However, in order to solve $\bar{W}_{ik} < 0$, one needs to know the neighboring nodes' control gains K_j, which is not available in the decentralized control approach. Therefore, in addition to transforming the bilinear matrix inequality $\bar{W}_{ik} < 0$ into a standard LMI through equivalent matrix operations, one also needs to find a way to eliminate the need for the matrices K_j. To tackle this problem, we define the following matrices

$$\tilde{M}_i = M_i^{-1} \qquad\qquad \tilde{P}_i = P_i^{-1}$$
$$\tilde{K}_{ji} = K_{ji}^+ \qquad\qquad \Lambda_i = diag\{\tilde{M}_i \ \ \tilde{P}_i \ \ \tilde{K}_{ji} \ \ 0\}$$

where K_{ji}^+ is the Moore-Penrose generalized inverse [103] of the matrix K_{ji}. By pre and post multiplying the matrix $\bar{W}_{ik}$ with Λ_i^T and Λ_i, respectively, the following matrix Ω_{ik} is then obtained

$$\Omega_{ik} \quad = \quad \Lambda_i^T \bar{W}_{ik} \Lambda_i = \begin{bmatrix} \bar{\Omega}_{ik} & 0 \\ 0 & 0 \end{bmatrix}$$

where:

$$\bar{\Omega}_{ik} \quad = \quad \begin{bmatrix} \tilde{M}_i^T Y_{ik} \tilde{M}_i & \tilde{M}_i^T - \tilde{P}_i + \tilde{M}_i^T (A_{ic}^k)^T N_i^T \tilde{P}_i & -B_{ji} \\ * & -\tilde{P}_i^T (2N_i^T + \bar{N}_i^T) \tilde{P}_i + \tilde{P}_i^T \bar{S}_i \tilde{P}_i & -\tilde{P}_i^T N_i^T B_{ji} \\ * & * & 0 \end{bmatrix}$$

Let us define

231

$$
\begin{aligned}
X_{ik} &= A_{i0}^k \tilde{M}_i & \tilde{Q}_i &= \tilde{M}_i^T Q_i \tilde{M}_i \\
Y_{ik} &= X_{ik}^T N_i^T \tilde{P}_i & \tilde{R}_i &= \tilde{M}_i^T K_i^T R_i K_i \tilde{M}_i \\
U_i &= B_{i0} K_i \tilde{M}_i & \tilde{S}_i &= \tilde{P}_i^T S_i \tilde{P}_i \\
V_i &= B_{ji} & \tilde{N}_i &= \tilde{P}_i^T N_i^T \tilde{P}_i \\
T_i &= \tilde{P}_i^T N_i^T B_{ji} & \bar{\bar{M}}_i &= \tilde{M}_i^T \bar{M}_i \tilde{M}_i \\
\bar{\bar{N}}_i &= \tilde{P}_I^T \bar{N}_i \tilde{P}_i
\end{aligned}
$$

Then the matrix $\bar{\Omega}_{ik}$ becomes

$$
\bar{\Omega}_{ik} = \begin{bmatrix} 2(X_{ik} + U_i) + \bar{\bar{M}}_i + \tilde{Q}_i + \tilde{R}_i & \tilde{M}_i^T - \tilde{P}_i + Y_{ik} & -V_i \\ * & -2\tilde{N}_i + \bar{\bar{N}}_i + \tilde{S}_i & -T_i \\ * & * & 0 \end{bmatrix}
$$

Since $\Omega_{ik} < 0 \Leftrightarrow \bar{\Omega}_{ik} < 0$, then by solving the LMI condition $\bar{\Omega}_{ik} < 0$, one can now obtain the control gain K_i (without requiring K_j) as well as the system matrices and the Lyapunov matrices as given below

$$
K_i = B_{i0}^+ U_i \tilde{M}_i^{-1} \tag{5.131}
$$

$$
P_i = \tilde{P}^{-1} \tag{5.132}
$$

$$
S_i = P_i^T \bar{S}_i P_i \tag{5.133}
$$

$$
A_{i0}^k = X_{ik} \tilde{M}^{-1} \tag{5.134}
$$

$$
B_{ji} = V_i \tag{5.135}
$$

This completes the proof of Lemma 5.6. ∎

Stability Analysis of the Premium Traffic

The stability conditions of the premium traffic flow as given in Lemma 5.6 under the decentralized controller guarantee the ultimate boundedness of each node and the robustness of the closed-loop performance with respect to the unknown multiple and time-varying delays from its neighboring nodes.

Stability Conditions Incorporating the Physical Constraints

The associated LMI conditions of the centralized congestion controller for the physical constraints, as given in Section 5.1.2, are now extended to the decentralized control case. The physical constraints of each node in the network and the corresponding LMI conditions are listed below.

- **Constraints of the states**

  The constraints of the states for node i incurred by the buffer size limitation are given as

  $$\bar{z}_{pi}^{min} \leq \bar{z}_{pi}(t) \leq \bar{z}_{pi}^{max} \tag{5.136}$$

  where $\bar{z}_{pi}^{min} = -x_{pi}^{ref}$ and $\bar{z}_{pi}^{max} = x_{pi}^{buffer} - x_{pi}^{ref}$

  Consider the following ellipsoid for a selected number $\varepsilon_i > 0$

  $$\mathbb{F}_i = \{\bar{z}_{pi}(t) | \bar{z}_{pi}^T \tilde{P}_i^{-1} \bar{z}_{pi} \leq \epsilon_i\} \tag{5.137}$$

  By following the similar lines as those given previously in Section 4.1.2, and the definition of non-negative system as given in Definition 5.1, the state constraints for the node i will be satisfied if the matrix X_{ik} in (5.131) satisfies the following conditions:

  $$
  \begin{aligned}
  X_{ik} &= \begin{bmatrix} X_{ik}^1 & X_{ik}^2 \\ X_{ik}^3 & X_{ik}^4 \end{bmatrix} \\
  X_{i1}^1 &= X_{i2}^1 = 0 \\
  X_{i1}^2 &= X_{i2}^2 = 0 \\
  X_{i2}^3 &= 0 \\
  X_{i1}^3 &> 0 \text{ and is diagonal} \\
  X_{i1}^4 &= X_{i2}^4 < 0 \text{ and is diagonal}
  \end{aligned}
  $$

233

and the following LMI conditions hold

$$\Omega_{c1i} \triangleq \gamma_i \Phi_i \le \epsilon_i \tag{5.138}$$

$$\Omega_{c2i} \triangleq \begin{bmatrix} \tilde{P}_i & \tilde{P}_i^T \\ \tilde{P}_i & \|\bar{z}_{pi}^{max}\|^2/\epsilon_i \end{bmatrix} \ge 0 \tag{5.139}$$

$$\Omega_{c3i} \triangleq (U_i)_{ij} \ge 0 \qquad i,j = 1,...2n \tag{5.140}$$

where λ_{pi} is adopted from the transmission constraint of node i, which indicates the maximum allowable external incoming traffic of the premium class.

- **Constraints of the input**

  The input constraints of each node i can be defined as follows

$$0 \le \bar{u}_{pi}(t) \le C_{server,i} \tag{5.141}$$

Following the similar lines as those given in Section 5.1.2 and considering the same ellipsoid as defined in (5.137), the input constraint for node i can be modified to the following LMI conditions

$$\Omega_{c4i} \triangleq \begin{bmatrix} I & K_i^T \\ K_i & (C_{server,i}^2/\epsilon_i)\tilde{P}_i \end{bmatrix} \ge 0$$

$$\Omega_{c5i} \triangleq (V_i^{-1})_{ij} \ge 0 \tag{5.142}$$

Therefore, the above results, as well as the LMI conditions that are given in Lemma 5.6 can be summarized in the following theorem.

Theorem 5.3. *A decentralized guaranteed cost congestion controller $\bar{u}_{pi} = K_i \bar{z}_{pi}$ for the premium traffic dynamical queuing model (5.120) is obtained by satisfying the LMI condition given in Lemma 5.5 subject to the positive definite diagonal matrix $\tilde{M}_i$, block matrix X_{ik} as defined in (5.138), and the LMI conditions Ω_{c1i}, Ω_{c2i}, Ω_{c3i}, Ω_{c4i}, and Ω_{c5i}, for $i = 1,...n$ and $k = 1,2$, as given in (5.138) to (5.141), respectively.*

    Proof: Follows along the same line as those derivations in Lemma 5.5, Lemma 5.6, and the LMI conditions for the physical constraints. ∎

5.2.2   Ordinary Traffic Control Strategy

The decentralized ordinary traffic model (2.27) is rewritten here again

$$\dot{x}_{ri}(t) = -f(x_{ri}(t))u_{ri}^1(t) + u_{ri}^2(t) + \sum_{\substack{j=1 \\ j \neq i}}^{n} f(x_{rj}(t - \tau_{ji}(t)))u_{rj}^1(t - \tau_{ji})g_r^{ji}(t) \quad (5.143)$$

Since the ordinary traffic has a less restrictive QoS requirements and lower priority than the premium traffic, the control specifications and objectives for the ordinary traffic is defined in terms of regulating the incoming traffic rate while monitoring the link capacity that is leftover after its utilization by the premium traffic. In the next two subsections, we will address the congestion control problems of the ordinary traffic through the dynamic *flow rate control* and the *bandwidth allocation control*. The nonlinear system model is first transformed into an equivalent system model through input-state feedback linearization technique. A state feedback control law is then derived to obtain the transformed system and guarantees the consequent closed-loop system's performance cost with respect to the unknown and time-varying delays. The stability conditions and the physical constraints of the ordinary traffic are presented as a group of LMIs conditions.

For the above nonlinear system, we apply the feedback linearization technique by introducing a new input signal and a state variable as follows:

$$z_{ri}(t) = x_{ri}(t) - x_{ri}^{ref}$$

$$u_{ri}(t) = F^{-1}(x_{ri}, t)\bar{u}_i(t)$$

$$F(x_{ri}(t)) = \begin{bmatrix} f(x_{ri}(t)) & 0 \\ 0 & 1 \end{bmatrix}$$

where $u_{ri}(t) = vec\{u_{ri}^1(t), u_{ri}^2(t)\}$ and $\bar{u}_{ri}(t) = vec\{\bar{u}_{ri}^1(t), \bar{u}_{ri}^2(t)\}$. The above feedback linearization controller implies that $u_{ri}^1 = f^{-1}(x_{ri}, t)\bar{u}_{ri}^1$ and $u_{ri}^2 = \bar{u}_{ri}^2$. Therefore, the transformed linear system of (5.142) can be written as

$$\dot{z}_{ri}(t) = B_{i0}\bar{u}_{ri}(t) + \sum_{\substack{j=1 \\ j \neq i}}^{n} B_j \bar{u}_{rj}(t - \tau_{ji}(t)), \qquad i, j = 1, ..., n \qquad (5.144)$$

where $B_{i0} \in R^{1 \times 2}$ and $B_j \in R^{1 \times 2}$ are the system matrices defined for node i. In fact, B_{i0} is equal to $\begin{bmatrix} -1 & 1 \end{bmatrix}$, and B_j denotes the compression rates between node i and its

235

neighboring nodes and is actually equal to $\begin{bmatrix} g_r^{ji} & 0 \end{bmatrix}$.

The proposed congestion control algorithm for the ordinary traffic is then recast as that of designing the controller $\bar{u}_{ri}(t) = K_i z_{ri}(t)$ so that the following objective function is upper bounded

$$J_{ri} = \int_0^\infty (z_{ri}^T(t) Q_i z_{ri}(t) + \bar{u}_{ri}^T(t) R_i \bar{u}_{ri}(t)) dt \tag{5.145}$$

where Q_i and R_i are given positive definite matrices.

By applying the state feedback controller $\bar{u}_{ri}(t) = K_i z_{ri}(t)$ to the ordinary traffic dynamical queuing model (5.144), the corresponding closed-loop system is obtained as

$$\dot{z}_{ri}(t) = B_{i0} K_i z_{ri}(t) + \sum_{\substack{j=1 \\ j \neq i}}^{n} B_j K_j z_{rj}(t - \tau_{ji}(t)), \qquad i, j = 1, ..., n \tag{5.146}$$

Following along the similar lines as in the synthesis of the centralized congestion controller, and as described in Section 5.2.3, the following lemma can be stated to show that the decentralized controller $\bar{u}_{ri}(t) = K_i z_{ri}(t)$, with a selected control gain K_i, is the guaranteed cost congestion controller for node i and the queuing errors of the premium traffic at each node is guaranteed to be bounded.

Lemma 5.7. *Given the cost function (5.144) and under Assumption 5.2, the state feedback control law $\bar{u}_{ri}(t) = K_i z_{ri}(t)$ is the guaranteed cost controller for the system (5.144), with the control gain $K_i = B_{i0}^+ \theta_{i1} \tilde{M}_i^{-1}$, if there exist symmetric positive definite matrices $\tilde{P}_i$, $\tilde{S}_i$, positive definite matrices $\tilde{M}_i$, $\tilde{N}_i$, $\tilde{S}_i$, $\tilde{Q}_i$, $\tilde{R}_i$, and matrices θ_{i1}, θ_{i2}, θ_{i3}, θ_{i4}, for $i = 1, ..., n$, such that the following LMI condition holds*

$$\bar{\Omega}_i = \begin{bmatrix} 2\theta_{i1} + \tilde{Q}_i + \tilde{R}_i & \tilde{M}_i^T - \tilde{P}_i + \theta_{i2} & -\theta_{i3} \\ * & -2\tilde{N}_i + \tilde{S}_i & -\theta_{i4} \\ * & * & 0 \end{bmatrix} < 0$$

Proof: The same Lyapunov-Krasovskii functional that is selected as before for the stability analysis of the ordinary traffic dynamics is considered below

$$V_i = V_{i1} + V_{i2} \tag{5.147}$$

$$V_{i1} = z_{ri}^T(t) P_i z_{ri}(t)$$

$$V_{i2} = \frac{1}{h} \int_{-h}^0 \int_{t+\theta}^t y_i^T(s) S_i y_i(s) ds d\theta$$

236

where P_i and S_i are sympatric positive definite matrices, and

$$\dot{z}_{ri}(t) = y_i(t) \tag{5.148}$$

$$y_i(t) = B_{i0}z_{ri}(t) + \sum_{\substack{j=1 \\ j \neq i}}^{n} B_j K_j z_{rj}(t) - \sum_{\substack{j=1 \\ j \neq i}}^{n} B_j K_j \int_{t-\tau_{ji}(t)}^{t} y_j(s)ds$$

Therefore, the time derivative of V along with the trajectories of the system (5.144) is given by

$$
\begin{aligned}
\dot{V}_i &= \dot{V}_{i1} + \dot{V}_{i2} \\
&= 2z_{ri}^T(t)P_i y_i(t) + y_i^T(t)S_i y_i(t) - \frac{1}{h}\int_{t-h}^{t} y_i^T(s)S_i y_i(s)ds \\
&= 2[z_{ri}^T(t) \; y_i^T(t)] \begin{bmatrix} P_i & M_i^T \\ 0 & N_i^T \end{bmatrix} \begin{bmatrix} y_i(t) \\ \dot{z}_{ri}(t) - y_i(t) \end{bmatrix} \\
&\quad + y_i^T(t)S_i y_i(t) - \frac{1}{h}\int_{t-h}^{t} y_i^T(s)S_i y_i(s)ds
\end{aligned}
$$

$$
\dot{V}_i = \begin{bmatrix} z_{ri}^T(t) \\ y_i^T(t) \\ Z_{rj}^T(t-\tau_{ji}(t)) \end{bmatrix}^T \begin{bmatrix} 2M_i^T B_{i0}K_i & P_i - M_i^T + K_i^T B_{i0}^T N_i^T & M_i^T B_{ji} K_{ji} \\ * & -2N_i^T & N_i^T B_{ji} K_{ji} \\ * & * & 0 \end{bmatrix} \begin{bmatrix} z_{ri}(t) \\ y_i(t) \\ Z_{rj}(t-\tau_{ji}(t)) \end{bmatrix}
$$

$$+ y_i^T(t)S_i y_i(t) - \frac{1}{h}\int_{t-h}^{t} y_i^T(s)S_i y_i(s)ds$$

where M_i and N_i are symmetric positive definite matrices, and $Z_{rj}(t-\tau_{ji}(t))$ is a vector that consists of the states of the nodes in the neighboring set of node i, with corresponding time-varying delays. The matrices B_{ji} and K_{ji} as well as the vector $Z_{rj}(t-\tau_{ji}(t))$ are defined as follows:

$$B_{ji} = vec\{B_j\}$$

$$K_{ji} = diag\{K_j\}$$

$$Z_{rj}(t-\tau_{ji}(t)) = vec\{z_j(t-\tau_{ji}(t))\}$$

In view of the above definitions, the derivative of the Lyapunov function V_i can be expressed according to

$$\dot{V}_i \leq \frac{1}{h}\int_{t-h}^{t} (\xi_{ri}^T(t,s)W_i\xi_{ri}(t,s)ds \tag{5.149}$$

237

where $\xi_{ri}(t,s) = [z_{ri}^T(t) \;\; y_i^T(t) \;\; Z_{rj}^T(t - \tau_{ji}(t)) \;\; y_i^T(s)]^T$ and the matrix W_i is given as

$$W_i = \begin{bmatrix} 2M_i^T B_{i0} K_i & P_i - M_i^T + K_i^T B_{i0}^T N_i^T & -M_i^T B_{ji} K_{ji} & 0 \\ * & -2N_i^T + S_i & -N_i^T B_{ji} K_{ji} & 0 \\ * & * & 0 & 0 \\ * & * & * & -S_i \end{bmatrix} \tag{5.150}$$

Let us define the following matrices

$$\tilde{M}_i = M_i^{-1} \qquad\qquad \tilde{P}_i = P_i^{-1}$$

$$\tilde{K}_{ji} = K_{ji}^+ \qquad\qquad \Lambda_i = diag\{\tilde{M}_i^T \;\; \tilde{P}_i^T \;\; \tilde{K}_{ji} \;\; 0\}$$

By pre and post multiplying the matrix W_i with Λ^T and Λ, we have

$$\Omega_i \;\; = \;\; \Lambda^T W_i \Lambda = \begin{bmatrix} \Psi_i & 0 \\ 0 & 0 \end{bmatrix}$$

$$\Psi_i \;\; = \;\; \begin{bmatrix} 2B_{i0}\tilde{M}_i & \tilde{M}_i^T - \tilde{P}_i + \tilde{M}_i^T K_i^T B_{i0}^T N_i^T \tilde{P}_i & -B_{ji} \\ * & -2\tilde{P}_i^T N_i^T \tilde{P}_i + \tilde{P}_i S_i \tilde{P}_i & -\tilde{P}_i^T N_i^T B_{ji} \\ * & * & 0 \end{bmatrix}$$

Comparing the matrices Ψ_i and $\bar{\Omega}_i$, one can note that $\Psi_i = \bar{\Omega}_i - (Q_i + K_i^T R_i K_i)$ if the following matrices are defined

$$\theta_{i1} \;\; = \;\; 2B_{i0} K_i \tilde{M}_i \qquad\qquad \tilde{N}_i = \tilde{P}_i^T N_i^T \tilde{P}_i$$

$$\theta_{i2} \;\; = \;\; \tilde{M}_i^T K_i^T B_{i0}^T N_i^T \tilde{P}_i \qquad\qquad \tilde{S}_i = \tilde{P}_i S_i \tilde{P}_i$$

$$\theta_{i3} \;\; = \;\; B_{ji}$$

$$\theta_{i4} \;\; = \;\; \tilde{P}_i^T N_i^T \theta_{i3}$$

Since Q_i and R_i are positive definite matrices, hence if the LMI condition $\Omega_i < 0$ as given in (5.146) is satisfied, we will have

$$\Psi_i \;\; < \;\; 0$$

$$\Rightarrow \;\; \Omega_i < 0$$

$$\Rightarrow \;\; W_i < 0$$

$$\Rightarrow \;\; \dot{V}_i < 0$$

That is, the dynamical system (5.144) is asymptotically stable. Now, notice that $W_i <$ $W_i + (Q_i + K_i^T R_i K_i)$, from the equation (5.149) one can obtain

$$\dot{V} < \frac{1}{h} \int_{t-h}^{t} (\xi_{ri}^T(t, s)(\bar{W}_i - Q_i - K_i^T R_i K_i)\xi_{ri}(t, s)ds \qquad (5.151)$$

where the matrix $\bar{W}_i$ is defined as $\bar{W}_i = W_i + (Q_i + K_i^T R_i K_i)$. Consequently, we have:

$$\dot{V} < -z T_{ri}(t)(Q_i + K_i^T R_i K_i)z_{ri}(t) \qquad (5.152)$$

Integrating both sides of (5.152) from 0 to ∞, one obtains

$$
\begin{aligned}
J_{ri} \quad &< \quad V_i(0) - V_i(\infty) = V_i(0) \\
&= \quad \varphi_{ri}^T(0)P_i\varphi_{ri}(0) + \frac{1}{h} \int_{-h}^{0} \int_{\theta}^{0} \dot{\varphi}_i^T(s)S_i\dot{\varphi}_i(s)dsd\theta = J_{ri}^*
\end{aligned}
$$

Therefore, the closed-loop system performance is guaranteed to be less than the upper bound, and the controller $\bar{u}_{ri}(t) = K_i z_{ri}(t)$ is the guaranteed cost controller of the system (5.144). This completes the proof of Lemma 5.7. ∎

Stability Analysis of the Ordinary Traffic

The physical constraints of the ordinary traffic dynamics are listed below

$$z_{ri}^{min} \leq z_r(t) \leq z_{ri}^{max} \qquad (5.153)$$

$$0 \leq \bar{u}_{ri}(t) \leq c_{ri}(t) \qquad (5.154)$$

where $z_{ri}^{maz} = x_{ri}^{buffer} - x_{ri}^{ref}$, $z_{ri}^{min} = -x_{ri}^{ref}$, x_{ri}^{ref} is the reference set point of the queuing length, $c_{ri}(t)$ is the maximum allowable bandwidth that can be allocated to the premium traffic at node i, which in fact is equal to the instantaneous leftover capacity from the premium traffic, that is $c_{ri}(t) = C_{server,i} - \bar{u}_{pi}(t)$.

To avoid any confusion, in the remainder of this section we utilize the notations of $\tilde{P}_i^p$ and $\tilde{P}_i^r$ to denote the matrix $\tilde{P}$ that is used in Lemma 5.6 for the premium traffic, and the other matrix $\tilde{P}$ that is used in Lemma 5.7 for the ordinary traffic, respectively. Also, we denote K_i^r and K_i^p for the control gains of the premium and the ordinary traffic, respectively.

Consider the following ellipsoid

$$\mathbb{S}_i = \{z_{ri}^T (\tilde{P}_i^r)^{-1} z_{ri} < \rho_i\} \tag{5.155}$$

where $Y_i = \tilde{P}_i$ and $\rho_i > 0$ is selected as a constant.

It follows that similar lines as in deriving the LMI conditions for the physical constraints in the centralized control approach, and as given previously in Section 5.1.2, the physical constraints in (5.153) will be satisfied if the following LMI conditions are satisfied:

$$\Omega_{c1i} \triangleq \begin{bmatrix} \tilde{M}_i & \tilde{M}_i^T \\ \tilde{M}_i & (z_{ri}^{max})^2/\rho_i \end{bmatrix} \geq 0 \tag{5.156}$$

$$\Omega_{c2i} \triangleq (\theta_{i1})_{ij} \geq 0, \qquad i,j = 1, ...2n \tag{5.157}$$

$$\Omega_{c3i} \triangleq \gamma_i \Phi_i \leq \epsilon_i \tag{5.158}$$

$$\Omega_{c4i} \triangleq \begin{bmatrix} I & K_i^r & K_i^p \\ (K_i^r)^T & \frac{C_{server,i}^2}{\epsilon_i + \rho_i} \tilde{P}_i^r & 0 \\ (K_i^p)^T & 0 & \frac{C_{server,i}^2}{\epsilon_i + \rho_i} \tilde{P}_i^p \end{bmatrix} \geq 0 \tag{5.159}$$

$$\Omega_{c5i} \triangleq (\theta_{i3}^{-1})_{ij} > 0, \qquad i,j = 1, ..., 2n \tag{5.160}$$

The following theorem can now be obtained

Theorem 5.4. *A decentralized guaranteed cost congestion controller for the dynamical queuing system of the ordinary traffic in each node i is obtained, if the conditions given in Lemma (5.7) are satisfied, subject to the LMIs of Ω_{c1i} to Ω_{c5i} as governed by (5.156) to (5.160), respectively.*

Proof: The proof follows along the same lines as those given in Lemma 5.7 and the derivations for the physical constraints as given in this section ∎

The decentralized congestion control strategies of the premium and the ordinary traffic classes derived in this section are summarized by the flow chart that is shown in Fig. 5.1. As shown in Fig. 5.1, the decentralized premium traffic controller first solves the local LMI conditions Ω_{ik} and Ω_{c1i} to Ω_{ci6} of each node to derive the decentralized control gains K_{pi}, and the decentralized adaptive control gains δ_{pi} and β_{pi}. The adaptive estimator $\hat{\lambda}_{pi}(t)$
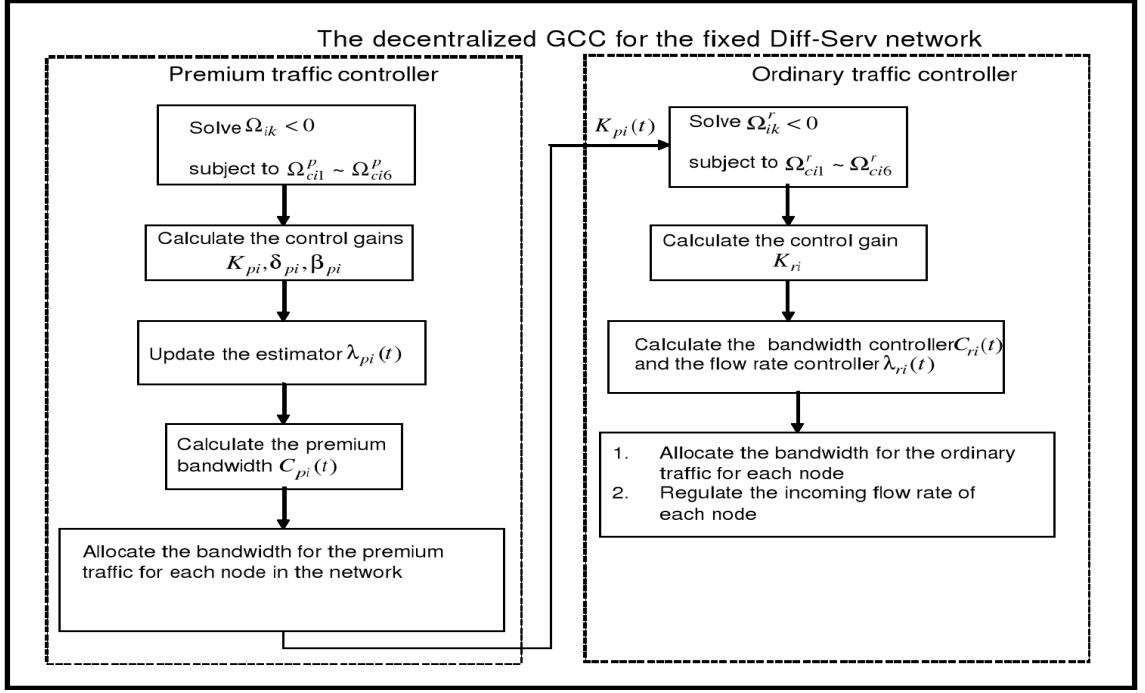
Figure 5.2: The flow chart of the decentralized guaranteed cost congestion controller (GCC) for the Diff-Serv network with fixed topology

is then updated based on the queuing state of each node, and the bandwidth controller $C_{pi}(t)$ is calculated according to the following

$$
\begin{aligned}
C_{pi}(t) &= f^{-1}(x_{pi}, t)\bar{u}|_{pi}(t) \\
&= f^{-1}(x_{pi}, t)K_{pi}(t)\bar{z}_{pi}(t) \\
&= f^{-1}(x_{pi}, t)K_{pi}(t)\begin{bmatrix} x_{pi}(t) - x_{pi}^{ref} \\ \hat{\lambda}_{pi}(t) \end{bmatrix}
\end{aligned}
\tag{5.161}
$$

where $f(x_{pi}(t)) = \mu \frac{x_{pi}(t)}{1+x_{pi}(t)}$, and $x_{pi}(t)$ is the queuing length of node i.

The bandwidth of the premium traffic is allocated at each node. Given the premium traffic control gain K_{pi} and the leftover capacity $C_{server,i} - C_{pi}(t)$, the decentralized controller of the ordinary traffic at each node first solves the corresponding LMI conditions as given by the Lemma 5.7 and the LMI conditions for the physical constraints. Therefore, the decentralized control gain K_{ri} for the ordinary traffic can be obtained. The bandwidth

241
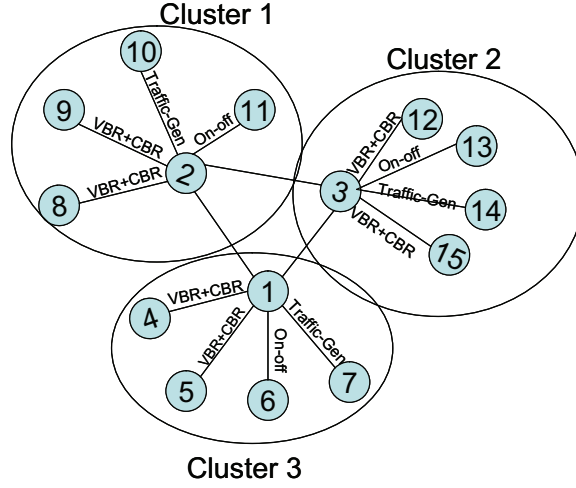
Figure 5.3: The Diff-Serv network consisting of three clusters and 15 nodes.

controller $C_{ri}(t)$ and the flow rate controller $\lambda_{ri}(t)$ can then be calculated as shown below

$$
\begin{bmatrix} C_{ri}(t) \\ \lambda_{ri}(t) \end{bmatrix} = F^{-1}(x_{ri}, t)\bar{u}_{ri}(t)
$$

$$
= \begin{bmatrix} f^{-1}(x_{ri}, t) & 0 \\ 0 & 1 \end{bmatrix} K_{ri} z_{ri}(t)
$$

$$
= \begin{bmatrix} f^{-1}(x_{ri}, t) & 0 \\ 0 & 1 \end{bmatrix} K_{ri}(x_{ri}(t) - x_{ri}^{ref}) \tag{5.162}
$$

where $x_{ri}(t)$ is the queuing length of the ordinary traffic at node i.

5.3 Simulation Results

In this section, we conduct a detailed simulation-based study to evaluate the performance of our proposed guaranteed cost congestion control strategy (GCC). In order to compare our proposed GCC algorithms with a state-of-the-art congestion control scheme in the control community, namely the IDCC approach [3], whose performance has been presented in Chapter 3, we adopt the same network model and the traffic configuration as applied in Section 3.3.2. The simulation network is shown in Fig. 5.3.

242

In the simulation results presented below, the physical constraints of the network are set to $x_{buffer,i} = 5$ Mbits, $C_{server,i} = 10$ Mbits, for $i = 1, ..., 15$. For the simulation studies we generate the Differentiated Services (Diff-Serv) traffic by the event-based simulator tool QualNet [133] and apply it then to the above network. The premium and the ordinary traffic are generated by the sources nodes that are dynamic. Each source node generates a premium random traffic with a mean packet size of 512 bytes and pace the packets into the network every 10 ms. The premium traffic is assumed to be bounded such that $\lambda_{pi}^{max} = 0.8$ Mbps. The source nodes also generate an ordinary traffic by pacing packets into the network according to a on-off mechanism. During the off-time period, no packets are generated. The length of the off-time is determined by an exponential distribution with a mean period of 5 ms. During the on-time, the source nodes generate packets with a constant rate of 100 packets/s with a mean packet size of 512 bytes.

In the remainder of this section we first present the queuing performance of the bottle neck nodes by utilizing our proposed centralized and decentralized GCC strategies. The simulation results are then compared with the corresponding IDCC approach, which was also derived based on the fluid flow model. Moreover, the stability of the network and the tracking errors of the premium and the ordinary traffic under different delay bounds are investigated. Finally, a comparative analysis of the centralized and the decentralized GCC approaches are presented. A numerical comparison on the packet loss rate, the average queuing delay, and the amount of the guaranteed cost J^* are also summarized.

As stated earlier, by utilizing the guaranteed cost congestion strategy, one need not to regulate the traffic compression rates for the stability purpose. Therefore, a higher traffic compression gains (less packet drop out) can be achieved when compared with the switching congestion control strategy (presented in Chapter 3). In this section, the performance of GCC strategy with high traffic compression gains are first illustrated. The comparative studies of GCC and SCC strategies with a lower traffic compression gains (as the average compression gains obtained in Chapter 3) are then presented and analyzed.

5.3.1 Simulation Results Using the Proposed Centralized GCC Strategy

Based on the above simulation model and the traffic configuration, we first present the simulation results by utilizing the centralized GCC strategy. The traffic compression gains among the nodes are set to $g_{ji} = 0.9$, for $i, j = 1, ..., 15$. The time delays among the nodes are taken as a random signal varying from 0 ms to 20 ms. That is $\tau = min\{0, max\{h_{max}, h\}\}$, where $h_{max} = 20$ ms is the maximum bound of delay in the network, $h \sim N(15ms, 10ms)$ is a normal distributed function with the mean value of 15 ms and the standard derivation of 10 ms. The control parameters of the three bottle neck nodes derived from Theorem 5.1 and Theorem 5.2 are given as follows

$$K_p = \begin{bmatrix} 4680 & 0.53 & 0 & 0 & 0 & 0 \\ 0 & 0 & 3610 & 0.10 & 0 & 0 \\ 0 & 0 & 0 & 0 & 2780 & 0.43 \end{bmatrix} \tag{5.163}$$

$$K_r = \begin{bmatrix} 4730 & 3.1 \times 10^3 & 0 & 0 & 0 & 0 \\ 0 & 0 & 6150 & 1.5 \times 10^3 & 0 & 0 \\ 0 & 0 & 0 & 0 & 2200 & 0.7 \times 10^3 \end{bmatrix}^T \tag{5.164}$$

Remark 5.7. *Although by utilizing the GCC strategy there is no limitation for the traffic compression gains g_{ji}. However, during the tasks of a NMAS traffic compression is essential for the network operations. Usually, processing data consumes much less power than transmitting data in communication medium, so it is effective to apply compression before transmitting data for reducing the total power consumption and extend the life time of the network. Therefore, the traffic compression gains are still applied to each node in this chapter. The traffic compression gains are assigned by network operator according to the other network requirements such as data processing and power consumption.*

Remark 5.8. *Different settings of g_{ji} yield different LMIs in Lemma 5.1 - Lemma 5.4 and hence result in different control gains K_p and K_r. On the other hand, the traffic compression gains among different nodes need not to be equal. In this section, the traffic*
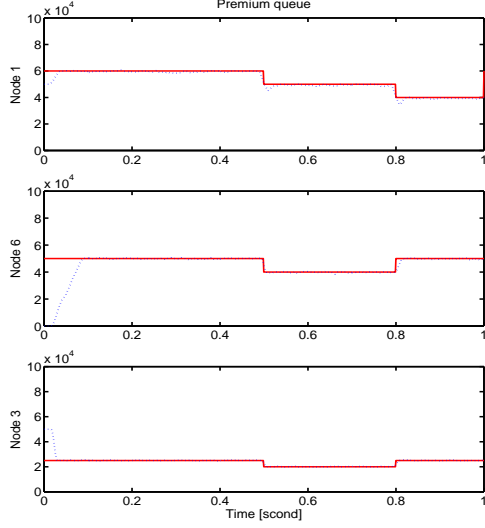
Figure 5.4: Premium queuing lengths (bits) by utilizing the centralized GCC approach. The solid lines denote the set point references and the dashed lines denote the actual queuing lengths.
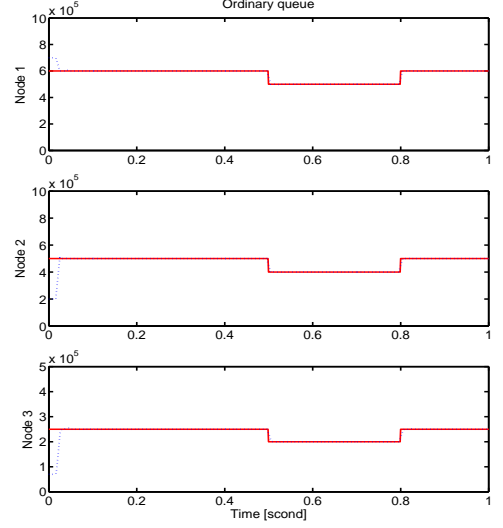
Figure 5.5: Ordinary queuing lengths (bits) by utilizing the centralized GCC approach. The solid lines denote the set point references and the dashed lines denote the actual queuing lengths.

compression gains are set to be the same and equal to 0.9, *while in the next section different values of g_{ji} are considered and the performance of our proposed GCC strategy is then evaluated.*

The queuing performance of the three bottle neck nodes are now shown in Fig. 5.4 to Fig. 5.5, for the premium and the ordinary traffic, respectively. By inspecting the plots presented in these figures, one may conclude that for both traffic classes our proposed centralized guaranteed cost congestion control strategy can stabilize the buffer queues.

Furthermore, as presented in Theorem 5.1, the GCC control strategy can only guarantee the ultimate boundedness of the premium traffic due to the unknown nature of the external incoming traffic $\lambda_p(t)$. On the contrary, for the ordinary traffic class, since both the bandwidth and the incoming traffic are available for control, the GCC control strategy can guarantee the asymptotically stability of the ordinary traffic by satisfying the LMI conditions in Theorem 5.2. As one can observe from the queuing performance of the premium and the ordinary traffic shown in Fig. 5.4 and Fig. 5.5, respectively, the above theoretical results are also validated by the simulations. Moreover, the mean percentage errors of the three bottle neck nodes under different values of maximum delays $h_{max} = [20 \ 40 \ 80]$ ms

245

Table 5.1: The queuing errors for both the traffic classes by utilizing the centralized GCC strategy with different delay levels.

h_{max}	20 ms		40 ms		80 ms	
Centralized GCC	P	O	P	O	P	O
Node 1	1.97%	0.07%	2.08%	0.08%	3.01%	0.10%
Node 2	4.47%	0.16%	5.30%	0.16%	5.30%	0.21%
Node 3	3.25%	0.41%	3.45%	0.42%	3.84%	0.43%

are summarized in the Table 5.1. As seen from the results in Table 5.1, our proposed GCC strategy stabilize both the traffic classes and the buffer queue performance remain robust to the multiple and time-varying delays up to 80 ms amplitude.

5.3.2 Simulation Results Using the Proposed Decentralized GCC Strategy

In order to evaluate in simulation our proposed guaranteed cost congestion control (GCC) strategy and compare its performance with respect to the IDCC [3] approach, we adopt the same network configuration as the one that was used in Chapter 3 and given in Fig. 5.3.

Our proposed decentralized GCC strategy is now evaluated in presence of multiple time-varying delays selected randomly with a maximum upper bound of $h = 20$ ms. In simulations presented below, the sampling time is set to $T_s = 1$ ms and the control parameters that are generated from the LMI conditions in Theorem 5.3 and Theorem 5.4 are $K_{p1} = [1730 \ 1.35]$, $K_{p2} = [7300 \ 3.74]$, $K_{p3} = [2630 \ 2.65]$, $K_{r1} = [1.41 \times 10^4 \ 1.53 \times 10^3]^T$, $K_{r2} = [3.22 \times 10^4 \ 2.31 \times 10^3]^T$, $K_{r3} = [7.14 \times 10^4 \ 5.32 \times 10^3]^T$.

The physical constraints of the network are selected as follows. The server capacity of each node is $C_{server,i} = 10$ Mbps and the buffer size for each traffic class at each node is set to $x_{buffer,i} = 5$ Mbits. The traffic compression gains among each node are set to $g_{ij} = 0.9$ for $i = 1, 2, 3$ and $g_{ij} = 0.7$ for $i = 4, ..., 15$. The simulation results are presented in Fig. 5.6 to Fig. 5.7.
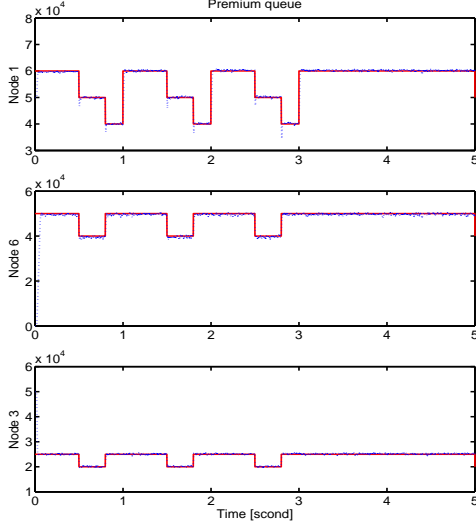
Figure 5.6: Premium queuing lengths (bits) by utilizing our proposed decentralized GCC approach. The solid lines denote the set point references and the dashed lines denote the actual queuing lengths.
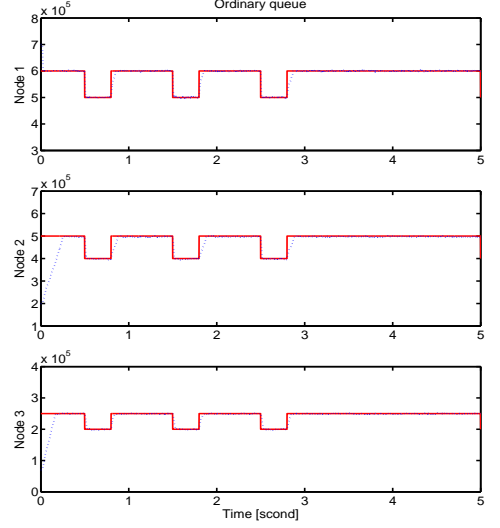
Figure 5.7: Ordinary queuing lengths (bits) by utilizing our proposed decentralized GCC approach. The solid lines denote the set point references and the dashed lines denote the actual queuing lengths.

Table 5.2: The queuing errors for both the traffic classes by utilizing the decentralized GCC strategy with different delay levels.

h_{max}	20 ms		40 ms		80 ms	
Decentralized GCC	P	O	P	O	P	O
Node 1	3.52%	0.84%	3.91%	1.11%	4.13%	1.62%
Node 2	3.56%	0.83%	3.74%	0.93%	3.98%	1.85%
Node 3	2.77%	0.58%	2.90%	0.62%	3.87%	1.14%

Fig. 5.6 and Fig. 5.7 show the buffer queue responses of both traffic classes at each sink node by using our proposed decentralized guaranteed cost congestion controller. By inspecting these results one can conclude that for both services our proposed decentralized GCC strategy stabilizes the network despite the presence of multiple and time-varying delays and a dynamic incoming traffic. When one compares the above results to that of the decentralized IDCC approach, as presented in Section 3.3.2, it follows that the performance of the network is significantly improved by utilizing our proposed GCC approach.

Table 5.2 summarizes the mean percentage errors of the three bottle neck nodes under different values of the maximum delay in the network. By inspecting these numerical

results, one can conclude that our proposed decentralized GCC strategy can stabilize the buffer queues despite the presence of multiple and time-varying delays even for values of delay up to 80 ms. Furthermore, if one compares the results in Table 5.2 with that under the centralized GCC strategy (Table 5.1), one can also conclude that the centralized GCC algorithm can obtain a better control performance in terms of the queuing errors.

5.3.3 Comparisons of the GCC and the SCC Strategies

It is worth noting that in the GCC approach, one <u>does not</u> require to regulate the traffic compression gains to ensure stability. Therefore, a higher traffic compression gains can be obtained. This is due to the fact that in the SCC approach one needs to regulate the traffic compression gains g_{ji} when the control input reaches its physical bounds to guarantee that the system remains stable. As presented in Sections 5.3.1 and 5.3.2, the traffic compression gains in the GCC strategy can be set up to as high as 0.9. On the other hand, the average traffic compression gains in the decentralized SCC approach, as obtained in Section 3.3.2, are as follows

$$\bar{G}_p = \begin{bmatrix} 0 & \bar{g}_{21}^p & \bar{g}_{31}^p \\ \bar{g}_{12}^p & 0 & \bar{g}_{32}^p \\ \bar{g}_{13}^p & \bar{g}_{23}^p & 0 \end{bmatrix} = \begin{bmatrix} 0 & 0.48 & 0.50 \\ 0.70 & 0 & 0.50 \\ 0 & 0.50 & 0 \end{bmatrix} \tag{5.165}$$

$$\bar{G}_r = \begin{bmatrix} 0 & \bar{g}_{21}^r & \bar{g}_{31}^r \\ \bar{g}_{12}^r & 0 & \bar{g}_{32}^r \\ \bar{g}_{13}^r & \bar{g}_{23}^r & 0 \end{bmatrix} = \begin{bmatrix} 0 & 0.50 & 0.50 \\ 0.50 & 0 & 0.50 \\ 0 & 0.30 & 0 \end{bmatrix} \tag{5.166}$$

It follows from equations (5.165) and (5.166) that the traffic compression gain that can be achieved in the decentralized SCC approach is about 0.5. In order to evaluate our proposed GCC and SCC approaches fairly, the following two cases are presented for the comparative studies.

Case 1: Decentralized GCC vs Decentralized SCC

248

Table 5.3: Packet loss rate by utilizing the decentralized IDCC, SCC, and GCC approaches with $h_{max} = 40$ ms.

Premium	IDCC [3]	SCC	GCC
Node 1	92.96%	0	0
Node 2	93.86%	0	0
Node 3	93.27%	0	0
Ordinary	IDCC [3]	SCC	GCC
Node1	87.93%	5.66%	0.52%
Node 2	96.08%	4.65%	0.99%
Node 3	96.13%	2.34%	0.91%

Table 5.4: Average queuing delay by utilizing the decentralized IDCC, SCC, and GCC approaches with $h_{max} = 40$ ms.

Premium	IDCC [3]	SCC	GCC
Node 1	∞	48.8 ms	41.5 ms
Node 2	∞	44.9 ms	37.4 ms
Node 3	∞	22.5 ms	20.9 ms
Ordinary	IDCC [3]	SCC	GCC
Node 1	∞	67.8 ms	57.28 ms
Node 2	∞	138.1 ms	46.28 ms
Node 3	∞	178.5 ms	23.36 ms

In this section, the performance of our proposed decentralized GCC strategy is compared with the decentralized SCC (as presented in Chapter 3) by using the same compression gains that are given in equations (5.165) and (5.166). The network configurations are the same as shown in Fig. 5.3. The time-delay among the nodes is generated as a random signal using a Gaussian distribution with mean value of 20 ms and the maximum bound of $h_{max} = 40$ ms. The physical constraints of the network are selected as follows. The server capacity of the nodes are set to $C_{server,1} = 20$ Mbps, $C_{server,2} = 10$ Mbps, $C_{server,3} = 5$ Mbps, and $C_{server,i} = 100$ Mbps for $i = 4, ..., 15$. The buffer size for each traffic class at each node is set to $x_{buffer,i} = 5$ Mbits.

Based on the above configurations, the comparative results obtained in Table 3.1 and Table 3.2 of Chapter 3 can now be extended to Table 5.3 and Table 5.4. It follows from the comparative results that the buffer queue performance by utilizing either the proposed SCC or the GCC strategies are greatly improved when compared with the IDCC [3].

Moreover, as shown in Table 5.3, the packet loss rate (PLR) of the ordinary traffic has been greatly improved by using our proposed GCC strategy. One possible reason is that in the GCC approach, by taking the incoming traffic $\lambda_{ri}(t)$ as an additional control input, the regulation is accomplished more readily with this extra degree of freedom and higher level of ordinary traffic flow is allowed into the network. Hence, less packets are dropped out during the flow rate regulation. On the other hand, as shown in Table 5.4, the average queuing delay of both traffic class by using the SCC and GCC approaches are

249

Table 5.5: Packet loss rate by utilizing the centralized IDCC, SCC, and GCC approaches with $h_{max} = 40$ ms.

Premium	IDCC [3]	SCC	GCC
Node 1	84.63%	0	0
Node 2	83.23%	0	0
Node 3	88.70%	0	0
Ordinary	IDCC [3]	SCC	GCC
Node 1	38.34%	1.61%	0.23%
Node 2	62.95%	0.94%	0.19%
Node 3	73.68%	1.43%	0.78%

Table 5.6: Average queuing delay by utilizing the centralized IDCC, SCC, and GCC approaches with $h_{max} = 40$ ms.

Premium	IDCC [3]	SCC	GCC
Node 1	∞	45.3 ms	34.5 ms
Node 2	∞	43.7 ms	27.4 ms
Node 3	∞	21.4 ms	20.6 ms
Ordinary	IDCC [3]	SCC	GCC
Node 1	∞	57.1 ms	53.6 ms
Node 2	∞	116.6 ms	44.5 ms
Node 3	∞	132.8 ms	22.7 ms

similar.

Case 2: Centralized GCC vs Centralized SCC

In this section, the performance of our proposed centralized GCC strategy is compared with the centralized SCC (as presented in Chapter 3) by using the same compression gains as follows

$$\bar{G}_p = \begin{bmatrix} 0 & 0.23 & 0.31 \\ 0.42 & 0 & 0.21 \\ 0 & 0.30 & 0 \end{bmatrix} \qquad \bar{G}_r = \begin{bmatrix} 0 & 0.41 & 0.25 \\ 0.52 & 0 & 0.12 \\ 0 & 0.28 & 0 \end{bmatrix}$$

The network configurations are the same as shown in Fig. 5.3. The time-delay among the nodes are set to be the same as in Case 1. Based on the above configurations, the comparative results in the buffer queues are now summarized in Table 5.5 and Table 5.6. By inspecting the numerical results in Table 5.5 and Table 5.6, one can conclude that the performance of the network has been greatly improved by utilizing our proposed SCC and GCC strategies when compared to the IDCC. On the other hand, by considering the traffic rate as the control input the packet loss rate of the ordinary traffic has also been improved in the centralized GCC.

5.3.4 Comparisons of the Proposed Decentralized GCC and the Centralized GCC Strategies

As mentioned earlier, the centralized and the decentralized control approaches both have distinct advantages as well as drawbacks. A centralized congestion control does yield an optimal and an accurate result since it makes use of the full information of the entire network. However, as the number of nodes in a network increases, there would be a significant increase of the traffic load onto the network. It would be very difficult to implement a centralized congestion control algorithm for a large scale traffic network which requires one to solve a set of LMIs with a significantly large dimensions.

In this section, comparative results and numerical analysis of our proposed decentralized and centralized guaranteed cost congestion control (GCC) strategies are presented based on the simulation results that are presented in the previous two subsections. The performances of these two strategies are compared on two aspects:

- Quality of service (QoS): encompassing metrics such as packet loss rate and average queuing delay, and

- Quality of control (QoC): encompassing metrics such as mean queuing error, settling time, and the upper bound of cost.

The number of LMIs that need to be solved and the maximum dimension of the LMIs are also considered as a measure of feasibility and scalability for these two congestion control algorithms.

Based on the same network scenarios and simulation results as presented in the previous two subsections, the performance of the buffer characteristics of node 3 for the premium and the ordinary traffic services in presence of the time-delay of 80 ms upper bound are summarized in Table 5.7 and Table 5.8, respectively. The definitions of the packet loss rate (PLR) and the average queuing delay are given in Section 3.3.1. The settling time is defined as the time t when the queuing error has decreased to less than 2% and has remained to less than 5% for the duration of the remaining simulation of its steady state value.

The last item in Table 5.7 and Table 5.8 are the upper bound of the cost. It should be noted that in order to compare the cost of the decentralized and the centralized GCC strategies fairly, one needs to apply the same cost function J. Recall the decentralized and the centralized cost functions:

$$J_i^{decen} = \int_{t=0}^{\infty} (z_i^T(t)R_i z_i(t) + u_i^T(t)Q_i u_i(t))dt \qquad (5.167)$$

$$J^{cen} = \int_{t=0}^{\infty} (z^T(t)Rz(t) + u^T(t)Qu(t))dt \qquad (5.168)$$

Now, let us set the quadratic matrices R and Q in equation (5.167) to be diagonal positive definite matrices, and set the decentralized quadratic matrices R_i and Q_i equals to the the corresponding diagonal elements in R and Q. The cost function for the entire network in the decentralized GCC can then be written as follows:

$$
\begin{aligned}
J_{total}^{decen} &= \sum_{i=1}^{n} J_i^{decen} \\
&= \int_{t=0}^{\infty} (z^T(t)Rz(t) + u^T(t)Qu(t))dt = J^{cen}
\end{aligned}
$$

Therefore, the total cost function for the entire network is the same and we can now compare the value of the guaranteed cost fairly. According to (5.39), the upper bound of the cost for the premium traffic by utilizing the centralized GCC approach is given by

$$J_p^* = \varphi^T(0)P\varphi(0) + \sum_{l=1}^{m} \frac{1}{h} \int_{-h}^{0} \int_{\theta}^{0} \dot{\varphi}^T(s)S_l\dot{\varphi}(s)dsd\theta + \gamma\lambda_{max}(\Phi)$$

where $\varphi(t)$ is a continuous time function defined in $[-h, \ 0]$ representing the initial value of the time-delay system. We assume that $\dot{\varphi}(t) = 0$ for $t \in [-h, \ 0]$, so that J_p^* becomes

$$J_p^* = \varphi^T(0)P\varphi(0) + \gamma\lambda_{max}(\Phi) \qquad (5.169)$$

where $\Phi = B_\lambda(\bar{M}+\bar{N})^{-1}B_\lambda$, and the matrices P, $\bar{M}$, and $\bar{N}$ are derived from Theorem 5.1. Note that γ is the bound of the integral of incoming traffic that satisfy the Assumption 5.1, by setting $\gamma = 2.0 \times 10^{14}$ we can calculate the value of J_p^*. Similar definitions and assumptions are applied to the ordinary traffic. The upper bound of the guaranteed cost J_r^* by utilizing the centralized and the decentralized GCC approach are given in Table. 5.8.

252

Table 5.7: The premium traffic performance of the node 3 with $h_{max} = 80$ ms, by utilizing the decentralized GCC and the centralized GCC approaches.

$h_{max} = 80$ ms		Decentralized GCC	Centralized GCC
QoS	PLR	0	0
	Queuing Delay	26.0 ms	24.5 ms
QoC	Mean Error	3.38%	2.87%
	Settling Time	0.09s	0.11s
	Max cost J_p^*	5.05×10^{20}	2.94×10^{20}
Feasibility	Num of LMIs	21	8
	Max dimension of LMIs	10×10	18×18

As can be inspected from the comparison results the centralized GCC approach can achieve a better QoS performance than the decentralized GCC. For the QoC, the centralized GCC can achieve a more accurate tracking in the queuing error with a smaller cost J^* when compared to the decentralized strategy. On the contrary, since the decentralized control approach only has access to the local state information, more control effort is needed to stabilize the buffer queues.

However, in the centralized GCC strategy, one needs to solve LMIs with higher dimensions. As the number of nodes increase in the network, it will become difficult or computationally challenging to find a feasible solution to the high dimensional LMI conditions. Actually, for a network with n node, the centralized GCC needs to deal with one $6n \times 6n$, one $4n \times 4n$, four $3n \times 3n$, two $2n \times 2n$, two $2n \times n$, and one $n \times n$ matrices obtained such that the LMI conditions in Theorem 5.1 and Theorem 5.2 are satisfied.

On the other hand, the decentralized controllers can be constructed locally at individual nodes and only need access to the local information. Therefore, a decentralized control approach is more preferable for practical purposes and implementation. Furthermore, by utilizing our proposed decentralized congestion control strategies for each node, there are two matrices with a dimension of $5 \times (m + 3)$, n matrices with dimension of $(2m + 2) \times (2m + 2)$, three matrices of 2×2 dimension, one matrix of 3×3 dimension, and one matrix of $2 \times m$ dimension, where m is the number of neighboring nodes of node i. If the network is fully connected, $m = n - 1$. Therefore, although the number of the

253

Table 5.8: The ordinary traffic performance of the node 3 with $h_{max} = 80$ ms, by utilizing the decentralized GCC and the centralized GCC approaches.

$h_{max} = 80$ ms		Decentralized GCC	Centralized GCC
QoS	PLR	0.98%	0.36%
	Queuing Delay	23.55 ms	23.14 ms
QoC	Mean Error	0.68%	0.43%
	Settling Time	0.09s	0.24s
	Max cost J_r^*	3.01×10^{20}	1.45×10^{20}
Feasibility	Num of LMIs	18	7
	Max dimension of LMIs	7×7	18×18

required matrices in the decentralized control scheme is higher than the centralized controller method, given that the dimensions of the corresponding matrices are lower than the centralized case, a solution to the decentralized scheme can be obtained by LMI technique much faster and more efficiently.

Based on the above observations, one can draw a conclusion that for a small scale network the complexity of the LMI conditions for the centralized GCC approach is close to the decentralized one, hence a centralized congestion controller is desired due to its higher accuracy. However, for large scale networks the decentralized congestion controller is preferred due to its preferred feasibility, practical and implementation considerations.

5.4   Conclusions

In this chapter, the Diff-Serv networks with fixed topology is considered. A novel guaranteed cost congestion control (GCC) strategy is developed for the premium and the ordinary traffic, respectively. By employing the guaranteed cost control scheme, the dynamic queuing systems of the network are stabilized and the robustness of the closed-loop systems with respect to the multiple and time-varying delays are guaranteed. The physical constraints of the network are guaranteed by satisfying extra LMI conditions. Comparative analysis shows that the GCC algorithm is less conservative than the SCC approach on the aspect of packet loss rate. Simulation results and numerical comparisons do illustrate

that the performances of the network has been greatly improved by applying our proposed GCC algorithms when compared to the other available methods in the literature.

Furthermore, comparative analysis is performed between the centralized and the decentralized congestion control strategies as developed in Chapters 3-5. One can conclude that each of these two schemes has their distinguished advantages and unavoidable disadvantages. However, since the decentralized controller is implemented at each node, therefore it is scalable to large scale networks and is more robust to the changes of the network topology. Therefore, the decentralized control scheme is selected for the guaranteed cost congestion control problem of mobile Diff-Serv networks that is investigated in the next chapter.

Chapter 6

Guaranteed Cost Congestion Control of Mobile Diff-Serv Networks

The aim of this chapter is to extend the guaranteed cost congestion controller (GCC), as discussed in Chapter 5, to the mobile Diff-Serv networks. As presented before, the mobility of nodes will change the neighboring set of each node in the network, and thus results in a changing network topology. The changes of the network topology can be modeled by a Markov chain α_t, and the queuing dynamics of the mobile network becomes a nonlinear time-delay system with Markovian jump parameters. Based on the dynamic queuing models of the mobile network that are given in Chapter 2, a jump quadratic cost function is defined in this chapter and a Markovian jump guaranteed cost congestion control (MJ-GCC) strategy is developed for the premium and the ordinary traffic of the mobile networks. By solving the corresponding LMI conditions, the stability of the system is guaranteed with a bounded performance cost. The physical constraints of the mobile network are considered and transformed into a group of complementary LMI conditions.

The remainder of this chapter is organized as follows. In Section 6.1, a brief introduction to guaranteed cost control of the Markovian jump linear systems (MJLS) is

provided and the definitions for the stochastic guaranteed cost is given. In Section 6.2, a decentralized guaranteed cost congestion controller is developed for the mobile Diff-Serv network based on a jump quadratic cost function and the stochastic control theory. In Section 6.3, simulation results are shown to evaluate our proposed MJ-GCC strategies. The conclusions are given in Section 6.4.

6.1   Guaranteed Cost Control of Markovian Jump Linear Systems with Time-Delay

In practice, a large number of dynamical systems have variable structures that are subject to random abrupt changes. This may be due to random failures and repairs of the components, changes in the interconnections of the subsystems, sudden environment changes, modifications of the operating points of a linearized model of a nonlinear system, etc. The hybrid systems, which involve both time-evolving and event-driven mechanisms may be employed to model these systems. A Markovian Jump Liner system (MJLS) is a hybrid system with multiple operating modes. Every mode corresponds to a deterministic dynamics. The switching system mode is governed by a Markov process. When the mode is fixed, the system state evolves according to a corresponding deterministic dynamics.

Control of MJLS with time-delays has been a research subject that has attracted a lot of interest during the past decade and has been extensively studied by many authors [119], [154], [155]. The guaranteed cost control (GCC) of uncertain systems was first put forward by the authors in [116] and has been studied by a number of researchers, which is to design a controller that robustly stabilizes the uncertain system and guarantees that the cost function has an upper bound. Recently the guaranteed cost control of Markovian jump linear systems (MJLS) with time-delays has also attracted great interest as seen from the works [156], [157], [158], [159], [139], [160].

Consider the following MJLS with time-delay:

$$\dot{x}(t) = A(\alpha_t)x(t) + A_d(\alpha_t)x(t - \tau(t)) + B(\alpha_t)u(t) + B_w(\alpha_t)w(t) \qquad (6.1)$$

$$x(t) = \phi(t), t \in [-h, 0]$$

where $x(t)$ is the system state, $u(t)$ is the input signal, $w(t)$ is the disturbance, $\tau(t)$ is the unknown time-varying delay, h is the upper bound of the delay which is known, $A(\alpha_t)$, $A_d(\alpha_t)$, $B(\alpha_t)$ and $B_w(\alpha_t)$ are the system matrices that depend on the mode α_t, and α_t is the Markov chain that represents the changes of the system or in our application network topology.

The transition probability between different modes α_t is determined by the following function:

$$P[\alpha_{t+\delta} = k \mid \alpha_t = l] = \begin{cases} \pi_{kl}\Delta + o(\Delta), & k \neq l; \\ 1 + \pi_{kk}\Delta + o(\Delta), & k = l. \end{cases} \tag{6.2}$$

where $\pi_{kl} \geq 0$ is the transition rate from mode k to mode l, $\pi_{kk} = -\sum\limits_{l=1,l\neq k}^{M} \pi_{kl}$, and $o(\Delta)$ is a function satisfying $\lim\limits_{\Delta \to 0} \frac{o(\Delta)}{\Delta} = 0$.

The guaranteed cost control (GCC) of the Markovian jump linear system is an extension of the GCC problem of the deterministic system, with the following jump quadratic cost function:

$$J \quad = \quad E\{\int_0^\infty [x^T(t)Q(\alpha_t)x(t) + u^T(t)R(\alpha_t)u(t)]dt\} \tag{6.3}$$

where $x(t)$ is the state of the system, $u(t)$ is the acclimated input, $Q(\alpha_t)$ and $R(\alpha_t)$ are the positive definite matrices, α_t is a finite state Markovian process representing the system mode, and α_t takes discrete values in a given finite set $\mathcal{S} = \{1, ..., M\}$.

Therefore, the guaranteed cost control problem of the MJLS (6.1) is to select the state feedback controller $u(t) = K(\alpha_t)x(t)$, for each mode, such that the Markovian jump time-delay system (6.1) is stable and the jump quadratic cost function (6.3) is bounded by a scalar J^*. The definitions corresponding to the stochastic stability are now presented as follows:

Definition 6.1. *[135]: The Markovian jump time-delay system (6.1) with $u(t) \equiv 0$ and $w(t) \equiv 0$ is said to be stochastically stable if there exists a constant $T(\phi(.), r_0)$ such that the following holds for any initial condition $(\phi(.), r_0)$:*

$$E[\int_0^\infty \|x(t)\|^2 dt \mid \phi(.), r_0] \leq T(\phi(.), r_0) \tag{6.4}$$

where ϕ is a function representing the initial condition.

Definition 6.2. *[156] For the Markovian jump time-delay system (6.1) and the jump quadratic cost function (6.3), if there exist a control law $u^*(t)$ and a positive scalar J^* such that the closed-loop system is stochastic stable and the cost function J satisfies:*

$$J \leq J^*$$

then J^* is the stochastic guaranteed cost *of the system (6.1) and $u^*(t)$ is the* guaranteed cost controller *of the system (6.1).*

6.2 A Markovian Jump Guaranteed Cost Congestion Control (MJ-GCC) Strategy for Mobile Diff-Serv Networks

In this section, the decentralized guaranteed cost congestion control (GCC) strategy presented in Chapter 5 is extended to the mobile networks. Consider a mobile network with n nodes where each node has three separate buffers for the premium, the ordinary, and the best-effort traffic, respectively. The control objective for the premium traffic is to allocate the output capacity $C_{pi}(t)$ of each node so that the premium queuing length of each node will be as close as possible to its reference set point value. On the other hand, the control objective for the ordinary traffic is to simultaneously allocate the bandwidth $C_{ri}(t)$ and regulate the incoming flow rate $\lambda_{ri}(t)$ of each node so that the ordinary queuing length is as close as possible to its corresponding reference value. Furthermore, the physical constraints of the mobile network need to also be considered. In the following subsections, Markovian jump guaranteed cost control strategies are presented for the premium and the ordinary traffic in the mobile network.

6.2.1 Premium Traffic Control

The decentralized dynamic model of the premium traffic flow in a mobile network is rewritten here again for convenience:

$$\dot{x}_{pi}(t) = -f(x_{pi}(t))u_{pi}(t) + \sum_{j \in \wp_i(\alpha_t)} f(x_{pj}(t - \tau_{ji}(t)))u_{pj}(t - \tau_{ji}(t))g_p^{ji}(t) + \lambda_{pi}(t) \quad (6.5)$$

where x_{pi} denotes the premium queueing length, $u_{pi}(t) = C_{pi}(t)$ is the bandwidth controller of the premium traffic at node i, $u_{pj}(t - \tau_{ji}(t))$ is the bandwidth controller of the neighboring node j with the unknown but bounded time-varying delay $\tau_{ji}(t)$, $\lambda_{pi}(t)$ is the external traffic flow, $g_p^{ji}(t)$ is the traffic compression gain between node j and i, $\wp_i$ is the neighboring set of node i, and α_t is the Markov process representing the changes of the network topology. The transition probabilities among different modes α_t are as defined in (6.2).

The multiple and time-varying delays $\tau_{ji}(t)$ in the queuing model of the premium traffic in the mobile network (6.5) are assumed to be upper bounded by different values h_{ji} and with the maximum upper bound h that is assumed to be known a priori. The above assumptions are the extension of the general assumptions of delays that was given in Chapter 2 and is presented below.

Assumption 6.1. *The unknown multiple and time-varying delays $\tau_{ji}(t)$ are upper bounded and the maximum upper bound is a known constant, that is*

$$0 \leq \tau_{ji}(t) \leq h_{ji} \quad (6.6)$$

$$h = max\{h_{ji}\} \quad (6.7)$$

Feedback linearization technique

Since the dynamic queuing model (6.5) is nonlinear, it can be transformed into an equivalent linear system model through the following feedback linearization stradegy

$$z_{pi}(t) = x_{pi}(t) - x_{pi}^{ref} \quad (6.8)$$

$$u_{pi}(t) = f^{-1}(x_{pi}, t)\bar{u}_{pi}(t) \quad (6.9)$$

where x_{pi}^{ref} is the reference queueing length at node i.

By using the above definitions and transformations, the premium queuing model (6.5) can be expressed as follows

$$\dot{z}_{pi}(t) = -\bar{u}_{pi}(t) + \lambda_{pi}(t) + \sum_{j \in \wp_i(\alpha_t)} \bar{u}_{pj}(t - \tau_{ji}(t)) g_p^{ji}(t) \tag{6.10}$$

In review of the above linear system model, the congestion control problem of the premium traffic can be viewed as that of selecting the decentralized state feedback controller $\bar{u}_{pi}(t) = K_{pi}(\alpha_t) z_{pi}(t)$, for each mode α_t, such that the Markovian jump system (6.10) is stable. However, due to the unknown external input signal $\lambda_{pi}(t)$, the state feedback controller is augmented by adding an adaptive estimator $\hat{\lambda}_{pi}(t)$ to estimate the unknown incoming traffic and compensate for its effect via feedback. Therefore, the state feedback controller $\bar{u}_{pi}(t)$ is modified to the following

$$\bar{u}_{pi}(t) = K_{pi}(\alpha_t) \bar{z}_{pi}(t) \tag{6.11}$$

$$\bar{z}_{pi}(t) = \begin{bmatrix} z_{pi}(t) & \hat{\lambda}_{pi}(t) \end{bmatrix}^T \tag{6.12}$$

where $\bar{z}_{pi}(t)$ is a new state variable and $\hat{\lambda}_{pi}(t)$ is the online estimation of the unknown external signal $\lambda_{pi}(t)$. The updating rule of the estimation process is selected based on the parameter projection method [128], namely

$$\dot{\hat{\lambda}}_{pi}(t) = \begin{cases} \delta_{pi}(\alpha_t) z_{pi}(t) - \beta_{pi}(\alpha_t) \hat{\lambda}_{pi}(t), & \text{if } 0 \leq \hat{\lambda}_{pi}(t) \leq \lambda_{pi}^{max} \text{ or} \\ & \qquad \hat{\lambda}_{pi}(t) = 0,\ z_{pi}(t) \geq 0 \text{ or} \\ & \qquad \hat{\lambda}_{pi}(t) = \lambda_{pi}^{max},\ z_{pi}(t) \leq 0 \\ -\beta_{pi}(\alpha_t) \hat{\lambda}_{pi}(t), & \text{otherwise} \end{cases} \tag{6.13}$$

where $\delta_{pi}(\alpha_t) > 0$ and $\beta_{pi}(\alpha_t) > 0$ are design parameters depending on the mode α_t.

Based on the definition of the new state representation (6.11), the Markovian jump linear system (6.10) can be re-written into the following hybrid switching system with multiple and time-varying delays:

$$\dot{\bar{z}}_{pi}(t) = A_{i0}^k(\alpha_t) \bar{z}_{pi}(t) + B_{i0} \bar{u}_{pi}(t) + \sum_{j \in \wp_i(\alpha_t)} B_j \bar{u}_j(t - \tau_{ji}(t)) + B_{\lambda_i} \lambda_{pi}(t) \tag{6.14}$$

$$\bar{z}_{pi}(t) = \varphi_i(t) \qquad \varphi_i(t) \in [-h, 0]$$

$$k \in \aleph,\ \aleph = 1, 2$$

$$\alpha_t \in \mathcal{S},\ \mathcal{S} = \{1, ..., M\}$$

where the system matrices $A_{i0}^k(\alpha_t)$, B_{i0}, B_j, and B_{λ_i}, for $i, j = 1, ..., n$ are defined as follows:

$$A_{i0}^1(\alpha_t) = \begin{bmatrix} 0 & 0 \\ \delta_{pi}(\alpha_t) & -\beta_{pi}(\alpha_t) \end{bmatrix} \qquad A_{i0}^2(\alpha_t) = \begin{bmatrix} 0 & 0 \\ 0 & -\beta_{pi}(\alpha_t) \end{bmatrix}$$

$$B_{i0} = \begin{bmatrix} -1 \\ 0 \end{bmatrix} \qquad B_j = \begin{bmatrix} g_{ji}^p \\ 0 \end{bmatrix} \qquad B_{\lambda_i} = \begin{bmatrix} 1 \\ 0 \end{bmatrix}$$

The above dynamical system is a hybrid switching system with both deterministic and stochastic switchings. The deterministic switching signal k is introduced by the adaptive estimator $\hat{\lambda}_{pi}(t)$ and has two values. The stochastic switching signal α_t is induced by the changes to the network topology in the mobile network, and takes value from the finite set $\mathcal{S}$.

Physical Constraints

The physical constraints of the new dynamical system (6.14) are listed as follows:

$$\bar{z}_{pi}^{min} \leq \bar{z}_{pi}(t) \leq \bar{z}_{pi}^{max} \tag{6.15}$$

$$0 \leq \bar{u}_{pi}(t) \leq C_{server,i}(\alpha_t) \tag{6.16}$$

where $\bar{z}_{pi}^{min} = [-x_{pi}^{ref} \ 0]^T$ is the minimum value of the new state, $\bar{z}_{pi}^{max} = [x_{pi}^{buffer} - x_{pi}^{ref}, \lambda_{pi}^{max}]^T$ is the maximum bound of the new state, and $C_{server,i}(\alpha_t)$ is the mode-dependent link capacity of node i.

Performance Cost Function

According to the definition of the guaranteed cost control for the MJLS, the performance cost function for the hybrid switching system (6.14) is selected as the following jump quadratic cost function:

$$J_{pi} = E\{\int_0^\infty (\bar{z}_{pi}^T(t)Q_i(\alpha_t)\bar{z}_{pi}(t) + \bar{u}_{pi}^T(t)R_i(\alpha_t)\bar{u}_{pi})dt\} \tag{6.17}$$

where $Q_i(\alpha_t)$ and $R_i(\alpha_t)$ are given positive definite matrices for each mode.

Therefore, the guaranteed cost congestion control problem of the premium traffic is recast as that of selecting the state feedback controller $\bar{u}_{pi}(t) = K_{pi}(\alpha_t)\bar{z}_{pi}(t)$, for each

mode with the understanding that a "centralized" knowledge on the network topology changes as represented by $\alpha(t)$ is available, such that the hybrid switching system (6.14) is ultimately bounded and the jump quadratic cost function (6.17) is upper bounded. Clearly, the "centralized" knowledge on $\alpha(t)$ does not impose any restrictive condition on the implementation of the decentralized controller $\bar{u}_{pi}(t)$ as the characteristics on the network topology changes are assumed to be known *a prior*.

In order to guarantee an upper bound of the corresponding cost function, in this chapter we adopt the same Assumption 5.2 as presented in Chapter 5. Then the following lemmas are now presented to show that the memoryless state feedback control law with the mode-dependent control gain $K_{pi}(\alpha_t)$ is a guaranteed cost controller for the hybrid switching system (6.14).

Lemma 6.1. *Given the cost function (6.17) and under Assumption 5.2, the controller $\bar{u}_{pi}(t) = K_{pi}(\alpha_t)\bar{z}_{pi}(t)$ is a guaranteed cost control law of system (6.14), if there exist symmetric positive definite matrices $P_i(\alpha_t)$, $S_i(\alpha_t)$, U_i, and positive definite matrices $M_i(\alpha_t)$ and $N_i(\alpha_t)$, $i = 1, ..., n$, such that the following matrix inequality condition is satisfied for all the modes $\alpha_t \in \mathcal{S}$, $\mathcal{S} = \{1, ..., M\}$:*

$$\bar{W}_{ik}(\alpha_t) = \begin{bmatrix} X_{ik}(\alpha_t) & h^2(A_{ic}^k)^T(\alpha_t)U_iB_{ji}K_{ji}(\alpha_t) + P_i(\alpha_t)B_{ji}K_{ji}(\alpha_t) & U_i \\ * & h^2B_{ji}K_{ji}(\alpha_t)(U_i + N_i(\alpha_t))B_{ji}K_{ji}(\alpha_t) & 0 \\ * & * & -U_i - (1-h)S_i(\alpha_t) \end{bmatrix} < 0$$

$$\Psi_i(\alpha_t) = B_{\lambda_i}(h^2U_i + M_i^{-1}(\alpha_t)Y_i(\alpha_t) + h^2N_i^{-1}(\alpha_t))B_{\lambda_i} < 0$$

where:

$$A_{ic}^k(\alpha_t) = A_{i0}^k(\alpha_t) + B_{i0}K_{pi}(\alpha_t)$$

$$Y_i(\alpha_t) = h^2A_{ic}^k(\alpha_t)U_i + P_i(\alpha_t)$$

$$X_{ik}(\alpha_t) = (2P_i(\alpha_t) + h^2(A_{ic}^k)^T(\alpha_t)U_i)A_{ic}^k(\alpha_t) + \sum_{l=1}^{M}\pi_{\alpha_t l}P_i(l) + (1+h)S_i(\alpha_t)$$

$$-U_i + M_i(\alpha_t) + Q_i(\alpha_t) + K_{pi}^T(\alpha_t)R_i(\alpha_t)K_{pi}(\alpha_t)$$

Proof: Consider the following stochastic Lyapunov-Krasovskii functional candidate:

$$V_i(\bar{z}_{pi}(t), \alpha_t) = V_{i1} + V_{i2} + V_{i3} + V_{i4} \tag{6.18}$$

$$V_{i1} = \bar{z}_{pi}(t)^TP_i(\alpha_t)\bar{z}_{pi}(t) \tag{6.19}$$

$$V_{i2} = \int_{t-h}^{t} \bar{z}_{pi}^T(s)S_i(\alpha_t)\bar{z}_{pi}(s)ds \tag{6.20}$$

$$V_{i3} = h \int_{-h}^{0} \int_{t+\theta}^{t} \dot{\bar{z}}_{pi}^T(s) U_i \dot{\bar{z}}_{pi}(s) ds d\theta \tag{6.21}$$

$$V_{i4} = \int_{-h}^{0} \int_{t+\theta}^{t} \bar{z}_{pi}^T(s) S_i(\alpha_t) \bar{z}_{pi}(s) ds d\theta \tag{6.22}$$

with $P_i(\alpha_t)$, $S_i(\alpha_t)$, U_i denoting positive definite matrices with appropriate dimensions. Let $\mathcal{L}$ be the infinitesimal generator of $\{\bar{z}_{pi}(t), \alpha_t\}$, $t \geq 0$. Then, for each $\alpha_t = k \in \mathcal{S}$ we have:

$$
\begin{aligned}
\mathcal{L}V_{i1} &= \lim_{\Delta \to 0^+} \frac{1}{\Delta} \{ E[V_{i1}(\bar{z}_{pi}(t+\Delta), \alpha_{t+\delta}, t+\Delta) | \bar{z}_{pi}(t), \alpha_t = k] - V_{i1}(\bar{z}_{pi}(t), k, t) \} \\
&= 2\bar{z}_{pi}^T(t) P_i(\alpha_t) \dot{\bar{z}}_{pi}(t) + \sum_{k=1}^{M} \pi_{\alpha_t k} \bar{z}_{pi}^T(t) P_i(k) \bar{z}_{pi}(t) \\
&= 2\bar{z}_{pi}^T(t) P_i(\alpha_t)[A_{ic}^k(\alpha_t) \bar{z}_{pi}(t) + \sum_{j \in \wp_i(\alpha_t)} B_j K_{pj}(\alpha_t) \bar{z}_{pj}(t - \tau_{ji}(t))] \\
&\quad + \bar{z}_{pi}^T(t) \sum_{k=1}^{M} \pi_{\alpha_t k} P_i(k) \bar{z}_{pi}(t) + 2\bar{z}_{pi}^T(t) P_i(\alpha_t) B_{\lambda_i} \lambda_{pi}(t)
\end{aligned}
$$

$$
\begin{aligned}
\mathcal{L}V_{i2} &= \int_{t-h}^{t} 2\bar{z}_{pi}^T(s) S_i(\alpha_t) \dot{\bar{z}}_{pi}(s) ds + \int_{t-h}^{t} \bar{z}_{pi}^T(s) \sum_{k=1}^{M} \pi_{\alpha_t k} S_i(k) \bar{z}_{pi}(s) ds \\
&= \bar{z}_{pi}^T(t) S_i(\alpha_t) \bar{z}_{pi}(t) - (1-h) \bar{z}_{pi}^T(t-h) S_i(\alpha_t) \bar{z}_{pi}(t-h) \\
&\quad + \int_{t-h}^{t} \bar{z}_{pi}^T(s) \sum_{k=1}^{M} \pi_{\alpha_t k} S_i(k) \bar{z}_{pi}(s) ds
\end{aligned}
$$

$$
\begin{aligned}
\mathcal{L}V_{i3} &= h^2 \dot{\bar{z}}_{pi}^T(t) U_i \dot{\bar{z}}_{pi}(t) - h \int_{t-h}^{t} \dot{\bar{z}}_{pi}^T(s) U_i \dot{\bar{z}}_{pi}(s) ds \\
&= h^2 [A_{ic}^k(\alpha_t) \bar{z}_{pi}(t) + \sum_{j \in \wp_i(\alpha_t)} B_j K_{pj}(\alpha_t) \bar{z}_{pj}(t - \tau_{ji}(t)) + B_{\lambda_i} \lambda_{pi}(t)]^T U_i \\
&\quad [A_{ic}^k(\alpha_t) \bar{z}_{pi}(t) + \sum_{j \in \wp_i(\alpha_t)} B_j K_{pj}(\alpha_t) \bar{z}_{pj}(t - \tau_{ji}(t)) + B_{\lambda_i} \lambda_{pi}(t)] \\
&\quad - h \int_{t-h}^{t} \dot{\bar{z}}_{pi}^T(s) U_i \dot{\bar{z}}_{pi}(t) ds
\end{aligned}
$$

$$
\mathcal{L}V_{i4} = h \bar{z}_{pi}^T(t) S_i(\alpha_t) \bar{z}_{pi}(t) - \int_{t-h}^{t} \bar{z}_{pi}^T(s) \sum_{k=1}^{M} \pi_{\alpha_t k} S_i(k) \bar{z}_{pi}(s) ds
$$

Adding up the above equations, one will have

$$
\begin{aligned}
\mathcal{L}V_i &\leq \bar{z}_{pi}^T(t)(2P_i(\alpha_t) A_{ic}^k(\alpha_t) + \sum_{k=1}^{M} \pi_{\alpha_t k} P_i(k) + (1+h) S_i(\alpha_t)) \bar{z}_{pi}(t) \\
&\quad + h^2 \bar{z}_{pi}^T(t)((A_{ic}^k)^T(\alpha_t) U_i A_{ic}^k(\alpha_t) - U_i) \bar{z}_{pi}(t) \\
&\quad + 2\bar{z}_{pi}^T(t)(h^2 (A_{ic}^k(\alpha_t))^T U_i + P_i(\alpha_t)) \sum_{j \in \wp_i(\alpha_t)} B_j K_{pj}(\alpha_t) \bar{z}_{pj}(t - \tau_{ji}(t))
\end{aligned}
$$

264

$$+h^2(\sum_{j\in\wp_i(\alpha_t)} B_j K_{pj}(\alpha_t)\bar{z}_{pj}(t-\tau_{ji}(t)))^T U_i(\sum_{j\in\wp_i(\alpha_t)} B_j K_{pj}(\alpha_t)\bar{z}_{pj}(t-\tau_{ji}(t)))$$

$$+2\bar{z}_{pi}^T(t)U_i\bar{z}_{pi}(t-h) - \bar{z}_{pi}^T(t-h)(U_i+(1-h)S_i(\alpha_t))\bar{z}_{pi}(t-h)$$

$$+h^2(B_{\lambda_i}\lambda_{pi}(t))^T U_i(B_{\lambda_i}\lambda_{pi}(t)) + 2\bar{z}_{pi}^T(t)(h^2 A_{ic}^k(\alpha_t)U_i + P_i(\alpha_t))B_{\lambda_i}\lambda_{pi}(t)$$

$$+2h^2(\sum_{j\in\wp_i(\alpha_t)} B_j K_{pj}(\alpha_t)\bar{z}_{pi}(t-\tau_{ji}(t)))^T(B_{\lambda_i}\lambda_{pi}(t))$$

Let us define

$$B_{ji} = vec\{B_j\} \tag{6.23}$$

$$K_{ji}(\alpha_t) = diag\{K_{pj}(\alpha_t)\} \tag{6.24}$$

$$\bar{Z}_{pj}(t-\tau) = vec\{\bar{z}_{pj}^T(t-\tau_{ji}(t))\} \qquad i=1,...,n \ \ j\in\wp_i(\alpha_t) \tag{6.25}$$

then the following equation holds:

$$B_{ji}K_{ji}(\alpha_t)\bar{Z}_{pj}(t-\tau) = \sum_{j\in\wp_i(\alpha_t)} B_j K_{pj}(\alpha_t)\bar{z}_{pj}(t-\tau_{ji}(t)) \tag{6.26}$$

By substituting $B_{ji}K_{ji}(\alpha_t)\bar{Z}_{pj}(t-\tau)$ into $\mathcal{L}V_i$, one will get

$$\begin{aligned}
\mathcal{L}V_i \leq\ & \bar{z}_{pi}^T(t)(2P_i(\alpha_t)A_{ic}^k(\alpha_t) + \sum_{k=1}^M \pi_{\alpha_t l}P_i(k) + (1+h)S_i(\alpha_t))\bar{z}_{pi}(t)\\
&+h^2\bar{z}_{pi}^T(t)((A_{ic}^k)^T(\alpha_t)U_i A_{ic}^k(\alpha_t) - U_i + M_i(\alpha_t))\bar{z}_{pi}(t)\\
&+2\bar{z}_{pi}^T(t)(h^2(A_{ic}^k)^T(\alpha_t)U_i + P_i(\alpha_t))B_{ji}K_{ji}(\alpha_t)\bar{Z}_{pj}(t-\tau)\\
&+h^2(B_{ji}K_{ji}(\alpha_t)\bar{Z}_{pj}(t-\tau))^T(U_i+N_i(\alpha_t))(B_{ji}K_{ji}(\alpha_t)\bar{Z}_{pj}(t-\tau))\\
&+2\bar{z}_{pi}^T(t)U_i\bar{z}_{pi}(t-h) - \bar{z}_{pi}^T(t-h)(U_i+(1-h)S_i(rt))\bar{z}_{pi}(t-h)\\
&+h^2(B_{\lambda_i}\lambda_{pi}(t))^T U_i B_{\lambda_i}\lambda_{pi}(t) + (B_{\lambda_i}\lambda_{pi}(t))^T Y_i^T(\alpha_t)M_i^{-1}(\alpha_t)Y_i(\alpha_t)B_{\lambda_i}\lambda_{pi}(t)\\
&+h^2(B_{\lambda_i}\lambda_{pi}(t))^T N_i^{-1}(\alpha_t)B_{\lambda_i}\lambda_{pi}(t)\\
=\ & \bar{z}_{pi}^T(t)(2P_i(\alpha_t)A_{ic}^k(\alpha_t) + \sum_{k=1}^M \pi_{\alpha_t l}P_i(k) + (1+h)S_i(\alpha_t))\bar{z}_{pi}(t)\\
&+h^2\bar{z}_{pi}^T(t)((A_{ic}^k)^T(\alpha_t)U_i A_{ic}^k(\alpha_t) - U_i + M_i(\alpha_t))\bar{z}_{pi}(t)\\
&+2\bar{z}_{pi}^T(t)(h^2(A_{ic}^k)^T(\alpha_t)U_i + P_i(\alpha_t))B_{ji}K_{ji}(\alpha_t)\bar{Z}_{pj}(t-\tau)\\
&+h^2\bar{Z}_{pj}^T(t-\tau)K_{ji}^T(\alpha_t)B_{ji}^T(U_i+N_i(\alpha_t))B_{ji}K_{ji}(\alpha_t)\bar{Z}_{pj}(t-\tau)\\
&+2\bar{z}_{pi}^T(t)U_i\bar{z}_{pi}(t-h) - z_{t-h}^T(U_i+(1-h)S_i(\alpha_t))\bar{z}_{pi}(t-h)\\
&+\lambda_{pi}^T(t)B_{\lambda_i}^T(h^2 U_i + Y_i^T(\alpha_t)M_i^{-1}(\alpha_t)Y_i(\alpha_t) + h^2 N_i^{-1}(\alpha_t))B_{\lambda_i}\lambda_{pi}(t)
\end{aligned}$$

$$
\begin{aligned}
&= \begin{bmatrix} \bar{z}_{pi}^T(t) \\ \bar{Z}_{pj}^T(t-\tau) \\ \bar{z}_{pi}^T(t-h) \end{bmatrix}^T \begin{bmatrix} w_{ik}^1(\alpha_t) & w_{ik}^2(\alpha_t) & U_i \\ * & w_i^3(\alpha_t) & 0 \\ * & * & -U_i - (1-h)S_i(\alpha_t) \end{bmatrix} \begin{bmatrix} \bar{z}_{pi}(t) \\ \bar{Z}_{pj}(t-\tau) \\ \bar{z}_{pi}(t-h) \end{bmatrix} \\
&\quad + \lambda_{pi}^T(t)\Psi_i(\alpha_t)\lambda_{pi}(t) \\
&= \eta_i^T(t,\tau,h)W_{ik}(\alpha_t)\eta_i(t,\tau,h) + \lambda_{pi}^T(t)\Psi_i(\alpha_t)\lambda_{pi}(t) \qquad (6.27)
\end{aligned}
$$

where $\eta_i(t,\tau,h) = [\bar{z}_{pi}^T(t)\ \bar{Z}_{pj}^T(t-\tau)\ \bar{z}_{pi}^T(t-h)]^T$, M_i and N_i are positive definite matrices, and $Y_i(\alpha_t) = h^2 A_{ic}^k(\alpha_t)U_i + P_i(\alpha_t))$. The matrices W_{ik} and Ψ_i are defined as

$$
W_{ik}(\alpha_t) = \begin{bmatrix} w_{ik}^1(\alpha_t) & w_{ik}^2(\alpha_t) & U_i \\ * & w_i^3(\alpha_t) & 0 \\ * & * & -U_i - (1-h)S_i(\alpha_t) \end{bmatrix} \qquad (6.28)
$$

$$
\Psi_i(\alpha_t) = B_{\lambda_i}^T(h^2 U_i + Y_i^T(\alpha_t)M_i^{-1}(\alpha_t)Y_i(\alpha_t) + h^2 N_i^{-1}(\alpha_t))B_{\lambda_i}
$$

$$
w_{ik}^1(\alpha_t) = (2P_i(\alpha_t) + h^2(A_{ic}^k)^T(\alpha_t)U_i)A_{ic}^k(\alpha_t) + \sum_{l=1}^{M}\pi_{\alpha_t l}P_i(l) + (1+h)S_i(\alpha_t) - U_i + M_i(\alpha_t)
$$

$$
w_{ik}^2(\alpha_t) = (h^2(A_{ic}^k)^T(\alpha_t)U_i + P_i(\alpha_t))B_{ji}K_{ji}(\alpha_t)
$$

$$
w_i^3(\alpha_t) = h^2 K_{ji}^T(\alpha_t)B_{ji}^T(U_i + N_i(\alpha_t))B_{ji}K_{ji}(\alpha_t)
$$

Comparing the matrices $W_{ik}(\alpha_t)$ and $\bar{W}_{ik}(\alpha_t)$, one can see that:

$$
W_{ik}(\alpha_t) = \bar{W}_{ik}(\alpha_t) - Q_i(\alpha_t) - K_{pi}^T(\alpha_t)R_i(\alpha_t)K_{pi}(\alpha_t)
$$

Since $\bar{W}_{ik}(\alpha_t) < 0$, one gets:

$$
\begin{aligned}
\mathcal{L}V_i &\leq \eta_i^T(t,\tau,h)[\bar{W}_{ik}(\alpha_t) - Q_i(\alpha_t) - K_{pi}^T(\alpha_t)R_i(\alpha_t)K_{pi}(\alpha_t)]\eta_i(t,\tau,h) \\
&\quad + \lambda_{pi}^T(t)\Psi_i(\alpha_t)\lambda_{pi}(t) \\
&\leq -\bar{z}_{pi}^T(t)(Q_i(\alpha_t) + K_{pi}^T(\alpha_t)R_i(\alpha_t)K_{pi}(\alpha_t))\bar{z}_{pi}(t) + \lambda_{pi}^T(t)\Psi_i(\alpha_t)\lambda_{pi}(t) \quad (6.29)
\end{aligned}
$$

Therefore, for any $\bar{z}_{pi}(t)$ that satisfies:

$$
\bar{z}_{pi}^T(t)(Q_i(\alpha_t) + K_{pi}^T(\alpha_t)R_i(\alpha_t)K_{pi}(\alpha_t))\bar{z}_{pi}(t) \geq \lambda_{pi}^T(t)\Psi_i(\alpha_t)\lambda_{pi}(t) \qquad (6.30)
$$

we will have $\mathcal{L}V_i < 0$. Therefore, according to the Definition 6.1, the system (6.14) is stochastically ultimately bounded and the radius of the ultimate bound region is given by:

$$
\frac{max\{\Psi_i(\alpha_t)\}}{\lambda_{min}(Q_i(\alpha_t) + K_{pi}^T(\alpha_t)R_i(\alpha_t)K_{pi}(\alpha_t))}\|\lambda_{pi}^{max}\|^2 \qquad (6.31)
$$

Furthermore, from (6.29) we have

$$
\begin{aligned}
J_{pi} &= E\{\int_0^\infty (\bar{z}_{pi}^T(t)Q_i(\alpha_t)\bar{z}_{pi}(t) + \bar{u}_{pi}^T(t)R_i(\alpha_t)\bar{u}_{pi})dt\} \\
&= E\{\int_0^\infty (\bar{z}_{pi}^T(t)[Q_i(\alpha_t) + K_{pi}^T(\alpha_t)R_i(\alpha_t)K_{pi}(\alpha_t)]\bar{z}_{pi}(t)dt\} \\
&\leq E\{\int_0^\infty (-\mathcal{L}V_i + \lambda_{pi}^T(t)\Psi_i(\alpha_t)\lambda_{pi}(t))dt\} \\
&= V_i(\bar{z}_{pi}(0),0,r_0) - \lim_{t\to\infty} V_i(\bar{z}_{pi}(t),t,\alpha_t) + E\{\int_0^\infty \Psi_i(\alpha_t)\lambda_{pi}^2(t)dt\} \\
&\leq V_i(\bar{z}_{pi}(0),0,r_0) - \bar{z}_{pi}^T(\infty)P_i(r_\infty)\bar{z}_{pi}(\infty) + \gamma_i max(\Psi_i(\alpha_t)) \qquad (6.32)
\end{aligned}
$$

According to the ultimate bounded region that is given by (6.31), we have

$$
0 \leq \|\bar{z}_{pi}(\infty)\|^2 \leq \frac{max\{\Psi_i(\alpha_t)\}}{\lambda_{min}(Q_i(\alpha_t) + K_i^T(\alpha_t)R_i(\alpha_t)K_i(\alpha_t))}(\lambda_{pi}^{max})^2 \qquad (6.33)
$$

so that the upper bound of the cost function J_{pi} is obtained as follows:

$$
J_{pi} < V_i(\bar{z}_{pi}(0),0,r_0) + \gamma_i max(\Psi_i(\alpha_t)) = J_{pi}^* \qquad (6.34)
$$

Therefore, the system (6.14) is robust with respect to any admissible time-varying delays that satisfy Assumption 6.1. The degradation of the closed-loop system performance incurred by delays is guaranteed to be less than the scalar J_{pi}^*. According to the Definition 6.1, the stochastic state feedback controller $\bar{u}_{pi}(t) = K_{pi}(\alpha_t)\bar{z}_{pi}(t)$ is the stochastic guaranteed cost controller of the system (6.14) and the scalar J_{pi}^* is the stochastic guaranteed cost of the system (6.14). This completes the proof of Lemma 6.1. ∎

Lemma 6.1 shows that the decentralized controller $\bar{u}_{pi}(t) = K_{pi}(\alpha_t)\bar{z}_{pi}(t)$ is a stochastic guaranteed cost controller for the hybrid time-delay system (6.14). The stability conditions (6.18) are dependent on the Markov chain α_t. That is, at each time when the network topology is changed, one needs to check the corresponding matrix inequality conditions again. However, the matrix inequality conditions in Lemma 6.1 is not linear with respect to the control gains K_{pi}, δ_{pi} and β_{pi}, hence can not be solved directly. Moreover, in order to solve the conditions in Lemma 6.1, one needs to known the control gains of neighboring nodes K_{pj} which are not available for the decentralized controller of node i. The following lemma is presented to tackle this problem.

Lemma 6.2. *Given the cost function (6.17) and under Assumption 5.2, if there exist symmetric positive definite matrices $\Lambda_{i1}^T(\alpha_t)$, $\bar{X}_{ik}(\alpha_t)$, $\bar{V}_{ii}(\alpha_t)$, $\bar{T}_i(\alpha_t)$, and matrices U_i, $N_i(\alpha_t)$, Λ_{i3}^T, and $\bar{S}_i(\alpha_t)$ for $k = 1, 2$, $i = 1, ...n$, and $\alpha_t \in \mathcal{S} = \{1, \ldots, M\}$ such that the following LMI conditions are satisfied:*

$$
\Omega_{ik}(\alpha_t) = \begin{bmatrix} \bar{X}_{ik}(\alpha_t) & h^2(\bar{V}_{ik}^T(\alpha_t) + \bar{T}_i(\alpha_t))B_{ji} + B_{ji} & \Lambda_{i1}^T(\alpha_t) \\ * & h^2 B_{ji}^T(U_i + N_i(\alpha_t))B_{ji} & 0 \\ * & * & -\Lambda_{i3}^T - (1-h)\bar{S}_i(\alpha_t) \end{bmatrix} < 0 \quad (6.35)
$$

then the controller $\bar{u}_{pi}(t) = K_{pi}(\alpha_t)\bar{z}_{pi}(t)$ is the stochastic guaranteed cost controller of system (6.14), and the decentralized control gain is given by $K_{pi}(\alpha_t) = B_{i0}^+ T_i(\alpha_t)\Lambda_{i1}^{-1}(\alpha_t)$.

Proof: Based on the matrix inequality conditions in Lemma 6.1, the objective is derive the control gains $K_{pi}(\alpha_t)$, and the adaptive control parameters $\delta_{pi}(\alpha_t)$, and $\beta_{pi}(\alpha_t)$. The adaptive control parameters are embedded in the closed-loop system matrices $A_{i0}^k(\alpha_t)$. To transform the nonlinear matrix inequality conditions into an equivalent linear one, the following matrices are defined:

$$\Lambda_{i1}(\alpha_t) = P_i^{-1}(\alpha_t) \qquad \Lambda_{i2}(\alpha_t) = K_{ji}^{-1}(\alpha_t)$$

$$\Lambda_{i3} = U_i^{-1} \qquad \Lambda_i(\alpha_t) = diag\{\Lambda_{i1}(\alpha_t), \Lambda_{i2}(\alpha_t), \Lambda_{i3}\}$$

By pre and post multiplying the matrix $\bar{W}_{ik}(\alpha_t)$ with Λ_i^T and Λ_i, respectively, the following matrix can be obtained:

$$
\begin{aligned}
\Omega_{ik}(\alpha_t) &= \Lambda_i^T(\alpha_t)\bar{W}_{ik}(\alpha_t)\Lambda_i(\alpha_t) \\
&= \begin{bmatrix} \Lambda_{i1}^T(\alpha_t)X_{ik}(\alpha_t)\Lambda_{i1}(\alpha_t) & h^2\Lambda_{i1}^T(\alpha_t)(A_{ic}^k)^T(\alpha_t)U_iB_{ji} + B_{ji} & \Lambda_{i1}^T(\alpha_t) \\ * & h^2 B_{ji}^T(U_i + N_i(\alpha_t))B_{ji} & 0 \\ * & * & -\Lambda_{i3}^T - (1-h)\Lambda_{i3}^T S_i(\alpha_t)\Lambda_{i3} \end{bmatrix}
\end{aligned}
$$

Let us define

$$A_{i0}^k(\alpha_t) = V_{ik}(\alpha_t)\Lambda_{i1}^{-1}(\alpha_t) \qquad \bar{V}_{ik}^T = V_{ik}^T U_i$$

$$B_{i0}K_{pi}(\alpha_t) = T_i\Lambda_{i1}^{-1}(\alpha_t) \qquad \bar{T}_i = T_i^T U_i$$

$$S_i(\alpha_t) = P_i(\alpha_t) \qquad M_i(\alpha_t) = U_i$$

$$\bar{U}_i(\alpha_t) = V_{ik}^T(\alpha_t)U_i V_{ik}(\alpha_t) \qquad \bar{S}_i(\alpha_t) = \Lambda_{i3}^T S_i\Lambda_{i3}^T$$

$$\bar{Q}_i(\alpha_t) = \Lambda_{i1}^T(\alpha_t)Q_i(\alpha_t)\Lambda_{i1}(\alpha_t) \qquad \bar{R}_i(\alpha_t) = \Lambda_{i1}^T(\alpha_t)K_{pi}^T(\alpha_t)R_i(\alpha_t)K_{pi}(\alpha_t)\Lambda_{i1}(\alpha_t)$$

268

Then, the matrix $\Omega_{ik}(\alpha_t)$ will become

$$\Omega_{ik}(\alpha_t) = \begin{bmatrix} \bar{X}_{ik}(\alpha_t) & h^2(\bar{V}_{ik}^T + \bar{T}_i)B_{ji} + B_{ji} & \Lambda_{i1}^T(\alpha_t) \\ * & h^2 B_{ji}^T(U_i + N_i(\alpha_t))B_{ji} & 0 \\ * & * & -\Lambda_{i3}^T - (1-h)\bar{S}_i(\alpha_t) \end{bmatrix} \quad (6.36)$$

where $\bar{X}_{ik}(\alpha_t) = V_{ik}(\alpha_t) + V_{ik}^T(\alpha_t) + T_i + T_i^T + h^2\bar{U}_i(\alpha_t) + (1 + h + \sum_{l=1}^{M} \pi_{\alpha_t l})\Lambda_{i1}^T(\alpha_t) + \bar{Q}_i(\alpha_t) + \bar{R}_i(\alpha_t)$. Therefore, if $\Omega_{ik}(\alpha_t) < 0$, one will also have $\bar{W}_{ik} < 0$. Then, by solving the LMI conditions $\Omega_{ik}(\alpha_t) < 0$, one can obtain the control gain $K_{pi}(\alpha_t)$ as well as the system matrices as follows:

$$K_{pi}(\alpha_t) = B_{i0}^+ T_i(\alpha_t)\Lambda_{i1}^{-1}(\alpha_t) \quad (6.37)$$

$$A_{i0}^k(\alpha_t) = V_{ik}(\alpha_t)\Lambda_{i1}^{-1}(\alpha_t) \quad (6.38)$$

This completes the proof of Lemma 6.2. ∎

6.2.2 Stability Conditions Incorporating the Physical Constraints

The LMI conditions associated with the physical constraints of the guaranteed cost congestion controller (GCC) of fixed network, as given in Section 5.2.2, are now extended to mobile networks.

Constraints of the state

As given in (6.15), the constraints of the states for the system (6.14) can be expressed as follows:

$$\bar{z}_{pi}^{min} \leq \bar{z}_{pi}(t) \leq \bar{z}_{pi}^{max} \quad (6.39)$$

where $\bar{z}_{pi}^{min} = [-x_{pi}^{ref} \ 0]^T$ denotes the minimum value of the new state, and $\bar{z}_{pi}^{max} = [x_{pi}^{buffer} - x_{pi}^{ref}, \lambda_{pi}^{max}]^T$ denotes the maximum bound of the new state.

By squaring (6.39) one will have

$$\bar{z}_{pi}^T(t)\bar{z}_{pi}(t) \leq \|\bar{z}_{pi}^{max}\|^2 \quad (6.40)$$

269

Consider the following ellipsoid for a selected number $\epsilon_{1i} > 0$,

$$\mathbb{F}_i(\alpha_t) = \{\bar{z}_{pi}(t) | \bar{z}_{pi}^T \Lambda_{i1}^{-1}(\alpha_t) \bar{z}_{pi} \leq \epsilon_{1i}\} \tag{6.41}$$

According to the definitions of the Lyapunov functional V_i in (6.18), since $\Lambda_{i1}^{-1}(\alpha_t) = P_i(\alpha_t)$, we have

$$\bar{z}_{pi}(t) | \bar{z}_{pi}^T \Lambda_{i1}^{-1}(\alpha_t) \bar{z}_{pi} \leq V_i(\bar{z}_{pi}(t), \alpha_t) \tag{6.42}$$

By integrating (6.29), from 0 to t and considering that $V_i(\bar{z}_{pi}(0), r_0) = 0$, we have

$$
\begin{aligned}
V_i \quad &\leq \quad -\int_0^t \bar{z}_{pi}^T(t)(Q_i(\alpha_t) + K_{pi}^T(\alpha_t)R_i(\alpha_t)K_{pi}(\alpha_t))\bar{z}_{pi}(t)dt + \int_0^t \lambda_{pi}^T(t)\Psi_i(\alpha_t)\lambda_{pi}(t)dt \\
&< \quad \int_0^t \lambda_{pi}^T(t)\Psi_i(\alpha_t)\lambda_{pi}(t)dt \\
&< \quad \int_0^\infty \lambda_{pi}^T(t)\Psi_i(\alpha_t)\lambda_{pi}(t)dt \\
&< \quad \gamma_i max(\Psi_i(\alpha_t)) \tag{6.43}
\end{aligned}
$$

Therefore, the state $\bar{z}_{pi}(t)$ will belong to the set $\mathbb{F}_i(\alpha_t)$ for all the modes α_t if

$$\gamma_i max(\Psi_i(\alpha_t)) \leq \epsilon_{1i} \tag{6.44}$$

Consequently, the right hand side of the state constraint (6.39) is satisfied if

$$\epsilon_{1i}/(\bar{z}_{pi}^{max})^2 \leq \Lambda_{i1}^{-1}(\alpha_t) \tag{6.45}$$

By applying the Schur complement to (6.45), the right hand side of the state constraint (6.39) will hold if the following LMI conditions are satisfied:

$$\Omega_{c1i}^p(\alpha_t) \triangleq \gamma_i max\{\Psi_i(\alpha_t)\} \leq \epsilon_{1i} \tag{6.46}$$

$$\Omega 6p_{c2i}(\alpha_t) \triangleq \begin{bmatrix} \Lambda_{i1}(\alpha_t) & \Lambda_{i1}^T(\alpha_t) \\ \Lambda_{i1}(\alpha_t) & \|\bar{z}_{pi}^{max}\|^2/\epsilon_{1i} \end{bmatrix} \geq 0 \tag{6.47}$$

On the other hand, the left hand side of the state constraint (6.39) can be rewritten as

$$\bar{z}_{pi}(t) - \bar{z}_{pi}^{min} \geq 0 \tag{6.48}$$

Therefore, according to the definition of non-negative system (5.1), by selecting the matrix $\Lambda_{i1}(\alpha_t)$ as a diagonal positive definite matrix and following along the similar lines

as those given previously in Section 5.2.2, the left hand side of the state constraint can be expressed as

$$\Omega_{c3i}^{p}(\alpha_t) \triangleq (T_i(\alpha_t))_{ij} \geq 0 \tag{6.49}$$

$$V_{ik}(\alpha_t) = \begin{bmatrix} V_{ik}^{1}(\alpha_t) & V_{ik}^{2}(\alpha_t) \\ V_{ik}^{3}(\alpha_t) & V_{ik}^{4}(\alpha_t) \end{bmatrix}$$

$$V_{i1}^{1}(\alpha_t) = V_{i2}^{1}(\alpha_t) = 0$$

$$V_{i1}^{2}(\alpha_t) = V_{i2}^{2}(\alpha_t) = 0$$

$$V_{i2}^{3}(\alpha_t) = 0$$

$$V_{i1}^{3}(\alpha_t) > 0 \text{ and is diagonal}$$

$$V_{i1}^{4}(\alpha_t) = V_{i2}^{4}(\alpha_t) < 0 \text{ and is diagonal}$$

Constraint of the input

The input constraint of the system (6.14) can be defined as follows:

$$0 \leq \bar{u}_{pi}(t) \leq C_{server,i}(\alpha_t) \tag{6.50}$$

Using (6.37), the decentralized congestion controller $\bar{u}_{pi}(t)$ can be written as

$$\bar{u}_{pi}(t) = B_{i0}^{+}T_i(\alpha_t)\Lambda_{i1}^{-1}(\alpha_t)\bar{z}_{pi}(t) \tag{6.51}$$

Therefore, the input constraint (6.50) becomes

$$0 \leq B_{i0}^{+}T_i(\alpha_t)\Lambda_{i1}^{-1}(\alpha_t)\bar{z}_{pi}(t) \leq C_{server,i}(\alpha_t) \tag{6.52}$$

Consider the ellipsoid (6.41), so that the right hand side of the input constraint will be satisfied if

$$(B_{i0}^{+}T_i(\alpha_t)\Lambda_{i1}^{-1}(\alpha_t))^{T}(\epsilon_{i1}/C_{server,i}^{2}(\alpha_t))B_{i0}^{+}T_i(\alpha_t)\Lambda_{i1}^{-1}(\alpha_t) \leq \Lambda_{i1}^{-1}(\alpha_t) \tag{6.53}$$

The above condition can be transformed into the following LMI condition:

$$\Omega_{c4i}^{p}(\alpha_t) \triangleq \begin{bmatrix} I & K_i^{T}(\alpha_t) \\ K_i(\alpha_t) & (C_{server,i}^{2}(\alpha_t)/\epsilon_{1i})\Lambda_{i1}(\alpha_t) \end{bmatrix} \geq 0 \tag{6.54}$$

271

The non-negative constraint of the input will be satisfied if the control gain $(K_{pi}(\alpha_t))_{ij} > 0$. Hence, by using $K_{pi}(\alpha_t) = B_{i0}^+ T_i(\alpha_t) \Lambda_{i1}^{-1}(\alpha_t)$ and noting that $\Lambda_{i1}^{-1}(\alpha_t)$ is set to be a diagonal positive definite matrix, then B_{i0} is negative definite. The left hand side of the input constraint can be transformed into the following LMI condition:

$$\Omega_{c5i}^p(\alpha_t) \quad \triangleq \quad (T_i(\alpha_t))_{ij} \le 0 \tag{6.55}$$

Therefore, the above results, as well as the LMI conditions that are given in Lemma 6.2 can be summarized into the following theorem.

Theorem 6.1. *The decentralized Markovian jump guaranteed cost congestion controller (MJ-GCC) for the premium traffic in a mobile network is determined by $\bar{u}_{pi} = K_{pi}(\alpha_t)\bar{z}_{pi}$, if the mode-dependent LMI conditions given in Lemma 6.2 subject to the positive definite diagonal matrix $\Lambda_{i1}^{-1}(\alpha_t)$ and the mode-dependent LMI conditions of $\Omega_{c1i}^p(\alpha_t)$, $\Omega_{c2i}^p(\alpha_t)$, $\Omega_{c3i}^p(\alpha_t)$, $\Omega_{c4i}^p(\alpha_t)$, and $\Omega_{c5i}^p(\alpha_t)$ for $i = 1, ...n$, $\alpha_t \in S = \{1, ..., M\}$, as given in (6.46), (6.48), (6.49), (6.54), and (6.55), respectively, are all satisfied.*

Proof: Follows along the same line as the derivations in Lemma 6.1, Lemma 6.2, and the above analysis for the physical constraints. ∎

6.2.3 Ordinary Traffic Control

The decentralized dynamic queuing model of the ordinary traffic in the mobile network is re-written here again for convenience:

$$\dot{x}_{ri}(t) = -f(x_{ri}(t))u_{ri}^1(t) + u_{ri}^2(t) + \sum_{j \in \wp_i(\alpha_t)} f(x_{rj}(t - \tau_{ji}(t)))u_{rj}^1(t - \tau_{ji})g_r^{ji}(t) \tag{6.56}$$

where $x_{ri}(t)$ is the ordinary queuing length of node i, u_{ri}^1 is the bandwidth controller, $u_{ri}^2(t)$ is the flow rate controller, g_{ji}^r is the traffic compression gains for the ordinary traffic, and $\wp_{ri}(\alpha_t)$ is the neighboring set of node i subject to the mode α_t.

Regarding the nonlinear dynamic system (6.56), we first apply the following feedback

linearization scheme by proposing the new state and input signal:

$$z_{ri}(t) = x_{ri}(t) - x_{ri}^{ref} \tag{6.57}$$

$$u_{ri}(t) = F^{-1}(x_{ri}, t)\bar{u}_{ri}(t) \tag{6.58}$$

$$F(x_{ri}(t)) = \begin{bmatrix} f(x_{ri}(t)) & 0 \\ 0 & 1 \end{bmatrix} \tag{6.59}$$

where $u_{ri}(t) = vec\{u_{ri}^1(t), u_{ri}^2(t)\}$ and $\bar{u}_{ri}(t) = vec\{\bar{u}_{ri}^1(t), \bar{u}_{ri}^2(t)\}$. Therefore, the dynamic queuing system (6.56) can be re-written into the following Markovian jump linear system with time-delay:

$$\dot{z}_{ri}(t) = B_{i0}\bar{u}_{ri}(t) + \sum_{j \in \wp_i(\alpha_t)} B_j \bar{u}_{rj}(t - \tau_{ji}(t)) \tag{6.60}$$

where $B_{i0} \in R^{1\times 2}$ and $B_j \in R^{1\times 2}$ are the system matrices defined for node i. In fact, B_{i0} is equal to $\begin{bmatrix} -1 & 1 \end{bmatrix}$, and B_j denotes the compression rates between node i and its neighboring nodes and is actually equal to $\begin{bmatrix} g_r^{ji} & 0 \end{bmatrix}$.

Physical Constraints

The physical constraints of the transformed system (6.60) are listed below:

$$z_{ri}^{min} \leq z_{ri}(t) \leq z_{ri}^{max} \tag{6.61}$$

$$0 \leq \bar{u}_{ri} \leq c_{ri}(\alpha_t) \tag{6.62}$$

$$c_{ri}(\alpha_t) = C_{server,i}(\alpha_t) - \bar{u}_{pi}(\alpha_t) \tag{6.63}$$

where $z_{ri}^{min} = -x_{ri}^{ref}$ is the minimum bound of the state, $z_{ri}^{max} = x_{ri}^{buffer} - x_{ri}^{ref}$ is the maximum bound of the state, and $c_{ri}(\alpha_t)$ is the maximum bound of input which is actually the leftover capacity from the premium traffic and is dependent on the Markov chain α_t.

Performance Cost Function

The performance cost function for the ordinary traffic in a mobile network is given by the following jump quadratic cost function:

$$J_{ri} = E\{\int_0^\infty (z_{ri}^T(t)Q_i(\alpha_t)z_{ri}(t) + \bar{u}_{ri}^T(t)R_i(\alpha_t)\bar{u}_{ri}(t))dt\} \tag{6.64}$$

273

where Q_i and R_i are given positive definite matrices.

The congestion control problem of the ordinary traffic is to select the stochastic state feedback controller $\bar{u}_{ri}(t) = K_{ri}(\alpha_t)z_{ri}(t)$ so that the system (6.60) is stable and the upper bound of the jump quadratic cost function (6.64) is guaranteed. The following lemma is then stated to show that the decentralized controller $\bar{u}_{ri}(t) = K_{ri}(\alpha_t)z_{ri}(t)$ is a stochastic guaranteed cost congestion controller for the system (6.60) and the queuing errors of the premium traffic at each node is guaranteed to be bounded.

Lemma 6.3. *Given the cost function (6.64) and under Assumption 5.2, the state feedback control law $\bar{u}_{ri}(t) = K_{ri}(\alpha_t)z_{ri}(t)$ is the stochastic guaranteed cost controller for the system (6.60), if there exist symmetric positive definite matrices $P_i(\alpha_t)$, $S_i(\alpha_t)$, U_i, positive definite matrices $Q_i(\alpha_t)$, and $R_i(\alpha_t)$, for $i = 1, ..., n$, $\alpha_t \in \mathcal{S} = \{1, ...M\}$, such that the following LMI condition holds*

$$\bar{W}_i(\alpha_t) = \begin{bmatrix} w_i^1(\alpha_t) & w_i^2(\alpha_t) & U_i \\ * & w_i^3(\alpha_t) & 0 \\ * & * & -U_i - (1-h)S_i(\alpha_t) \end{bmatrix}$$

where:

$$\begin{aligned} w_i^1(\alpha_t) &= (2P_i(\alpha_t) + h^2(B_{i0}K_{ri})^T(\alpha_t)U_i)B_{i0}K_{ri}(\alpha_t) + \sum_{l=1}^{M}\pi_{\alpha_t l}P_i(l) + (1+h)S_i(\alpha_t) \\ &\quad -U_i + Q_i(\alpha_t) + K_{ri}^T(\alpha_t)R_i(\alpha_t)K_{ri}(\alpha_t) \\ w_i^2(\alpha_t) &= (h^2(B_{i0}K_{ri})^T(\alpha_t)U_i + P_i(\alpha_t))B_{ji}K_{ji}(\alpha_t) \\ w_i^3(\alpha_t) &= h^2 K_{ji}^T(\alpha_t)B_{ji}^T U_i B_{ji}K_{ji}(\alpha_t) \end{aligned}$$

Proof: Consider the following stochastic Lyapunov-Krasovskii functional candidate:

$$V_i(z_{ri}(t), \alpha_t) = V_{i1} + V_{i2} + V_{i3} + V_{i4}$$

$$V_{i1} = z_{ri}(t)^T P_i(\alpha_t)z_{ri}(t)$$

$$V_{i2} = \int_{t-h}^{t} z_{ri}^T(s)S_i(\alpha_t)z_{ri}(s)ds$$

$$V_{i3} = h\int_{-h}^{0}\int_{t+\theta}^{t} \dot{z}_{ri}^T(s)U_i\dot{z}_{ri}(s)dsd\theta$$

$$V_{i4} = \int_{-h}^{0}\int_{t+\theta}^{t} z_{ri}^T(s)S_i(\alpha_t)z_{ri}(s)dsd\theta$$

274

with $P_i(\alpha_t)$, $S_i(\alpha_t)$, U_i are positive definite matrices with appropriate dimensions. Let $\mathcal{L}$ be the infinitesimal generator of $\{z_{ri}(t), \alpha_t\}$, $t \geq 0$. Then, for each $\alpha_t = k \in \mathcal{S}$ we have

$$
\begin{aligned}
\mathcal{L}V_{i1} &= \lim_{\Delta \to 0^+} \frac{1}{\Delta} \{ E[V_{i1}(z_{ri}(t+\Delta), \alpha_{t+\delta}, t+\Delta)|z_{ri}(t), \alpha_t = k] - V_{i1}(z_{ri}(t), k, t) \} \\
&= 2z_{ri}^T(t)P_i(\alpha_t)\dot{z}_{ri}(t) + \sum_{k=1}^{M} \pi_{\alpha_t k} z_{ri}^T(t) P_i(k) z_{ri}(t) \\
&= 2z_{ri}^T(t)P_i(\alpha_t)[B_{i0}K_{ri}(\alpha_t)z_{ri}(t) + \sum_{j \in \wp_i(\alpha_t)} B_j K_{rj}(\alpha_t) z_{rj}(t - \tau_{ji}(t))] \\
&\quad + z_{ri}^T(t) \sum_{k=1}^{M} \pi_{\alpha_t k} P_i(k) z_{ri}(t)
\end{aligned}
$$

$$
\begin{aligned}
\mathcal{L}V_{i2} &= \int_{t-h}^{t} 2z_{ri}^T(s)S_i(\alpha_t)\dot{z}_{ri}(s)ds + \int_{t-h}^{t} z_{ri}^T(s) \sum_{k=1}^{M} \pi_{\alpha_t k} S_i(k) z_{ri}(s)ds \\
&= z_{ri}^T(t)S_i(\alpha_t)z_{ri}(t) - (1-h)z_{ri}^T(t-h)S_i(\alpha_t)z_{ri}(t-h) \\
&\quad + \int_{t-h}^{t} z_{ri}^T(s) \sum_{k=1}^{M} \pi_{\alpha_t k} S_i(k) z_{ri}(s)ds
\end{aligned}
$$

$$
\begin{aligned}
\mathcal{L}V_{i3} &= h^2 \dot{z}_{ri}^T(t)U_i\dot{z}_{ri}(t) - h\int_{t-h}^{t} \dot{z}_{ri}^T(s)U_i\dot{z}_{ri}(s)ds \\
&= h^2[B_{i0}K_{ri}(\alpha_t)z_{ri}(t) + \sum_{j \in \wp_i(\alpha_t)} B_j K_{rj}(\alpha_t)z_{rj}(t - \tau_{ji}(t))]^T U_i \\
&\quad [B_{i0}K_{ri}(\alpha_t)z_{ri}(t) + \sum_{j \in \wp_i(\alpha_t)} B_j K_{rj}(\alpha_t)z_{rj}(t - \tau_{ji}(t))] \\
&\quad - h\int_{t-h}^{t} \dot{z}_{ri}^T(s)U_i\dot{z}_{ri}(t)ds
\end{aligned}
$$

$$
\mathcal{L}V_{i4} = hz_{ri}^T(t)S_i(\alpha_t)z_{ri}(t) - \int_{t-h}^{t} z_{ri}^T(s) \sum_{k=1}^{M} \pi_{\alpha_t k} S_i(k) z_{ri}(s)ds
$$

By adding up the above equations, we will have

$$
\begin{aligned}
\mathcal{L}V_i &\leq z_{ri}^T(t)(2P_i(\alpha_t)B_{i0}K_{ri}(\alpha_t) + \sum_{k=1}^{M} \pi_{\alpha_t k} P_i(k) + (1+h)S_i(\alpha_t))z_{ri}(t) \\
&\quad + h^2 z_{ri}^T(t)((B_{i0}K_{ri})^T(\alpha_t)U_i B_{i0}K_{ri}(\alpha_t) - U_i)z_{ri}(t) \\
&\quad + 2z_{ri}^T(t)(h^2(B_{i0}K_{ri}(\alpha_t))^T U_i + P_i(\alpha_t)) \sum_{j \in \wp_i(\alpha_t)} B_j K_{rj}(\alpha_t)z_{rj}(t - \tau_{ji}(t)) \\
&\quad + h^2(\sum_{j \in \wp_i(\alpha_t)} B_j K_{rj}(\alpha_t)z_{rj}(t - \tau_{ji}(t)))^T U_i(\sum_{j \in \wp_i(\alpha_t)} B_j K_{rj}(\alpha_t)z_{rj}(t - \tau_{ji}(t))) \\
&\quad + 2z_{ri}^T(t)U_i z_{ri}(t-h) - z_{ri}^T(t-h)(U_i + (1-h)S_i(\alpha_t))z_{ri}(t-h)
\end{aligned}
$$

By defining that:

$$B_{ji} = vec\{B_j\}$$

$$K_{ji}(\alpha_t) = diag\{K_{rj}(\alpha_t)\}$$

$$Z_{rj}(t-\tau) = vec\{z_{rj}^T(t-\tau_{ji}(t))\}$$

we will have

$$
\begin{aligned}
\mathcal{L}V_i \;\leq\; & z_{ri}^T(t)(2P_i(\alpha_t)B_{i0}K_{ri}(\alpha_t) + \sum_{k=1}^{M}\pi_{\alpha_t l}P_i(k) + (1+h)S_i(\alpha_t))z_{ri}(t) \\
& + h^2 z_{ri}^T(t)((B_{i0}K_{ri})^T(\alpha_t)U_i B_{i0}K_{ri}(\alpha_t) - U_i)z_{ri}(t) \\
& + 2z_{ri}^T(t)(h^2(B_{i0}K_{ri})^T(\alpha_t)U_i + P_i(\alpha_t))B_{ji}K_{ji}(\alpha_t)z_{rj}(t-\tau) \\
& + h^2(B_{ji}K_{ji}(\alpha_t)z_{rj}(t-\tau))^T U_i(B_{ji}K_{ji}(\alpha_t)z_{rj}(t-\tau)) \\
& + 2z_{ri}^T(t)U_i z_{ri}(t-h) - z_{ri}^T(t-h)(U_i + (1-h)S_i(rt))z_{ri}(t-h) \\
=\; & z_{ri}^T(t)(2P_i(\alpha_t)B_{i0}K_{ri}(\alpha_t) + \sum_{k=1}^{M}\pi_{\alpha_t l}P_i(k) + (1+h)S_i(\alpha_t))z_{ri}(t) \\
& + h^2 z_{ri}^T(t)((B_{i0}K_{ri})^T(\alpha_t)U_i B_{i0}K_{ri}(\alpha_t) - U_i)z_{ri}(t) \\
& + 2z_{ri}^T(t)(h^2(B_{i0}K_{ri})^T(\alpha_t)U_i + P_i(\alpha_t))B_{ji}K_{ji}(\alpha_t)z_{rj}(t-\tau) \\
& + h^2 \bar{Z}_{pj}^T(t-\tau)K_{ji}^T(\alpha_t)B_{ji}^T U_i B_{ji}K_{ji}(\alpha_t)z_{rj}(t-\tau) \\
& + 2z_{ri}^T(t)U_i z_{ri}(t-h) - z_{t-h}^T(U_i + (1-h)S_i(\alpha_t))z_{ri}(t-h)
\end{aligned}
$$

$$
= \begin{bmatrix} z_{ri}^T(t) \\ \bar{Z}_{rj}^T(t-\tau) \\ z_{ri}^T(t-h) \end{bmatrix}^T \begin{bmatrix} w_i^1(\alpha_t) & w_i^2(\alpha_t) & U_i \\ * & w_i^3(\alpha_t) & 0 \\ * & * & -U_i - (1-h)S_i(\alpha_t) \end{bmatrix} \begin{bmatrix} z_{ri}(t) \\ Z_{rj}(t-\tau) \\ z_{ri}(t-h) \end{bmatrix}
$$

$$
= \eta_i^T(t,\tau,h)W_i(\alpha_t)\eta_i(t,\tau,h) \tag{6.65}
$$

where $\eta_i(t,\tau,h) = [z_{ri}^T(t)\ \bar{Z}_{rj}^T(t-\tau)\ z_{ri}^T(t-h)]^T$. The matrices W_{ik} and Ψ_i are defined as

$$
W_i(\alpha_t) = \begin{bmatrix} w_i^1(\alpha_t) & w_i^2(\alpha_t) & U_i \\ * & w_i^3(\alpha_t) & 0 \\ * & * & -U_i - (1-h)S_i(\alpha_t) \end{bmatrix}
$$

$$w_i^1(\alpha_t) = (2P_i(\alpha_t) + h^2(B_{i0}K_{ri})^T(\alpha_t)U_i)B_{i0}K_{ri}(\alpha_t) + \sum_{l=1}^{M}\pi_{\alpha_t l}P_i(l) + (1+h)S_i(\alpha_t) - U_i$$

$$w_i^2(\alpha_t) = (h^2(B_{i0}K_{ri})^T(\alpha_t)U_i + P_i(\alpha_t))B_{ji}K_{ji}(\alpha_t)$$

$$w_i^3(\alpha_t) = h^2 K_{ji}^T(\alpha_t)B_{ji}^T U_i B_{ji}K_{ji}(\alpha_t)$$

Therefore, since $\bar{W}_i(\alpha_t) < 0$, we have $W_i(\alpha_t) < 0$ and $\mathcal{L}V_i < 0$. Hence, according to the Definition 6.1, the system (6.60) is stochastically stable. Furthermore, according to (6.65), the following inequality also holds for $\mathcal{L}V_i$, namely

$$
\begin{aligned}
\mathcal{L}V_i &\leq \eta_i^T(t,\tau,h)[\bar{W}_{ik}(\alpha_t) - Q_i(\alpha_t) - K_{pi}^T(\alpha_t)R_i(\alpha_t)K_{pi}(\alpha_t)]\eta_i(t,\tau,h) \\
&\leq -z_{ri}^T(t)(Q_i(\alpha_t) + K_{pi}^T(\alpha_t)R_i(\alpha_t)K_{pi}(\alpha_t))z_{ri}(t)
\end{aligned} \tag{6.66}
$$

Consequently, we can obtain

$$
\begin{aligned}
J_{ri} &= E\{\int_0^\infty (z_{ri}^T(t)Q_i(\alpha_t)z_{ri}(t) + \bar{u}_{pi}^T(t)R_i(\alpha_t)\bar{u}_{pi})dt\} \\
&= E\{\int_0^\infty (z_{ri}^T(t)[Q_i(\alpha_t) + K_{pi}^T(\alpha_t)R_i(\alpha_t)K_{pi}(\alpha_t)]z_{ri}(t)dt\} \\
&\leq -E\{\int_0^\infty (\mathcal{L}V_i(z_{ri}(t),\alpha_t))dt\} \\
&= V_i(z_{ri}(0),0,r_0) - \lim_{t\to\infty} V_i(z_{ri}(t),t,\alpha_t) \\
&\leq V_i(z_{ri}(0),0,r_0) = J_{ri}^*
\end{aligned} \tag{6.67}
$$

Therefore, the jump quadratic cost function (6.64) is upper bounded. The closed-loop system (6.60) is stochastically stable. The performance of the closed-loop system is guaranteed for any admissible time-varying delays under Assumption 6.1. According to the Definition 6.2, the state feedback controller $\bar{u}_{ri}(t)$ is the stochastic guaranteed cost controller of the system (6.60) and the scalar J_{ri}^* is the stochastic guaranteed cost of the system (6.60). This completes the proof of Lemma 6.3. ∎

The following lemma is now presented to derive the control gain $K_{ri}(\alpha_t)$.

Lemma 6.4. *Given the cost function (6.64) and under Assumption 5.2, if there exist symmetric positive definite matrices $\Lambda_{i1}^T(\alpha_t)$, $\bar{X}_i(\alpha_t)$, $\bar{V}_{ii}(\alpha_t)$, $\bar{T}_i(\alpha_t)$, and matrices U_i, $N_i(\alpha_t)$, Λ_{i3}^T, and $\bar{S}_i(\alpha_t)$ for $i = 1,....n$, and $\alpha_t \in \mathcal{S} = \{1,\ldots,M\}$ such that the following LMI conditions are satisfied:*

$$
\Omega_i(\alpha_t) = \begin{bmatrix} \bar{X}_{ik}(\alpha_t) & h^2(\bar{V}_{ik}^T(\alpha_t) + \bar{T}_i(\alpha_t))B_{ji} + B_{ji} & \Lambda_{i1}^T(\alpha_t) \\ * & h^2 B_{ji}^T U_i B_{ji} & 0 \\ * & * & -\Lambda_{i3}^T - (1-h)\bar{S}_i(\alpha_t) \end{bmatrix} < 0 \tag{6.68}
$$

then the controller $\bar{u}_{ri}(t) = K_{ri}(\alpha_t)z_{ri}(t)$ is the stochastic guaranteed cost controller of the system (6.60), and the decentralized control gain is given by $K_{ri}(\alpha_t) = B_{i0}^+ T_i(\alpha_t)\Lambda_{i1}^{-1}(\alpha_t)$.

Proof: Based on the matrix inequality conditions in Lemma 6.1, the objective is derive the control gains $K_{pi}(\alpha_t)$, and the adaptive control parameters $\delta_{pi}(\alpha_t)$ and $\beta_{pi}(\alpha_t)$. The adaptive control parameters are presented in the closed-loop system matrices $A_{i0}^k(\alpha_t)$. To transform the nonlinear matrix inequality conditions into an equivalent linear one, the following matrices are defined:

$$\Lambda_{i1}(\alpha_t) = P_i^{-1}(\alpha_t) \qquad \Lambda_{i2}(\alpha_t) = K_{ji}^{-1}(\alpha_t)$$

$$\Lambda_{i3} = U_i^{-1} \qquad \Lambda_i(\alpha_t) = diag\{\Lambda_{i1}(\alpha_t), \Lambda_{i2}(\alpha_t), \Lambda_{i3}\}$$

By pre and post multiplying the matrix $\bar{W}_{ik}(\alpha_t)$ with Λ_i^T and Λ_i, respectively, the following matrix can be obtained:

$$\Omega_i(\alpha_t) = \Lambda_i^T(\alpha_t)\bar{W}_i(\alpha_t)\Lambda_i(\alpha_t)$$

$$= \begin{bmatrix} \Lambda_{i1}^T(\alpha_t)X_{ik}(\alpha_t)\Lambda_{i1}(\alpha_t) & h^2\Lambda_{i1}^T(\alpha_t)(B_{i0}K_{ri})^T(\alpha_t)U_iB_{ji} + B_{ji} & \Lambda_{i1}^T(\alpha_t) \\ * & h^2B_{ji}^T(U_i + N_i(\alpha_t))B_{ji} & 0 \\ * & * & -\Lambda_{i3}^T - (1-h)\Lambda_{i3}^TS_i(\alpha_t)\Lambda_{i3} \end{bmatrix}$$

Let us define

$$B_{i0}K_{ri}(\alpha_t) = T_i\Lambda_{i1}^{-1}(\alpha_t) \qquad \bar{T}_i = T_i^TU_i$$

$$S_i(\alpha_t) = P_i(\alpha_t) \qquad M_i(\alpha_t) = U_i$$

$$\bar{Q}_i(\alpha_t) = \Lambda_{i1}^T(\alpha_t)Q_i(\alpha_t)\Lambda_{i1}(\alpha_t) \qquad \bar{S}_i(\alpha_t) = \Lambda_{i3}^TS_i\Lambda_{i3}^T$$

$$\bar{R}_i(\alpha_t) = \Lambda_{i1}^T(\alpha_t)K_{ri}^T(\alpha_t)R_i(\alpha_t)K_{ri}(\alpha_t)\Lambda_{i1}(\alpha_t)$$

The matrix $\Omega_{ik}(\alpha_t)$ will then become

$$\Omega_i(\alpha_t) = \begin{bmatrix} \bar{X}_i(\alpha_t) & h^2\bar{T}_iB_{ji} + B_{ji} & \Lambda_{i1}^T(\alpha_t) \\ * & h^2B_{ji}^TU_iB_{ji} & 0 \\ * & * & -\Lambda_{i3}^T - (1-h)\bar{S}_i(\alpha_t) \end{bmatrix} \qquad (6.69)$$

where $\bar{X}_i(\alpha_t) = T_i + T_i^T + (1 + h + \sum_{l=1}^M \pi_{\alpha_t l})\Lambda_{i1}^T(\alpha_t) + \bar{Q}_i(\alpha_t) + \bar{R}_i(\alpha_t)$. Therefore, if $\Omega_i(\alpha_t) < 0$, one will also have $\bar{W}_i < 0$. By solving the LMI conditions $\Omega_i(\alpha_t) < 0$, we can then obtain the control gain $K_{ri}(\alpha_t)$ as $K_{ri}(\alpha_t) = B_{i0}^+T_i(\alpha_t)\Lambda_{i1}^{-1}(\alpha_t)$. This completes the proof of Lemma 6.4. ∎

6.2.4 Stability Conditions Incorporating the Physical Constraints

The closed-loop system (6.60) after applying the stochastic state feedback controller $\bar{u}_{ri}(t)$ can be written as follows:

$$\dot{z}_{ri}(t) = B_{i0}K_{ri}(\alpha_t)z_{ri}(t) + \sum_{j \in \wp_i(\alpha_t)} B_j K_{rj}(\alpha_t)z_{rj}(t - \tau_{ji}(t)) \tag{6.70}$$

The physical constraints for the ordinary traffic in a mobile network are listed as below:

$$z_{ri}^{min} \le z_r(t) \le z_{ri}^{max} \tag{6.71}$$

$$0 \le \bar{u}_{ri}(t) \le c_{ri}(\alpha_t) \tag{6.72}$$

where $z_{ri}^{maz} = x_{ri}^{buffer} - x_{ri}^{ref}$ and $z_{ri}^{min} = -x_{ri}^{ref}$.

To avoid confusion, in the remainder of this section we use the notations Λ_{pi1} and Λ_{ri1} to denote the Lyapunov matrix Λ_{i1} used in Lemma 6.2 and Lemma 6.4, for the premium and the ordinary traffic and the following analysis of the physical constraints can be obtained.

Constraints of the State

For the state constraints (6.71), consider the following ellipsoid for a selected $\epsilon_{i2} > 0$:

$$\mathbb{S}_i = \{z_{ri}^T(\tilde{P}_{ri})^{-1}(\alpha_t)z_{ri} < \epsilon_{i2}\} \tag{6.73}$$

From the definition of the Lyapunov function given in (6.65), if the stability conditions are satisfied, we will have

$$z_r^T(t)\Lambda_{ri1}^{-1}z_r(t) \le V_i(z_{ri}(t), \alpha_t) \tag{6.74}$$

Now, by integrating (6.66) on both sides from 0 to t and considering $V(z_{ri}(0), r_0) = 0$, we will have

$$V_i \le -\int_0^t z_{ri}^T(t)(Q_i(\alpha_t) + K_{pi}^T(\alpha_t)R_i(\alpha_t)K_{pi}(\alpha_t))z_{ri}(t)dt < 0 \tag{6.75}$$

Therefore, $z_{ri}(t)$ belongs to the set $\mathbb{S}_i$ for all $t > 0$. Consequently, the right hand side of the state constraint (6.71) can be expressed as the following LMI condition:

$$\Omega_{c1i}^r(\alpha_t) \triangleq \begin{bmatrix} \Lambda_{ri1}(\alpha_t) & \Lambda_{ri1}^T(\alpha_t) \\ \Lambda_{ri1}(\alpha_t) & (z_{ri}^{max})^2/\epsilon_{i2} \end{bmatrix} \geq 0 \tag{6.76}$$

On the other hand, the left hand side of the state constraint can be considered by the following nonnegative constraint:

$$z_{ri}(t) - z_{ri}^{min} \geq 0 \tag{6.77}$$

Following the similar lines as those in deriving the LMI conditions for the physical constraints of the premium traffic, and noting that the matrix Λ_{ri1} is set to be a diagonal positive definite, and given that $B_{i0} < 0$, the non-negative constraint of the state can be expressed by the following LMI conditions:

$$\Omega_{c2i}^r(\alpha_t) \triangleq (T_i(\alpha_t))_{ij} \leq 0, \qquad i, j = 1, ... 2n \tag{6.78}$$

Constraints of the Input

For the constraints of the input, by using $\bar{u}_{ri}(t) = K_{ri}(\alpha_t)z_{ri}(t)$, it can be stated that follows:

$$0 \leq B_{i0}^+ T_i(\alpha_t)\Lambda_{ri1}^{-1}(\alpha_t)z_{ri}(t) \leq c_{ri}(\alpha_t) \tag{6.79}$$

Note that:

$$c_{ri}(\alpha_t) = C_{server,i}(\alpha_t) - K_{pi}(\alpha_t)\bar{z}_{pi}(t) \tag{6.80}$$

where $K_{pi}(\alpha_t)$ is the control gain of the premium traffic controller. Therefore, the input constraint of the ordinary traffic (6.80) can be expressed as follows:

$$0 \leq K_{ri}(\alpha_t)z_{ri}(t) \leq C_{server,i}(\alpha_t) - K_{pi}(\alpha_t)\bar{z}_{pi}(t) \tag{6.81}$$

From the right hand side of (6.81) one can have

$$K_{ri}(\alpha_t)z_{ri}(t) + K_{pi}(\alpha_t)\bar{z}_{pi}(t) \leq C_{server,i}(\alpha_t) \tag{6.82}$$

By squaring (6.82) we have

$$\begin{bmatrix} z_{ri}^T(t) \\ z_{pi}^T(t) \end{bmatrix} \begin{bmatrix} K_{ri}^T \\ K_{pi}^T \end{bmatrix} \begin{bmatrix} K_{ri} & K_{pi} \end{bmatrix} \begin{bmatrix} z_{ri}(t) \\ z_{pi}(t) \end{bmatrix} \leq \|C_{server,i}(\alpha_t)\|^2 \tag{6.83}$$

Therefore, by considering the ellipsoid $\mathbb{F}_i$ and the set $\mathbb{S}_i$, the right hand side of the input constraint will be satisfied if the following LMI conditions hold

$$\Omega^r_{c3i}(\alpha_t) \triangleq \gamma_i max\{\Psi_i(\alpha_t)\} \leq \epsilon_{i1} \tag{6.84}$$

$$\Omega^r_{c4i}(\alpha_t) \triangleq \begin{bmatrix} I & K_{ri}(\alpha_t) & K_{pi}(\alpha_t) \\ K^T_{ri}(\alpha_t) & \frac{C^2_{server,i}(\alpha_t)}{\epsilon_{i1}+\epsilon_{i2}}\Lambda_{ri1}(\alpha_t) & 0 \\ K^T_{pi}(\alpha_t) & 0 & \frac{C^2_{server,i}(\alpha_t)}{\epsilon_{i1}+\epsilon_{i2}}\Lambda_{pi1}(\alpha_t) \end{bmatrix} \geq 0 \tag{6.85}$$

The LMI conditions derived above together with the stability conditions in Lemma 6.4 can be summarized by the following theorem.

Theorem 6.2. *A decentralized Markovian jump guaranteed cost congestion controller (MJ-GCC) for the dynamical queuing system for the ordinary traffic in each node i is obtained provided that the mode-dependent conditions that are given in Lemma 6.4 are satisfied, subject to the mode-dependent LMIs $\Omega^r_{c1i}(\alpha_t)$ to $\Omega^r_{c4i}(\alpha_t)$ that are governed by equations (6.76), (6.78), (6.84), and (6.85), respectively.*

Proof: The proof follows along the same lines as those given in Lemma 6.3 and Lemma 6.4, and the derivations for the physical constraints that are given in this section. ∎

The decentralized guaranteed cost congestion control strategy of the premium and the ordinary traffic classes that are derived in this section are summarized by the flow chart that is shown in Fig. 6.1.

As shown in the Fig. 6.1, given a mobile network with changing network topologies $\alpha_t \in \mathcal{S} = \{1,...,M\}$, the decentralized premium traffic controller first solves the mode-dependent LMI conditions $\Omega_{ik}(\alpha_t)$ and $\Omega_{c1i}(\alpha_t)$ to $\Omega_{ci6}(\alpha_t)$ of each node, so that the stochastic control gains $K_{pi}(\alpha_t)$ and the adaptive control gains $\delta_{pi}(\alpha_t)$ and $\beta_{pi}(\alpha_t)$ can be obtained. The adaptive estimator $\hat{\lambda}_{pi}(t)$ is then updated based on the switching conditions that are given by (6.13). The stochastic bandwidth controller $C_{pi}(t)$ is calculated as follows:
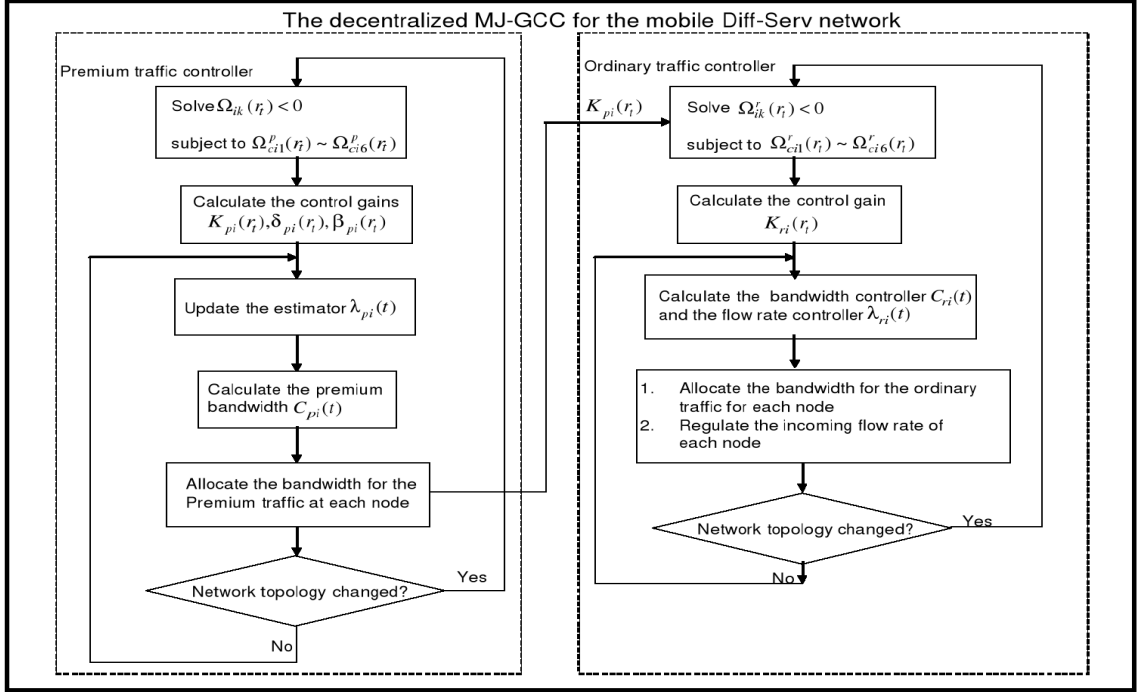
Figure 6.1: The flow chart of the decentralized guaranteed cost congestion controller (GCC) for the Mobile Diff-Serv network.

$$
\begin{aligned}
C_{pi}(\alpha_t) &= f^{-1}(x_{pi}, t)\bar{u}|_{pi}(\alpha_t) \\
&= f^{-1}(x_{pi}, t)K_{pi}(\alpha_t)\bar{z}_{pi}(t) \\
&= f^{-1}(x_{pi}, t)K_{pi}(\alpha_t)\left[\begin{array}{c} x_{pi}(t) - x_{pi}^{ref} \\ \hat{\lambda}_{pi}(t) \end{array}\right]
\end{aligned}
\tag{6.86}
$$

where $x_{pi}(t)$ is the queuing length of node i.

Given the premium traffic control gain $K_{pi}(\alpha_t)$ and the leftover capacity $C_{server,i}(\alpha_t) - C_{pi}(t)$, the decentralized controller of the ordinary traffic first solves the corresponding LMI conditions to derive the mode-dependent control gain $K_{ri}(\alpha_t)$. The bandwidth controller $C_{ri}(\alpha_t)$ and the flow rate controller $\lambda_{ri}(\alpha_t)$ are then calculated as follows

$$
\begin{aligned}
\left[\begin{array}{c} C_{ri}(\alpha_t) \\ \lambda_{ri}(\alpha_t) \end{array}\right] &= F^{-1}(x_{ri}, t)\bar{u}_{ri}(\alpha_t) = \left[\begin{array}{cc} f^{-1}(x_{ri}, t) & 0 \\ 0 & 1 \end{array}\right] K_{ri}(\alpha_t)z_{ri}(t) \\
&= \left[\begin{array}{cc} f^{-1}(x_{ri}, t) & 0 \\ 0 & 1 \end{array}\right] K_{ri}(\alpha_t)(x_{ri}(t) - x_{ri}^{ref})
\end{aligned}
\tag{6.87}
$$

282
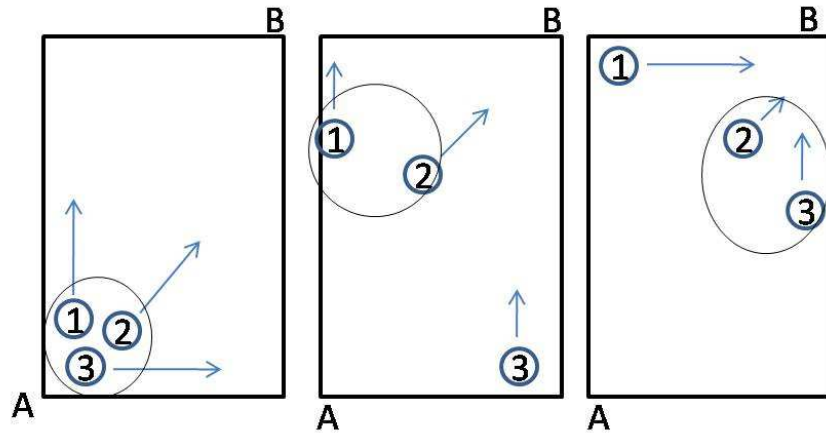
Figure 6.2: The schematic of the network configuration for three "typical" modes of a mobile network in Example 6.1.

where $x_{ri}(t)$ is the queuing length of the ordinary traffic at node i.

It should be noted that, different from the guaranteed cost congestion control algorithms of the fixed network, as shown in the Fig. 5.2, the Markovian jump guaranteed cost congestion control (MJ-GCC) algorithm needs to re-calculate all the mode-dependent parameters such as the state feedback control gain $K_{pi}(\alpha_t)$ and $K_{ri}(\alpha_t)$ and the adaptive control gains $\delta_{pi}(\alpha_t)$ and $\beta_{pi}(\alpha_t)$, at each time when the network topology is changed. The congestion controller are then updated based on the new control parameters.

6.3　Simulations

The simulation results presented in this section are intended to demonstrate the effectiveness and the capabilities of our proposed decentralized Markovian jump guaranteed cost congestion (MJ-GCC) strategy to mobile Diff-Serv networks. We adopt the same performance metrics, namely the packet loss rate and the average queuing delay with respect to the mobile network, as defined in Section 4.3.1. The simulations are conducted by two examples where our proposed decentralized MJ-GCC strategy is compared and evaluated with another benchmark scheme as before, namely the IDCC [3] approach.

Example 6.1. In this example, the network topology and the scenario considered in Section 4.5.1 is repeated. The NMAS have 3 nodes that are supposed to explore a rectangular area from point A to point B. As shown in Fig. 6.2. The first node moves towards north first and then towards east, the second node moves towards northeast directly, and the third node moves towards east and then towards north. It is assumed that the network is fully connected at the start. The capacity of each link is 10 Mbps, and the maximum buffer size is 5 Mbits. The simulation time duration is selected as $30s$. A total of 5 switching modes are defined based on the network topology. In other words we consider the following network modes $M_1 = \{1, 2, 3\}$, $M_2 = \{1, 2\}, \{3\}$, $M_3 = \{1\}, \{2, 3\}$, $M_4 = \{1, 3\}, \{2\}$, and $M_5 = \{1\}, \{2\}, \{3\}$.

The transition probabilities π_{kl} among different modes are random and following transition probability matrix is considered for the Markovian jump model of the changes in network topologies

$$
\Pi = \begin{bmatrix} \pi_{11} & \cdots & \pi_{15} \\ \vdots & \ddots & \vdots \\ \pi_{51} & \cdots & \pi_{55} \end{bmatrix} = \begin{bmatrix} 0.2 & 0.1 & 0.3 & 0.3 & 0.1 \\ 0.1 & 0.4 & 0.2 & 0.15 & 0.15 \\ 0.15 & 0.15 & 0.6 & 0.05 & 0.05 \\ 0.2 & 0.6 & 0.05 & 0.1 & 0.05 \\ 0.2 & 0.2 & 0.2 & 0.2 & 0.2 \end{bmatrix} \tag{6.88}
$$

Based on the above configurations, the following two cases are then considered for evaluating the performance of our decentralized MJ-GCC strategy.

Remark 6.1. *The Markovian jump model is simulated through a Monte carlo method [152]. A Markov chain is generated by using the MatLab function randsrc based on the transition matrix (6.88).*

Case 1: Queuing Performances of Each Node

The input Diff-Serv traffic for each node is defined as follows. The premium traffic is defined based on a Poisson distribution with the mean traffic rate of $\lambda_{pi}(t) = 5$ Mbits per second. The ordinary traffic is defined as an on-off signal with the maximum traffic rate of 10 Mbits per second. The average off-time of the ordinary traffic is defined based
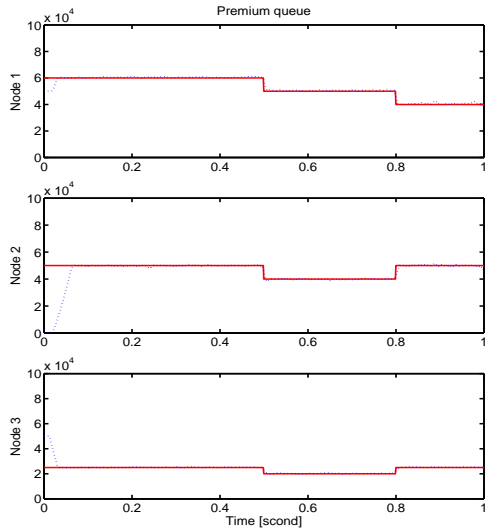
Figure 6.3: Premium queuing length (bits) by utilizing our proposed decentralized MJ-GCC approach. The solid lines denote the set point references and the dashed lines denote the actual queuing lengths.
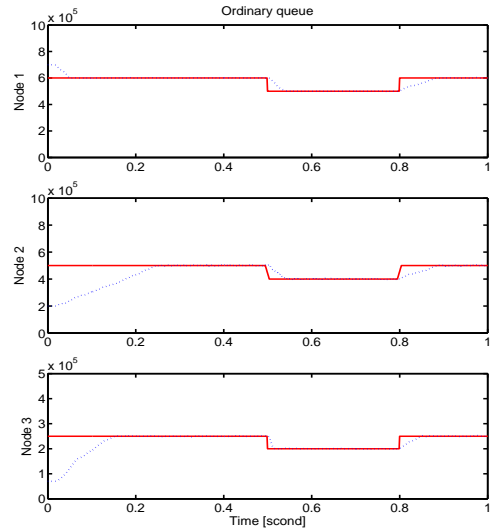
Figure 6.4: Ordinary queuing length (bits) by utilizing our proposed decentralized MJ-GCC approach. The solid lines denote the set point references and the dashed lines denote the actual queuing lengths.

on an exponential distribution with a mean period of 2 ms. The best-effort traffic load is defined as a random signal varying from 0.5 Mbps to 2 Mbps. The delay among the nodes is defined as a random signal as $\tau = min\{0, max\{h_{max}, h\}\}$ where $h_{max} = 20$ ms is the maximum bound of delay, and $h \sim N(10ms, 5ms)$ is a Gaussian distributed function with mean value of 10 ms and standard derivation of 5 ms.

Fig. 6.3 and Fig. 6.4 depict the queuing length of the three nodes by utilizing our proposed MJ-GCC strategy. The left and the right column are devoted to the premium and the ordinary traffic services, respectively. The results confirm that our proposed MJ-GCC strategy is effective in stabilizing the buffer queues in the presence of changing network topology and time-varying delays.

The numerical results of the packet loss rate and the average queuing delays of each node are summarized in Table. 6.1. If one compares the results with that of the Markovian jump switching congestion controller (MJ-SCC), given in Table. 4.1 and Table. 4.2, one can see that the packet loss rate of the ordinary traffic by utilizing the MJ-GCC strategy is greatly decreased. The reason is that in the switching congestion control (SCC) strategy, one needs to regulate the traffic compression gains so to guarantee the network is working

Table 6.1: The queuing performance by utilizing the proposed decentralized MJ-GCC approach with $h_{max} = 20$ ms

Premium	PLR	Queuing Delay
Node 1	0.012%	42.70 ms
Node 2	0.032%	44.80 ms
Node 3	0.011%	23.70 ms
Ordinary	PLR	Queuing Delay
Node1	2.61%	65.41 ms
Node 2	1.32%	48.22 ms
Node 3	1.41%	26.10 ms

in the safe operating range (within the physical constraints). However in the guaranteed cost congestion control (GCC) strategy, the physical constraints are expressed as a set of complementary LMIs that affect the control parameters so that a higher traffic compression gains, which in turn results in a lower packet loss rate, may be obtained.

Case 2: Performance Under Different Delay levels

The performance of our proposed congestion control algorithm is evaluated based on different levels of the time-delays having maximum bounds of $h = \{20; \ 40; \ 80\}$ ms. Table 6.2 presents the buffer characteristics of each node for both the premium and the ordinary traffic services.

By inspecting the above numerical results one can observe that as the level of the delay increases our proposed decentralized MJ-GCC approach can still maintain a robust performance on the packet loss rate and the average queuing delay, despite the changes in dynamical network topologies. Indeed, the packet loss rate in the network remains less than 0.1% for the premium traffic and less than 6% for the ordinary traffic. The average queuing delay for the premium traffic remains less than 53 ms and for the ordinary traffic remains less than 70 ms.

Table 6.2: The queuing performance by utilizing the proposed decentralized MJ-GCC approach with different delay levels.

PLR	Node 1		Node 2		Node 3	
h	P	O	P	O	P	O
20 ms	0.012%	2.61%	0.032%	1.32%	0.011%	1.41%
40 ms	0.012%	2.91%	0.034%	4.66%	0.013%	2.12%
80 ms	0.099%	3.42%	0.037%	5.95%	0.034%	5.57%
Delay	Node 1		Node 2		Node 3	
h	P	O	P	O	P	O
20 ms	42.70 ms	65.41 ms	44.80 ms	48.22 ms	23.70 ms	26.10 ms
40 ms	51.30 ms	66.56 ms	44.90 ms	49.64 ms	24.80 ms	27.87 ms
80 ms	52.60 ms	67.03 ms	47.70 ms	50.12 ms	25.80 ms	30.48 ms

6.4   Conclusions

In this chapter, the congestion control problem of mobile Diff-Serv networks is considered. By utilizing the guaranteed cost control theory, a novel decentralized Markovian jump guaranteed cost congestion control (MJ-GCC) algorithm is developed for the premium and the ordinary traffic in the presence of changing network topology and time-varying delays. By employing the Markovian process, the changes of the network topology are modeled as a stochastic process. The dynamic queuing model of each traffic is then modeled as a Markovian jump system. The proposed MJ-GCC strategy is shown to be capable of stabilizing the buffer queues and maintaining the robustness of the system with respect to the admissible time-varying delays. The stability conditions of the mobile network are represented by a set of mode-dependent LMIs. Furthermore, the mode-dependent physical constraints of the mobile network are guaranteed by satisfying a set of complementary LMIs. Comparative analysis shows that the MJ-GCC algorithm is less conservative than the MJ-SCC strategy in the sense of traffic compression gains. The simulation results and numerical comparisons shows that the performance of our proposed MJ-GCC algorithms has great superiority when compared to the conventional IDCC method (which in general results in an unstable closed-loop system for the applications considered in this thesis).

Part III

Distributed Congestion Control

Scheme

Chapter 7

Distributed Congestion Control of Mobile DiffServ Networks

As presented in the previous chapters, for both the switching congestion control (SCC) approach (Chapters 3-4) and the guaranteed cost congestion control (GCC) approach (Chapters 5-6), we have investigated and developed congestion control solutions for a network of multi-agent systems (NMAS) with differentiated services (Diff-Serv) through two control schemes, namely

- *Centralized control scheme*, and

- *Decentralized control scheme*

for both fixed Diff-Serv networks and mobile Diff-Serv networks.

However, since the network of multi-agent systems (NMAS) is a highly coupled system, several limitations will quickly be encountered with practical deployments of both centralized and decentralized control schemes as the dimension of the network increases. In general, the following three main drawbacks of a centralized control scheme are the main reasons of why one might want to avoid centralized controllers:

- Deployment Cost. Centralized controllers typically need all the state information of the global system even for controller design, which requires modifying the underlying interconnections to implement such controllers. This may be undesirable for

applications such as communication networks, when introducing new channels between subsystems can normally be less practical and more expensive than increasing the transmission rates over the pre-existing ones.

- Communication Cost. By the same reason of the information-structure requirement of centralized controllers, a centralized controller needs all the sub-systems to communicate their own state to one central station in order for the centralized controller to generate appropriate control signal for each subsystem. Due to the communication limitations, some stringent specification of the Quality of Service (OS) are needed for the network. Practical networks used in networked control systems sometimes cannot provide this service; for example, in wireless sensor networks it is impractical for controllers to subscribe such services because of the fading issues. Besides, communication leads to longer delays, which is a situation that one wants to avoid as a control engineer.

- Computational Cost. By their own nature, centralized controllers are bound to have a large number of states, inputs and outputs, which is precisely the situation why classical control design algorithms can not handle the problem effectively. Moreover higher computational power is normally required to implement these design, not to mention that convergence of the computation of larger dimension matrices with large condition numbers is always a difficult numerical problem.

Because of all the above centralized control limitations for high dimensional distributed system, one option is to adopt a fully decentralized architecture where a local controller is attached to each node and where the local control action is based on only local measurements. From the communication point view, this approach greatly reduces the communication burden, and from the implementation point of view, the decentralized controllers are easy to deploy.

However, the performance of a decentralized controller is normally conservative due to the fact that the decisions are only based on local information while the entire system is generally highly coupled. To balance and have a trade-off between these two extreme

290
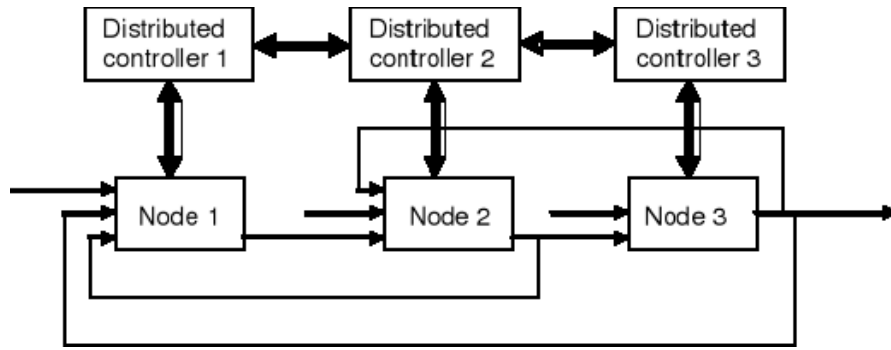
Figure 7.1: The distributed control framework for a NMSA with three nodes.

control philosophies, it is natural to introduce an approach which respects the underlying interconnection, adopts a distributed architecture and scales well to large scale systems. We consider the congestion control problem of a NMAS through a distributed control scheme, by incorporating the possibility of communications among the controllers.

The aim of this chapter is to develop a distributed congestion control strategies for the mobile NMAS subject to Diff-Serv traffic based on the guaranteed cost control approach. The changes of the network topology is defined by the Markov chain $\alpha_t \in \mathcal{S}$, $\mathcal{S} = \{1, ..., M\}$, where M is the number of modes (different topologies) that the mobile network may experience. It should be noted that the fixed network can be viewed as a special case of mobile networks when $M = 1$. Therefore, we only consider the congestion control problem of mobile Diff-Serv networks in this chapter.

The proposed distributed congestion controller is shown to be in fact equivalent to a local state feedback control plus a nearest neighboring controllers' adjustment with proportional gains. The resulting guaranteed cost control problem is then cast as a quadratic regulation problem of a time-delay system with free parameters (gains) that need to be selected. With this methodology, the distributed control approach yields an algorithm that significantly enhances the scalability of the centralized algorithm and improves the performance of the decentralized approach to a large scale traffic network. The basic concept of the distributed control scheme is shown in Fig. 7.1. As shown in Fig. 7.1, the controller is implemented at each local node. The controllers can communication with

291

each others. Therefore, the decisions of each controller is based on the local information of each node and the adjusting information from the nearest neighboring controllers.

The remainder of this chapter is organized as follows. The congestion control strategies for the premium and the ordinary traffic classes are presented in Section 7.1 and 7.2, respectively, and both are developed based on the guaranteed cost control approach and the dynamical models that are given in Chapter 2. The proposed distributed GCC strategies are then evaluated and compared with the centralized and decentralized GCC approaches on the performance of QoS and control through comprehensive simulations in Section 7.4. Finally, conclusions are provided in Section 7.5.

7.1 Distributed Guaranteed Cost Congestion Control (DGCC) for the Premium Traffic Class

The congestion control objective of the premium traffic is to regulate the link capacity $C_{pi}(t)$ so that the premium queueing length $x_{pi}(t)$ is as close as possible to the reference set point x_{pi}^{ref}. Recall that the decentralized dynamic queuing model of the premium traffic in a mobile network is given by:

$$\dot{x}_{pi}(t) = -f(x_{pi}(t))u_{pi}(t) + \lambda_{pi}(t) + \sum_{j \in \wp_i(\alpha_t)} f(x_{pj}(t - \tau_{ji}(t)))u_{pj}(t - \tau_{ji}(t))g_{ji}^p \quad (7.1)$$

where $\lambda_{pi}(t)$ is the external incoming premium traffic, g_{ji}^p is the traffic compression gain from node j to node i, $\wp_i(\alpha_t)$ is the neighboring set of node i which depends on the mode of network topology α_t, α_t is a Markov process indicating the changes of the neighboring set of node i which takes values from the finite set $\mathcal{S} = \{1, ..., M\}$ and the transition probability between different modes in $\mathcal{S}$ is governed by the following distribution function:

$$P[\alpha_{t+\delta} = k \mid \alpha_t = l] = \begin{cases} \pi_{kl}\Delta + o(\Delta), & k \neq l; \\ 1 + \pi_{kk}\Delta + o(\Delta), & k = l. \end{cases} \quad (7.2)$$

where $\pi_{kl} \geq 0$ is the transition rate from mode k to mode l, $\pi_{kk} = -\sum_{l=1,l\neq k}^{M} \pi_{kl}$, and $o(\Delta)$ is a function satisfying $\lim_{\Delta \to 0} \frac{o(\Delta)}{\Delta} = 0$. Furthermore, the unknown and time-varying delays $\tau_{ji}(t)$ between node j to node i satisfy the same assumptions as defined in (2.12)-(2.14).

292

Feedback Linearization

The nonlinear system model (7.1) is first transformed into an equivalent linear system by applying the following input to state feedback transformations:

$$z_{pi}(t) = x_{pi}(t) - x_{pi}^{ref}$$

$$u_{pi}(t) = f^{-1}(x_{pi}, t)\bar{u}_{pi}(t)$$

where x_{pi}^{ref} is the reference set point of the queuing length for the premium traffic. Consequently, the dynamic queuing model of the premium traffic (7.1) can be rewritten as follows:

$$\dot{z}_{pi}(t) = -\bar{u}_{pi}(t) + \lambda_{pi}(t) + \sum_{j \in \wp_i(\alpha_t)} \bar{u}_{pj}(t - \tau_{ji}(t))g_{ji}^p \tag{7.3}$$

Based on the decentralized dynamic model (7.3), the distributed congestion controller of the premium traffic is selected as:

$$\bar{u}_{pi}(t) = \bar{u}_{pi}^{de}(t) + \sum_{j \in \wp_i(\alpha_t)} w_{ji}^p(\alpha_t)\bar{u}_{pj}^{de}(t) \tag{7.4}$$

$$\bar{u}_{pi}^{de}(t) = K_{pi}^1(\alpha_t)z_{pi}(t) + K_{pi}^2(\alpha_t)\hat{\lambda}_{pi}(t) \tag{7.5}$$

$$\dot{\hat{\lambda}}_{pi}(t) = \begin{cases} \delta_{pi}(\alpha_t)z_{pi}(t) - \beta_{pi}(\alpha_t)\hat{\lambda}_{pi}(t), & \text{if } 0 \le \hat{\lambda}_{pi}(t) \le \lambda_{pi}^{max} \text{ or} \\ & \hat{\lambda}_{pi}(t) = 0,\ z_{pi}(t) \ge 0 \text{ or} \\ & \hat{\lambda}_{pi}(t) = \lambda_{pi}^{max},\ z_{pi}(t) \le 0 \\ -\beta_{pi}(\alpha_t)\hat{\lambda}_{pi}(t), & \text{otherwise} \end{cases} \tag{7.6}$$

where the notation $\bar{u}_{pi}^{de}(t)$ indicates the decentralized controller, $w_{ji}^p(\alpha_t)$ is the distributed control gains for the premium traffic between node j and i which is dependent on the mode of network topology α_t, $\hat{\lambda}_{pi}(t)$ is an adaptive estimator used to estimate the unknown external incoming premium traffic $\lambda_{pi}(t)$ and compensates for its effect via feedback.

Therefore, if we view the estimator $\hat{\lambda}_{pi}(t)$ as an extra state and define a new state space as $\bar{z}_{pi}(t) = [z_{pi}(t) \quad \hat{\lambda}_{pi}(t)]^T$, the dynamic queuing model of the premium traffic

(7.3) can be expressed by the following hybrid system:

$$\dot{\bar{z}}_{pi}(t) = A_{i0}^k(\alpha_t)\bar{z}_{pi}(t) + B_{i0}\bar{u}_{pi}(t) + \sum_{j \in \wp_i(\alpha_t)} B_j \bar{u}_{pj}(t - \tau_{ji}(t)) + B_{\lambda_i}\lambda_{pi}(t) \quad (7.7)$$

$$\bar{z}_{pi}(t) = \varphi_i(t) \qquad \varphi_i(t) \in [-h, 0]$$

$$k \in \aleph, \aleph = 1, 2$$

$$\alpha_t \in \mathcal{S}, \mathcal{S} = \{1, ..., M\}$$

where $A_{i0}^k(\alpha_t)$, B_{i0}, B_j, and B_{λ_i}, for $i, j = 1, ..., n$ are the system matrices that are defined as follows:

$$A_{i0}^1(\alpha_t) = \begin{bmatrix} 0 & 0 \\ \delta_{pi}(\alpha_t) & -\beta_{pi}(\alpha_t) \end{bmatrix} \qquad A_{i0}^2(\alpha_t) = \begin{bmatrix} 0 & 0 \\ 0 & -\beta_{pi}(\alpha_t) \end{bmatrix}$$

$$B_{i0} = \begin{bmatrix} -1 \\ 0 \end{bmatrix} \qquad B_j = \begin{bmatrix} g_{ji}^p \\ 0 \end{bmatrix} \qquad B_{\lambda_i} = \begin{bmatrix} 1 \\ 0 \end{bmatrix}$$

The distributed controller (7.4) can then be expressed as:

$$\bar{u}_{pi}(t) = \bar{u}_{pi}^{de}(t) + \sum_{j \in \wp_i(\alpha_t)} w_{ji}^p(\alpha_t)\bar{u}_{pj}^{de}(t) \tag{7.8}$$

$$\bar{u}_{pi}^{de}(t) = K_{pi}(\alpha_t)\bar{z}_{pi}(t) \tag{7.9}$$

Therefore, the distributed controller is actually a local state feedback control $K_{pi}(\alpha_t)\bar{z}_{pi}(t)$ plus a nearest neighboring controllers' adjustment $\bar{u}_{pj}^{de}(t)$ with proportional gains w_{ji}^p or a weighted combination of the local neighboring controllers. Hence, the decentralized controller proposed in Chapter 6 is indeed a special case of the distributed controller (7.8) when we set $w_{ji}^p = 0$. Let us define:

$$W_{ji}(\alpha_t) = vec\{w_{ji}^p(\alpha_t)\}$$

$$K_{ji}(\alpha_t) = diag\{K_{pj}(\alpha_t)\}$$

$$\bar{Z}_{pj}(t - \tau) = vec\{\bar{z}_{pj}^T(t - \tau_{ji}(t))\}$$

then the distributed controller $\bar{u}_{pi}(t)$ in (7.8) can be re-written as:

$$\bar{u}_{pi}(t) = K_{pi}(\alpha_t)\bar{z}_{pi}(t) + W_{ji}(\alpha_t)K_{ji}(\alpha_t)\bar{Z}_{pj}(t) \qquad i = 1, ..., n \ \ j \in \wp_i(\alpha_t) \quad (7.10)$$

Consequently, the closed-loop system of the premium traffic (7.7) after applying the distributed controller (7.8) becomes:

$$
\begin{aligned}
\dot{\bar{z}}_{pi}(t) &= A_{i0}^k(\alpha_t)\bar{z}_{pi}(t) + B_{\lambda_i}\lambda_{pi}(t) + B_{i0}[K_{pi}(\alpha_t)\bar{z}_{pi}(t) + \sum_{j\in\wp_i(\alpha_t)} w_{ji}^p(\alpha_t)\bar{u}_{pj}^{de}(t)] \\
&\quad + \sum_{j\in\wp_i(\alpha_t)} B_j[K_{pj}(\alpha_t)\bar{z}_{pj}(t-\tau_{ji}(t)) + \sum_{k\in\wp_j(\alpha_t)} w_{kj}^p \bar{u}_{pk}^{de}(t-\tau_{ji}(t))] \\
&= A_{ic}^k(\alpha_t)\bar{z}_{pi}(t) + B_{\lambda_i}\lambda_{pi}(t) + \sum_{j\in\wp_i(\alpha_t)} B_j K_{pj}(\alpha_t)\bar{z}_{pj}(t-\tau_{ji}(t)) \\
&\quad + \sum_{j\in\wp_i(\alpha_t)} B_{i0}w_{ji}^p(\alpha_t)\bar{u}_{pj}^{de}(t) + \sum_{j\in\wp_i(\alpha_t)}\sum_{k\in\wp_j(\alpha_t)} B_j w_{kj}^p \bar{u}_{pk}^{de}(t-\tau_{ji}(t)) \\
&= A_{ic}^k(\alpha_t)\bar{z}_{pi}(t) + \sum_{j\in\wp_i(\alpha_t)} B_j K_{pj}(\alpha_t)\bar{z}_{pj}(t-\tau_{ji}(t)) + B_{\lambda_i}\lambda_{pi}(t) \qquad (7.11) \\
&\quad + \sum_{j\in\wp_i(\alpha_t)} B_{i0}w_{ji}^p(\alpha_t)K_{pj}(\alpha_t)\bar{z}_{pj}(t) + \sum_{\substack{j\in\wp_i(\alpha_t) \\ k\in\wp_j(\alpha_t)}} B_j w_{kj}^p K_{pk}(\alpha_t)\bar{z}_{pk}(t-\tau_{ji}(t))
\end{aligned}
$$

where $A_{ic}^k(\alpha_t) = A_{i0}^k(\alpha_t) + B_{i0}K_{pi}(\alpha_t)$, $\wp_j(\alpha_t)$ is the neighboring set of node j, $\bar{u}_{pk}^{de}(t)$ is the decentralized controller of node k which is the neighboring set $\wp_j(\alpha_t)$. As we can seen from the dynamics of the premium traffic (7.11), the closed-loop dynamics of node i is affected by its nearest neighbors $j \in \wp_i$ and the nearest neighbors of neighbors $k \in \wp_j$. Therefore, the effect of more neighboring nodes are indeed taken into account.

The control range of the centralized, the decentralized, and the distributed congestion control algorithms can be illustrated by the example that is given in Fig. 7.2. As shown in Fig. 7.2, there are a total of 11 nodes in the network which may be mobile. Let us take the node 1 as an example. In order to obtain the control input for node 1, a centralized control algorithm needs to consider all the nodes in the network simultaneously and which is to be implemented as a central commander. Therefore, the control range of the centralized controller is 11, as shown by the solid square in Fig. 7.2.

The decentralized controller of node 1 only needs to consider the local information at node 1, and is implemented locally. As shown in the figure, the nearest neighboring nodes of node 1 are the nodes 2 and 3, as shown by the small solid circle. Due to the delayed inputs from nodes 2 and 3, the closed-loop dynamics of node 1 will have the coupling states of nodes 2 and 3 with the corresponding delays $\bar{z}_{pj}(t - \tau_{ji}(t))$. Therefore, the decentralized controller actually considers the dynamics of nodes 2 and 3 indirectly.
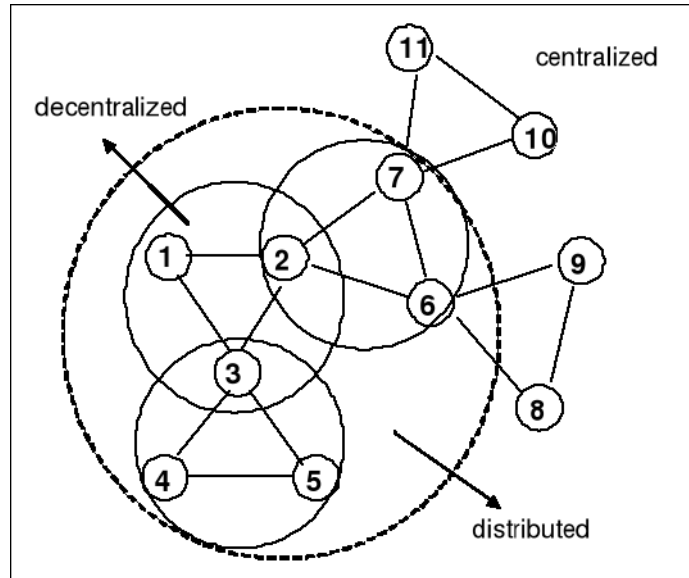
Figure 7.2: The control range of the centralized, the decentralized, and the distributed congestion control strategies.

The control range of the decentralized controller of node 1 equals to 3.

Finally, the distributed control algorithm is also implemented at each node. However, the distributed controller of node 1 incorporates the decentralized controllers of nodes 2 and 3, with proper weights $w_{ji}(\alpha_t)$. The decentralized controllers of nodes 2 and 3 will take into account the coupling effect of their nearest neighboring nodes, respectively. Therefore, the distributed controller of node 1 actually considers the dynamics of nodes 2 and 3, and their neighboring nodes 4, 5, 6, and 7, indirectly. That is, the dynamics of the neighbors of the neighboring nodes are indeed taken into account. Therefore, the control range of the distributed controller of node 1 is equal to 7, as shown by the large dashed circle in Fig. 7.2.

In reviewing the closed-loop system (7.11), the control objective of the distributed guaranteed cost congestion control (DGCC) problem is actually to select the local state feedback control gain $K_{pi}(\alpha_t)$ and the adjusting weights of the neighboring controllers $W_{ji}(\alpha_t)$, such that the system (7.11) is stable and the following jump quadratic cost

function is bounded:

$$J_{pi} = E\{\int_0^\infty (\bar{z}_{pi}^T(t)Q_i(\alpha_t)\bar{z}_{pi}(t) + \bar{u}_{pi}^T R_i(\alpha_t)\bar{u}_{pi}(t))dt\} \tag{7.12}$$

where $Q_i(\alpha_t)$ and $R_i(\alpha_t)$ are positive definite matrices with respect to each mode $\alpha_t \in \mathcal{S} = \{1, ..., M\}$.

In order to guarantee an upper bound of the cost function, we adopt the same Assumption 5.2 as presented in Chapter 5. Then, the following lemma is now presented to show that the distributed controller $\bar{u}_{pi}(t) = K_{pi}(\alpha_t)\bar{z}_{pi}(t) + W_{ji}(\alpha_t)K_{ji}(\alpha_t)\bar{Z}_j(t)$, is a stochastic guaranteed cost controller for the system (7.7).

Lemma 7.1. *Given the cost function (7.12) and under Assumption 5.2, the distributed controller $\bar{u}_{pi}(t) = K_{pi}\bar{z}_{pi}(t) + W_{ji}K_{ji}\bar{Z}_{pj}(t)$ is a stochastic guaranteed cost control law for the system (7.7), if there exist symmetric positive definite matrices $P_i(\alpha_t)$, $S_i(\alpha_t)$, U_i and positive definite matrices $M_{ik}(\alpha_t)$, $i = 1, ..., n$, such that the following matrix inequality conditions are satisfied for all the modes $\alpha_t \in \mathcal{S}$, $\mathcal{S} = \{1, ..., M\}$:*

$$\bar{W}_{ik} = \begin{bmatrix} \sigma_1 + Q_i + K_{pi}^T R_i K_{pi} & \sigma_2 & [P_i + h^2(A_{ic}^k)^T U_i]B_{ji}K_{ji} \\ * & \sigma_4 + K_{ji}^T W_{ji}^T R_i W_{ji}K_{ji} & h^2 K_{ji}^T W_{ji}^T B_{i0}^T U_i B_{ji}K_{ji} \\ * & * & h^2 K_{ji}^T B_{ji}^T U_i B_{ji}K_{ji} \\ * & * & * \\ * & * & * \end{bmatrix}$$

$$\begin{matrix} \sigma_3 & U_i \\ \sigma_5 & 0 \\ \sigma_6 & 0 \\ \sigma_7 & 0 \\ * & -U_i - (1-h)S_i \end{matrix} \tag{7.13}$$

where:

$$\sigma_1 = 2P_i(\alpha_t)A_{ic}^k(\alpha_t) + \sum_{k=1}^M \pi_{\alpha_t k}P_i(k) + h^2(A_{ic}^k(\alpha_t))^T U_i A_{ic}^k(\alpha_t) + (1+h)S_i(\alpha_t) - U_i$$

$$\sigma_2 = P_i(\alpha_t)B_{i0}W_{ji}(\alpha_t)K_{ji}(\alpha_t) + h^2(A_{ic}^k(\alpha_t))^T U_i B_{i0}W_{ji}(\alpha_t)K_{ji}(\alpha_t)$$

$$\sigma_3 = [P_i(\alpha_t) + h^2(A_{ic}^k(\alpha_t))^T U_i]B_{kj}W_{kj}(\alpha_t)K_{kj}(\alpha_t)$$

$$\sigma_4 = h^2 K_{ji}^T(\alpha_t)W_{ji}^T(\alpha_t)B_{i0}^T U_i B_{i0}W_{ji}(\alpha_t)K_{ji}(\alpha_t)$$

$$\sigma_5 = h^2 K_{ji}^T(\alpha_t)W_{ji}^T(\alpha_t)B_{i0}^T U_i B_{kj}W_{kj}(\alpha_t)K_{kj}(\alpha_t)$$

297

$$\sigma_6 = h^2 K_{ji}^T(\alpha_t) B_{ji}^T U_i B_{kj} W_{kj}(\alpha_t) K_{kj}(\alpha_t)$$

$$\sigma_7 = h^2 K_{kj}^T(\alpha_t) W_{kj}^T(\alpha_t) B_{kj}^T U_i B_{kj} W_{kj}(\alpha_t) K_{kj}(\alpha_t)$$

$$B_{ji} = vec\{B_j\} \qquad\qquad B_{kj} = vec\{[B_j \ \ B_j]\}$$

$$W_{kj} = diag\{w_{kj}^p\} \qquad\qquad K_{kj}(\alpha_t) = diag\{K_{pk}(\alpha_t)\}$$

Proof: Consider the following stochastic Lyapunov-Krosovskii functional candidate:

$$V_i(\bar{z}_{pi}(t), \alpha_t) = V_{i1} + V_{i2} + V_{i3} + V_{i4}$$

$$V_{i1} = \bar{z}_{pi}(t)^T P_i(\alpha_t) \bar{z}_{pi}(t)$$

$$V_{i2} = \int_{t-h}^{t} \bar{z}_{pi}^T(s) S_i(\alpha_t) \bar{z}_{pi}(s) ds$$

$$V_{i3} = h \int_{-h}^{0} \int_{t+\theta}^{t} \dot{\bar{z}}_{pi}^T(s) U_i \dot{\bar{z}}_{pi}(s) ds d\theta$$

$$V_{i4} = \int_{-h}^{0} \int_{t+\theta}^{t} \bar{z}_{pi}^T(s) S_i(\alpha_t) \bar{z}_{pi}(s) ds d\theta$$

and $P_i(\alpha_t)$, $S_i(\alpha_t)$, U_i are positive definite matrices with appropriate dimensions. For each mode $\alpha_t = k \in \mathcal{S}$, the infinitesimal generator of the Lyapunov function can be derived as follows:

$$
\begin{aligned}
\mathcal{L}V_{i1} &= \lim_{\Delta \to 0^+} \frac{1}{\Delta} \{E[V_{i1}(\bar{z}_{pi}(t+\Delta), \alpha_{t+\delta}, t+\Delta)|\bar{z}_{pi}(t), \alpha_t = k] - V_{i1}(\bar{z}_{pi}(t), k, t)\} \\
&= 2\bar{z}_{pi}^T(t) P_i(\alpha_t) \dot{\bar{z}}_{pi}(t) + \sum_{k=1}^{M} \pi_{\alpha_t k} \bar{z}_{pi}^T(t) P_i(k) \bar{z}_{pi}(t) \\
&= 2\bar{z}_{pi}^T(t) P_i(\alpha_t) [A_{ic}^k(\alpha_t) \bar{z}_{pi}(t) + \sum_{j \in \wp_i(\alpha_t)} B_j K_{pj}(\alpha_t) \bar{z}_{pj}(t - \tau_{ji}(t)) \\
&\quad + \sum_{j \in \wp_i(\alpha_t)} B_{i0} w_{ji}^p(\alpha_t) K_{pj}(\alpha_t) \bar{z}_{pj}(t) + \sum_{\substack{j \in \wp_i(\alpha_t) \\ k \in \wp_j(\alpha_t)}} B_j w_{kj}^p K_{pk}(\alpha_t) \bar{z}_{pk}(t - \tau_{ji}(t))] \\
&\quad + \bar{z}_{pi}^T(t) \sum_{k=1}^{M} \pi_{\alpha_t k} P_i(k) \bar{z}_{pi}(t) + 2\bar{z}_{pi}^T(t) P_i(\alpha_t) B_{\lambda_i} \lambda_{pi}(t) \\
\mathcal{L}V_{i2} &= \int_{t-h}^{t} 2\bar{z}_{pi}^T(s) S_i(\alpha_t) \dot{\bar{z}}_{pi}(s) ds + \int_{t-h}^{t} \bar{z}_{pi}^T(s) \sum_{k=1}^{M} \pi_{\alpha_t k} S_i(k) \bar{z}_{pi}(s) ds \\
&= \bar{z}_{pi}^T(t) S_i(\alpha_t) \bar{z}_{pi}(t) - (1-h) \bar{z}_{pi}^T(t-h) S_i(\alpha_t) \bar{z}_{pi}(t-h) \\
&\quad + \int_{t-h}^{t} \bar{z}_{pi}^T(s) \sum_{k=1}^{M} \pi_{\alpha_t k} S_i(k) \bar{z}_{pi}(s) ds
\end{aligned}
$$

298

$$
\begin{aligned}
\mathcal{L}V_{i3} \;=\;& h^2 \dot{z}_{pi}^T(t) U_i \dot{\bar{z}}_{pi}(t) - h \int_{t-h}^{t} \dot{z}_{pi}^T(s) U_i \dot{\bar{z}}_{pi}(s)\, ds \\[4pt]
\;=\;& h^2 [A_{ic}^k(\alpha_t)\bar{z}_{pi}(t) + \sum_{j\in\wp_i(\alpha_t)} B_j K_{pj}(\alpha_t)\bar{z}_{pj}(t-\tau_{ji}(t)) + B_{\lambda_i}\lambda_{pi}(t) \\[4pt]
& + \sum_{j\in\wp_i(\alpha_t)} B_{i0} w_{ji}^p(\alpha_t) K_{pj}(\alpha_t)\bar{z}_{pj}(t) + \sum_{\substack{j\in\wp_i(\alpha_t)\\ k\in\wp_j(\alpha_t)}} B_j w_{kj}^p K_{pk}(\alpha_t)\bar{z}_{pk}(t-\tau_{ji}(t))]^T U_i \\[4pt]
& [A_{ic}^k(\alpha_t)\bar{z}_{pi}(t) + \sum_{j\in\wp_i(\alpha_t)} B_j K_{pj}(\alpha_t)\bar{z}_{pj}(t-\tau_{ji}(t)) + B_{\lambda_i}\lambda_{pi}(t) \\[4pt]
& + \sum_{j\in\wp_i(\alpha_t)} B_{i0} w_{ji}^p(\alpha_t) K_{pj}(\alpha_t)\bar{z}_{pj}(t) + \sum_{\substack{j\in\wp_i(\alpha_t)\\ k\in\wp_j(\alpha_t)}} B_j w_{kj}^p K_{pk}(\alpha_t)\bar{z}_{pk}(t-\tau_{ji}(t))] \\[4pt]
& - h \int_{t-h}^{t} \dot{z}_{pi}^T(s) U_i \dot{\bar{z}}_{pi}(t)\, ds \\[6pt]
\mathcal{L}V_{i4} \;=\;& h \bar{z}_{pi}^T(t) S_i(\alpha_t)\bar{z}_{pi}(t) - \int_{t-h}^{t} \bar{z}_{pi}^T(s) \sum_{k=1}^{M} \pi_{\alpha_t k} S_i(k)\bar{z}_{pi}(s)\, ds
\end{aligned}
$$

Let us define:

$$
\bar{Z}_{pk}(t-\tau) = vec\{\bar{z}_{pk}^T(t-\tau_{ji}(t))\} \quad k\in\wp_j(\alpha_t)
$$

Then the following equations will hold:

$$
B_{ji} K_{ji}(\alpha_t) \bar{Z}_{pj}(t-\tau) = \sum_{j\in\wp_i(\alpha_t)} B_j K_{pj}(\alpha_t)\bar{z}_{pj}(t-\tau_{ji}(t))
$$

$$
B_{kj} W_{kj}(\alpha_t) K_{kj}(\alpha_t) \bar{Z}_{pk}(t-\tau) = \sum_{\substack{j\in\wp_i(\alpha_t)\\ k\in\wp_j(\alpha_t)}} B_j w_{kj}^p(\alpha_t) K_{pk}(\alpha_t)\bar{z}_{pk}(t-\tau_{ji}(t))
$$

Therefore, by adding up $\mathcal{L}V_{i1}$ to $\mathcal{L}V_{i4}$ and considering the above definitions, one can obtain :

$$
\begin{aligned}
\mathcal{L}V_i \;\leq\;&
\begin{bmatrix}
\bar{z}_{pi}^T(t)\\
\bar{Z}_{pj}^T(t)\\
\bar{Z}_{pj}^T(t-\tau)\\
\bar{Z}_{pk}^T(t-\tau)\\
\bar{z}_{pi}^T(t-h)
\end{bmatrix}^T
\Sigma_{ik}(\alpha_t)
\begin{bmatrix}
\bar{z}_{pi}(t)\\
\bar{Z}_{pj}(t)\\
\bar{Z}_{pj}(t-\tau)\\
\bar{Z}_{pk}(t-\tau)\\
\bar{z}_{pi}(t-h)
\end{bmatrix}
+
\begin{bmatrix}
\bar{z}_{pi}^T(t)\\
\bar{Z}_{pj}^T(t)\\
\bar{Z}_{pj}^T(t-\tau)\\
\bar{Z}_{pk}^T(t-\tau)\\
\bar{z}_{pi}^T(t-h)
\end{bmatrix}^T
\Theta_{ik}(\alpha_t) B_{\lambda_i}\lambda_{pi}(t) \\[6pt]
& + h^2 \lambda_{pi}^T(t) B_{\lambda_i}^T U_i B_{\lambda_i}\lambda_{pi}(t) \\[4pt]
\;=\;& \eta_i^T(t,\tau,h)\Sigma_{ik}(\alpha_t)\eta_i(t,\tau,h) + \eta_i^T(t,\tau,h)\Theta_{ik}(\alpha_t) B_{\lambda_i}\lambda_{pi}(t) + h^2 \lambda_{pi}^T(t) B_{\lambda_i}^T U_i B_{\lambda_i}\lambda_{pi}(t) \\[4pt]
\;\leq\;& \eta_i^T(t,\tau,h)[\Sigma_{ik}(\alpha_t) + M_{ik}(\alpha_t)]\eta_i(t,\tau,h) + \lambda_{pi}^T(t) B_{\lambda_i}^T [\Theta_{ik}^T M_{ik}^{-1}\Theta_{ik}(\alpha_t) + h^2 U_i] B_{\lambda_i}\lambda_{pi}(t) \\[4pt]
\;=\;& \eta_i^T(t,\tau,h) W_{ik}(\alpha_t)\eta_i(t,\tau,h) + \lambda_{pi}^T(t)\Psi_{ik}\lambda_{pi}(t) \hspace{4cm} (7.14)
\end{aligned}
$$

where $\eta_i(t,\tau,h) = [\bar{z}_{pi}^T(t)\ \bar{Z}_{pj}^T(t)\ \bar{Z}_{pj}^T(t-\tau)\ \bar{Z}_{pk}^T(t-\tau)\ \bar{z}_{pi}^T(t-h)]^T$; $M_{ik}(\alpha_t)$ is a positive definite matrix, and the matrices Σ_{ik} and Θ_{ik} are defined as:

$$\Sigma_{ik}(\alpha_t) = \begin{bmatrix} \sigma_1 & \sigma_2 & [P_i(\alpha_t)+h^2(A_{ic}^k(\alpha_t))^T U_i]B_{ji}K_{ji}(\alpha_t) & \sigma_3 & U_i \\ * & \sigma_4 & h^2 K_{ji}^T(\alpha_t)W_{ji}^T(\alpha_t)B_{i0}^T U_i B_{ji}K_{ji}(\alpha_t) & \sigma_5 & 0 \\ * & * & h^2 K_{ji}^T(\alpha_t)B_{ji}^T U_i B_{ji}K_{ji}(\alpha_t) & \sigma_6 & 0 \\ * & * & * & \sigma_7 & 0 \\ * & * & * & * & -U_i-(1-h)S_i(\alpha_t) \end{bmatrix}$$

$$\Theta_{ik}(\alpha_t) = \begin{bmatrix} \theta_1 & \theta_2 & \theta_3 & \theta_4 & 0 \end{bmatrix}^T$$

$$W_{ik}(\alpha_t) = \Sigma_{ik}(\alpha_t) + M_{ik}(\alpha_t)$$

$$\Psi_i(\alpha_t) = B_{\lambda_i}^T[\Theta_{ik}^T M_{ik}^{-1}\Theta_{ik}(\alpha_t)+h^2 U_i]B_{\lambda_i}$$

$$\theta_1 = 2P_i(\alpha_t)+2h^2(A_{ic}^k(\alpha_t))^T U_i$$

$$\theta_2 = 2h^2 K_{ji}^T(\alpha_t)W_{ji}^T(\alpha_t)B_{i0}^T U_i$$

$$\theta_3 = 2h^2 K_{ji}^T(\alpha_t)B_{ji}^T U_i$$

$$\theta_4 = 2h^2 K_{kj}^T(\alpha_t)W_{kj}^T(\alpha_t)B_{kj}^T U_i$$

By comparing the matrices $W_{ik}(\alpha_t)$ and $\bar{W}_{ik}(\alpha_t)$, one can see that:

$$W_{ik}(\alpha_t) = \bar{W}_{ik}(\alpha_t) - \begin{bmatrix} Q_i(\alpha_t)+K_{pi}^T(\alpha_t)R_i(\alpha_t)K_{pi}(\alpha_t) & 0 & 0 & 0 & 0 \\ * & K_{ji}^T W_{ji}^T R_i W_{ji}K_{ji} & 0 & 0 & 0 \\ * & * & 0 & 0 & 0 \\ * & * & * & 0 & 0 \\ * & * & * & * & 0 \end{bmatrix}$$

Since $\bar{W}_{ik}(\alpha_t) < 0$, one will have $W_{ik}(\alpha_t) < 0$. From (7.14), it then yields that:

$$\begin{aligned} \mathcal{L}V_i \ \leq\ & -\bar{z}_{pi}^T(t)(Q_i(\alpha_t)+K_{pi}^T(\alpha_t)R_i(\alpha_t)K_{pi}(\alpha_t))\bar{z}_{pi}(t) && (7.15) \\ & -\bar{Z}_{pj}^T K_{ji}^T W_{ji}^T R_i W_{ji}K_{ji}\bar{Z}_{pj}(t)+\lambda_{pi}^T(t)\Psi_i(\alpha_t)\lambda_{pi}(t) \end{aligned}$$

Therefore, for any $[\bar{z}_{pi}(t)\ \bar{Z}_{pj}(t)]$ that satisfies:

$$\begin{bmatrix} \bar{z}_{pi}^T(t) \\ \bar{Z}_{pj}^T(t) \end{bmatrix}^T \underbrace{\begin{bmatrix} Q_i(\alpha_t)+K_{pi}^T(\alpha_t)R_i(\alpha_t)K_{pi}(\alpha_t) & 0 \\ 0 & K_{ji}^T W_{ji}^T R_i W_{ji}K_{ji} \end{bmatrix}}_{\mathbb{C}_{ik}} \begin{bmatrix} \bar{z}_{pi}(t) \\ \bar{Z}_{pj}(t) \end{bmatrix} \geq \Psi_i(\alpha_t)\lambda_{pi}^2(t)$$

one will have $\mathcal{L}V_i < 0$. Therefore, according to the Definition 6.1, the system (7.4) is stochastically ultimate bound and the ultimately bounded region is given by:

$$\|\bar{z}_{pi}(t)\|^2 + \|\bar{Z}_{pj}(t)\|^2 \geq \frac{max(\Psi_i(\alpha_t))}{\lambda_{min}(\mathbb{C}_{ik})}\lambda_{pi}^2(t) \tag{7.16}$$

On the other hand, from (7.15), we have

$$
\begin{aligned}
J_{pi} &= E\{\int_0^\infty (\bar{z}_{pi}^T(t)Q_i(\alpha_t)\bar{z}_{pi}(t) + \bar{u}_{pi}^T(t)R_i(\alpha_t)\bar{u}_{pi})dt\} \\
&= E\{\int_0^\infty (\bar{z}_{pi}^T(t)[Q_i(\alpha_t) + K_{pi}^T(\alpha_t)R_i(\alpha_t)K_{pi}(\alpha_t)]\bar{z}_{pi}(t) + \bar{Z}_{pj}^T(t)K_{ji}^T W_{ji}^T R_i W_{ji}K_{ji}\bar{Z}_{pj}(t)dt\} \\
&\leq E\{\int_0^\infty (-\mathcal{L}V_i + \lambda_{pi}^T(t)\Psi_i(\alpha_t)\lambda_{pi}(t))dt\} \\
&= V_i(\bar{z}_{pi}(0),0,r_0) - \lim_{t\to\infty} V_i(\bar{z}_{pi}(t),t,\alpha_t) + E\{\int_0^\infty \Psi_i(\alpha_t)\lambda_{pi}^2(t)dt\} \\
&\leq V_i(\bar{z}_{pi}(0),0,r_0) - \bar{z}_{pi}^T(\infty)P_i(r_\infty)\bar{z}_{pi}(\infty) + \gamma_i max(\Psi_i(\alpha_t))
\end{aligned}
$$

According to the ultimate bound region of the system (7.16), we have:

$$0 \leq \|\bar{z}_{pi}(\infty)\|^2 \leq \frac{max(\Psi_i(\alpha_t))}{\lambda_{min}(\mathbb{C}_{ik})}(\lambda_{pi}^{max})^2 - \|\bar{Z}_{pj}(\infty)\|^2 \tag{7.17}$$

Therefore, the upper bound of the cost function J_{pi} is

$$J_{pi} < V_i(\bar{z}_{pi}(0),0,r_0) + \gamma_i max(\Psi_i(\alpha_t)) = J_{pi}^* \tag{7.18}$$

From the Definition 6.2, we known that J_{pi}^* is the stochastic guaranteed cost of the system (6.1). This completes the proof of Lemma 7.1. ∎

Lemma 7.1 shows that the distributed controller $\bar{u}_{pi}(t) = K_{pi}(r_t)\bar{z}_{pi}(t) + W_{ji}(\alpha_t)K_{ji}(\alpha_t)\bar{Z}_{pj}(t)$ is a stochastic guaranteed cost controller for the system (7.7). The following lemma gives the expression of the control gain $K_{pi}(\alpha_t)$ and the distributed weights $W_{ji}(\alpha_t)$ for all the modes $\alpha_t \in \mathcal{S}$.

Lemma 7.2. *Given the cost function (7.13), if there exist symmetric positive definite matrices* $\Lambda_{i1}^T(\alpha_t)$, $\bar{X}_{ik}(\alpha_t)$, $\bar{V}_{ii}(\alpha_t)$, $\bar{T}_i(\alpha_t)$, *and matrices* U_i, $N_i(\alpha_t)$, Λ_{i3}^T, *and* $\bar{S}_i(\alpha_t)$ *for* $k = 1, 2$, $i = 1, ...n$, *and* $\alpha_t \in S = \{1, \ldots, M\}$ *such that the following LMI conditions are*

satisfied:

$$
\bar{\Omega}_{ik} = \begin{bmatrix} Y_{ik} & B_{i0}W_{ji} + h^2\bar{W}_{ji} & I + h^2(\bar{V}_{ik} + \bar{T}_i) & I + h^2(\bar{V}_{ik} + \bar{T}_i) \\ * & h^2\tilde{W}_{ji} + \tilde{R}_i & h^2\hat{W}_{ji} & h^2\hat{W}_{ji} \\ * & * & h^2U_i & h^2U_i \\ * & * & * & h^2U_i \end{bmatrix} < 0
$$

$$
Y_{ik} = 2(V_{ik} + T_i) + \sum_{k=1}^{M} \pi_{\alpha_t k}\Lambda_{i1} + h^2\tilde{V}_{ik}(\alpha_t) + (1+h)\bar{S}_i - \bar{U}_i + \bar{Q}_i + \bar{R}_i
$$

then the distributed controller (7.8) is a stochastic guaranteed cost controller of the system

(7.7), and the state feedback control gain is given by $K_{pi}(\alpha_t) = B_{i0}^+ T_i(\alpha_t)\Lambda_{i1}^{-1}(\alpha_t)$.

Proof: Consider the following matrices:

$$\Lambda_{i1}(\alpha_t) = P_i^{-1}(\alpha_t) \qquad\qquad \Lambda_{i2}(\alpha_t) = K_{ji}^+(\alpha_t)$$

$$\Lambda_{i3}(\alpha_t) = [B_{ji}K_{ji}(rt)]^{-1} \qquad \Lambda_{i4}(\alpha_t) = [B_{kj}W_{kj}(\alpha_t)K_{ji}(\alpha_t)]^{-1}$$

$$\Lambda_{i5}(\alpha_t) = 0 \qquad\qquad \Lambda_i(\alpha_t) = diag\{\Lambda_{ij}(\alpha_t)\} \quad j = 1,\dots.5$$

By pre and post multiplying the matrix $\bar{W}_{ik}(\alpha_t)$ with Λ_i^T and Λ_i, respectively, we will obtain:

$$
\Omega_{ik}(\alpha_t) = \Lambda_i^T(\alpha_t)\bar{W}_{ik}(\alpha_t)\Lambda_i(\alpha_t) = \begin{bmatrix} \bar{\Omega}_{ik} & 0 \\ 0 & 0 \end{bmatrix} \tag{7.19}
$$

where:

$$
\bar{\Omega}_{ik} = \begin{bmatrix} X_{ik} & B_{i0}W_{ji} + h^2A_{ic}^k U_i B_{i0}W_{ji} & I + h^2A_{ic}^k U_i & I + h^2A_{ic}^k U_i \\ * & h^2W_{ji}^T B_{i0}^T U_i B_{i0}W_{ji} + W_{ji}^T R_i W_{ji} & h^2W_{ji}^T B_{i0}^T U_i & h^2W_{ji}^T B_{i0}^T U_i \\ * & * & h^2U_i & h^2U_i \\ * & * & * & h^2U_i \end{bmatrix}
$$

$$
\begin{aligned}
X_{ik} =\ & 2A_{ic}^k\Lambda_{i1} + \sum_{k=1}^{M} \pi_{\alpha_t k}\Lambda_{i1} + h^2\Lambda_{i1}^T(A_{ic}^k)^T U_i A_{ic}^k \Lambda_{i1} + (1+h)\Lambda_{i1}^T S_i \Lambda_{i1} \\
& -\Lambda_{i1}^T U_i \Lambda_{i1} + \Lambda_{i1}^T(Q_i + K_{pi}^T R_i K_{pi})\Lambda_{i1}
\end{aligned}
$$

Therefore, if we define:

$$A_{i0}^k(\alpha_t) = V_{ik}(\alpha_t)\Lambda_{i1}^{-1}(\alpha_t) \qquad B_{i0}K_{pi}(\alpha_t) = T_i(\alpha_t)\Lambda_{i1}^{-1}(\alpha_t)$$

$$\bar{V}_{ik}(\alpha_t) = V_{ik}^T(\alpha_t)U_i \qquad\qquad \bar{T}_i^T(\alpha_t) = T_i^T(\alpha_t)U_i$$

$$\bar{R}_i = \Lambda_{i1}^T K_{pi}^T R_i K_{pi}\Lambda_{i1} \qquad\qquad \tilde{R}_i = W_{ji}^T R_i W_{ji}$$

$$\bar{W}_{ji} = A_{ic}^k U_i B_{i0} W_{ji} \qquad\qquad \hat{W}_{ji} = W_{ji}^T B_{i0}^T U_i$$

$$\tilde{W}_{ji} = \hat{W}_{ji} B_{i0} W_{ji} \qquad\qquad \bar{S}_i = \Lambda_{i1}^T S_i \Lambda_{i1}$$

$$\bar{Q}_i = \Lambda_{i1}^T Q_i \Lambda_{i1} \qquad\qquad \bar{U}_i = \Lambda_{i1}^T U_i \Lambda_{i1}$$

$$\tilde{V}_{ik}(\alpha_t) = (\bar{V}_{ik}(\alpha_t) + \bar{T}_i^T(\alpha_t))(V_{ik}(\alpha_t) + T_i(\alpha_t))$$

then, the matrix $\bar{\Omega}_{ik}(\alpha_t)$ will becomes:

$$\bar{\Omega}_{ik} = \begin{bmatrix} Y_{ik} & B_{i0}W_{ji} + h^2 \bar{W}_{ji} & I + h^2(\bar{V}_{ik} + \bar{T}_i) & I + h^2(\bar{V}_{ik} + \bar{T}_i) \\ * & h^2 \tilde{W}_{ji} + \tilde{R}_i & h^2 \hat{W}_{ji} & h^2 \hat{W}_{ji} \\ * & * & h^2 U_i & h^2 U_i \\ * & * & * & h^2 U_i \end{bmatrix}$$

$$Y_{ik} = 2(V_{ik} + T_i) + \sum_{k=1}^{M} \pi_{\alpha_t k} \Lambda_{i1} + h^2 \tilde{V}_{ik}(\alpha_t) + (1+h)\bar{S}_i - \bar{U}_i + \bar{Q}_i + \bar{R}_i$$

Therefore, if $\bar{\Omega}_{ik}(\alpha_t) < 0$, one will have $\Omega_{ik} < 0$, and hence $\bar{W}_{ik} < 0$. Furthermore, by solving the LMI conditions $\bar{\Omega}_{ik}(\alpha_t) < 0$, the weight matrix $W_{ji}(\alpha_t)$ can be obtained directly. The state feedback control gain $K_{pi}(\alpha_t)$ and the system matrix A_{i0}^k can be expressed as follows:

$$K_{pi}(\alpha_t) = B_{i0}^+ T_i(\alpha_t) \Lambda_{i1}^{-1}(\alpha_t)$$

$$A_{i0}^k(\alpha_t) = V_{ik}(\alpha_t) \Lambda_{i1}^{-1}(\alpha_t)$$

This completes the proof of Lemma 7.2. ∎

7.1.1 Stability Analysis

Lemmas 7.1 and 7.2 show that the distributed congestion control law is a stochastic guaranteed cost controller of the premium traffic in a mobile network. It should be noted that the ultimate bound region (7.16) is a hyper surface defined by the state space of the node $\bar{z}_{pi}(t)$ and the state space of its nearest neighboring nodes $\bar{Z}_{pj}(t) \in \wp_i(\alpha_t)$. That is, by applying the distributed congestion control strategy, the queuing errors of the nodes that are in the same neighboring set are guaranteed to be uniformly ultimately bounded, simultaneously.

Furthermore, the stability conditions in Lemmas 7.1 and 7.2 are dependent on the

Markovian jump process α_t. Therefore, at each time when the network topology changes, one needs to recalculate the control gain $K_{pi}(\alpha_t)$ and the weight matrix $W_{ji}(\alpha_t)$ again.

Stability Conditions Incorporating The Physical Constraints

The LMI conditions associated with the physical constraints for the guaranteed cost congestion controller (GCC) of fixed network, as given in Section 5.2.2, are now extended to the mobile networks.

- **Constraints of the states**

  The constraints of the states for node i incurred by the buffer size limitation are given as follows:

  $$\bar{z}_{pi}^{min} \leq \bar{z}_{pi}(t) \leq \bar{z}_{pi}^{max} \tag{7.20}$$

  where $\bar{z}_{pi}^{min} = -x_{pi}^{ref}$ and $\bar{z}_{pi}^{max} = x_{pi}^{buffer} - x_{pi}^{ref}$.

  Consider the following ellipsoid for a selected number $\varepsilon_i > 0$

  $$\mathbb{F}_i = \{\bar{z}_{pi}(t) | \bar{z}_{pi}^T \tilde{P}_{ir}^{-1} \bar{z}_{pi} \leq \epsilon_i\} \tag{7.21}$$

  By following along the similar lines as that given previously in Section 5.2.2, and the definition of non-negative systems as given in Definition 5.1, the state constraint (7.20) will be satisfied if the matrices $V_{ik}(\alpha_t)$ and $T_i(\alpha_t)$ in (7.20) satisfy the following conditions:

  $$
  \begin{aligned}
  V_{ik}(\alpha_t) &= \begin{bmatrix} V_{ik}^1(\alpha_t) & V_{ik}^2(\alpha_t) \\ V_{ik}^3(\alpha_t) & V_{ik}^4(\alpha_t) \end{bmatrix} \\
  V_{i1}^1(\alpha_t) &= V_{i2}^1(\alpha_t) = 0 \\
  V_{i1}^2(\alpha_t) &= V_{i2}^2(\alpha_t) = 0 \\
  V_{i2}^3(\alpha_t) &= 0 \\
  V_{i1}^3(\alpha_t) &> 0 \text{ and is diagonal} \\
  V_{i1}^4(\alpha_t) &= V_{i2}^4(\alpha_t) < 0 \text{ and is diagonal}
  \end{aligned}
  $$

and the following LMI conditions hold:

$$\Omega_{c1i} \triangleq \gamma_i max(\Psi_i(\alpha_t)) \leq \epsilon_i \tag{7.22}$$

$$\Omega_{c2i} \triangleq \begin{bmatrix} \tilde{P}_{ir} & \tilde{P}_{ir}^T \\ \tilde{P}_{ir} & \|\bar{z}_{pi}^{max}\|^2/\epsilon_i \end{bmatrix} \geq 0 \tag{7.23}$$

$$\Omega_{c3i} \triangleq (T_i(\alpha_t))_{ij} \geq 0 \qquad i, j = 1, ...2n \tag{7.24}$$

where λ_{pi} is adopted from the transmission constraints of the node i, which indicates the maximum allowable external incoming traffic of the premium class.

- **Constraints of the input**

The input constraint of each node i can be defined as follows

$$0 \leq \bar{u}_{pi}(t) \leq C_{server,i}(\alpha_t) \tag{7.25}$$

By following along the similar lines as that given previously in Section 5.2.2, and considering the same ellipsoid as defined in (7.21), the right hand side of the input constraint (7.25) can be expressed by the following LMI conditions

$$\Omega_{c4i} \triangleq \begin{bmatrix} I & K_i^T \\ K_i & (C_{server,i}^2(\alpha_t)/\epsilon_i)\tilde{P}_{ir} \end{bmatrix} \geq 0$$

$$\Omega_{c5i} \triangleq (V_i^{-1})_{ij} \geq 0 \tag{7.26}$$

The non-negative constraint of the input $\bar{u}_{pi}(t)$ can be ensured if the control gain $K_{pi}(\alpha_t) > 0$. Noting that the control gain $K_{pi} = B_{i0}^+ T_i \Lambda_{i1}^{-1}$, then by setting the matrix Λ_{i1}^{-1} to be a diagonal positive definite, the non-negative side of the input constraint (6.50) can now be expressed by the following LMI conditions:

$$\Omega_{c6i} = (B_{i0}^+ T_i)_{ij} \geq 0, \qquad i, j = 1, ..., n \tag{7.27}$$

Therefore, the above results, as well as the LMI conditions that are given in Lemma 6.2 can be summarized by the following theorem.

Theorem 7.1. *The distributed guaranteed cost congestion controller (DGCC) for the premium traffic in a mobile network can be obtained according to*

305

$$\bar{u}_{pi} = K_{pi}(\alpha_t)\bar{z}_{pi} + W_{ji}(\alpha_t)K_{ji}(\alpha_t)\bar{Z}_{pj}(t) \qquad (7.28)$$

if the LMI conditions that are given in Lemma 7.2 subject to the positive definite diagonal matrix $\Lambda_{i1}^{-1}(\alpha_t)$ and the LMI conditions Ω_{c1i}, Ω_{c2i}, Ω_{c3i}, Ω_{c4i}, Ω_{c5i} and Ω_{c6i}, for $i = 1, ...n$, $k = 1, 2$, $\alpha_t \in \mathcal{S} = \{1, ..., M\}$, as given in (7.22) to (7.27), respectively, are satisfied.

Proof: Follows along the same lines as that is the derivations in Lemma 7.1, Lemma 7.2, and the above analysis for the physical constraints. ∎

7.2 Distributed Guaranteed Cost Congestion Control (DGCC) for the Ordinary Traffic Class

The control objective for the ordinary traffic is to regulate the incoming traffic $\lambda_{ri}(t)$ and the link capacity $C_{ri}(t)$ so that the queueing length $x_{ri}(t)$ is as close as possible to the reference set point x_{ri}^{ref}. Let us re-write the dynamic queuing model of the ordinary traffic in a mobile network as follows:

$$\dot{x}_{ri}(t) = -f(x_{ri}, r)u_{ri}^1(t) + u_{ri}^2(t) + \sum_{j \in \wp_i(\alpha_t)} f(x_{rj}(t - \tau_{ji}(t)))u_{rj}^1(t - \tau_{ji}(t))g_{ji}^r(t) \quad (7.29)$$

Let us define the input vector of the ordinary traffic $u_{ri} = [u_{ri}^1, u_{ri}^2]^T$, and the nonlinear matrix $F(x_{ri}(t)) = diag\{f(x_{ri}(t)), 1\}$. The dynamical system (7.29) can be transformed into an equivalent linear system through the application of the following input-state feedback transformations:

$$z_{ri}(t) = x_{ri}(t) - x_{ri}^{ref} \qquad (7.30)$$

$$u_{ri}(t) = F^{-1}(x_{ri}, t)\bar{u}_{ri} \qquad (7.31)$$

where x_{ri}^{ref} is the reference set point of the queuing length at node i. The above equations imply that $u_{ri}^1 = f^{-1}(x_{ri}, t)\bar{u}_{ri}^1$ and $u_{ri}^2 = \bar{u}_{ri}^2$. Therefore, the nonlinear dynamics (7.29) becomes

$$\begin{aligned}
\dot{z}_{ri}(t) &= -\bar{u}_{ri}^1(t) + \bar{u}_{ri}^2(t) + \sum_{j \in \wp_i(\alpha_t)} \bar{u}_{rj}^1(t - \tau_{ji}(t))g_{ji}^r(t) \\
&= B_{i0}\bar{u}_{ri}(t) + \sum_{j \in \wp_i(\alpha_t)} B_{ij}\bar{u}_{rj}(t - \tau_{ji}(t)) \qquad (7.32)
\end{aligned}$$

306

where $B_{i0} = \begin{bmatrix} -1 & 1 \end{bmatrix}^T$, $B_{ij} = \begin{bmatrix} g_{ji}^r & 0 \end{bmatrix}^T$. Based on the decentralized model (7.32), the distributed congestion controller for the ordinary traffic is selected as follows:

$$\bar{u}_{ri}(t) = \bar{u}_{ri}^{de}(t) + \sum_{j \in \wp_i(\alpha_t)} w_{ji}^r \bar{u}_{rj}^{de}(t) \tag{7.33}$$

$$\bar{u}_{ri}^{de}(t) = K_{ri} z_{ri}(t)$$

Therefore the distributed congestion controller of the ordinary traffic can be written as

$$\bar{u}_{ri}(t) = K_{ri}(\alpha_t) z_{ri}(t) + W_{ji}(\alpha_t) K_{ji}(\alpha_t) Z_{rj}(t) \tag{7.34}$$

where $W_{ji}(\alpha_t) = vec\{w_{ji}^r(\alpha_t)\}$ and $K_{ji}(\alpha_t) = diag\{K_{ri}(\alpha_t)\}$.

Therefore, the control objective for the ordinary traffic is to select the distributed control gain $K_{ri}(\alpha_t)$ and the distributed weight matrix W_{ji} such that the system (7.32) is stochastically stable and the following cost function is upper bounded:

$$J_{ri} = E\{ \int_0^\infty (z_{ri}^T(t) Q_i(\alpha_t) z_{ri}(t) + \bar{u}_{ri}^T(t) R_i(\alpha_t) \bar{u}_{ri}(t)) dt \} \tag{7.35}$$

where $Q_i(\alpha_t)$ and $R_i(\alpha_t)$ are given positive definite matrices.

Lemma 7.3. *Given the cost function (7.35) and under Assumption 5.2, the state feedback control law (7.38) is the stochastic guaranteed cost controller for the system (7.32), if there exist symmetric positive definite matrices $\Lambda_{i1}(\alpha_t)$, $\bar{S}_i(\alpha_t)$, U_i, $\bar{U}_i$, $\bar{Q}_i(\alpha_t)$, $\bar{R}_i(\alpha_t)$, positive definite matrices $T_i(\alpha_t)$, $\tilde{T}_i(\alpha_t)$, $\bar{W}_{ji}(\alpha_t)$, $\hat{W}_{ji}(\alpha_t)$, and $W_{ji}(\alpha_t)$, for $i = 1, ..., n$, $\alpha_t \in \mathcal{S} = \{1, ...M\}$, such that the following LMI conditions are satisfied:*

$$\Sigma_i(\alpha_t) = \begin{bmatrix} \sigma_1 + Q_i(\alpha_t) + K_i^T(\alpha_t) R_i(\alpha_t) K_i(\alpha_t) & \sigma_2 \\ * & \sigma_4 + +K_{ji}^T(\alpha_t) W_{ji}^T(\alpha_t) R_i W_{ji}(\alpha_t) K_{ji}(\alpha_t) \\ * & * \\ * & * \\ * & * \end{bmatrix}$$

$$\begin{bmatrix} [P_i(\alpha_t) + h^2 (B_{i0} K_{ri}(\alpha_t))^T U_i] B_{ji} K_{ji}(\alpha_t) & \sigma_3 & U_i \\ h^2 K_{ji}^T(\alpha_t) W_{ji}^T(\alpha_t) B_{i0}^T U_i B_{ji} K_{ji}(\alpha_t) & \sigma_5 & 0 \\ h^2 K_{ji}^T(\alpha_t) B_{ji}^T U_i B_{ji} K_{ji}(\alpha_t) & \sigma_6 & 0 \\ * & \sigma_7 & 0 \\ * & * & -U_i - (1-h) S_i(\alpha_t) \end{bmatrix} < 0 \tag{7.36}$$

307

where

$$
\begin{aligned}
\sigma_1 &= 2P_i(\alpha_t)B_{i0}K_{ri}(\alpha_t) + \sum_{k=1}^{M}\pi_{\alpha_t k}P_i(k) + h^2 K_{ri}^T(\alpha_t)B_{i0}^T U_i B_{i0}K_{ri}(\alpha_t) \\
&\quad + (1+h)S_i(\alpha_t) - U_i \\[4pt]
\sigma_2 &= P_i(\alpha_t)B_{i0}W_{ji}(\alpha_t)K_{ji}(\alpha_t) + h^2 K_{ri}^T B_{i0}^T U_i B_{i0}W_{ji}(\alpha_t)K_{ji}(\alpha_t) \\[4pt]
\sigma_3 &= [P_i(\alpha_t) + h^2 K_{ri}^T B_{i0}^T U_i]B_{kj}W_{kj}(\alpha_t)K_{kj}(\alpha_t) \\[4pt]
\sigma_4 &= h^2 K_{ji}^T(\alpha_t)W_{ji}^T(\alpha_t)B_{i0}^T U_i B_{i0}W_{ji}(\alpha_t)K_{ji}(\alpha_t) \\[4pt]
\sigma_5 &= h^2 K_{ji}^T(\alpha_t)W_{ji}^T(\alpha_t)B_{i0}^T U_i B_{kj}W_{kj}(\alpha_t)K_{kj}(\alpha_t) \\[4pt]
\sigma_6 &= h^2 K_{ji}^T(\alpha_t)B_{ji}^T U_i B_{kj}W_{kj}(\alpha_t)K_{kj}(\alpha_t) \\[4pt]
\sigma_7 &= h^2 K_{kj}^T(\alpha_t)W_{kj}^T(\alpha_t)B_{kj}^T U_i B_{kj}W_{kj}(\alpha_t)K_{kj}(\alpha_t)
\end{aligned}
$$

Proof: Consider the following stochastic Lyapunov-Krosovskii functional candidate:

$$V_i(\bar{z}_{ri}(t), \alpha_t) = V_{i1} + V_{i2} + V_{i3} + V_{i4}$$

$$V_{i1} = \bar{z}_{ri}(t)^T P_i(\alpha_t)z_{ri}(t)$$

$$V_{i2} = \int_{t-h}^{t} z_{ri}^T(s)S_i(\alpha_t)z_{ri}(s)ds$$

$$V_{i3} = h\int_{-h}^{0}\int_{t+\theta}^{t} \dot{z}_{ri}^T(s)U_i\dot{z}_{ri}(s)dsd\theta$$

$$V_{i4} = \int_{-h}^{0}\int_{t+\theta}^{t} z_{ri}^T(s)S_i(\alpha_t)z_{ri}(s)dsd\theta$$

and $P_i(\alpha_t)$, $S_i(\alpha_t)$, U_i are positive definite matrices with appropriate dimensions. For each mode $\alpha_t = k \in \mathcal{S}$, the infinitesimal generator of the Lyapunov function can then be derived as follows:

$$
\begin{aligned}
\mathcal{L}V_{i1} &= \lim_{\Delta\to 0^+}\frac{1}{\Delta}\{E[V_{i1}(z_{ri}(t+\Delta), \alpha_{t+\delta}, t+\Delta)|z_{ri}(t), \alpha_t = k] - V_{i1}(z_{ri}(t), k, t)\} \\
&= 2z_{ri}^T(t)P_i(\alpha_t)\dot{z}_{ri}(t) + \sum_{k=1}^{M}\pi_{\alpha_t k}z_{ri}^T(t)P_i(k)z_{ri}(t) \\
&= 2z_{ri}^T(t)P_i(\alpha_t)[B_{i0}K_{ri}(\alpha_t)z_{ri}(t) + \sum_{j\in\wp_i(\alpha_t)}B_j K_{rj}(\alpha_t)z_{rj}(t-\tau_{ji}(t)) \\
&\quad + \sum_{j\in\wp_i(\alpha_t)}B_{i0}w_{ji}^p(\alpha_t)K_{rj}(\alpha_t)z_{rj}(t) + \sum_{\substack{j\in\wp_i(\alpha_t) \\ k\in\wp_j(\alpha_t)}}B_j w_{kj}^p K_{rk}(\alpha_t)z_{rk}(t-\tau_{ji}(t))] \\
&\quad + z_{ri}^T(t)\sum_{k=1}^{M}\pi_{\alpha_t k}P_i(k)z_{ri}(t)
\end{aligned}
$$

$$
\begin{aligned}
\mathcal{L}V_{i2} &= \int_{t-h}^{t} 2z_{ri}^{T}(s)S_i(\alpha_t)\dot{z}_{pi}(s)ds + \int_{t-h}^{t} z_{ri}^{T}(s)\sum_{k=1}^{M}\pi_{\alpha_t k}S_i(k)z_{ri}(s)ds \\
&= z_{ri}^{T}(t)S_i(\alpha_t)z_{ri}(t) - (1-h)z_{ri}^{T}(t-h)S_i(\alpha_t)z_{ri}(t-h) \\
&\quad + \int_{t-h}^{t} z_{ri}^{T}(s)\sum_{k=1}^{M}\pi_{\alpha_t k}S_i(k)z_{ri}(s)ds \\
\mathcal{L}V_{i3} &= h^2\dot{z}_{ri}^{T}(t)U_i\dot{z}_{ri}(t) - h\int_{t-h}^{t}\dot{z}_{ri}^{T}(s)U_i\dot{z}_{ri}(s)ds \\
&= h^2[B_{i0}K_{ri}(\alpha_t)z_{ri}(t) + \sum_{j\in\wp_i(\alpha_t)} B_j K_{rj}(\alpha_t)z_{rj}(t-\tau_{ji}(t)) \\
&\quad + \sum_{j\in\wp_i(\alpha_t)} B_{i0}w_{ji}^{p}(\alpha_t)K_{rj}(\alpha_t)z_{rj}(t) + \sum_{\substack{j\in\wp_i(\alpha_t)\\k\in\wp_j(\alpha_t)}} B_j w_{kj}^{p}K_{rk}(\alpha_t)z_{rk}(t-\tau_{ji}(t))]^T U_i \\
&\quad [B_{i0}K_{ri}(\alpha_t)z_{ri}(t) + \sum_{j\in\wp_i(\alpha_t)} B_j K_{rj}(\alpha_t)z_{rj}(t-\tau_{ji}(t)) \\
&\quad + \sum_{j\in\wp_i(\alpha_t)} B_{i0}w_{ji}^{p}(\alpha_t)K_{rj}(\alpha_t)z_{rj}(t) + \sum_{\substack{j\in\wp_i(\alpha_t)\\k\in\wp_j(\alpha_t)}} B_j w_{kj}^{p}K_{rk}(\alpha_t)z_{rk}(t-\tau_{ji}(t))] \\
&\quad - h\int_{t-h}^{t}\dot{z}_{ri}^{T}(s)U_i\dot{z}_{ri}(t)ds \\
\mathcal{L}V_{i4} &= hz_{ri}^{T}(t)S_i(\alpha_t)z_{ri}(t) - \int_{t-h}^{t} z_{ri}^{T}(s)\sum_{k=1}^{M}\pi_{\alpha_t k}S_i(k)z_{ri}(s)ds
\end{aligned}
$$

Let us define that:

$$
Z_{rk}(t-\tau) = vec\{\bar{z}_{rk}^{T}(t-\tau_{ji}(t))\} \quad k\in\wp_j(\alpha_t)
$$

$$
B_{ji}K_{ji}(\alpha_t)z_{rj}(t-\tau) = \sum_{j\in\wp_i(\alpha_t)} B_j K_{rj}(\alpha_t)z_{rj}(t-\tau_{ji}(t))
$$

$$
B_{kj}W_{kj}(\alpha_t)K_{kj}(\alpha_t)z_{rk}(t-\tau) = \sum_{\substack{j\in\wp_i(\alpha_t)\\k\in\wp_j(\alpha_t)}} B_j w_{kj}^{p}(\alpha_t)K_{rk}(\alpha_t)z_{rk}(t-\tau_{ji}(t))
$$

Therefore, by adding up $\mathcal{L}V_{i1}$ to $\mathcal{L}V_{i4}$ and considering the above definitions, one can obtain

$$
\mathcal{L}V_i \leq \eta_i^{T}(t,\tau,h)\Sigma_i(\alpha_t)\eta_i(t,\tau,h) \tag{7.37}
$$

where $\eta_i(t,\tau,h) = [z_{ri}^{T}(t)\ \bar{Z}_{rj}^{T}(t)\ \bar{Z}_{rj}^{T}(t-\tau)\ \bar{Z}_{rk}^{T}(t-\tau)\ z_{ri}^{T}(t-h)]^{T}$, and Σ_i is given by

$$\Sigma_i(\alpha_t) = \begin{bmatrix} \sigma_1 & \sigma_2 & [P_i(\alpha_t) + h^2(B_{i0}K_{ri}(\alpha_t))^T U_i]B_{ji}K_{ji}(\alpha_t) & \sigma_3 & U_i \\ * & \sigma_4 & h^2 K_{ji}^T(\alpha_t)W_{ji}^T(\alpha_t)B_{i0}^T U_i B_{ji}K_{ji}(\alpha_t) & \sigma_5 & 0 \\ * & * & h^2 K_{ji}^T(\alpha_t)B_{ji}^T U_i B_{ji}K_{ji}(\alpha_t) & \sigma_6 & 0 \\ * & * & * & \sigma_7 & 0 \\ * & * & * & * & -U_i - (1-h)S_i(\alpha_t) \end{bmatrix}$$

Since $\bar{\Sigma}_{ik}(\alpha_t) < 0$ one will have

$$\Sigma_i(\alpha_t) = \bar{\Sigma}_{ik}(\alpha_t) - \begin{bmatrix} Q_i + K_i^T R_i K_i & 0 \\ 0 & K_{ji}^T W_{ji}^T R_i W_{ji} K_{ji} \end{bmatrix} < 0 \tag{7.38}$$

hence $\mathcal{L}V_i < 0$. According to the Definition 6.1, the system (7.32) is stochastically stable. Moreover, from (7.37) and (7.38) we also have

$$\mathcal{L}V_i \leq -z_{ri}^T[Q_i + K_{ri}^T R_i K_{ri}]z_{ri} - Z_{rj}^T(t)K_{ji}^T W_{ji}^T R_i W_{ji} K_{ji} Z_{rj}(t)) < 0 \tag{7.39}$$

According the the cost function (7.35), one will obtain

$$\begin{aligned} J_{ri} &= E\{\int_0^\infty (z_{ri}^T Q_i z_{ri} + \bar{u}_{ri}^T R_i \bar{u}_{ri})dt\} \\ &= E\{\int_0^\infty (z_{ri}^T[Q_i + K_{ri}^T R_i K_{ri}]z_{ri} + Z_{rj}^T(t)K_{ji}^T W_{ji}^T R_i W_{ji} K_{ji} Z_{rj}(t))dt\} \\ &\leq -E\int_0^\infty \mathcal{L}V_i dt \\ &= V(z_{ri}(0), 0, r_0) = J_{ri}^* \end{aligned} \tag{7.40}$$

Therefore, according to the Definition 6.2, the scaler J_{ri}^* is the stochastic guaranteed cost of the system (7.32). This completes the proof of Lemma 7.3. ∎

Lemma 7.4. *Given the cost function (7.35), the distributed controller (7.33) is the stochastic guaranteed cost controller for the system (7.32), if there exist symmetric positive definite matrices $\Lambda_{i1}(\alpha_t)$, $\bar{S}_i(\alpha_t)$, U_i, $\bar{U}_i$, $\bar{Q}_i(\alpha_t)$, $\bar{R}_i(\alpha_t)$, positive definite matrices $T_i(\alpha_t)$, $\tilde{T}_i(\alpha_t)$, $\bar{W}_{ji}(\alpha_t)$, $\hat{W}_{ji}(\alpha_t)$, and $W_{ji}(\alpha_t)$, for $i = 1, ..., n$, $\alpha_t \in \mathcal{S} = \{1, ...M\}$, such that the following LMI conditions are satisfied:*

$$\tilde{\Sigma}_{ik}(\alpha_t) = \begin{bmatrix} Y_{ik} & B_{i0}W_{ji} + h^2\bar{W}_{ji} & I + h^2\bar{T}_i & I + h^2\bar{T}_i \\ * & h^2\tilde{W}_{ji} & h^2\hat{W}_{ji} & h^2\hat{W}_{ji} \\ * & * & h^2U_i & h^2U_i \\ * & * & * & h^2U_i \end{bmatrix} < 0$$

$$Y_{ik} = 2T_i(\alpha_t) + \sum_{k=1}^{M}\pi_{\alpha_t k}\Lambda_{i1} + h^2\tilde{T}_i(\alpha_t) + (1+h)\bar{S}_i - \bar{U}_i + \bar{Q}_i + \bar{R}_i$$

and the distributed control gain is given by $K_{ri}(\alpha_t) = B_{i0}^{+}T_i(\alpha_t)\Lambda_{i1}^{-1}(\alpha_t)$.

Proof: Regarding the nonlinear matrix inequality condition (7.38), let us define

$$\Lambda_{i1}(\alpha_t) = P_i^{-1}(\alpha_t) \qquad \Lambda_{i2}(\alpha_t) = K_{ji}^{+}(\alpha_t)$$

$$\Lambda_{i3}(\alpha_t) = [B_{ji}K_{ji}(rt)]^{-1} \qquad \Lambda_{i4}(\alpha_t) = [B_{kj}W_{kj}(\alpha_t)K_{ji}(\alpha_t)]^{-1}$$

$$\Lambda_{i5}(\alpha_t) = 0 \qquad \Lambda_i(\alpha_t) = diag\{\Lambda_{ij}(\alpha_t)\} \quad j = 1,....5$$

By pre and post multiplying the matrix $\Sigma_i(\alpha_t)$ with Λ_i^T and Λ_i, respectively, one will obtain

$$\bar{\Sigma}_{ik}(\alpha_t) = \Lambda_i^T(\alpha_t)\Sigma_i(\alpha_t)\Lambda_i(\alpha_t) = \begin{bmatrix} \tilde{\Sigma}_{ik} & 0 \\ 0 & 0 \end{bmatrix} \tag{7.41}$$

where:

$$\tilde{\Sigma}_{ik} = \begin{bmatrix} X_{ik} & B_{i0}W_{ji} + h^2B_{i0}K_{ri}U_iB_{i0}W_{ji} & I + h^2B_{i0}K_{ri}U_i & I + h^2B_{i0}K_{ri}U_i \\ * & h^2W_{ji}^TB_{i0}^TU_iB_{i0}W_{ji} + W_{ji}^TR_iW_{ji} & h^2W_{ji}^TB_{i0}^TU_i & h^2W_{ji}^TB_{i0}^TU_i \\ * & * & h^2U_i & h^2U_i \\ * & * & * & h^2U_i \end{bmatrix}$$

$$X_{ik} = 2B_{i0}K_{ri}\Lambda_{i1} + \sum_{k=1}^{M}\pi_{\alpha_t k}\Lambda_{i1} + h^2\Lambda_{i1}^T(B_{i0}K_{ri})^TU_iB_{i0}K_{ri}\Lambda_{i1} + (1+h)\Lambda_{i1}^TS_i\Lambda_{i1}$$
$$-\Lambda_{i1}^TU_i\Lambda_{i1} + \Lambda_{i1}^T(Q_i + K_{pi}^TR_iK_{pi})\Lambda_{i1}$$

Therefore, if we define

$$B_{i0}K_{ri}(\alpha_t) = T_i(\alpha_t)\Lambda_{i1}^{-1}(\alpha_t) \qquad \bar{T}_i^T(\alpha_t) = T_i^T(\alpha_t)U_i$$

$$\bar{W}_{ji} = B_{i0}K_{ri}U_iB_{i0}W_{ji} \qquad \hat{W}_{ji} = W_{ji}^TB_{i0}^TU_i$$

$$\tilde{W}_{ji} = \hat{W}_{ji}B_{i0}W_{ji} \qquad \bar{R}_i = \Lambda_{i1}^TK_{pi}^TR_iK_{pi}\Lambda_{i1}$$

$$\bar{S}_i = \Lambda_{i1}^TS_i\Lambda_{i1} \qquad \bar{U}_i = \Lambda_{i1}^TU_i\Lambda_{i1}$$

$$\bar{Q}_i = \Lambda_{i1}^TQ_i\Lambda_{i1} \qquad \tilde{T}_i(\alpha_t) = \bar{T}_i^T(\alpha_t)T_i(\alpha_t))$$

then, the matrix $\tilde{\Sigma}_{ik}(\alpha_t)$ becomes

$$\tilde{\Sigma}_i(\alpha_t) = \begin{bmatrix} Y_{ik} & B_{i0}W_{ji} + h^2\bar{W}_{ji} & I + h^2\bar{T}_i & I + h^2\bar{T}_i \\ * & h^2\tilde{W}_{ji} & h^2\hat{W}_{ji} & h^2\hat{W}_{ji} \\ * & * & h^2 U_i & h^2 U_i \\ * & * & * & h^2 U_i \end{bmatrix}$$

$$Y_{ik} = 2T_i + \sum_{k=1}^{M} \pi_{\alpha_t k}\Lambda_{i1} + h^2\tilde{T}_i(\alpha_t) + (1+h)\bar{S}_i - \bar{U}_i + \bar{Q}_i + \bar{R}_i$$

Therefore, if $\tilde{\Sigma}_i(\alpha_t) < 0$, one will have $\Sigma_i(\alpha_t) < 0$, and the system (7.32) is stochastically stable. By solving the LMI conditions $\bar{\Omega}_{ik}(\alpha_t) < 0$, the weight matrix $\tilde{\Sigma}_{ik}(\alpha_t) < 0$, one can obtain that:

$$K_{ri}(\alpha_t) = B_{i0}^+ T_i(\alpha_t)\Lambda_{i1}^{-1}(\alpha_t)$$

This completes the proof of Lemma 7.4. ∎

7.2.1 Stability Analysis

Lemma 7.3 shows that the distributed congestion control law is a stochastic guaranteed cost controller for the ordinary traffic in a mobile network. Due to the nodes mobility, the network topology is time-varying in a mobile network, hence the stability conditions in Lemma 7.3 and the distributed control gains are now mode-dependent. Therefore, similar to the premium traffic controller, at each time when the network topology is changed one needs to re-calculate the distributed control gain $K_{ri}(\alpha_t)$ and the distributed weights $w_{ji}^r(\alpha_t)$, and the distributed controller $\bar{u}_{ri}(t)$ needs to be updated for the new network conditions.

Moreover, since the external incoming traffic of the ordinary traffic $\lambda_{ri}(t)$ is considered as an input in the guaranteed cost control approach, the distributed congestion control strategy can guarantee the stability of the ordinary traffic of each node as well as its nearest neighbors, simultaneously.

Stability Conditions Incorporating The Physical Constraints

The physical constraints of the ordinary traffic in a mobile network are listed as

$$z_{ri}^{min} \leq z_r(t) \leq z_{ri}^{max} \tag{7.42}$$

$$0 \leq \bar{u}_{ri}(t) \leq c_{ri}(\alpha_t) \tag{7.43}$$

where $z_{ri}^{maz} = x_{ri}^{buffer} - x_{ri}^{ref}$, $z_{ri}^{min} = -x_{ri}^{ref}$, x_{ri}^{ref} is the reference set point of the queuing length, $c_{ri}(\alpha_t)$ is the maximum allowable bandwidth that can be allocated to the ordinary traffic at node i which in fact is equal to the instantaneous leftover capacity from the premium traffic $c_{ri}(t) = C_{server,i}(\alpha_t) - \bar{u}_{pi}(t)$.

To avoid any confusions, in the remainder of this section, we utilize the notations of P_{pi} and P_{ri} to denote the Lyapunov matrices $P_i(\alpha_t)$ that are used in Lemma 6.1 for the premium traffic, and the other matrices $P_i(\alpha_t)$ that are used in Lemma 6.3 for the ordinary traffic, respectively.

Consider the following ellipsoid

$$\mathbb{S}_i = \{z_{ri}^T (\tilde{P}_{ri})^{-1}(\alpha_t) z_{ri} < \rho_i\} \tag{7.44}$$

where $\rho_i > 0$ is a selected constant.

Now, it follows along the lines similar to deriving the LMI conditions for the physical constraints in the decentralized congestion controller for the fixed network, as given previously in Section 5.2.2, that physical constraints in (6.71) are satisfied if the following LMI conditions are satisfied, namely

$$\Omega_{c1i} \triangleq \begin{bmatrix} \tilde{M}_i & \tilde{M}_i^T \\ \tilde{M}_i & (z_{ri}^{max})^2/\rho_i \end{bmatrix} \geq 0 \tag{7.45}$$

$$\Omega_{c2i} \triangleq (T_i(\alpha_t))_{ij} \geq 0, \qquad i,j = 1,...2n \tag{7.46}$$

$$\Omega_{c3i} \triangleq \gamma_i max(\Psi_i(\alpha_t)) \leq \epsilon_i \tag{7.47}$$

$$\Omega_{c4i} \triangleq \begin{bmatrix} I & K_{ri} & K_{pi} \\ (K_{ri})^T & \frac{C_{server,i}^2(\alpha_t)}{\epsilon_i+\rho_i}\tilde{P}_{ri}(\alpha_t) & 0 \\ (K_{pi})^T & 0 & \frac{C_{server,i}^2(\alpha_t)}{\epsilon_i+\rho_i}\tilde{P}_{pi}(\alpha_t) \end{bmatrix} \geq 0 \tag{7.48}$$

The following theorem can now be obtained.

Theorem 7.2. *A distributed guaranteed cost congestion controller (DGCC) for the ordinary traffic in a mobile network can be determined if the conditions given in Lemma 7.3 is satisfied subject to the LMIs Ω_{c1i} to Ω_{c4i} that are governed by (7.45) to (7.47), respectively.*
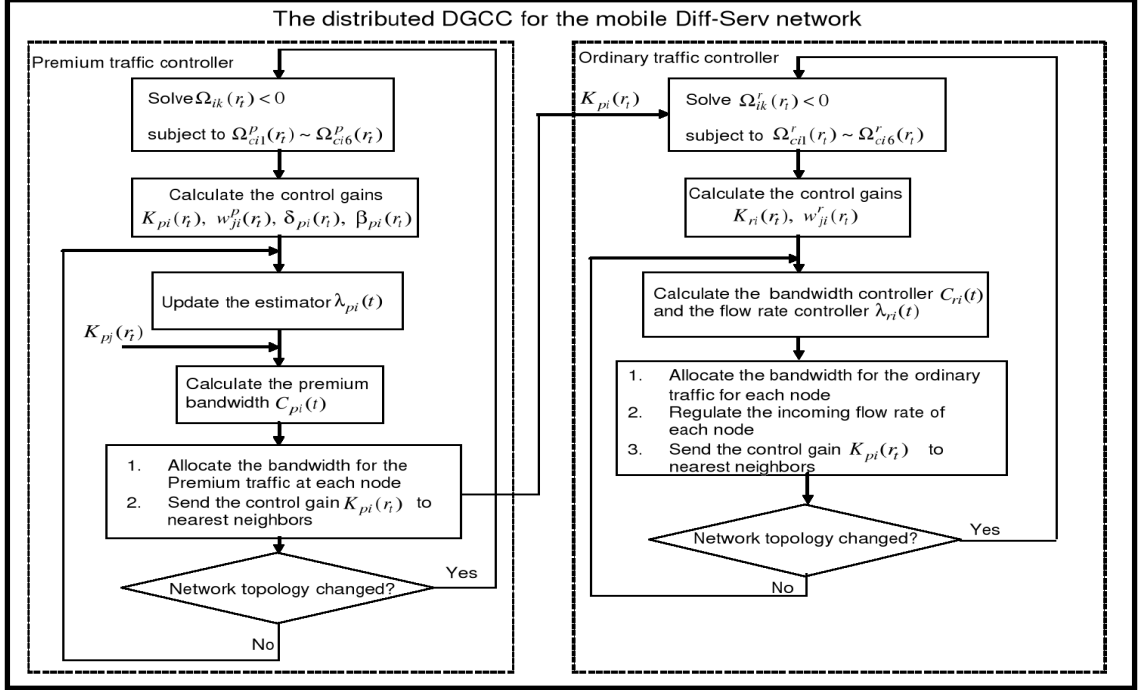
313

Figure 7.3: The flow chart of the distributed guaranteed cost congestion controller (DGCC) for a Mobile Diff-Serv network.

Proof: The proof follows along the same lines as given in Lemma 7.3 and the derivations for the physical constraints as given in this section. ∎

The distributed guaranteed cost congestion control strategies of a mobile Diff-Serv network that are proposed in this chapter can be summarized by the flowchart shown in Fig. 7.3. As shown in the distributed congestion control scheme the controller is implemented at each node. The controllers of the nodes that are in the same neighboring set are able to communicate with each other and share information. That is, the control gain $K_{pi}(\alpha_t)$, the state information $\bar{z}_{pi}(t)$ and $\hat{\lambda}_{pi}(t)$ are available to all the nodes in its neighboring set.

Therefore, given a node i in a mobile Diff-Serv network, the premium traffic controller first solves the corresponding LMI conditions to derive the distributed control gains $K_{pi}(\alpha_t)$, the distributed weights of the neighboring nodes $w_{ji}^p(\alpha_t)$, and the adaptive control gains $\delta_{pi}(\alpha_t)$ and $\beta_{pi}(\alpha_t)$. The adaptive estimator of the premium traffic $\hat{\lambda}_{pi}(t)$ can then be updated. Given the local control parameters and the control gains of the nearest

314

neighboring nodes $K_{pj}(\alpha_t)$, for $j \in \wp_i(\alpha_t)$, the bandwidth allocated to the premium traffic of node i is calculated as follows:

$$
\begin{aligned}
C_{pi}(t) &= u_{pi}(t) = f^{-1}(x_{pi}, t)\bar{u}_{pi}(t) \qquad\qquad\qquad\qquad\qquad\qquad (7.49)\\
&= f^{-1}(x_{pi}, t)[K_{pi}(\alpha_t)\bar{z}_{pi}(t) + W_{ji}(\alpha_t)K_{ji}(\alpha_t)\bar{Z}_j(t)] \qquad i = 1, ..., n \ \ j \in \wp_i(\alpha_t)\\
&= f^{-1}(x_{pi}, t)[K_{pi}(\alpha_t)\begin{bmatrix} x_{pi}(t) - x_{pi}^{ref} \\ \hat{\lambda}_{pi}(t) \end{bmatrix} + W_{ji}(\alpha_t)K_{ji}(\alpha_t)\begin{bmatrix} X_{pj}(t) - X_{pj}^{ref} \\ \hat{\Lambda}_{pj}(t) \end{bmatrix}]
\end{aligned}
$$

where $x_{pi}(t)$ is the queuing length of node i, x_{pi}^{ref} is the reference point of the queuing length of node i which is selected by the network operator, $X_{pj}(t) = vec\{x_{pj}(t)\}$ is the queuing length of the nearest neighboring nodes in the set $\wp_i(\alpha_t)$, X_{pj}^{ref} is the reference queuing length of the neighboring nodes, $\hat{\lambda}_{pi}(t) = vec\{\hat{\lambda}_{pi(t)}\}$ is the estimator of the neighboring nodes, $K_{pi}(\alpha_t)$ and $W_{ji}(\alpha_t)$ are the control gains that can be derived from the LMI conditions of node i and $K_{pj}(\alpha_t)$ is the control gain of the neighboring nodes which are sent from the neighbors.

On the other hand, given the bandwidth controller $C_{pi}(\alpha_t)$ of the premium traffic, the ordinary traffic controller first solves the LMI conditions and derives the local control gains $K_{ri}(\alpha_t)$ as well as the distributed wights $w_{ji}^r(\alpha_t)$. Given the information of the neighboring nodes, the bandwidth controller and the flow rate controller for the ordinary traffic of node i are then obtained as follows:

$$
\begin{aligned}
\begin{bmatrix} C_{ri}(t) \\ \lambda_{ri}(t) \end{bmatrix} &= F^{-1}(x_{ri}, t)\bar{u}_{ri}(t) \qquad\qquad\qquad\qquad\qquad\qquad (7.50)\\
&= \begin{bmatrix} f^{-1}(x_{ri}, t) & 0 \\ 0 & 1 \end{bmatrix}[K_{ri}(\alpha_t)(x_{ri}(t) - x_{ri}^{ref}) + W_{ji}^r(\alpha_t)K_{ji}^r(\alpha_t)(Z_{ri}(t) - Z_{ri}^{ref})
\end{aligned}
$$

where $x_{ri}(t)$ is the ordinary queuing length of node i, x_{ri}^{ref} is the reference point of the ordinary queuing length of node i, $X_{rj}(t) = vec\{x_{rj}(t)\}$ is the ordinary queuing length of the neighboring nodes, X_{rj}^{ref} is the reference ordinary queuing length of the neighboring nodes, $K_{ri}(\alpha_t)$ and $W_{ji}^r(\alpha_t)$ are the control gains that can be derived from the LMI conditions of node i, and $K_{rj}(\alpha_t)$ is the control gain of the neighboring nodes which are sent from the neighbors.

At each time when the network changs, the distributed congestion controllers of the premium and the ordinary traffic need to re-calculate all their mode-dependent parameters, and update the corresponding bandwidth controllers and flow rate controllers with the new parameters, respectively. It is worth nothing that by setting $M = 1$ the distributed guaranteed cost congestion control (DGCC) strategy proposed in this chapter becomes applicable to the fixed Diff-Serv network trivially.

7.3 Simulation Results

In this section, simulation results are provided to evaluate the performance of our proposed distributed guaranteed cost congestion control strategy (DGCC) in a NMAS with Diff-Serv traffic. Although, the DGCC strategy was developed based on the decentralized queuing model of the node in a mobile network, however, if we set the number of modes to $M = 1$, then the DGCC approach proposed in this chapter can also be applied to the NMAS with a fixed topology. Furthermore, if we set the distributed control gains to $w_{ji}(\alpha_t) = 0$, then the DGCC approach will become identical to the decentralized GCC approach that are presented in Chapter 6.

Therefore, the simulations that are conducted in this section are intended to demonstrate the advantages and improvements of the congestion control by incorporating the adjustments from the nearest neighboring nodes. The performance of our proposed DGCC are evaluated through two examples and are compared with the centralized GCC and the decentralized GCC approaches.

Example 7.1. Mobile Network. In this example, the network topology and the scenario that are considered in Section 5.3 are repeated. However, the nodes in the network are now mobile. The initial configuration of the network is shown in Fig. 3.5. The network has 15 nodes and is divided into three clusters. These three clusters are supposed to search a rectangular area from the point A to point B, as shown in Fig. 7.4. The first cluster C_1 that includes the nodes $1 - 5$ moves towards north first and then towards east; the second cluster C_2 including the nodes $6 - 10$ moves towards north-east directly; the third cluster

C_3 with the nodes $11 - 15$ moves towards east first and then towards north. The nodes 1, 6, and 11 are the decision makers which can communicate with each other, if connected. The other nodes in the network are sensors which are responsible for collecting data. It is assumed that the nodes within the same group are always connected with the decision maker and keep the same formation during the task. On the other hand, during the movement, the connected nodes between different groups are changed depending on the relative positions of the groups. For example, Fig. 7.4 illustrates three typical modes of the mobile network during the mission. The capacity of each link is assumed to be 10 Mbps and the buffer size for each traffic class in each node is set to 5 Mbits. A total of 12 switching modes are defined based on the network topology. In other words, we consider the following network modes $M_1 = \{1, ..., 15\}$; $M_2 = \{1, ..., 7\}$, $\{6, ..., 15\}$; $M_3 = \{1, ..., 6\}$, $\{6, ..., 15\}$; $M_4 = \{1, ..., 7\}$, $\{6, ..., 11\}$, $\{11, ..., 15\}$; $M_5 = \{1, ..., 6\}$, $\{6, ..., 11\}$, $\{11, ..., 15\}$; $M_6 = \{1, ..., 5\}$, $\{6, ..., 11, 15\}$, $\{11, ..., 15\}$; $M_7 = \{1, ..., 5\}$, $\{6, ..., 10\}$, $\{11, ..., 15\}$; $M_8 = \{1, ..., 6\}$, $\{6, ..., 10\}$, $\{11, ..., 15\}$; $M_9 = \{1, ..., 7\}$, $\{6, ..., 10\}$, $\{11, ..., 15\}$; $M_{10} = \{1, ..., 10\}$, $\{10, ..., 15\}$; $M_{11} = \{1, ..., 10\}$, $\{6, ..., 11\}$ $\{10, ..., 15\}$; and $M_{12} = \{1, ..., 10\}$ $\{6, ..., 15\}$. The transition probabilities for the Markovian jump model of changes in the network topologies are assumed to be $\pi_{kl} = 0.002$ for $l \neq k$. The following two cases are considered for evaluating the performance of our proposed decentralized MJ-GCC strategy.

Remark 7.1. *As stated earlier, the transition probability π_{kl} depends on the velocity, the communication range of nodes and the distance among them. The transition probabilities need not to be the same, and still the performances of our proposed congestion control strategy remains similar with different settings of π_{kl}. Therefore, without loss of generality, we assume that the transition rates are $\pi_{kl} = 0.002$, for $k \neq l$ in this chapter. It should be noted that different transition probabilities have been considered in the previous Chapters 4 and 6. Moreover, the Markovian jump model is simulated through a Monte carlo method [152] by using the MatLab function randsrc based on the transition probabilities π_{kl}.*

    Case 1: Queuing Lengths of the Bottle Neck Nodes

In the network model shown above, the premium traffic load is defined based on a
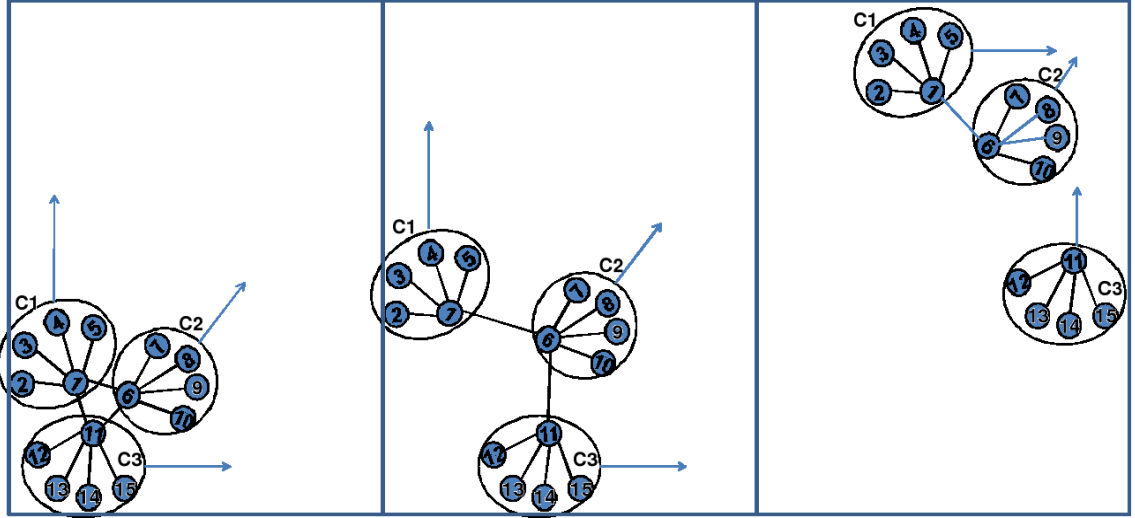
Figure 7.4: The schematic of the network configuration for three "typical" modes of the mobile network in Example 7.1.

Poisson distribution with the rate of $\lambda_{pi}(t) = 10$ Mbps, the ordinary traffic is set according to an on-off traffic with the maximum rate of 20 Mbps and the off-time is defined based on the exponential distribution with a mean period of $5ms$, the best-effort traffic is set to a random signal varying from 0.5 Mbps to 2 Mbps. The delays among the nodes are defined as a random signal as $\tau = min\{0, max\{h_{max}, h\}\}$, where $h \sim N(20ms, 10ms)$ is a normal distribution function and $h_{max} = 40$ ms is the maximum bound of the delay.

During the network operation, the sink nodes 1, 6, and 11 are the bottle neck nodes. The queuing length of the bottle neck nodes are shown in Fig. 7.5 and Fig. 7.6, for the premium and the ordinary traffic, respectively. The simulation results indeed confirm that our proposed distributed GCC strategy can stabilize the buffer queues despite the changing network topology and the time-varying delays.

Case 2: Performance Under Different Delays Levels

The performance of the bottle neck nodes are also evaluated based on different levels of time delays with maximum bound of $h = [20 \ 40 \ 80]$ ms. Table 7.1 presents the buffer characteristics, namely the packet loss rate (PLR) and the average queuing delay, of the bottle neck nodes by utilizing our proposed DGCC approach. It should be noted that these two performance metrics are calculated according to the definitions given in Section 4.3.1.
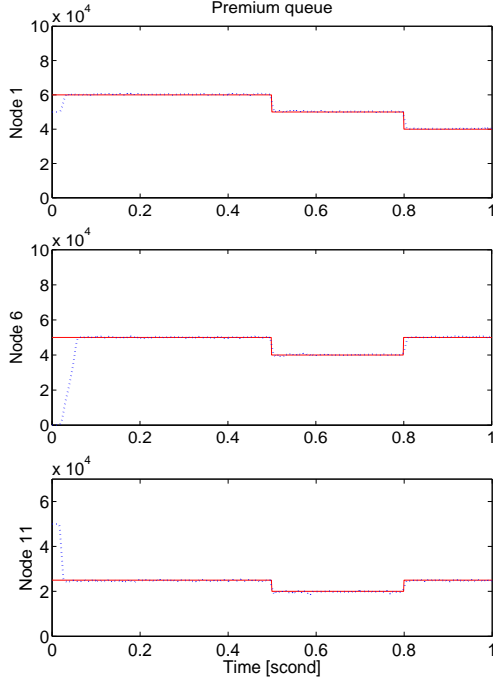
Figure 7.5: Premium queuing length (bits) by utilizing our proposed DGCC approach in Example 7.1.
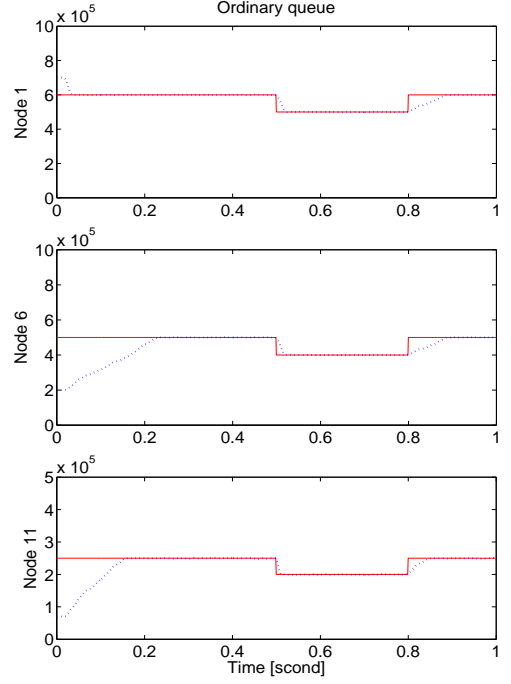
Figure 7.6: Ordinary queuing length (bits) by utilizing our proposed DGCC approach in Example 7.1.

By inspecting these results it follows that the packet loss rate of both traffic class remain less than 0.05% for the premium traffic and less than 5% for the ordinary traffic in the mobile network despite the increasing levels of delays in the network. The average queuing delay in each node is also robust with respect to the different levels of the time-delays.

Example 7.2. Fixed Network. In this example, the performance of the DGCC is compared with the decentralized and centralized GCC strategies that were proposed in Chapter 5. By setting the number of modes to $M = 1$ in the DGCC algorithm, the congestion control strategy proposed in this chapter can be applied to a fixed network topology directly. The network topology and scenario presented in Section 5.3 is repeated. The physical constraints of the network are set to $x_{buffer,i} = 5$ Mbits, $C_{server,i} = 10$ Mbits, for $i = 1, ..., 15$. Each source node generates a premium random traffic with a mean packet size of 512 bytes and pace the packets into the network every 10ms. The premium traffic is assumed to be bounded such that $\lambda_{pi}^{max} = 0.8$ Mbps. The source nodes also generate an ordinary traffic by pacing packets into the network according to an on-off mechanism.

Table 7.1: The queuing performance of the bottle neck nodes in Ex. 7.1 by utilizing the proposed DGCC approach with different delay levels.

PLR	Node 1		Node 6		Node 11	
h_{max}	P	O	P	O	P	O
20 ms	0.011%	2.05%	0.026%	1.01%	0.006%	1.33%
40 ms	0.012%	2.33%	0.028%	4.16%	0.007%	1.42%
80 ms	0.013%	2.48%	0.035%	4.57%	0.026%	3.70%
Queuing Delay	Node 1		Node 2		Node 3	
h_{max}	P	O	P	O	P	O
20 ms	33.0 ms	56.4 ms	42.5 ms	42.1 ms	20.3 ms	21.8 ms
40 ms	50.8 ms	56.6 ms	44.1 ms	42.5 ms	24.3 ms	22.6 ms
80 ms	52.4 ms	57.0 ms	45.9 ms	45.0 ms	25.2 ms	24.9 ms

During the off-time period there are no packets generated. The length of the off-time is determined by an exponential distribution with a mean period of 5ms. During the on-time, the source nodes generate packets with a constant rate of 100 packets/s with the mean packet size of 512 bytes.

Fig. 7.7 shows the buffer responses of both traffic classes in node 1 by utilizing the DGCC strategy. By inspecting these plots, one may readily conclude that for both traffic classes our proposed distributed guaranteed cost congestion (DGCC) strategy stabilizes the network despite the multiple time-varying delays. Moreover, it can be seen from the simulation results that not only the buffer queues convergence to their references set points, but also the transient responses are also fast.

Fig. 7.8 shows the comparison of the buffer responses in node 1 by utilizing the DGCC, the centralized GCC, and the decentralized GCC strategies, for the premium and the ordinary traffic, respectively. The plots are corresponding to the zoomed period of 0.1 seconds for the premium traffic and 0.05 seconds for the ordinary traffic corresponding to the transients of Fig. 7.7. During this time period, the reference set point of the premium traffic is 6×10^4 bits and the reference set point for the ordinary traffic is 6×10^5 bits. In Fig. 7.8, the solid line indicates the buffer response by utilizing the centralized GCC algorithm; the dashed line corresponds to the buffer response with the distributed GCC
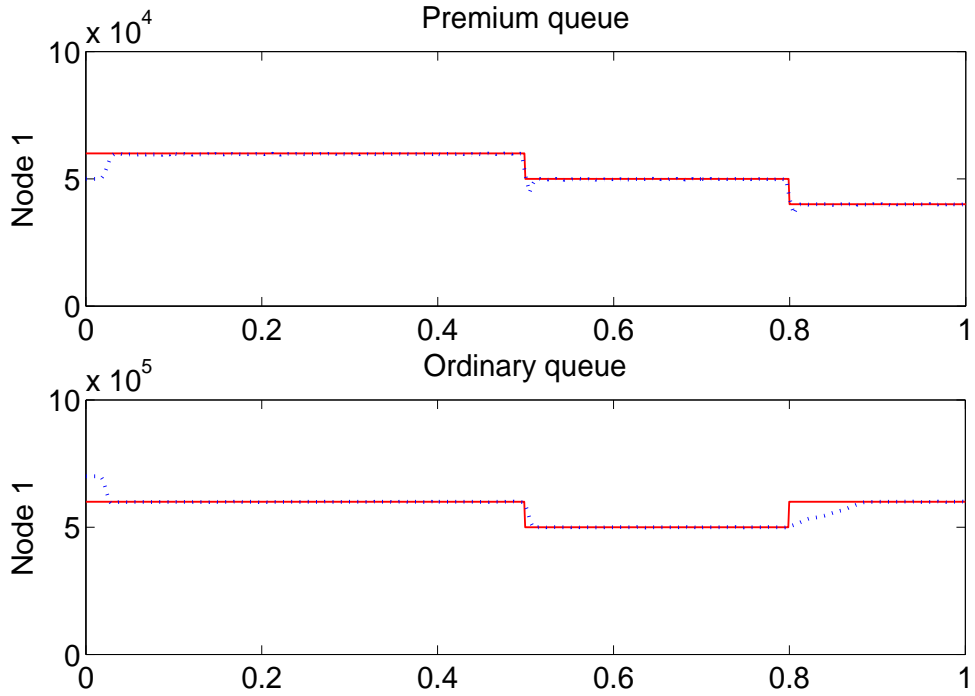
Figure 7.7: The buffer response of node 1 in Example 7.2 by utilizing the proposed DGCC approach.

algorithm; and the dotted line denotes the buffer response with the decentralized GCC algorithm.

On the other hand, the performance of the buffer characteristics of node 11 for the premium and the ordinary traffic services in presence of time-delay of 80ms is summarized in Table 7.2 and Table 7.3.

As can be inspected from the plots in Fig. 7.8 and the numerical comparisons in the tables, one can readily observe that:

- The buffer queues by utilizing all the three congestion control strategies do converge to their reference set points. The QoS performance of the network by utilizing the three GCC strategies are similar;

- The DGCC strategy can obtain a more accurate control result (mean error) than the decentralized GCC algorithm, and respond faster (settling time) than the centralized GCC. The reason is that by incorporating the adjustments from the nearest neighboring nodes, the coupling effects of the neighboring states are considered
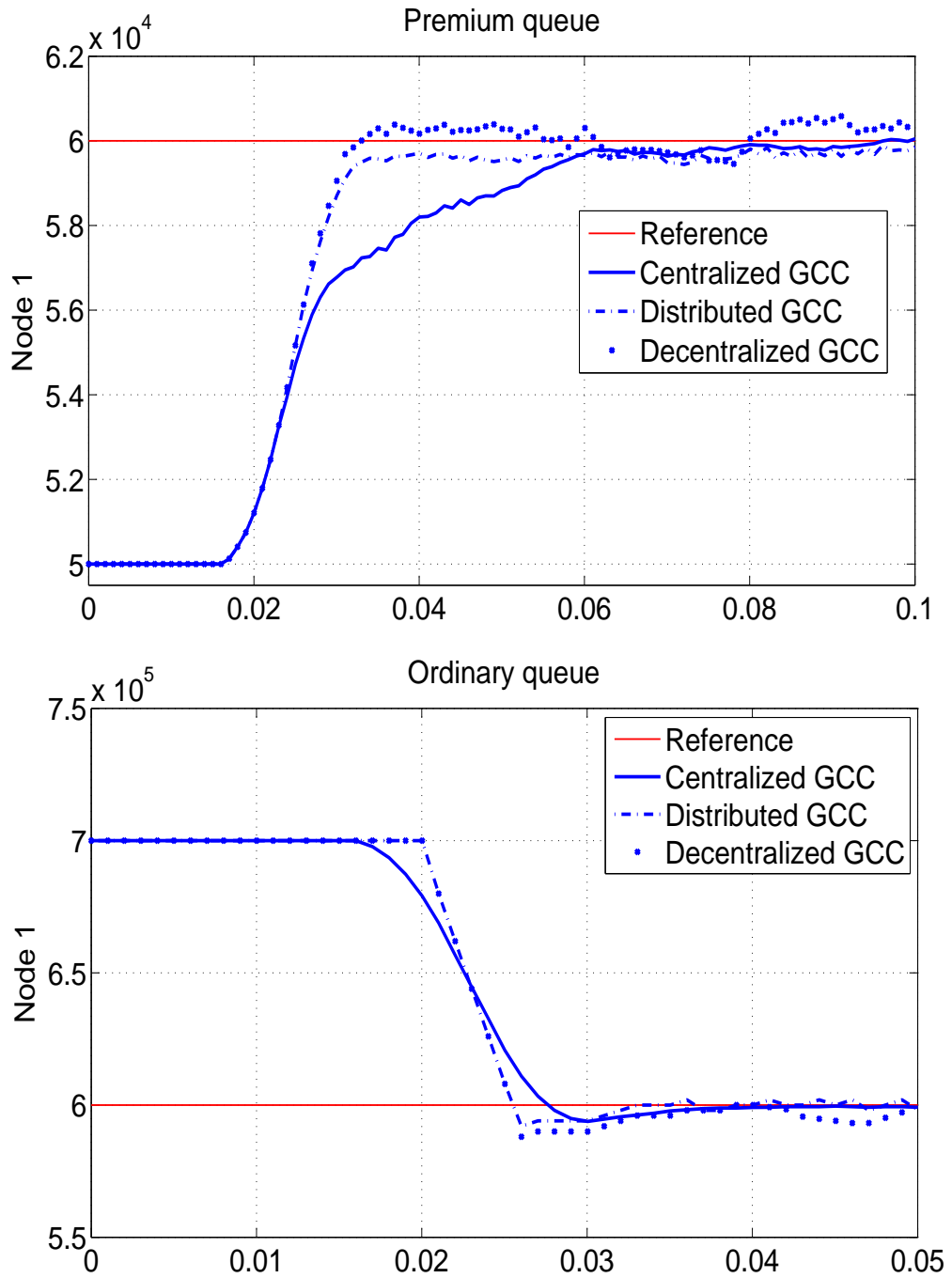
Figure 7.8: The comparison of the buffer response in node 1 by utilizing the decentralized GCC, the centralized GCC, and the distributed GCC approaches.

Table 7.2: The premium traffic performance of the node 11 in Example 7.2 with $h_{max} = 80$ ms, by utilizing the decentralized GCC, the centralized GCC, and the distributed GCC (DGCC) approaches.

$h_{max} = 80$ ms		Decentralized GCC	Centralized GCC	Distributed GCC (DGCC)
QoS	PLR	0	0	0
	Queuing Delay	26.0 ms	24.5 ms	24.6 ms
QoC	Mean Error	3.83%	2.87%	2.93%
	Settling Time	0.09s	0.11s	0.09s
	Max cost J_p^*	5.05×10^{20}	2.94×10^{20}	3.27×10^{20}
Feasibility	Num of LMIs	21	8	18
	Max dimension of LMIs	10×10	18×18	10×10

explicitly. Therefore, by properly selecting the distributed weights, the DGCC approach can obtain a more effective control than the decentralized one. On the other hand, the DGCC controller is implemented at each node and updated only based on the local information. Therefore, the buffer response of the DGCC is faster than the centralized one, and

- The upper bound of the guaranteed cost by utilizing the DGCC approach is between the decentralized and the centralized GCC approaches. However, the number of LMIs and the maximum dimension of the LMIs by utilizing the DGCC approach is similar to the decentralized one. These results confirm again that the DGCC approach is also scalable to large scale networks.

7.4 Conclusions

In this chapter, the guaranteed cost congestion control strategy for a NMAS with Diff-Serv traffic that are proposed in Chapter 5 and Chapter 6 are generalized. The extension consists mainly of incorporating the communication capabilities of the local congestion controllers and adding adjustment controls from the nearest neighboring nodes. By taking the advantages of the Markovian jump and the guaranteed cost control principles, the proposed distributed guaranteed cost congestion controller (DGCC) is shown to be in fact

Table 7.3: The ordinary traffic performance of the node 11 in Example 7.2 with $h_{max} = 80$ ms, by utilizing the decentralized GCC, the centralized GCC, and the distributed GCC (DGCC) approaches.

$h_{max} = 80$ ms		Decentralized GCC	Centralized GCC	Distributed GCC
QoS	PLR	0.98%	0.36%	0.78%
	Queuing Delay	23.55ms	23.14ms	23.16ms
QoC	Mean Error	0.68%	0.43%	0.65%
	Settling Time	0.09s	0.24s	0.11s
	Max cost J_r^*	3.01×10^{20}	1.45×10^{20}	2.04×10^{20}
Feasibility	Num of LMIs	18	7	15
	Max dimension of LMIs	7×7	18×18	10×10

equivalent to a local state feedback control plus a nearest neighboring controllers that are adjusted with proportional gains. The resulting congestion control problem is then cast as a quadratic regulation problem of a time-delay system with free parameters (gains) that need to be selected. The analytical results are confirmed through a number of simulation studies. The comparative results demonstrate that the DGCC strategy significantly enhances the scalability of the centralized algorithm and improves the performance of the decentralized approach to large scale traffic networks.

Part IV

Robustness Evaluations

Chapter 8

Robustness Evaluations

The aim of this chapter is to evaluate the robustness of the congestion control strategies that are proposed in this thesis through extensive simulations. The system uncertainty can be represented in two distinctly different forms, namely the parametric uncertainty and the unstructured uncertainty [161]. Therefore, in order to evaluate and compare the robustness capabilities of all the proposed switching congestion control (SCC) strategies and the guaranteed cost congestion control (GCC) strategies, the simulations in this chapter are conducted under the following two aspects:

- The uncertainty in system parameters. The parametric uncertainty typically arises from a physical model that has uncertain or changing parameters. In this thesis, there is only one system parameter in the queuing model, namely the average queue service rate μ. Therefore, in this section, the robustness to the average queue service rate will be investigated with different levels of uncertainties in μ.

- The unstructured uncertainties. The unstructured uncertainty is typically used to account for neglected or unmodelled dynamics, and both magnitude and phase are are considered to be uncertain. In this thesis, the congestion control strategies are developed based on the standard M/M/1 queue. Therefore, in order to check the robustness to unstructured uncertainties, two other kinds of queuing models, namely the $M/D/1$ and $M/E_k/1$ queuing models are utilized.
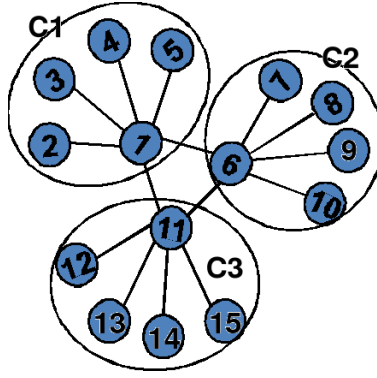
Figure 8.1: The network with a fixed topology that is utilized for robustness evaluations.

On the other hand, the congestion control strategies proposed in this thesis are developed for both fixed and mobile networks. Therefore, different network simulation models and scenarios need to be defined for robustness evaluations.

A. Simulation Model for a Fixed Network

For the SCC, GCC, and the DGCC strategies for networks with fixed topology, the network model and scenario shown in Fig. 8.1 are utilized. The network scenario is the same as that defined in Example 7.2. The physical constraints of the network are set to $x_{buffer,i} = 5Mbits$ and $C_{server,i} = 10Mbits$, for $i = 1, ..., 15$. Each source node generates a premium random traffic with a mean packet size of 512 bytes and pace the packets into the network every 10ms. The premium traffic is assumed to be bounded such that $\lambda_{pi}^{max} = 0.8$ Mbps. The source nodes also generate an ordinary traffic by pacing packets into the network according to an on-off mechanism. During the off-time period, no packets are generated. The length of the off-time is determined by an exponential distribution with a mean period of 5ms. During the on-time, the source nodes generate packets with a constant rate of 100 packets/s with the mean packet size of 512 bytes. The delays among the nodes are defined as a random signal as $\tau = min\{0, max\{h_{max}, h\}\}$ with a maximum bound of $h_{max} = 20$ ms, where $h \sim N(\mu, \sigma^2)$ is a normal distributed function with mean value of $\mu = 15$ ms and standard derivation of $\sigma^2 = 10$ ms. The reference queuing length for the premium and the ordinary traffic in the bottle neck nodes 1, 6, and 11 are selected
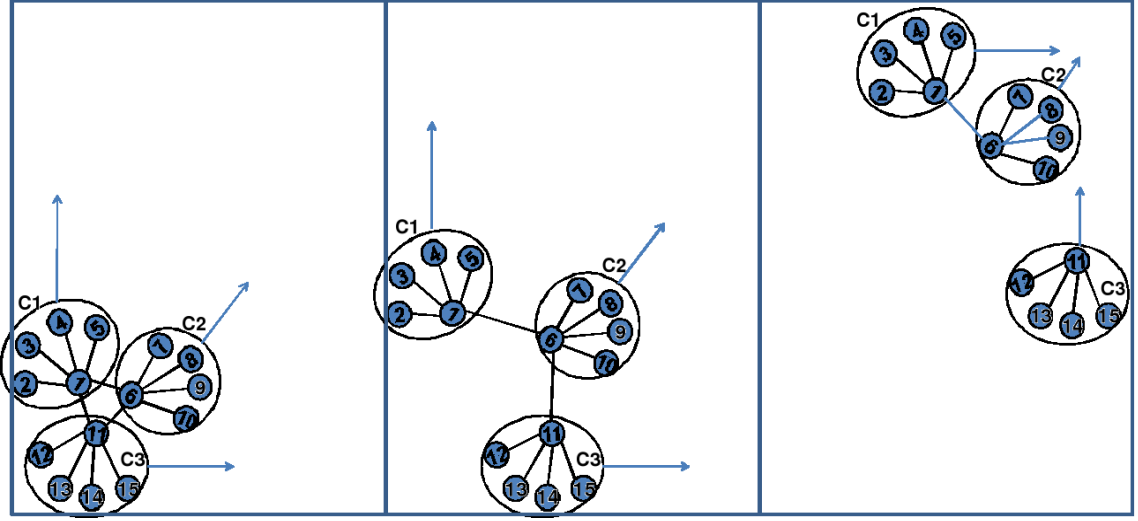
327

Figure 8.2: The schematic of the network configuration for three "typical" modes of a mobile network that is utilized for robustness evaluations.

to be a sinusoidal function of time,that is:

$$x_{p1}^{ref}(t) = 30 + 30sin(5t)kbits, \qquad x_{r1}^{ref}(t) = 3 + 3sin(5t)Mbits$$

$$x_{p2}^{ref}(t) = 25 + 25sin(5t)kbits, \qquad x_{r2}^{ref}(t) = 2.5 + 2.5sin(5t)Mbits$$

$$x_{p3}^{ref}(t) = 12.5 + 12.5sin(5t)kbits, \qquad x_{r3}^{ref}(t) = 1.25 + 1.25sin(5t)Mbits$$

B. Simulation Model for Mobile Networks

For the MJ-SCC, MJ-GCC, and the DGCC strategies for mobile networks, the network model shown in Fig. 8.2 is utilized. The network scenario is the same as that defined in Example 7.1. The 15 nodes that are divided into three clusters are supposed to search a rectangular area from point A to point B. The first cluster C_1 moves towards north first and then towards east; the second cluster C_2 moves towards north-east directly; the third cluster C_3 moves towards east first and then towards north. The nodes 1, 6, and 11 are the decision makers which can communicate with each other, if connected. It is assumed that the nodes within the same group always keep the same formation during the mission. Fig. 8.2 only illustrates three "typical" modes of the mobile network during the movement. The capacity of each link is assumed to be 5 Mbps and the buffer size for

each traffic class in each node is set to 5 Mbits. The incoming premium traffic is defined based on a Poisson distribution with the rate of $\lambda_{pi}(t) = 10$ Mbps and the ordinary traffic is set according to an on-off traffic with the maximum rate of 20 Mbps, the off-time is defined based on the exponential distribution with a mean period of $5ms$; the best-effort traffic is set to a random signal varying from 0.5 Mbps to 2 Mbps. The delays among the nodes are defined as the same as in the fixed network. The reference queuing length for the premium and the ordinary traffic in the bottle neck nodes are set to be same as before.

The total simulation duration is selected as $30s$ and the switching modes are defined the same as in Example 7.1. That is, the following neighboring sets of the network during nodes mobility are considered: $M_1 = \{1, ..., 15\}$; $M_2 = \{1, ..., 7\}$, $\{6, ..., 15\}$; $M_3 = \{1, ..., 6\}$, $\{6, ..., 15\}$ $M_4 = \{1, ..., 7\}$, $\{6, ..., 11\}$, $\{11, ..., 15\}$; $M_5 = \{1, ..., 6\}$, $\{6, ..., 11\}$, $\{11, ..., 15\}$; $M_6 = \{1, ..., 5\}$, $\{6, ..., 11, 15\}$, $\{11, ..., 15\}$; $M_7 = \{1, ..., 5\}$, $\{6, ..., 10\}$, $\{11, ..., 15\}$; $M_8 = \{1, ..., 6\}$, $\{6, ..., 10\}$, $\{11, ..., 15\}$; $M_9 = \{1, ..., 7\}$, $\{6, ..., 10\}$, $\{11, ..., 15\}$; $M_{10} = \{1, ..., 10\}$, $\{10, ..., 15\}$; $M_{11} = \{1, ..., 10\}$, $\{6, ..., 11\}$, $\{10, ..., 15\}$; and $M_{12} = \{1, ..., 10\}$, $\{6, ..., 15\}$. The transition probabilities for the Markovian jump model of changes in the network topologies are assumed to be $\pi_{kl} = 0.002$ for $l \neq k$.

8.1 Robustness to Parametric Uncertainty

The dynamic queuing fluid flow model corresponding to the M/M/1 queue in the network as presented in Chapter 2 is re-written here for convenience:

$$\dot{x}_i(t) = -\mu_i \frac{x_i(t)}{1 + x_i(t)} C_i(t) + \lambda_i(t) + \sum_{\substack{j=1 \\ j \neq i}}^{n} \mu \frac{x_j(t - \tau_{ji}(t))}{1 + x_j(t - \tau_{ji}(t))} C_j(t - \tau_{ji}(t)) g_{ji}(t) \quad (8.1)$$

where x_i is the average queuing length of node i, C_i is the output capacity, λ_i is the average incoming traffic rate, g_{ji} is the traffic compression gains from node j to node i, n is the number of neighboring nodes of node i, τ_{ji} is the unknown time-varying delay from node j to node i, and μ_i is the average queue service rate at node i. In this thesis, we assume that the nominal value of the average queue service rate for the M/M/1 queue is $\mu = 1$. In order to evaluate and compare the robustness capabilities of all our proposed

congestion control algorithms with respect to uncertainty in the queue service rate, we define the uncertainties in μ_i through percentage errors of $[-100\%, 100\%]$ with respect to the nominal value. The corresponding simulation results are presented below.

A. Simulation Results for a Fixed Network

The simulation results of the decentralized SCC, the decentralized GCC, and the distributed GCC for a fixed network shown in Fig. 8.1 with $+20\%$, $+80\%$, -50%, and -80% uncertainties in the average queue service rate μ are depicted in Fig. 8.3 to Fig. 8.8, respectively.

B. Simulation Results for a Mobile Network

The simulation results of the decentralized MJ-SCC, the decentralized MJ-GCC, and the distributed GCC for a mobile network shown in Fig. 8.2 with $+20\%$, $+80\%$, -50%, and -80% uncertainties in the average queue service rate μ are depicted in Fig. 8.9 to Fig. 8.14, respectively.

By inspecting from the above simulation results, the following observations and comparisons can be summarized:

- The proposed congestion control strategies perform well only subject to "small" parametric uncertainties that are less than 20%;

- Within the robust range, the proposed congestion control strategies perform well to both positive uncertainties ($+20\%$) and negative uncertainties (-20%);

- When the uncertainty level increases, the SCC and GCC algorithms perform better than the MJ-SCC and MJ-GCC algorithms for both traffic classes;

- The proposed distributed guaranteed cost congestion control (DGCC) strategy performs very well in both the fixed and mobile networks subject to "small" parametric uncertainties that are less than 20%;
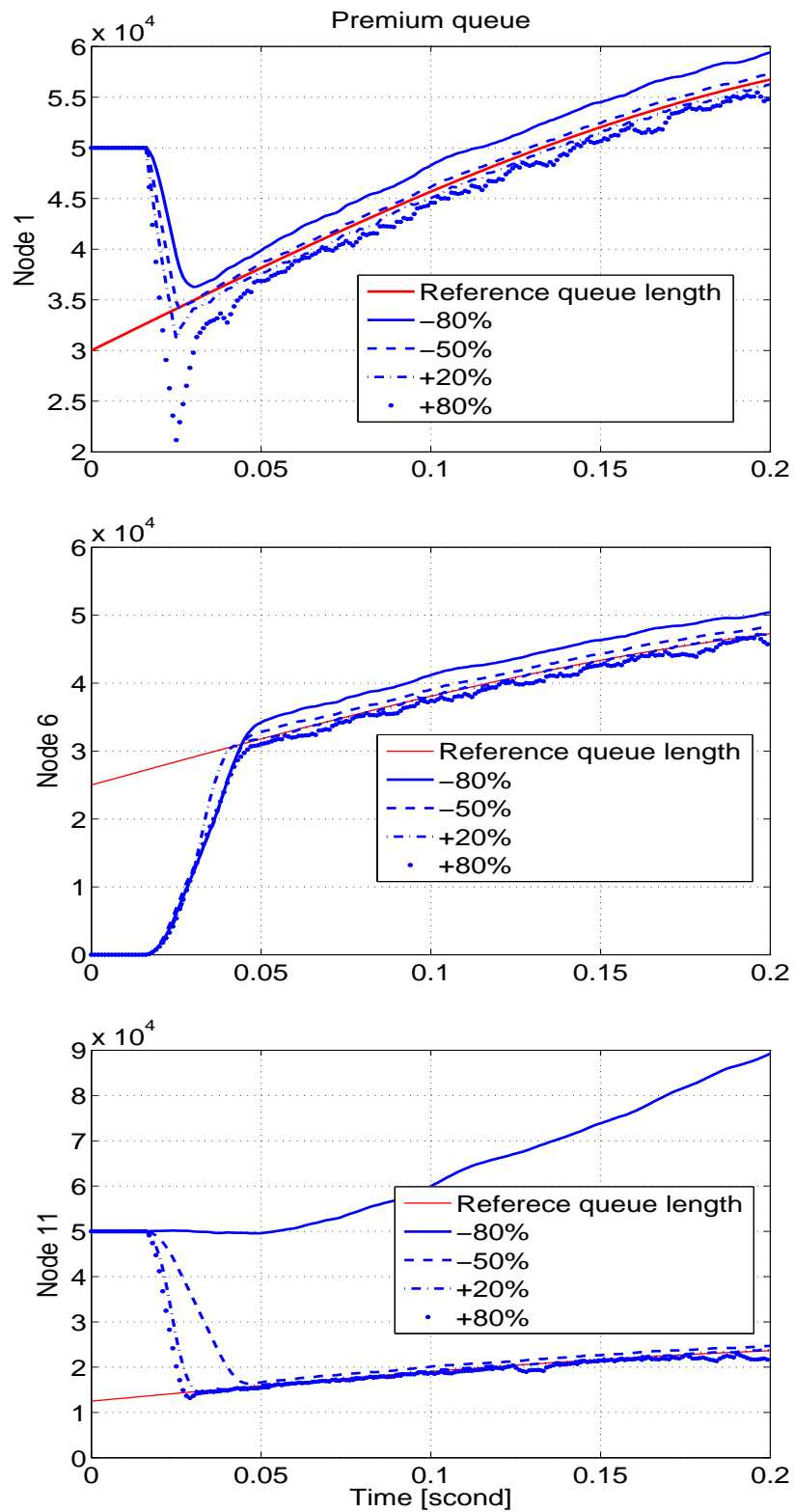
Figure 8.3: Premium queuing length (bits) under different levels of uncertainties in μ by utilizing the decentralized SCC approach.
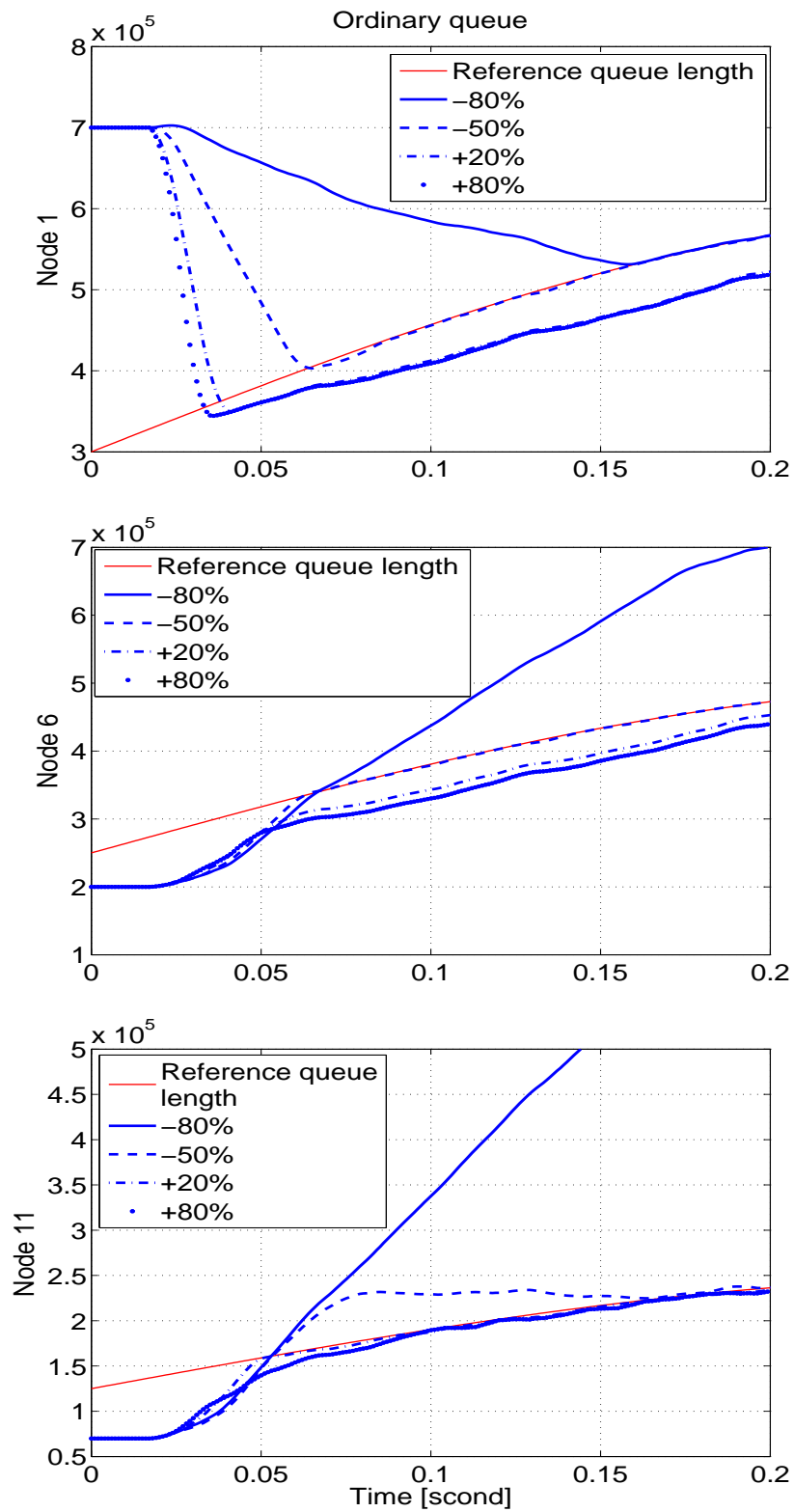
Figure 8.4: Ordinary queuing length (bits) under different levels of uncertainties in μ by utilizing the decentralized SCC approach.
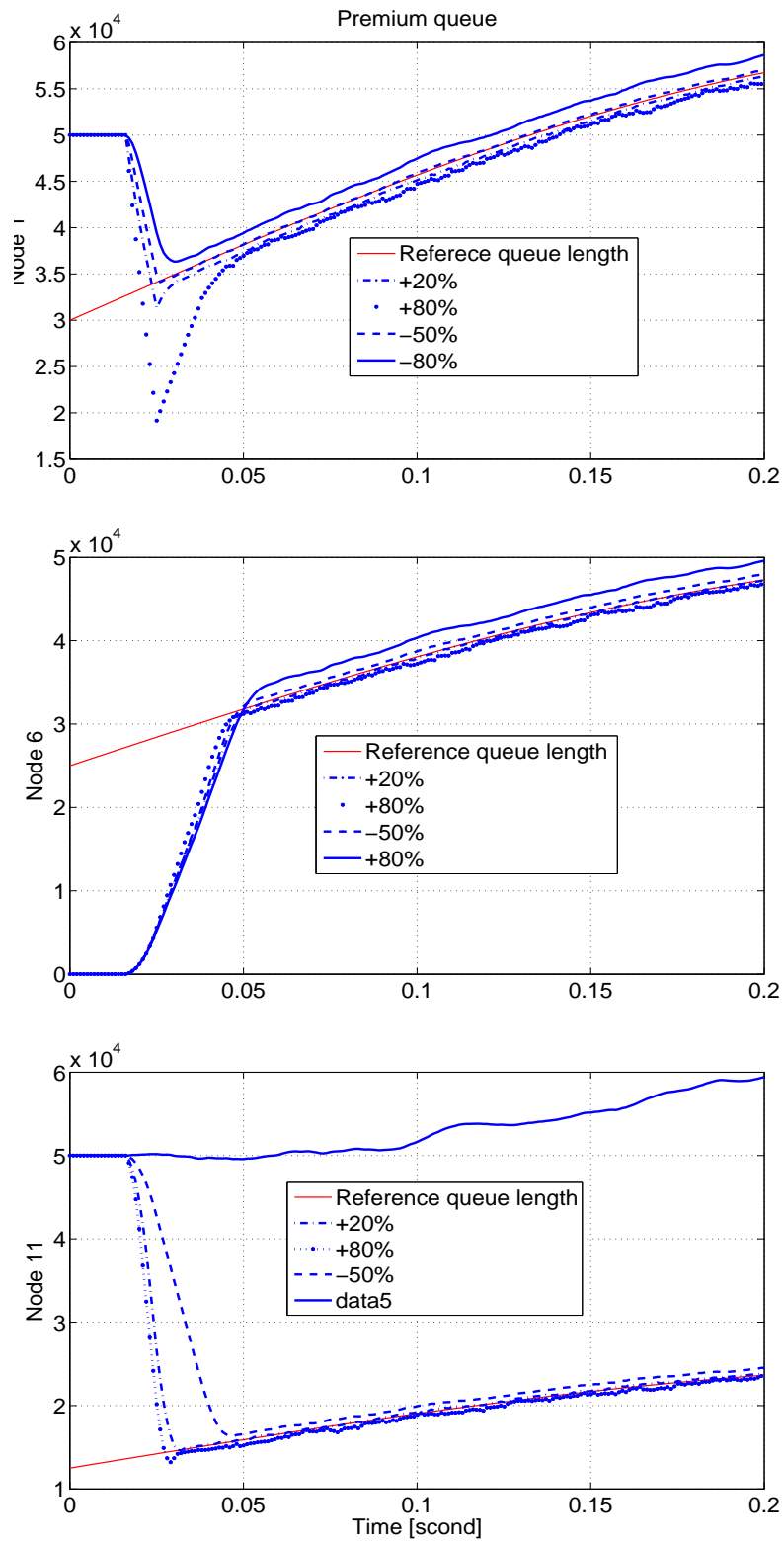
Figure 8.5: Premium queuing length (bits) under different levels of uncertainties in μ by utilizing the decentralized GCC approach.
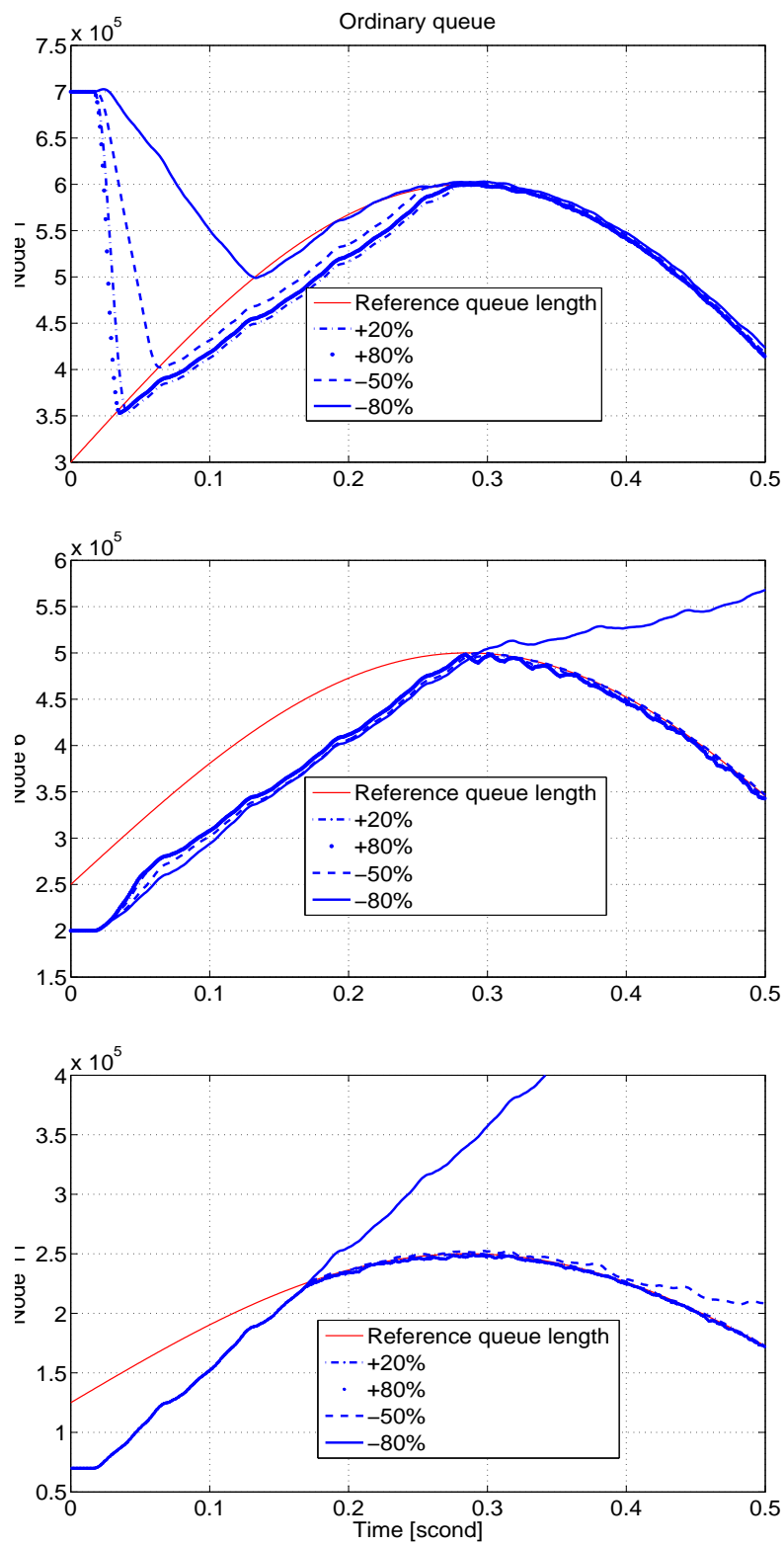
333

Figure 8.6: Ordinary queuing length (bits) under different levels of uncertainties in μ by utilizing the decentralized GCC approach.
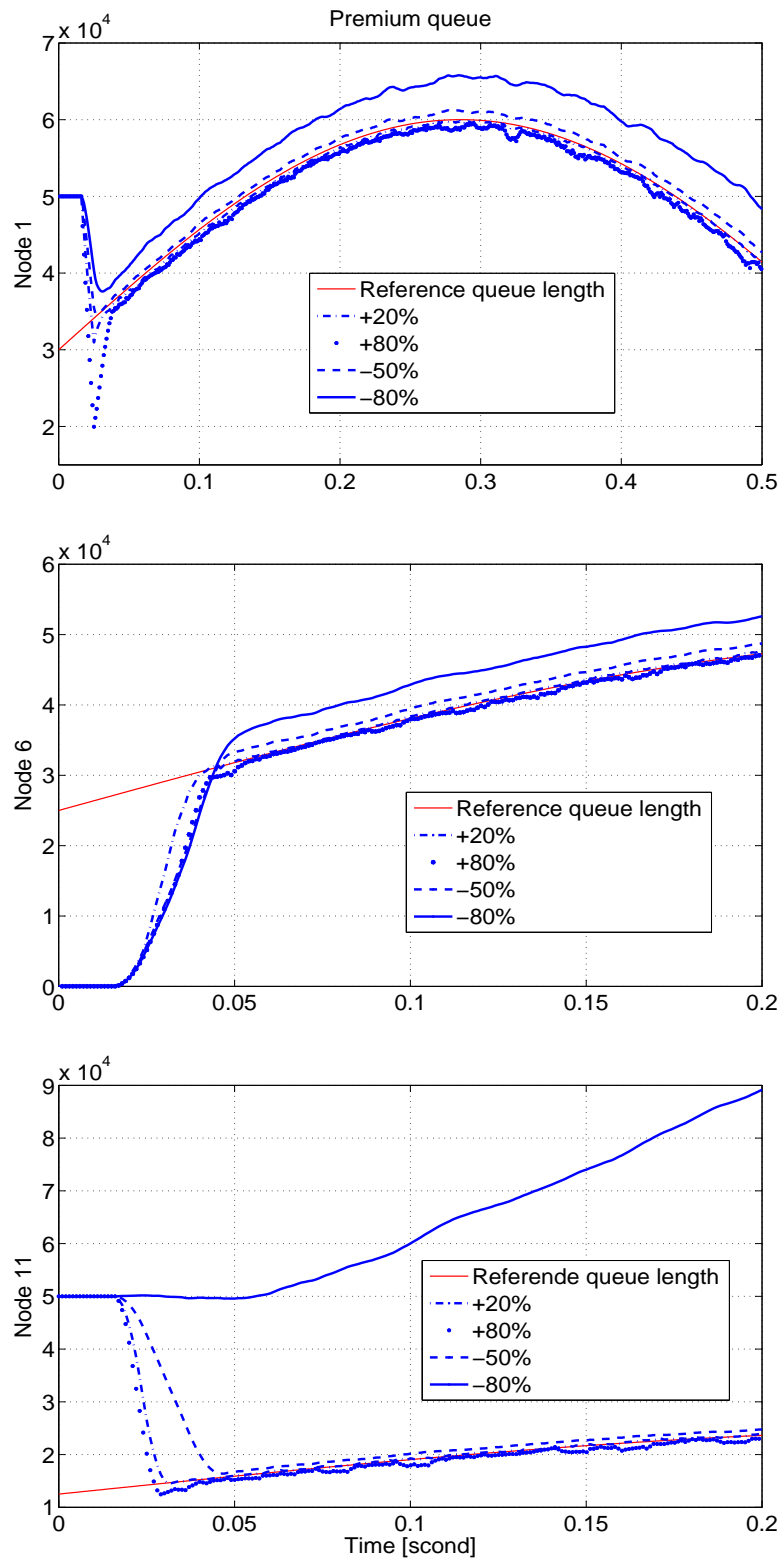
Figure 8.7: Premium queuing length (bits) under different levels of uncertainties in μ by utilizing the distributed GCC approach.
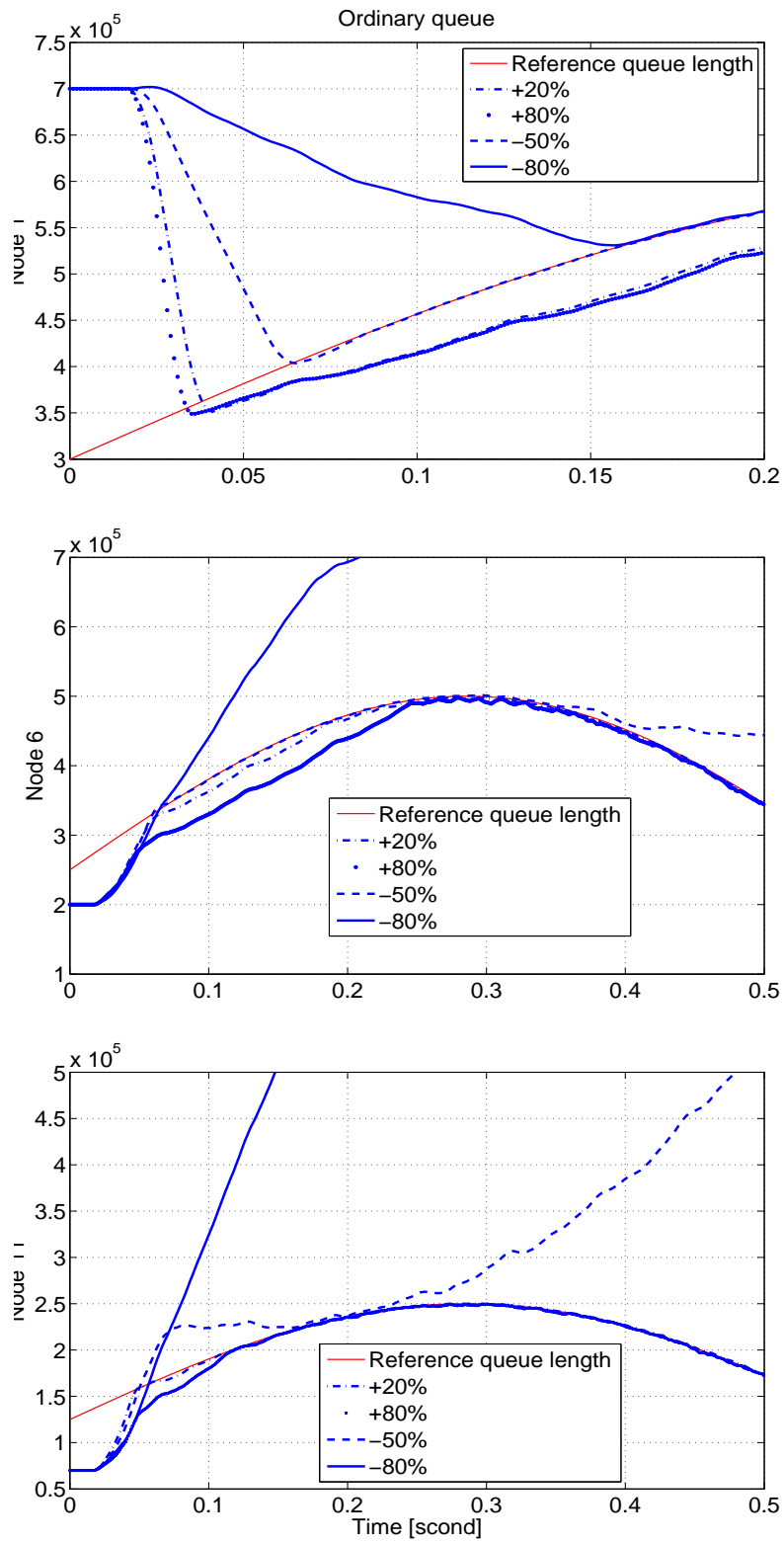
Figure 8.8: Ordinary queuing length (bits) under different levels of uncertainties in μ by utilizing the distributed GCC approach.
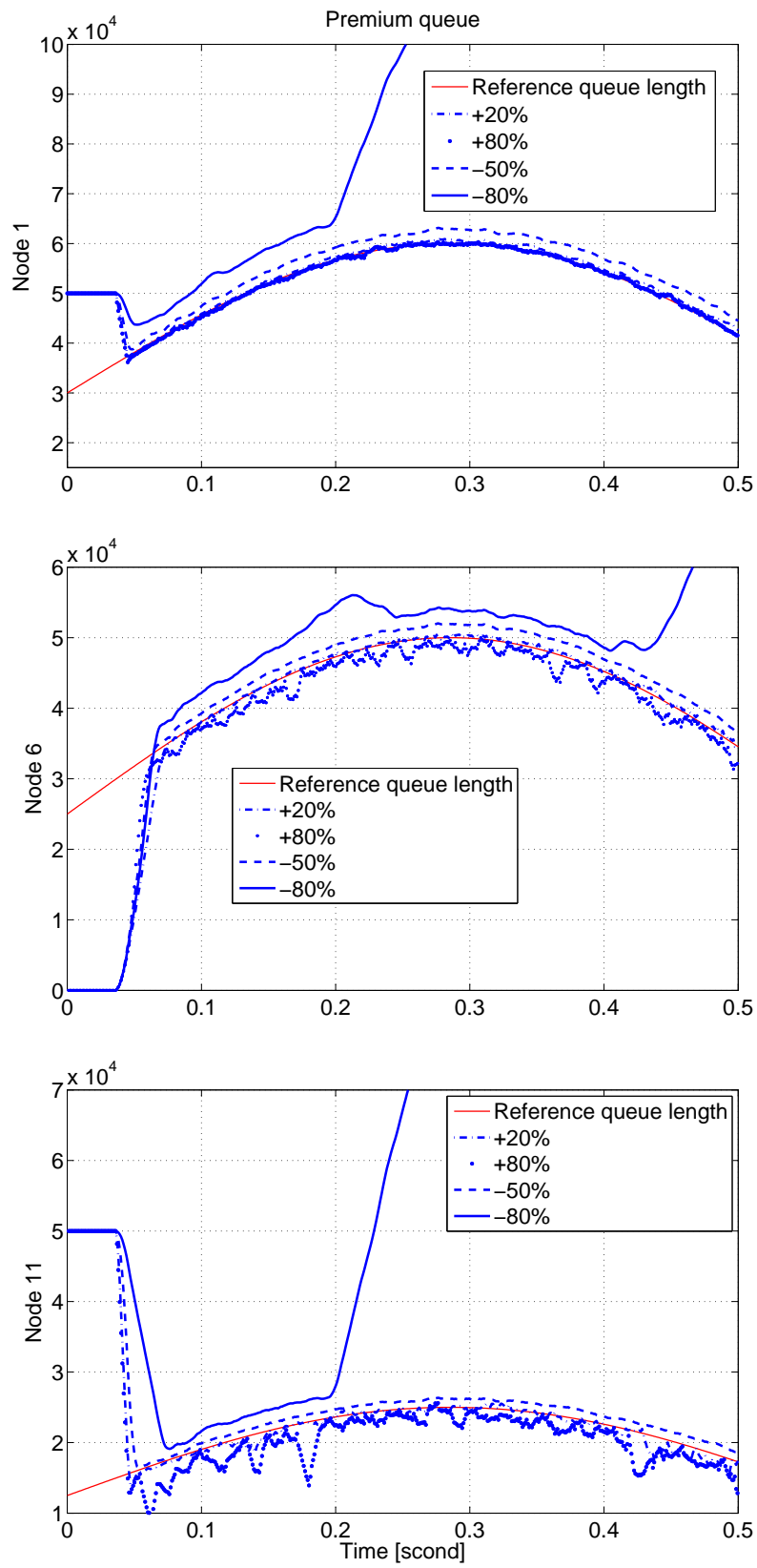
Figure 8.9: Premium queuing length (bits) under different levels of uncertainties in μ by utilizing the decentralized MJ-SCC approach.
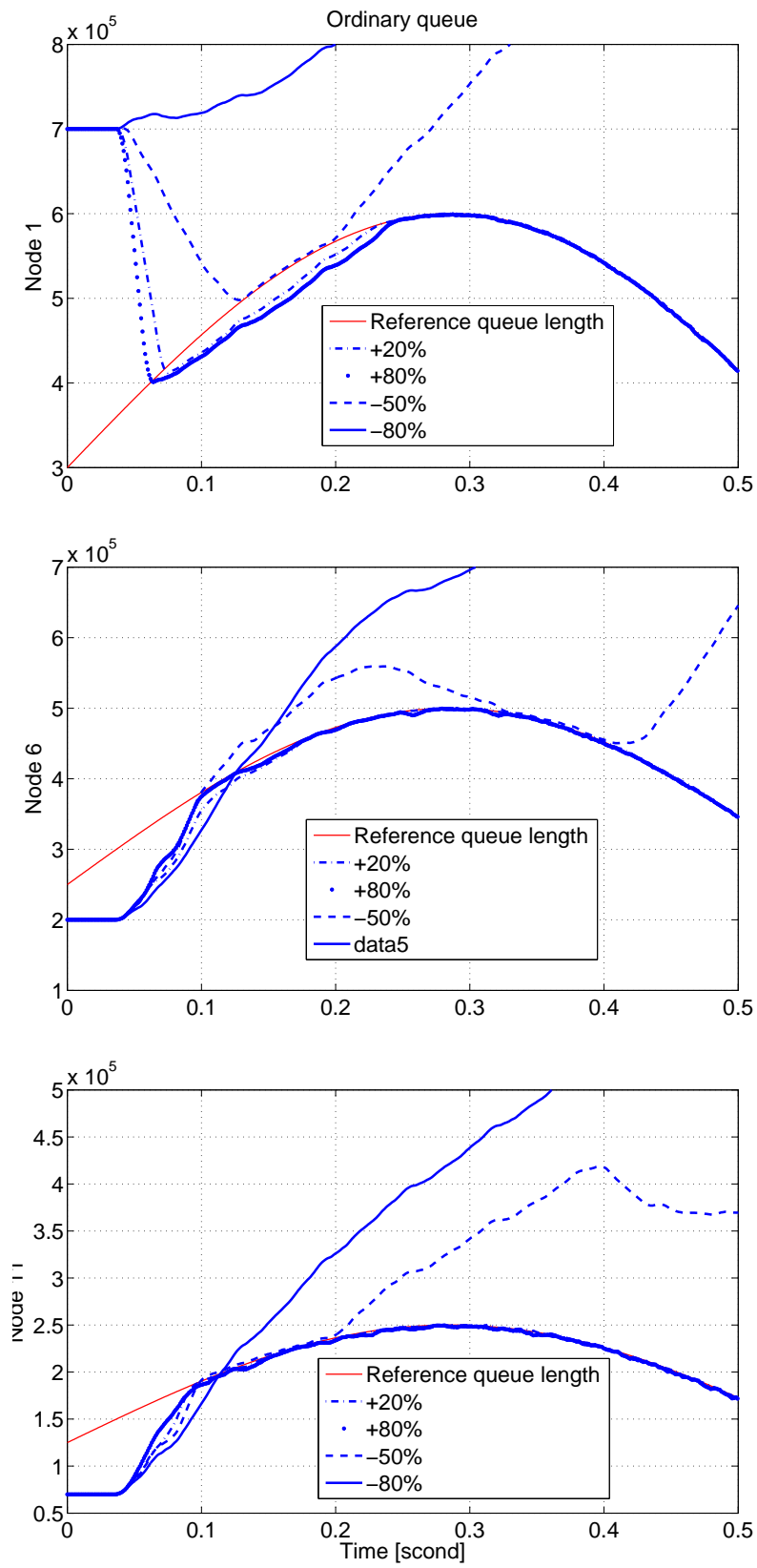
Figure 8.10: Ordinary queuing length (bits) under different levels of uncertainties in μ by utilizing the decentralized MJ-SCC approach.

338

Figure 8.11: Premium queuing length (bits) under different levels of uncertainties in μ by utilizing the decentralized MJ-GCC approach.

Figure 8.12: Ordinary queuing length (bits) under different levels of uncertainties in μ by utilizing the decentralized MJ-GCC approach.

Figure 8.13: Premium queuing length (bits) under different levels of uncertainties in μ by utilizing the distributed GCC approach.

Figure 8.14: Ordinary queuing length (bits) under different levels of uncertainties in μ by utilizing the distributed GCC approach.
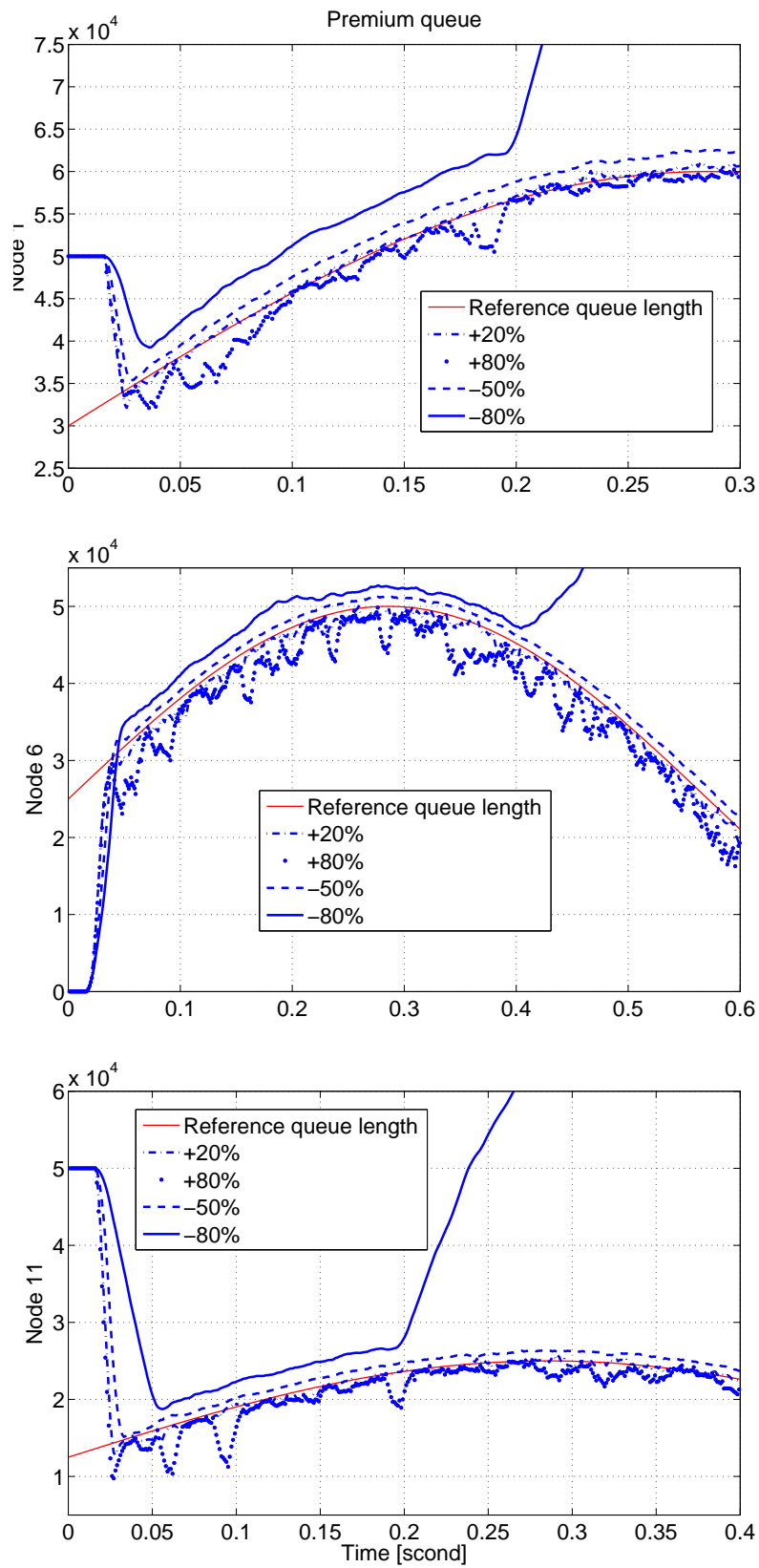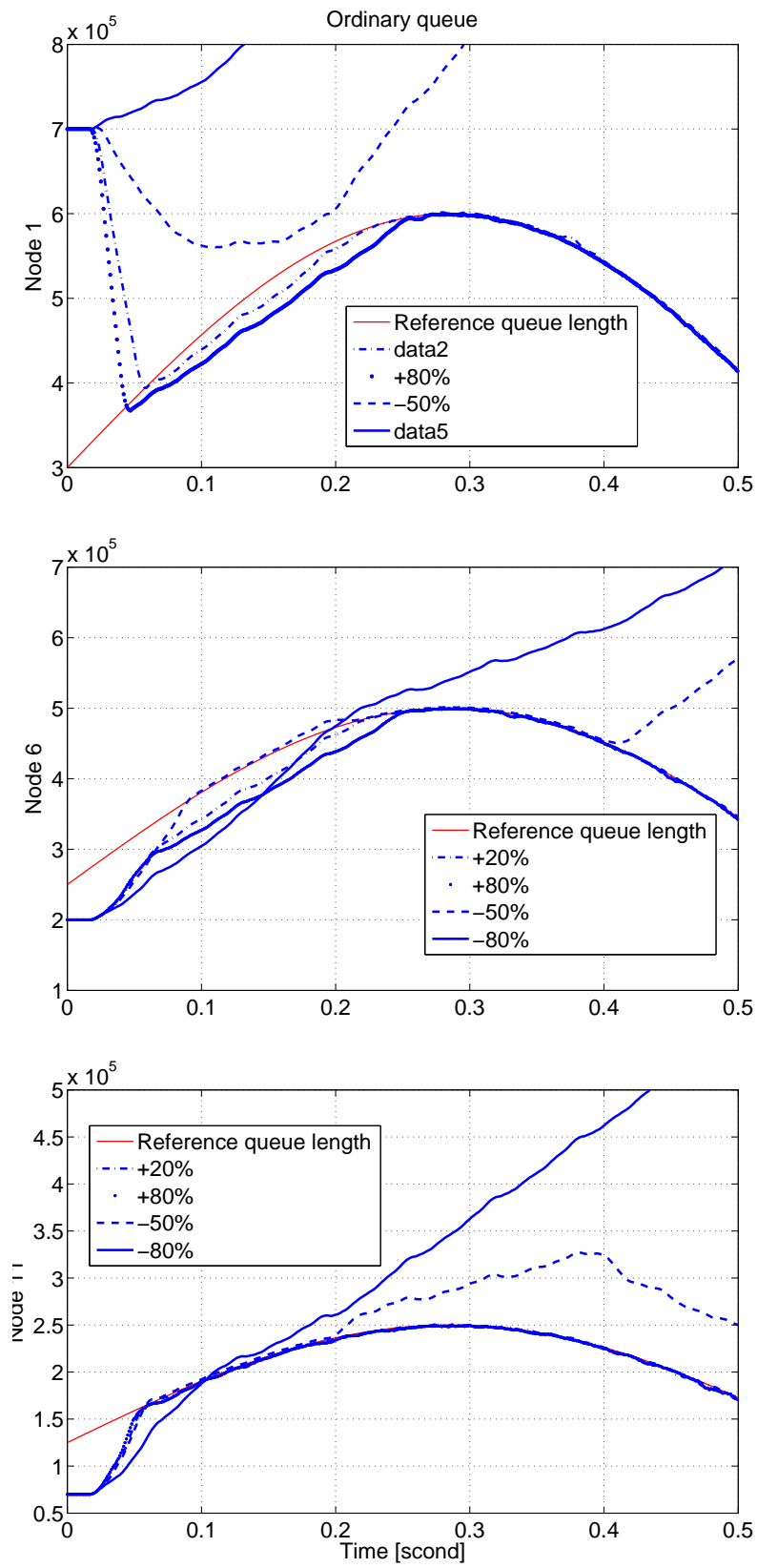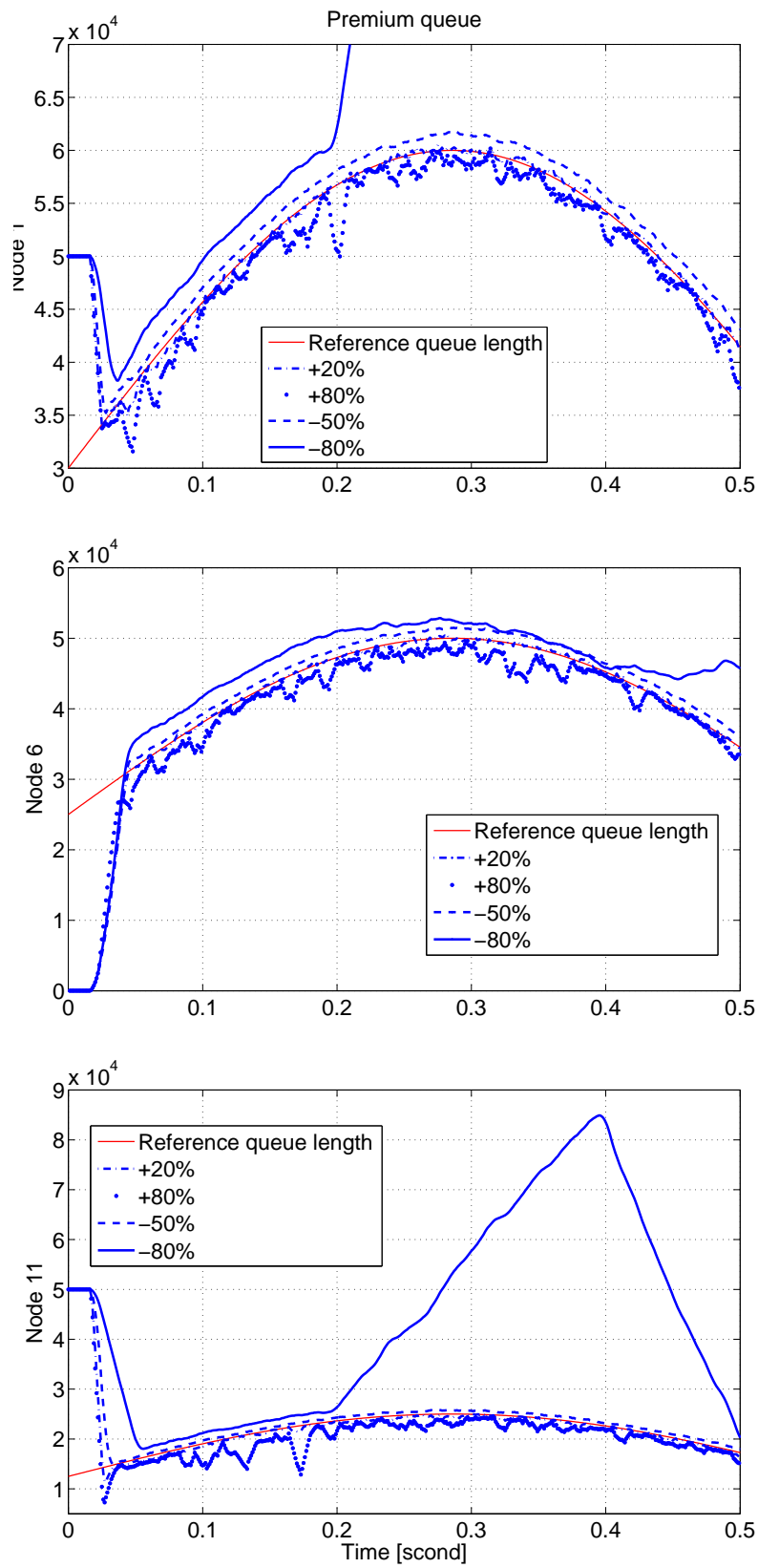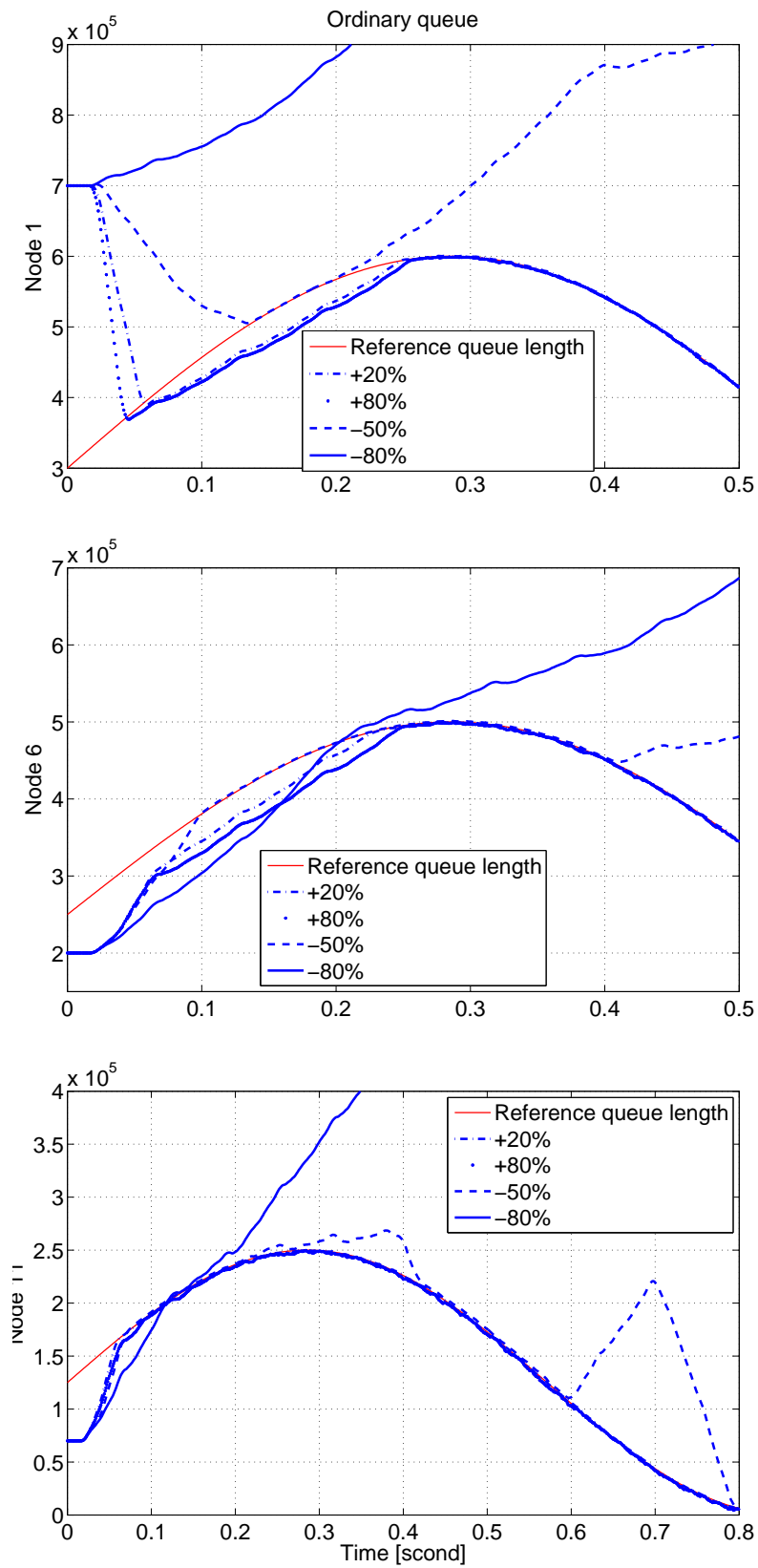
8.2 Robustness to Unstructured Uncertainty

In this section, unstructured uncertainties in the queuing model are considered for robustness evaluations. As discussed in Chapter 2, the dynamic fluid flow model (8.1) is developed based on the conservation law:

$$\dot{x}(t) = -f_{out}(t) + f_{in}(t) \tag{8.2}$$

The above conservation law is commonly refereed to as the fluid flow or dynamic flow equation. The flow out of the system f_{out} can be related to the ensemble average utilization of the server $\rho(t)$ by $f_{out} = \mu\rho(t)$. If the buffer size of the system is assumed to be infinite, then the flow into the system is just the arrival rate, that is $f_{in}(t) = \lambda(t)$ and the fluid flow model (8.2) becomes:

$$\dot{x}(t) = -\mu\rho(t) + \lambda(t) \tag{8.3}$$

The expression of $\rho(t)$ is dependent on the queuing system under study. However, determining an exact expression for $\rho(t)$ is quite difficult even for the simplest queues. Therefore, an approximation method based on the point wise approximation (PSA) method is generally adopted. The general idea is to determine the values of $\rho(t)$ at a particular time by a point wise mapping from the current value of $x(t)$ into $\rho(t)$ by using the steady- state queuing relationships. The value of $\rho(t)$ is then used to numerically solve the equation (8.3) over a small time interval. Thus a new $x(t)$ is obtained and the procedure is repeated for the next time step. The dynamic queuing model 8.1 that is used in this thesis is an approximation of the M/M/1 queue by mapping the queuing state $x(t)$ at steady state.

Therefore, in order to evaluate and compare the robustness capabilities of our proposed congestion control strategies, we use other types of queuing models as the nominal system model but still apply our proposed congestion control strategies to these "unseen" models. By applying the same mapping procedure and utilizing the pointwise stationary the fluid flow approximation (PSFFA) modeling technique [97], the following two special cases of the M/G/1 queue for various common service time distributions can be obtained [97]:

343

Table 8.1: Average queuing error with different nominal queueing models in fixed network.

Nominal model	Node	Decentralized SCC		Decentralized GCC		Distributed GCC	
		Pre.	Ord.	Pre.	Ord.	Pre.	Ord.
M/D/1	1	1.32%	1.44%	1.46%	0.85%	2.25%	1.05%
	6	1.27%	2.21%	2.08%	1.70%	1.89%	2.89%
	11	1.93%	1.65%	2.82%	0.82%	2.73%	1.48%
$M/E_k/1$	1	0.84%	0.14%	1.33%	1.21%	1.48%	2.67%
	6	1.18%	2.13%	1.12%	1.73%	1.75%	2.74%
	11	1.56%	2.87%	3.63%	2.97%	2.12%	1.29%

- $M/D/1$ queue, where D refers to deterministic service times:

$$\dot{x}_i(t) = -\mu_i[x_i(t) + 1 - \sqrt{x_i^2 + 1}]C_i(t) + \lambda_i(t) \qquad (8.4)$$

- $M/E_k/1$ queue, where E_k refers to the Erlang-k distributed service times:

$$\dot{x}_i(t) = -\mu_i[\frac{k(x_i(t) + 1)}{k - 1} - \frac{\sqrt{k^2 x_i^2 + 2kx + k^2}}{k - 1}]C_i(t) + \lambda_i(t) \qquad (8.5)$$

where $k \geq 1$ is a constant. In the following simulations k is set to $k = 2$.

A. Simulation Results for Fixed Network

The simulation results of the network model shown in Fig. 8.1 by utilizing our proposed decentralized SCC, the decentralized GCC, and the distributed GCC strategies are illustrated in Fig. 8.15 to Fig. 8.17, respectively. In Fig. 8.15 to Fig. 8.17, the solid line represents the reference queuing length, the dashed line indicates the buffer response with the nominal model of the $M/D/1$ queue, and the dotted line denotes the buffer response with the nominal model of the $M/E_k/1$ queue.

In order to compare the overall performance of the three algorithms in a more comprehensible manner, the numerical results are summarized in Table 8.1. This summary of the results is made based on the mean percentage queuing errors corresponding to the nominal models of the M/D/1 and the $M/E_k/1$ queuing systems.

B. Simulation Results for Mobile Network
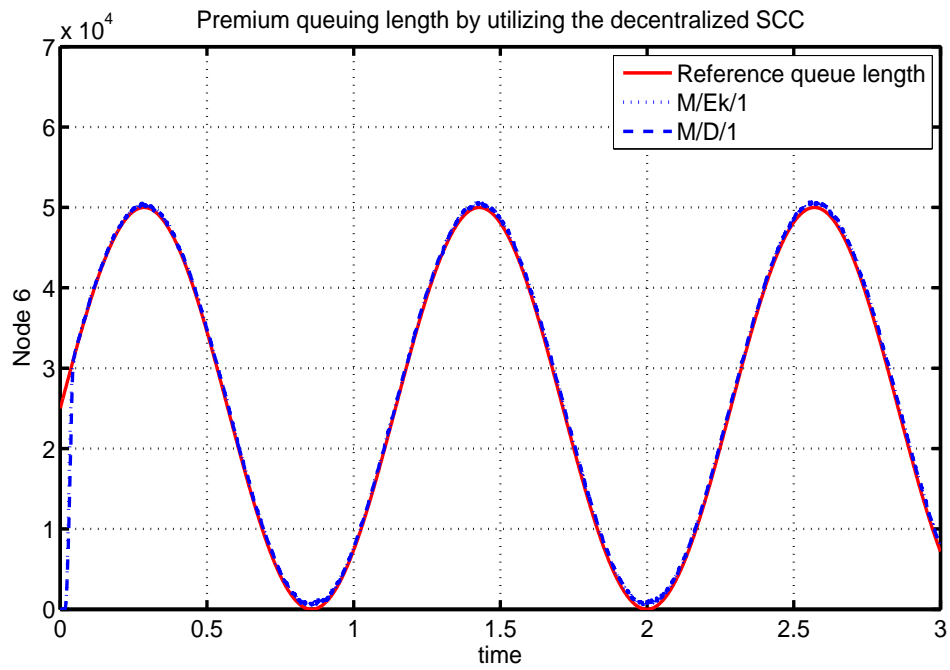
(a)
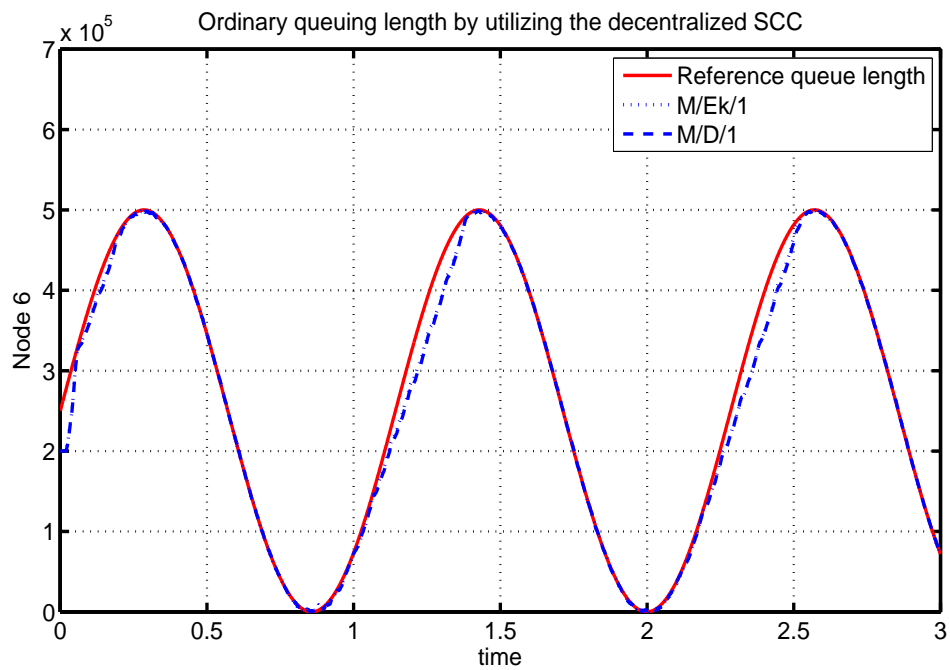
(b)

Figure 8.15: Buffer responses of node 6 subject to the decentralized SCC strategy that is designed based on the M/M/1 model but applied to the M/D/1 and the $M/E_k/1$ models. The solid line is the reference queuing length, the dashed line is the buffer response with the M/D/1 model, and the dotted line is the buffer response with the $M/E_k/1$ model.

(a)

(b)

Figure 8.16: Buffer responses of node 11 subject to the decentralized GCC strategy that is designed based on the M/M/1 model but applied to the M/D/1 and the $M/E_k/1$ models. The solid line is the reference queuing length, the dashed line is the buffer response with the M/D/1 model, and the dotted line is the buffer response with the $M/E_k/1$ model.

(a)

(b)

Figure 8.17: Buffer responses of node 6 subject to the DGCC strategy that is designed based on the M/M/1 model but applied to the M/D/1 and the $M/E_k/1$ models. The solid line is the reference queuing length, the dashed line is the buffer response with the M/D/1 model, and the dotted line is the buffer response with the $M/E_k/1$ model.

Table 8.2: Average queuing error with different nominal queuing models in mobile network.

Nominal model	Node	Decentralized MJ-SCC		Decentralized MJ-GCC		Distributed GCC	
		Pre.	Ord.	Pre.	Ord.	Pre.	Ord.
M/D/1	1	1.64%	0.11%	1.97%	3.47%	1.76%	3.45%
	6	1.61%	1.28%	1.64%	4.19%	1.71%	2.85%
	11	3.04%	0.32%	4.19%	4.37%	1.93%	4.47%
$M/E_k/1$	1	1.72%	0.84%	2.12%	2.53%	1.41%	3.45%
	6	1.45%	1.31%	1.58%	5.18%	1.67%	2.36%
	11	3.93%	3.26%	3.77%	5.35%	1.77%	2.51%

The simulation results for the network model shown in Fig. 8.2 by utilizing our proposed decentralized MJ-SCC, the decentralized MJ-GCC, and the distributed GCC strategies for the mobile network are presented in Fig. 8.18 to Fig. 8.20. The solid line represents the reference queuing length, the dashed line indicates the buffer response with the nominal model of the $M/D/1$ queue, and the dotted line denotes the buffer response with the nominal model of the $M/E_k/1$ queue.

For comparing the robustness capabilities of the three congestion control strategies in mobile networks with respect to different nominal queuing models, the average queuing errors of all the bottle neck nodes are summarized in Table 8.2.

C. Observations and Conclusions

From the simulation results shown in Fig. 8.15 to Fig. 8.20 and the numerical comparisons in Tables 8.1 to 8.2, one can summarize the following conclusions for the three congestion control strategies, namely the decentralized SCC, with respect to the robustness to the model uncertainties

- As shown in Fig. 8.15 and Fig. 8.18, the SCC and the MJ-SCC algorithms converge with both the M/D/1 and the $M/E_k/1$ queuing models, for the fixed and the mobile networks environment, respectively.

- The SCC algorithm can achieve an overall queuing error of less than 3% and the MJ-SCC algorithm can achieve an overall queuing error of less than 4%.
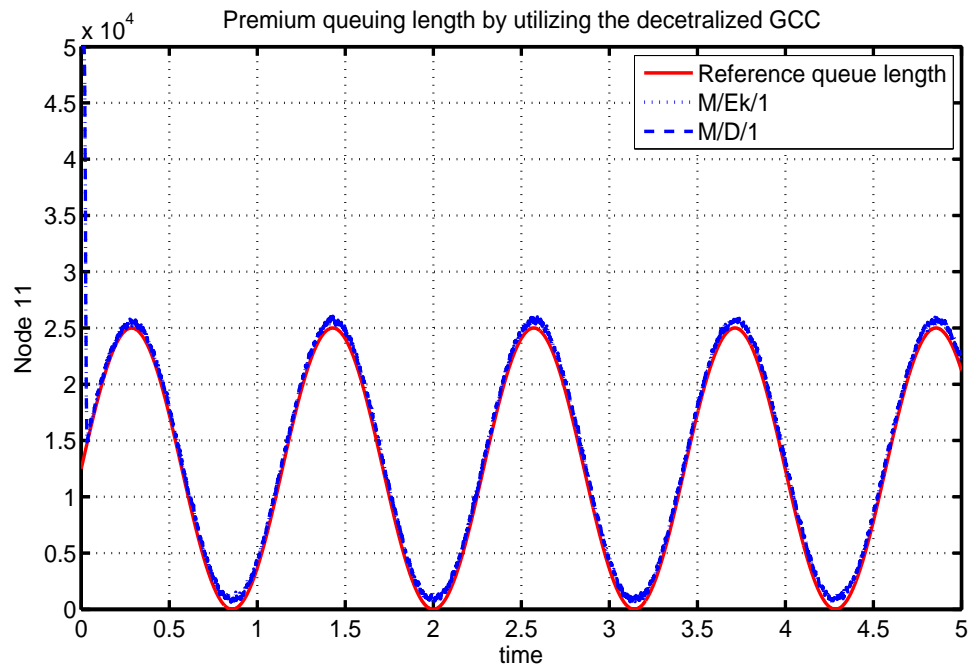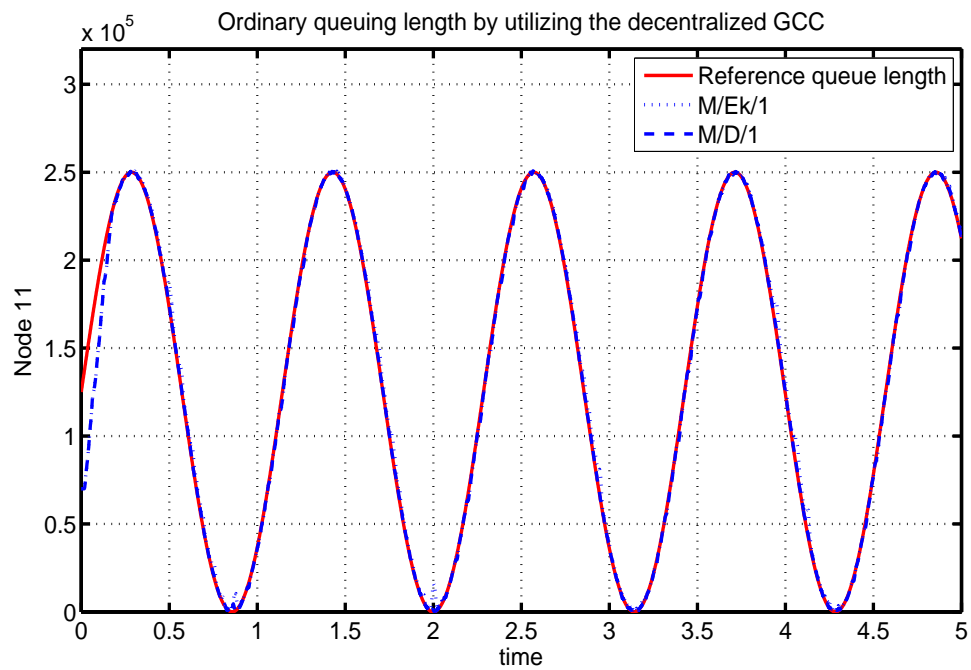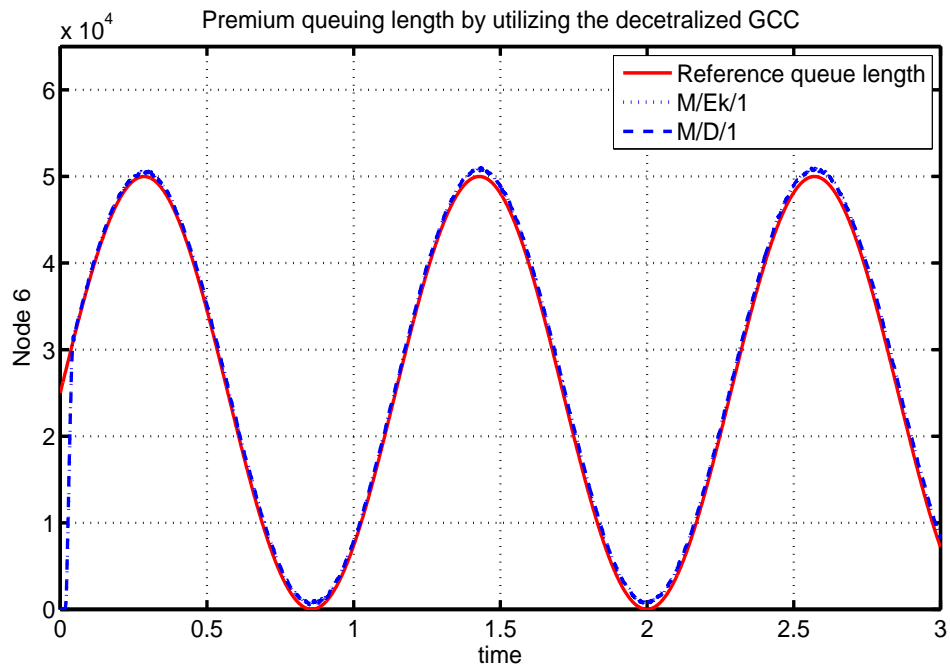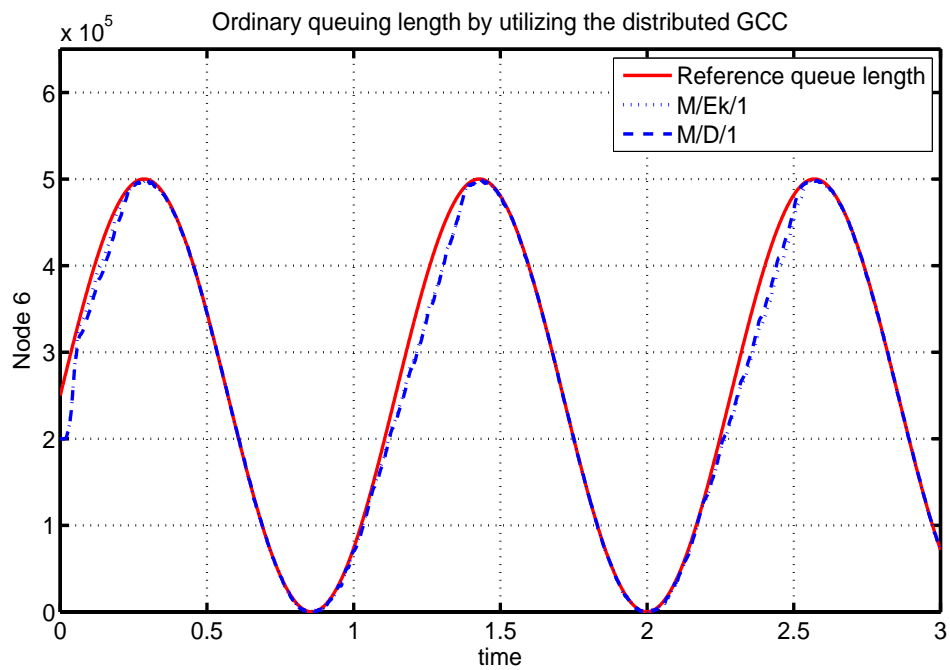
348
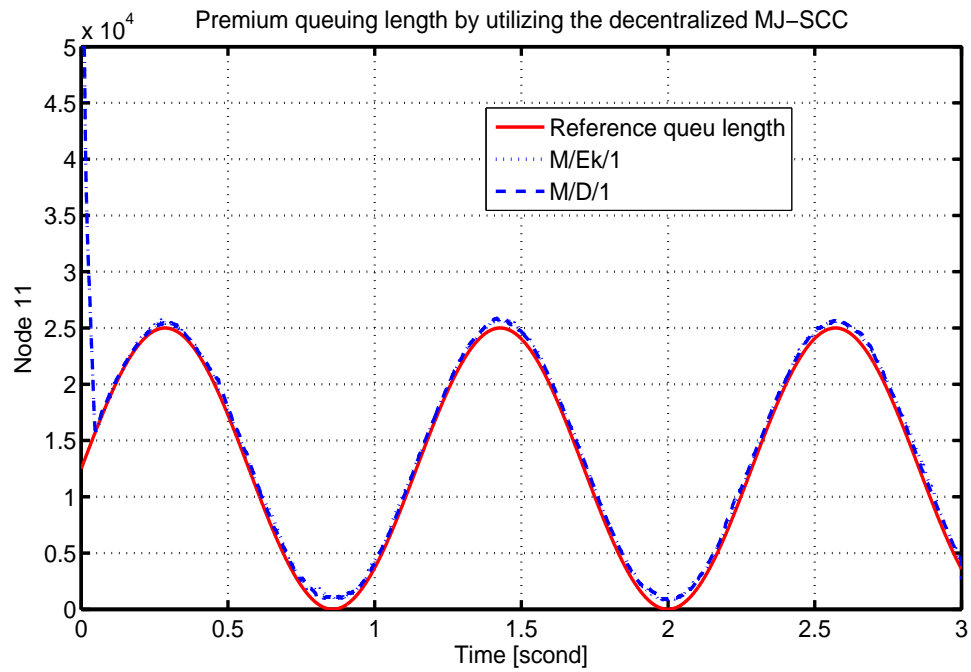
(a)
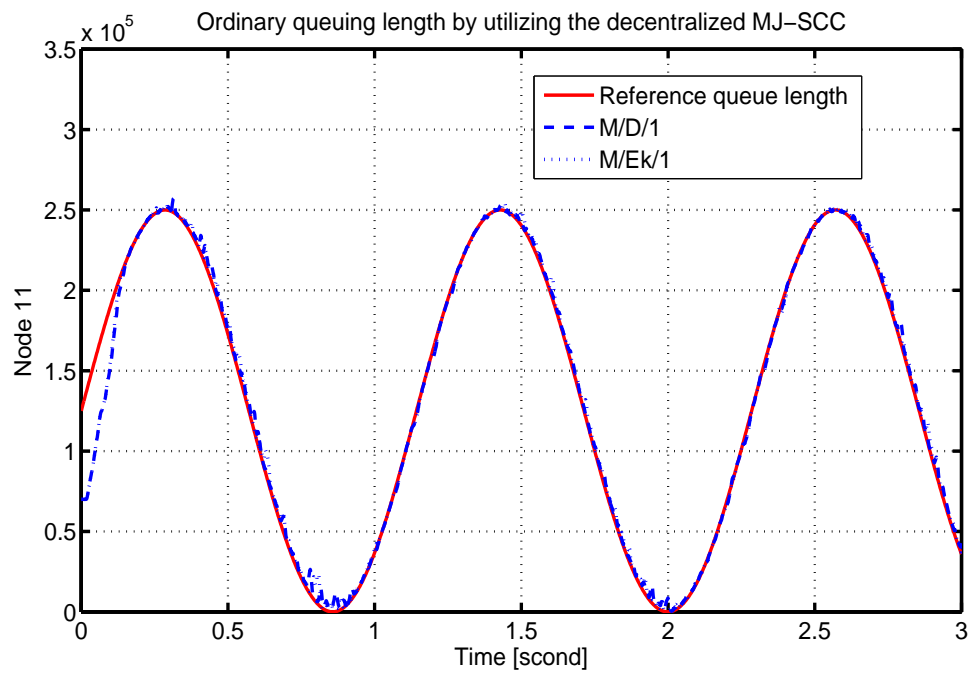
(b)

Figure 8.18: Buffer responses of node 11 subject to the decentralized MJ-SCC strategy that is designed based on the M//M/1 model but applied to the M/D/1 and the $M/E_k/1$ models. The solid line is the reference queuing, the dashed line is the buffer response with the M/D/1 model, and the dotted line is the buffer response with the $M/E_k/1$ model.
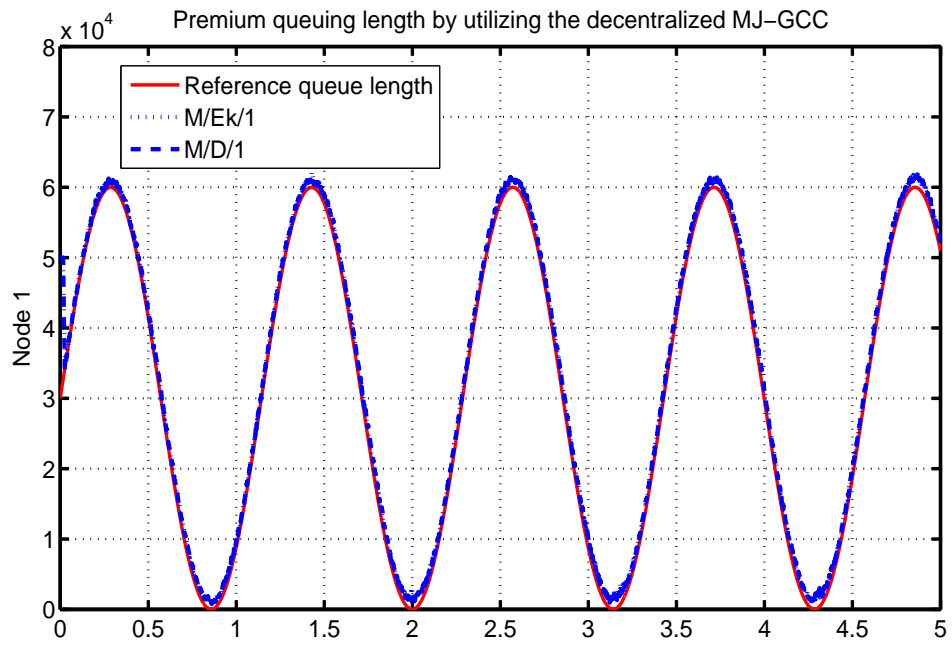
(a)
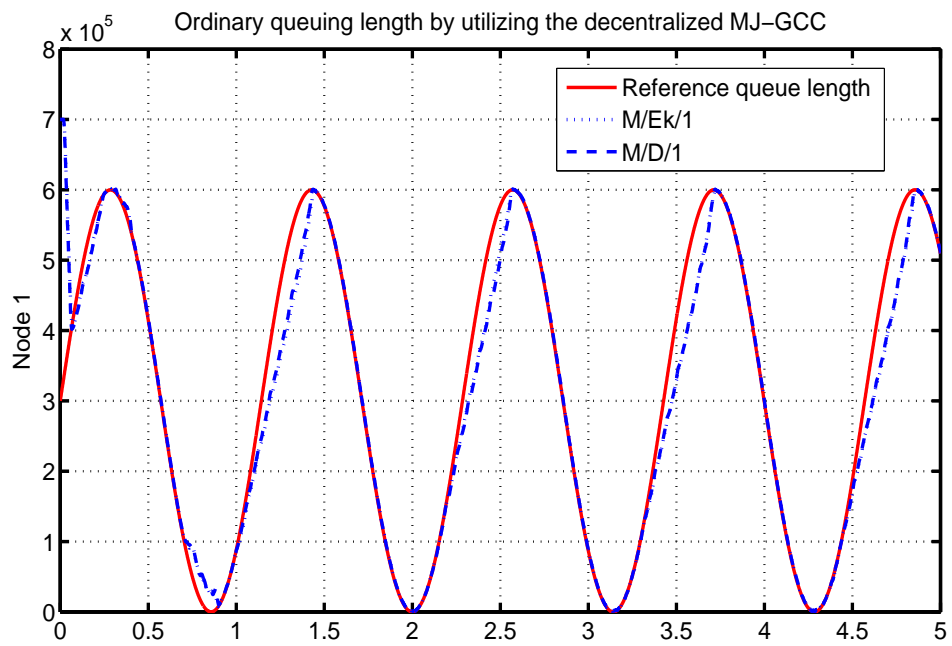
(b)

Figure 8.19: Buffer responses of node 1 subject to the decentralized MJ-GCC strategy that is designed based on the M//M/1 model but applied to the M/D/1 and the $M/E_k/1$ models. The solid line is the reference point, the dashed line is the buffer response with the M/D/1 model, and the dotted line is the buffer response with the $M/E_k/1$ model.

(a)

(b)

Figure 8.20: Buffer responses of node 6 subject to the decentralized DGCC strategy that is designed based on the M//M/1 model but applied to the M/D/1 and the $M/E_k/1$ models. The solid line is the reference point, the dashed line is the buffer response with the M/D/1 model, and the dotted line is the buffer response with the $M/E_k/1$ model.

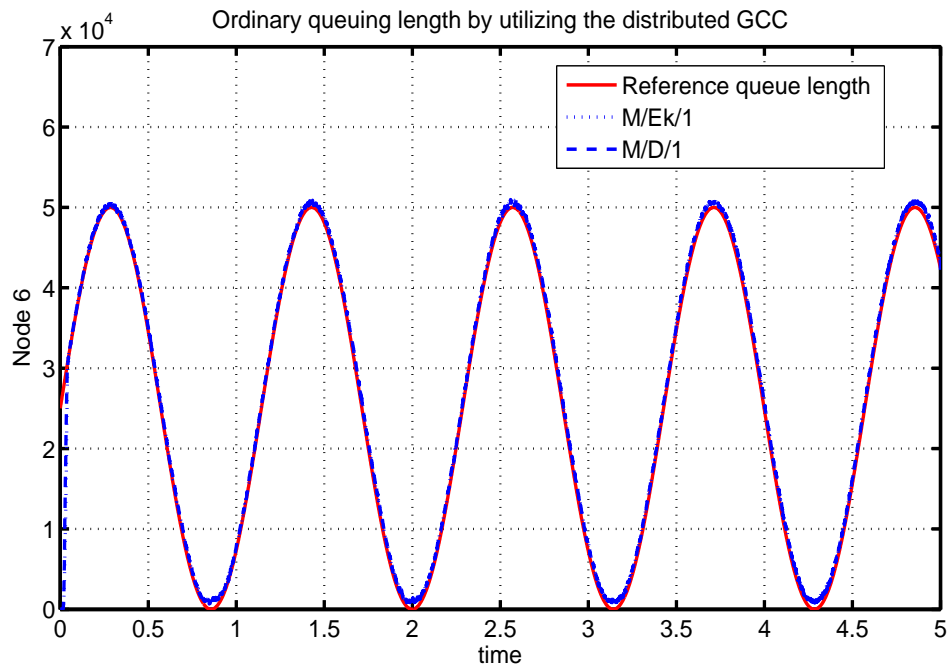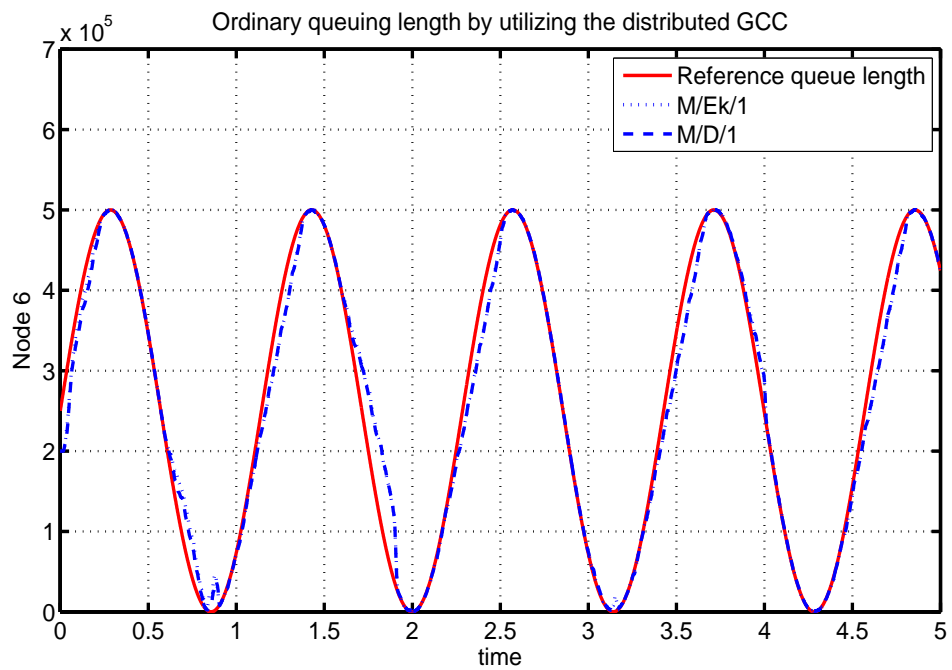- As shown in Fig. 8.16, the GCC algorithm converges for both the premium and the ordinary traffic classes with the two queuing models. However, the performance of the ordinary traffic is more robust than the premium traffic class. The overall queuing error of the GCC algorithm is less than 4%.

- As shown in Fig. 8.19, the MJ-GCC algorithm converges for both the traffic classes. On the other hand, the buffer response of the ordinary traffic has large discrepancies during when the queuing length increases. However, the overall queuing errors of the ordinary traffic by utilizing the MJ-GCC algorithm remains less than 6%.

- As shown in Fig. 8.17, the DGCC algorithm converges in the fixed network with both the M/D/1 and the $M/E_k/1$ queuing models. The average queuing errors by utilizing the DGCC strategy is less than 3% for the fixed network.

- As shown in Fig. 8.20, the DGCC algorithm performs very well for the premium traffic in a mobile network. However, the buffer response of the ordinary traffic class has large discrepancies when the queuing length increases. The overall queuing errors of the DGCC algorithm in mobile networks is less than 2% for the premium traffic and less than 5% for the ordinary one.

8.3   Conclusions

In this chapter, the robustness capabilities of the decentralized SCC, the decentralized GCC, and the distributed GCC strategies are evaluated and compared through a comprehensive simulations for the network with a fixed topology as well as for a mobile network. The simulation results show that all the three congestion control strategies are robust when the queue service rate μ has a relatively small uncertainty of less than 20%, for both the traffic classes. However, when the parametric uncertainty increases, the performance of all the congestion control strategies deteriorate and the controllers are still able to stabilize the buffer queues.

On the other hand, the robustness evaluations for the unstructured uncertainties

show that all the three congestion control strategies for the fixed network are highly robust with the nominal system of $M/D/1$ and $M/E_k/1$ queueing models. For the mobile network, the MJ-SCC strategy is robust for both the premium and the ordinary traffic classes. But, the MJ-GCC and the DGCC strategies are only robust for the premium traffic but have large discrepancies during the transient of buffer responses for the ordinary traffic.

Chapter 9

Conclusions and Future Work

This chapter discuss the conclusions of the thesis followed by some suggestions for future research work.

9.1 Conclusions and Main Contributions

In this dissertation, we have been focused on the congestion control problem in a network of multi-agent system(NAMS) subject to differentiated services (Diff-Serv)traffic. To achieve this goal, the following are the main contributions of this thesis:

- The analytical and quantitative queuing models of the networks of multi-agent systems(NMAS) based on the conservation law for each traffic class, as defined in the Diff-Serv architecture [56], are considered. The dynamic queuing model for a single node system was generalized to a large scale network where the inter-node traffic is considered explicitly with multiple and time-varying delays. For the congestion control design purposes, the models are developed in two different frameworks, namely the centralized and the decentralized model for fixed network as well as for mobile networks. In the centralized model, the entire network is considered as a whole for each traffic class. The unknown and time-varying delays are considered as inherent characteristics in the model. In the decentralized model, dynamics of each node is

modeled as a coupling system with unknown and time-varying delays in the coupling states and inputs from the neighboring nodes.

- In Chapter 3, a novel switching congestion control (SCC) strategy is proposed for a fixed network. The physical constraints of the communication network are considered during the controller synthesis. Multiple controllers are designed based on the system constraints, and the congestion control problem of each traffic class is recast as a switching controller based on the characteristics of the system state. The closed-loop system is shown to experience multiple modes and the stability conditions under each mode are derived and expressed by a set of Linear Matrix Inequalities (LMIs). For each traffic class, a centralized and a decentralized switching congestion control strategy are developed.

In Chapter 4, a mobile NMAS is considered. To address the random node mobility, and consequently the stochastic changes of the network topology, a Markovian jump process was considered. A Markovian jump switching congestion controller (MJ-SCC) is then developed to stochastically stabilize the Markovian jump systems with time-varying delays. The closed-loop system is shown to be represented as a hybrid switching system with both deterministic and stochastic switchings. A set of mode-dependent LMIs are then provided to ensure the stability of the closed-loop system.

- Our second proposed congestion control approach is introduced in Chapters 5 and 6 that is known as the guaranteed cost congestion control (GCC) strategy. The congestion controller is first developed without consideration of physical constraints. A robust congestion control strategy is developed based on a quadratic cost function. An upper bound on the cost is guaranteed by satisfying a corresponding set of linear matrix inequality (LMI) conditions. The physical constraints of the system are then considered and are expressed as a group of complementary LMIs. The proposed guaranteed cost congestion controller is generalized to the mobile network. The resulting guaranteed cost control problem for each traffic class is considered as a jump linear quadratic regulation (JLQR) problem and a Markovian jump guaranteed

cost congestion control (MJ-GCC) strategy is proposed.

- The proposed centralized and decentralized approaches are evaluated and compared on a given performance index in terms of both the QoS and the control, such as the packet loss rate, the queuing delay, the size of the LMIs, and the upper bound of the cost. The distinct advantages of each approach have revealed through comparative evaluations to the idea of a mixed control scheme, namely the distributed congestion control (DGCC) strategy. By incorporating the capability of the communication among the controller, the DGCC strategy is in fact equivalent to a local state feedback control plus a nearest neighboring controller's that are adjusted with proportional gains. The DGCC approach has shown to significantly enhance the scalability of the centralized algorithm and improves the performance of the decentralized approach to a large scale traffic network.

- Finally, in order to investigate the robustness of all the proposed congestion control strategies in this thesis, comprehensive simulations are conducted to evaluate our proposed SCC and GCC strategies for both the fixed and mobile NMAS with respect to uncertainties of system parameters and uncertainties in the model dynamics. The robustness performance characteristics of the centralized, the decentralized, and the distributed schemes for the premium and the ordinary traffic are investigated and evaluated extensively through numerical simulation studies. It is shown that our proposed solution are strongly robust to unmodeled dynamics but to a lower degree is robust to parametric uncertainties.

9.2   Future Work

The research presented in this thesis has provided several strategies for congestion control problem of NMAS with Diff-Serv traffic. In order to extend the current work, some of the open problems and prospective future researches are listed below:

- Throughout the thesis, the performance of our proposed congestion control strategies are only compared with a fluid flow model based congestion controller, namely the integrated dynamic congestion controller (IDCC) [3]. Comparisons with other common congestion control schemes in the literature will be interesting and essential for the purpose of complete evaluation. Possible approaches for future comparative studies include the sliding mode based congestion control [131], [162], the PID based congestion control [163], [164], and the TCP window based congestion control strategies [165], [166].

- The proposed congestion control schemes in this thesis are derived based on a fluid flow model with an assumption of M/M/1 queue. Considering other kinds of queuing systems, such as the $M/E_k/1$ and the G/M/1 and designing stabilizing corresponding controllers can be an interesting extension of our proposed congestion control schemes.

- To improve the robustness capabilities of our proposed congestion control strategies, a formal synthesis and development by utilizing the robust control theory are needed for the congestion control problem of Diff-Serv networks, especially with multiple and time-varying delays. Recently, much attention has been shown to robust congestion control problem and significant research has been presented in the literature. In [167], a robust congestion control scheme is developed based on the analytical fluid flow model for a packet switching network. In [168], the congestion control problem of ATM networks is considered and a robust H_∞ controller is developed. On the other hand, the robust stability and control of time-delay systems has become an attractive topic in the literature. In [169], [170], the authors presented some similar and most often used delay-dependent methods, yet these methods are too conservative in some cases, particularly when applied to a system which is stabilizable independent of the size of the delay. Furthermore, they are often very complex and can only deal with small delays. In [85], an improved method for the previous results is proposed. Our next step will focus on extending the proposed congestion

357

control strategies by utilizing a formal robust stabilization and control framework.

- The time-delays considered in this thesis are assumed to be unknown and time varying for both fixed and mobile networks. However, in a mobile network, the time-delays are often mode-dependent due to the changes of distance between two nodes and the changes of the network topology. Although, the stabilization problem of Markovian jump systems (MJS) with time-delays has been well investigated, there has been very little literature on the mode-dependent time-delays. In some cases, the time-delays may even be more complicated comprising of distributed ones, which is referred to as mixed mode-dependent (MDD) time-delays [171]. Therefore, more investigation will be necessary in the future on finding stabilizing controllers for a Markovian jump system with mode-dependent delay.

Appendix A

Integrated Dynamic Congestion Controller (IDCC)

The integrated dynamic congestion controller (IDCC) was first presented by the researchers in [3]. The basic idea is to control the traffic by using information on the status of each queue in the network, based on a nonlinear model of the network that is generated by using fluid flow considerations. The IDCC method is treated as the benchmark of model-based analytical congestion control approach in the control community and has been shown great performances in ATM based networks. In [3], the IDCC approach was presented in a decentralized framework. In this Appendix, we first review the decentralized IDCC approach as presented in [3], and then extendeded it to a centralized formulation.

A.1   Decentralized IDCC

The dynamic queuing model of a single ATM switch with the assumption of an M/M/1 queue is given by

$$\dot{x}_i(t) = -\mu_i \frac{x_i(t)}{1 + x_i(t)} C_i(t) + \lambda_i(t) \tag{A.1}$$

$$x(0) = 0$$

where $x_i(t)$ is the queuing state, $C_i(t)$ is defined as the capacity of queue server, $\lambda_i(t)$ is the incoming traffic rate, and μ_i is the average queue services rate which is assumed to

be 1 in [3]. The model (A.1) is applicable to both the premium and the ordinary traffic classes.

The integrated congestion control strategy for the premium and the ordinary traffic is then given as follows:

$$C_{pi}(t) = max\{0, min\{C_{i,server}, \rho \frac{1 + x_{pi}(t)}{x_{pi}(t)}[\alpha_{pi}(\bar{x}_{pi}(t)) + k_{pi}(t)]\}\} \qquad (A.2)$$

$$C_{ri} = max\{0, C_{i,server} - C_{pi}(t)\} \qquad (A.3)$$

$$\lambda_{ri}(t) = max\{0, min\{C_{ri}(t), C_{ri}(t)\frac{x_{ri}(t)}{1 + x_{ri}(t)} - \alpha_{ri}\bar{x}_{ri}(t)\}\} \qquad (A.4)$$

where "p" denotes the premium traffic, "r" denotes the ordinary traffic, $C_{pi}(t)$ is the capacity allocated for the premium traffic, $C_{ri}(t)$ is the maximum allowable capacity for the ordinary traffic, $\lambda_{ri}(t)$ is the regulated incoming traffic for the ordinary traffic, $C_{i,server}$ is the maximum possible service rate, $\bar{x}_i(t) = x_i(t) - x_{i,ref}$ is the the queuing error, α_i is the control gain, and $k_{pi}(t)$ is the adaptive estimator for the premium traffic which is updated according to

$$\dot{k}_{pi}(t) = Pr[\delta_{pi}\bar{x}_{pi}(t)] \qquad (A.5)$$

$$Pr[\delta_{pi}\bar{x}_{pi}(t)] = \begin{cases} \delta_{pi}\bar{x}_{pi}(t), & \text{if } 0 \leq k_{pi}(t) \leq \hat{k}_{pi}; \\ & \text{or } k_{pi}(t) = \hat{k}_{pi}, \bar{x}_{pi} \leq 0 \\ & \text{or } k_{pi}(t) = 0, \bar{x}_{pi}(t) \geq 0 \\ 0, & \text{else.} \end{cases} \qquad (A.6)$$

where $\hat{k}_{pi}$ is the maximum allowable traffic rate for the premium traffic.

Remark A.1. *As indicated from (A.2), the IDCC controller does consider the physical constraints of the network and has been shown to be stable for a single node model (A.1) [3]. Therefore, it is applicable to a cascade type of networks. However, when it is applied to the fully connected networks, such as the NMAS, the nonlinear coupling states of the neighboring nodes with multiple and time-varying delays are no longer negligible and can lead to the main resource of instability. This has been shown by the simulations in our thesis.*

A.2 Centralized IDCC

In order to compare the IDCC approach with our proposed centralized congestion controllers (SCC, GCC, MJ-SCC, MJ-GCC) fairly, we extend the decentralized IDCC in [3] to a centralized framework.

Based on the decentralized queuing model (A.1), the centralized queuing model of a network with an M/M/1 queue can be written as

$$\dot{X}(t) = -F(X,t)C(t) + \lambda(t) \tag{A.7}$$

$$F(X,t) = diag\{\mu_i \frac{x_i(t)}{1 + x_i(t)}\} \tag{A.8}$$

$$X(0) = 0$$

where $X(t) = vec[x_i(t)]$ is the vector of queuing state, $C(t) = vec[C_i(t)]$ is the vector of the capacities of the queue server, and $\lambda(t) = vec[\lambda_i(t)]$ is the vector of the incoming traffic rate. The above (A.13)-(A.8) is applicable to both the premium and the ordinary traffic classes of traffic.

The decentralized IDCC strategies (A.2) can then be extended to the following centralized one:

$$C_p(t) = max\{0, min\{C_{server}, F^{-1}(X_p,t)[A_p(\bar{X}_p(t)) + K_p(t)]\}\} \tag{A.9}$$

$$C_r = max\{0, C_{server} - C_p(t)\} \tag{A.10}$$

$$\lambda_r(t) = max\{0, min\{C_r(t), F(X_r,t)C_r(t) - A_r\bar{X}_r(t)\}\} \tag{A.11}$$

where "p" denotes the premium traffic, "r" denotes the ordinary traffic, $C_p(t)$ is the centralized capacity controller for the premium traffic, $C_r(t)$ is the maximum allowable capacity for the ordinary traffic, $\lambda_r(t)$ is the centralized flow rate controller for the ordinary traffic, $C_{server} = vec[C_{i,server}]$ is the vector of maximum service rate, $\bar{X}(t) = vec\{\bar{x}_i(t)\}$ is the vector of queuing errors, A_p and A_r are the centralized control gain matrices, and $K_p(t)$ is the centralized adaptive estimator for the premium traffic which is defined as $K_p(t) = vec\{k_{pi}(t)\}$ and is updated according to

$$\dot{K}_p(t) = Pr[\Delta_p\bar{X}_p(t)] \tag{A.12}$$

$$Pr[\Delta_p \bar{X}_p(t)] = \begin{cases} \Delta_p \bar{X}_p(t), & \text{if } 0 \leq K_p(t) \leq \hat{K}_p; \\ & \quad \text{or } K_p(t) = \hat{K}_p, \bar{X}_p \leq 0 \\ & \quad \text{or } K_p(t) = 0, \bar{X}_p(t) \geq 0 \\ 0, & \text{else.} \end{cases} \tag{A.13}$$

where $\hat{K}_p = vec\{\hat{k}_{pi}\}$ is the vector of maximum allowable traffic rate for the premium traffic.

Remark A.2. *The switching conditions in the above projection algorithm (A.13) are based on the comparisons of vectors $K_p(t)$ and $\hat{K}_p$, and also on the value of vector $\bar{X}_p(t)$. According to Definition 2.4, only when all the elements in the vector $K_p(t)$ satisfy the corresponding conditions will the estimator be updated. For example, the condition $K_p(t) = \hat{K}_p$ is valid only when $k_{pi}(t) = \hat{k}_{pi}$ for all $i = 1, ..., n$, and the condition $\bar{X}_p \leq 0$ is valid only when $\bar{x}_{pi}(t) \leq 0$ for all $i = 1, ..., n$.*

Remark A.3. *In our proposed centralized SCC, centralized MJ-SCC, and centralized GCC strategies, as presented in Chapters 3, 4, and 5, respectively, the switching conditions of the estimators $\hat{\lambda}_p(t)$ and $\hat{\lambda}_r(t)$ are also based on the comparisons of vectors. It should be noted that the vectors are also compared according to the Definition 2.4.*

Appendix B

QualNet Simulator

QualNet is the next generation of the scalable GloMoSim (Global Mobile Information Systems Simulator) simulator. GloMoSim was designed to simulate large-scale wireless networks with thousands of mobile nodes, each of which may have different communication capabilities via multi-hop ground, aircraft and satellite media. QualNet has extended GloMoSims capabilities to wired networks as well as mixed wired and wireless networks. Like its predecessor, QualNet uses the parallel simulation kernel provided by the PARSEC discrete-event simulation language. Consequently, QualNet is among the few simulators for wireless and wired networks that have been implemented on sequential and parallel architectures.

QualNet software includes detailed models of commonly used protocols at each of the primary layers of OSI model. In each layer, the commonly used protocols in both wired and wireless networks have been modeled [133]. The following QualNet features provide a unique capability for accurate, efficient simulation of large-scale heterogeneous networks [133]:

- Robust set of wired and wireless network protocol and device models, useful for simulating diverse types of networks,

- Optimized for speed and scalability on one processor, QualNet executes equivalent scenarios 5-10x times faster than commercial alternatives,

- Designed from the ground-up as a parallel simulator, QualNet executes your simulation multiples faster as you add processors.

- A robust graphical user interface covers all aspects of the simulation, from scenario creation and topology setup, integration of custom protocols, through real-time execution of network models from within the GUI, animation, to post-simulation statistical analysis.

- QualNet has been used to simulate high-fidelity models of wireless networks with as many as 50,000 mobile nodes.

B.1 Integration of QualNet Traffic in MatLab

In order to incorporate the QualNet traffic into MatLab, we need to implement the traffic flow in MatLab according to the protocol models that are defined in QualNet. This mainly involves the conversion of the features from QualNet to input needed for the fluid flow model, which is the dynamic system model that is used in this thesis. Packets from data sources need to be converted to flows entering the analytical model, and then used for simulations of our proposed congestion control strategies in MatLab.

In the QualNet simulator, the system entity is the *node-queue*; the system events are *packets-arrival* and *packets-departure*; and the system state which is changed according to and by these events is the *number-of-packets-in-the-queue*. This is represented as a discrete-event system with continuous-time state space representation. The random variables that need to be specified to model this system stochastically are *packet-size* and *packet-inter-arrival-time*, which are the characteristics of the incoming traffic.

In the simulations of fixed network, the only entities that will change the events (*packets-arrival* and *packets-departure*) are the *traffic generator* that are invoked in the application layer of the QualNet software. Once the variables are set, such as the *packet-size* and *average-inter-arrival-time*, the packets characteristics are subsequently determined. In other words, the chronological sequence of events are determined. Therefore, our approach to this problem is to first construct a simulation scenario and generate the traffics

by using the QualNet software environment, and then convert the packet characteristics, as determined by the entities set in the QualNet, into data flows with the form that is required by the fluid flow model. The fluid flow analytical model will make use of these data flows and other parameters to obtain network statistics by solving the corresponding differential equations. In particular, the queue lengths of the nodes are obtained. The fluid flow model is the part that is implemented in MatLab. Therefore, we can state that the discrete behavior of the packets as generated by the QualNet software environment is integrated with the fluid flow model that is implemented by the MatLab software environment.

On the other hand, in a mobile network, besides the *traffic generator*, the other important entity that will change the events (*packets-arrival* and *packets-departure*) is the connectivity between two nodes which is based on the network topology. In this thesis, the changes of the network topology is modeled as a stochastic process of Markov chain. Different neighboring sets are represented as different network modes α_t. The transition probability from mode l to mode k is defined by the variable π_{kl}. In this thesis, we assume that the transition probabilities among different modes are given. The Markov chain is then generated by using the MatLab function *randsrc* [152].

For example, a 5 mode mobile network is represented by an index vector $[1, 2, 3, 4, 5]$. Suppose the current mode is $mode(k) = 2$, and the transition probabilities from mode 2 to the other modes are $\pi_{l2} = [0.1, 0.6, 0.1, 0.05, 0.15]$. Then, the following command is applied to predict the next mode $mode(k + 1)$, that is

$$s = randsrc(1, N, [1, 2, 3, 4, 5; \ 0.1, 0.6, 0.1, 0.05, 0.15])$$

$$mode(k + 1) = s(k + 1)$$

where N is the simulation time. The above command will generate an $1 \times N$ vector s with numbers 1 to 5. The sequence of the numbers are random but the occurrence probability of each number is the same as given by π_{l2}. Hence, in each round of simulation, the sequence of switching modes can be obtained and the chronological sequence of events is then determined.

Therefore, our approach is to run the simulations for multiple rounds (e.g. 10

rounds). In each round, the data flows are converted from the QualNet traffics as in the fixed network. The queuing length at each instant is then determined as the average value over these 10 rounds. As a result, one can state that the discrete behavior of the packets generator and the changes of the network topology are implemented in the MatLab software environment.

Bibliography

[1] DARPA, *Joint Unmanned Combat Air Systems J-UCAS Overview*, March 2004.

[2] D. Buis, "Key technologies for uav interoperability," in *41st Annual NDIA Symposium*, The Boeing Company, November 2003.

[3] A. Pitsillides, P. Ioannou, M. Lestas, and L. Rossides, "Adaptive nonlinear congestion controller for a differentiated-service framework," in *IEEE/ACM Transactions on networking*, vol. 13 of *1*, pp. 94–107, February 2005.

[4] S. Corley, M. Tesselaar, J. Cooley, J. Meink, F. Malabocchia, and F. J. Garijo, "The application of intelligent and mobile agents to networks and service management," in *Proceedings of the 5th International Conference on Intelligence and Services in Networks*, vol. 1430, pp. 127 – 138, 1998.

[5] C. Tomlin, G. J. Pappas, and S. Sastry, "Conflict resolution for air traffic management: a study in multi-agent hybrid systems," in *IEEE Transactions on Automatic Control*, vol. 43 of *4*, pp. 509–521, April 1998.

[6] K. Akkaya and M. Younis, "A survey on routing protocols for wireless sensor networks," in *Ad Hoc Network Journal*, vol. 3 of *3*, pp. 325–349, May 2004.

[7] FOUNDATION FOR INTELLIGENT PHYSICAL AGENTS (FIPA), *Agent Communication Language*, October 1997.

[8] J. Hill, "System architecture directions for networked sensors," in *Proceedings ACM International Conference on Architectural Support of Programming Languages and Operating Systems*, vol. 35 of *11*, pp. 93–104, November 2000.

[9] D.Gay, "A holistic approach to networked embedded systems," in *Proceedings of the ACM conference on Programming language design and implementation (SIGPLAN)*, vol. 38, pp. 1–11, May 2003.

[10] C. Borcea, "Spatial programming using smart messages: Design and implementation," in *Proceedings of the 24th International Conference on Distributed Computing Systems (ICDCS)*, pp. 690–699, 2004.

[11] B. Greenstein, "A distributed index for features in sensor networks.," in *Proceedings of the First IEEE International Workshop on Sensor Network Protocols and Applications*, pp. 163–173, 2003.

[12] D. Niculescu, "Positioning in ad hoc sensor networks," vol. 18 of *4*, pp. 24–29, 2004.

[13] G. L. Mariottini, F. Morbidi, D. Prattichizzo, N. V. Valk, N. Michael, G. Pappas, and K. Daniilidis, "Vision-based localization for leader-follower formation control," in *IEEE Transactions on Robotics*, vol. 25 of *6*, pp. 1431 – 1438, December 2009.

[14] B. Sinopoli, C. Sharp, L. Schenato, S. Schaffert, and S. S. Sastry, "Distributed control applications within sensor networks," in *Proceedings of the IEEE*, vol. 91 of *8*, pp. 1235–1245, August 2003.

[15] C. Han, "A dynamic operating system for sensor nodes," in *Proceedings of the 3rd international conference on Mobile systems, applications, and services(MobiSys.)*, pp. 163–176, 2005.

[16] B. J. Culpepper, L. Dung, and M. Melody, "Design and analysis of hybrid indirect transmissions (hit) for data gathering in wireless micro sensor networks," in *ACM Mobile Computing and Communications Review (SIGMOBILE)*, vol. 8 of *1*, p. 6183, January 2004.

[17] A. Helmy, "Capture: location-free contact-assisted power-efficient query resolution for sensor networks," in *ACM Mobile Computing and Communications Review (SIG-MOBILE)*, vol. 8 of *1*, pp. 27–47, January 2004.

[18] X. Hu, Y. Liu, M. J. Lee, and T. N. Saadawi, "A novel route update design for wireless sensor networks," in *ACM Mobile Computing and Communications Review (SIGMOBILE)*, vol. 8 of *1*, pp. 18–26, January 2004.

[19] P. Traakadas, T. Zahariadis, S. Voliotis, and C. Manasis, "Efficient routing in pan and sensor networks," in *ACM Mobile Computing and Communications Review (SIGMOBILE)*, vol. 8 of *1*, pp. 10–17, January 2004.

[20] T. Melodia, D. Pompili, and I. F. Akyildiz, "Optimal local topology knowledge for energy efficient geographical routing in sensor networks," in *Prodeedings of Twenty-third AnnualJoint Conference of the IEEE Computer and Communications Societies (INFOCOM)*, vol. 3, pp. 1705–1716, 2004.

[21] K. Seada, M. Zuniga, A. Helmy, and B. Krishnamachari, "Energy-efficient forwarding strategies for geographic routing in lossy wireless sensor networks," in *Proceedings of the 2nd international conference on Embedded networked sensor systems (SenSys)*, pp. 108–121, 2004.

[22] Q. Fang, J. Gao, and L. J. Guibas, "Locating and bypassing routing holes in sensor networks," in *Proceedings of Twenty-third AnnualJoint Conference of the IEEE Computer and Communications Societies (INFOCOM)*, vol. 4, pp. 2458–2468, 2004.

[23] L. Chen, S. H. Low, M. Chiang, and J. C. Doyle, "Cross-layer congestion control, routing and scheduling design in ad hoc wireless networks," in *25th IEEE International Conference on Computer Communications,(INFOCOM)*, pp. 1–13, April 2006.

[24] F. Paganini, Z. Wang, J. Doyle, and S. Low, "Congestion control for high performance, stability and fairness in general networks," in *IEEE/ACM Transactions on Networking*, vol. 13 of *1*, pp. 43–56, February 2005.

[25] S. Floyd and V. Jacobson, "Random early detection gateways for congestion avoidance," in *IEEE/ACM Transaction on Networking*, vol. 1 of *4*, pp. 397–413, August 1993.

[26] B. K. Lee, L. K. John, and E. John, "Architectural enhancements for network congestion control applications," in *IEEE Transactions on Very Large Scale Systems*, vol. 14 of *6*, pp. 609–615, June 2006.

[27] M. Baines, B. Nandy, P. Pieda, N. Seddigh, and M. Devetsikiotis, "Using tcp models to understand bandwidth assurance in a differentiated services network," in *Proceeding of IEEE Global Telecommunications Conference(GLOBECOM)*, vol. 3, pp. 1800–1805, 2001.

[28] F. Xia, "Qos challenges and opportunities in wireless sensor/actuator networks," in *Sensors*, vol. 8 of *2*, pp. 1099–1110, February 2008.

[29] J. Nagle, "Congestion control in tcp/ip internetworks," in *ACM Computer Communication Review*, vol. 14 of *4*, pp. 11–17, October 1984.

[30] S. Kunniyur and R. Srikant, "Analysis and design of an adaptive virtual queue (avq) algorithm for active queue management," in *ACM Annual Conference of Special Interest Group on Data Communications*, pp. 123–134, August 2001.

[31] C. Hollot, V. Misra, D. Towsley, and W. Gong, "On designing improved controllers for aqm routers supporting tcp flows," in *Proceedings of Twentieth Annual Joint Conference of the IEEE Computer and Communications Societies (INFOCOM)*, vol. 3, pp. 1726–1734, April 2001.

[32] S. Athuraliya, S. Low, V. Li, and Q. Yin, "Rem: active queue management," in *IEEE Network Magazine*, vol. 15 of *3*, pp. 48–53, May 2001.

[33] V. Jacobson, "Congestion avoidance and control," in *ACM Annual Conference of Special Interest Group of Data Commnicaitons*, pp. 314–329, August 1988.

[34] B. Braden and et al., "Recommendations on queue management and congestion avoidance in the internet," tech. rep., RFC 2309, April 1998.

[35] H. Salim, "A proposal for backward ecn for the internet protocol (ipv4/ipv6)," techn. report, ATM Forum, Traffic Management Specification, 1999.

[36] W. Feng, D. D. Kandlur, D. Saha, and K. G. Shin, "A self-configuring red gateway," in *Proceedings of 8th Annual Joint Conference of IEEE Computer and Communication Societies*, vol. 3, pp. 1320–1328, March 1999.

[37] S. Floyd, R. Gummadi, and S. Shenker, "Adaptive red: an algorithm for increasing the robustness of red's active queue management," in *http://www.icir.org/floyd/papers/adaptiveRed.pdf*, August 2001.

[38] W. Feng, D. D. Kandlur, D. Saha, and K. Shi, "The blue active queue management algorithms," in *IEEE/ACM Transactions on Networking*, vol. 10 of *4*, pp. 513–528, August 2002.

[39] C. G. Wang, J. C. Liu, B. Li, K. Sohraby, and Y. T. Hou, "Lred: A robust and responsive aqm algorithm using packet loss ratio measurement," in *IEEE Transactions on Parallel and Distributed Systems*, vol. 18 of *1*, pp. 29–43, January 2007.

[40] C. Y. Wan, S. B. Eisenman, and A. T. Campbell, "Coda: Congestion detection and avoidance in sensor networks," in *Proceedings of the 1st international conference on Embedded networked sensor systems (SenSys)*, pp. 266–279, November 2003.

[41] P. Mishra and H. Kanakia, "A hop by hop rate-based congestion control scheme," in *Conference proceedings on Communications architectures & protocols(SIGCOMM)*, pp. 112–123, 1992.

[42] B. Hull, K. Jamieson, and H. Balakrishnan, "Mitigating congestion in wireless sensor networks," in *Proceeding of International Conference on Embedded Networked Sensor Systems (SenSys)*, pp. 134–147, November 2004.

[43] Y. Sankarasubramaniam, A. Ozgur, and I. Akyildiz, "Esrt: Event-to-sink reliable transport in wireless sensor networks," in *Proceedings of the 4th ACM international symposium on Mobile ad hoc networking & computing (MobiHoc)*, pp. 177–188, 2003.

[44] C. Wang, K. Sohraby, V. Lawrence, B. Li, and Y. Hu, "Priority-based congestion control in wireless sensor networks," in *Proceedings of the IEEE International Conference on Sensor Networks, Ubiquitous, and Trustworthy Computing*, vol. 1, June 2006.

[45] M. Rashid, M. M. Alam, M. A. Razzaque, and C. S. Hong, "Reliable event detection and congestion avoidance in wireless sensor networks," vol. 4782, pp. 521–532, Springer Berlin / Heidelberg, September 2007.

[46] C. Ee and R. Bajcsy, "Congestion control and fairness for many-to-one routing in sensor networks," in *Proceedings of the 2nd international conference on Embedded networked sensor systems (SenSys)*, pp. 148–161, November 2004.

[47] C. Y. Wan, A. T. Campbell, and L. Krishnamurthy, "Psfq: a reliable transport protocol for wireless sensor networks," in *Proceedings of the 1st ACM international workshop on Wireless sensor networks and applications (WSNA)*, pp. 1–11, September 2002.

[48] S. Chen and N. Yang, "Congestion avoidance based on lightweight buffer management in sensor networks," in *Parallel and Distributed Systems, IEEE Transactions on*, vol. 17 of *9*, pp. 934–946, September 2006.

[49] A. Segall, "The modeling of adaptive routing in data communication networks," in *IEEE Transactions on Communications*, vol. 25 of *1*, pp. 85–95, January 1977.

[50] A. Kolarov and G. Ramamurthy, "A control theoretic approach to the design of closed loop rate based flow control for high speed atm networks," in *IEEE/ACM Transactions on Networking*, vol. 1, pp. 293–301, 1997.

[51] T. P. Ha and D. B. Hoang, "Ficc-diffserv: A new qos architecture supporting resources discover," in *Information Technology and Applications, Third International Conference*, vol. 2, pp. 710–715, July 2005.

372

[52] C. Chrysostomou, A. Pitsillides, L. Rossides, and A. Sekercioglu, "Fuzzy logic controlled red: congestion control in tcp/ip differentiated services networks," in *Journal of Soft Computing*, vol. 8 of *2*, pp. 79–92, December 2003.

[53] A. Pitsillides and J. Lambert, "Adaptive congestion control in atm based networks: Quality of service with high utilization," in *Journal of Computer Communications*, vol. 20, pp. 129–139, 1997.

[54] H. Wu, K. Long, S. Cheng, and J. Ma, "Direct congestion control scheme (dccs) for differentiated services ip networks," in *IEEE global telecommunications conference (GLOBECOM)*, vol. 4, pp. 2290–2294, November 2001.

[55] S. Hongjun and M. Atiquzzaman, "End-to-end qos for differentiated services and atm internetworking," in *Proceedings of Ninth International Conference on Computer Communications and Networks*, pp. 557–562, October 2000.

[56] K. Chan, J. Babiarz, and F. Baker, "Aggregation of diffserv service classes," tech. rep., RFC 5127, February 2008.

[57] N. Zhang, G. Wang, L. Zhao, Y. Jing, and X. Li, "Sliding mode congestion control algorithm for a class of large-scale networks based on t-s model," in *Chinease Control and Decision Conference, (CCDC)*, pp. 3504–3508, July 2008.

[58] N. Zhang, M. Yang, Y. Jing, and S. Zhang, "Congestion control for diffserv network using second-order sliding mode control," in *IEEE Transactions on Industrial Electronics*, vol. 56 of *9*, pp. 3330–3336, September 2009.

[59] V. Utkin and L. Hoon, "Chattering problem in sliding mode control systems variable structure systems," in *International Workshop on VSS'06*, pp. 346–350, June 2006.

[60] R. R. Chen and K. Khorasani, "An adaptive congestion control technique for networked control systems," in *IEEE Conference on Industrial Electronics and Applications*, pp. 2791–2796, May 2007.

[61] A. Pitsillides, J. Lambert, and D. Tipper, "Dynamic bandwidth allocation in broadband-isdn using a multilevel optimal control approach," in *IEEE 14th Annual Joint Conference of Computer and Communications Societies: Bringing Information to People*, vol. 3, pp. 1086–1094, 1995.

[62] A. Pitsillides, P. Ioannou, and D. Tipper, "Integrated control of connection admission, flow rate, and bandwidth for atm based networks," in *Proceedings of Fifteenth Annual Joint Conference of the IEEE Computer Societies. Networking the Next Generation(INFOCOM)*, vol. 2, pp. 785–793, 1996.

[63] M. Handley, S. Floyd, J. Padhye, and J. Widmer, "Tcp friendly rate control (tfrc): Protocol specification," tech. rep., RFC 3448, January 2003.

[64] S. Floyd, "Congestion control principles," tech. rep., RFC 2914, September 2000.

[65] F. Ordonez and B. Krishnamachari, "Optimal information extraction in energy-limited wireless sensor networks," in *IEEE Journal on Selected Areas in Communications*, vol. 22 of *6*, pp. 1121–1129, August 2004.

[66] N. Sadagopan and B. Krishnamachari, "Maximizing data extraction in energy-limited sensor networks," in *Proceedings of Twenty-third AnnualJoint Conference of the IEEE Computer and Communications Societies (INFOCOM)*, vol. 3, pp. 1717–1727, March 2004.

[67] C. Brandauer, G. Iannaccone, C. Diot, T. Ziegler, S. Fdida, and M. May, "Comparison of tail drop and active queue management performance for bulk-data and web-like internet traffic," in *Sixth IEEE Symposium on Computers and Communications*, pp. 122–129, March 2001.

[68] M. Karsten and J. Schmitt, "Packet marking for integrated load control," in *9th IFIP/IEEE International Symposium on Integrated Network Management*, pp. 499–512, May 2005.

374

[69] R. W. Thommes and M. J. Coates, "Deterministic packet marking for congestion price estimation," in *Twenty-third AnnualJoint Conference of the IEEE Computer and Communications Societies (INFOCOM)*, vol. 1, pp. 76–85, March 2004.

[70] C. Simon, A. Vidacs, I. Moldovan, A. Torok, K. Ishibashi, A. Koike, and H. Ichikawa, "End-to-end relative differentiated services for ip networks," in *Proceedings of Seventh International Symposium on Computers and Communications (ISCC)*, pp. 783–788, November 2002.

[71] V. Jacobson, K. Nichols, and K. Poduri, "An expedited forwarding phb," tech. rep., RFC 2598, June 1999.

[72] J. Heinamen, F. Baker, W. Weiss, and J. Wroclawski, "Assured forwarding phb group," tech. rep., RFC 2597, June 1999.

[73] J. Little, "A proof for the queuing formula: $l = \lambda w$," in *Operations Research*, vol. 9 of *3*, pp. 383–387, May 1961.

[74] J. Filipiak, *Modeling and Control of Dynamic Flows in Communication Networks*. New York: Springer-Verlag, 1988.

[75] K. Pawlikowski, T. Bell, H. Emberson, and P. Ashton, "Compression of data traffic in packet-based lans," in *Proceedings of Data Compression Conference (DCC)*, pp. 430–430, March 1995.

[76] K. C. Chua and D. T. Nguyen, "Analysis of combined priority and bit-rate compression traffic access control strategy for integrated services networks," in *Electronics Letters*, vol. 25 of *8*, pp. 489–490, April 1989.

[77] O. Alatas, O. Javed, and M. Shah, "Video compression using spatiotemporal regularity flow," in *IEEE Transactions on Image Processing*, vol. 15 of *12*, pp. 3812–3823, December 2006.

[78] H. K. Khalil, *Nonlinear Systems, third edition*. Prentice Hall, 2001.

[79] V. S. Chellaboina, A. Kamath, and W. M. Haddad, "Frequency domain sufficient conditions for stability analysis of linear neutral time-delay systems," in *44th IEEE Conference on Decision and Control and European Control Conference (CDC-ECC)*, pp. 4330–4335, December 2005.

[80] V. Rassvan, D. Danciu, and D. Popescu, "Frequency domain stability inequalities for nonlinear time delay systems," in *15th IEEE Mediterranean Electrotechnical Conference (MELECON)*, pp. 1398–1401, April 2010.

[81] E. Fridman, "New lyapunov-krasovskii functionals for stability of linear retarded and neutral type system," in *System Control Letters*, vol. 43 of *4*, pp. 309–319, July 2001.

[82] E. Fridman and U. Shaked, "New bounded real lemma representations for time-delay systems and their application," in *IEEE Transactions on Automatic Control*, vol. 46 of *12*, pp. 1973–1979, December 2001.

[83] K. Benjelloun and E. K. Boukas, "Independent delay sufficient conditions for robust stability of uncertain linear time-delay systems with jumps," in *Proceedings of the American Control Conference*, vol. 6, pp. 3814–3815, June 1997.

[84] W. Cuihong and H. Tianmin, "Delay-independent variable structure control of time-delay systems with mismatched uncertainties," in *46th IEEE Conference on Decision and Control*, pp. 2065–2070, December 2007.

[85] E. Fridman, "Descriptor discretized lyapunov functional method: analysis and design," in *IEEE Transactions on Automatic control*, vol. 51 of *5*, pp. 890–897, May 2006.

[86] S. P. Boyd, L. E. Ghaoui, E. Feron, and V. Balakrishnan, *Linear Matrix Inequalities in System and Control Theory*, vol. 15. SIAM, 1994.

[87] A. J. L. P. Gahinet, A. Nemirovski and M. Chilali, *LMI Toolbox for User with Matlab*. The MathWorks Inc, 2001.

[88] J. K. Tar, I. J. Rudas, J. F. Bito, and J. A. T. Machado, "Centralized and decentralized applications of a novel adaptive control," in *Proceedings of IEEE International Conference on Intelligent Engineering Systems (INES)*, pp. 87–92, September 2005.

[89] P. Fraisse, D. Andreu, R. Zapata, J. P. Richard, and T. Divoux, "Remote decentralized control strategy for cooperative mobile robots," in *8th Control, Automation, Robotics and Vision Conference*, vol. 2, pp. 1011–1016, December 2004.

[90] K. Malakian and A. Vidmar, "Comparison of centralized and decentralized linear-quadratic-gaussian path control problems," in *Proceedings of 10th IEEE/AIAA Conference on Digital Avionics Systems*, pp. 68–78, October 1991.

[91] C. Agnew, "Dynamic modeling and control of congestion-prone systems," in *Operation Research*, vol. 24 of *3*, pp. 400–419, May 1976.

[92] K. L. Rider, "A simple approximation to the average queue size in the time-dependent m/m/l queue," in *Journal of the ACM Homepage table of contents archive*, vol. 23 of *2*, pp. 361–367, April 1976.

[93] W.K.Grassmann, *Computational Methods in Probability Theory: Handbooks in Operations Research and Management Science*, vol. 2. North Holland, 1990.

[94] S. G. Eick, W. A. Massey, and W. Whitt, "Nonstationarity in offered traffic to the at/t long distance network," in *AT/T Joint Symposium on Performance Analysis and Teletraffic Research*, December 1990.

[95] S. Floyd, "Metrics for the evaluation of congestion control mechanism," tech. rep., RFC 5166, March 2008.

[96] N. Dukkipati and N. McKeow, "Why flow-completion time is the right metric for congestion control," in *ACM Computer Communication Review (SIGCOMM)*, vol. 36 of *1*, pp. 59–62, January 2006.

[97] D. Tipper and M. K. Sundareshan, "Numerical methods for modeling computer networks under nonstationary conditions," in *IEEE Journal of Selected Areas in Communications*, vol. 8 of *9*, pp. 1682–1695, December 1990.

[98] H. Bin-Abbas and D. Tipper, "A call level adaptive bandwidth allocation scheme based on lyapunov control theory," in *IEEE 11th Symposium on Computers and Communications*, pp. 655–661, 2006.

[99] Y. Fan, Z. P. Jiang, and H. Zhang, "Stabilizing queues in large-scale networks," in *IEEE 62nd Vehicular Technology Conference*, vol. 2, pp. 937–941, 2005.

[100] D. Tipper, Y. Qian, and X. Hou, "Modeling the time-varying behavior of mobile ad hoc networks," in *Proceedings of ACM International Workshop on Modeling Analysis and Simulation of Wireless and Mobile Systems*, pp. 12–19, 2004.

[101] G. Bastin and V. Guffens, "Congestion control in compartmental network systems," in *Systems and Control Letters*, vol. 55 of *8*, pp. 689–696, August 2006.

[102] D. T. A. Pitsillides, J. Lambert, "Optimal bandwidth control in atm based multimedia networks," in *International Conference on Telecommunications ICT'95*, April 1995.

[103] H. Lutkepohl, *Handbook of matrices.* John Wiley and Sons, 1996.

[104] H. Ranjzad, A. Ghaffar, and P. Rahbar, "A new analytical model and protocol for mobile ad-hoc networks based on time varying behavior of nodes," in *Communications in Computer and Information Science*, vol. 36, pp. 57–67, 2009.

[105] E. G. Gilbert, "Linear control systems with pointwise-in-time constraints: What do we do about them?," in *Proceedings of the American Control Conference*, pp. 2565 – 2565, 1992.

[106] E. G. Gilbert and K. T. Tan, "Linear systems with state and control constraints: The theory and application of maximal output admissible sets," in *IEEE Transactions on Automatic control*, vol. 36 of *9*, pp. 1008–1020, September 1991.

378

[107] K. Hirata and M. Fujita, "Analysis of conditions for non-violation fo constraints on linear discrete-time systems with exogenous inputs," in *Proceedings of the 36th Conference on Decision and Control*, vol. 2, pp. 1477–1478, December 1997.

[108] I. Kolmanovsky and E. G. Gilbert, *Multimode regulators for systems with state & control constraints and disturbance inputs, Control using logic-based switching*, vol. 222. Lecture Notes in Control and Information Sciences, Springer, 1997.

[109] I. Kolmanovsky and E. G. Gilbert, "Maximal output admissible sets for discrete-time systems with disturbance inputs," in *Proceedings of American Control Conference*, vol. 3, pp. 1995–1999, June 1995.

[110] A. S. Morse, "Control using logic-based switching," in *Lecture Notes in Control and Information Sciences, Springer*, p. 276, 1997.

[111] G. F. Wredenhagen and P. R. BClanger, "Piecewise-linear lq control for systems with input constraints," in *Automatica*, vol. 30 of *3*, pp. 403–416, March 1994.

[112] K. Hirata and M. Fujita, "Multimode switching state feedback control of constrained linear discrete-time systems," in *Proceedings of the IEEE International Conference on Control Applications*, vol. 1, pp. 148–152, September 1998.

[113] K. Hirata and M. Fujita, "Controller switching strategies for constrained mechanical systems with applications to the remote control over networks," in *Proceedings of the IEEE International Conference on Control Applications*, vol. 1, pp. 480–484, September 2004.

[114] A. Okuyama and T.Yamaguchi, "Controller switching strategy for constrained systems and its application to hard disk drives," in *9th IEEE International Workshop on Advanced Motion Control*, pp. 143–148, 2006.

[115] A. H. Glattfelder and W. Schaufellberger, *Control systems with input and output constraints.* Springer, 2003.

379

[116] S. S. L. Chang and T. K. C. Peng, "Adaptive guaranteed cost control of systems with uncertain parameters," in *IEEE Transactions on Automatic Control*, vol. 17 of *4*, pp. 474–483, April 1972.

[117] I. R. Petersen and D. C. McFarlane, "Optimal guaranteed cost control and filtering for uncertain linear systems," in *IEEE Transactions on Automatic Control*, vol. 39 of *9*, pp. 1971–1977, September 1994.

[118] G. H. Yang, J. L. Wang, and Y. C. Soh, "Guaranteed cost control for discrete-time linear systems under controller gain perturbations," in *Application of Linear Algebra*, vol. 312 of *1-3*, pp. 161–180, June 2000.

[119] E. F. Costa and V. A. Oliveira, "On the design of guaranteed cost controllers for a class of uncertain linear systems," in *Systems and Control Letters*, vol. 46 of *1*, pp. 17–29, May 2002.

[120] G. C. L. Yu and M. Yang, "Optimal guaranteed cost control of linear uncertain systems: Lmi approach," in *Proceedings of the 14th IFAC World Congress*, pp. 541–546, June 1999.

[121] S. Xu, J. Lam, C. Yang, and E. I. Verriest, "An lmi approach to guaranteed cost control for uncertain linear neutral delay systems," in *International Journal of Robust and Nonlinear Control*, vol. 13 of *1*, pp. 35–53, January 2003.

[122] S. H. Esfahani, S. O. R. Moheimani, and I. R. Petersen, "Lmi approach to suboptimal guaranteed cost control for uncertain time-delay systems," in *IEEE Proceedings of Control, Theory and Applications*, vol. 145 of *6*, pp. 491–498, November 1998.

[123] Y. S. Lee, Y. S. Moon, and W. H. Kwon, "Delay-dependent guaranteed cost control for uncertain state-delayed systems," in *Proceedings of the American control conference*, vol. 5, pp. 3376–3381, June 2001.

[124] W. H. Chen, J. X. Xu, and Z. H. Guan, "Guaranteed cost control for uncertain markovian jump systems with mode-dependent time-delays," in *IEEE Transactions on Automatic Control*, vol. 48 of *12*, pp. 2270–2277, December 2003.

[125] J. H. Park, "Delay-dependent criterion for guaranteed cost control of neutral delay systems," in *Journal of optimization theory and applications*, vol. 124 of *2*, pp. 491–502, February 2005.

[126] D. Liberzon, *Switching in systems and control*. Boston: Birkhauser, 2003.

[127] P. A. Ioannou, *Adaptive control tutorial*. Society for Industrial and Applied Mathematics, 2006.

[128] P. A. Ioannou and J. Sun, *Robust adaptive control*. Upper Saddle River, 1996.

[129] P. Park, "A delay-dependent stability criterion for systems with uncertain time-invariant delays," in *IEEE Transactions on Automatic Control*, vol. 44 of *4*, pp. 876–877, April 1999.

[130] K. Bouyoucef and K. Khorasani, "A robust distributed congestion control strategy for differentiated-services network," in *IEEE Transactions on Industrial Electronics*, vol. 56 of *3*, pp. 608–617, March 2009.

[131] K. Bouyoucef and K. Khorasani, "A sliding mode-based congestion control for time delayed differentiated-services networks," in *Proceedings of the IEEE Mediterranean Conference on Control and Automation*, vol. T31-022, pp. 1–6, July 2007.

[132] R. R. Chen and K. Khorasani, "A markovian jump congestion control strategy for mobile ad-hoc networks with differentiated services traffic," in *Proceedings of the* 29th *Chinese Control Conference*, pp. 4701–4708, July 2010.

[133] Scalable Networks, *QualNet 4.0 Product Tour*, 2006.

[134] M. Mariton, *Jump Linear Systems in Automatic Control*. New York: Marcel Dekker, 1990.

[135] E. K. Boukas and Z. K. Liu, *Deterministic and Stochastic Time Delay Systems.* Birkhauser, 2002.

[136] E. K. Boukas, *Stochastic Switching Systtems.* Birkhauser, 2006.

[137] P. Shi and E. K. Boukas, "Control of markovian jump discrete-time systems with norm bounded uncertainty and unknown delay," in *IEEE Transactions on Automatic Control*, vol. 44 of *11*, pp. 2139–2144, November 1999.

[138] M. S. Mahmoud and P. Shi, "Robust kalman filtering for continuous time-lag systems with markovian jump parameters," in *IEEE Transactions on Circuits and Systems I-Fundamental Theory and Applications*, vol. 50 of *1*, pp. 98–105, January 2003.

[139] E. K. Boukas and P. Shi, "Guaranteed cost control of discrete-time markovian jumping uncertain systems," in *IEEE American Control Conference*, vol. 2, pp. 733–737, 1998.

[140] E. K. Boukas and Z. K. Liu, "Robust stability and h_∞ control of discrete-time jump linear systems with time-delay: an lmi approach," in *Proceedings of the 39th IEEE Conference on Decision and Control*, vol. 2, pp. 1527–1532, December 2000.

[141] E. K. Boukas, Z. K. Liu, and P. Shi, "Delay-dependent stability and output feedback stabilisation of markov jump linear system with time-delay," in *IEE Proceedings on Control Theory and Applications*, vol. 149 of *5*, pp. 379–386, September 2002.

[142] E. K. Boukas and H. Liu, "Delay-dependent stabilization of stochastic discrete-time systems with time-varying time-delay," in *American Control Conference*, pp. 2448–2453, July 2007.

[143] A. Haidar and E. K. Boukas, "Robust stability criteria for markovian jump singular systems with time-varying delays," in *IEEE 47th Conference on Decision and Control*, pp. 4657–4662, December 2008.

[144] L. Zhang, E. K. Boukas, and J. Lam, "Analysis and synthesis of markov jump linear systems with time-varying delays and partially known transition probabilities," in

IEEE Transactions on Automatic Control, vol. 53 of *10*, pp. 2458–2464, November 2008.

[145] S. Ma and E. K. Boukas, "A descriptor system approach to sliding mode control for uncertain markov jump systems," in *7th Asian Control Conference*, pp. 182–187, August 2009.

[146] L. Wu, P. Shi, and H. Gao, "State estimation and sliding-mode control of markovian jump singular systems," in *IEEE Transactions on Automatic Control*, vol. 55 of *5*, pp. 1213–1219, May 2010.

[147] J. Xiong, V. A. Ugrinovskii, and I. R. Petersen, "Local mode dependent decentralized stabilization of uncertain markovian jump large-scale systems," in *IEEE Transactions on Automatic Control*, vol. 54 of *11*, pp. 2632–2637, November 2009.

[148] Y. Y. Cao and J. Lam, "Stochastic stabilizability and h_∞ control for discretetime jump linear systems with time delay," in *Journal of The Franklin Institute*, vol. 336 of *8*, pp. 1263–1281, 1999.

[149] Y. Y. Cao and J. Lam, "Robust h_∞ control of uncertain markovian jump systems with time-delay," in *IEEE Transactions on Automatic Control*, vol. 45 of *1*, pp. 77–83, January 2000.

[150] S. Y. Xu, J. Lam, and X. R. Mao, "Delay-dependent h_{infty} control and filtering for uncertain markovian jump systems with time-varying delays," in *IEEE Transactions on Circuits and Systems I-Regular Papers*, vol. 54 of *9*, pp. 2070–2077, September 2007.

[151] K. Gu, "An integral inequality in the stability problem of time-delay systems," in *Proceedings of 39th IEEE Conference on Decision and Control*, vol. 3, pp. 2805–2810, December 2000.

[152] Z. He, Y. Wang, F. W. Meng, and M. Shao, "Monte carlo simulation of markovian jump system," in *Electric Machine and Control*, vol. 12 of *1*, pp. 80–83, January 2008.

[153] W. S. Haddad and V. S. Chellabiona, "Stability theory for nonnegative and compartmental dynamical systems with time delay," in *IEEE American Control Conference*, vol. 2, pp. 1422–1427, June 2004.

[154] Y. Ji and H. J. Chizeck, "Controllability, stabilizability, and continuous time markovian jump linear quadratic control," in *IEEE Transactions on Automatic Control*, vol. 35 of *7*, pp. 777–788, July 1990.

[155] Z. Wu, H.Su, and J. Chu, "Delay-dependent h_∞ control for singular markovian jump systems with time delay," in *Optimal Control Applications and Methods*, vol. 30 of *5*, pp. 443–461, 2008.

[156] E. K. Boukas, Z. K. Liu, and F. Al-Sunni, "Guaranteed cost control of a markov jump linear uncertain system using a time-multiplied cost function," in *Journal of optimization theory and applictions*, vol. 116 of *1*, pp. 183–204, January 2003.

[157] E. K. Boukas and Z. K. Liu, "Guaranteed cost control for discrete-time markovian jump linear system with mode-dependent time-delays," in *Proceedings of the 41st IEEE Conference on Decision and Control*, vol. 4, pp. 3794 – 3798, December 2002.

[158] Y. Zhou and H. Li, "Guaranteed cost control for singular markovian jump systems with time delay," in *2010 Chinese Control and Decision Conference (CCDC)*, pp. 1971–1975, 2010.

[159] Y. Luo, M. Zhou, X. W. X. Zhang, andX. Qi, and R. Chen, "Robust guaranteed cost control for markovian jump systems with time delay," in *IEEE International Conference on Information and Automation (ICIA)*, pp. 323–328, June 2010.

[160] W. H. Chen, J. X. Xu, and Z. H. Guan, "Guaranteed cost control for uncertain markovian jump systems with mode-dependent time-delays," in *IEEE Transactions on Automatic Control*, vol. 48 of *12*, pp. 2270–2277, December 2003.

[161] A. Jegen, *Robust Control: The Parameter Space Approach*. Series: Communications and Control Engineering, Springer, 2002.

[162] Y. Fan, Z. P. Jiang, and X. Wu, "A control theoretic approach to stabilizing queues in large-scale networks," in *IEEE Communications Letters*, vol. 9 of *10*, pp. 951–953, 2005.

[163] Y. Qian and Q. Li, "A robust nonlinear pid congestion control algorithm for time-delay network with parametric uncertainty," in *The Sixth World Congress on Intelligent Control and Automation*, vol. 1, pp. 2398–2402, June 2006.

[164] L. Tan, M. Yin, and L. Chen, "A new framework for congestion control of integrated services in computer networks," in *International Conference on Communication Technology Proceedings*, vol. 1, pp. 361–367, 2003.

[165] M. Barbera, A. Lombardo, C. Panarello, and G. Schembra, "Queue stability analysis and performance evaluation of a tcp-compliant window management mechanism," in *IEEE/ACM Transactions on Networking*, vol. 18 of *4*, pp. 1275–1288, 2010.

[166] H. Balakrishnan, N. Dukkipati, N. McKeown, and C. J. Tomlin, "Stability analysis of explicit congestion control protocols," in *IEEE Communications Letters*, vol. 11 of *10*, pp. 823 – 825, 2007.

[167] H. Wang, W. Y, Y. Mao, Y. Jing, and L. Guo, "Robust congestion control for uncertain time-varying delay network systems," in *Control and Decision Conference(CCDC)*, pp. 739–743, 2008.

[168] Y. Gao, X. Guan, B. Yang, and C. Long, "A novel algorithm of robust congestion control in multi-virtual-circuit atm networks," in *Fifth World Congress on Intelligent Control and Automation*, vol. 2, pp. 1502–1505, June 2004.

[169] X. Li and C. E. D. souza, "Delay-dependent robust stability and stabilization of uncertain linear delay systems: a linear matrix inequality approach," in *IEEE Transactions on Automatic Control*, vol. 42 of *8*, pp. 1144–1148, August 1997.

[170] Y. Y. Cao, Y. X. Sun, and J. Lam, "Delay-dependent robust h_∞ control of uncertain systems with time-varying delays," in *IEEE Proceedings of Control Theory Applications*, vol. 145 of *3*, pp. 338–344, 1998.

[171] Z. Wang, Y. Liu, and X. Liu, "Exponential stabilization of a class of stochastic system with markovian jump parameters and mode-dependent mixed time-delays," in *IEEE Transactions on Automatic Control*, vol. 55 of *7*, pp. 1656–1662, July 2010.